Investigation of New Intermolecular and Intramolecular Trapping Reactions of 1,2-Cyclohexadienes.

by

Verner Alexander Lofstrand

A thesis submitted in partial fulfillment of the requirements for the degree of

Doctor of Philosophy

Department of Chemistry
University of Alberta

Abstract

Small carbocyclic allenes are one of many reactive intermediates though their use in the formation of strategic bonds in organic chemistry is limited. While a vast literature exists detailing the generation and trapping of these species very little has been dedicated to investigating the synthetic potential. This thesis will discuss several new advancements toward the development of small-carbocyclic allenes as strategic intermediates in the synthesis of heterocyclic compounds.

Chapter 1 provides a detailed recount of the generation, trapping, and reactive mechanistic inspection of 1,2-cyclohexadiene and derivatives thereof. This is to act as a comprehensive review of the chemistry associated with six-membered cyclic allenes to contrast with the research results presented in this thesis.

Chapter 2 will describe the development and use of a robust method to cyclic allene precursor synthesis using copper mediated nucleophilic silylation. The allylic silanes synthesized were presumed to form cyclic allenes *in situ* based upon the formation of new and previously described cycloadducts. The cyclic allene precursors were used further in the synthesis of nitrogen containing heterocycles via the reaction of 1,3-dipolar compounds with 1,2-cyclohexadiene and derivatives. The cycloaddition proved to be general for a number of 1,3-dipolar compounds with high regio-, site-, and diastereoselectivity.

Chapter 3 then expands upon the formation of nitrogen containing heterocycles by exploring attempts to transfer/conserve the central chirality of allene precursors to cycloadducts via axially chiral cyclic allene intermediates.Within this context we sought to investigate the mechanism of the cycloaddition, with a focus on whether it occurs by a concerted or stepwise process.

Chapter 4 discusses the attempts made toward a general intramolecular trapping strategy. Via the Stork-Danheiser alkylation, a number of β-subsituted 2-bromo-2-cyclohexen-1-ones were synthesized, silylated, and subjected to fluoride-mediated elimination conditions. With a number of tethered trapping molecules attached at the β-position the ability to trap a cyclic allene in an intramolecular manner was evaluated.

Finally, Chapter 5 discusses some strategy and synthetic efforts toward asphaltene model compounds. The synthetic stratagem relied upon a [2+2+2] cycloaddition of nitriles and 1,2-dipropargylic arenes. Effort towards new archipelago asphaltene model compounds is discussed.

Acknowledgements

First of all I am inconceivably indebted to Professor Frederick G. West. Two and a half years ago he gave me a second chance to rediscover my passion for chemistry through a crazy, complicated, frustrating, but perfect project involving too many new reactions and processes to even count. Without your guidance I would not be here today and for that I couldn't begin to repay you. You have taught me many things I hope to be able to pass along. Thank you.

This thesis should be dedicated to my family though. For without them it would have been over long before it began. Seriously it would have been done years ago. The unwavering support I get each night when I come home from my kids (Simon, 4, and Sasha, 1) and my wife Erika (29) compels me to quit, stay home, and be in our pajamas together. But they also drive me to keep going, to finish my dream, and make a new life for us wherever that may be. I love you very much.

To my mom and brother, thank you for being extremely supportive and keeping me on my path. More importantly you kept me humble.

I started my graduate studies with many people but it seemed like I finished with only a few. Yonghoon Kwon, you are amazing, but that’s not my problem. We will meet again and it will be good.

Thomas, thanks for all the support and help keeping me sane. I fully expect you to live tweet the lab day-to-day goings on. Bren, thank you for being naïve and easily persuaded, but also very patient with an old dog while he learns how to talk to people. Owen, have a nice life. Ryan, thanks for being my double and helping me survive this experience. Finally thank you to my group, the West group. You all helped me get to where I am and I am forever grateful.

Dr. Roy Jensen. I am almost certain that the beginning of my journey can be traced to a classroom in Grant MacEwan University where I learned chemistry from you. In that classroom I knew I wanted to continue doing chemistry. Thank you for teaching me.

This is by far the most difficult thing I have ever done. I don't think anyone would expect any different though. My understanding of perseverance and failure has matured significantly over the past eleven years to the point that I doubt people would recognize

me. It is worth doing as long as it makes you happy. I made things no person ever has, I made some things in a way nobody considered, and I accomplished some things some people said couldn't be done (some would say that was graduating).

For any person I may have missed this last line is for you. Though you may not be present here, your influence will stay with me forever.

Table of Contents

List of Figures

Chapter 5

List of Tables

Chapter 1

Chapter 2

Chapter 3

Chapter 4

Chapter 5

List of Equations

Chapter 1

List of Schemes

Chapter 1

Chapter 2

Chapter 3

Chapter 4

Chapter 5

List of Symbols and Abbreviations

^{1}H	proton
^{13}C	carbon-13
Å	angstrom
AA	acetic acid
Ac	acetyl
Ac_2O	acetic anhydride
Anal.	elemental analysis
app.	apparent (spectral)
aq	aqueous solution
Ar	aryl
B:	unspecified base
BBN	borobicyclononane
BHT	butylated hydroxytoluene
Bn	benzyl
br	broad (spectral)
Bu	butyl
°C	degrees Celsius
calcd	calculated
cat.	indicates that the reagent was used in a catalytic amount
CBS	Corey-Bakshi-Shibata
cm^{-1}	wave numbers
COSY	H-H correlation spectroscopy

conc.	concentrated
CsF	cesium fluoride
Cy	cyclohexyl
d	day(s); doublet (spectral)
DBU	1,8-diazabicyclo[5.4.0]undec-7-ene
DCC	N,N’-dicyclohexylcarbodiimide
DCE	1,2-dichloroethane
DCM	dichloromethane
dd	doublet of doublets (spectral)
ddd	doublet of doublet of doublets (spectral)
DFT	density functional theory
DIBAL-H	diisobutylaluminum hydride
DIPA	diisopropylamine
DIPEA	diisopropylethylamine (Hunig's Base)
DMAP	4-dimethylaminopyridine
DMF	N,N-dimethylformamide
DMSO	dimethylsulfoxide
DMP	Dess-Martin periodinane
DMPU	1,3-Dimethyl-3,4,5,6-tetrahydro-2-pyrimidinone
DMS	Doering-Moore-Skattebøl
DPIBF	1,3-diphenylisobenzofuran
d.r.	diastereomeric ratio
dt	doublet of triplets (spectral)

dtd	doublet of triplets of doublets (spectral)
E^+	unspecified electrophile
EDG	electron-donating group
e.e.	enantiomeric excess
EI	electron impact (mass spectrometry)
ent	enantiomer
e.r.	enantiomeric ratio
ESI	electrospray ionization (mass spectrometry)
Et	ethyl
EtOAc	ethyl acetate
equiv	equivalent(s)
EWG	electron-withdrawing group
F^-	fluoride anion
FVP	flash vacuum pyrolysis
g	gram(s)
$\Delta G^‡$	Transition-state Gibbs free energy change
h	hour(s)
Hex	hexyl
HFIP	hexafluoroisopropanol
HMBC	heteronuclear multiple bond coherence (spectral)
HMPA	hexamethylphosphoramide
HSQC	heteronuclear single quantum coherence (spectral)
HRMS	high resolution mass spectrometry

hν	light
Hz	hertz
IPA	isopropanol
i-Pr	isopropyl
IR	infrared
J	coupling constant
kcal	kilocalories
KHMDS	potassium bis(trimethylsilyl)amide
L	litre(s); unspecified ligand
LA	Lewis acid
LAH	lithium aluminum hydride
LDA	lithium diisopropylamide
LHMDS	lithium bis(trimethylsilyl)amide
Ln*	chiral ligand
LUMO	lowest unoccupied molecular orbital
M	molar
m	multiplet (spectral)
M^+	generalized Lewis acid; molecular ion
Me	methyl
Mes	mesityl
mg	milligram(s)
MHz	megahertz
MLn	unspecified metal-ligand pair

μL	microlitre(s)
μW	microwave(s)
min	minute(s)
mL	millilitre(s)
mm	millimeter(s)
mmol	millimole(s)
mol	mole(s)
MOM	methoxymethyl
mp	melting point
MS	molecular sieves
Ms	methanesulfonyl
m/z	mass to charge ratio
n-Bu	normal butyl
nm	nanometer
NMR	nuclear magnetic resonance
NOE	nuclear overhauser effect
n-Pr	normal propyl
Nuc	unspecified nucleophile
OMOM	methoxymethyl ether
ORTEP	Oak Ridge Thermal-Ellipsoid Plot
Ph	phenyl
ppm	parts per million
Pr	propyl

R	generalized alkyl group of substituent
R_f	retention factor (in chromatography)
rOe	rotating-frame Overhauser enhancement
rt	room temperature
s	singlet (spectral)
SARA	Saturate, Aromatic, Resin, and Asphaltene separation
sat'd	saturated
$\Delta S^{\ddagger}$	Transition state entropy change
t	triplet (spectral)
T	temperature
TBAF	tetrabutylammonium fluoride
TBAT	tetrabutylammonium triphenyldifluorosilicate
TBS	tert-butyldimethylsilyl
t-Bu	tert-butyl
TEA	triethylamine
TES	triethylsilyl
Tf	trifluoromethanesulfonyl
TFA	trifluoroacetic acid
TFAA	trifluoroacetic anhydride
TFE	2,2,2-trifluoroethanol
THF	tetrahydrofuran
THP	2-tetrahydropyranyl
TIPS	triisopropylsilyl

TLC	thin layer chromatography
TMEDA	tetramethylenediamine
TMS	trimethylsilyl
Tol	tolyl
TROESY	transverse rotating-frame Overhauser enhancement spectroscopy
Ts	p-toluenesulfonyl
TsOH	p-toluenesulfonic acid
VSEPR	Valence Shell Electron Pair Repulsion model
X	variable substituent (alkyl, heteroatom, proton, etc.)
XPHOS	2-dicyclohexylphosphino-2′,4′,6′-triisopropylbiphenyl
δ	chemical shift
Δ	heated to reflux

1. 1,2-Cyclohexadiene: Generation, Trapping, and Mechanism

1.1 Reactive Intermediates

Carbon-carbon bond formation relies heavily upon the generation of reactive intermediates. Molecular orbital analysis shows that increasing the energy of the HOMO of the nucleophilic partner or lowering the LUMO of the electrophile will facilitate a faster reaction under milder reaction conditions (Figure 1.1).[1] There are a number of strategies that have been employed previously to generate reactive intermediates *in situ* via the formation of anions, cations, radicals, or carbenes. A molecule that contains a sterically crowded bond or contains a functional group forced to adhere to non-ideal bonding angles is also activating due to the introduction of strain.

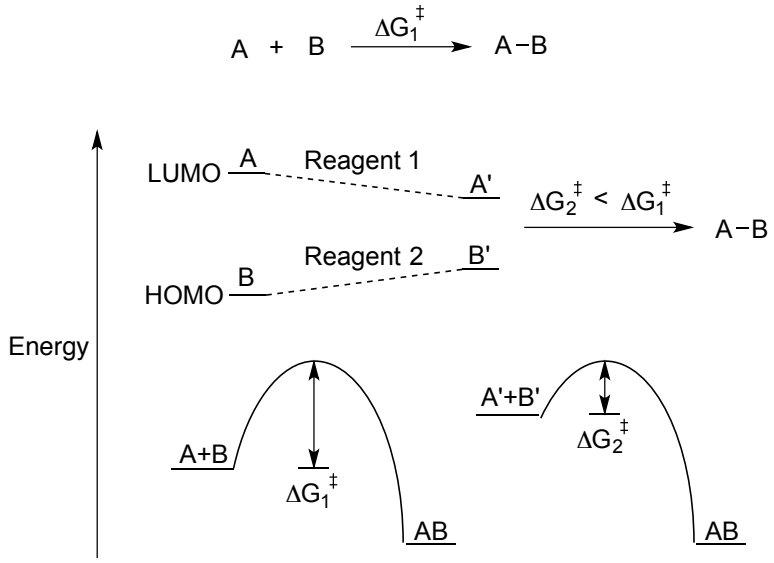

Figure 1.1 - Activation of substrates via the formation of a reactive intermediate.

1.2 Using Strain to Activate an Intermediate

1.2.1 Ring Strain

One method of introducing strain into a molecule is via the use of small rings.[2] VSEPR theory predicts an ideal bond angle of 109.5 ° around an sp^3 hybridized carbon atom. A six-membered carbocycle with all sp^3 hybridized carbon atoms is predicted to have ideal internal bond angles when adopting a chair conformation and be the only carbocycle free of strain.[3] Decreasing the number of carbon atoms within the ring

decreases the internal bond angles, forcing a rehybridization of the atoms. From Walsh's depiction (Figure 1.2) the internal carbon-carbon bonds of cyclopropane are derived almost exclusively from p-orbital overlap.[4] The exocyclic carbon-hydrogen bonds are significantly more acidic than those of a non-functionalized, straight chain alkane, and shorter due to the increase in s-character.

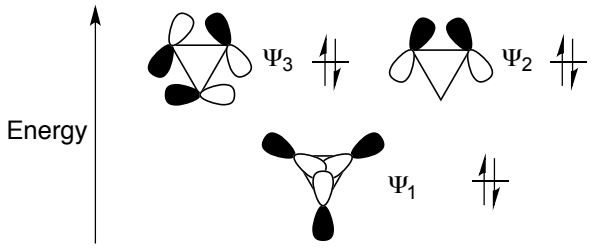

Figure 1.2 - Walsh's depiction of σ bonding orbitals of cyclopropane.

In a similar fashion to carbocycle reactivity, the reactivity of functional groups constrained within a small ring can be changed based upon strain. Olefins are generally considered to be nucleophilic, however, an anti-Bredt's olefin[5] such as **4** has poor overlap between the two adjacent sp^2 carbon centers due to the conformational constraints of the bridgehead carbon.[6] The decrease in π overlap between the two olefin carbons makes the olefin significantly more receptive to nucleophilic attack that extinguishes the strain and generates new complexity under mild reaction conditions.

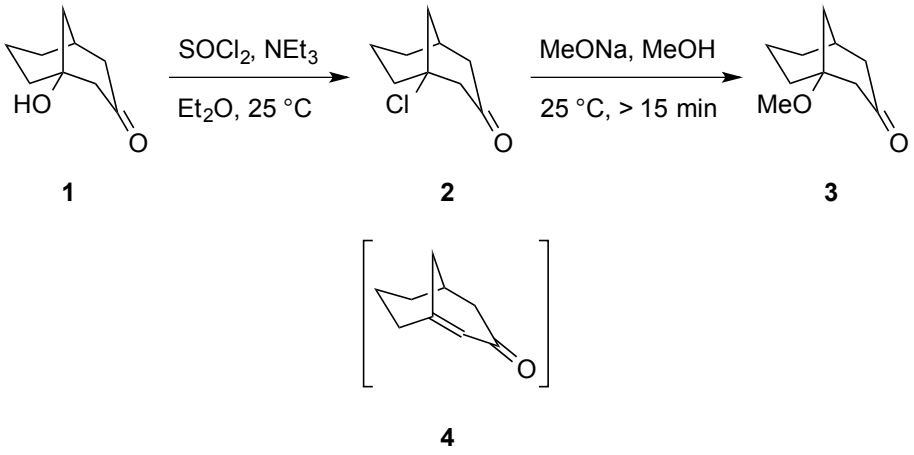

Scheme 1.1 - House's *in situ* generation of anti-Bredt's olefin 4.

1.2.2 Cyclic Alkynes

The preferred dihedral angle of an sp hybridized carbon atom is 180 °. Alkynes have two sp hybridized carbon atoms that are adjacent thus four atoms that have a preferred linear geometry. The strain associated with cyclic alkynes (and other constrained π systems) comes from forcing the adoption of bond angles less than the ideal 180 °, leading to decreased molecular overlap, and in turn greater reactivity. The significant amount of literature dedicated to understanding and harnessing the power of cyclic alkynes cannot be thoroughly discussed within this review; however, it is worth mentioning select examples.[7] Within the context of total synthesis, Carreira and coworkers have used the high reactivity of cyclic alkynes to generate complex polycycles from the [2+2] cycloaddition of cyclic alkynes and enolates.[8] Functionalized cyclobutenols undergo ring opening in the presence of a Lewis acid or base to give a formal two-carbon ring expansion and the addition of one degree of unsaturation to the larger carbocycle. The 5-7-6 carbon skeleton of guanacastapenes N and O was assembled in a linear fashion via this method in the recent total synthesis (Scheme 1.2).[9] Diiron (0) nonacarbonyl was found to be the ideal Lewis acid precursor, as it was selective to the ring opening of cyclobutenol **7** without significant side reactions with the acetal.

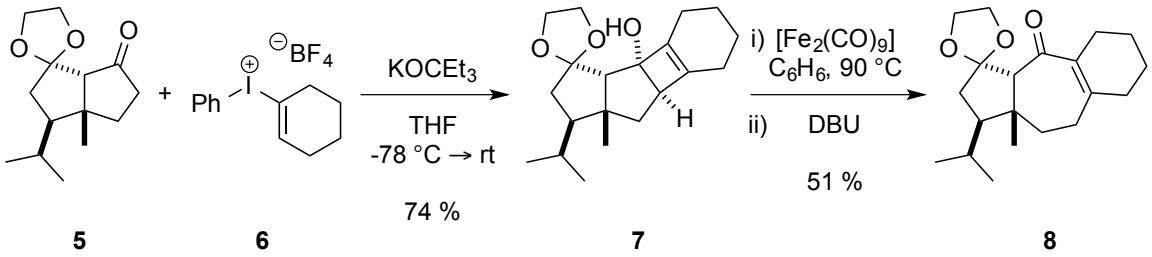

Scheme 1.2 – Key steps in Carreira's total synthesis of guanacastapenes N and O using cyclic alkynes.

Interest in the discovery of "click" reactions[10] to further augment the biochemical investigation of living systems has driven the development of strain-promoted cycloadditions. The Huisgen [3+2] dipolar cycloaddition of alkynes with azides[11,12] has proved to be extremely efficient in the presence of a copper catalyst; however, high catalyst loading and biocompatibility have raised questions as to its *in vivo* applicability.

Wittig and Krebs were the first to report that constraining alkynes in medium-sized carbocycles allows for their spontaneous cycloaddition with azides.[13] To circumvent the need for a catalyst, Bertozzi reported the application of Wittig's strain promoted Huisgen cycloaddition to *in vivo* labeling of cellular structures.[14,15]

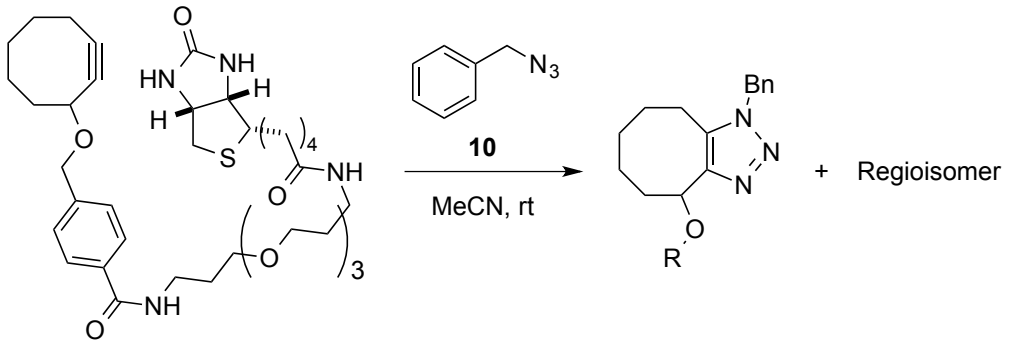

Scheme 1.3 - Strain promoted Huisgen cycloaddition.

1.2.3 Reactivity of Cyclic Allenes in Comparison to Cyclic Alkynes

If the ring is further decreased in size, cyclic alkynes constrained within six or seven-membered rings are not isolable under non-specialized conditions. Regardless of the fleeting existence of cyclic alkynes in a reaction there still exists a breadth of literature on the generation and synthetic utility of cyclohexynes,[16,17] which strongly contrasts with the relative dearth of study on 1,2-cyclohexadiene. The initial generation and definitive intermediacy of 1,2-cyclohexadiene lagged behind the *in situ* synthesis of cyclohexyne by 5 years regardless of their comparably strained structures.[13,18] The facile oligomerization of 1,2-cyclohexadiene warranted careful examination of reaction mixtures, which led finally to the employment of the highly reactive trapping molecule 1,3-diphenylisobenzofuran (DPIBF, **14**) to provide **17** and its diastereomer **17'**, giving definitive evidence of the cyclic allene intermediate (Scheme 1.4).

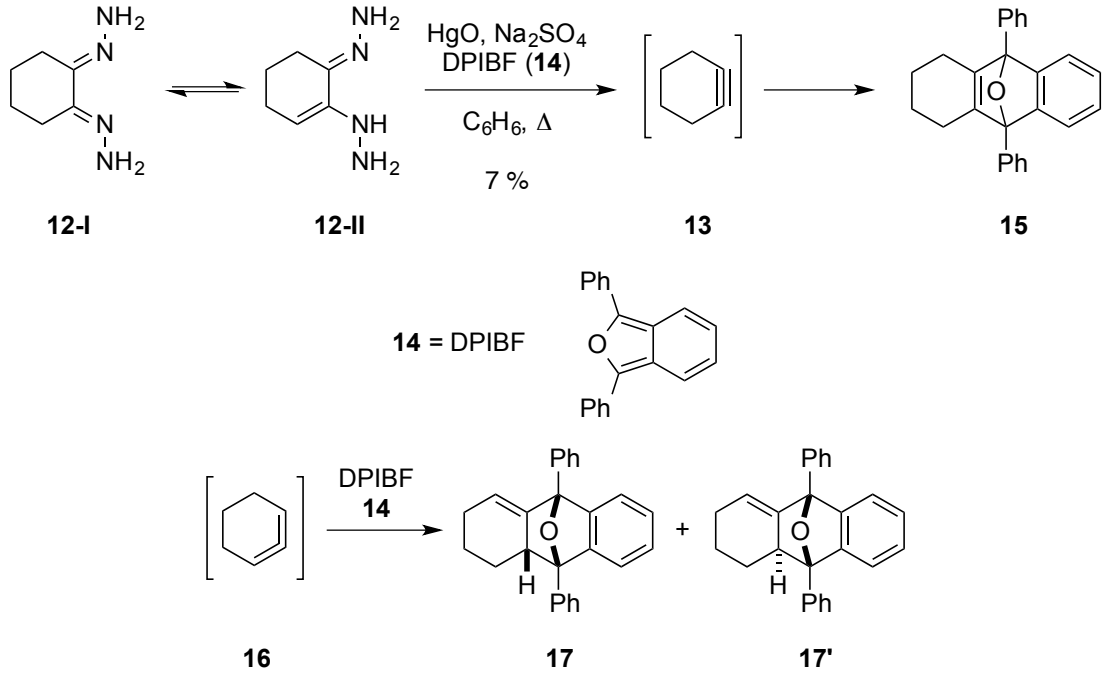

Scheme 1.4 - Generation and trapping of cyclohexyne and 1,2-cyclohexadiene with DPIBF.

The cycloaddition of strained carbocyclic allenes or alkynes with DPIBF (**14**) each gives a characteristic isomeric cycloadduct, **15** and **17/17'** respectively, differing only by the position of the olefin (Scheme 1.4).[13,18] Products **17** and **17'** were hypothesized to be accessible via a base-mediated isomerization of the allylic proton in **15** (formal [1,3] proton shift). However, if the cyclohexyne adduct **15** was subjected to the reaction conditions used to generate cyclic allene adducts **17/17'** no isomerization was detected and vice versa.[18]

One of the main differences in reactivity between cyclic allenes and cyclic alkynes is dimerization (Scheme 1.5). Formation of homodimer **19** quenches the strain of 1,2-cyclohexadiene (**16)** whilst generating a relatively less strained product (**19**).[18] Cyclohexyne homodimerization initially generates antiaromatic butadiene **22**, which undergoes further reactions to dispel the high-energy, anti-aromatic system.[19] Importantly, homodimerization of cyclic allene **16** is diastereoselective and leads to conjugated diene **19**, and not isomers **20** or **21** (Scheme 1.5). The *trans*-isomer **19** is less sterically hindered as the two substituents on the dialkylidenecyclobutane are on opposite sides of the ring (discouraging the formation of *cis*-isomer **21**), although the two fused

rings being *trans* to one another on the cyclobutane introduces a ring strain on the tricyclic system. The orientation of the two approaching allenes in the dimerization along the orthogonal trajectory (**18**) rather than a parallel approach would favor the formation of **19** over **21**. The greater reactivity of central carbon of the cyclic allene leads to exclusive formation of bis(allyl) diradical **18** and precludes the formation of **20**.

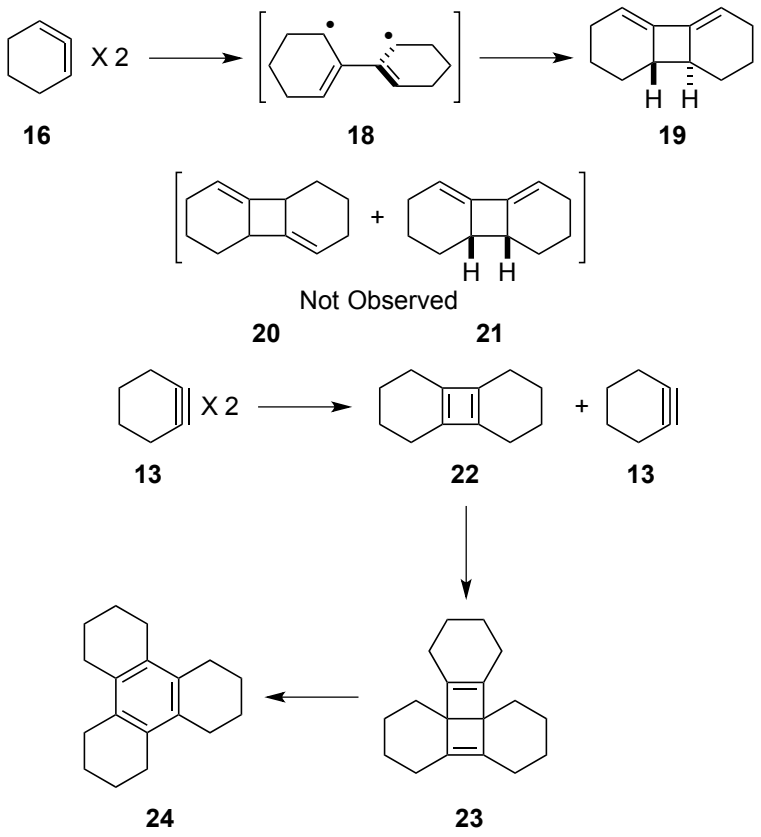

Scheme 1.5 - Dimerization and trimerization reactions of cyclic allenes and alkynes.

1.3 Dimerization of Cyclic Allenes

The dimerization of cyclic allenes has been observed by many research groups and is seemingly an unavoidable side reaction in any reaction involving these intermediates.[20-22] Part of the significant propensity of cyclic allenes to dimerize is derived from the strain energy that is released when diradical **18** forms (~64 kcal/mol based upon the strain relieved in two molecules of cyclic allene **16**).[23] Starting from the assumption of a closed shell cyclic allene (weak double bonds), formation of a bond between the two central carbons rehybridizes the central carbons to sp^2 thus relieving the ring strain associated with having an sp hybridized carbon in a ring and relaxing the

geometric preference of the allene to having two orthogonal double bonds. The diradical intermediate **18** gains significant stability from the rehybridization as the SOMO-π orbital is conjugated with the adjacent olefin to form an allyl-like fragment, though the two allyl fragments are not conjugated due to lack of planarity (Scheme 1.6).

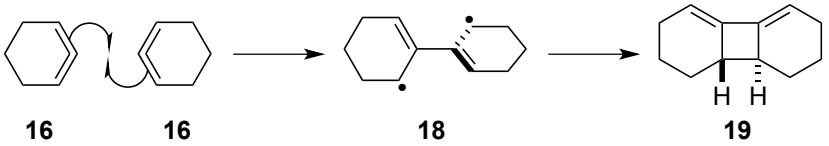

Scheme 1.6 - Dimerization of 1,2-cyclohexadiene

Johnson has recently investigated the dimerization of acyclic allenes and computations suggest a radical dimerization pathway analogous to the mechanism proposed for cyclic allenes.[24] Experimentally, Kiefer and Levek demonstrated that the dimerization of 1,1-dimethylallene (**25**) provides the same products and product ratios as the thermolysis or photolysis of 4,5-dimethylene-3,3,6,6-tetramethyl-3,4,5,6-tetrahydropyridazine **30**, which is also a precursor to tetramethylene-ethane diradical **26** (Scheme 1.7).[25] The decomposition of tetrahydropyridazines is known to proceed via extrusion of dinitrogen to form a diradical species.[26,27]

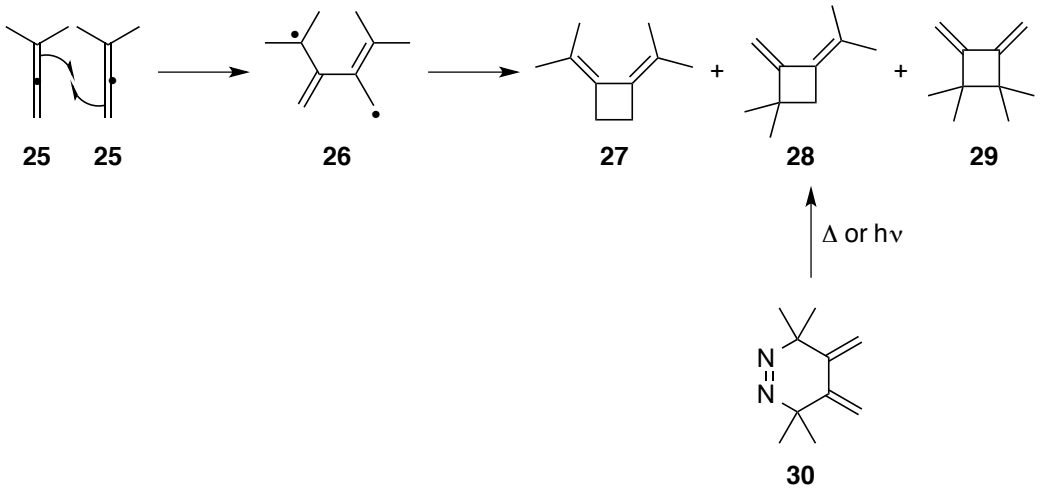

Scheme 1.7 - Dimerization of acyclic allenes.

The radical nature of cyclic allene dimerization is further supported by the addition of a radical scavenger. Bottini and Cabral reported the formation of the 1:1 allene:nitroxide adduct **33** in 19 % yield when the generation of methyl-cyclic allene **31**

was performed in the presence of the di-*t*-butylnitroxide (**34**), without any trace of dimer **32** (Scheme 1.8).[28] In the absence of nitroxide the reaction proceeds to provide 30 % yield of dimer **32**. The yield of the trapped product decreased slightly in the presence of nitroxide **34** regardless of the fact that the radical scavenger fails to react with the monomeric cyclic allene. Nitroxide **34** was reported to only intercept the longer-lived cross-conjugated bisallyl radical system **33**. This implies minimal radical character on the cyclic allene, suggesting a closed-shell cyclic allene.

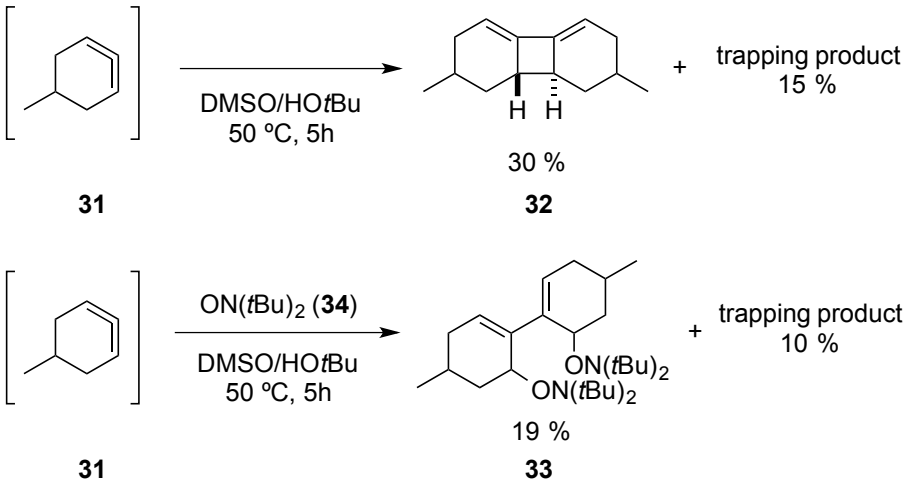

Scheme 1.8 - Interruption of cyclic allene dimerization by nitroxide radicals.

Similarly, temperature plays an important role in the dimerization/oligomerization of cyclic allenes. Moore and Moser report the isolation of tetramers **35** and **36** when 1,2-cyclohexadiene **16** was generated at low temperature with only trace amounts of dimer **19** being formed.[29] When the diethyl ether solvent was heated to reflux during the reaction, dimer **19** was the major product (Scheme 1.9). The temperature dependence is possibly due to the energy associated with forming a cyclobutane ring with two sp^2 carbon centers constrained.

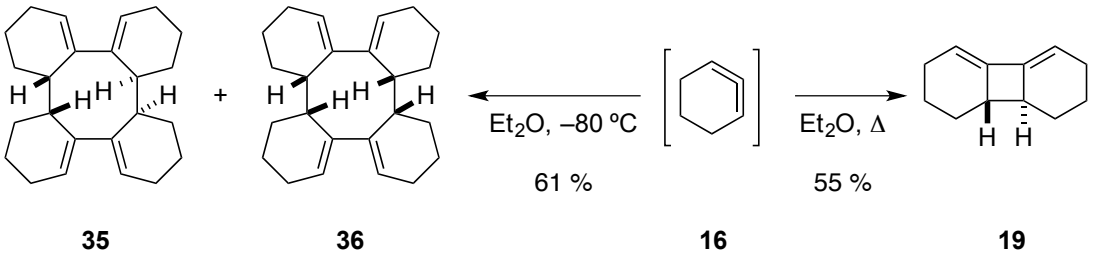

Scheme 1.9 - Temperature effects on cyclic allene dimerization.

The [2+2] dimerization of 1,2-cyclohexadienes is a common reaction and the cyclobutane containing products have been reported for a number of substituted intermediates including, but not limited to 1-methyl,[30] 5-methyl,[28] 1-cyclopropyl, and 1-(3-phenylpropyl).[20] In light of the observation of the many different dimers, the observation of the homodimer is dependent upon the method of generation that will be addressed in later sections.

Interestingly, 1-phenyl-1,2-cyclohexadiene was reported to react very differently when investigated by different groups. Budak and Ceylan,[31] as well as Johnson and Tolbert[32] reported the generation of biphenyl **39** from the *in situ* prepared cyclic allene **37**. The authors proposed that the strain of phenyl-subsituted allene **37** promoted a [1,3]-hydrogen shift and subsequent auto-oxidation of phenyl-1,3-cyclohexadiene **38** (Scheme 1.10). In contrast, Christl and coworkers did not detect any traces of biphenyl when studying the reactivity of 1-phenyl-1,2-cyclohexadiene in the absence of a trap. The cyclic allene appears to follow the expected dimerization pathway with interruption by one of the phenyl substituents, forming dimer **40** in 31 % yield.[33] Interestingly, if the same cyclic allene was generated *in situ* at a lower temperature via a different method, neither biphenyl nor dimer **40** was detected but rather the open trimer **42** in 18 % yield. The authors proposed the formation of **42** arose from dearomatized intermediate **41** undergoing an Alder-ene reaction[34] with a third equivalent of cyclic allene **37** or radical hydrogen atom abstraction and recombination; both reactions are unprecedented for cyclic allenes. These examples again highlight the temperamental nature of cyclic allene generation.

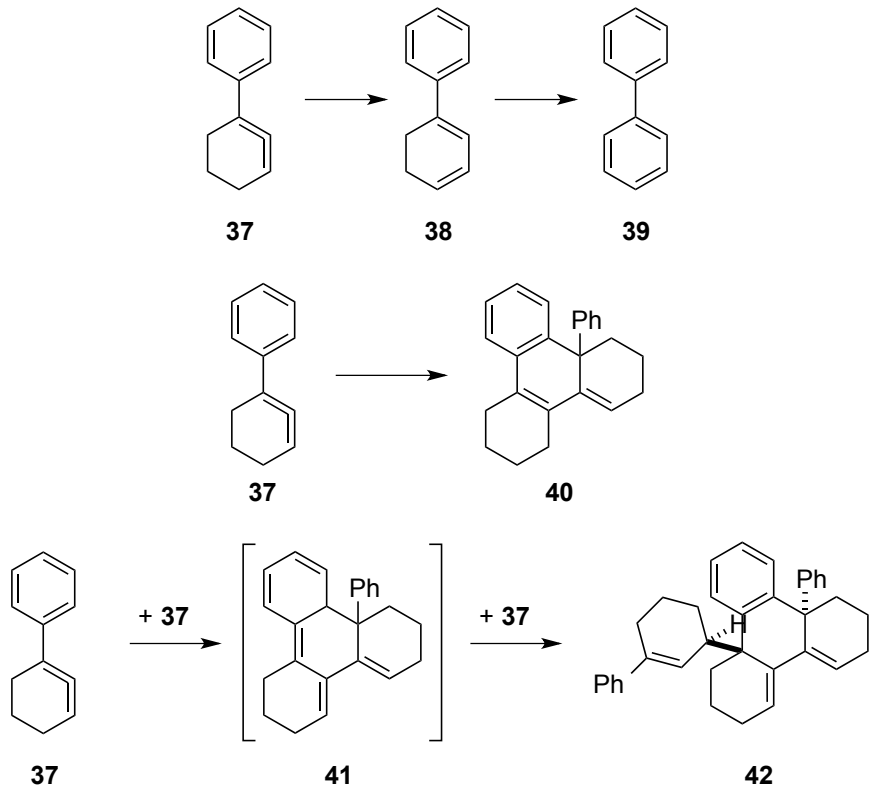

Scheme 1.10 – Different decomposition/oligomerizations of 1-phenyl-1,2-cyclohexadiene.

From these studies there are two characteristics indicative of the generation of a cyclic allene intermediate. The first point of interest is the propensity of the cyclic allene to quench the cyclic allenes strain via its dimerization or oligomerization, and its proposed occurrence via a diradical intermediate. Secondly, from the early work of Wittig and Fritze, cyclic allenes will undergo a formal Diels-Alder reaction with DPIBF (**14**) to generate a stable mixture of diastereomeric cycloadducts. These are important aspects, as the isolation of a 6-membered cyclic allene intermediate has never been reported; therefore, the only evidence of the intermediacy of a cyclic allene (by any method) is the observation of trapping products. The validation of a method to generate cyclic allenes comes from these observations.

1.4 Generation of 1,2-Cyclohexadiene as a Reactive Intermediate

The use of reactive intermediates in synthetically useful applications requires the development of reaction conditions where the species is persistent long enough for

observation or for a subsequent reaction to take place. Several methods have been developed and applied to the generation of cyclic allenes, many of which are still routinely used.

1.4.1 Base-Mediated Eliminative Methods to Generate 1,2-Cyclohexadienes

1.4.1.1 E2 Elimination of Vinyl Leaving Groups

Wittig and Fritze were the first to demonstrate the intermediacy of a cyclic allene via the isolation of both dimerization products and DPIBF trapping products. [18,35] Their work also established base-mediated elimination as a versatile method to generate cyclic allenes *in situ*. Regardless of its prevalence in the literature, the intricacy of the elimination is not to be underestimated. The number of acidic protons on or adjacent to the olefin as shown in Figure 1.3 complicates the selective generation of the cyclic allene.

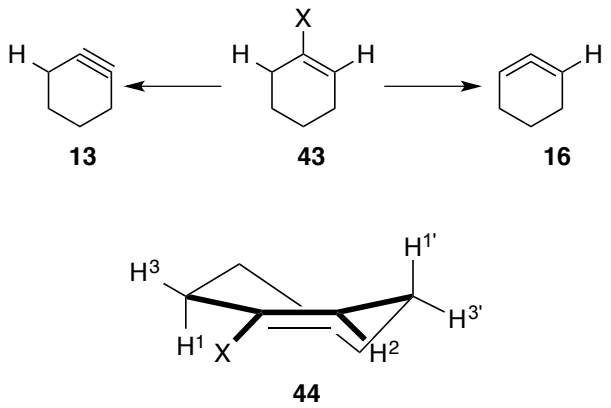

Figure 1.3 - Acidic protons on the cyclohexene skeleton of 43 and the two possible elimination outcomes.

In order to promote elimination of the vinylic leaving group on **43** (X), the hindered base must selectively attack the allylic pseudo-equatorial proton (H^3) (Figure 1.3). Deprotonation of axial proton (H^1) would not lead to elimination via the desired E2 elimination of HX, due to the stereoelectronic requirement for an anti-periplanar or syn-periplanar geometry of the proton and the leaving group. The base must not be so strong as to irreversibly generate allylic anions from the deprotonation of the more acidic pseudo-axial allylic protons (H^1 and $H^{1\prime}$). Favorable orbital overlap suggests attack on the adjacent sp^2-hybridized proton (H^2) would cause the elimination of HX from the

cyclohexene framework, though deprotonation of H^2 would lead to the structurally isomeric cyclic alkyne (**13)**.

The elimination has been successfully controlled using moderately strong, reversible bases, such as potassium *t*-butoxide (Scheme 1.11). The base used is too weak to irreversibly deprotonate the axial proton and successfully eliminated HBr to generate 1,2-cyclohexadiene, which was irreversibly trapped by DPIBF as, reported by Wittig and Fritze.[18,35]

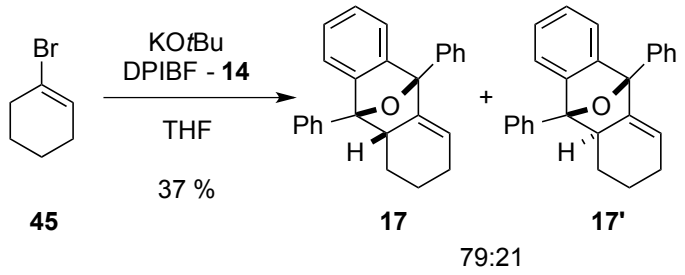

Scheme 1.11 - First report of 1,2-cyclohexadiene generation by Wittig and Fritze.

The slight bias toward *endo* selectivity could be rationalized as a kinetic phenomenon similar to that observed in concerted Diels-Alder reactions.[36-38] In the case of the cyclic allenes reported, steric encumbrance appears to be a greater contributor to the selectivity observed considering that 1,2-cyclohexadiene has no clear secondary conjugation or overlap with incoming dienes; the adjacent π system is orthogonal to the approaching diene.

Reducing the steric bulk and reactivity of the diene relative to DPIBF, Bottini and coworkers showed furan to be a proficient trap for 1,2-cyclohexadiene (Scheme 1.12).[39] In this seminal publication expanding the cycloaddition chemistry of cyclic allenes, Bottini reported a much greater *endo*/*exo* selectivity of 10:1 versus the reaction with DPIBF, again favoring the *endo* isomer, **46**. When the reaction was run using 2-methylfuran a mixture of two regioisomeric cycloadducts **47** and **48** are observed. Both regioisomers are reported as single *endo* diastereomers, which could be a consequence of the detection limits of the scale of this reaction.

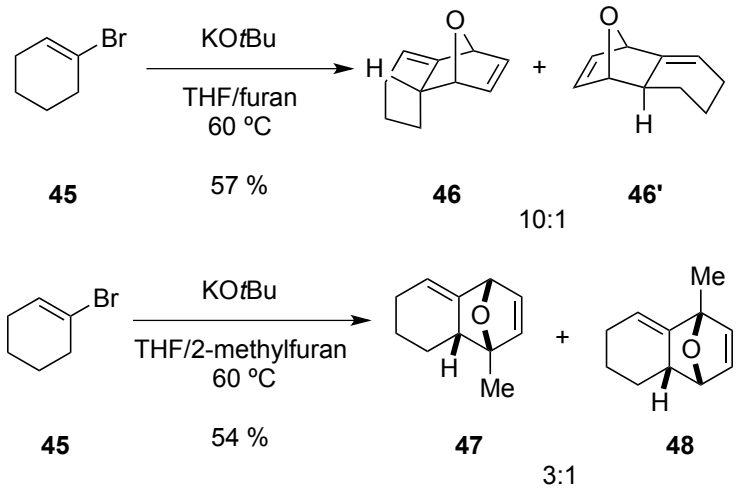

Scheme 1.12 - Trapping of 1,2-cyclohexadiene with furan and substituted furans.

Intriguingly, Moore and Moser report the attempted trapping of 1,2-cyclohexadiene with furan in 1970 with no success.[29] Bottini addresses this as a possible temperature dependence on the cycloaddition.[39] Bottini reported the cycloaddition of furan with 1,2-cyclohexadiene using a base mediated elimination (as well as other methods) at 0 °C and above, while Moore and Moser performed their reactions at –80 °C.

1.4.1.1.1 Using Chiral Precursors to Generate Chiral Cyclic Allenes

Using the known cycloaddition of 1,2-cyclohexadiene with DPIBF, Balci and Jones reported the first evidence supporting the idea that 1,2-cyclohexadiene is a closed shell bent allene intermediate.[40] Given the strain that was present in 1,2-cyclohexadiene, it was assumed the intermediate existed as a diradical, or zwitterion that would readily undergo inversion. If both double bonds of the cyclic allene are true double bonds the cyclic allene could be chiral as suggested by calculations.[23,41-47]

Enantiomerically enriched 1-bromo-6-deuterocyclohex-1-ene **D-45** was synthesized from bromo enone **49** in 3 steps (Scheme 1.13), where the chiral center was introduced via an enantioselective reduction of enone **49** with quinine and LAH.[40] Treating enantiomerically enriched vinyl bromide **D-45** with KO*t*Bu in the presence of DPIBF gave enantiomerically enriched cycloadducts **D-17** and **D-17'** though the degree of enantiomeric enrichment was never quantified. The optical rotation of the cycloadducts was dependent upon the reaction temperature; the use of higher temperatures led eventually to the loss of optical activity.

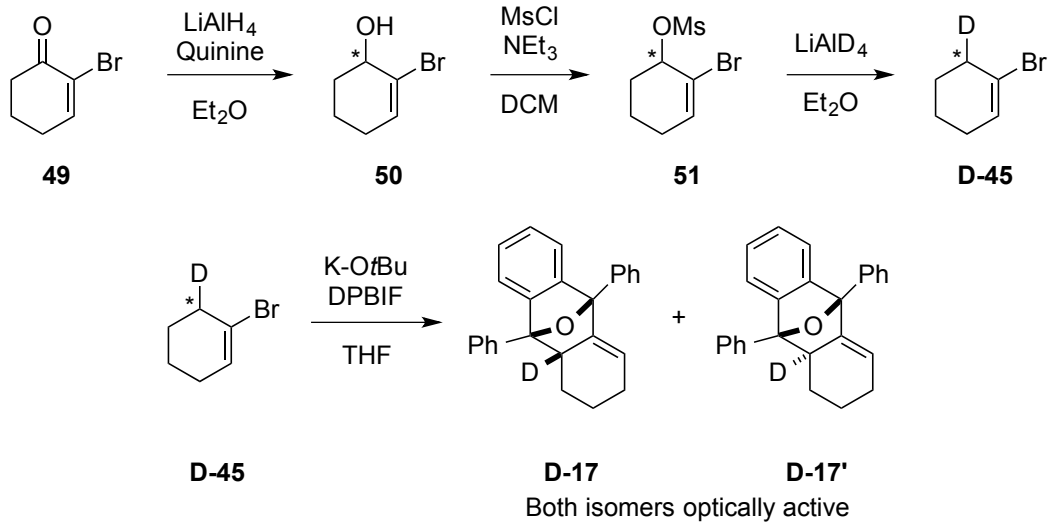

Scheme 1.13 - Chiral fidelity from the elimination of HBr from 1-bromo-6-deuterocyclohexene.

The work of Balci and Jones with chiral cyclic allene precursors agrees with the complementary study using potassium menthoxide and a number of racemic halocycloalkenes. The enantiomeric enrichment of the cyclic allene intermediates was derived from stereoselective distinction between enantiomeric protons using the chiral alkoxide base, potassium menthoxide. Similar chiral cycloadducts and decomposition products were obtained via asymmetric induction rather than the previously established enantiomeric fidelity study (Scheme 1.14).[48] Interestingly, enantiomerically enriched bicyclic vinyl bromide **52** was reported to racemize under strongly basic conditions by Bergman;[49] however, in the presence of potassium menthoxide, optically active cycloadducts **53** and optically active decomposition product **54** were obtained. The ability for enantiomeric enrichment to be transferred from the starting material to the cycloadducts via both enantiomeric induction as well as enantiomeric fidelity strongly suggests a closed-shell cyclic allene structure.

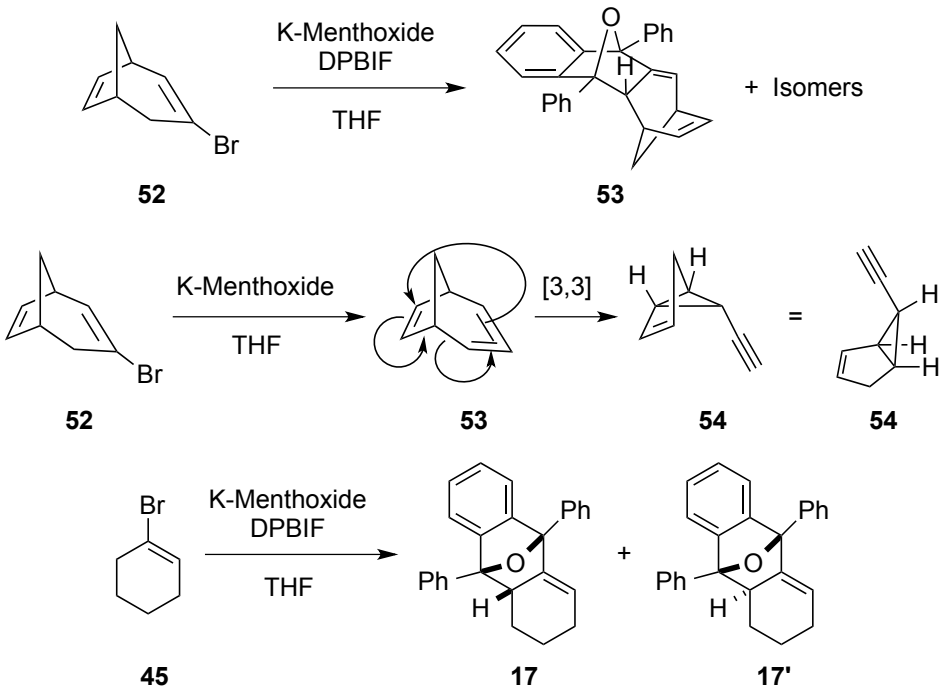

Scheme 1.14 - Optically active cycloadducts from the trapping of chiral cyclic allenes generated by the menthoxide-mediated elimination of racemic vinyl bromides.

1.4.1.1.2 Anomalous Reactivity of E2-Generated Cyclic Allenes

The base-mediated elimination reaction of bromo dihydronaphthalene **55** highlights the electron deficiency of a cyclic allene intermediate. As shown in Scheme 1.15 the elimination of hydrogen bromide is suggested by the intermolecular trapping with furan. The low yield of trapping products is due to the deprotonation of the cyclic allene intermediate to form naphthalene anion **57**. Anion **57** has been reported to deprotonate other cyclic allenes or precursors to generate naphthalene **60** in addition to other side reactions. Further proof for the formation of anion **57** was provided when the reaction was run in the presence of benzophenone, from which (2-naphthyl)diphenylmethanol **59** and isomer **58** were reported in 13 and 4 % yield respectively.[50]

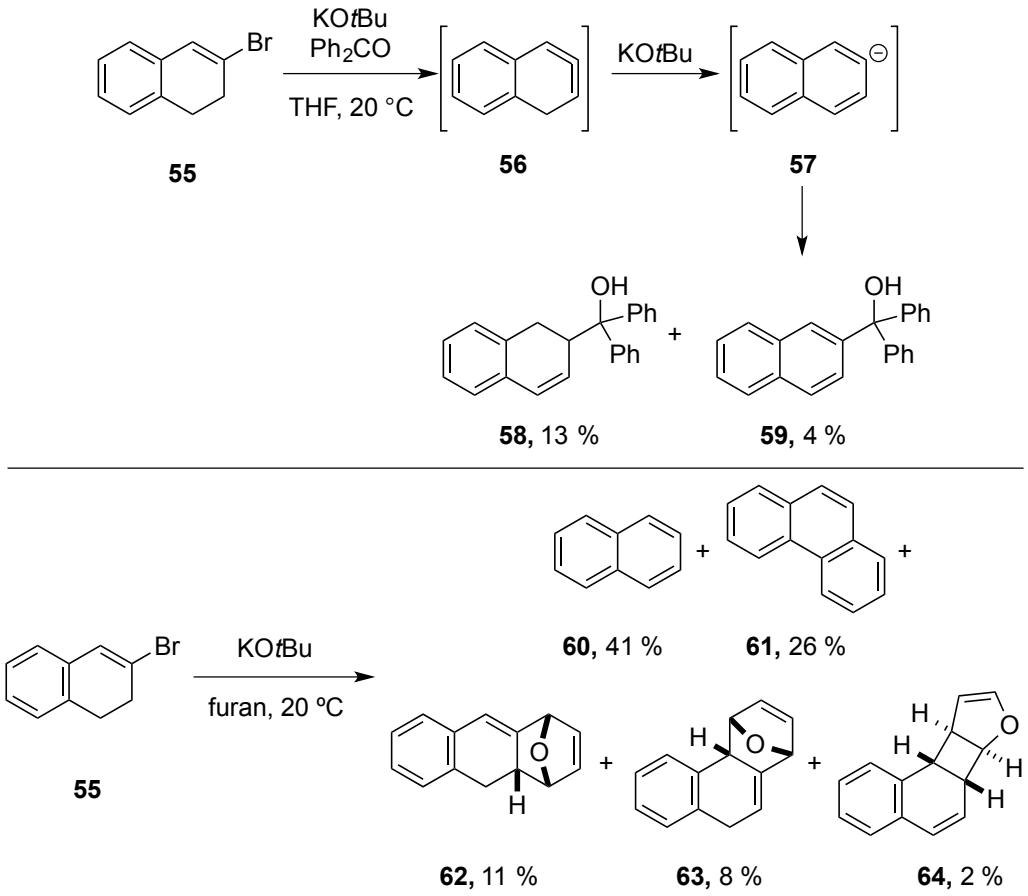

Scheme 1.15 - Trapping of parent isonaphthalene cyclic allene.

Isonaphthalene cyclic allene **56** appears to have anomalous reactivity with cyclopentadienes as well. Christl and coworkers have shown that in addition to the previously observed Diels-Alder reactivity with furan (**62**/**63**), furan will undergo a [2+2] cycloaddition to give fused-cyclobutane containing **64** (Scheme 1.15).[50] Cyclopentadiene **68** did not undergo a typical Diels-Alder cycloaddition to any observable extent. Only [2+2] cycloaddition products **65–67** were observed in addition to other decomposition products (Scheme 1.16). The authors do not speculate into the origin of this novel reactivity.

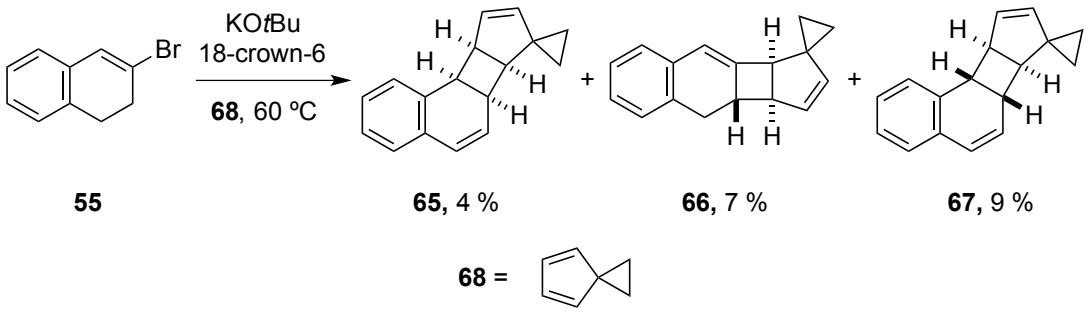

Scheme 1.16 - Anomalous reactivity of isonaphthalene cyclic allene with cyclopentadiene 68.

The decomposition of isonaphthalene cyclic allene **56** was avoided by blocking the benzylic positions with a *gem*-dimethyl group as in vinyl bromides **69–70**. Miller and Shi reported that dihydronaphthalenes **69** and **70** (used as an inseparable mixture) formed a cyclic allene intermediate upon treatment with KO*t*Bu from isolation and characterization of the trapping products with DPIBF **71** and **72** (Scheme 1.17).[51] The methyl groups prevent the base-mediated decomposition of the cyclic allene intermediate but interestingly do not inhibit the preferential formation of the more congested linear regioisomer **71**.

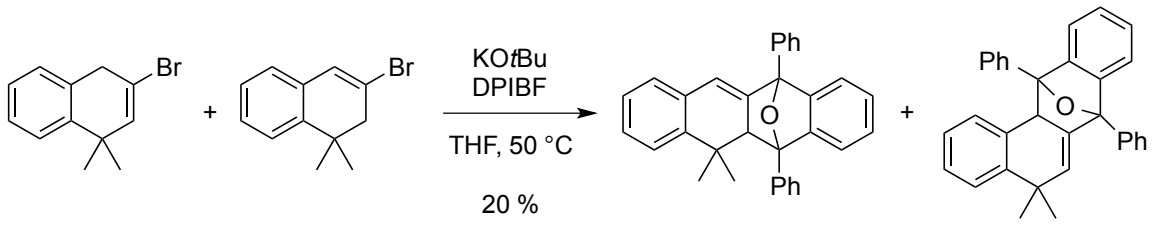

Scheme 1.17 - Trapping of *gem*–dimethyl isonaphthalene cyclic allenes.

Intriguingly, the use of 1-bromocyclohexa-1,4-diene **73** did not produce similar side products when isobenzene cyclic allene **74** was generated in the presence of excess base (Scheme 1.18).[52] Under conditions analogous to those employed by Miller and Shi, Christl and Groetsch observed furan cycloadduct **75** when furan was used as the solvent. In the presence of excess base and benzophenone only minor amounts of triphenyl methanol were obtained. The anionic trapping of benzophenone, furnishing triphenylmethanol (**76**) was reported to occur in only 5 % yield and the authors suggest

the poor yield could be attributed to premature protonation of phenyl anion, generating benzene.

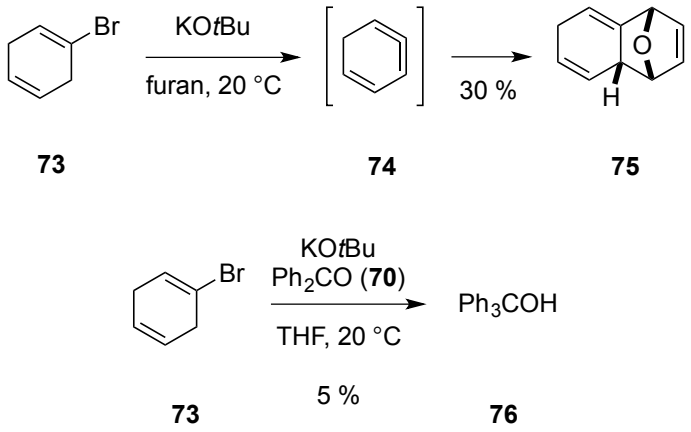

Scheme 1.18 - Generation and capture of isobenzene from HBr elimination.

1.4.1.1.3 Nucleophilic Capture of 1,2-Cyclohexadienes from E2 Elimination

In the course of studying the elimination-addition mechanism of cyclic vinyl chlorides (Scheme 1.19) Wittig,[53] Roberts,[54-56] and Montgomery[57,58] compiled extensive evidence for a cycloalkyne intermediate (**78**) using predicted ^{13}C scrambling, deuterium labeling studies, and isotope effects (**79**).

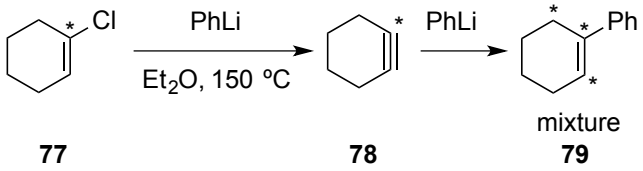

Scheme 1.19 - Elimination/addition on ^{13}C-labeled chlorocyclohexene with phenyllithium.

Bottini and coworkers investigating the base-mediated elimination of chlorocyclohexene **80** with weaker bases than phenyllithium found a solvent, base, and leaving group dependence upon the product mixture between **83** and **84** (Scheme 1.20).[59] It was previously known that cyclic alkynes could be attacked by the base used to generate the reactive intermediate;[60-62] however, the biased formation of enol ether **83** suggested another mechanism was taking place. Enol ether **84** is best described as being formed from the nucleophilic attack of *t*-butoxide anion on C2 of 4-methyl-1-cyclohexyne (**81**); however, assuming no stereoelectronic or steric effects from the distal

methyl group a relative 1:1 distribution of nucleophilic attack at C1 and C2 would be predicted. Assuming no influence from the attached methyl group, the large predominance of enol ether **83** can best be explained by nucleophilic attack of *t*-butoxide anion on the central carbon of a 5-methyl-1,2-cyclohexadiene (**82**).

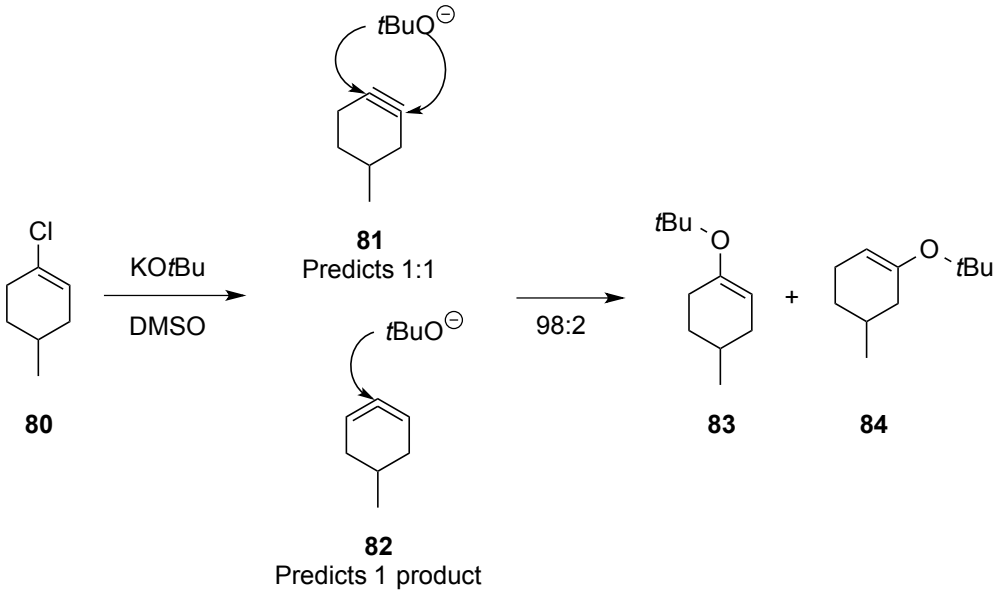

Scheme 1.20 - Two possible mechanisms for elimination of HCl from chlorocyclohexene 80.

Using a poor leaving group in highly polar solvents with a reversible base gives products most consistent with cyclic allene intermediate, as the ratio of **83** to **84** is 98:2 (Table 1.1). This outcome correlates to at least 4 % of the product arising from the formation of a cyclic alkyne, while 96 % is more likely derived from a cyclic allene. Counter to this, the combination of vinyl iodide **86** with potassium *t*-butoxide in THF gave a 55:45 mixture of **83** and **84**; essentially the entire result could be accounted for by a cyclic alkyne intermediate.[59] The work by Bottini and coworkers suggests the elimination is a delicate balance between alkyne and allene generation (Table 1.1).

Table 1.1 - Leaving group and solvent effects on cyclic allene generation.

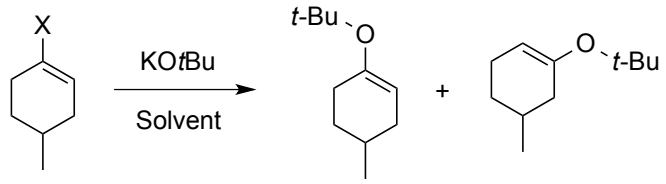

80, 85, 86 **83** **84**

Substrate	Leaving Group (X)	Solvent	Ratio of **31:32**
80	Cl	DMSO	98:2
80	Cl	Diglyme	90:10
85	Br	DMSO	86:14
86	I	DMSO	75:25
86	I	THF	55:45

[a] Ratios were determined by comparison of integration in the ^{1}H NMR spectrum.

In order to remove any conformational preferences or bias that could be introduced by the distal methyl group, the reaction of deuterium-labeled halocyclohexene derivatives **D3-87** and **D3-88** with strong base was studied (Table 1.2). The deuterated substrates elimination and trapping agree with the previous study using methyl cyclohexenes **80** and **86**.[59] The use of a deuterium label rather than an alkyl-substituent removes any gauche interactions or conformational instabilities the alkyl group may impart upon the cycloallene/cycloalkyne intermediate. Subjecting vinylic-halides **D3-87** to strong alkoxide base in DMSO led to the formation of dideuterated enol ethers **6-D2-89**, **3-D2-89**, and **D2-90** differing only in the position of the two deuterium labels (Table 1.2). 2,6-Dideuterated ether **D2-90** is derived solely from a cyclic allene intermediate, and the 6,6-dideuterated (**6-D2-89**) and 3,3-dideuterated ethers (**3-D2-89**) are derived solely from a cyclic alkyne intermediate. Using chloride derivative **D3-87**, a 0:2:98 ratio was reported, identical to the result when methyl chlorocyclohexene **80** was used (Scheme 1.20). Using iodide derivative **D3-88** however generates a 2:34:64 distribution

between the two products, indicative of a large shift toward generating the cyclic alkyne intermediate.

Table 1.2 - Results of deuterium labeled vinyl halides with alkoxide elimination/addition.

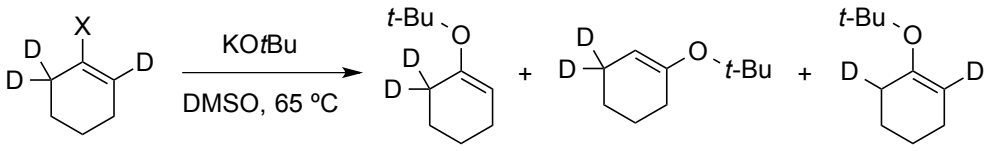

D3-87 (X = Cl) or **D3-88** (X = I) | **6-D2-89** | **3-D2-89** | **D2-90**

Starting material	X =	**6-D2-89**	**3-D2-89**	**D2-90**
D3-87	Cl	0 %	2 %	98 %
D3-88	I	2 %	34 %	64 %

1.4.1.1.4 Trapping of Cyclic Allenes with Ketone Enolates

Simultaneously to the work done with alkoxide bases trapping cyclic allenes, Caubère and coworkers were studying the capture of unsaturated reactive intermediates with amides and thiolates. The group initially believed the preponderance of the products were derived from cyclic alkynes; however, in 1969 a single instance of the elimination product of 1-chlorocyclohexene was trapped by a ketone enolate (**91**) (Scheme 1.21).[62] In the case of furan, a single example exists of a [2+2] cycloaddition across one of the aromatic double bonds;[50] however, the enolates of many different cyclic and acyclic ketones react with 1,2-cyclohexadiene.

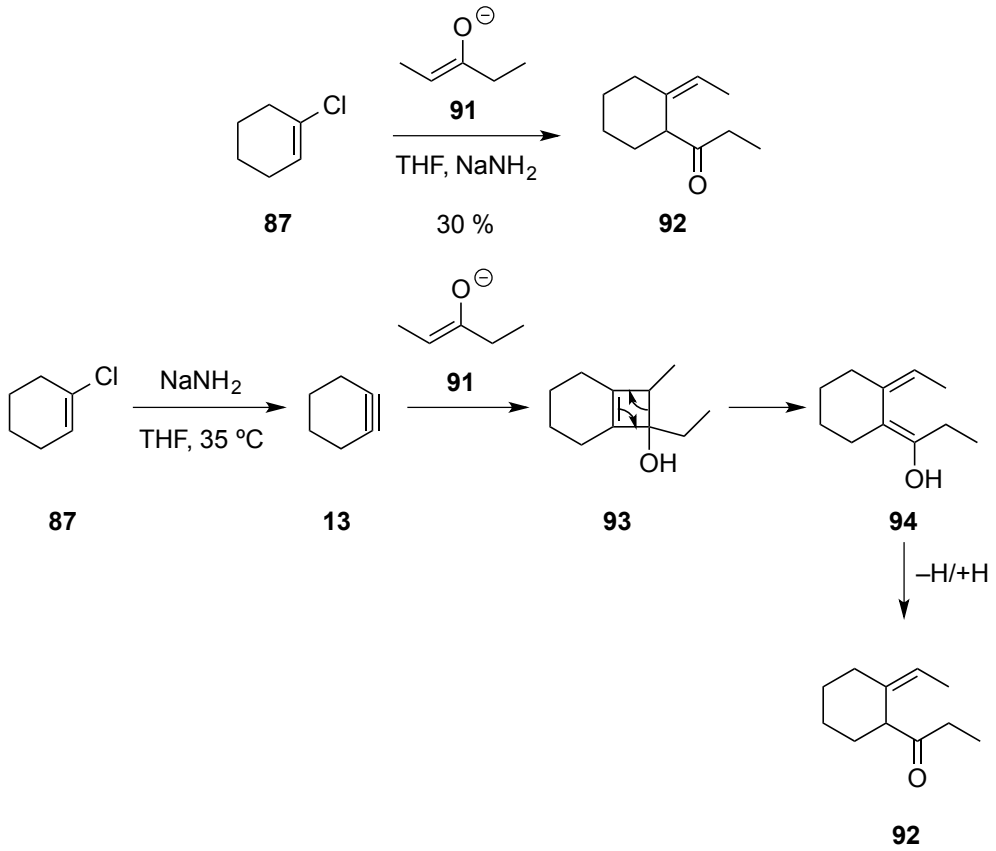

Scheme 1.21 - Caubère's trapping of proposed cyclic alkynes with enolates.

In order to account for the β,γ-unsaturated ketone products **92**, a cyclic alkyne intermediate was proposed which was captured by the enolate in a [2+2] cycloaddition to form cyclobutanols like **93** (Scheme 1.21). The cyclobutenols (**93**) formed *in situ* can undergo a 4-electron-electrocyclic ring opening to form the observed β,γ-unsaturated ketones. Investigating the scope of the reaction, it was found that cyclohexene-fused-cyclobutanol **96** was the major product using the enolate of 2,4-dimethylpentan-3-one (**95**) as the trap (Scheme 1.22). Furthermore, in the reaction of cyclic ketone enolate **100**, alkylidene cyclobutanol **101** was the major product formed. A 4-electron-electrocyclic ring opening cannot occur from alcohols **96** or **101**.

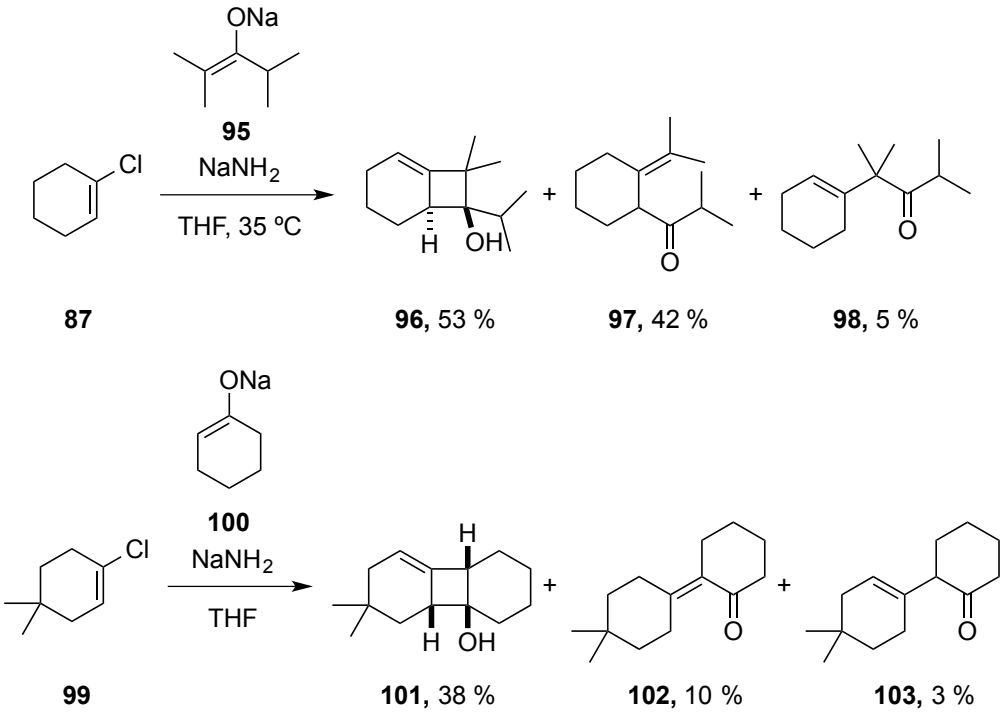

Scheme 1.22 – Formation of alkylidene cyclobutanols (96/101) inconsistent with a cyclic alkyne intermediate.

The previously proposed cyclic alkyne mechanism cannot explain the formation of the alkylidene cyclobutanols (**96/101**). Similar to the products of DPIBF cycloaddition with 1,2-cyclohexadiene the olefin is exocyclic to the cyclobutane and likely not isomerized under the reaction conditions. Alkylidene cyclobutanol **101** suggests a cyclic allene intermediate was operative in these instances rather than a cyclic alkyne intermediate. Elimination of HCl from the methylated cyclohexene derivative **104** can only occur through a cyclic alkyne intermediate (Scheme 1.23), mechanistically similar to the more recent work of Carreira (Scheme 1.2). Caubère's use of methyl-derivative **106** provides significant evidence that cyclic allenes can undergo similar processes via the observation of alkylidene cyclobutanol **107**.

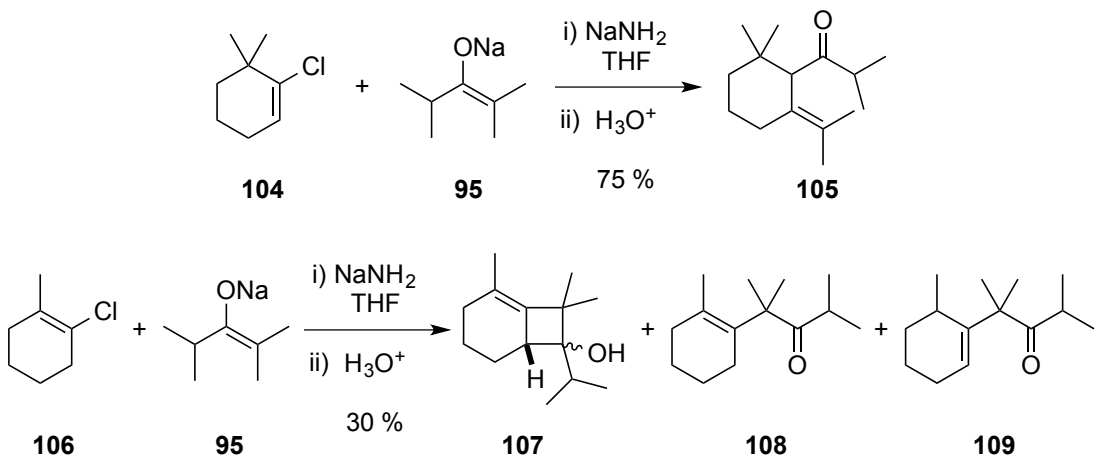

Scheme 1.23 - Caubère and coworkers demonstrate definitive cyclic allene intermediates from substituted cyclohexenes.

The proposed mechanism as shown in Scheme 1.24 has several processes equilibrating under the reaction conditions. Initial stepwise capture of the cyclic allene by the enolate generates new anion **110**, which can be protonated to form linear β,γ-unsaturated ketone **98** or it can undergo ring closure to generate alkylidene cyclobutoxide **111**. Alkylidene cyclobutoxide **111** can be protonated to form the cyclobutanol product observed (**96**) or undergo ring opening and subsequent protonation to generate the isomeric β,γ-unsaturated ketone **97**.[63-65]

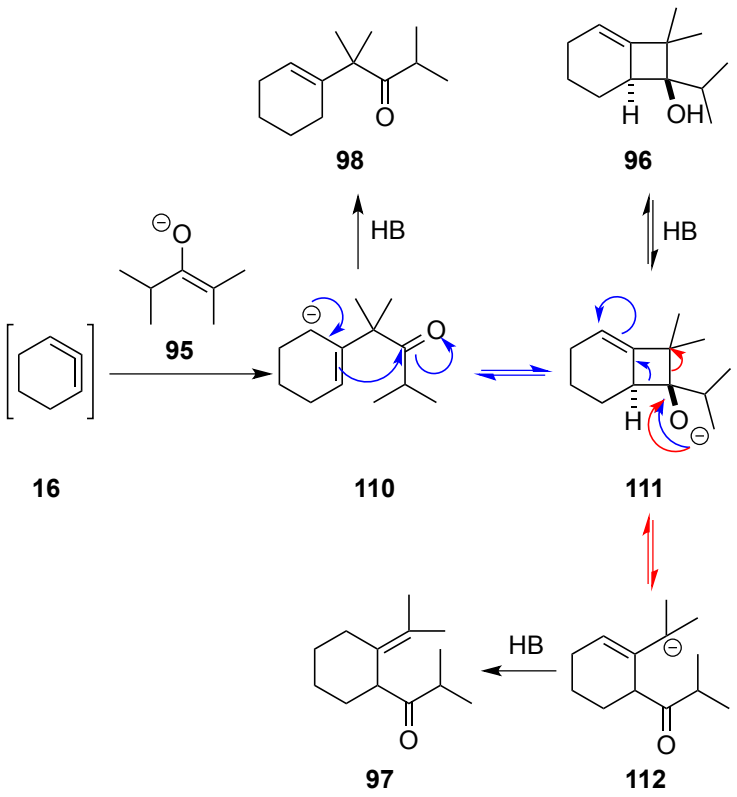

Scheme 1.24 - Cyclic allene mechanism for enolate trapping.

In the reaction of 4,4-dimethyl-1-chlorocyclohex-1-ene (**99**) and the enolate of 2,4-dimethylpentan-3-one (**95**), a mixture of **113**–**116** was reported (Scheme 1.25). β,γ-Unsaturated enone **115** (obtained in 20 percent of the mass balance) was most likely derived from a cyclic alkyne intermediate. This implies up to 40 % of the reactivity of this substrate can be attributed to a cyclic alkyne rather than a cyclic allene. Although the majority of the mass balance was derived from a cyclic allene intermediate, this example demonstrates the complex effect the solvent, substrate, and base ultimately have on the formation of possible reactive intermediates.[66]

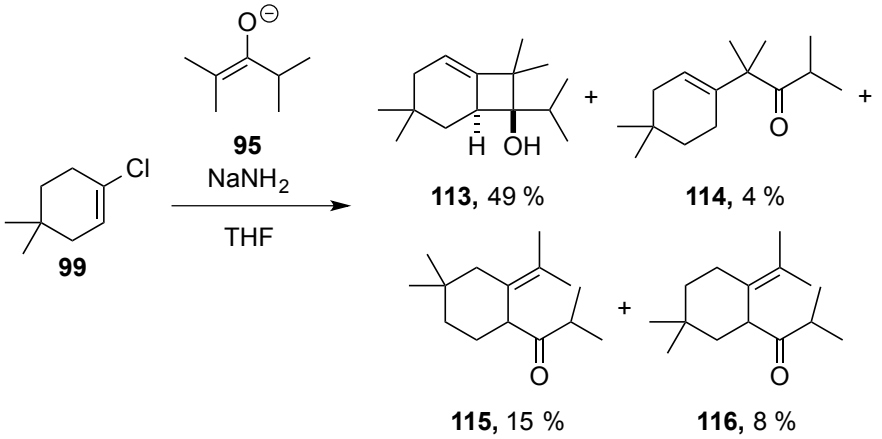

Scheme 1.25 - Products derived from both a cyclic alkyne intermediate as well as derived from a cyclic allene intermediate were observed in the same reaction mixture using the enolate of 2,4-dimethylpentan-3-one.

A full understanding of all the nuances of capturing a cyclic allene with an enolate is lacking considering that only base-mediated elimination methods have been used to investigate the reaction. The work done by the Caubère group showed that beyond olefins and aryl groups, oxygen atoms would activate an olefin to trap cyclic allenes in a [2+2] cycloaddition. Interestingly, the mass balance obtained was good even when highly substituted enolates, such as the enolate of 2,4-dimethylpentan-3-one **95**, were used.

In light of the mechanistic work done and the new trapping modalities discovered while generating cyclic allenes using a base-mediated E2 elimination, there are a number of drawbacks to the method. The strongly basic conditions can lead to the decomposition of the targeted intermediate as in the case of Christl and coworkers when they attempted to efficiently generate isonaphthalene cyclic allene **56** (Scheme 1.15).[50] The work of the Bottini group and the Caubère group demonstrated a delicate relationship between the reaction conditions and the ability to definitively generate either a cyclic alkyne or a cyclic allene intermediate. As the identity of the reactive intermediate that is being generated in a reaction will have profound effects on the reactivity and products that are observed, careful experimental planning must be exercised.

1.4.1.2 $E1_{CB}$ Elimination of Vinyl Leaving Groups

Earlier, the E2 elimination of a vinyl leaving group on a cyclohexene scaffold was described as being complicated by the presence of the more acidic pseudo-axial protons (Figure 1.3). A collaborative effort between Tolbert and Johnson revealed that the presumed unproductive anions generated from axial deprotonation can in fact lead to cyclic allene generation with the application of either photolytic or thermal stress (Scheme 1.26).[32] The authors reported the deprotonation of **117** or **118** was complete from the expedient generation of a darkly colored solution. The anion generated, due to orthogonal orbital overlap between the allyl orbital system and the leaving group's σ* orbital, should not undergo an elimination to generate a cyclic allene. Upon photolysis in DMSO (λ > 450 nm) or heating at reflux in THF for 20 h in the presence of the furan, cycloadducts **119** and **120** were observed (Scheme 1.26). Both cycloadducts are consistent with a cyclic allene intermediate and particular attention is drawn to product **120**, one of the few tetra-substituted cyclic allene cycloadducts reported.

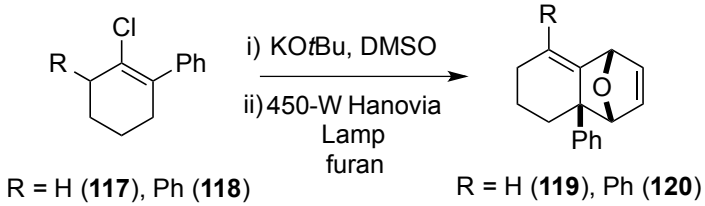

Scheme 1.26 - Cyclic allene generated by photolysis of allylic anion.

More recently, Houk and Tolbert found an ester-conjugated cyclic allene intermediate to form via thermal elimination in a 1:2, THF:furan mixed-solvent system with strong alkoxide base (Scheme 1.27).[43] Similar to cycloadduct **119** reported by Johnson and Tolbert (Scheme 1.26), cycloaddition favors reactivity at the more substituted double bond of the allene **124**. This is consistent with Johnson and Tolbert's inference that the frontier molecular orbitals have larger coefficients on the double bond conjugated with the substituent.[32]

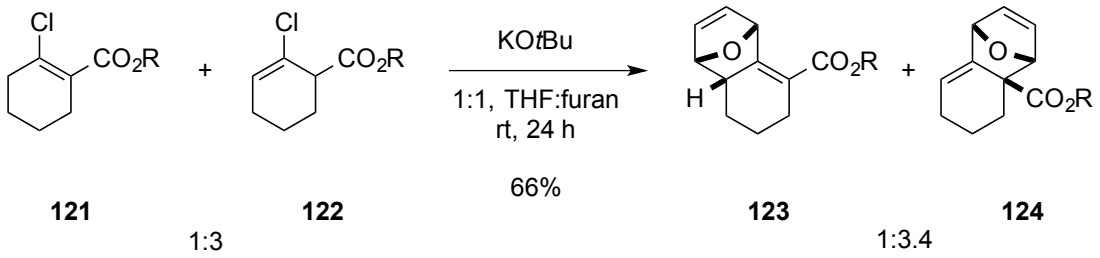

Scheme 1.27 - Generation and trapping of an ester-conjugated cyclic allene.

Elimination in the phenyl- and ester-conjugated systems is hampered by the bias toward axial deprotonation to generate stabilized anions. The π system stabilizing the anion is orthogonal to the σ* orbital of the leaving group (**125–I,** Figure 1.4), thus preventing elimination. Photolysis or thermal activation facilitates the elimination event by encouraging the change in configuration of the anionic carbon, breaking conjugation with the stabilizing groups. Inversion at an allylic carbanion is generally very fast as the barrier was predicted to be <2 kcal/mol.[3]

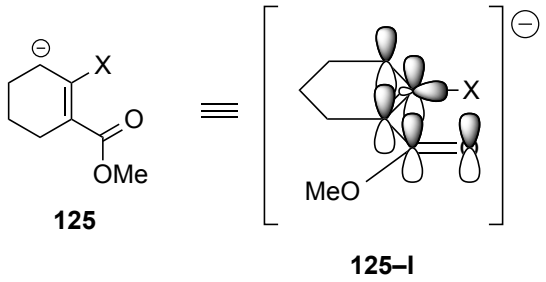

Figure 1.4 – Tolbert and Houk's anionic intermediates, stabilized by conjugation.

When investigating the furan cycloaddition with methyl 1,2-cyclohexadienoate (Scheme 1.28), Houk and Tolbert found computationally that the *endo* adducts (**123**/**124**) were favored both thermodynamically by 0.8 kcal/mol, but also kinetically by 0.9 kcal/mol if the reaction proceeds via a highly asynchronous concerted pathway.[43] Unfortunately transition states for all of the diradical intermediate steps could not be found, though preliminary results suggest the diradical pathway would be lower in energy. The computations could not provide reasoning for the diastereoselectivity that was observed.

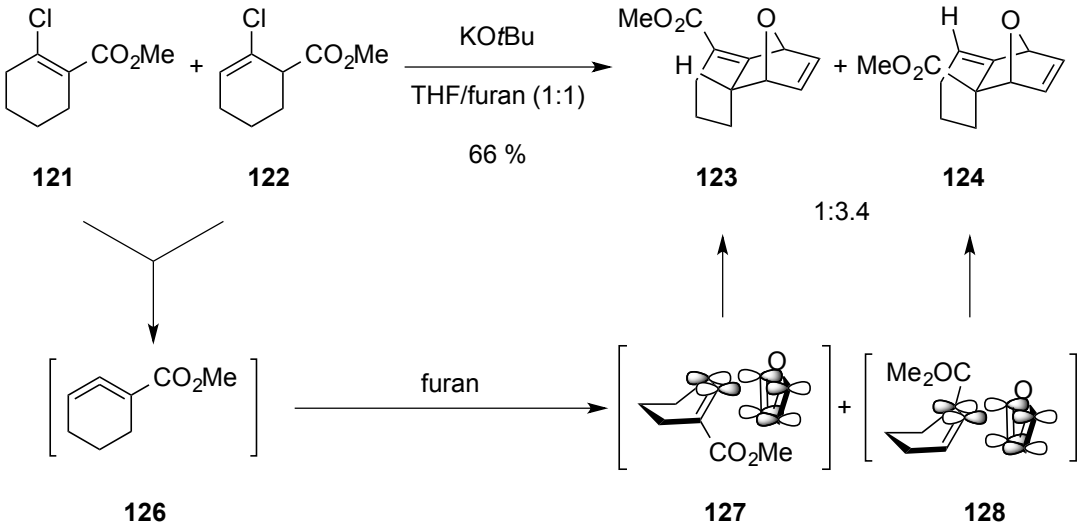

Scheme 1.28 – Possible geometries for furan approach and the formation of the two regioisomers 123 and 124.

The base-mediated elimination of vinyl leaving groups was established very early on as a fruitful method for generating cyclic allenes and discovering interesting trapping modalities. The generation of chiral cyclic allenes, in turn allowed a mechanistic investigation into the physical description of a cyclic allene as a closed shell, highly bent cyclic allene, rather than a 1,2-diradical species. The use of strongly basic conditions and high temperatures encouraged the decomposition of several different cyclic allene intermediates and trapping products. Further methods build upon the foundation of the elimination method.

1.4.2 The Doering-Moore-Skattebøl (DMS) Reaction

The Doering-Moore-Skattebøl reaction has proved to be an efficient means to generate cyclic allenes in a complementary manner to the base-mediated elimination method. The DMS reaction allowed the discovery of new trapping modalities, partially derived from the milder reaction temperatures that were used in the reaction. Most interesting may be the more rigorous work done on the trapping of chiral cyclic allenes.

1.4.2.1 Developing the DMS Reaction

In 1954 Doering and Hoffman hypothesized the generation of allenes using 1,1-dihalocyclopropanes (**130**) (Scheme 1.29).[67,68] Quickly following this challenge, the rearrangement of dihalocyclopropanes to allenes was then independently reported by

Doering,[69] Moore,[70] and Skattebøl.[71] Dibromocyclopropanes in the presence of reactive elemental metals (sodium or magnesium) or alkyl lithium reagents furnish allenes in good yields. Skattebøl pushed the limits of the method and prepared 1,2-cyclononadiene (**135**), the smallest carbocyclic allene that is stable under ambient conditions. [72]

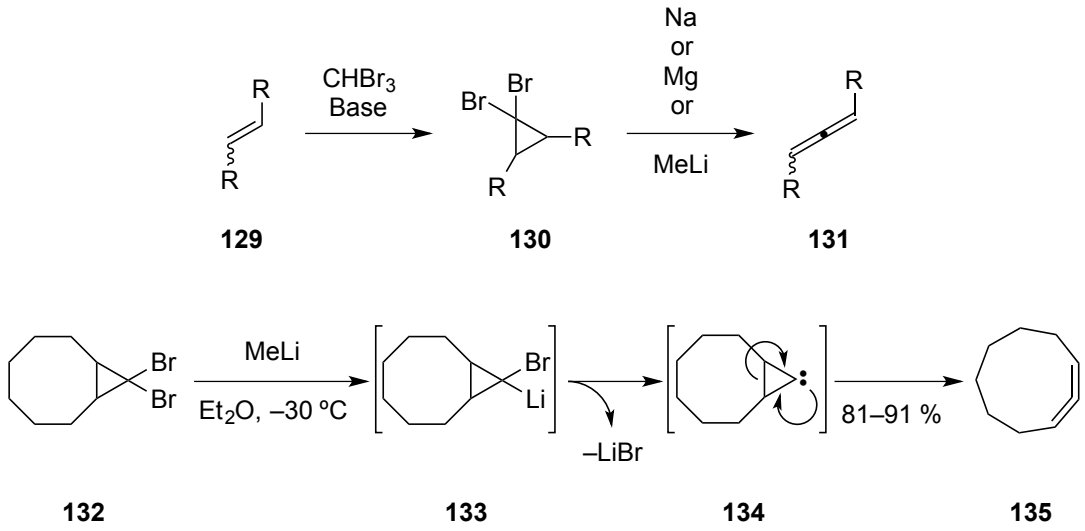

Scheme 1.29 - The general DMS reaction and application to cyclic allenes.

The DMS reaction is believed to be a three-step mechanism (Scheme 1.29).[73] The first step is a fast lithium/halogen exchange to generate the metallated species **133**. The dichlorinated species are generally unreactive in the DMS reaction, attributed to the strength of the carbon-halogen bond. The formation of the free carbene **134** and final ring opening to form the allene are closely coupled, with calculations suggesting the two may occur simultaneously.[73] Regardless of the timing of the events, a four-electron ring opening of the cyclopropane furnishes the allene **135**.

Immediately following the report of the large-scale preparation of 1,2-cyclononadiene, Moore and Moser reported the *in situ* generation of 1,2-cyclohexadiene from the reaction of 6,6-dibromobicyclo[3.1.0]hexane (**136**) with methyl-lithium (Scheme 1.30).[29] The intermediacy of a cyclic allene was supported by the formation of tetramers **35** and **36** at low temperatures (–80 °C) and the formation of dimer **19** at higher temperatures (35 °C).

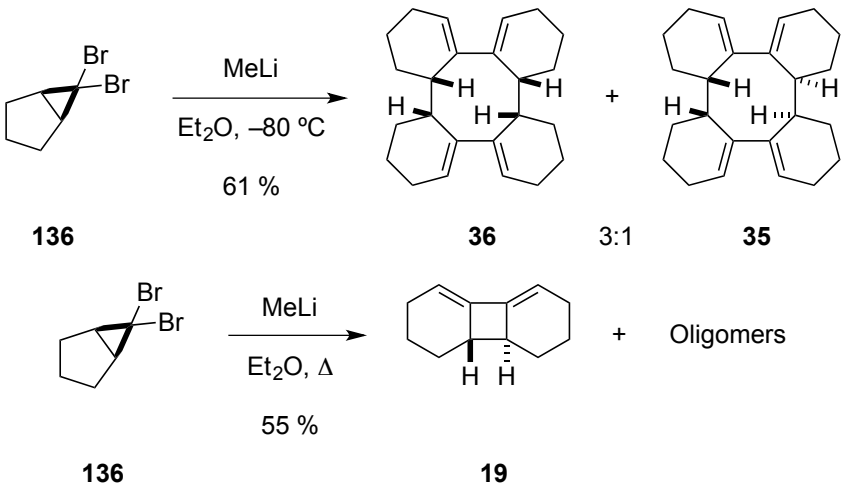

Scheme 1.30 - Tetramers, and dimerization of 1,2-cyclohexadiene using the DMS reaction.

1.4.2.2 Trapping of 1,2-Cyclohexadiene with Styrenes

Further supporting the application of the DMS method to the generation of cyclic allenes, Moore and Moser simultaneously reported the trapping of 1,2-cyclohexadiene with styrene in 1970 when applying the DMS reaction to the generation of small carbocyclic allenes (Scheme 1.31).[74] Styrene was not previously used to trap cyclic allenes, as the strong bases used in the eliminative method for cyclic allene generation were incompatible with styrene. Styrene trapping showed a lack of selectivity giving cycloadducts **137** and **137'** in a 2.2:1 ratio and a 76 % combined yield. In addition to the trapping products, small amounts of the previously discussed dimer **19** and tetramers **35/36** were observed, and gratifyingly no sign of polymeric styrene. [30]

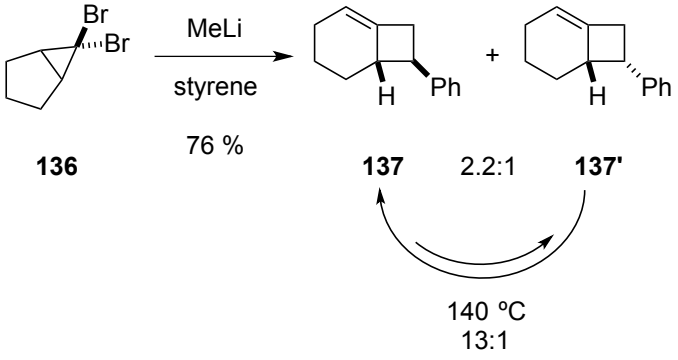

Scheme 1.31 - Trapping of styrene by Moore and Moser.

Christl and Schreck found that a thermodynamic mixture of the styrene adducts **137** and **137'** could be achieved by heating the mixture to 140 °C, establishing a 13:1 ratio favoring trans-isomer **137** (Scheme 1.31). The 13:1 ratio agrees with the calculated product energy difference of ~0.9 kcal/mol.[30] The difference between the thermally established ratio of products and the ratio observed in the reaction mixture by Moore and Moser suggests the trapping reaction of 1,2-cyclohexadiene with styrene is under kinetic control.

Waali and coworkers trapped cyclic allene **16** with electronically modulated styrenes (**138**) enabling the generation of a Hammett plot and the subsequent determination of a ρ parameter of +0.79 (Scheme 1.32).[75] The authors suggest this was consistent with a slightly nucleophilic allene attacking the styrene to first generate diradical intermediate **139**. Following the generation of cyclic allene **16**, the electrophilic character of the trap will influence the rate of nucleophilic addition, and in turn the efficiency of the reaction.

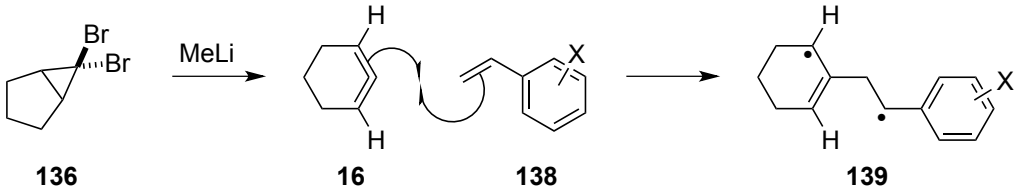

Scheme 1.32 - Diradical intermediate from the trapping of 1,2-cyclohexadiene with styrene.

The steric environment of the styrene olefin plays a significant role in the efficiency of the reaction. α-Methylstyrene (**140**) reacts analogously to styrene with 1,2,4-cyclohexatriene **74** to give cyclohexene-fused cyclobutane **141**, however β-methylstyrene (**142**) gives cycloadduct **143** in only 5 % yield (Scheme 1.33).[76] Congestion of the electrophilic reaction center causes a significant decrease in the efficiency of the cycloaddition.

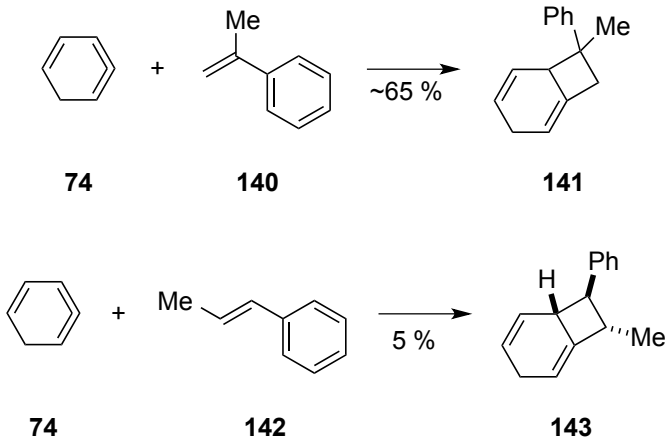

Scheme 1.33 - Reaction of isobenzene cyclic allene with methyl-substituted styrenes.

1.4.2.3 Trapping of Cyclic Allenes with Dienes

The mildness of the DMS reaction conditions facilitated the study of 1,2-cyclohexadiene trapping with a broader range of π electrophiles. Cyclic dienes, 1,3-cyclopentadiene and 1,3-cyclohexadiene, underwent [4+2] Diels-Alder cycloadditions with 1,2-cyclohexadiene **16** to give mixtures of the *endo* and *exo* cycloadducts (Scheme 1.34).[39] The observed diastereoselectivity was very poor in comparison to the cycloaddition reported with furan (the closest related cyclic diene, Scheme 1.12).[39] In the case of 1,3-cyclohexadiene two different cycloadditions take place; the [4+2] Diels-Alder reaction provides *endo* and *exo* isomers **145** and **145'** in 63 % yield as well as a [2+2] cycloaddition to generate cyclohexene-fused cyclobutane **146** in 20 % yield.[20] Given the poor diastereoselectivity and regioselectivity of the reaction of 1,3-cyclohexadiene it is likely the reaction proceeds in step-wise fashion.

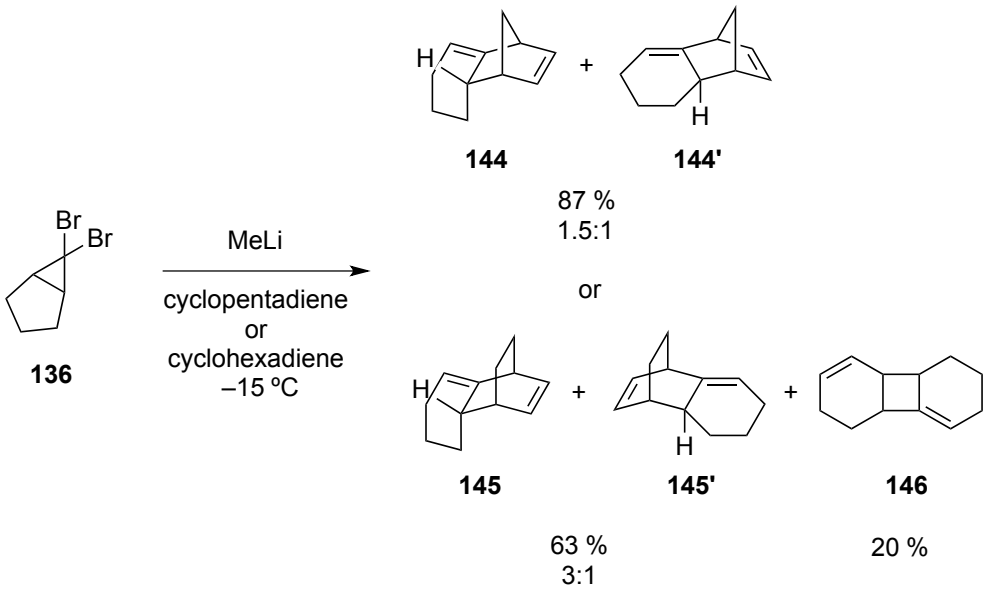

Scheme 1.34 - Reaction of 1,2-cyclohexadiene with conjugated cyclic dienes.

1.4.2.4 Trapping of Cyclic Allenes with Butadienes

Similar to the cycloaddition reaction of 1,2-cyclohexadiene with 1,3-cyclohexadiene, the cycloaddition of 1,2-cyclohexadiene with 1,3-butadiene resulted in cycloadducts **147** and **147'**, and **148** isolated in a 31 %, 4 % and 8 % yield, respectively (Scheme 1.35). The *endo* stereochemistry was assigned in comparison to the known phenyl-substituted derivatives **81/81'**.[30]

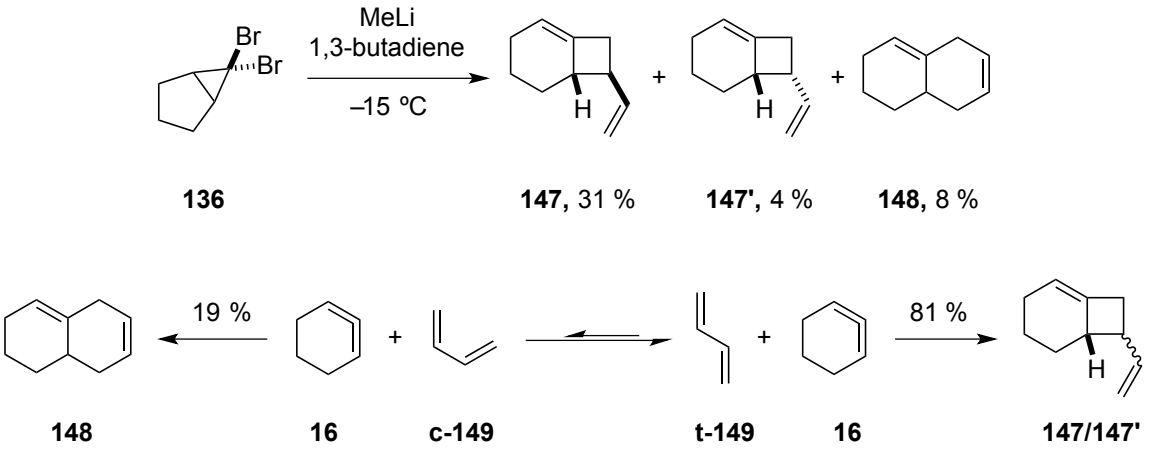

Scheme 1.35 - Trapping of 1,2-cyclohexadiene with 1,3-butadiene.

In addition to the [2+2] cycloadducts, a small fraction of the formal Diels-Alder adduct, **148,** was obtained. The energy barrier to the diene being in the *s*-cis conformation

c-149 (~2.8 kcal/mol)[77] predisposes the diene to a [2+2] mechanism; this barrier is not present in 1,3-cyclohexadiene and the majority of the product is derived from a [4+2] cycloaddition. The step-wise [4+2] is also disfavored by the rotational barrier of the allyl radical (~15 kcal/mol),[78] likely much higher than cyclobutane-ring closure. Christl and Schreck report the thermal isomerization of either [2+2] adduct **147** or **147'** results in the formation of hexahydronaphthalene **148** (Scheme 1.36).[79] Similar to the styrene cycloadducts, the thermal isomerization was proposed to take place via the participation of diradical intermediates **150/151**.

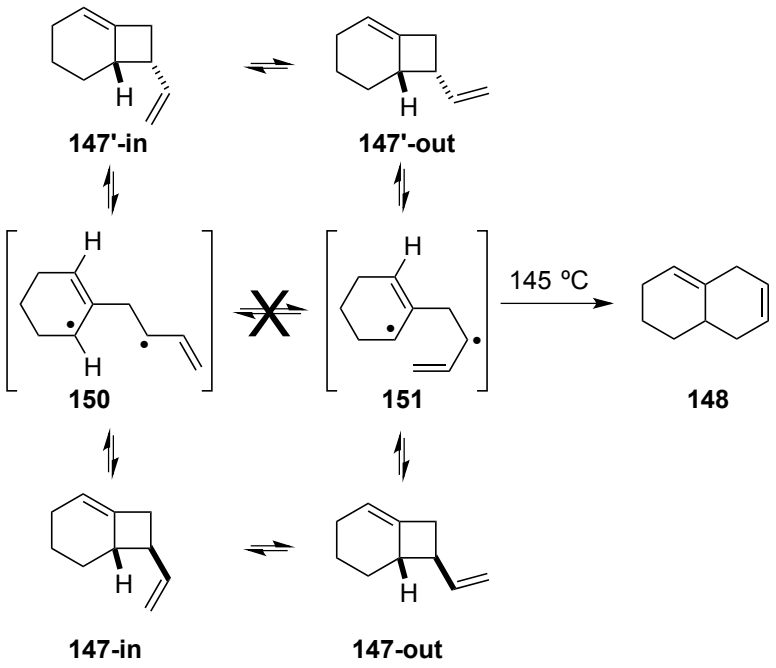

Scheme 1.36 - Thermal isomerization of *endo* and *exo* [2+2] cycloadducts to hexahydronaphthalene 229.

Alkyl-substituted butadienes favor the formation of the [2+2] cycloadducts especially in the case of *cis*-1,3-pentadiene **152** and 2,3-dimethyl-1,3-butadiene **153**, furnishing single products, **154** and **155** respectively (Scheme 1.37). Backbone substituents on these acyclic dienes used strongly disfavor the *s*-cis configuration of the diene, which prevented the possible [4+2] cycloaddition and only the [2+2] adduct **155** was observed. A terminal methyl group was shown to control both the regiochemistry of the attack on the olefin as well as provide a single diastereomer. Interestingly the *cis* stereochemistry of the internal olefin was conserved, though the mass balance for the

reaction was quite poor.[39,79,80] The cycloaddition of isoprene (**156)** furnished a mixture of regioisomers where cycloaddition preferentially occurred at C1 to give alkylidene cyclobutane **157**. Mechanistically addition to C1 generates a tertiary allylic radical whereas addition to C4 generates simply an allylic radical. The initial bond formed the more stable radical intermediate at the expense of generating a more congested quaternary carbon in alkylidene cyclobutane **157**.[79]

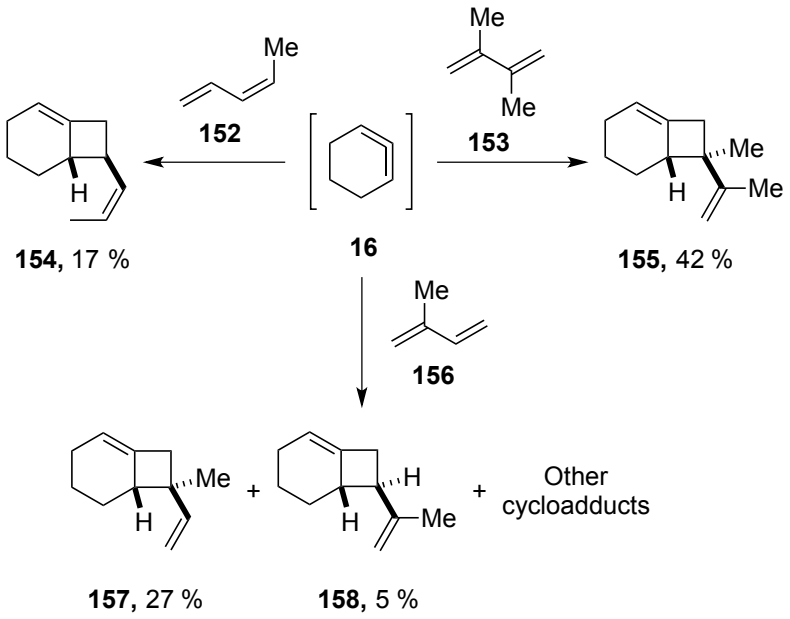

Scheme 1.37 - 1,2-Cyclohexadiene reactions with substituted acyclic dienes.

1.4.2.5 Mechanistic Insight into Cyclic Allene Capture with Olefins

There are few examples of concerted [2+2] cycloadditions, which suggests the reactions studied with cyclic allenes are stepwise. Using stereochemically pure (*Z*)-β-deuterostyrene (**βD-159**), both the Christl[30] and Waali[75] groups independently found scrambling of the stereochemical information of the olefin in the cycloaddition with 1,2-cyclohexadienes (Scheme 1.38). The cycloaddition of (*Z,Z*)-1,4-dideutero-1,3-butadiene **D_2-149** with 1,2-cyclohexadiene gave a complex mixture of the three possible cycloadducts. The stereochemistry of the deuterium labels was not conserved in either the [2+2] cycloadditions (**D_2-147/D_2-147'**), nor the [4+2] cycloadduct **D_2-148**.[20] The lack of stereochemical fidelity with respect to the deuterium labels is in agreement with the step-wise mechanism predicted computationally by Houk.[43]

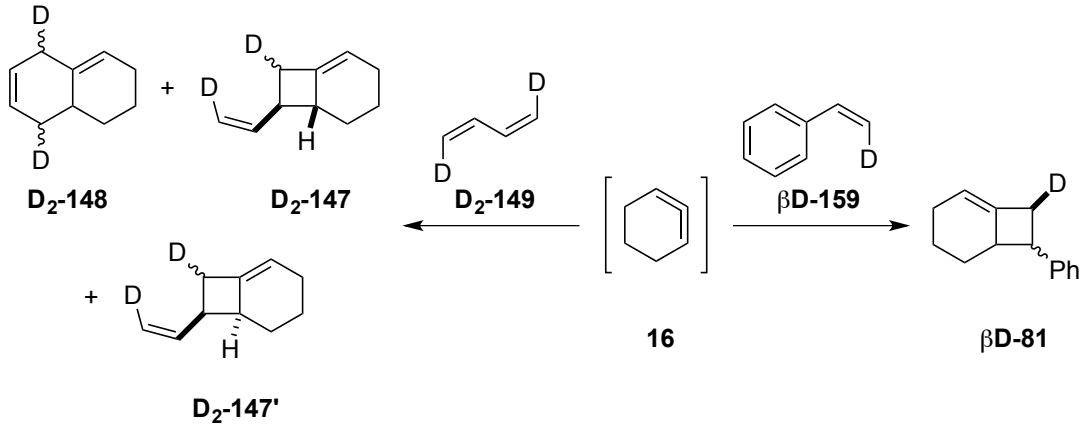

Scheme 1.38 - Stereochemical scrambling of deuterium labels in [2+2] and [4+2] cycloadditions of activated olefins.

1.4.2.6 Limitations of the DMS Reaction

There are a number of limitations associated with cyclic allene generation by the DMS reaction that are similar to those previously discussed for the base-mediated elimination method. The reliance upon alkyl lithium reagents means that acidic or electrophilic functional groups are not tolerated by the reaction. In the DMS reaction where strong alkyl lithium bases are used, metalation of the cyclic dienes can take place, complicating the reaction mixture.[39] In the case of furan this has been circumvented via the use of 2,5-dialkylfuran derivatives.

In some cases, the thermal instability of the dihalocyclopropanes can be overcome by preparing the compounds *in situ* without isolation.[71,81,82] The synthesis and isolation of dibromo precursor **161** was low yielding due to its thermal instability (Scheme 1.39). When both steps were performed in a single pot, anhydrous conditions were necessary with strong bases to induce cyclopropanation and subsequent ring opening, but the procedure gave access to interesting cyclic allene derivatives in higher overall yields (Scheme 1.39).[76] Isonaphthalene cyclic allene **56** was previously synthesized via the elimination of HBr from dihydronaphthalene derivative **55** (Scheme 1.15),[50] however the reaction mixture was very complicated due to side reactions of the cyclic allene with the excess base required for the reaction. The DMS reaction circumvented the undesired decomposition pathways encountered previously to give good yields of several cycloadducts (e.g. **162** and **163,** Scheme 1.39) and the most prevalent side products **165**.

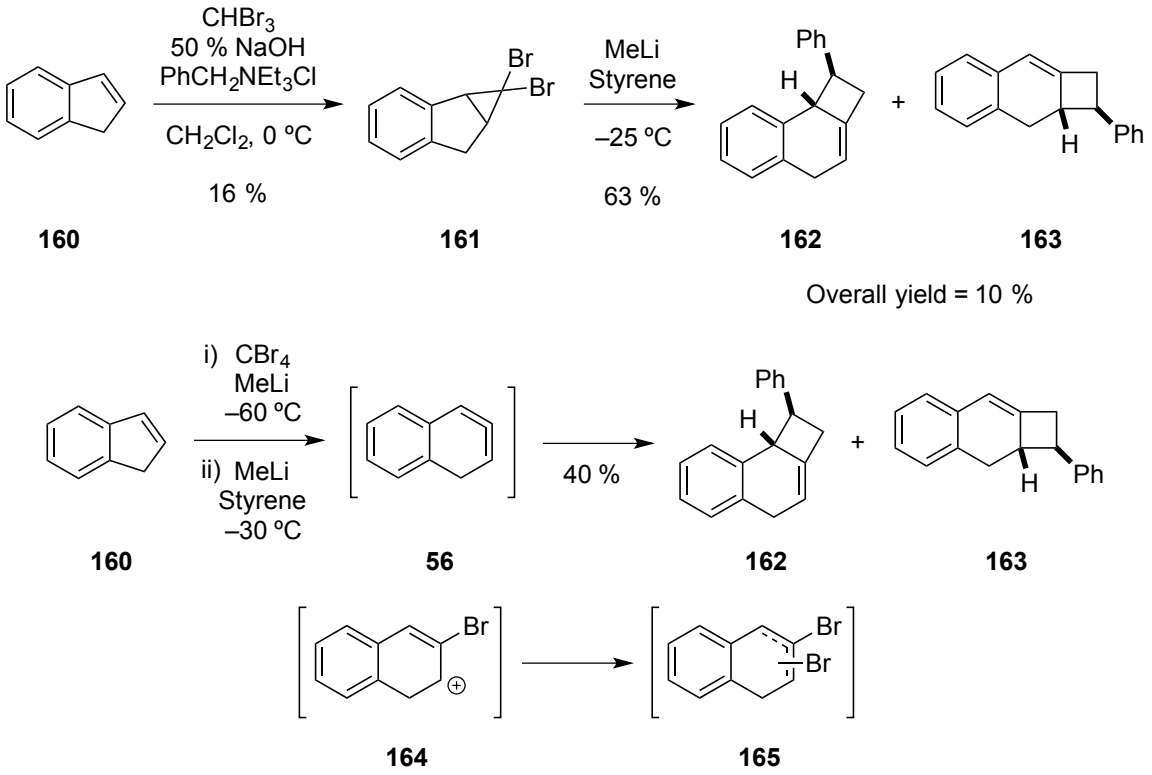

Scheme 1.39 - Comparison of *in situ* synthesis and reaction of thermally sensitive dibromocyclopropane derivatives.

The lithium halogen exchange of a bromine atom using 6,6-dihalocyclopropane **166** is much faster than the similar reaction with a chlorine atom due to the relative bond strengths.[71] Unfortunately the thermal stability of the starting dibromocyclopropanes decreases as the cyclopropane ring is further substituted (Scheme 1.40). Dibrominated cyclopropanes like **166** have been reported to spontaneously ionize and undergo a 2-electron-electrocylic ring opening to structural isomer **167** (Scheme 1.40).[81,83] With 6-fluoro-6-bromocyclopropane **170/171**, only the *endo*-bromo isomer of the dihalocyclopropane **171** could undergo rearrangement. The ring opening and ionization of the leaving group have to occur simultaneously thus having the leaving group *syn* to the fused ring facilitates ring opening. Diastereomer **170** failed to undergo thermal ring opening because the carbon-fluorine bond is much stronger than the carbon-bromine bond, and fluoride anion is a poor leaving group (Scheme 1.40).

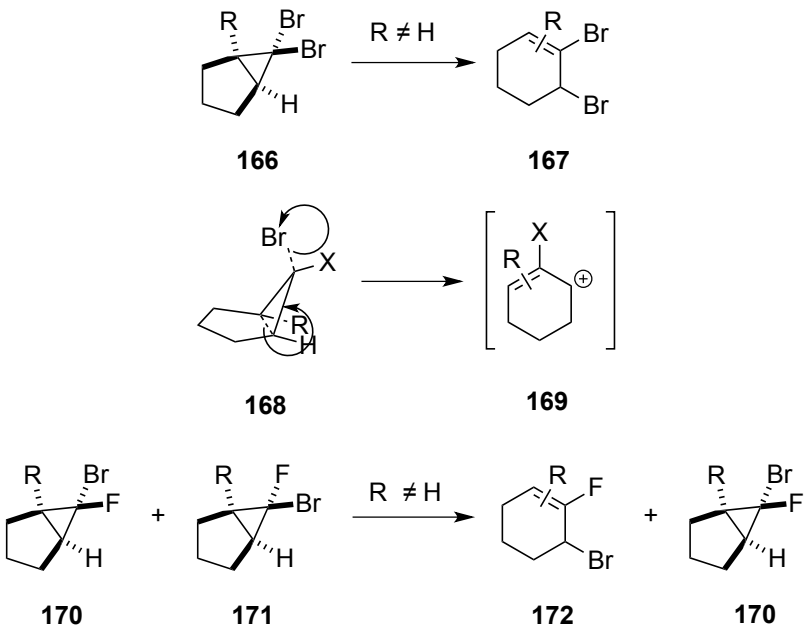

Scheme 1.40 - Thermal decomposition of dihalocyclopropanes.

1.4.2.7 Mechanistic Investigation of Cyclic Diene Reactions with Cyclic Allenes

Several examples illustrate the practicality of the bromofluoro derivatives, including phenyl-substituted derivative **173** reported by Christl and Stalke.[33] A phenyl group would have a stabilizing effect toward the allyl cation intermediate of dihalocyclopropane ring opening (**172**); however, the strength of the carbon-fluorine bond disfavors thermal ring opening of one isomer, allowing the authors to isolate the needed starting material as a single diastereomer **174** (Scheme 1.41).

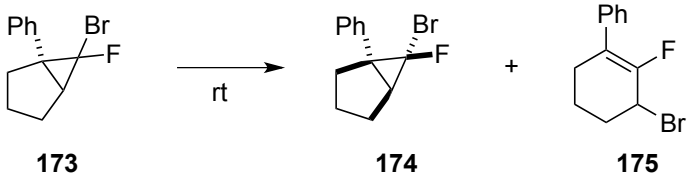

Scheme 1.41 – A phenyl-substituted dihalocyclopropane that is stable to ring opening.

The tendency of one diastereomer to decompose was used in the ultimate demonstration of the generation of chiral cyclic allenes. To test the rate of ring closure with furan and stereochemical fidelity of DMS derived chiral cyclic allenes, Christl and coworkers used enantiopure bromofluoro-derivative **176** in a Diels-Alder cycloaddition with dimethylfuran.[84] The isolation of bromofluoro derivative **176** was possible due to

the decomposition of one of the diastereomers (similar to Scheme 1.41) and the use of preparative scale chiral HPLC to obtain both enantiomers of the starting dihalocyclopropane (**176**). Upon subjecting **176** to MeLi at -78 °C in 2,5-dimethyl furan, fused-cyclopropylcarbene **178** formed and opened to isonaphthalene cyclic allene isomer **179** or its enantiomer **180**, which was trapped by 2,5-dimethylfuran forming *endo* cycloadduct **177** in 40 % yield and a single regioisomer (Scheme 1.42).

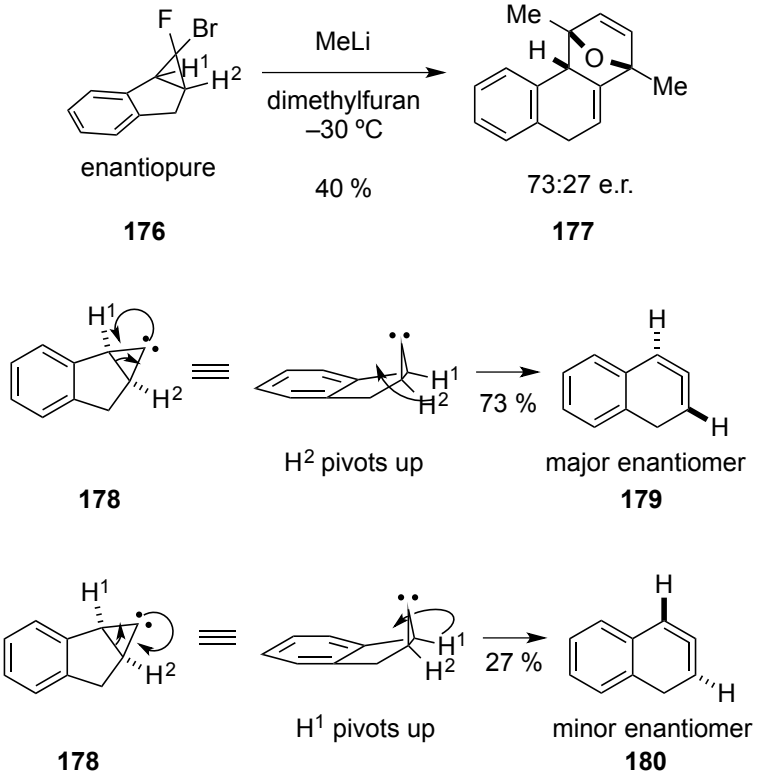

Scheme 1.42 - DMS ring opening of chiral isonaphthalene precursor.

Upon investigating the enantiomeric excess of the cycloadducts, the product was found to have an enantiomeric ratio of 73:27. To determine if the loss in enantiomeric excess was occurring during the allene generation or the allene trapping, experiments were run under higher dilution, higher temperature, and finally using traps of increasing steric demand (from dimethylfuran, to bis-*t*-butylfuran) (Table 1.3). In all of these cases similar enantiomeric ratios were obtained leading researchers to conclude the loss of enantiomeric enrichment was derived from the generation of the allene. Upon the addition of MeLi, free carbene **178** forms (Scheme 1.42). It was assumed the fused benzene ring would rigidify the ring system and control the torquoselectivity of the

cyclopropane ring opening absolutely. The ring opening fails to occur with 100 % fidelity, proceeding in a reproducible 73:27 ratio.

Table 1.3 - Enantiomeric excess from cycloaddition of benzo-fused cyclic allene and substituted furans.

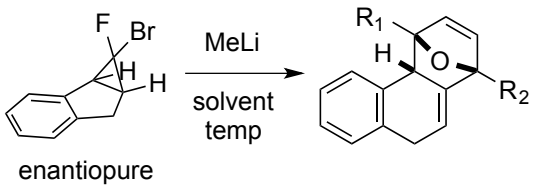

enantiopure

176 **177 and 181**

Solvent	Temperature (°C)	Dilution	Enantiomeric Excess[a]	Product
Dimethylfuran	–30	No cosolvent	73:27	**177**
Dimethylfuran	rt	No cosolvent	72:28	**177**
Dimethylfuran	–30	furan:ether (1:1)	73:27	**177**
Di-*t*-butylfuran	–30	No cosolvent	74:26	**181**

[a] Enantiomeric excess of the products determined by chiral HPLC of the purified cycloadducts.

Christl and Engels were able to improve the torquoselectivity of the cyclopropane rearrangement by substituting the allene with a phenyl group.[84] Enantiopure bromofluorocyclopropane **174** was subjected to MeLi in the presence of 2,5-dimethylfuran to give cycloadduct **182** in 31 % yield with 100 % enantiomeric fidelity (Scheme 1.43). The phenyl group showed much greater propensity to control the torquoselectivity of the ring opening of cyclopropyl carbene **183**. Of note was the preference for the more substituted cycloadduct **182** as a single diastereomer. In the previously discussed ester-substituted cycloadducts **123/124** (Scheme 1.27)[43] the more substituted double bond was more reactive. Substitution of the cyclic allene functionality increases the diastereoselectivity beyond the 10:1 diastereoselectivity previously described for 1,2-cyclohexadiene.

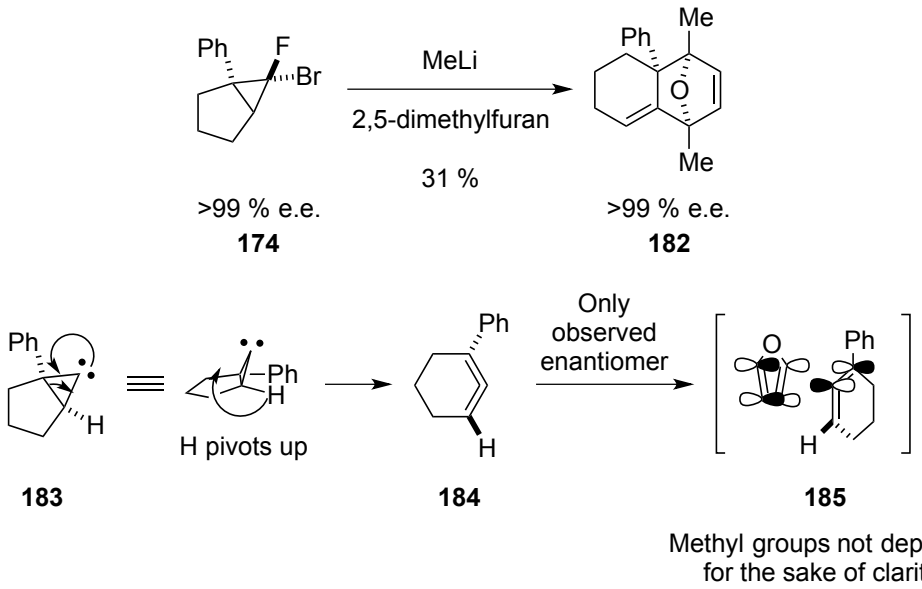

Scheme 1.43 – 2,5-Dimethylfuran trapping of an enantiopure cyclic allene.

Studying the enantiomeric fidelity of cyclic allene cycloadditions with styrene, Christl and Engels found minor erosion of enantiomeric enrichment using phenyl-substituted cyclic allene precursor **174**.[47] Unlike the reaction with dimethylfuran (Scheme 1.43), styrene failed to conserve absolutely the stereochemistry of enantioenriched precursor **174** (Scheme 1.44). *Syn* and *anti* diastereomers **186** and **187**, respectively, were formed in a 1:1 ratio and upon inspection of the enantiomeric excess the *syn* isomer was found to have an e.r. of 94:6 (minimal erosion of stereochemical information), and the *anti* isomer was found to have an e.r. of 85:15 (more significant enantiomeric erosion). Unlike the cycloaddition with furan only the less-substituted isomers were formed due to the high spin-density on the terminus of the proposed phenyl-substituted allyl radical **V-VIII** (more likely in a step-wise reaction) (Scheme 1.44). To explain the high degree of enantiomeric fidelity, the authors propose a pseudo-concerted transition state, whereby the nucleophilic attack of the allene on the styrene can have 4 different orientations **I-IV**, with fast subsequent ring closure on the same face. Ring closure must be faster than racemization/equilibration to maintain such a high e.e. in the products, further supported by the 1:1 mixture of diastereomers when the thermal equilibrium is known to favor a 1:10 ratio of **186:187**.[33]

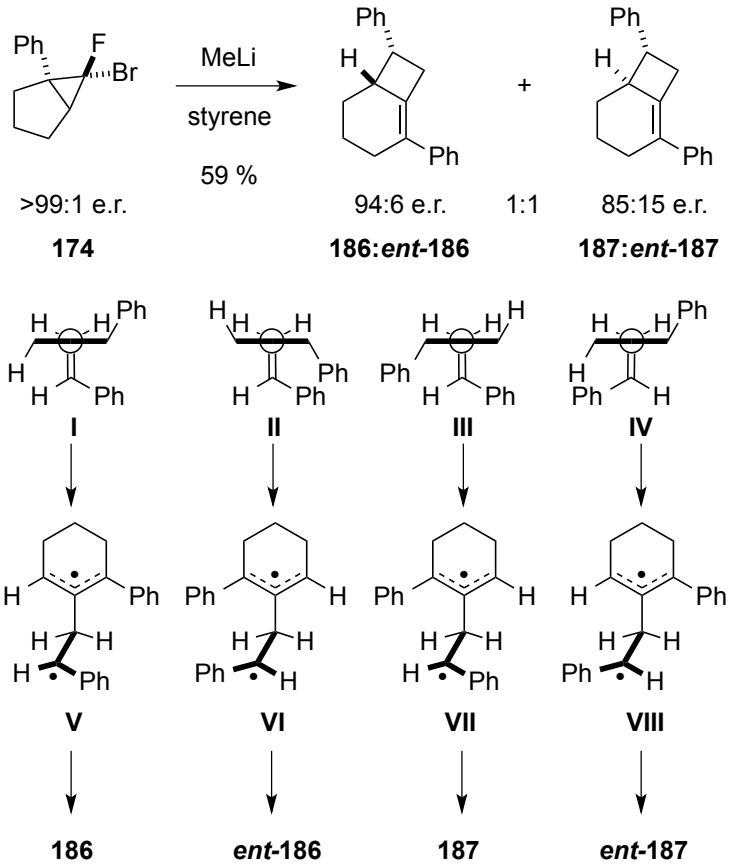

Scheme 1.44 - Enantiomeric fidelity in styrene/cyclic allene [2+2] cycloadditions.

1.4.2.8 Application of the DMS reaction to the Smallest Carbocyclic Allene Trapped

As a final note on the DMS reaction, the stability of the fluorobromocyclopropane derivatives enabled the first synthesis and trapping of a five-membered cyclic allene **192**, (Scheme 1.45).[85] Though outside the scope of this review, trapping the cyclic allene **192** as the furan cycloadduct **191** stands as a hallmark achievement of the applicability of the DMS reaction to cyclic allene generation.

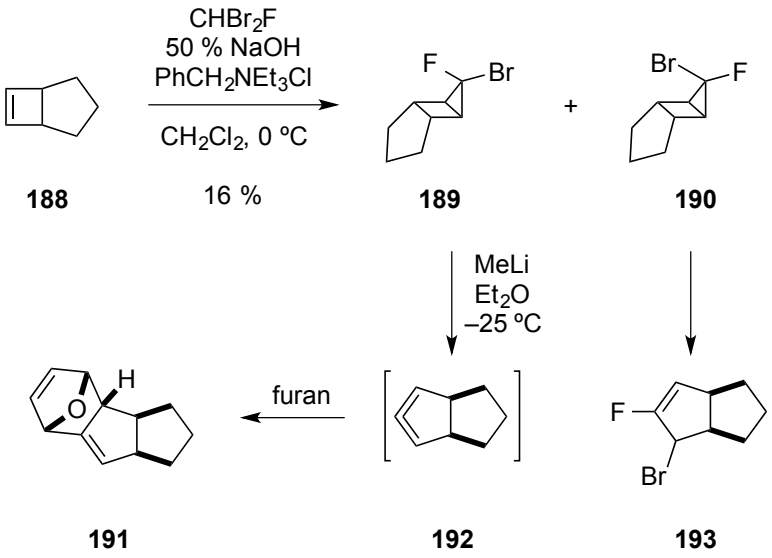

Scheme 1.45 - First trapping of a five-membered cyclic allene.

1.4.3 1,6-Dihalocyclohexenes for Cyclic Allene Generation

Dibromocyclohexene **194** was derived from the thermal decomposition of the dihalocyclopropanes used in the DMS reaction. Boyden demonstrated that **194** in the presence of a THF dispersion of magnesium metal and diphenylisobenzofuran would provide known cycloadducts **17** and **17'** (Scheme 1.46).[86]

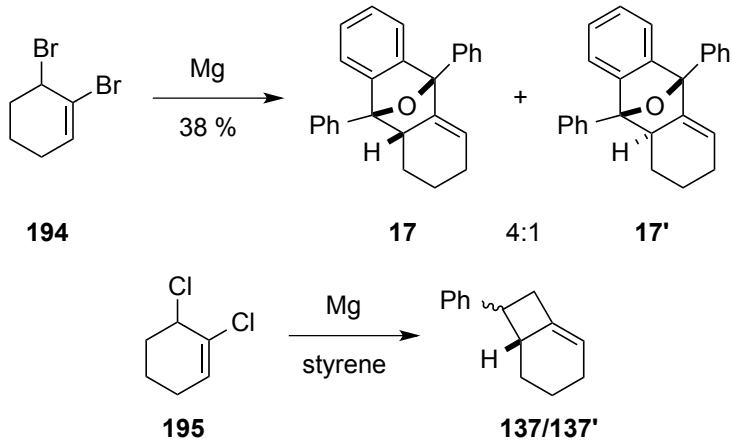

Scheme 1.46 - Magnesium reduction of dihalocyclohexenes.

Though reported sparingly, the 1,6-dichloro derivatives **195**, derived from the 6,6-dichlorobicyclo[3.1.0]hexane that were generally inert to DMS reaction conditions, were equally efficient in the generation of 1,2-cyclohexadiene as inferred from the trapping experiments with styrene.[39] The strongly reducing conditions are not compatible with

electron-rich heteroaromatic furans. For similar reasons, dienes such as cyclohexadiene and cyclopentadiene undergo reduction and were not amenable to trapping the cyclic allene generated with this method.

1.4.4 Fluoride-Mediated Allylic Silane Elimination

The generation of cyclic allenes using a base-mediated elimination was in part hampered by the limited ability of the base to distinguish between all the protons on the cyclohexene scaffold. Selective deprotonation of the pseuodo-equatorial allylic proton (H^3) is necessary to generate 1,2-cyclohexadiene in the absence of an anionic stabilizing group (Figure 1.3). This selectivity could be mediated by the use of alkyl silanes, which could chemoselectively initiate the elimination by the addition of a fluoride anion source (e.g. tetrabutylammonium fluoride or cesium fluoride). The large silyl group is preferentially situated in a pseudo equatorial configuration, pre-organizing the substrate to elimination. Johnson and Shakespeare first demonstrated the fluoride mediated elimination method using 1-bromo-6-trimethylsilylcyclohexene **196** (Scheme 1.47).[87]

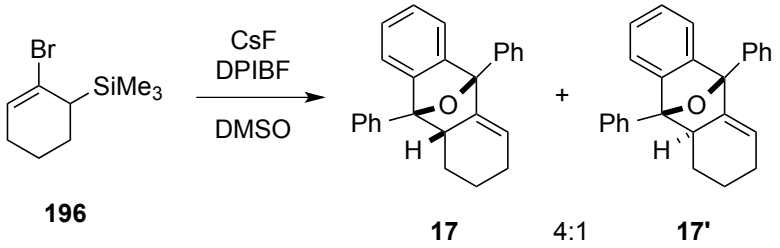

Scheme 1.47 - Fluoride-mediated desilylative elimination generating cyclic allenes.

Peña and coworkers further elaborated upon the fluoride-mediated silyl-elimination by exchanging the vinyl bromide employed by Johnson for a vinyl triflate leaving group.[88] The authors hypothesized that the triflate leaving group would lead to a more efficient elimination and thus greater yields in the trapping events. The reported synthesis of the starting material allowed the incorporation of substituents on the allene (Scheme 1.48). In addition to the parent 1,2-cyclohexadiene, 1-methyl-1,2-cyclohexadiene was also demonstrated to react with furans, though the regioselectivity between the two olefins was poor. DPIBF cycloadducts **202/202'** and **203** were isolated in a 1.5:1 ratio with reactivity at the methyl substituted double bond being the major product (**202/202'**).

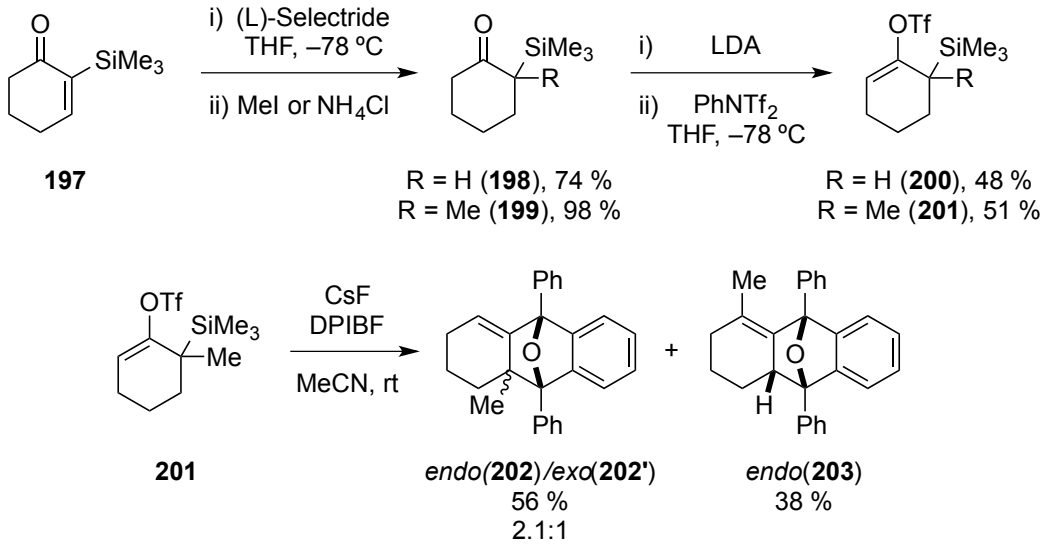

Scheme 1.48 - Desilylative elimination of a vinyl-triflate.

1.4.5 Cyclic Allenes from Cycloaddition: the Dehydro-Diels-Alder

The strongly reducing conditions employed in the previous methods contrast with the redox neutral pericyclic methods that are available. The use of cycloadditions and electrocyclizations to generate cyclic allenes is an attractive strategy given that thermal activation is sufficient to form the reactive intermediates and the tolerance for functional groups is therefore high. A number of different methods to generate cyclic allenes and trap cyclic allenes have been developed utilizing different pericyclic reactions.

The dehydro-Diels-Alder dimerization of vinylacetylene was reported to involve the intermediacy of a vinyl-substituted cyclic allene.[89] Dykstra reinvestigated the thermal polymerization of vinylacetylene in the presence of acid catalysts and assigned the structure of the dimer formed as styrene (Scheme 1.49). The yield ranged from 20 - 50 % depending upon the catalyst employed. The author proposed the reaction proceeds through cyclic allene intermediate **205**, although he was quick to address the controversy of the proposed structure: "*The structure of IV* (**205**)*, which is shown as a six-membered ring containing a pair of contiguous double bonds, appears to be practically impossible stereochemically. It is conceivable that IV* (**205**) *is not actually formed as an intermediate but that a triad shift* [a [1,3]-hydrogen shift across three atoms] *occurs concurrently with the combination so that styrene is formed directly*."[89]

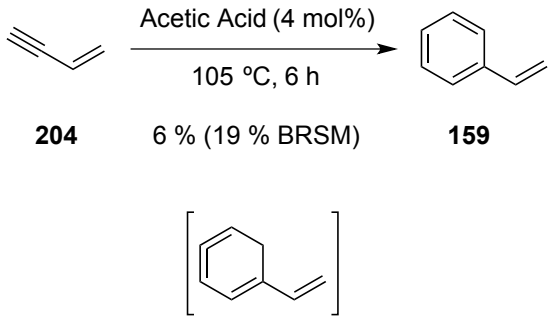

Scheme 1.49 - Dimerization of vinyl acetylene via an intermolecular dehydro-Diels-Alder cycloaddition.

1.4.5.1 Butz's Cascade Dehydro-Diels-Alder

Inspired by the observation of Marvel and Blomquist that ene-enyes react with maleic anhydride,[90] Butz and coworkers investigated the dehydro-Diels-Alder reaction on more complex substrates under the pretense of trapping the cyclic allenes generated *in situ*.[91-96] Conjugated diene-yne **206** underwent a facile [4+2] cycloaddition reaction with maleic anhydride at 130 °C to generate cyclic allene **208** (Scheme 1.50). The subsequent Diels-Alder reaction of **208** with **207** was accelerated by the strain imposed on the system by the cyclic allene incorporated into the cycloadduct. Butz and coworkers further applied the Diels-Alder cascade to the synthesis of steroid-like carbon frameworks **211** (Scheme 1.50).

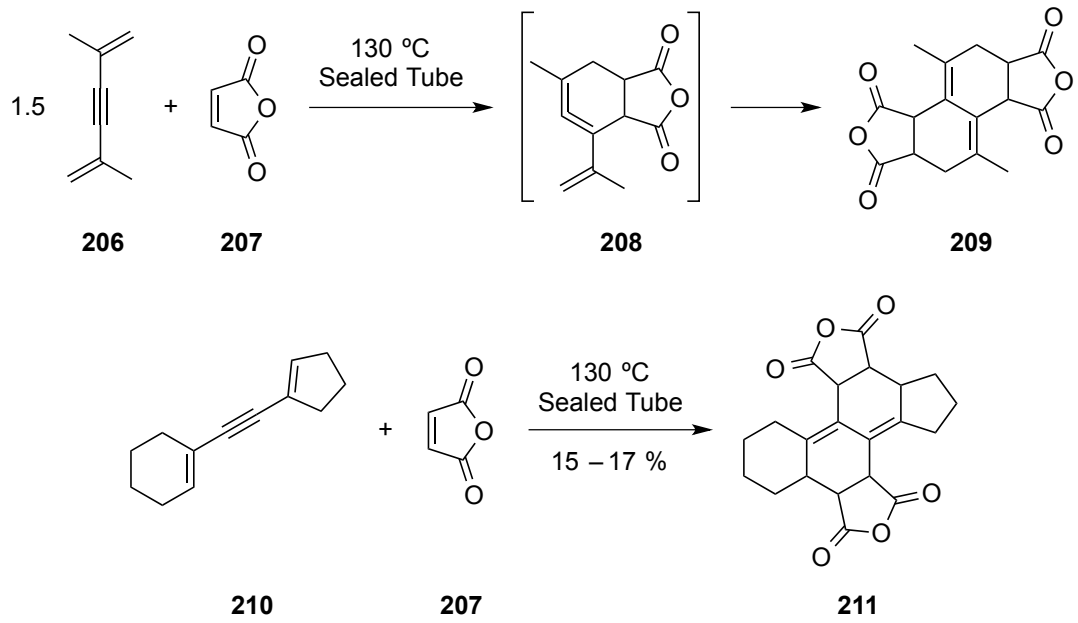

Scheme 1.50 - Intermolecular dehydro-Diels-Alder reaction with maleic anhydride.

1.4.5.2 Danheiser's Intramolecular Dehydro-Diels-Alder

More recently Danheiser and coworkers reported on the synthetic capabilities of the tetradehydro-Diels-Alder reaction via the intramolecular cycloaddition of ene-ynes with electronically activated alkynes (Table 1.4).[97] Similar to Dykstra's report,[89] the isobenzene **213** rearomatizes via a formal [1,3]-hydrogen shift to furnish poly-substituted aromatics. Lewis acid, Brønsted acid, or thermal activation facilitated the cycloaddition of **212** to give the desired cycloadduct, with aluminum trichloride delivering the highest yield under the mildest reaction conditions (Table 1.4).

Table 1.4 - Intramolecular dehydro-Diels-Alder cycloaddition under various conditions.

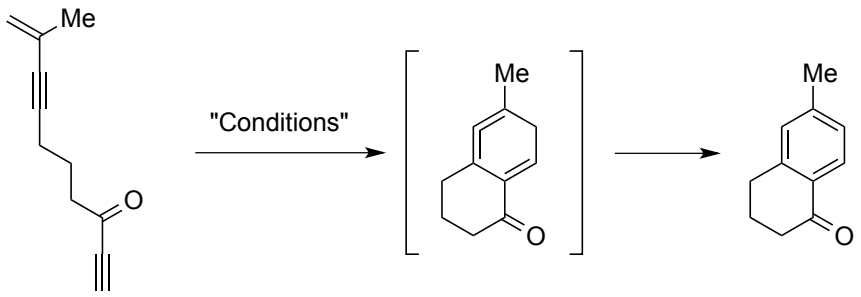

212 **213** **214**

Entry	Conditions	Yield (%)[a]
1	BHT, $PhCH_3$, 180 °C	78
2	$MeSO_3H$, DCM, 0 °C	87
3	$AlCl_3$, DCM, 0 °C	90
4	Me_2AlCl, DCM, –78 °C → rt	49

[a] Yields reported were of isolated compounds.

Changing the electronic demand of the cycloaddition, Danheiser employed ynamides in the tetradehydro-Diels-Alder reactions (Scheme 1.51).[97] Heating the ynamide-tethered ene-ynes (**215** or **217**) in toluene (temperatures ranging from 110 – 210 °C) gave good yields of polysubsituted indolines (Scheme 1.51), though the reactants gave no products under the Lewis acidic conditions employed previously ($AlCl_3$, DCM). Satisfyingly the amide nitrogen could be conjugated to either the ene-ynophile (**215**) or could be conjugated to the ene-yne moiety (**217**), allowing access to a variety of substitution patterns. In the case of ynoate **219**, Lewis acid catalysts could again be employed at relatively low temperatures to mediate the cyclization.

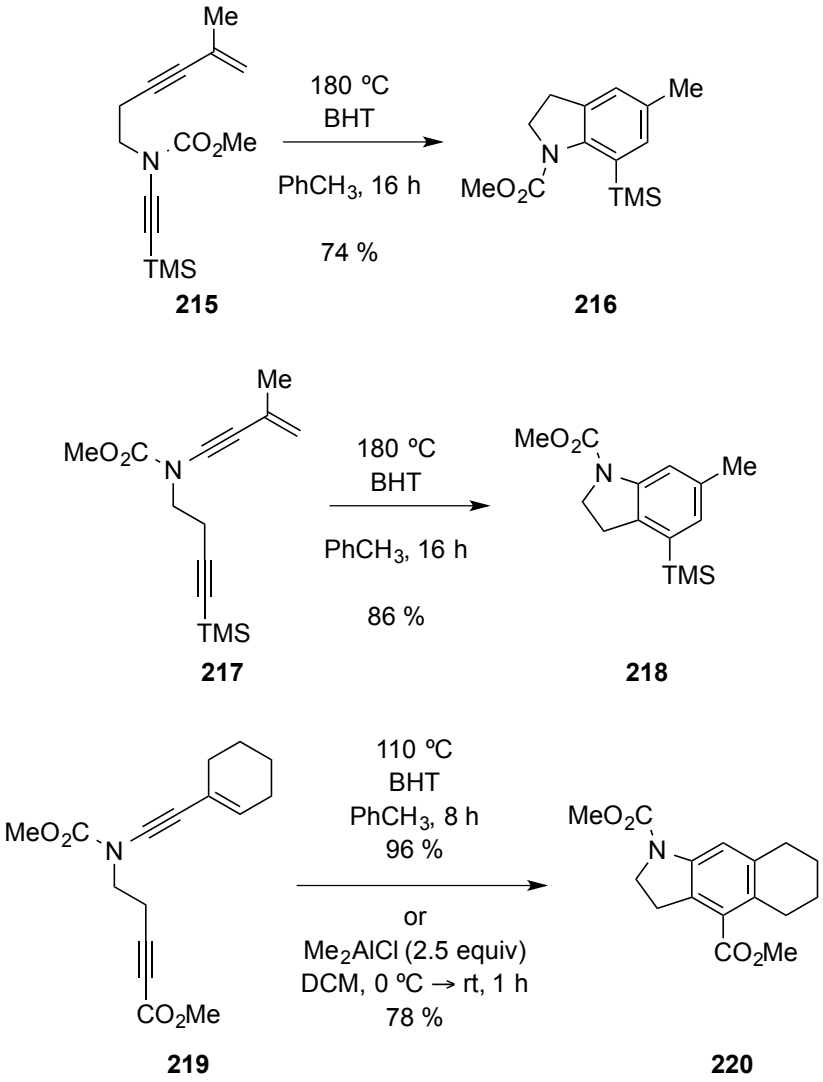

Scheme 1.51 - Tetradehydro-Diels-Alder reaction of ynamides.

Within Danheiser's previous reports was a single example of ene-yne **221** acting as an ene-yneophile furnishing α,β,γ,δ-cyclohexadienone **222** (Scheme 1.52).[97] By reacting an activated olefin with an ene-yne, non-aromatic products were obtained, and if the olefin were substituted, the diastereoselectivity of the reaction could be evaluated.

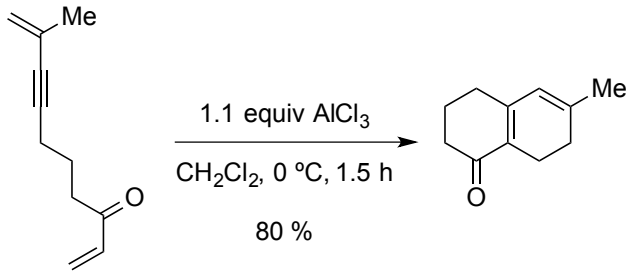

221 **222**

Scheme 1.52 - Intramolecular dehydro-Diels-Alder.

Danheiser and coworkers returned to the ene-yne as a ene-yneophile in 2011, demonstrating the Lewis acid-mediated dehydro-Diels-Alder reaction of cyclobutenones with tethered ene-ynes (Scheme 1.53).[98] Following the cycloaddition, fused cyclobutane **225** could be opened to cyclooctatriene **226** by simple thermal activation. Interestingly, cyclobutenone substrate **227** presumably underwent an intramolecular dehydro-Diels-Alder reaction but only the one pot tandem dehydro-Diels-Alder/6p-electrocyclic ring opening product, cyclooctatrienone **228,** was reported.

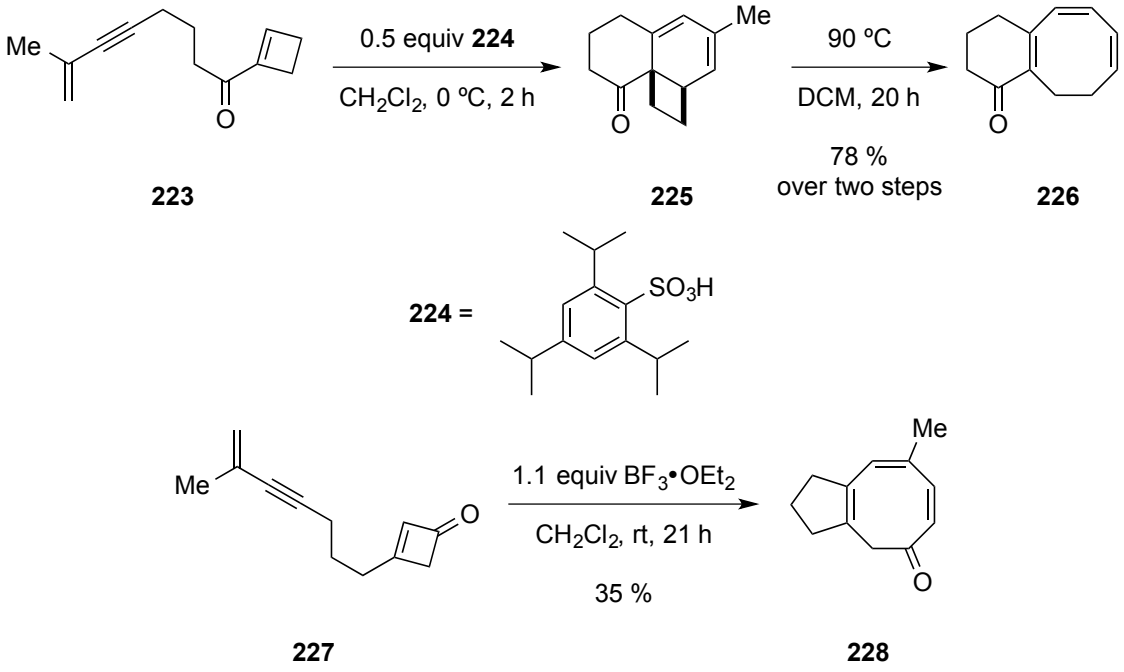

Scheme 1.53 - Dehydro-Diels-Alder with carbonyl-conjugated cyclobutenes.

Finally, the use of benzyne circumvented the barrier to the thermal tetradehydro-Diels-Alder reaction. Danheiser and coworkers used tetrabutylammonium

triphenyldifluorosilicate (TBAT) to initiate a fluoride-mediated desilylative elimination of an adjacent triflate on aryl-tethered ene-yne **229** to generate benzyne **233**. Isonapthalene cyclic allene **234** was formed from the intramolecular dehydro-Diels-Alder reaction (Scheme 1.54).[99] A BHT-mediated hydrogen transposition furnished the polysubstituted naphthalenes (**231**/**232**) in good yields under mild reaction conditions. The reaction was tolerant to many different functional groups and the olefin of the ene-yne functionality could even be part of a heteroaromatic ring (**236**). Unfortunately the yields were lower when the ene-yne olefin was not substituted at R^1 (**231** versus **232**).

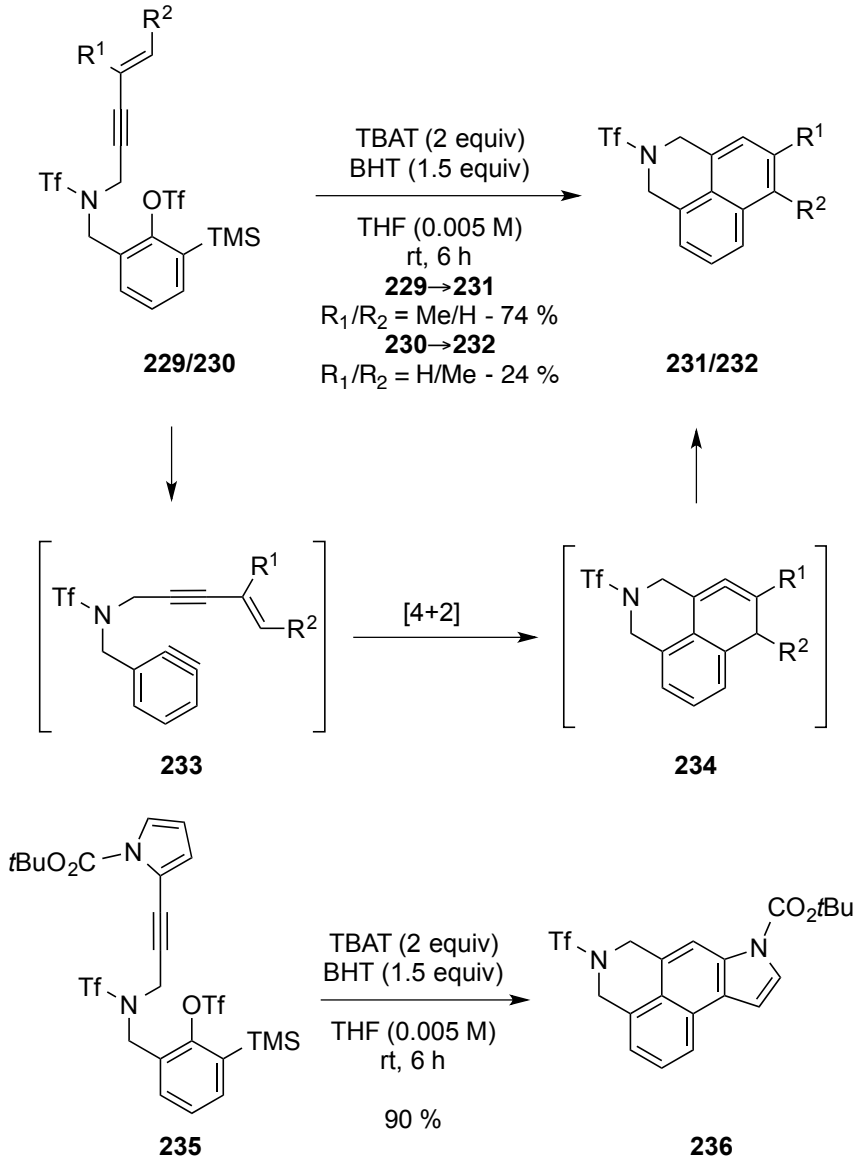

Scheme 1.54 - Tetradehydro-Diels-Alder reaction employing benzyne.

1.4.6 1,2-Cyclohexadiene from Diels-Alder Cycloreversion

Furan cycloadduct **46/46'** was used by Werstiuk and coworkers to generate 1,2-cyclohexadiene via the retro-Diels-Alder reaction (Scheme 1.55).[100] A continuous wave carbon dioxide laser enabled the generation of the intermediate **16** along with the recording of its photoelectron spectrum while removing background furan and 1,3-cyclohexadiene contaminant signals. The reactions were driven toward the cyclic allene using high nozzle temperatures (550 °C – 850 °C) and dilute solutions of the precursor. Unfortunately, intermolecular trapping of cyclic allenes generated using flash vacuum pyrolysis was only applieed to the physical investigation of the intermediate and not trapping reactions.

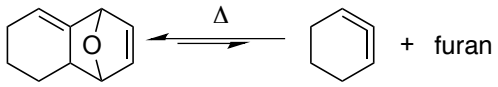

46/46' **16**

Scheme 1.55 - Pyrolysis of the furan cycloadduct (46/46') allows the photoelectron spectrum of 1,2-cyclohexadiene (16).

1.4.7 Dehydro-Electrocyclizations to Generate Cyclic Allenes

1.4.7.1 The Hopf Cyclization

In a similar fashion to the dehydro-Diels-Alder, the dehydro-electrocyclization of dieneyne **237** provides isobenzene cyclic allene **74** as an intermediate (Scheme 1.56).[101] In the absence of a trap, isobenzene **74** undergoes a [1,3]-hydrogen shift to yield benzene. Known as the Hopf cyclization, it has been used in several cases to synthesize bowl-shaped fused-benzene derivatives such as corranulene using flash-vacuum pyrolysis (FVP),[102,103] although it was not definitive in these cases whether the cyclization occurs via a Hopf cyclization pathway through an isobenzene intermediate or via an alkyne-vinylidene isomerization/carbon-hydrogen bond insertion (**242** versus **243**); first theorized by Brown and coworkers.[104]

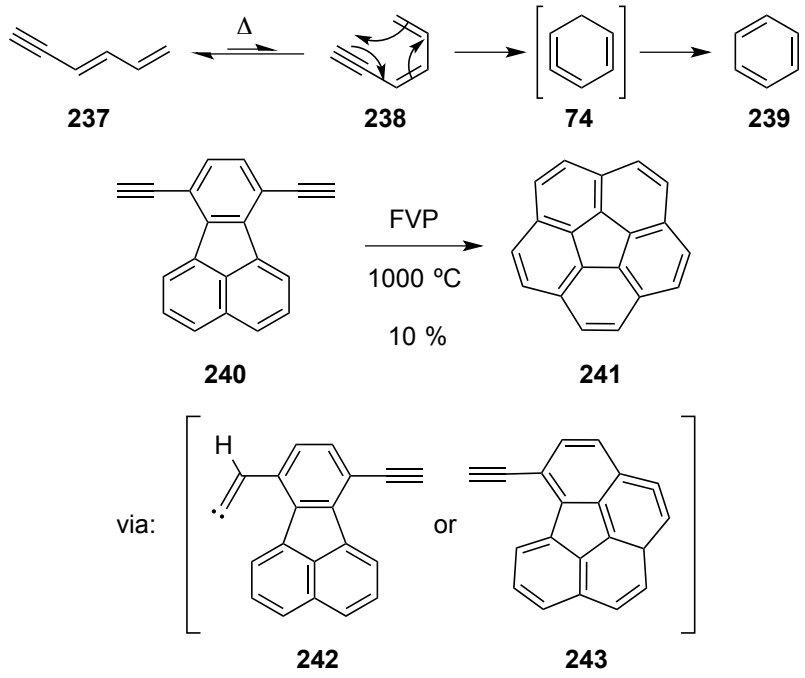

Scheme 1.56 - Hopf cyclization and application to corranulene synthesis.

Support for the cyclic allene intermediate in the Hopf cyclization was provided by a trapping experiment using styrene as a cosolvent. Investigating the mechanism of the reaction, Hopf and coworkers pyrolyzed diene-yne **237** in the presence of excess styrene and were able to isolate the [2+2] cycloadducts, **244** and **245** (Scheme 1.57) along with the significant byproducts **246**, and **239**.[105] Fukuzumi and coworkers calculated that the radical spin density is greatest on the central carbon of a pentadienyl radical,[106] explaining the observed greater ratio of non-conjugated regioisomer **245** (3:7, **244**:**245)**. Christl and coworkers reported the kinetic preference for cycloadduct **245** was much higher than the ratio reported by Hopf. They were able to use the DMS reaction to generate isobenzene **74** in the presence of styrene and obtained a ratio of 19:1, **244:245**,[76] thus highlighting the harshness of the reaction temperatures needed to facilitate the Hopf cyclization.

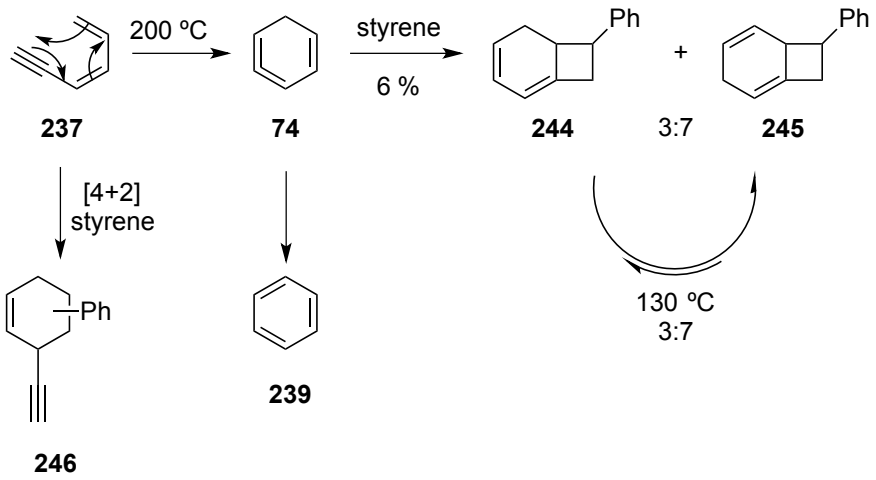

Scheme 1.57 - Trapping of isobenzene cyclic allene by styrene accessed by the Hopf cyclization.

Fernández and coworkers reported the intramolecular trapping of cyclic allenes via an electrocyclic ring opening/Hopf-like cyclization of cyclohexadienones in alcoholic solvents, (Scheme 1.58).[107] Photolysis of dienone **247** generated ketene **248** via a 6π-electrocyclic-ring opening, which quickly reacted with the alcoholic solvent to generate diene-yne **249**. A Hopf-like 6π-electrocyclic-ring closure produced cyclic allene **250**, which underwent a [1,3]-retro-Brook rearrangement to furnish silylated cyclohexadienone **251**. If the reaction was run in the presence of di-*i*-propyl amine, hydrogen atom abstraction/Michael-addition was favored over silyl-migration (**252**).

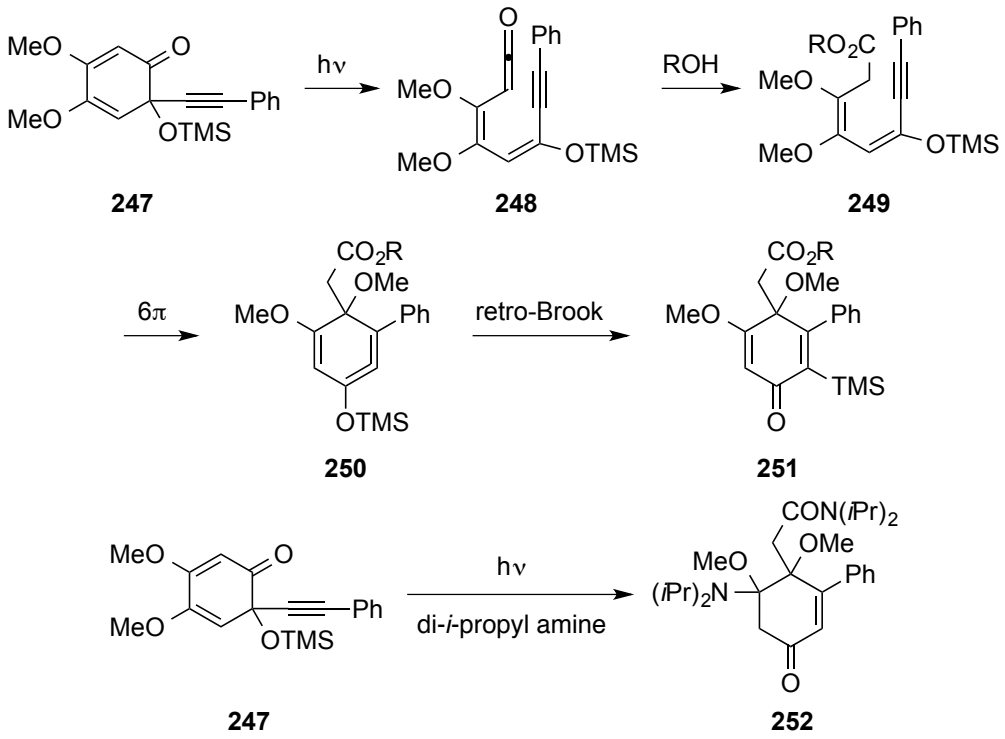

Scheme 1.58 - Photolytic Hopf cyclization with retro-Brook rearrangement to quench.

1.4.7.2 The Moore Cyclization

Elaborating upon the Hopf cyclization, Moore demonstrated the application of the 6π-electrocyclization of ene-yne-ketenes to the synthesis of polyfunctionalized quinones.[108] The Moore cyclization generates highly substituted 1,2,4-cyclohexatrienes (**255)** that are sterically shielded as well as highly delocalized. The observed high yields of the trapping reactions and broad reactivity of the Moore cyclization intermediates suggest the substituents enhance the reactivity of the cyclic allene significantly while preventing unwanted side reactions (Scheme 1.59). Two general methods were developed to gain access to the polyfunctionalized 1,2,4-cyclohexatriene cyclic allene **255**. The 4π-electrocyclic ring opening/6π-electrocyclic ring closure of alkyne substituted cyclobutanones (**253**), and the thermolysis of azido-substituted-1,2-benzoquinones **256**. Both showed high efficiency in a number of interesting transformations.[108-111]

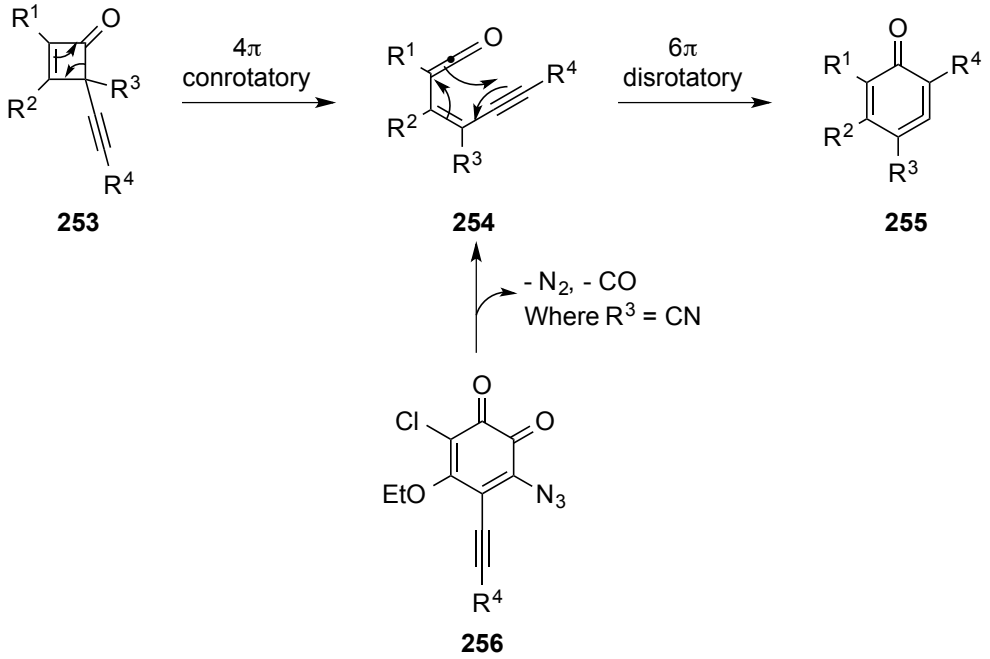

Scheme 1.59 - Moore cyclization of ketene-ene-ynes gives cyclic allene intermediates.

Recent investigation by Fernández and coworkers show the closed-shell cyclic allene to be lower in energy compared to the diradical proposed originally by Moore.[107,112] Using *ab initio* methods for the optimization of both **257** and **258** in Figure 1.5, the group found the diradical proposed by Moore to be approximately 19 kcal/mol higher in energy than the cyclic allene structure **257**. This is supported by calculations performed on other cyclic allene structures by Engels,[42] and Johnson.[23,44,113]

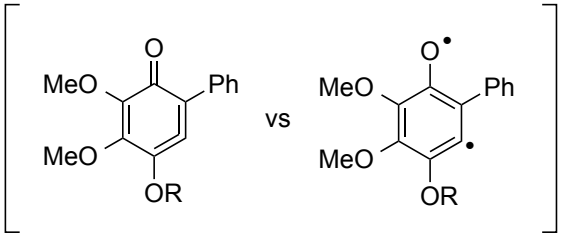

Figure 1.5 - Two proposed structures for the Moore electrocyclization intermediate.

1.4.7.2.1 Intramolecular Trapping of Cyclic Allenes Derived from the Moore Electrocyclization

The cyclic allenes generated from the Moore electrocyclization show unique reactivity compared to the cyclic allenes generated by any other method. Attractively,

Moore reported the first examples of intramolecular trapping of a cyclic allene intermediate. In the case of the isopropenyl-substituted cyclic allene **259**, alkylidene cyclobutane fused quinone **260** was proposed to arise from a 4π-electrocyclic ring closure (Scheme 1.60).[114] Tautomerization furnished the final aromatic phenol **261**. *O*-Allyl allene **262**, rearranged via a Claisen [3,3]-sigmatropic rearrangement to give allylated derivative **263**.[110]

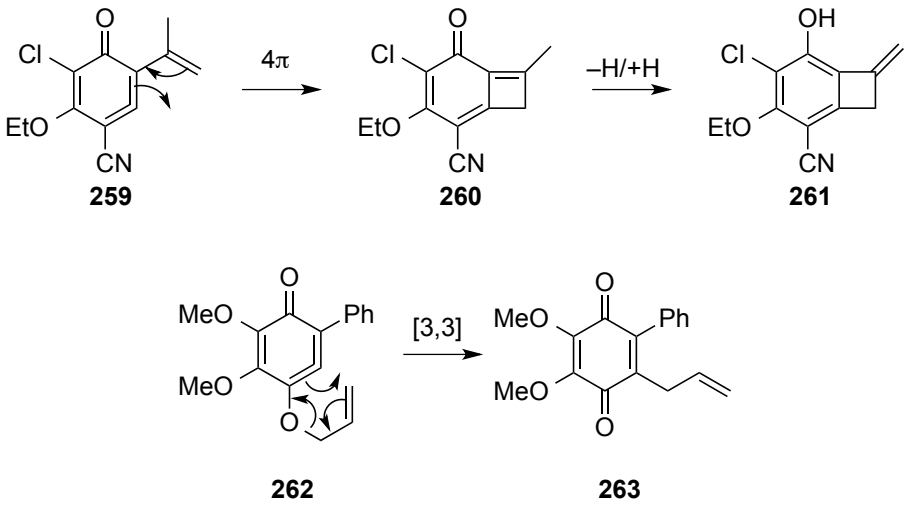

259 **260** **261** **262** **263**

Scheme 1.60 - Intramolecular pericyclic reactions of Moore cyclization intermediates.

Using tethered alkynes, such as **264**, the formation of alkylidenecyclopentene fused benzoquinone **268** was reported (Scheme 4.2).[115] The intramolecular capture of cyclic allene **266** could occur via either a stepwise mechanism (shown as a polar reaction in red) or a concerted Conia-ene process (shown in blue) in Scheme 4.2. The intramolecular alkyne trapping strategy was amenable to the incorporation of heteroatoms in the linker such as nitrogen, and oxygen to make fused-aza/oxynaphthalene derivatives.[116]

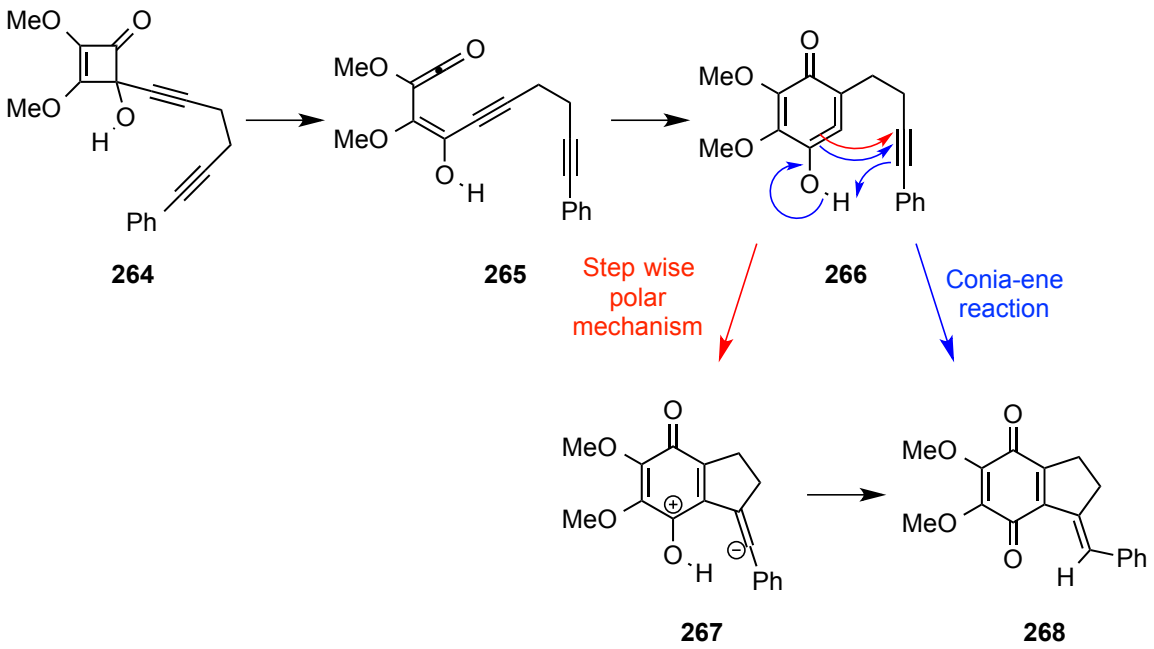

Scheme 1.61 – Intramolecular capture of cyclic allenes with alkynes.

There are a number of examples whereby a pendant aryl group traps a Moore cyclization cyclic allene by a Friedel-Crafts reaction (Scheme 4.3). Interestingly, only mild selectivity between the five-membered ring (**270**) and the 6-membered ring (**271**) arylation product was observed in the case of indole derivative **269**.[108,116] In the case of naphthyl-derivative **272** exclusive C8 alkylation was observed (**275**).[108]

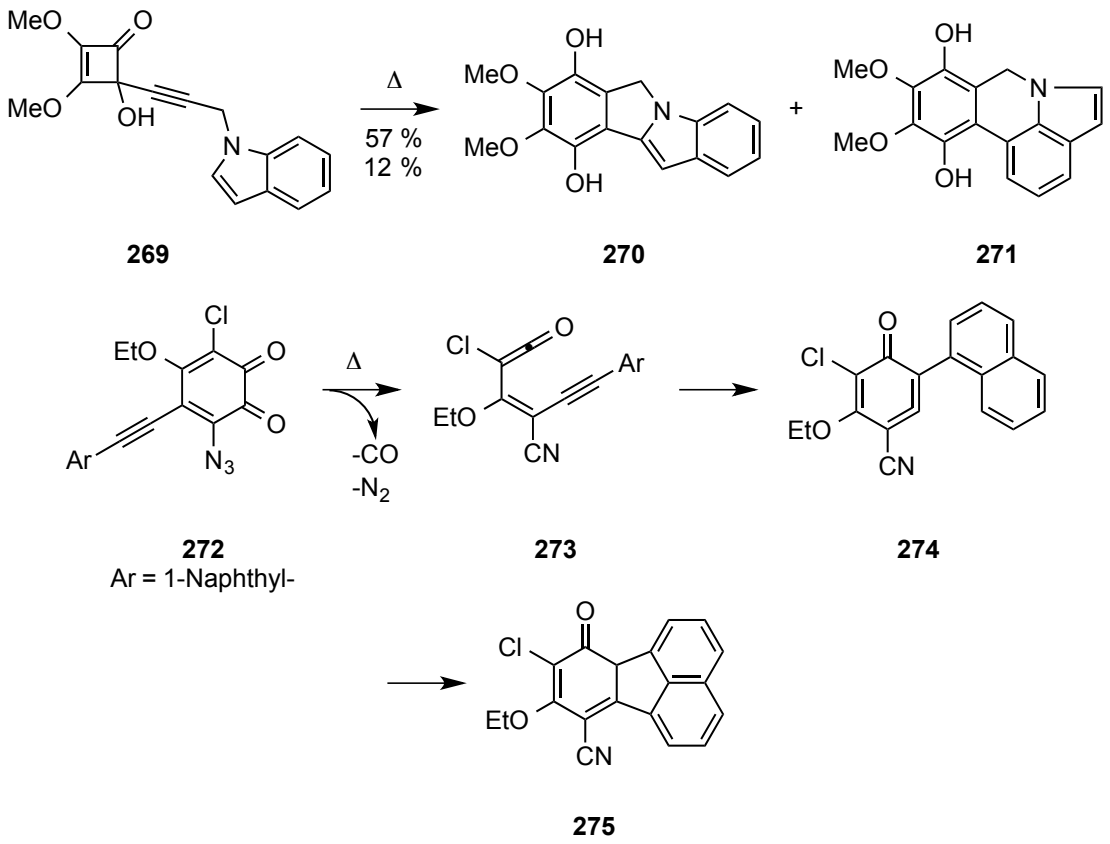

Scheme 1.62 - Intramolecular trapping of cyclic allenes by arene rings.

In the case of alkyl substituted derivatives, a hydrogen atom-transfer mechanism was proposed to explain the mixture of products (Scheme 1.63).[108] Diradical intermediate **279** could be formed in a step-wise fashion as a key intermediate, which was proposed to undergo a number of different elimination and cyclization reactions to furnish **280–283**.

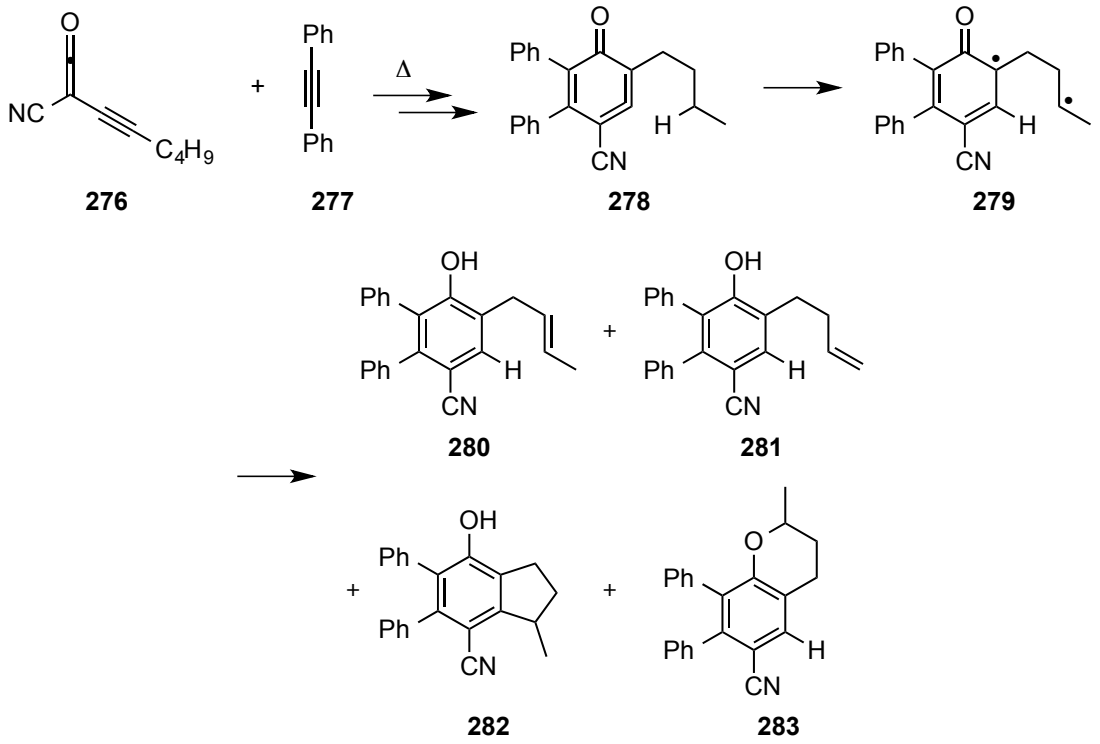

Scheme 1.63 - Intramolecular C-H insertion of cyclic allene into a pendant alkyl group.

1.4.7.2.2 Intermolecular Trapping of the Moore Cyclization Intermediate

A number of different intermolecular processes were also demonstrated including the trapping with styrene (**286**), alkynes (**287**) and the reaction with THF/TMS-Cl to give alkoxy-substituted phenol **284**.[108] The reaction with styrene was reported to proceed in a complementary fashion to that of phenylpropyne. A formal Diels-Alder occurs across the cyclic allene and the adjacent arene ring to give cycloadduct **286** with styrene while the reaction with phenylpropyne provided the [2+2] cycloadduct **287**. The reaction of phenylpropyne is further contrasted by the previously discussed intramolecular trapping of cyclic allene **266** with a pendant alkyne, which gave the formal-ene product **268** (Scheme 4.2).

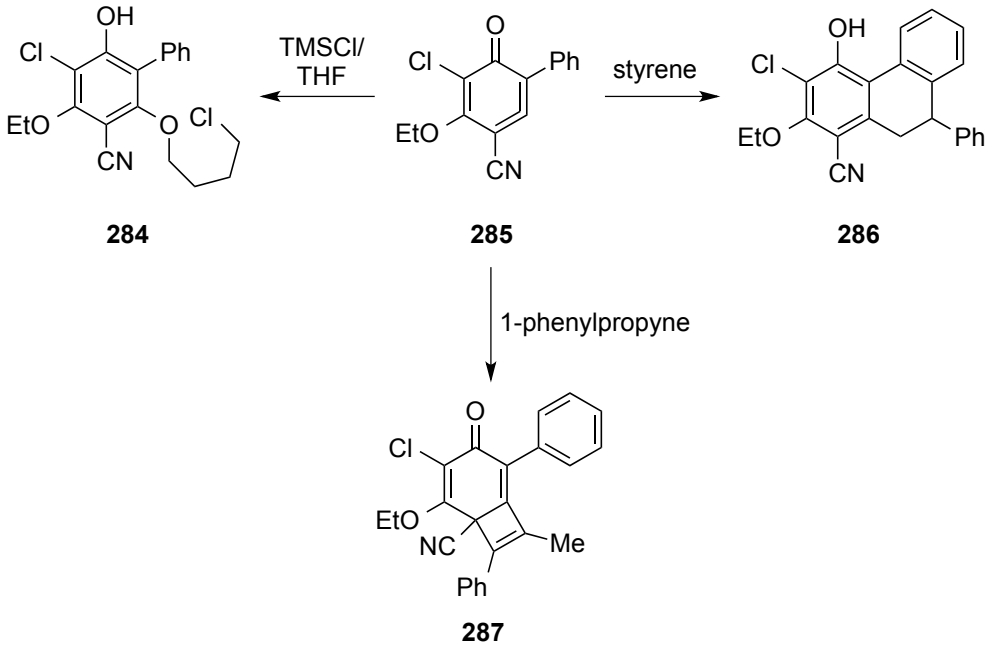

Scheme 1.64 – Interesting intermolecular trapping of the Moore cyclization's cyclic allene intermediates.

1.4.8 Cyclic Allenes from 1,2-Hydride Migration of Carbenes

The generation of an enantiomerically enriched version of cyclic allene **53** by Balci and Jones was discussed previously (Scheme 1.14).[48] The same cyclic allene has been generated via a number of different methods including the pyrolysis of tosylhydrazone derivative **289**[117] and the reaction of norbornadiene (**293**) with carbon suboxide reported by Klumpp and van Dijk (Scheme 1.65).[118] When salt **290** was pyrolyzed or photolyzed variable yields of a number of C-H insertion products of the proposed intermediate carbene **292** were obtained in addition to alkyne substituted bicyclic structure **54 (**Scheme 1.65). This structure was first observed by Bergman when they treated vinylbromide **52** with strong base.[49] It was originally proposed to be the doubly homoaromatic carbene **291** but the more recent investigation from Balci and Jones suggests the identity of the intermediate to be a cyclic allene **53**.[48]

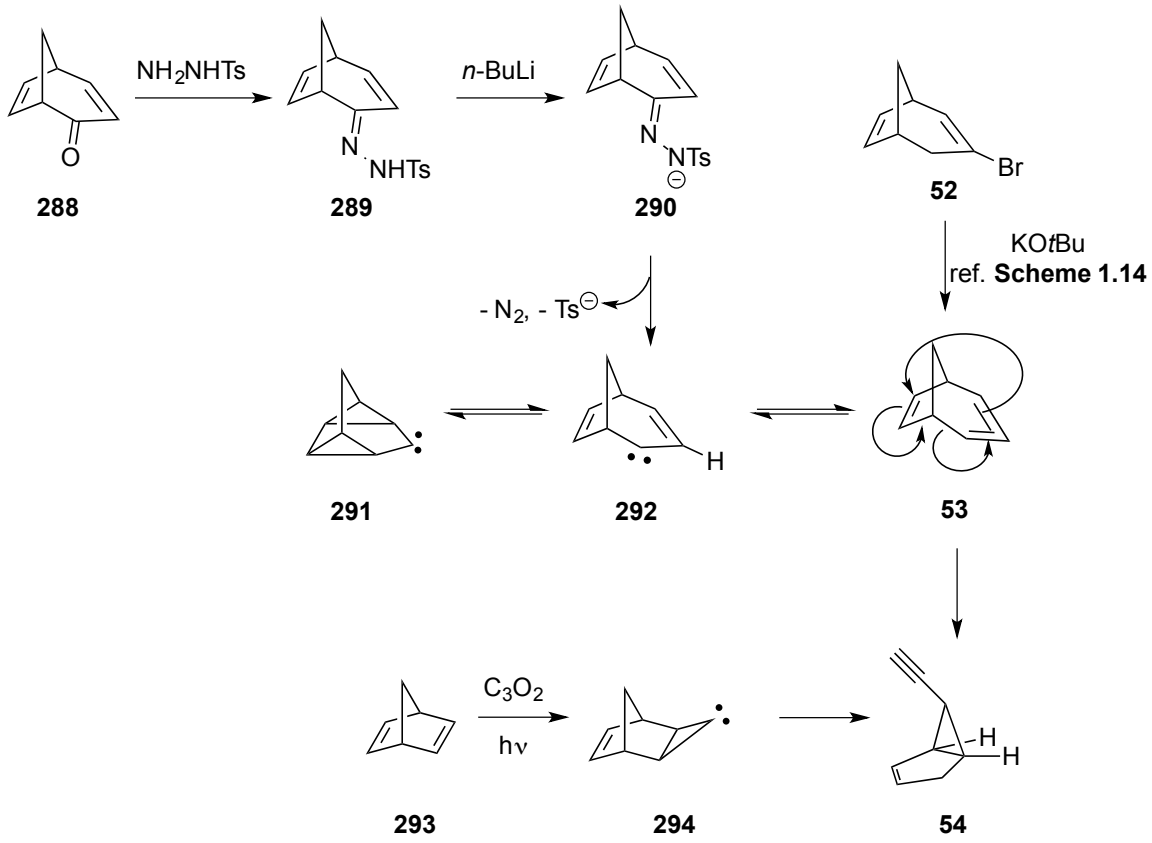

Scheme 1.65 – Generation of cyclic allene 53 by various methods.

The limitation of the carbene insertion method is the greater propensity of the insertion to occur at more readily available carbon-hydrogen bonds on less sterically encumbered and less conformationally constrained molecules. In the case of the tosylhydrazone **295**, when treated with methyl lithium the only product obtained was that of deuterated-1,3-cyclohexadiene **296** (Scheme 1.66).[119]

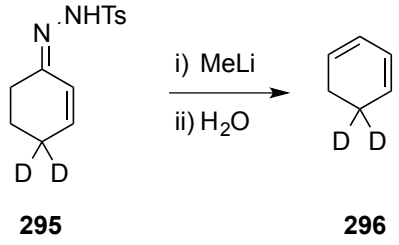

Scheme 1.66 - Decomposition of simple α,β-unsubstituted tosyl hydrazone.

1.5 Transition Metal-Mediated Transformations

Stabilization of reactive species through coordination to transition metals requires understanding the electronic demand of the system at hand.[120] For example in the case of an electron-deficient cyclic allene an electron-rich, low-valent metal systems capable of donating electron density should bond tightly to one of the olefins of the allene to alleviate the strain of the cyclic allene. Electron donation to the allene allows rehybridization of the carbons, relieving some of the strain of the reactive functional group, and enabling persistence of the intermediate in order to do further reactions.

The chemistry of coordinated cyclic alkynes is based upon the initial observations of Sonogashira and coworkers whereby heating diphenyl titanocene (**297**) in the presence of diphenylacetylene gave benzotitanocyclopentene **299** (Scheme 1.67).[121] Work from Vol'pin and Boekel later strongly suggested that stabilized benzyne intermediate **300** was being formed.[122-124]

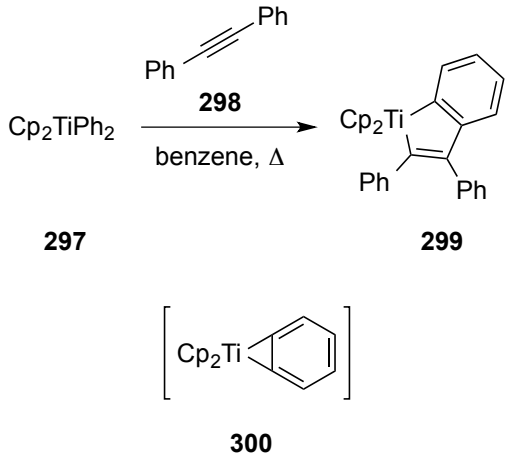

Scheme 1.67 - Formation of benzene-fused titanocyclopropane and reactivity.

Later, Buchwald developed generalized methods for the synthesis of coordinated cyclohexynes from readily available 1-chlorocyclohexene (**87**) (Scheme 1.68).[125] This was instrumental in the discovery of a large amount of olefin/alkyne addition chemistry known previously using coordinated benzyne as well as electrophilic quenching chemistry.[126] From the lithium-halogen exchange with **87**, transmetallation to zirconium, and elimination of methane formed zirconocyclopropene **302**. This reagent could be used *in situ* and reacted with a number of unsaturated compounds expanding the metallocycle,

or upon the addition of trimethylphosphine formed the thermally stable metal complex **304**.

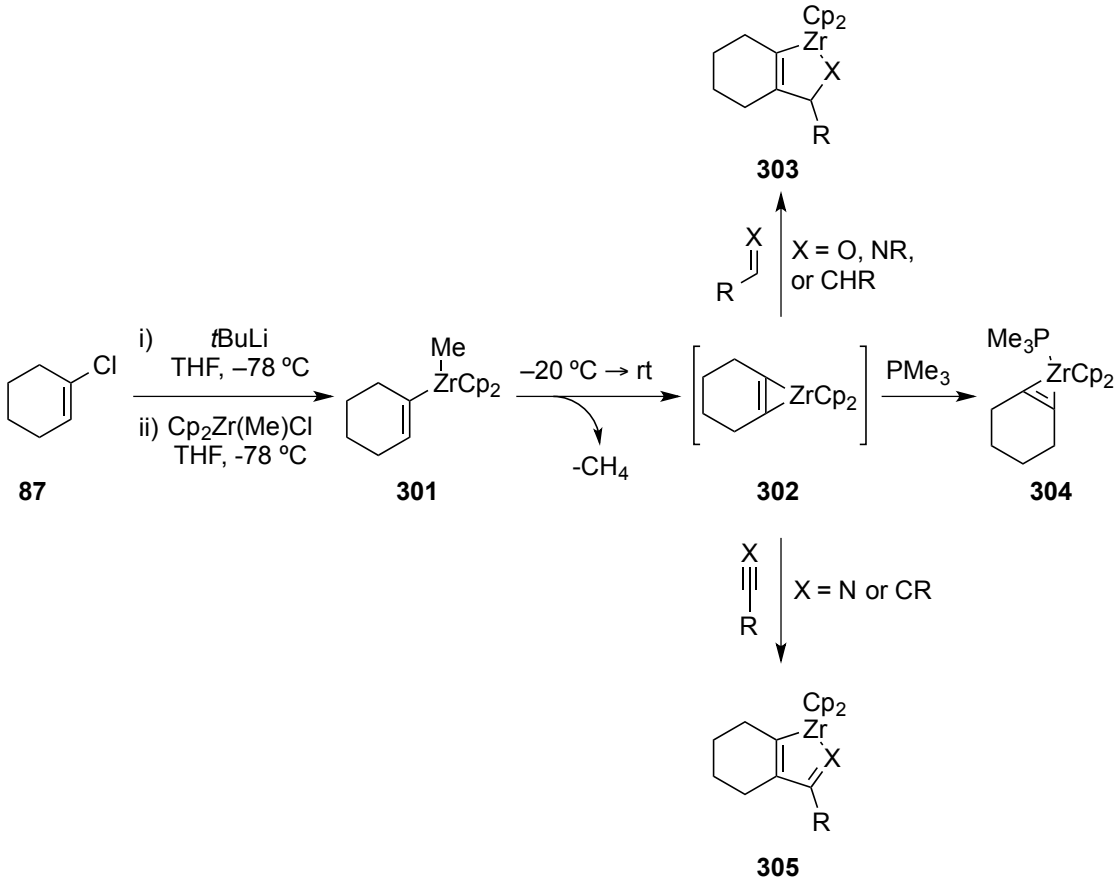

Scheme 1.68 - Zirconium stabilized cyclic alkynes as demonstrated by Buchwald.

It was from the observations of Buchwald and coworkers that Jones and coworkers were able to synthesize the first transition metal-stabilized 1,2-cyclohexadiene complex (**308**).[127] Similar to Buchwald's synthesis of cyclic alkyne complexes, dialkylzirconocene **306** was synthesized and, in the presence of trimethylphosphine, one equivalent of methylcyclohexene **307** was expelled leaving coordinated cyclic allene **308** (Scheme 1.69). Coordinated allene **308** underwent ring expansion to metallopentacycles such as **309** in the presence of activated olefins that could be demetalated under mildly acidic conditions (**310**).

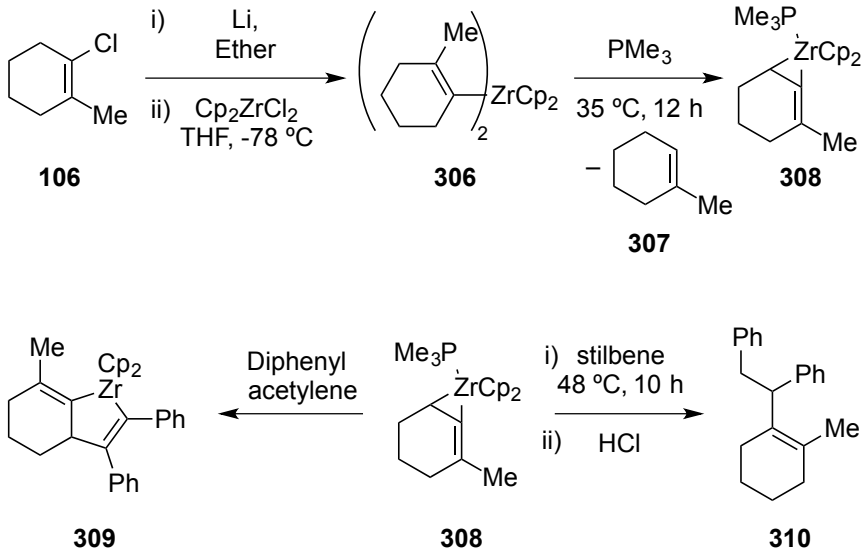

Scheme 1.69 - Zirconium-mediated cyclic allene generation and reactivity.

The same method was further applied to the generation of 4-phenyl-1,2,3-cyclohexatriene **312** (Scheme 1.70).[128] It is important to note the need for a blocking group on the adjacent olefin position, or cyclohexyne complexes **315/316** form preferentially. The crystal data and reactivity suggest that complexes **308/312** should be viewed similarly to an alkylidene metallocyclopropane, with strain promoted migratory insertions being the main reaction pathway.

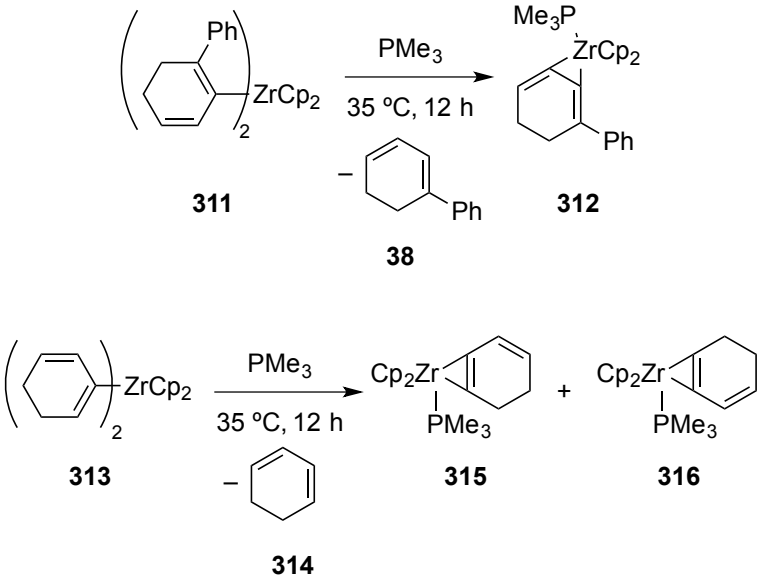

Scheme 1.70 - Phenyl-isobenzene zirconium-coordinated cyclic allene and isobenzene zirconium-coordinated cyclic alkyne.

More recently, Peña and coworkers reported that catalytic quantities of palladium could be used to harness the reactivity of 1,2-cyclohexadiene.[88] In the presence of cesium fluoride and excess dimethylacetylenedicarboxylate (**317**) the (2+2+2) cyclization took place to give tetrasubsituted-tetrahydronaphthalene **318** (Scheme 1.71). The major isolated allene:alkyne adduct **319** is likely derived from a base mediated isomerization/aromatization that captures excess DMAD in solution from anion **321**. Surprisingly, the palladium catalyst operated in the fluoride-containing medium although the yield of the cycloadducts was low.

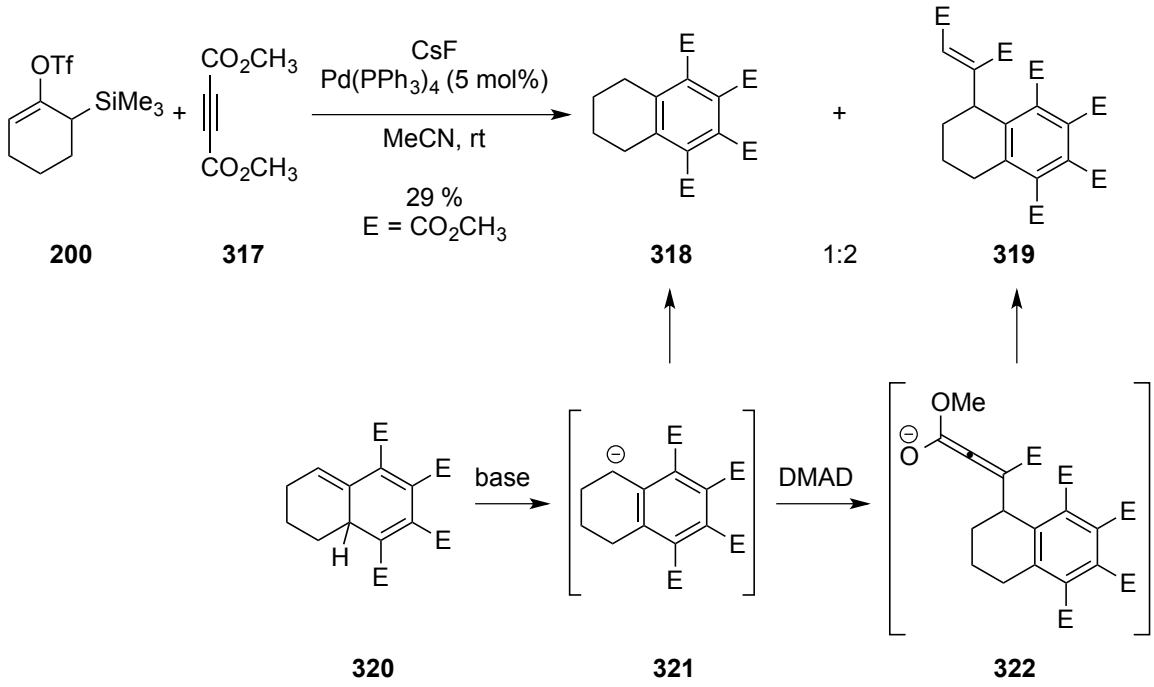

Scheme 1.71 - Palladium-catalyzed cyclotrimerization of alkynes with 1,2-cyclohexadiene.

1.6 Conclusions and Thesis Objective

The generation and trapping of cyclic allenes has been investigated for a substantial period owing to their high reactivity and the ability to make strained polycyclic organic frameworks via novel mechanisms. Several methods have been developed to generate cyclic allene intermediates efficiently under a variety of complementary reaction conditions. While the trapping of the intermediates has provided important evidence for the chiral nature of cyclic allene intermediates and diverse mechanisms detailing the generation and capture of cyclic allenes, little has been reported

on investigation of the synthetic utility of the intermediates. The field of cyclic allene generation and trapping modalities is due for a revolution.

In the context of 1,2-cyclohexadiene research, three objectives were outlined. A mild method to generating cyclic allenes was sought, keeping in mind the functional group tolerance of the method as well as the ready and scalable synthesis of the starting precursors. With a reliable method to generating cyclic allenes *in situ*, further exploration of the reactivity of the intermediates with heteroatom containing traps was proposed. Finally, the mechanism of these reactions would be further investigated using substituent effects and other methods.

In Chapter 2 a new method to the synthesis of cyclic allene precursors will be discussed that relies heavily upon copper-mediated nucleophilic silylation reactions. These allylic silanes were then used in subsequent fluoride-mediated elimination reactions to generate cyclic allenes *in situ*. Establishing their intermediacy, the trapping of these intermediates was demonstrated using 1,3-dipolar compounds to synthesize a variety of heterocyclic compounds. Chapter 3 will further explore the previously mentioned cycloadditions mechanistically, via the transference of enantiomeric excess from an enantiomerically enriched allylic silane to a cycloadduct via a chiral cyclic allene intermediate. Chapter 4 will outline our efforts toward the development of the first intramolecular capture of 1,2-cyclohexadiene. Finally, Chapter 5 will discuss efforts toward the synthesis of asphaltene model compounds, unrelated to the previous discussion on cyclic allenes.

1.7 References

(1) Allen, A. E.; MacMillan, D. W. C. *Chem. Sci.* **2012**, *3*, 633.

(2) Gillespie, R. J.; Nyholm, R. S. *Q. Rev., Chem. Soc.* **1957**, *11*, 339.

(3) Anslyn, E. V.; Dougherty, D. A. *Modern Physical Organic Chemistry.* University Science: Sausalito, CA, **2006**.

(4) Walsh, A. D. *Nature* **1947**, *159*, 712.

(5) Shea, K. J. *Tetrahedron* **1980**, *36*, 1683–1715.

(6) House, H. O.; Kleschick, W. A.; Zaiko, E. J. *J. Org. Chem.* **1978**, *43*, 3653–3661.

(7) Gampe, C. M.; Carreira, E. M. *Angew. Chemie. Int. Ed.* **2012**, *51*, 3766–3778.

(8) Gampe, C. M.; Boulos, S.; Carreira, E. M. *Angew. Chemie. Int. Ed.* **2010**, *49*, 4092–4095.

(9) Gampe, C. M.; Carreira, E. M. *Angew. Chemie. Int. Ed.* **2011**, *50*, 2962–2965.

(10) Kolb, H. C.; Finn, M. G.; Sharpless, K. B. *Angew. Chem. Int. Ed. Engl.* **2001**, *40*, 2004–2021.

(11) Huisgen, R. *Proc Chem. Soc.***1961**, 357–396.

(12) Huisgen, R. *Angew. Chem. Int. Ed. Engl.* **1963**, *2*, 565–598.

(13) Wittig, G.; Krebs, A. *Chem. Ber.* **1961**, *94*, 3260–3275.

(14) Baskin, J. M.; Prescher, J. A.; Laughlin, S. T.; Agard, N. J.; Chang, P. V.; Miller, I. A.; Lo, A.; Codelli, J. A.; Bertozzi, C. R. *Proc. Natl. Acad. Sci. U S A* **2007**, *104*, 16793–16797.

(15) Agard, N. J.; Prescher, J. A.; Bertozzi, C. R. *J. Am. Chem. Soc.* **2004**, *126*, 15046–15047.

(16) Hoffmann, R. W. *Dehydrobenzene and Cycloalkynes*; 1st ed.; Elsevier, 2012.

(17) Moss, R. A.; Platz, M. S.; Maitland Jones, J. *Reactive Intermediate Chemistry*; John Wiley & Sons, 2004.

(18) Wittig, G.; Fritze, P. *Angew. Chemie. Int. Ed.* **1966**, *5*, 846.

(19) Wittig, G.; Mayer, U. *Chem. Ber.* **1963**, *96*, 342–348.

(20) Christl, M. Cyclic Allenes up to Seven-Membered Rings. In *Modern Allene Chemistry*, Vol. 1; Krause, N., Hashmi A. K. S., Ed.; Wiley-VCH: Weinheim, Germany, 2005; 243–357.

(21) Johnson, R. P. *Chem. Rev.* **1989**, *89*, 1111–1124.

(22) Balci, M.; Taskesenligil, Y. In *Advances in Strained and Interesting Organic Molecules*; Halton, B., Ed.; JAI Press: Stamford, Connecticut, 1999; Vol. 8, pp. 43–82.

(23) Angus, R. O., Jr; Schmidt, M. W.; Johnson, R. P. *J. Am. Chem. Soc.* **1985**, *107*, 532–537.

(24) Skraba, S. L.; Johnson, R. P. *J. Org. Chem.* **2012**, *77*, 11096–11100.

(25) Levek, T. J.; Kiefer, E. F. *J. Am. Chem. Soc.* **1976**, *98*, 1875–1879.

(26) Dowd, P. *J. Am. Chem. Soc.* **1966**, *88*, 2587–2589.

(27) Dowd, P.; Chang, W.; Paik, Y. H. *J. Am. Chem. Soc.* **1986**, *108*, 7416–7417.

(28) Bottini, A. T.; Cabral, L. J.; Dev, V. *Tetrahedron Lett.* **1977**, 615–618.

(29) Moore, W. R.; Moser, W. R. *J. Am. Chem. Soc.* **1970**, *92*, 5469–5474.

(30) Christl, M.; Schreck, M. *Chem. Ber.* **1987**, *120*, 915–920.

(31) Ceylan, M.; Budak, Y. *J. Chem. Res.* **2002**, *2002*, 416–419.

(32) Tolbert, L. M.; Islam, M. N.; Johnson, R. P.; Loiselle, P. M.; Shakespeare, W. C. *J. Am. Chem. Soc.* **1990**, *112*, 6416–6417.

(33) Christl, M.; Schreck, M.; Fischer, T.; Rudolph, M.; Moigno, D.; Fischer, H.; Deuerlein, S.; Stalke, D. *Chem. Eur. J.* **2009**, *15*, 11256–11265.

(34) Hoffmann, H. *Angew. Chem. Int. Ed. Engl.* **1969**, *8*, 556–577.

(35) Wittig, G.; Fritze, P. *Liebigs Ann. Chem.* **1968**, *711*, 82–87.

(36) Martin, J. G.; Hill, R. K. *Chem. Rev.* **1961**, *61*, 537–562.

(37) Williamson, K. L.; Hsu, Y.-F. L. *J. Am. Chem. Soc.* **1970**, *92*, 7385–7389.

(38) Kobuke, Y.; Sugimoto, T.; Furukawa, J.; Fueno, T. *J. Am. Chem. Soc.* **1972**, *94*, 3633–3635.

(39) Bottini, A. T.; Hilton, L. L.; Plott, J. *Tetrahedron* **1975**, *31*, 1997–2001.

(40) Balci, M.; Jones, W. M. *J. Am. Chem. Soc.* **1980**, *102*, 7607–7608.

(41) Schöneboom, J. C.; Groetsch, S.; Christl, M.; Engels, B. *Chem. Eur. J.* **2003**, *9*, 4641–4649.

(42) Engels, B.; Schöneboom, J. C.; Münster, A. F.; Groetsch, S.; Christl, M. *J. Am. Chem. Soc.* **2002**, *124*, 287–297.

(43) Nendel, M.; Tolbert, L. M.; Herring, L. E.; Islam, M. N.; Houk, K. N. *J. Org. Chem.* **1999**, *64*, 976–983.

(44) Schmidt, M. W.; Angus, R. O.; Johnson, R. P. *J. Am. Chem. Soc.* **1982**, *104*, 6838–6839.

(45) Daoust, K. J.; Hernandez, S. M.; Konrad, K. M.; Mackie, I. D.; Winstanley, J.; Johnson, R. P. *J. Org. Chem.* **2006**, *71*, 5708–5714.

(46) Burrell, R. C.; Daoust, K. J.; Bradley, A. Z.; DiRico, K. J.; Johnson, R. P. *J. Am. Chem. Soc.* **1996**, *118*, 4218–4219.

(47) Christl, M.; Fischer, H.; Arnone, M.; Engels, B. *Chem. Eur. J.* **2009**, *15*, 11266–11272.

(48) Balci, M.; Jones, W. M. *J. Am. Chem. Soc.* **1981**, *103*, 2874–2876.

(49) Bergman, R. G.; Rajadhyaksha, V. J. *J. Am. Chem. Soc.* **1970**, *92*, 2163–2164.

(50) Groetsch, S.; Spuziak, J.; Christl, M. *Tetrahedron* **2000**, *56*, 4163–4171.

(51) Miller, B.; Shi, X. *J. Am. Chem. Soc.* **2001**, *109*, 578–579.

(52) Christl, M.; Groetsch, S. *Eur. J. Org. Chem.* **2000**, 1871–1874.

(53) Wittig, G.; Harborth, G. *Chem. Ber.* **1944**, *77*, 306–314.

(54) Scardiglia, F.; Roberts, J. D. *Tetrahedron* **1957**, *1*, 343–344.

(55) Roberts, J. D. *J. Am. Chem. Soc.* **1960**, *82*, 4750–4751.

(56) Montgomery, L. K.; Scardiglia, F.; Roberts, J. D. *J. Am. Chem. Soc.* **1965**, *87*, 1917–1925.

(57) Montgomery, L. K.; Applegate, L. E. *J. Am. Chem. Soc.* **1967**, *89*, 2952–2960.

(58) Montgomery, L. K.; Clouse, A. O.; Crelier, A. M.; Applegate, L. E. *J. Am. Chem. Soc.* **1967**, *89*, 3453–3457.

(59) Bottini, A. T.; Corson, F. P.; Fitzgerald, R.; Frost, I. K. A. *Tetrahedron* **1972**, *28*, 4883–4904.

(60) Wittig, G. *Naturwissenschaften* **1942**, *30*, 696–703.

(61) Roberts, J. D.; Simmons, H. E., Jr.; Carlsmith, L. A.; Vaughan, C. W. *J. Am. Chem. Soc.* **1953**, *75*, 3290–3291.

(62) Caubère, P.; Brunet, J. J. *Tetrahedron Lett.* **1969**, *14,* 3323–3326.

(63) Caubère, P.; Brunet, J. J. *Tetrahedron* **1972**, *28*, 4835–4845.

(64) Caubère, P.; Brunet, J. J. *Tetrahedron* **1972**, *28*, 4847–4857.

(65) Brunet, J. J.; Fixari, B.; Caubère, P. *Tetrahedron* **1974**, *30*, 1237–1243.

(66) Fixari, B.; Brunet, J. J.; Caubère, P. *Tetrahedron* **1976**, *32*, 927–934.

(67) Doering, W. V. E.; Hoffman, A. K. *J. Am. Chem. Soc.* **1954**, *76*, 6162–6165.

(68) Skell, P. S.; Garner, A. Y. *J. Am. Chem. Soc.* **1956**, *78*, 5430–5433.

(69) Doering, W. V. E.; LaFlamme, P. M. *Tetrahedron* **1958**, *2*, 75–79.

(70) Moore, W. R.; Ward, H. R. *J. Org. Chem.* **1960**, *25*, 2073.

(71) Skattebol, L. *Tetrahedron Lett.* **1961**, *5*, 167–172.

(72) Skattebol, L.; Solomon, S. *Org. Synth.* **1969**, *49*, 35–38.

(73) Voukides, A. C.; Cahill, K. J.; Johnson, R. P. *J. Org. Chem.* **2013**, *78*, 11815–11823.

(74) Moore, W. R.; Moser, W. R. *J. Org. Chem.* **1970**, *35*, 908–912.

(75) Harnos, S.; Tivakornpannarai, S.; Waali, E. E. *Tetrahedron Lett.* **1986**, *27*, 3701–3704.

(76) Christl, M.; Braun, M.; Müller, G. *Angew. Chem. Int. Ed. Engl.* **1992**, *31*, 473–476.

(77) Squillacote, M. E.; Sheridan, R. S.; Chapman, O. L.; Anet, F. *J. Am. Chem. Soc.* **1979**, *101*, 3657–3659.

(78) Viehe, H. G.; Janousek, Z.; Merényi, R. *Substituent Effects in Radical Chemistry*; D. Reidel Publishing Company: Dordrecht, Holland, 1986.

(79) Christl, M.; Schreck, M. *Angew. Chem. Int. Ed. Engl.* **1987**, *26*, 449–451.

(80) Bottini, A. T.; Hilton, L. L. *Tetrahedron* **1975**, *31*, 2003–2004.

(81) Kostikov, R.; Molchanov, A.; Hopf, H. *Top. Curr. Chem.* **1990**, *155*, 41–73.

(82) Untch, K. G.; Martin, D. J.; Castellucci, N. T. *J. Org. Chem.* **1965**, *30*, 3572–3573.

(83) Fedoryński, M. *Chem. Rev.* **2003**, *103*, 1099–1132.

(84) Christl, M.; Braun, M.; Fischer, H.; Groetsch, S.; Müller, G.; Leusser, D.; Deuerlein, S.; Stalke, D.; Arnone, M.; Engels, B. *Eur. J. Org. Chem.* **2006**, 5045–5058.

(85) Algi, F.; Ozen, R.; Balci, M. *Tetrahedron Lett.* **2002**, *43*, 3129–3131.

(86) Boyden, F. M. Ph.D. Dissertation, University of the Pacific: Stockton, California, 1969.

(87) Shakespeare, W. C.; Johnson, R. P. *J. Am. Chem. Soc.* **1990**, *112*, 8578–8579.

(88) Quintana, I.; Peña, D.; Pérez, D.; Guitián, E. *Eur. J. Org. Chem.* **2009**, *2009*, 5519–5524.

(89) Dykstra, H. B. *J. Am. Chem. Soc.* **1934**, *56*, 1625–1628.

(90) Blomquist, A. T.; Marvel, C. S. *J. Am. Chem. Soc.* **1933**, *55*, 1655–1662.

(91) Butz, L. W.; Gaddis, A. M.; Butz, E. W.; Davis, R. E. *J. Org. Chem.* **1940**, *5*, 379–388.

(92) Butz, L. W.; Joshel, L. M. *J. Am. Chem. Soc.* **1941**, *63*, 3344–3347.

(93) Butz, L. W.; Joshel, L. M. *J. Am. Chem. Soc.* **1942**, *64*, 1311–1313.

(94) Nudenberg, W.; Butz, L. W. *J. Am. Chem. Soc.* **1943**, *65*, 2059–2060.

(95) Butz, L. W.; Gaddis, A. M.; Butz, E. W. *J. Am. Chem. Soc.* **1947**, *69*, 924–925.

(96) Joshel, L. M.; Butz, L. W.; Feldman, J. *J. Am. Chem. Soc.* **1941**, *63*, 3348–3349.

(97) Danheiser, R. L.; Gould, A. E.; Fernandez de la Pradilla, R.; Helgason, A. L. *J. Org. Chem.* **1994**, *59*, 5514–5515.

(98) Robinson, J. M.; Tlais, S. F.; Fong, J.; Danheiser, R. L. *Tetrahedron* **2011**, *67*, 9890–9898.

(99) Hayes, M. E.; Shinokubo, H.; Danheiser, R. L. *Org. Lett.* **2005**, *7*, 3917–3920.

(100) Werstiuk, N. H.; Roy, C. D.; Ma, J. *Can. J. Chem.* **1996**, *74*, 1903–1905.

(101) Hopf, H.; Musso, H. *Angew. Chem. Int. Ed. Engl.* **1969**, *8*, 680–680.

(102) Scott, L. T.; Hashemi, M. M.; Meyer, D. T.; Warren, H. B. *J. Am. Chem. Soc.* **1991**, *113*, 7082–7084.

(103) Rabideau, P. W.; Abdourazak, A. H.; Folsom, H. E.; Marcinow, Z.; Sygula, A.; Sygula, R. *J. Am. Chem. Soc.* **1994**, *116*, 7891–7892.

(104) Brown, R. F. C.; Harrington, K. J.; McMullen, G. L. *J. Chem. Soc., Chem. Commun.* **1974**, 123.

(105) Hopf, H.; Berger, H.; Zimmermann, G.; Nüchter, U.; Jones, P. G.; Dix, I. *Angew. Chem. Int. Ed. Engl.* **1997**, *36*, 1187–1190.

(106) Kitaguchi, H.; Ohkubo, K.; Ogo, S.; Fukuzumi, S. *J. Am. Chem. Soc.* **2005**, *127*, 6605–6609.

(107) Fernández-Zertuche, M.; Hernández-Lamoneda, R.; Ramírez-Solís, A. *J. Org. Chem.* **2000**, *65*, 5207–5211.

(108) Moore, H. W.; Decker, O. H. *Chem. Rev.* **1986**, *86*, 821–830.

(109) Chow, K.; Van, N. N.; Moore, H. W. *J. Org. Chem.* **1990**, *55*, 3876–3880.

(110) Perri, S. T.; Foland, L. D.; Decker, O. H.; Moore, H. W. *J. Org. Chem.* **1986**, *51*, 3067–3068.

(111) Karlsson, J. O.; Nguyen, N. V.; Foland, L. D.; Moore, H. W. *J. Am. Chem. Soc.* **1985**, *107*, 3392–3393.

(112) Fernandez, M.; Hernandez, R.; Ramirez, A.; Ordonez, M. *J. Mex. Chem. Soc.* **2002,** *46,* 136-139.

(113) Angus, R. O. J.; Johnson, R. P. *J. Org. Chem.* **1984**, *49*, 2880–2883.

(114) Moore, H. W.; Chow, K.; Nguyen, N. V. *J. Org. Chem.* **1987**, *52*, 2530–2537.

(115) Xiong, Y.; Xia, H.; Moore, H. W. *J. Org. Chem.* **1995**, *60*, 6460–6467.

(116) Xiong, Y.; Moore, H. W. *J. Org. Chem.* **1996**, *61*, 9168–9177.

(117) Freeman, P. K.; Swenson, K. E. *J. Org. Chem.* **1982**, *47*, 2033–2039.

(118) Klumpp, G. W.; van Dijk, P. M. *Recl. Trav. Chim. Pays B.* **1971**, *90*, 381–384.

(119) Wehage, H.; Heesing, A. *Chem. Ber.* **1992**, *125*, 209–215.

(120) Hartwig, J. F., Ed. *Organotransition Metal Chemistry*; Univ Science Books: Sausalito, CA., 2010.

(121) Masai, H.; Sonogashira, K.; Hagihara, N. *Bull. Chem. Soc. Jpn.* **1968**, *41*, 750–751.

(122) Kolomnikov, I. S.; Loveeva, T. S.; Gorbachevskaya, V. V.; Aleksandrov, G. G.; Struckhov, Y. T.; Vol'pin, M. E. *J. Chem. Soc. D* **1971**, 972.

(123) Boekel, C. P.; Teuben, J. H.; de Liefde Meijer, H. J. *J. Organomet. Chem.* **1975**, *102*, 161–165.

(124) Boekel, C. P.; Teuben, J. H.; de Liefde Meijer, H. J. *J. Organomet. Chem.* **1974**, *81*, 371–377.

(125) Buchwald, S. L.; Lum, R. T.; Dewan, J. C. *J. Am. Chem. Soc.* **1986**, *108*, 7441–7442.

(126) Buchwald, S. L.; Nielsen, R. B. *Chem. Rev.* **1988**, *88*, 1047–1058.

(127) Yin, J.; Abboud, K. A.; Jones, W. M. *J. Am. Chem. Soc.* **1993**, *115*, 3810–3811.

(128) Yin, J.; Jones, W. M. *Tetrahedron* **1995**, *51*, 4395–4406.

2. Intermolecular Trapping of Cyclic Allenes with 1,3-Dipolar Compounds

2.1. [3+2] Dipolar Cycloadditions

There is a long history of dipolar cycloadditions in organic chemistry, beginning with the reaction of ozone with alkenes, originally investigated by Schönbein over 150 years ago.[1] Since this time a range of 1,3-dipolar compounds, including but not limited to nitrones, nitrile oxides, azides, carbonyl ylides, nitrous oxide, and azomethine imines have been discovered and used in cycloadditions to generate heterocyclic compounds.[2] The isolation or *in situ* generation of charged and often unstable building blocks has hampered the use of dipolar cycloadditions in synthesis. The dipolar cycloadditions often display poor regio-, chemo-, and diastereoselectivity due to the high energy of the dipolar compounds used, though careful frontier molecular orbital analysis allows one to explain distribution of products observed in the reaction mixture.

2.2. 1,3-Dipolar Cycloadditions of Acyclic Allenes

With regard to acyclic allenes as dipolarophiles, a high number of regiochemical outcomes are possible when compared with simple olefins and alkynes as both cumulated double bonds are reactive toward cycloaddition. Depending upon the substitution of the allene, regioselectivity of the dipolar compound as well as the regioselectivity on the allene become important as shown in Figure 2.1. Regioselectivity with respect to which double bond of the allene undergoes a reaction will be referred to as site selectivity.

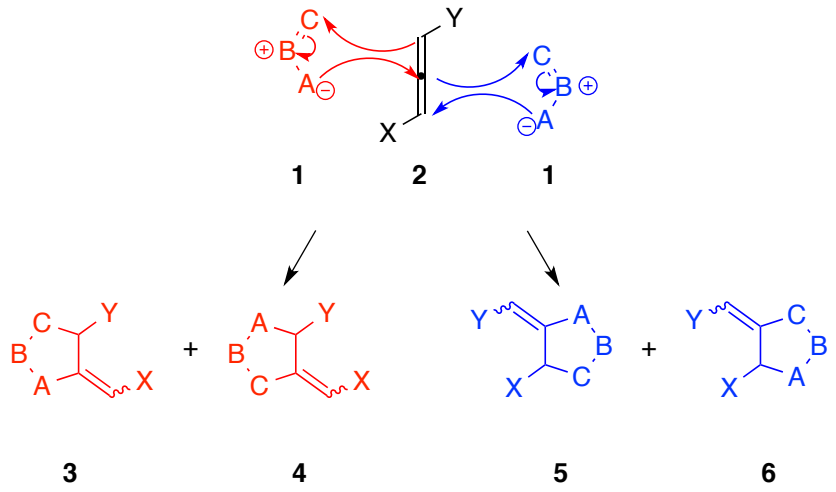

Figure 2.1 - Site- and regiochemical diversity associated with [3+2] dipolar cycloadditions of acyclic allenes.

Frontier molecular orbital theory is not useful for predicting (1,3)-dipolar/allene cycloaddition chemistry of non-substituted allenes. Non-polarized, acyclic allenes have two degenerate HOMOs and two degenerate LUMOs as shown in Figure 2.2. The molecular coefficients are almost identical for the terminus versus the central carbon; in terms of an orbital-controlled reaction, little regioselectivity is expected. The regiochemical outcome can be influenced by the degree of substitution on the allene, by electron-donating and electron-withdrawing groups, or by using an intramolecular reaction partner.

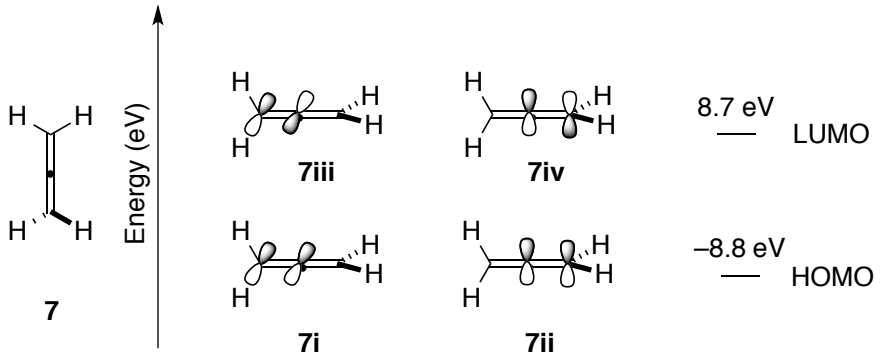

Figure 2.2 - Molecular orbital energies of 1,2-propanediene's HOMO and LUMO.

The reactivity of sulfone-substituted allenes has been well documented by Padwa and coworkers. The strong polarization the sulfone imparts to the allene controls both the

regio- and site selectivity.[3] CNDO calculations showed a significant lowering of the LUMO (3.7 eV) of the allene double bond conjugated with the sulfone as well as an increase in the size of the coefficient on the central carbon (Figure 2.3), manifested in greater control of the regiochemistry in the dipolar cycloadditions which are described later in Scheme 2.8 and Scheme 2.12.[4] The topic of allenes as dipolarophiles has been reviewed previously;[5] however, a selection of relevant examples is included below as an introduction to the cyclic allenes discussed in this chapter.

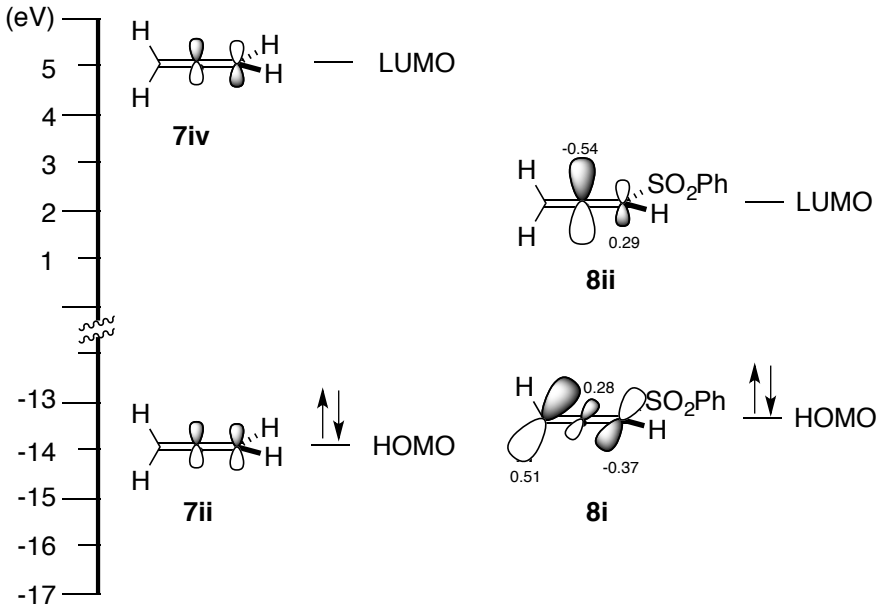

Figure 2.3 - Relative energy levels of perturbed allene with sulfone substituent.

2.2.1. Dipolar Cycloaddition of Allenes with Azides

Triazole synthesis has seen resurgence in the literature considering its application in bio-orthogonal labeling of cellular components.[6,7] The analogous alkylidene triazoline synthesis with allenes has lagged behind acetylenes. Buried within the paper discussing the reaction of diazo compounds with allenes is the first report of phenyl azide reacting with cyano-substituted allene by Ried and Mengler (Scheme 2.1).[8]

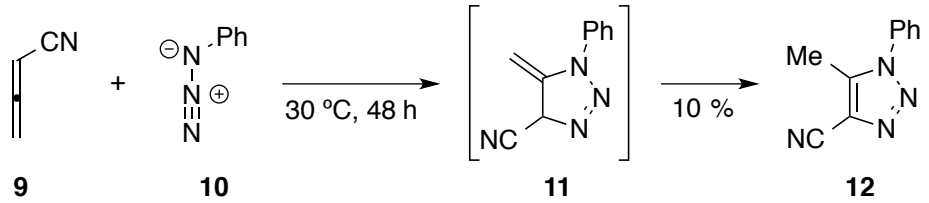

Scheme 2.1 - Reaction of 1-cyano-1,2-propandiene with phenylazide.

Electronically delocalized azides and allenes significantly decrease the need for harsh reaction conditions while simultaneously increasing the yield of the wanted cycloadducts. Bleiholder and Shechter further explored the reaction with electronically activated azides using symmetrical tetramethylallene and picryl azide (Scheme 2.2); alkylidene triazoline **15a** was isolated as a single regioisomer in 72 % yield.[9] In contrast, the reaction with phenyl azide proceeded considerably more slowly, requiring 4 days to consume the azide in excess boiling tetramethylpropadiene to yield **15b** in 29 % yield.

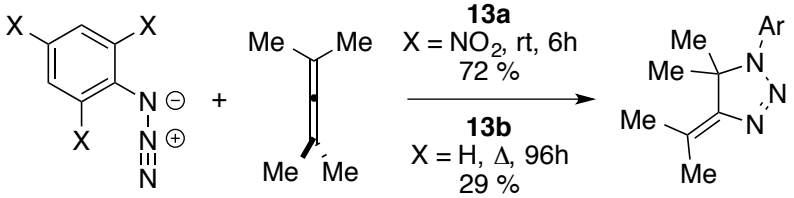

Scheme 2.2 - Reaction of aryl azides with symmetrical allenes.

Azides, as well as the azide/allene cycloadducts will decompose under the forcing reaction conditions used to facilitate the reaction. The reaction of ethyl azido formate with 2,4-dimethyl-2,3-propadiene resulted in the formation of two cycloadducts **17** and **18** (Scheme 2.3).[9] Alkylidene oxazoline **18** is not derived from alkylidene triazoline **17**: heating triazoline **17** does not produce any of the oxazoline. Oxazoline **18** is derived from the thermal decomposition of azide **16** to the corresponding nitrene and subsequent reaction of the nitrene with the allene. Tetramethylallene gives complicated mixtures in the cycloaddition with azides, partially due to the steric bulk around the allene.

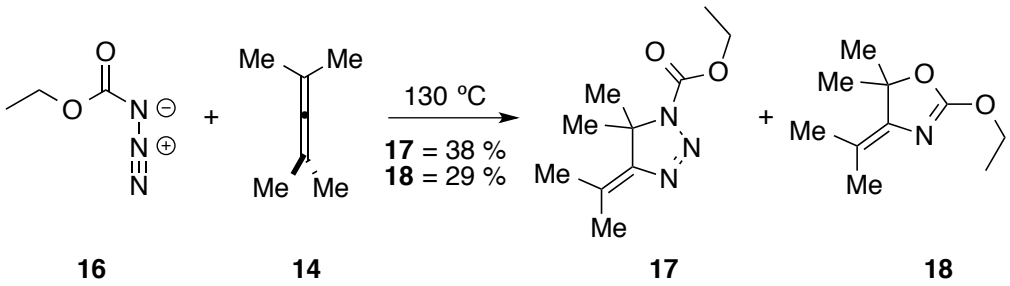

Scheme 2.3 - Thermally sensitive azides give mixtures of products with allenes in dipolar cycloadditions.

If instead the unsubstituted allene propadiene is used, the reaction of propadiene with phenyl azide in boiling benzene for over three weeks forms a mixture of two regioisomers derived from dipolar cycloaddition of the azide and allene dipolarophiles (Scheme 2.4).[10] Diamine cyclopropane **21** is also observed though in trace amounts. Diamine **21** is assumed to arise from a second cycloaddition with phenyl azide and subsequent decomposition, although the mechanism is not well understood.

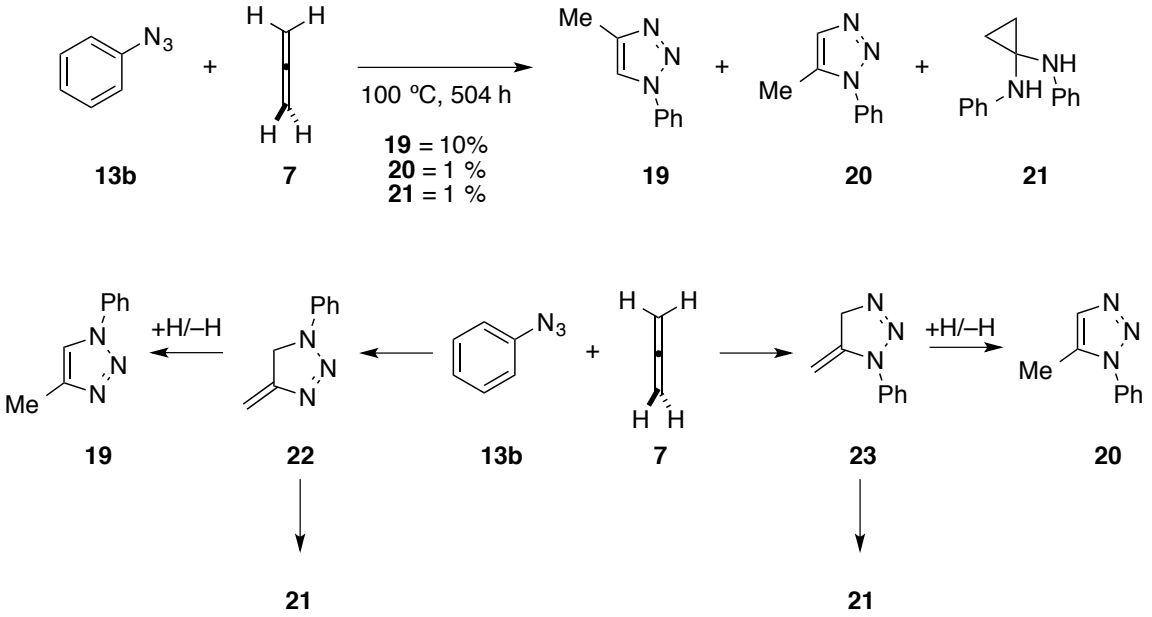

Scheme 2.4 - Reaction of phenyl azide with propadiene.

The analogous reaction with 1,2-cyclononadiene (**24**) in contrast gives a single regioisomer in 21 % yield (Scheme 2.5). To help elucidate the mechanism of the cycloaddition, optically enriched 1,2-cyclononadiene was used. The optically active triazoline isolated strongly suggests a concerted mechanism for the cycloaddition.

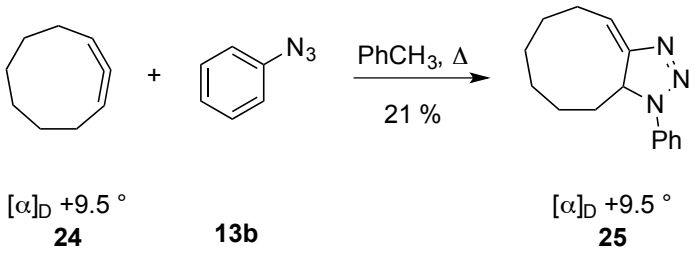

Scheme 2.5 - Reaction of phenyl azide with 1,2-cyclononadiene.

Recently, the Feldman group detailed the intramolecular cycloaddition of aliphatic azides with conjugated allenes.[11] The mechanism is proposed to involve formation of aza-trimethylene methane fragment **28** from spontaneous extrusion of nitrogen.[12] Radical recombination provides tricyclic imine **29** that was trapped with trimethylsilylcyanide, to furnish tricyclic product **31** in 50 % yield.

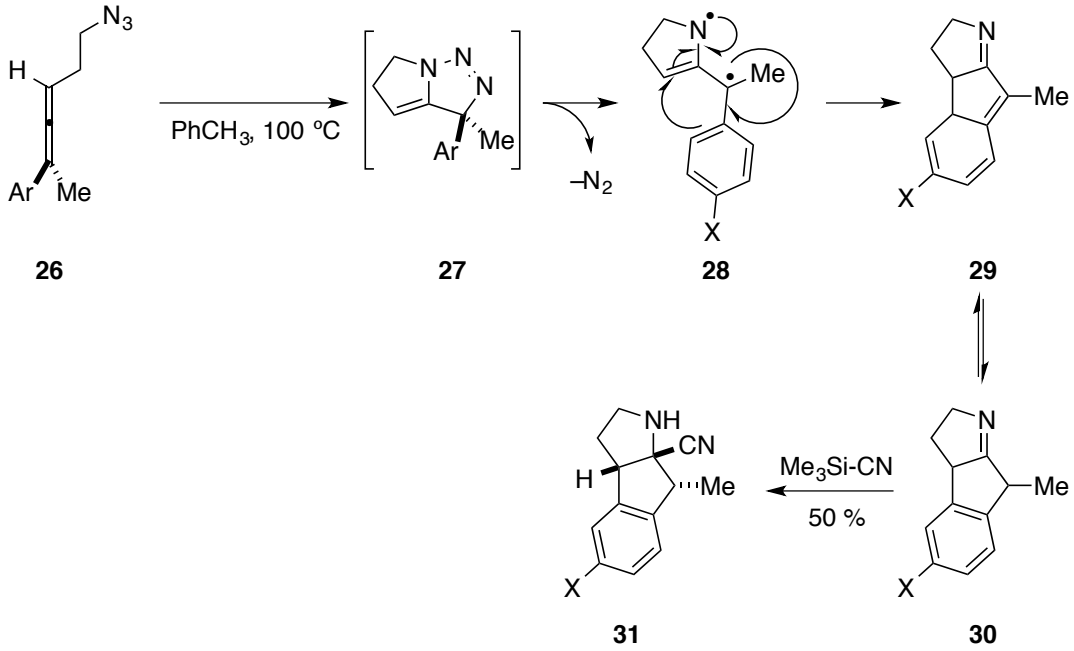

Scheme 2.6 - Intramolecular allene/azide dipolar cycloaddition.

Electron-deficient substituents on the *para* position of the aryl group showed a decreased yield of cycloadducts **31** when compared to neutral or electron-rich substituents. Diminished yields in these cases highlight the importance for a nucleophilic allene in this reaction. The Feldman group also found that the allene could be conjugated to an olefin to furnish bicyclic structures **33** (Scheme 2.7), though the same dependence on substitution was not observed.

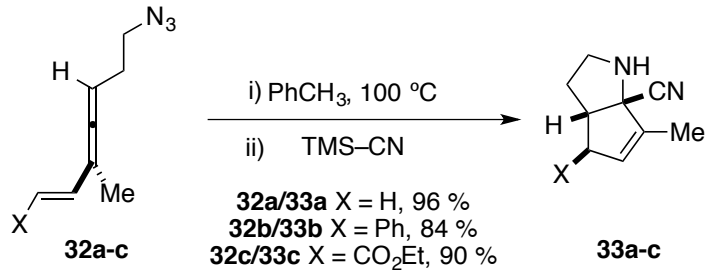

Scheme 2.7 - Intramolecular azide/allene cycloaddition with vinylic stabilizing group.

2.2.2. Cycloadditions of Allenes with Nitrile-Based 1,3-Dipolar Compounds

The reaction of allenes and azides has traditionally required harsh reaction conditions, significant stabilizing substitutents to promote the reaction, and suffered from poor yields and decomposition. This is not the case for other dipolarophiles such as nitrile oxides and nitrile imines, although they are isoelectronic with azides.

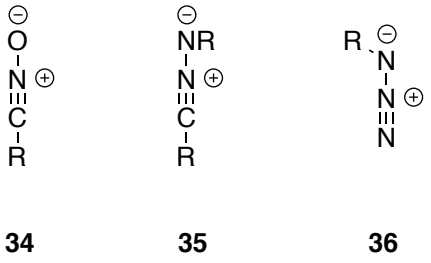

34 **35** **36**

Figure 2.4 - Nitrile oxides, nitrile imines, and azides.

As mentioned previously, substitution has profound effects on the allene's reactivity; the effects are best displayed by the difference in selectivity in the reaction with nitrile oxides as shown in Scheme 2.8. Padwa and coworkers observed a significant bias towards cycloadduct **38**,[13] rationalized by a [3+2] cycloaddition on the more reactive sulfonyl-conjugated bond followed by a (1,3)-sulfur shift, consistent with the FMO analysis done by Kanematsu.[4] In contrast, a related cycloaddition reported by Zecchi and coworkers showed little site selectivity with geminally substituted allene **41**.[14]

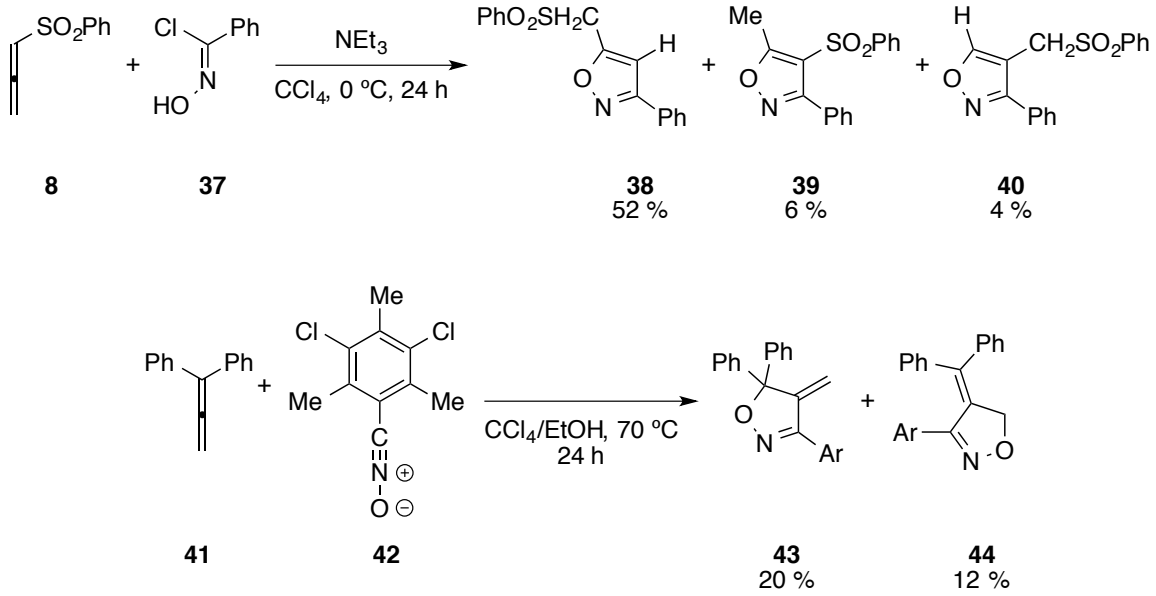

Scheme 2.8 - Padwa[13] and Zecchi[14] allene cycloadditions with nitrile oxides.

The isoelectronic nitrile imines fail to show any regiochemical differentiation with sulfone-substituted allenes. In the same manner as nitrile oxides, nitrile imines give two adducts with sulfonyl allene **45** (Scheme 2.9), though in a nearly 1:1 ratio.[15] Cycloadduct **49** could arise from a Mislow-Evans-like rearrangement of cycloadduct **50** followed by hydrolysis (Scheme 2.9). A similar rearrangement first being reported independently by Braverman[16] and Stirling[17].

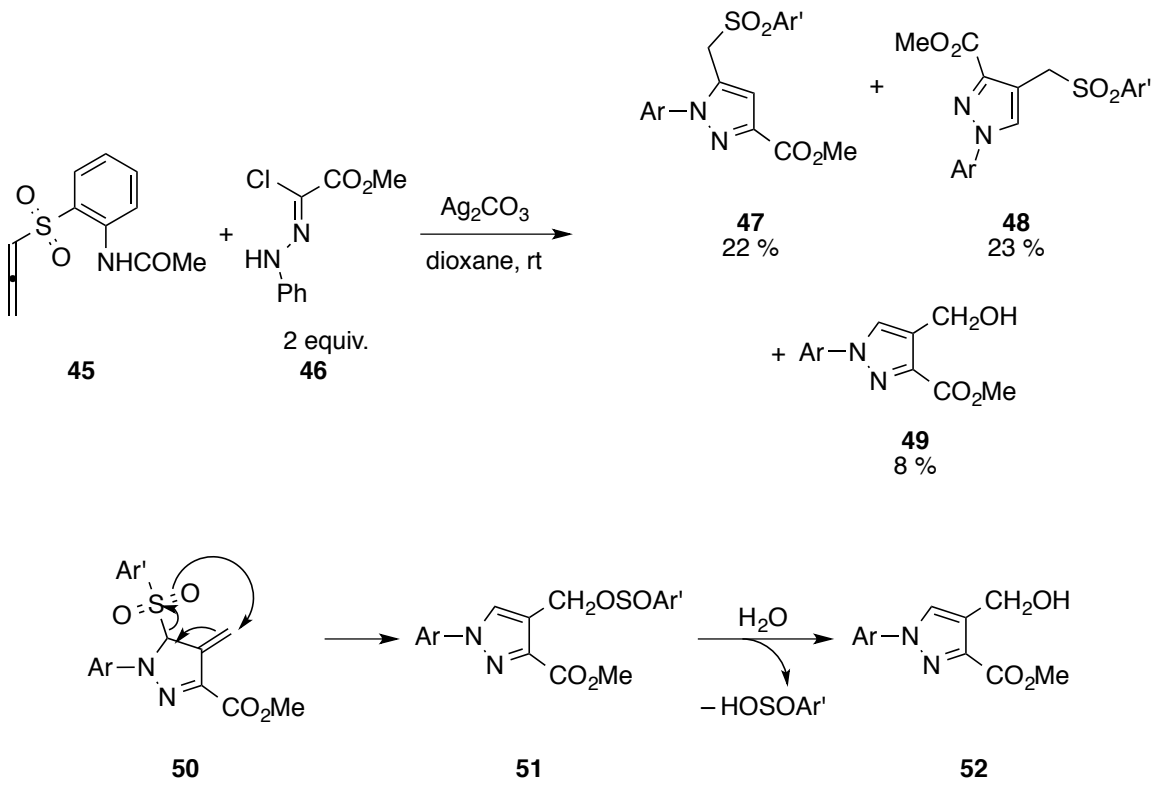

Scheme 2.9 - Sulfonyl-allene cycloaddition with nitrile imines and hydrolysis product.

2.2.3. Dipolar Cycloadditions of Allenes with Nitrones

Changing the bond order between the central nitrogen atom and the carbon terminus of the 1,3-dipole has a profound effect on the regio- and site selectivity of cycloadditions with allenes. Taylor reported that the reaction between perfluoropropadiene and *C*-phenyl-*N*-methylnitrone gave alkylidene isoxazolidine **55** in 71 % yield with exclusive regioselectivity for the C2(allene)-C(dipole) isomer (Scheme 2.10).[18] The HOMO of nitrones has a negligible difference on the coefficient size on oxygen and carbon, predicting a nearly equal mixture of cycloadduct regioisomers.[19,20] Depending upon the allene-substituents, if the LUMO of the nitrone is accessible, a much larger coefficient difference is calculated (Scheme 2.10), predicting a more selective reaction consistent with the observed regioselectivity.[20]

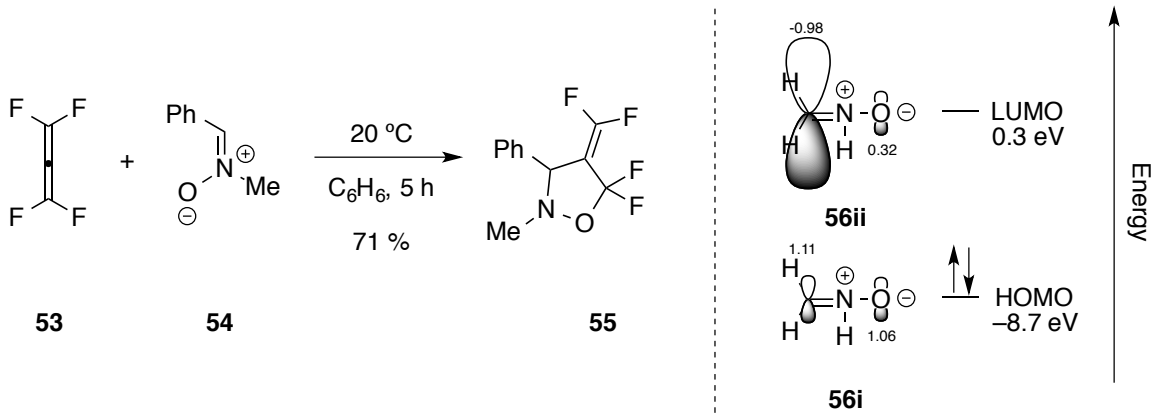

53 **54** **55** **56ii** **56i**

Scheme 2.10 – Reaction of perfluoropropadiene with *C*-phenyl-*N*-methyl nitrone and frontier molecular orbitals of generic nitrone.

Following the work on perfluoropropadiene, Dolbier and coworkers reported the analogous nitrone/allene cycloadditions with both 1,1-difluoropropadiene and 1-fluoropropadiene.[21-23] Both the difluoro and monofluoro allenes reacted with C-phenyl-N-methylnitrone to give cycloadducts with exclusively C2(allene)-C(dipole) regiochemistry as well as exclusive site-selectivity (Scheme 2.11). From the exceptional regio- and site selectivity the authors proposed the cycloadditions to be electrostatically controlled; the aversion of the fluorine substituents and the formally negatively charged oxygen are consistent with the high selectivity observed.[23]

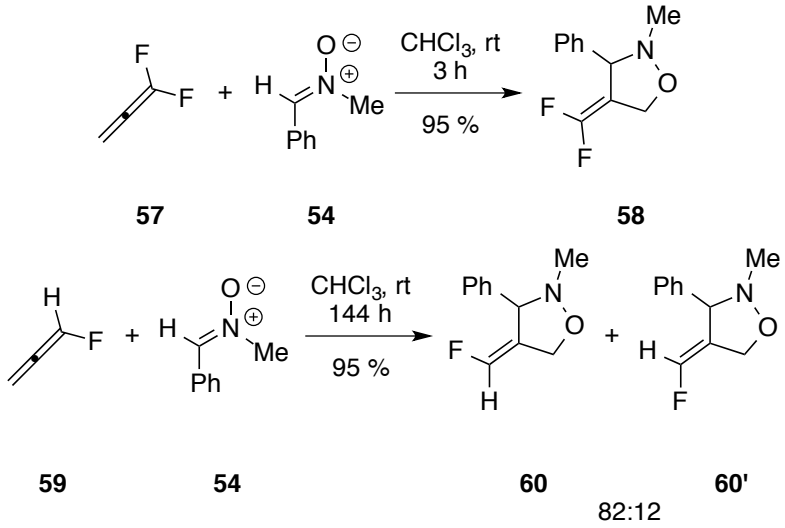

57 **54** **58**

59 **54** **60** **60'**

Scheme 2.11 - Nitrone/fluoroallene dipolar cycloadditions.

Padwa and coworkers also found high regioselectivity and site-selectivity with phenylsulfone substituted allenes, however reactions occurred across the conjugated double bond and the otherwise unreported C1(allene)-C(dipole) regioisomer was isolated.[3] 5-Alkylidene-isoxazolidine **61** formed exclusively using *C*-phenyl-*N*-methylnitrone in high yield and was tautomerized to isoxazoline **62** with simple heating.

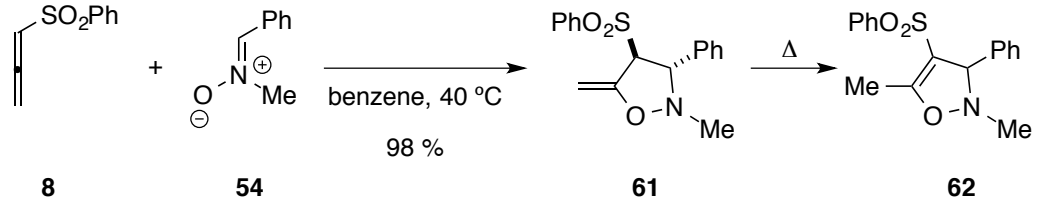

8 **54** **61** **62**

Scheme 2.12 - Reactivity of sulfone-substituted allenes with nitrones.

The same C1(allene)/C(dipole) regiochemistry was observed with a number of differently substituted nitrones and the authors suggest the high selectivity arose from an electrostatic interaction between the nitrone and allene reactants (orientating the dipoles of the two reactants *anti* to one another),[24] although the previous example by Dolbier showed the regio- and site selectivity can be explained by an allene/nitrone-LUMO/HOMO interaction using the frontier molecular orbitals predicted by Houk, and Hayakawa (Figure 2.5).[4,19]

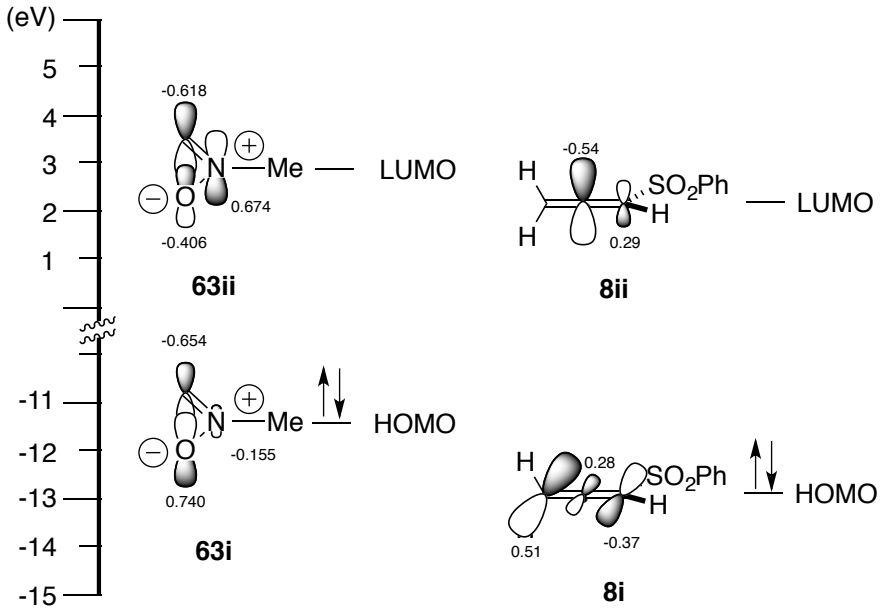

Figure 2.5 - Frontier molecular orbital analysis of nitrones and sulfone-substituted allenes.

Interestingly, the reaction of nitrone **54** with 1-methoxypropandiene resulted in the opposite regiochemistry as well as site-selectivity when compared to the similar cycloaddition with electron poor allenes (Scheme 2.13).[25] An elimination/addition mechanism accounts for the observed products via the isomerization of the kinetically formed cycloadduct, **66**.

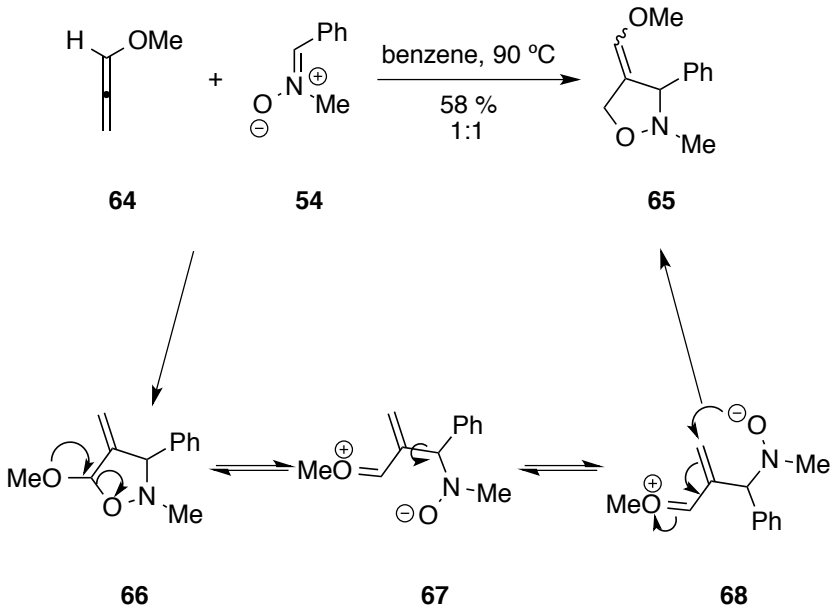

Scheme 2.13 - Formation of unpredicted methoxypropandiene/nitrone cycloadduct.

2.3. Background

The generation and trapping of cyclic allenes has led to interesting carbocyclic frameworks.[26-28] From the initial generation and capture study successfully carried out by Wittig and Fritze,[29] to the more recent findings of Christl, and Johnson, the involvement of cyclic allenes in pericyclic-like cycloadditions has been elaborated to include a variety of methods and trapping strategies.

Interestingly, literature concerning reactivity of cyclic allenes with 1,3-dipolar compounds is almost nonexistent. This is surprising as zwitterionic compounds have increased reactivity compared to the neutral traps previously employed which could allow the need for a large excess of the trapping molecule to be circumvented. The high reactivity of small carbocyclic allenes could allow interesting regio-, site, and diastereoselectivity.

2.3.1. Desilylative Methods to Generating Cyclic Allenes

Upon consideration of all the methods available for generating a cyclic allene (E2 elimination, Doering-Moore-Skattebøl reaction, Hopf electrocyclization, etc.) the fluoride-mediated desilylative elimination has a number of advantages. The elimination is promoted chemoselectively via the addition of fluoride anion and the elimination is reported to occur at room temperature or below (very mild temperatures). The method

was first introduced by Shakespeare and Johnson as an alternative to the base-mediated E2 elimination method.[30] Ready synthesis of the silylated precursors enabled efficient access to the precursors, **75** and **70**, for two previously unreported strained hexacarbocycles, in addition to the parent 1,2-cyclohexadiene.

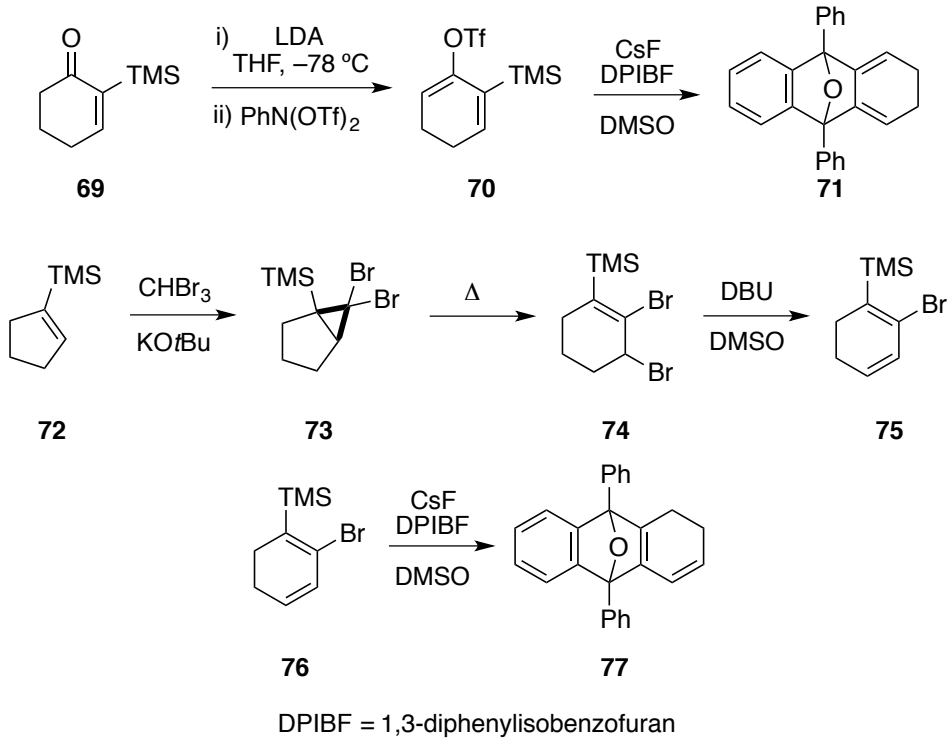

DPIBF = 1,3-diphenylisobenzofuran

Scheme 2.14 - Desilylative elimination method developed by Johnson and Shakespeare.

Following Johnson's success, Peña and coworkers applied a similar method to access 1,2-cyclohexadiene precursor **79a** and its 1-methyl derivative **79b** (Scheme 2.15).[31] By incorporating a triflate leaving group rather than a bromide, the group reported fast consumption of the starting material to generate known cycloadduct **80** in similar yield and diastereoselectivity to that reported originally by Wittig.[29,32]

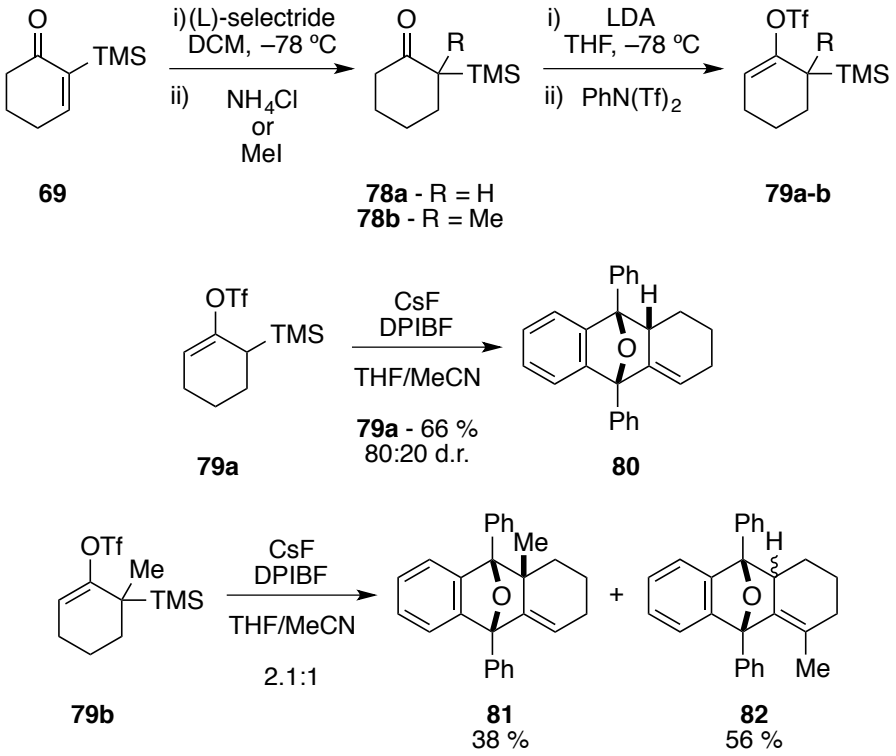

Scheme 2.15 - Peña and coworkers elaboration upon Johnson's desilylative method to allene generation.

The Peña group found that the mild desilylative reaction conditions for cyclic allene generation were compatible with the palladium-catalyzed cyclotrimerization of cyclic allenes with alkynes. In the presence of palladium tetrakis(triphenylphosphine) and dimethylacetylenedicarboxylate (DMAD), [2+2+2] cycloadduct **83** as well as cycloadduct **84** were obtained, although in poor yields (Scheme 2.16**)**.

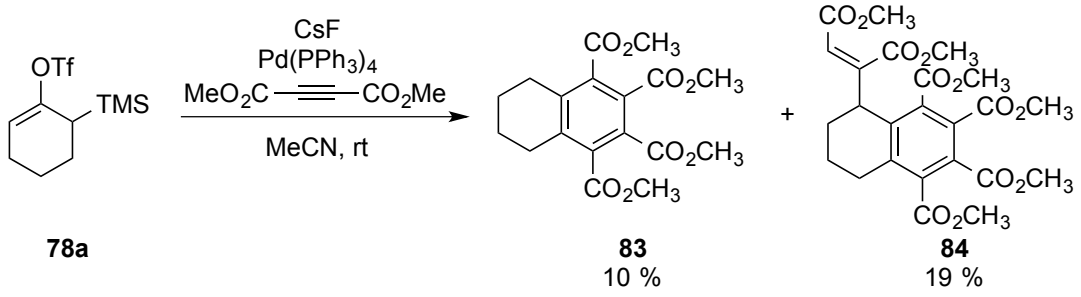

Scheme 2.16 - Reaction of 1,2-cyclohexadiene with DMAD in the presence of palladium catalyst.

The purpose of this chapter is to explore new reactivity of cyclic allenes, possibly with greater synthetic utility than that previously reported. Within this broad statement are a number of smaller goals we hoped to achieve. First the development of a method to generate cyclic allenes from readily available starting materials was required. The method to generate the cyclic allene should be operationally simple, tolerant to the presence of many different functional group, and applicable to trapping by a broad range of nucleophiles and electrophiles. Simultaneously the strategy by which the starting allene precursors are made should be operationally simple, high yielding, and able to access a broad range of substitution patterns and functionalized substrates.

Secondly, we wanted to discover new trapping processes of small carbocyclic allenes. The increased reactivity of 1,3-dipoles relative to the traps traditionally employed coupled with the ability to make new carbon-heteroatom bonds made 1,3-dipolar cycloadditions a seemingly tangible and desirable objective. As discussed in Section 2.2, the reaction of 1,3-dipoles with acyclic allenes has been plagued by low regio-, diastereo-, and site selectivity. By using the high-energy cyclic allenes in dipolar cycloadditions, not only can the reaction conditions be mild in comparison but also it may induce greater selectivity by polarizing the allene. The results of our investigation are discussed herein.

2.4. Results and Discussion

2.4.1. Copper-Mediated Nucleophilic Silane Addition

Upon inspection of the methods used by Johnson,[30] and Peña[31] to synthesize the needed precursors we were dismayed by the length, overall yield of the synthesis and reproducibility of the sequence. The lengthy introduction of the silyl group, in addition to the final introduction of the triflate-leaving group led to consideration of the opposite introduction of leaving group and silyl handle. The enone functionality of 2-bromo-2-cyclohexenone is consumed upon reduction with (L)-Selectride, and we hypothesized that the analogous conjugate addition of a silyl anion would enable expedient access to the desired cyclic allene precursors.

Inspired by the methods of Hanessian,[33] and Chorannat[34] we believed that the conjugate addition into the triflate derived from 1,2-cyclohexandione could be possible, contingent upon trapping the oxygen of the enolate to maintain the carbon-carbon double

bond. While *C*-alkylation is well precedented for copper-enolates, trapping of the oxygen occurs only with hard, polarized electrophiles.[35] Piers and coworkers reported the *in situ* protection of a cuprate enolate during the total synthesis of racemic seychellene.[36] The authors found, consistent with the results of Marshall,[37] *O*-acetylation of the copper enolate and isolation of enol acetate **86** using acetyl chloride.

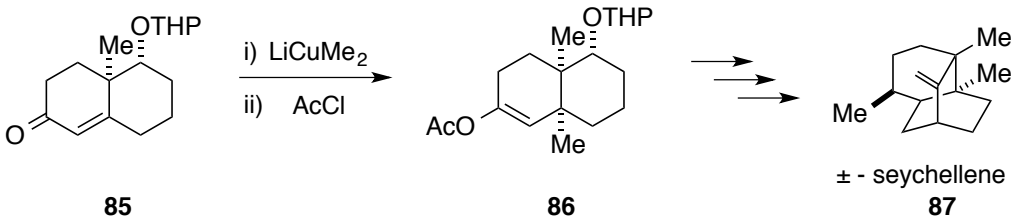

Scheme 2.17 - Enol acetate formation in the total synthesis of Seychellene.

We applied the method of Chorannat[34] and Piers[36] for the conjugate addition of silyl anion using copper bromide-dimethyl sulfide complex with an acetic anhydride quench to give acetoxy-substituted allene precursor (**90a**). This reaction proceeded in excellent yield from known enone-triflate **89** (Scheme 2.18).

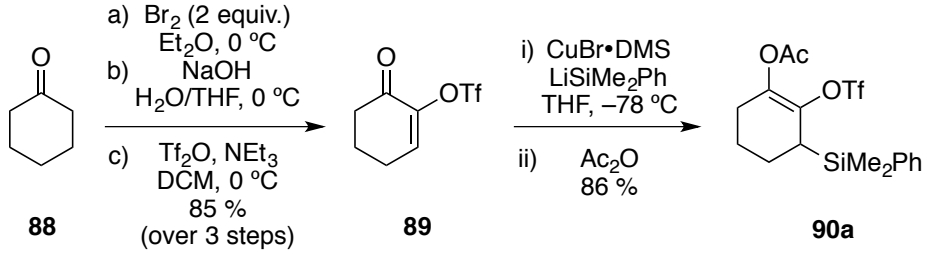

Scheme 2.18 - Synthesis of enol acetate-substituted allylic silanes.

A slightly longer sequence (Scheme 2.19) enables access to the parent 1,2-cyclohexadiene precursor, **90b**, via a 1,2-Luche reduction, tosylation, and finally copper-mediated allylic displacement. Tosylate **92** was used for the allylic displacement as the analogous allylic acetate showed no reactivity.

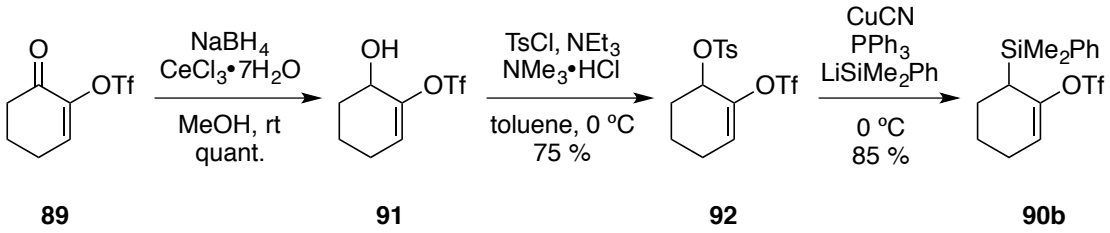

Scheme 2.19 - Synthesis of parent 1,2-cyclohexadiene precursor by allylic substitution.

Previous studies use the cycloaddition of furans with proposed cyclic allenes to establish the allene intermediacy under the reaction conditions employed.[28] Similar to the results of Peña and coworkers, when silyl triflate **90a** or **90b** is dissolved in furan and exposed to tetrabutylammonium fluoride (TBAF), furan/cyclic allene cycloadducts **93a/93b** formed in 33 % and 80 % yield respectively, as mixtures of *endo*/*exo* isomers (Scheme 2.20). Interestingly the major isomer characterized was from cycloaddition across the non-oxygenated carbon-carbon double bond, though from minor peaks in the ^{1}H NMR, formation of cycloadducts across the oxygenated carbon-carbon double bond cannot be completely refuted.

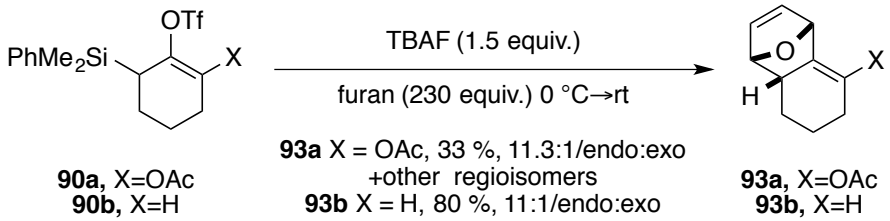

Scheme 2.20 - Furan/allene [4+2] cycloaddition.

2.4.2. Reaction of Cyclic Allenes with Nitrile Oxides

Having established a method for generating the needed allylic silanes **90a/90b** and having verified the intermediacy of 1,2-cyclohexadiene, the reaction of different dipolar compounds with cyclic allenes was then explored. We were driven to the investigation by the generation of new heterocyclic compounds and the reports that the use of cyclic alkynes greatly increase the rate of cycloaddition with nitrones[38] and azides.[6] The reaction of cyclic allene precursors **90a** and **90b** with mesityl nitrile oxide was performed. Mesityl nitrile oxide was chosen as the first 1,3-dipole partner due to it

bench-top stability and the absence of diastereomeric mixtures should cycloadducts be formed.

Exposure of a solution of nitrile oxide **94** and either allylic silane **90a** or **90b** to cesium fluoride resulted in the efficient capture of the cyclic allene generated by the nitrile oxide. In both cases 4-alkylidene-2-isoxazolines were isolated from the reaction mixture (**95a** and **95b** respectively). Only a single regioisomer was observed wherein C2 of the cyclic allene bonds to the carbon of the nitrile oxide, similar to the cycloadducts reported by Zecchi and coworkers (Scheme 2.8).[14] Unfortunately, the reaction did not tolerate the use of nitrile oxides generated *in situ*. When chlorinated oxime **96** was tested using reaction conditions comparable to those employed by Larock for nitrile oxide generation,[39] only the dimerization products could be observed (Scheme 2.21).

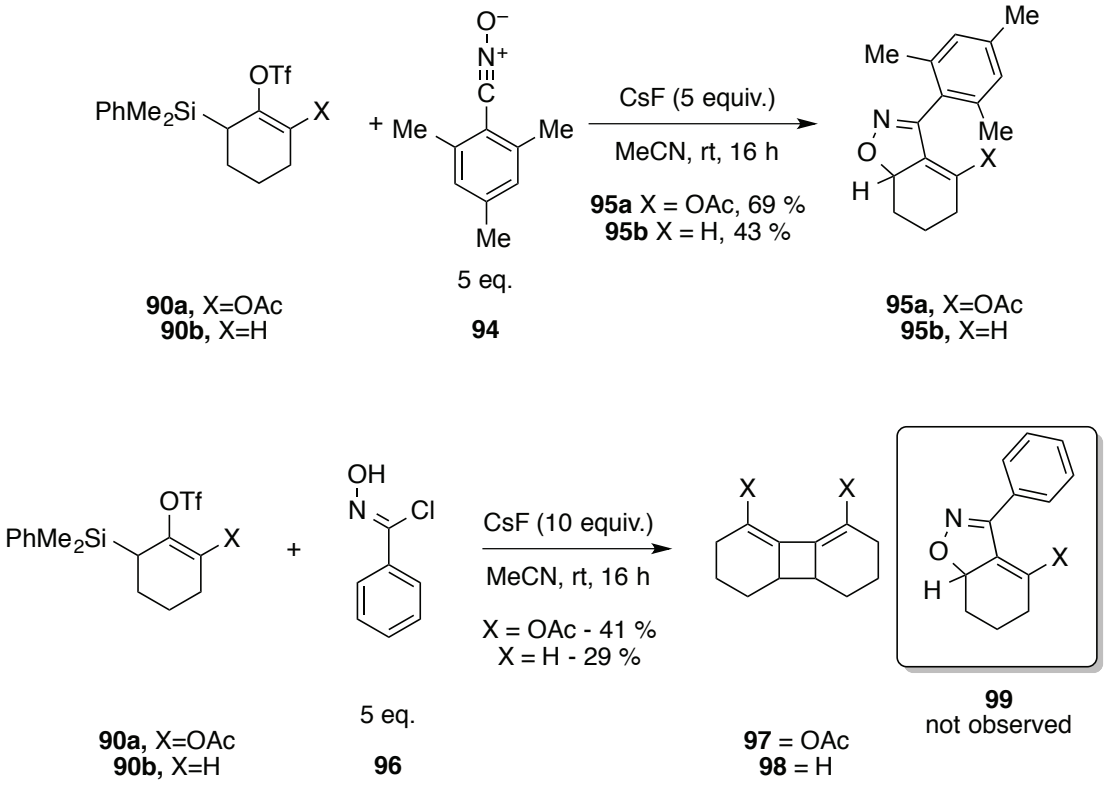

Scheme 2.21 - Reaction of cyclic allenes with nitrile oxides.

In order to rationalize the reactivity observed it is best to consider the perturbations of the FMO to the allene once constrained in a ring. Although the structure of cyclic allenes is a contentious subject, several experiments using chiral allenes,[26,40-42] as well as computational studies,[43-45] suggest the ground state of 1,2-cyclohexadiene is a

chiral, twisted allene. The barrier to inversion of a chiral 1,2-cyclohexadiene has been calculated to be ~14.2 kcal/mol.[46]

The calculated HOMO of 1,2-cyclohexadiene shows a larger coefficient on the central carbon relative to the two terminal carbons as calculated by Werstiuk *et. al.*.[47] This is consistent with the proposed mechanism of dimerization or trapping of cyclic allenes with activated olefins, whereby the central carbon reacts first in a stepwise cyclization reaction.

Substituents have a profound effect on the reactivity of cyclic allenes and the predicted HOMO and LUMO of the cyclic allene. Isobenzene cyclic allene **100** was shown to have greater orbital coefficients on the allene double bond conjugated with the endocyclic olefin, again with a larger coefficient on the central carbon relative to the coefficients on the terminal carbons (Figure 2.6).[45] The related pyran system calculated by Engels and Christl provides a similar result with an even larger coefficient on the central carbon, presumably due to the influence of the oxygen lone pair.[45] Indeed, a natural resonance theory (NRT) analysis suggests significant contribution of the canonical zwitterionic resonance structures **101^{I} – 101^{II}** to the ground state of cyclic allene **101**. The cyclic allene will have substantial dipolar content with a formal negative charge on the central carbon of the allene as shown by the contributing resonance structures in Figure 2.6.

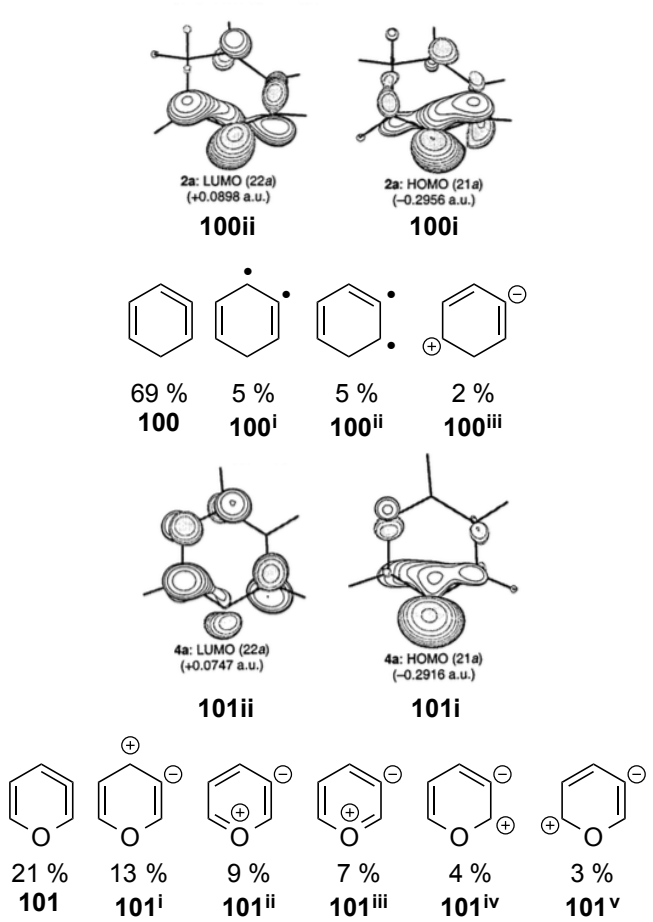

Figure 2.6 - HOMO/LUMO diagrams of substituted cyclic allenes and results of NRT analysis (Portions of Figure 2.6 adapted by the author from Engels *et. al. J. Am. Chem. Soc.* 2002, *124*, 287–297.

During the mechanistic investigation of the cycloaddition between furan and ester-conjugated cyclic allene precursor **102**, Houk and Tolbert proposed that the conjugated cyclic allene undergoes a stepwise, radical, formal Diels-Alder cyclization whereby bond formation first occurs at the central carbon of the allene.[48] The majority of the strain energy of cyclic allenes is derived from the hybridization and deformation of the bond angle of the central carbon of the cyclic allene. The formation of a bond at this center rehybridizes the carbon from sp to sp^2 and alleviates approximately 32 kcal/mol of strain energy.[44]

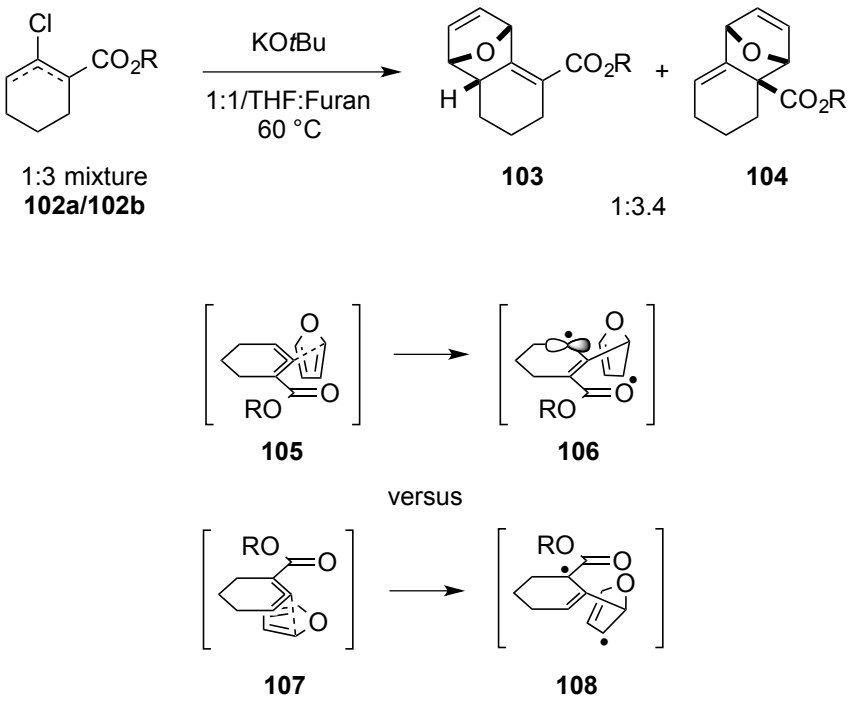

Scheme 2.22 - Step-wise radical mechanism for the formation of furan/allene cycloadducts 103 and 104.

From the work of Christl, similar to pyran cyclic allene **101,** the acetoxy-substituted cyclic allene should have a larger coefficient on C2 of the allene in the HOMO and nucleophilic character.[45] The unsubstituted 1,2-cyclohexadiene will have a large coefficient on C2 of the HOMO of the allene, but will not be as nucleophilic as the acetoxy-substituted allene as there is a weaker polarization of the electron density.

Nitrile oxides have carbon-based LUMO's,[19] and a HOMO(allene)/LUMO(dipole) interaction explains the observed regioselectivity and suggests an allene-nucleophilic attack on the dipolar trap (Figure 2.7). The partial negative charge on the central carbon of the allene will have an electrostatic attraction to the carbon of the nitrile oxide, consistent with the regioselectivity observed.

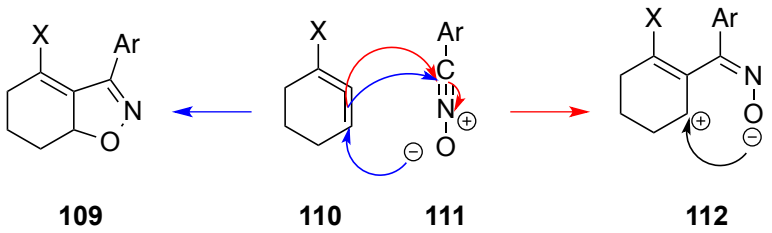

Figure 2.7 - Nucleophilic attack of cyclic allenes on nitrile oxides.

2.4.3. Reaction of Cyclic Allenes with Nitrones and Azomethine Imines

Nitrones are, in general, thermally stable, non-hygroscopic 1,3-dipolar compounds that produce isoxazolidines when used in cycloadditions with allene dipolarophiles. The reaction of 1,2-cyclohexadiene precursors **90a** and **90b** with nitrones yielded 4-alkylidene isoxazolidines in good yield (Table 2.1). Both aliphatic and conjugated nitrones gave the same regiochemistry observed with mesityl nitrile oxide (Scheme 2.21). Regrettably, the reaction of 1-acetoxy-1,2-cyclohexadiene with either geminally disubstituted nitrone **113c** or (*E*)-styryl substituted nitrones **113d** failed. Product **116a** was initially observed in poor yield however subsequent reproduction of the reaction failed repeatedly and only the dimer was observed. The increased reactivity of the acetoxy substituted cyclic allene intermediate (given the calculations of Christl and coworkers[45]) relative to the unsubstituted system is most likely responsible for the failed reaction.

Table 2.1 - Reaction of 1,2-cyclohexadienes with nitrones.

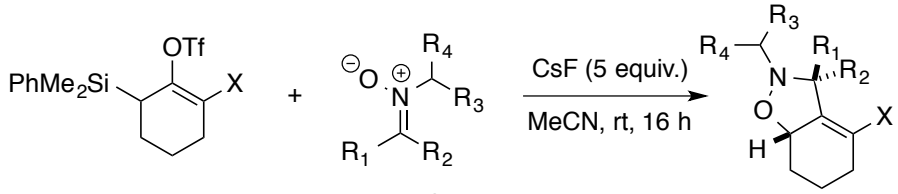

90a, X=OAc
90b, X=H

5 equiv.

113a-d

114-117

Nitrone	R^1	R^2	R^3	R^4	Compound	X	d.r.	Yield (%)[a]
113a	Ph	H	Ph	H	**114a**	OAc	>20:1	34
113a	Ph	H	Ph	H	**114b**	H	>20:1	62
113b	*i*Pr	H	*i*Pr	H	**115a**	OAc	>20:1	40
113b	*i*Pr	H	*i*Pr	H	**115b**	H	>20:1	54
113c	Me	Me	Me	Me	**116a**	OAc	NA	0
113c	Me	Me	Me	Me	**116b**	H	NA	58
113d	(*E*)-styryl	H	H	H	**117a**	OAc	0	0
113d	(*E*)-styryl	H	H	H	**117b**	H	2:1	42

[a] Products were isolated as a mixture. [b] Yields are of isolated compounds.

Encouraged by our results with nitrones we investigated the reaction with bench-stable azomethine imines with cyclic allenes. Dorn initially reported the synthesis of bench stable azomethine imines derived from the condensation of pyrazolidin-3-one with aldehydes in the 1960's.[49,50] Using a number of differently substituted pyrazolidin-3-one-derived azomethine imines the reaction with cyclic allene dipolarophiles proved efficient with good diastereoselectivity (Table 2.2). Similar to that observed with nitrones, the reaction with azomethine imines tolerated aliphatic, and conjugated azomethine imines, though a significantly large decrease in the diastereoselectivity was observed upon reacting the allenes with the (*E*)–styryl substituted azomethine imine **118d**.

Table 2.2 - Synthesis of pyrazolo[1,2-*a*]indazol-3-ones via dipolar cycloaddition with cyclic allenes.

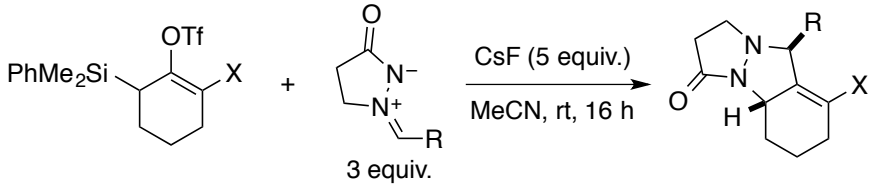

90a/90b **118a-d** **119-122**

Azomethine Imine	R	Compound	X	d.r.[a]	Yield (%)[b]
118a	Ph	**119a**	OAc	>20:1	44
118a	Ph	**119b**	H	>20:1	63
118b	*i*Pr	**120a**	OAc	>20:1	51
118b	*i*Pr	**120b**	H	11:1	46
118c	$(CH_2)_2Ph$	**121a**	OAc	>20:1	51
118c	$(CH_2)_2Ph$	**121b**	H	8:1	76
118d	(*E*)-styryl	**122a**	OAc	1:1	65
118d	(*E*)-styryl	**122b**	H	1:1	quant

[a] Products were isolated as a mixture. [b] Yields are of isolated compounds.

Fortuitously, the crystal structure of the cycloadduct of 1,2-cyclohexadiene and phenyl azomethine imine **118a** could be obtained and confirmed the relative stereochemistry as *anti,* as well as the C(2)allene/C(dipole) regiochemistry (Figure 2.8).

The stereochemistry of the major cycloadducts with nitrones **114 – 117**, and the cycloadducts with azomethine imines **119 – 122** was assigned using TROESY correlations as shown in Figure 2.9.

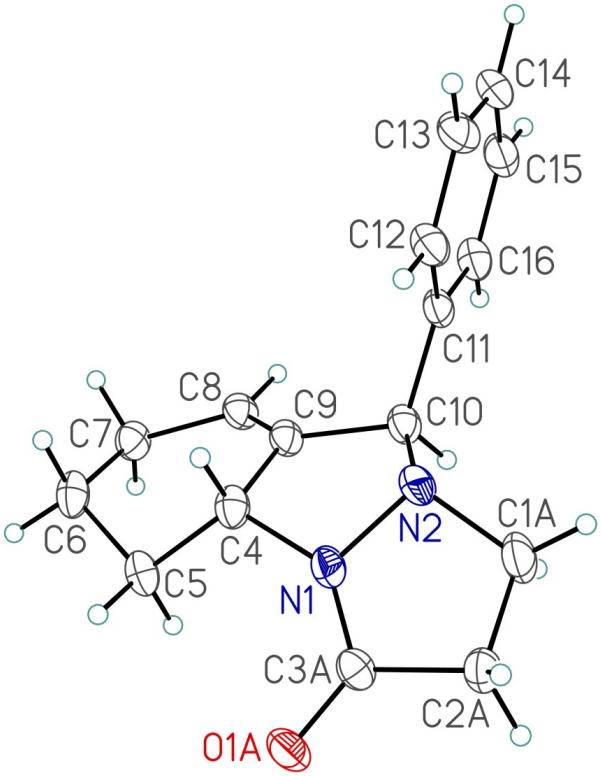

Figure 2.8 - Crystal structure of azomethine imine 1,2-cyclohexadiene cycloadduct 119b, Gaussian ellipsoids at 30% probability level. Hydrogen atoms are shown with arbitrarily small thermal parameters.

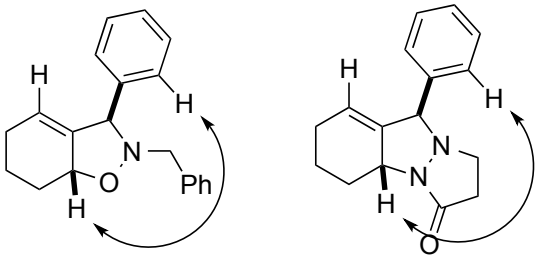

114b **119b**

Figure 2.9 - TROESY correlations strongly suggesting the relative stereochemistry of different [3+2] dipolar cycloadducts.

In addition to the electronic factors, there is also a steric bias to both the regiochemistry and the diastereoselectivity that is observed in the above cycloadditions. Very little crowding is expected from placement of the dipole C-terminus in proximity to the central sp-hybridized allene carbon. Furthermore, the constraints of the 6-membered ring force the non-hydrogen allene substituents away from the reacting centers (Figure 2.10). Using dipolar traps with known stereochemistry,[51,52] and assuming the pseudo-C_2 symmetric structure of a closed cyclic allene to be the correct ground state geometry, the transition state for the *anti* product would situate the carbon substituent away from the ring (***A*-124** and ***A*-124'**). The dipole substituent is on the opposite side of the 1,2-cyclohexadiene as the proton on the allene it is pointing toward, Figure 2.10.

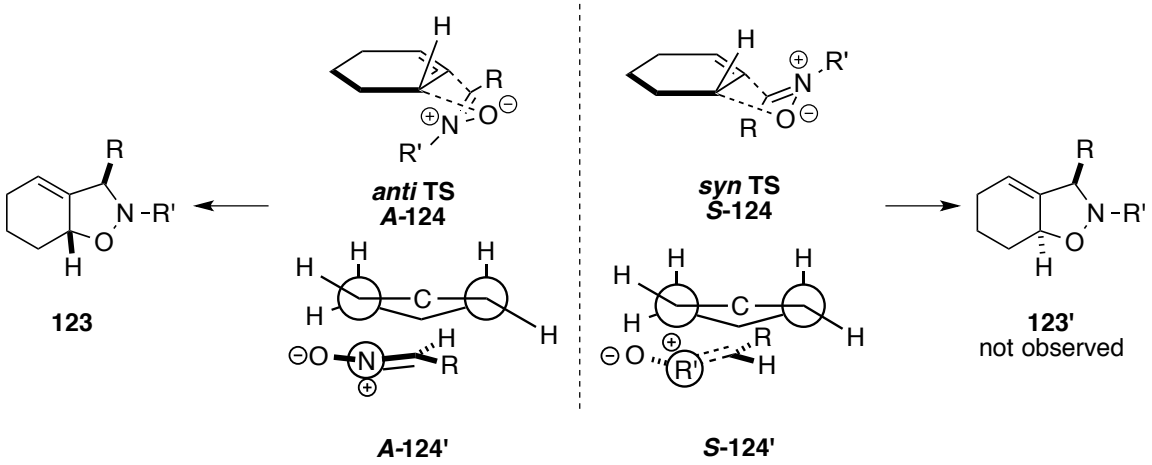

Figure 2.10 - *Anti* and *syn* transition states for the [3+2] dipolar cycloaddition of nitrones with cyclic allenes.

Unfortunately, the high selectivity is eliminated upon extension of the conjugation in the 1,3-dipole reactant. The (*E*)-styryl substituted azomethine imines and nitrones investigated gave approximately 1:1 and 2:1 diastereomeric ratios respectively (Scheme 2.23). This is a significant departure from the almost exclusive formation of the *anti* isomer when less conjugated (1,3)-dipoles are used. Reaction with 2-phenylethyl azomethine imine **118c** (Table 2.2) gave almost exclusively the *anti*-isomers further suggesting the change in selectivity can be attributed to conjugation rather than steric effects. The increased conjugation in the trap may perturb the mechanism from a concerted-asynchronous reaction to a stepwise cycloaddition, similar to the cycloaddition

with styrene.[53] However, conjugative stabilization of intermediates in an alternative stepwise process can only apply if C-N bond formation precedes C-C bond formation (i.e., **126** vs **125**, Scheme 2.23). This observation is further explored in Chapter 3 via the use of chiral precursors.

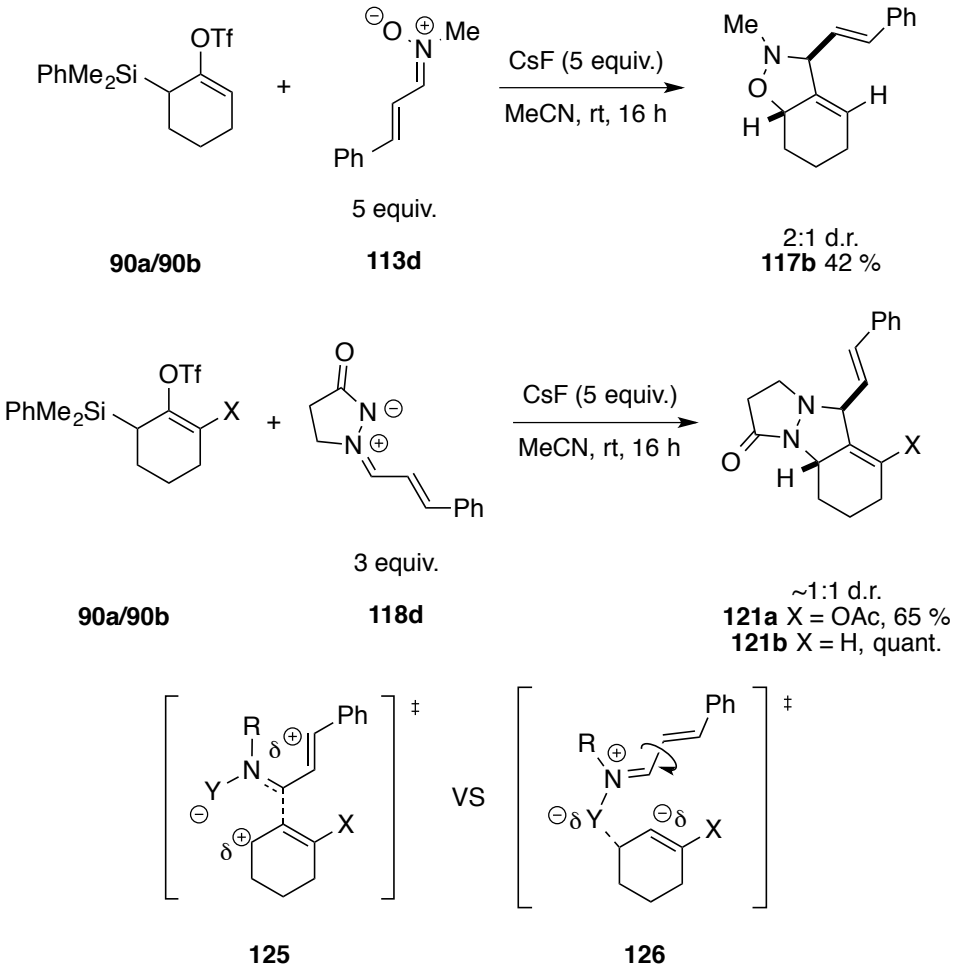

Scheme 2.23 – Loss of diastereoselectivity using (*E*)-styryl substituted traps.

2.4.4. Reaction of Cyclic Allenes with Azides

Organic azides were the final class of 1,3-dipolar compound investigated. Triazolines similar to that synthesized by Cristie[10] were not isolated from the reaction of *p*-nitrophenyl azide with 1,2-cyclohexadiene. Tricyclic aziridine **128** was formed in 52 % yield as shown in Table 2.3. One equivalent of azide reacts with two equivalents of cyclic allene though the reaction is anticipated to proceed through diradical aza-trimethylene methane intermediates similar to those proposed by Feldman (Scheme 2.6).[12] The reaction was limited to the use of electron-deficient azides. The use of *p*-

methylphenylazide led to complicated mixtures of products, none of which contained nitrogen. Use of acidic workup conditions led to the decomposition of aziridine **128** to the β-hydroxyamine **135**.

Table 2.3 - Conjugated azides reaction with 1,2-cyclohexadiene.

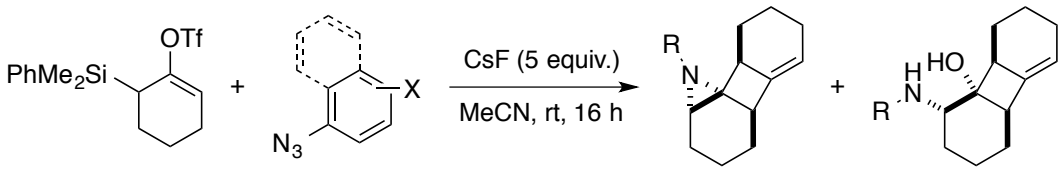

5 equiv.

90b **127a-g** **128-134** **135**

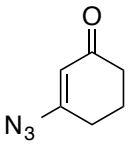

127f

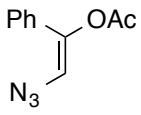

127g

Azide used	Product obtained	Yield (%)[c]
p-$NO_2C_6H_4$ – **127a**	**128**	52
p-$NO_2C_6H_4$ – **127a**	**135**[a]	34
p-$EtO_2CC_6H_4$ – **127b**	**129**	48
p-$MeOC_6H_4$ – **127c**	**130**	0
p-MeC_6H_4 – **127d**	**131**	0
1-azidonapthalene – **127e**	**132**	0
(*E*)-β-azidostyryl acetate[b] – **127f**	**133**	20
3-azidocyclohex-2-en-1-one – **127g**	**134**	18

[a] Acidic workup was done with 1M HCl. [b] Product decomposed upon prolonged exposure to $CHCl_3$. [c] Yields are of isolated compounds.

Extensive 2D NMR experiments allowed the assignment of the structure **128**. Cycloadducts **129 – 134** were assigned by spectral analogy to **128**. The stereochemistry was defined via TROESY correlations as shown in Figure 2.11.

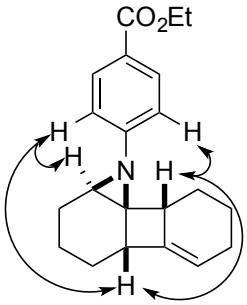

129

Figure 2.11 - TROESY correlations allowing assignment of relative stereochemistry to azide [2+1+2] cycloadduct.

If the azide/allene LUMO/HOMO overlap scenario is assumed in a similar sense to the previous dipolar cycloadditions, initial attack of the allene occurs on the terminal nitrogen of azide **127** (Scheme 2.24). The high energy of vinyl radical species **143** would hamper the extrusion of nitrogen gas, regardless of the previous results of Feldman.[11] The results of Houk's calculations[20] and Huisgen's experiments[54] confirm that cycloadditions of conjugated azides and electron-deficient olefins give 4-subsituted triazoline products. Therefore, the cycloaddition is likely occurring as an azide/allene, HOMO/LUMO interaction to first form alkylidene triazoline **138**, and upon nitrogen extrusion provides azatrimethylenemethane fragment **139** in a similar fashion to the mechanism proposed by Feldman and coworkers.[12] A reversible ring-closure generates the nucleophilic alkylidene aziridine, **140**. Similar to the work by Caubére,[55] the enolate equivalent can then undergo a formal [2+2] cycloaddition with a second equivalent of cyclic allene to generate aziridine tricycle **128**.

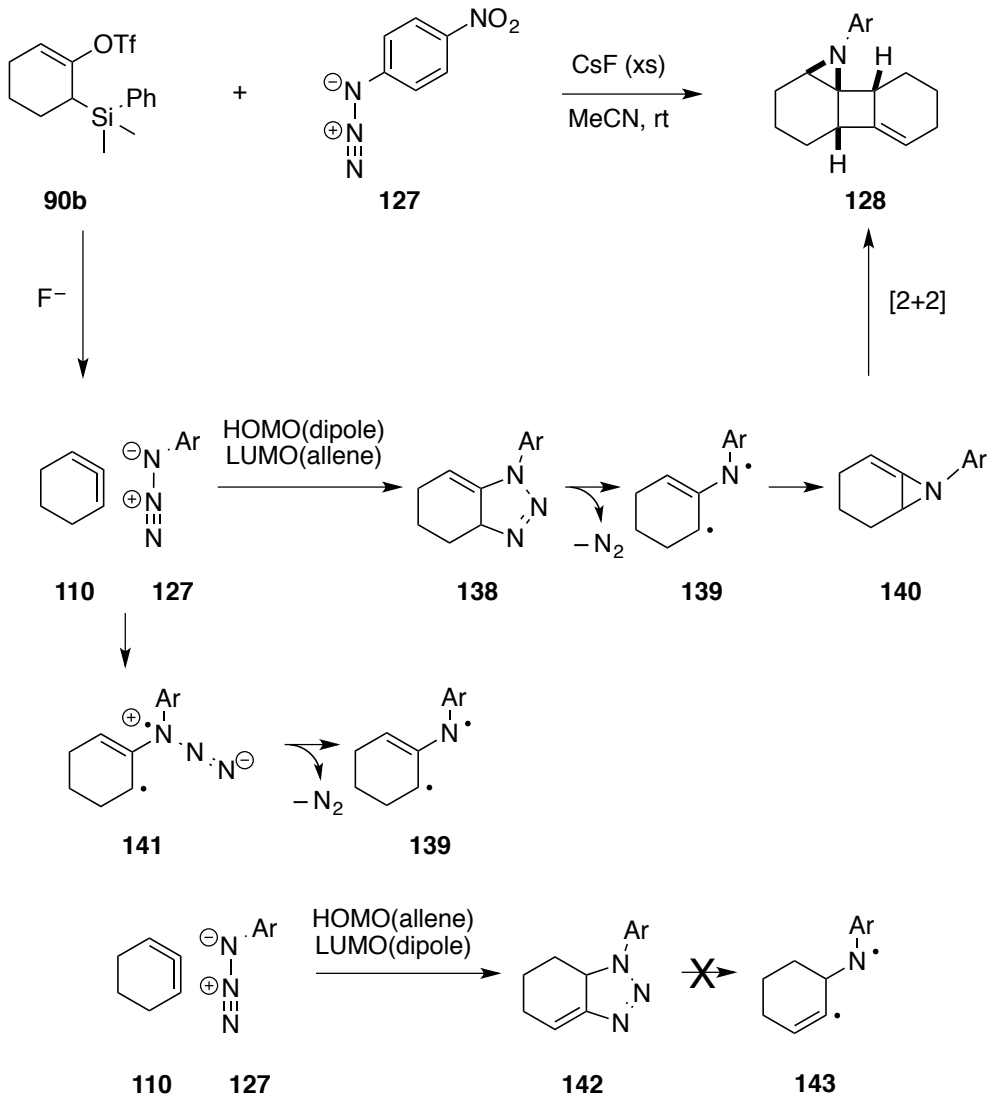

Scheme 2.24 - Possible mechanism for the formation of azide/allene cycloadduct.

The extrusion of nitrogen from the azide cycloadditions suggests the participation of radicals in the mechanism.[56] The loss of nitrogen, decomposition, and rearrangement of azide/allene cycloadducts does not occur at low temperatures (Scheme 2.25). This suggests a step-wise radical mechanism (**110 – 141,** Scheme 2.24), different from the cycloaddition/cycloreversion-like mechanism proposed by Feldman.[9,10,12]

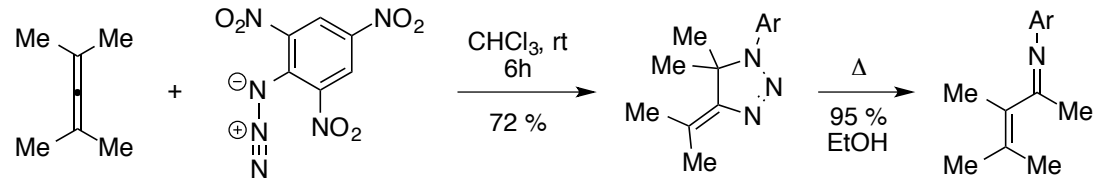

14 **13a** **15a** **144a**

Scheme 2.25 - Schecter azide/allene cycloaddition followed by thermal degradation.[9]

An azide functional group conjugated to a benzene ring is known to have higher HOMO than an unconjugated azide, while having a comparable LUMO energy level.[19,57] The extra conjugation and electron-withdrawing potential of the substituents contributes to a higher HOMO, changing the selectivity of dipolar/cyclic allene cycloaddition from LUMO(dipole)/HOMO(allene) to the opposite case, HOMO(dipole)/LUMO(allene). Electron rich azides gave complex mixtures that could not be resolved into single compounds for definitive characterization. The acetoxy-substituted allene failed to provide any products other than the dimer when subjected to the same trapping conditions. The HOMO of the acetoxy-substituted allene is raised when compared to the parent cyclic allene due to the conjugation with the oxygen lone pairs, making the allene less electrophilic. We hypothesize that the more nucleophilic cyclic allene fails to react with any azides as they are attempting to react as nucleophiles as well.

Styrene was added in an attempt to intercept any intermediates in the reaction of azides and cyclic allenes; however, the competition between azides and styrene strongly favors the cycloaddition reaction with styrene. As shown in Scheme 2.26 the addition of styrene to the standard reaction conditions resulted only in formation of known styrene adducts **137**/**137'**.[53]

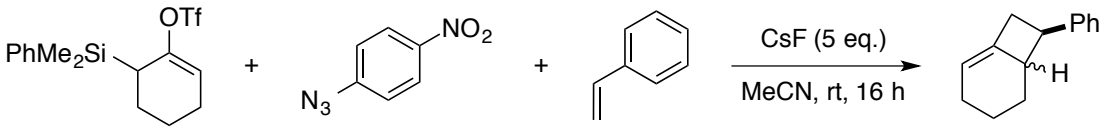

90b **127a** **136** ***anti* = 137** ***syn* = 137'**

Scheme 2.26 - Addition of styrene to intermolecular trapping study with aryl azides.

If a styrene and an azide moiety are combined into the same molecule, (α-azidostyrene **145b**), rather than a [2+2] cycloaddition with the styrene or a [2+1+2] cycloaddition with the azide a formal [3+2] cycloaddition takes place to give tetrahydroindole derivatives **146 – 149** (Table 2.4). As shown in Table 2.4, the [3+2] cycloaddition with α-azidostyrenes tolerated both electron-deficient and electron-rich substituents on the aryl ring. The reaction was amenable to the use of TBAF as the fluoride source rather than cesium fluoride, which permitted much shorter reaction times (~24 h versus 1.5 h). The attempted optimization of the reaction is outlined in Table 2.4, entries 1 - 8.

Table 2.4 - Optimization and scope of α-azidostyrene cycloaddition with 1,2-cyclohexadiene.

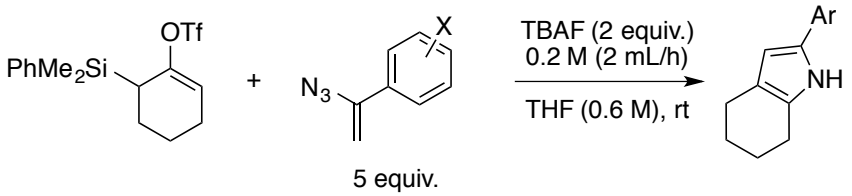

90b **145a-d** **146-149**

X = H, *m*-NO_2, *p*-OMe, 2-pyridyl

Entry	X = (Substituent)	Product	Solvent	Azide Equiv.	Temp. (°C)	Fluoride source	Yield (%)[b]
1	*p*-OMe **145a**	**146**	MeCN	5	rt	CsF (5 - 7 equiv.)	53
2	*p*-OMe **145a**	**146**	MeCN	5	–40	TBAF (2 equiv.)	52
3	*p*-OMe **145a**	**146**	MeCN	5	rt	TBAF (2 equiv.)	53
4	*p*-OMe **145a**	**146**	MeCN	3	rt	TBAF (2 equiv.)	25
5	*p*-OMe **145a**	**146**	$PhCH_3$	5	–78	TBAF (2 equiv.)	0
6	*p*-OMe **145a**	**146**	MeOH	5	rt	TBAF (2 equiv.)	0

7	*p*-OMe	**146**	THF	5	rt	TBAF	32
	145a					(2 equiv.)	
8	*p*-OMe	**146**	THF	5	rt	TBAF[a]	66
	145a		(0.6 M)			(2 equiv.)	
9	H	**147**	THF	5	rt	TBAF[a]	47
	145b		(0.6 M)			(2 equiv.)	
10	2-Pyridyl	**148**	THF	5	rt	TBAF[a]	15
	145c		(0.6 M)			(2 equiv.)	
11	*p*-NO_2	**149**	THF	5	rt	TBAF[a]	34
	145d		(0.6 M)			(2 equiv.)	
12	*p*-NO_2	**149**	THF	5	rt	CsF	43
	145d		(1.2 M)			(5 - 7 equiv.)	

[a] TBAF was diluted to 0.3 M from its original 1 M solution with THF and added at a rate of 2 mL/h. [b] Yield is of isolated compounds.

The reaction of 1,2-cyclohexadiene with styrene reported by Moore and Moser gave a 1:1 mixture of diastereomers **137** and **137'** (Scheme 2.27).[53] Christl later showed the two products could be thermally equilibrated to an 97:3 ratio.[58] It was hypothesized that the cycloaddition takes place in a stepwise fashion through diradical **150**. The isomerization could take place by the reversible formation of **150**.

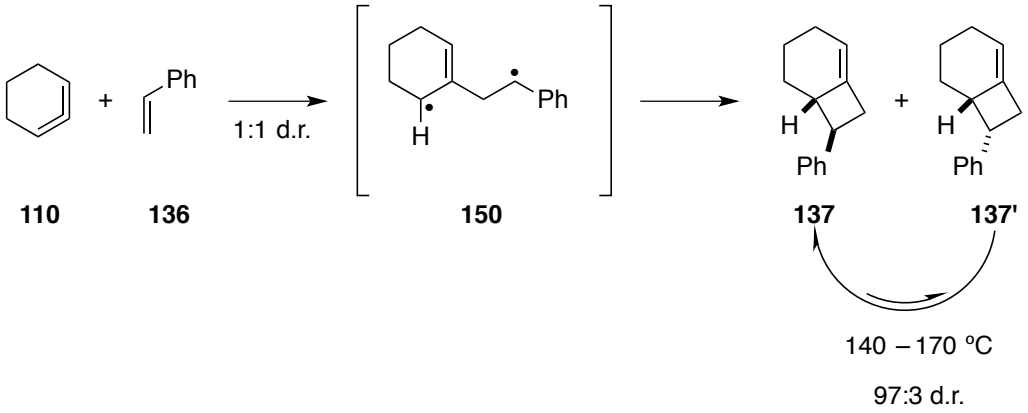

Scheme 2.27 - Investigation of the thermal equilibrium in styrene/cyclic allene cycloaddition.

The reaction with azidostyrenes could progress with a similar mechanism to the styrene cycloaddition, since a competition experiment between aryl azides and styrene resulted in only the [2+2] cycloadduct of styrene and 1,2-cyclohexadiene (Scheme 2.26). It is assumed that the ring closure to form pyrroline **152** occurs faster than the [2+2] cycloaddition with the α-substituted styrene. From pyrroline **152** the loss of nitrogen gas and a series of proton transfers furnishes tetrahydroindole **138**.

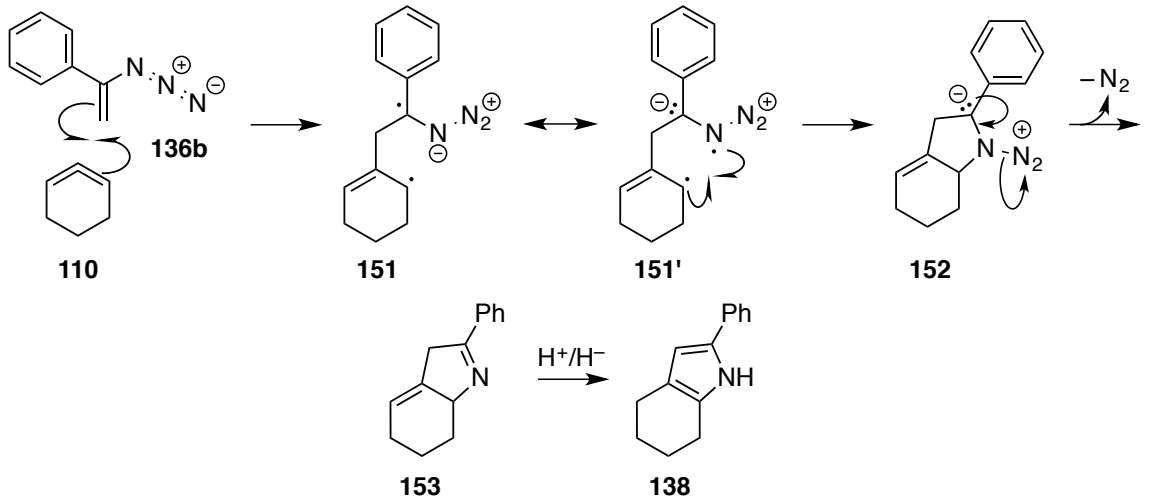

Scheme 2.28 – Proposed mechanism for the formation of tetrahydroindoles.

The extrusion of nitrogen from both the aryl azide and styryl azide cycloadditions under mild reaction conditions suggests both reactions occur through a radical mechanism (Scheme 2.24 and Scheme 2.28). While the simple azide cycloaddition showed a limited substrate scope with respect to the azide substituents tolerated. The reaction with azidostyrenes showed more tolerance to substitution on the aryl ring due to the greater reactivity of cyclic allenes with styrenes versus azides or the greater propensity of styrenes to act as electrophilic radical acceptors similar to the mechanism proposed by Waali and coworkers.[59] Interestingly, 2-azido-2-cyclohexenone gave only the [2+1+2] cycloadduct (**127g**) rather than a formal [3+2]. Ethyl 2-azidoacrylate failed to give either a [2+1+2] cycloadduct or a [3+2] adduct.

In order to expand the substitution patterns accessible via the formal [3+2] cycloaddition of styryl azides, β-alkyl-α-azidostyrenes were synthesized and subjected to the reaction conditions. Sadly, the tetrahydroindole products could never be isolated cleanly from the reaction mixtures. They appeared to be forming in minor amounts

according to thin layer chromatography analysis of the reaction mixture;[60] however, upon work-up and attempted purification, the product could never be isolated/observed. The major product had no indication of a cyclohexyl ring structure by ^{1}H NMR; thus no incorporation of the cyclic allene was apparent and characterization of the side-product was abandoned. The reaction was attempted with simple a simple phenyl group in addition to *m*-nitrophenyl-, and *o*-methoxyphenyl-substituted styrylazides.

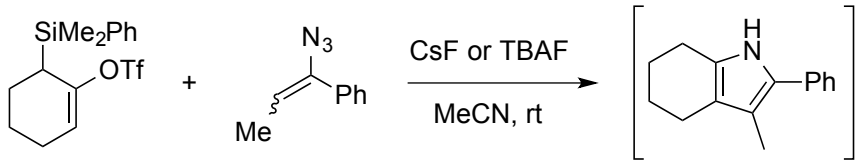

90b **154** trace/decomposed **155**

Scheme 2.29 - Use of alkyl-substituted α-azidostyrene.

In addition to the limited scope of azides amenable to trapping, the acetoxy-substituted cyclic allene failed to provide any products containing nitrogen. Although the starting material is consumed, no single compound could be isolated other than dimer **97**. It is possible the lack of isolable products was from decomposition of the products due to the presence of acid-sensitive functionalities, similar to Feldman's observation.[11] To mitigate this possible decomposition a reductive work-up was done, however, the outcome of the reaction remained unchanged.

2.5. Conclusions

Given the range of 1,3-dipolar compounds that proved to be effective at trapping cyclic allenes, it is apparent that cyclic allenes are potent dipolarophiles. The development of synthetic sequences employing either a silyl-cuprate allylic displacement or a silyl-cuprate conjugate addition permitted the synthesis of the targeted allylic silanes. The fluoride-mediated generation of cyclic allenes was found to be efficient given the yields of the trapped products obtained, even for the previously unreported acetoxy-substituted precursor **90a**. The [3+2] dipolar cycloadditions proceeded in good yields and with a high site-selectivity, high regioselectivity, and high diastereoselectivity. The reaction with azides proved to be more complicated due to the rearrangements and the loss of nitrogen gas. It did, however, spawn the formal [3+2] cycloaddition with α-

azidostyrene to give tetrahydroindoles in good yields. Easy access to large-quantities of stable cyclic allene precursor will enable even further reactivity screening to be carried out. In all of the reactions studied a low trap concentration was employed; using 5 – 3 equivalents rather than using the trap as a solvent as in the case with furan, styrene or other studies.[28]

2.6. Future Directions

With the success found trapping cyclic allenes with 1,3-dipolar compounds, the process appears to be a general way to make heterocyclic compounds of varying functionalization as pure diastereomers. An investigation into the reactivity of cyclic allenes bearing electron-withdrawing groups would complement the results discussed above.

Known 2-bromo-3-cyano-2-cyclohexenone (Scheme 2.30) was synthesized by a modified procedure of Agosta and Lowrance,[61] whereby diethylaluminum cyanide reacted with bromoethoxyenone **156**. This material was reduced to give alcohol **157**, which was esterified with picolinic acid under Steglich esterification conditions.[62] The final silylation step gave a complicated mixture of products,[63] which was not further investigated.

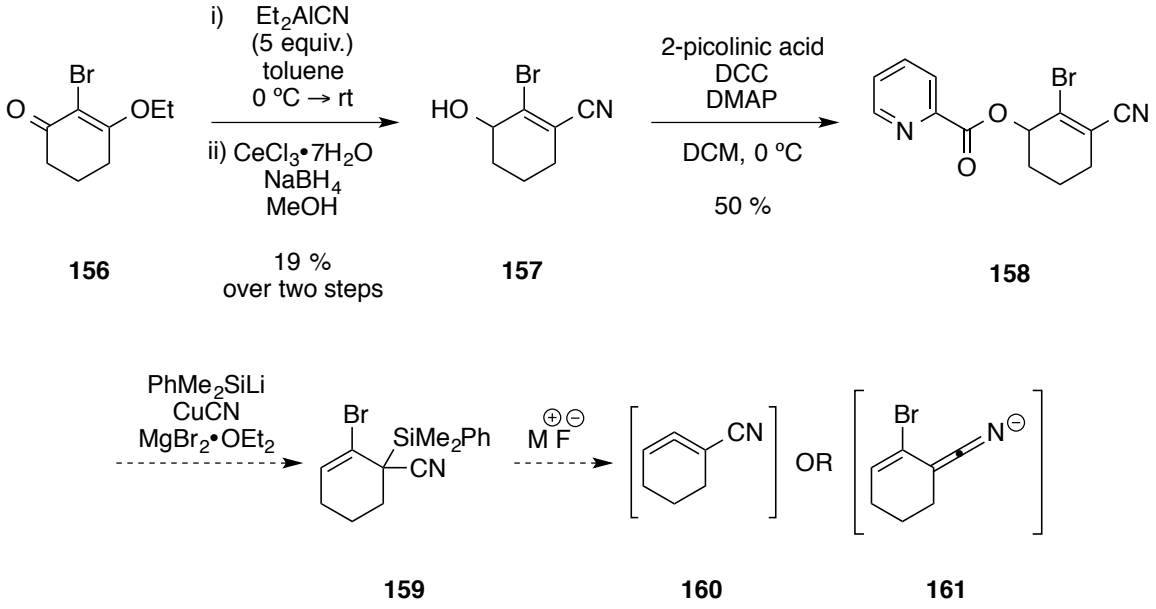

Scheme 2.30 - Attempted synthesis of cyano-substituted cyclic allene precursor.

In case the desilylation is complicated by conjugation with the cyano group on C1 (formation of **161** rather than **160**), cyanoacetate **164** was targeted (Scheme 2.31). This proved to be difficult due to the sensitivity of the cyanohydrin **163** to decomposition. Further work is warranted to complete the reactivity spectrum for monosubstituted-1,2-cyclohexadienes, from neutral, to electron-rich, and to electron-poor.

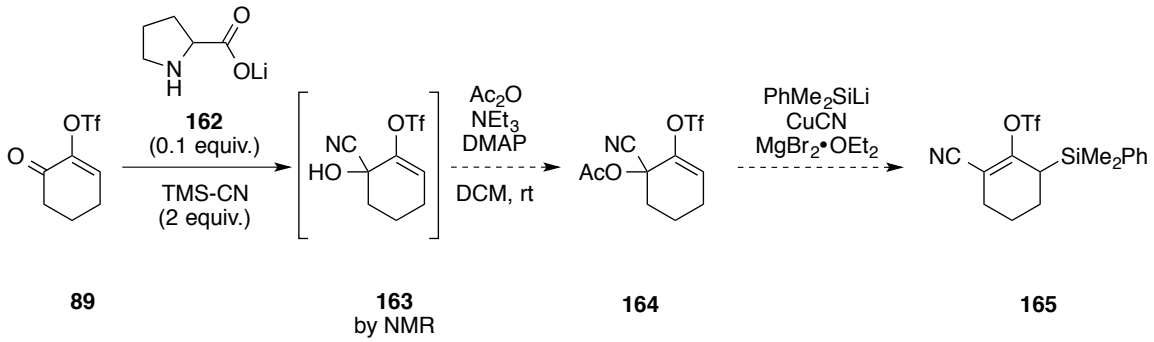

Scheme 2.31 - Attempted synthesis of cyanohydrin-derived silylation precursor.

Furthermore, in Chapter 3 and Chapter 4 the development of asymmetric allene generation and intramolecular reactions warranted the application of silyl-cuprate conjugate-addition/allylic-displacement to sterically crowded systems with variable degrees of substitution. With this in mind, the investigation of different substituents and substitution patterns on the cyclic allene skeleton may provide interesting reactivity as was observed by Moore during the development of the Moore cyclization.[64]

The heteroatom substituted cyclic allenes show high reactivity with good selectivity in a number of cycloadditions.[28] One such class that has never been reported has an iminium nitrogen as the central atom of the cumulated system (Scheme 2.32). This should be very reactive but also very interesting from a reactivity perspective, such that any bond forming reaction with the central nitrogen atom does not quench the positive charge on the allene, opening the substrates up to extravagant cascade reactions or multi-component reactions. One proposed synthesis could be the chloride abstraction from chlorinated aziridines to give an intermediate isoelectronic with that proposed for the DMS reaction. It would be a significant observation in terms of mechanism and bond forming reactions if the resulting cation opened to a diimine, either cyclic diimine **167** or a generic acyclic diimine.

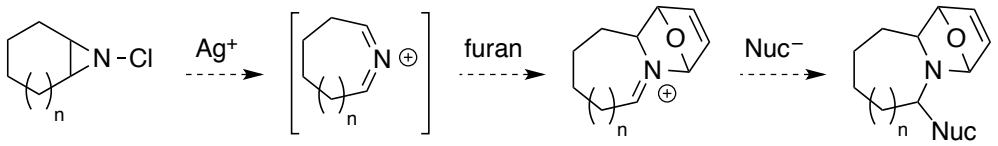

166 167 168 169

Scheme 2.32 - Possible nitrogen-substituted cyclic allene synthesis and trapping.

Finally, the ability to generate cyclic allenes under mild reaction conditions, with high functional group tolerance from different functional groups is highly sought after. In the instances whereby the cuprate addition failed or showed attenuated yields a different approach could be taken using 1,2-addition of a silyl anion to α,β-unsaturated ketones. As demonstrated by Koreeda and Koo, the 1,2-addition of dimethylphenylsilyl lithium to cyclohexenone gives high yields of the 1,1-silylcarbinols, even in more substituted examples (Scheme 2.33). The addition of a leaving group alpha to the ketone allows the possibility of a 1,2-Brook rearrangement/elimination to generate the cyclic allene is possible.

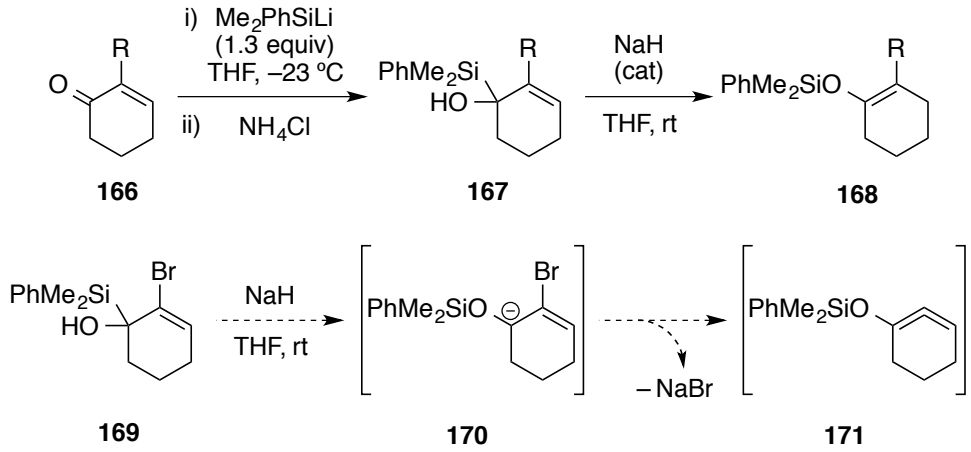

166 167 168 169 170 171

Scheme 2.33 - Possible cyclic allene generation by Brook rearrangement.

2.7. Experimental

2.7.1. General Information

Reactions were carried out in glassware that was oven (120 °C) or flame-dried under a positive argon atmosphere unless otherwise stated. Transfer of anhydrous reagents was accomplished with oven-dried syringes or cannulae. Solvents were distilled before use: acetonitrile (CH_3CN), triethylamine (NEt_3), and dichloromethane (CH_2Cl_2)

from calcium hydride, diethyl ether (Et_2O), and tetrahydrofuran (THF) from sodium/benzophenone; toluene, and benzene (C_6H_6) from sodium metal. Thin layer chromatography was performed on glass plates pre-coated with 0.25 mm Kieselgel 60 F254 (Merck). Flash chromatography columns were packed with 230-400 mesh silica gel (Silicycle). Proton nuclear magnetic resonance spectra (^{1}H NMR) were recorded at 300 MHz, 400 MHz, or 500 MHz and coupling constants (*J*) are reported in Hertz (Hz). Carbon nuclear magnetic resonance spectra (^{13}C NMR) were recorded at 100 MHz or 125 MHz. The chemical shifts are reported on the δ scale (ppm) and referenced to the residual solvent peaks: $CDCl_3$ (7.26 ppm, ^{1}H; 77.06 ppm, ^{13}C) as internal standards. Standard notation is used to describe the multiplicity of the signals observed in ^{1}H NMR spectra: broad (br), apparent (app), multiplet (m), singlet (s), doublet (d), triplet (t), quartet (q), pentet (p), etc. Infrared (IR) spectra were measured with a Mattson Galaxy Series FT-IR 3000 spectrophotometer. High-resolution mass spectrometry (HRMS) data (APPI/APCI/ESI technique) were recorded using an Agilent Technologies 6220 oaTOF instrument. HRMS data (EI technique) were recorded using a Kratos MS50 instrument.

Enone **89**,[65] cycloadduct **93b**,[31] nitrile oxide **94** and chloro-oxime **96**, [66] dimer **98**,[67] nitrones **113a-d**,[51] azomethine imines **118a-d**,[52] azides **127a-g**,[68-70] and α-azidostyrenes **145a-d** and β-methyl-α-azidostyrene**154**,[71] are all known literature compounds, ^{1}H NMR and ^{13}C NMR spectral data matched those reported in the literature.

Phenyldimethylsilyl lithium

Reagent was prepared by a procedure similar to that employed by Gilman and coworkers[72]:

Lithium wire (7 equiv) was rinsed with hexanes, weighed, and cut into roughly 2mm x 2mm pieces under a stream of argon into a oven dried, round-bottom flask. The flask was then capped with a rubber septum, vented, and flame dried again with a Bunsen burner under a stream of argon to ensure dryness. Once cooled, the flask was charged with THF, (0.6 M in silyl-chloride) and cooled to 0 °C using an ice-water bath. Dry phenyldimethylsilyl chloride was added via syringe and the septum was covered with parafilm two times to ensure no exchange of atmosphere after the argon supply needle

was removed. The flask was then stored in a freezer for 48 h, resulting in a dark red, slightly viscous solution, which could be stored at freezer temperatures for up to 4 weeks.

3-(Phenyldimethylsilyl)-2-{[(trifluoromethyl)sulfonyl]oxy}cyclohex-1-en-1-yl acetate (90a)

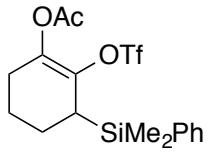

To a dry flask under argon atmosphere was added copper bromide•dimethyl sulfide complex (1.25 equiv) which was suspended in THF, (0.15 M) and the flask was cooled to 0 °C using an ice-water bath. To this flask was added previously prepared lithium phenyldimethylsilyl anion (see previous entry, 2.5 equiv) via cannula transfer giving a deep red solution. The resulting silyl cuprate reagent was stirred for 30 min maintaining the temperature at 0 °C.

The cuprate solution was then cooled to -78 °C using a dry ice/acetone bath, and a cooled solution of enone **89** (1 equiv, 0.4 M in THF) was added via cannula (for reactions in which the scale was in excess of 500 mg of enone, the solution of enone was added via a syringe pump over the course of 30 min). This solution was stirred at -78 °C for 5 hours. After 5 hours, freshly distilled acetic anhydride (5 equiv) was added via syringe. The solution was maintained at -78 °C for a further 5 hours.

To the solution was added a 30 mL portion of diethyl ether and a 25 mL portion of distilled water. The phases were separated and the aqueous layer was further extracted with diethyl ether (3 x 40 mL). The organic layer was washed with distilled water and brine, then dried over magnesium sulfate, and filtered. The organic layer was filtered, concentrated, and subjected to flash column chromatography on silica using a gradient eluent (3:1 hexanes:DCM → 1:1 hexanes:DCM) afforded the title compound.

Using 200 mg of enone **7**, 296 mg of acetoxy silyl compound **90a** was isolated as a clear, colorless oil, (86 % yield).

R_f = 0.5 (1:1, hexanes:DCM); ^{1}H NMR (400 MHz, $CDCl_3$) δ 7.55 – 7.51 (m, 2H), 7.41 – 7.36 (m, 3H), 2.36 – 2.18 (m, 3H), 2.19 (s, 3H), 1.86 – 1.78 (m, 1H), 1.67 – 1.54 (m, 3H), 0.46 (s, 3H), 0.45 (s, 3H); ^{13}C NMR (125 MHz, $CDCl_3$) δ 167.8, 139.9, 138.9, 136.4,

133.9, 129.5, 128.0, 118.3 (q, $^{1}J_{CF}$ = 318.2 Hz, 1C), 27.7, 27.1, 25.4, 21.1, 20.6, -2.9, -4.1; IR (cast film, cm^{-1}) 3072, 3050, 3022, 2954, 2864, 1771; HRMS (ESI) calcd for $[M+Na]^{+}$ $C_{17}H_{21}F_3NaO_5SSi$: 445.0723, found: 445.0717.

2-{[(Trifluoromethyl)sulfonyl]oxy}cyclohex-2-en-1-yl 4-methylbenzenesulfonate (92)

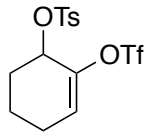

Enone **89**, cerium trichloride heptahydrate (1.1 equiv), and methanol (0.4 M) were added to a round bottom flask. The solution was stirred to homogeneity, and sodium borohydride (1.2 equiv) was added slowly. Once the vigorous bubbling had subsided, the solution was stirred for an additional 20 min. After this time the reaction was quenched with 5 mL sat. ammonium chloride and 5 mL 1M HCl and the solution was extracted with diethyl ether (5 x 25 mL). The organic layer was then washed with distilled water (2 x 25 mL) and brine (25 mL). The organic layer was dried over magnesium sulfate, filtered, and concentrated to afford alcohol **91**. This material was then used directly in the next step.

R_f = 0.21 (9:1, hexanes:ethyl acetate); ^{1}H NMR (500 MHz, $CDCl_3$) δ 5.95 (dd, *J* = 5.0, 4.0 Hz, 1H), 4.35 (app dd, *J* = 4.5, 1.5 Hz, 1H), 2.31 (app dtd, *J* = 18.5, 5.0, 1.5 Hz, 1H), 2.19 (ddddd, *J* = 18.5, 9.0, 5.0, 3.5, 1.5 Hz, 1H), 2.06 (br d, *J* = 7.0 Hz, OH), 1.94 – 1.90 (m, 2H), 1.80 – 1.61 (m, 2H); ^{13}C NMR (100 MHz, $CDCl_3$) δ 149.4, 122.3, 118.5 (q, *J* = 318.1 Hz, C–F_3), 65.3, 31.9, 24.4, 17.1; IR (cast film, cm^{-1}) 3368, 2948, 2872, 1681; HRMS (ESI) calcd for $[M]^{+}$ $C_7H_9NaO_4S$: 269.0174, found: 269.0065.

The procedure used for synthesizing allylic tosylate **92** was adapted from a literature procedure.[73] The flask was purged with argon and the allylic alcohol **91** was then dissolved in toluene (0.2 M). Solid trimethylamine hydrochloride was added (1 equiv) and the solution was cooled to 0 °C. To the cooled solution was added triethylamine (3 equiv) and the reaction was stirred for 20 min. Solid *p*-toluenesulfonyl chloride was added (0.75 equiv) and the solution was stirred for 2 hours. A second portion of *p*-toluenesulfonyl chloride (0.75 equiv) was added and the reaction was kept at 0 °C until TLC analysis (9:1, hexanes:ethyl acetate) showed complete consumption of the starting

alcohol. The reaction was quenched with 1 M HCl and extracted with diethyl ether (3 x 50 mL). The organic layers were washed with saturated sodium bicarbonate, brine, and dried over magnesium sulfate, and filtered. The organic layer was concentrated and careful gradient flash column chromatography on silica (hex:ethyl acetate, 95:5 → 85:15) provided allylic tosylate **92**, as a thermally unstable solid. The product was stored in the freezer if not used immediately.

Using 1.05 g of enone **89** 1.29 g of allylic tosylate **92** was isolated (75 % yield).

R_f = 0.23 (9:1, hexanes:ethyl acetate); ^{1}H NMR (500 MHz, $CDCl_3$) δ 7.85 (d, J = 8.4 Hz, 2H), 7.38 (d, J = 8.4 Hz, 2H), 6.14 (dd, J = 5.4, 2.8 Hz, 1H), 5.08 (br s, 1H), 2.49 (s, 3H), 2.39 – 2.29 (m, 2H), 2.25 – 2.17 (m, 1H), 1.93 – 1.86 (m, 1H), 1.83 – 1.68 (m, 2H); ^{13}C NMR (125 MHz, $CDCl_3$) δ 145.2, 143.9, 133.4, 129.9, 127.9, 126.5, 118.4 (q, $^1J_{CF}$ = 319.0 Hz, 1C) 74.4, 29.9, 24.1, 21.7, 15.6; IR (cast film, cm^{-1}) 3070, 2941, 2873, 1679, 1598; HRMS (ESI) calcd for $[M+Na]^+$ $C_{14}H_{15}F_3NaO_6S_2$: 423.0154, found: 423.0143.

6-(Phenyldimethylsilyl)cyclohex-1-en-1-yl trifluoromethanesulfonate (90b)

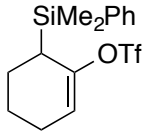

Use of catalytic copper conditions: To a dry flask under argon atmosphere was added copper cyanide (0.1 equiv), triphenylphosphine (0.2 equiv), and allylic tosylate **92**. The flask was charged with diethyl ether (0.15 M) and cooled to 0 °C using an ice/water bath. The previously prepared silyl anion solution was added to the flask via a syringe pump at a rate which allows the addition to be complete in 1 h.

Once the addition was complete, the reaction was kept at 0 °C for an additional 1 h. While cold the reaction was quenched with equal volumes of pH 7 - phosphate buffer and hexanes. The layers were separated and the aqueous layer was further washed with hexanes (3 x 40 mL). The organic layer was washed with brine and dried over magnesium sulfate, and filtered. Concentrating the organic layer, careful flash column chromatography on silica (hex:DCM, 95:5 → 90:10) afforded allylic silane **90b**.

Using 3.55 g of allylic tosylate **92,** 2.74 g of allylic silane **90b** was isolated as a clear, colorless oil (85 % yield).

R_f = 0.4 (9:1, hexanes:DCM); ^{1}H NMR (400 MHz, $CDCl_3$) δ 7.54 – 7.50 (m, 2H), 7.43 – 7.35 (m, 3H), 5.69 – 5.67 (m, 1H), 2.21 – 2.12 (m, 2H), 2.05 – 1.95 (m, 1H), 1.87 – 1.80 (m, 1H), 1.62 – 1.49 (m, 2H), 1.46 – 1.36 (m, 1H), 0.46 (s, 3H), 0.42 (s, 3H); ^{13}C NMR (125 MHz, $CDCl_3$) δ 152.2, 136.5, 133.9, 129.4, 127.9, 118.6 (q, $^1J_{CF}$ = 312.5 Hz, 1C), 115.9, 28.9, 25.7, 24.1, 20.8, -3.0, -3.9; IR (cast film, cm^{-1}) 3071, 3052, 2947, 2861, 1673; HRMS (EI) calcd for $[M]^+$ $C_{15}H_{19}F_3O_3SSi$: 364.0776, found: 364.0777.

Procedure using stoichiometric preformed silyl cuprate reagent: copper cyanide (1.3 equiv), and triphenylphosphine (2.6 equiv) were added to an oven-dried flask under an argon atmosphere. The reaction flask was charged with dry diethyl ether (0.2 M) with high stirring to help establish a finely divided suspension and cooled to 0 °C. To the cooled flask was added a solution of previously prepared dimethylphenylsilyl lithium via a cannula (2.55 equiv). The homogenous solution was allowed to stir for 10-15 min at 0 °C before allylic tosylate **92** (1 equiv) dissolved in diethyl ether (0.6 M) was added over 1 hour via syringe pump.

Once the addition was complete, the reaction was kept at 0 °C for an addition 1 h. While cold the reaction was quenched with equal volumes of pH 7 - phosphate buffer and hexanes. The layers were separated and the aqueous layer was further washed with hexanes (3 x 40 mL). The organic layer was washed with brine and dried over magnesium sulfate, and filtered. Concentrating the organic layer, careful flash column chromatography on silica (hex:DCM, 95:5 → 90:10) afforded allylic silane **90b**.

Using 126 mg of allylic tosylate **92,** 83 mg of allylic silane **90b** was isolated as a clear, colorless oil (85 % yield).

Characterization was the same as previously obtained.

In order to obtain high purity product three times the recommended silica was used and a column twice the diameter suggested for the scale according the paper by Still *et. al.*.[74]

8-(Acetyloxy)-2,3,4,4a,4b,5,6,7-octahydrobiphenylen-1-yl acetate (97)

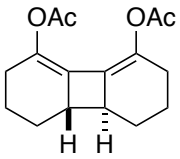

Acetoxy allylic silane **90a** was added to a flask and an argon atmosphere was established via a purge needle. Freshly distilled acetonitrile (1.6 mL) was added and tetrabutylammonium fluoride (1M THF, 2 equiv) was added dropwise via syringe. Concentration of the reaction mixture and subjecting the crude mixture to flash column chromatography on silica (9:1:1, hexanes:ethylacetate:DCM) to afforded dimer **97**.

Using 37 mg of acetoxy silane **90a** 5.0 mg of dimer **97** was isolated in a 41 % yield.

R_f = 0.43 (8:2, hexanes:ethyl acetate); ^{1}H NMR (500 MHz, $CDCl_3$) δ 2.59 (m, 2H), 2.30 (br dd, *J* = 17.4, 6.6 Hz, 2H), 2.19 – 2.11 (m, 2H), 2.14 (s, 6H), 1.95 – 1.89 (m, 4H), 1.63 – 1.53 (m, 2H), 1.25 – 1.17 (m, 2H); ^{13}C NMR (125 MHz, $CDCl_3$) δ 169.2, 137.0, 125.6, 47.1, 27.0, 26.6, 22.7, 20.8; IR (cast film, cm^{-1}) 2933, 2855, 1760, 1693; HRMS (EI) calcd for $[M+Na]^+$ $C_{16}H_{20}NaO_4$: 299.1254, found: 299.1247.

***Endo*-11-oxatricyclo[6.2.1.0^{2,7}]undeca-2,9-dien-3-yl acetate (93a)**

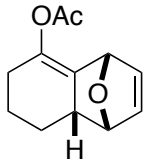

Acetoxy allylic silane **90a** was added to a flask and an argon atmosphere was established via a purge needle. Freshly distilled furan (230 equiv) was added and the reaction was cooled to 0 °C using an ice/water bath. Tetrabutylammonium fluoride (1M THF, 2 equiv) was added dropwise via syringe and the reaction was allowed to warm to room temperature. Concentration of the reaction mixture and subjecting the crude oil to flash column chromatography (9:1:1, hexanes:ethyl acetate:DCM) on silica afforded cycloadduct **93a**.

Using 43 mg of acetoxy silane **90a** 7.0 mg of cycloadduct **93a** was isolated (33 % yield) as a clear, colorless oil.

R_f = 0.23 (8:2, hexanes:ethyl acetate); ^{1}H NMR (MHz, $CDCl_3$) δ 6.42 (dd, (*J* = 5.7, 1.7 Hz, 1H), 6.14 (dd, *J* = 5.8, 1.7 Hz, 1H) 5.21 (s, 1H), 5.03 (br s, 1H), 2.61 – 2.56 (m, 1H), 2.30 (ddd, *J* = 16.7, 7.0, 2.0 Hz, 1H), 2.16 (s, 3H), 2.05 – 1.91 (m, 3H), 1.75 – 1.64 (m, 1H), 0.49 – 0.40 (m, 1H); ^{13}C NMR (125 MHz, $CDCl_3$) δ 169.2, 139.3, 135.4, 130.3,

126.6, 81.4, 77.9, 41.6, 26.4, 26.3, 23.4, 20.9; IR (cast film, cm^{-1}) 3005, 2937, 2865, 1753; HRMS (ESI) calcd for $[M+Na]^+$ $C_{12}H_{14}NaO_3$: 229.0835, found: 229.0832.

***Endo*-11-oxatricyclo[6.2.1.$0^{2,7}$]undeca-2,9-diene (93b)**

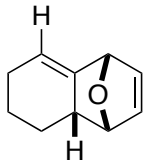

Allylic silane **90b** was added to a flask and an argon atmosphere was established via a purge needle. Freshly distilled furan (0.06 M in **90b**) was added and the reaction was cooled to 0 °C using an ice/water bath. Tetrabutylammonium fluoride (1M THF, 2 equiv) was added dropwise via syringe and the reaction was allowed to warm to room temperature. Concentration and careful flash column chromatography (19:1:1, hexanes:ethyl acetate:DCM) on silica afforded known cycloadduct **93b**.

^1H and ^{13}C NMR spectral data matched those reported for compound **93b**.[31]

The product is volatile and can easily be lost when concentrated on a rotary evaporator therefore the compound was not concentrated to dryness but redissolved in chloroform and further evaporated.

3-(2,4,6-Trimethylphenyl)-5,6,7,7a-tetrahydro-1,2-benzoxazol-4-yl acetate (95a)

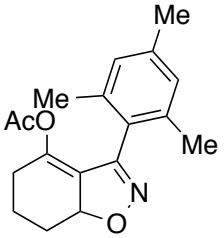

Allylic silane **90a**, and nitrile oxide **94** (5 equiv) were added to a flask and an argon atmosphere was established via a purge needle. Acetonitrile (0.2 M) was added and cesium fluoride (5 equiv) was added to the reaction flask while maintaining the argon atmosphere. The reaction was stirred at room temperature and the reaction progress was monitored by TLC analysis until the starting material was consumed. The reaction mixture was then concentrated and careful flash column chromatography on silica

afforded cycloadduct **95a**. The product is unstable, and decomposes uncontrollably upon concentration.

Using 55 mg of acetoxy silane **90a** and 105 mg of nitrile oxide **94,** 27 mg of cycloadduct **95a** (69 % yield) was isolated.

R_f = 0.3 (8:2, hexanes:ethyl acetate); ^{1}H NMR (500 MHz, $CDCl_3$) δ 6.91 (s, 1H), 6.89 (s, 1H), 5.12 (app sextet, *J* = 5.0 Hz, 1H), 2.50 (tdd, *J* = 11.7, 4.9, 3.3 Hz, 1H), 2.31 – 2.27 (m, 1H), 2.29 (s, 3H), 2.20 (s, 3H), 2.19 (s, 3H), 2.13 – 2.07 (m, 2H), 1.85 – 1.75 (m, 1H), 1.70 – 1.62 (m, 1H), 1.32 (s, 3H); ^{13}C NMR (100 MHz, $CDCl_3$) δ 168.4, 154.7, 142.2, 138.7, 137.5, 137.4, 128.1, 128.0, 127.9, 125.6, 80.1, 26.5, 26.2, 20.6, 19.3, 19.2, 18.8, 18.6; IR (cast film, cm^{-1}) 2954, 2867, 1767, 1699; HRMS (EI) calcd for $[M]^+$ $C_{18}H_{21}NO_3$: 299.1521, found: 299.1529.

3-(2,4,6-Trimethylphenyl)-5,6,7,7a-tetrahydro-1,2-benzoxazole (95b)

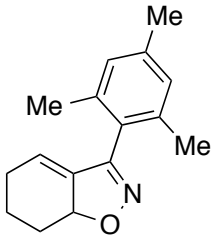

The allylic silane **90b**, and nitrile oxide **94** (5 equiv) were added to a flask and an argon atmosphere was established via a purge needle. Acetonitrile (0.2 M) was added and cesium fluoride (5 equiv) was added to the reaction flask maintaining the argon atmosphere. The reaction progress was monitored by TLC analysis, and upon consumption of the starting material the reaction mixture was concentrated, and the crude oil was subjected to careful flash column chromatography (10:1:1, hexanes:ethyl acetate:DCM) on silica to afford cycloadduct **95b** as a clear and colorless oil.

Using 25 mg of allylic silane **90b** and 56 mg of nitrile oxide **94,** 9.1 mg of cycloadduct **95b** (43 % yield) was isolated.

R_f = 0.17 (9:1, hexanes:ethyl acetate); ^{1}H NMR (500 MHz, $CDCl_3$) δ 6.92 (s, 1H), 6.92 (s, 1H), 5.53 (app q, *J* = 3.5 Hz, 1H), 4.92 (dqd, *J* = 10.1, 5.0, 3.8 Hz, 1H), 2.52 (ddt, *J* = 11.4, 4.9, 3.2 Hz, 1H), 2.32 (s, 3H), 2.25 – 2.19 (m, 2H), 2.22 (s, 3H), 2.19 (s, 3H), 1.98 (ddt, *J* = 17.7, 6.3, 3.5 Hz, 1H), 1.72 – 1.61 (m, 1H), 1.60 – 1.52 (m, 1H); ^{13}C NMR (125

MHz, $CDCl_3$) δ 157.6, 142.2, 138.8, 137.6, 137.2, 128.3, 128.3, 124.6, 122.7, 79.6, 29.7, 27.3, 24.2, 21.1, 19.9, 19.6, 18.7; IR (cast film, cm^{-1}) 2949, 2923, 2865, 1612; HRMS (EI) calcd for $[M]^+$ $C_{16}H_{19}NO$: 241.1466, found: 241.1463.

General procedure for allene/nitrone cycloaddition

The allylic silane **90a** or **90b**, and the appropriate nitrone **113a-d** (5 equiv) were added to a flask and an argon atmosphere was established via a purge needle. Acetonitrile (0.1 M) was added and cesium fluoride (5 equiv) was added to the reaction flask while maintaining the argon atmosphere via steady stream of argon from a purge needle. The reaction was monitored by TLC until completion, concentrated, and subjected to flash column chromatography on silica affording cycloadducts **114-117**.

***Anti*-2-Benzyl-3-phenyl-2,3,5,6,7,7a-hexahydro-1,2-benzoxazol-4-yl acetate (114a)**

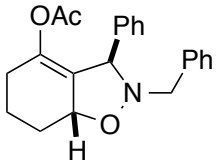

Using 50 mg of acetoxy silane **90a** and 130 mg of nitrone **113a** generated 15.3 mg of cycloadduct **114a** (34 % yield) was isolated as a clear, colorless oil.

R_f = 0.49 (8:2, hexanes:ethyl acetate); ^1H NMR (400 MHz, $CDCl_3$) δ 7.42 – 7.20 (m, 10H), 4.67 – 4.61 (m, 1H), 4.35 (app q, J = 2.5 Hz, 1H), 4.05, 3.95 (ABq, J_{AB} = 14.0 Hz, 2H), 2.33 – 2.11 (m, 3H), 2.00 (ddtd, J = 13.8, 6.9, 3.5, 1.1 Hz, 1H), 1.83 (s, 3H), 1.71 (qdd, J = 14.1, 6.9, 3.1 Hz, 1H), 1.40 (dddd, J = 13.8, 11.7, 10.3, 3.3 Hz, 1H); ^{13}C NMR (125 MHz, $CDCl_3$) δ 168.2, 141.3, 138.7, 137.5, 132.2, 128.9, 128.5, 128.3, 128.2, 127.8, 127.2, 71.1, 60.5, 27.0, 26.3, 20.3, 19.5; IR (cast film, cm^{-1}) 3087, 3061, 2949, 2866, 2943, 1755; HRMS (EI) calcd for $[M]^+$ $C_{22}H_{23}NO_3$: 349.1677, found: 349.1673.

Pertinent ROESY correlations for stereochemistry:

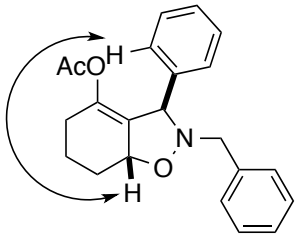

***Anti*-2-Benzyl-3-phenyl-2,3,5,6,7,7a-hexahydro-1,2-benzoxazole(114b)**

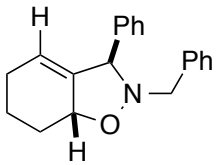

Using 50 mg of allylic silane **90b** and 145 mg of nitrone **113a** generated 24.6 mg of cycloadduct **114b** (62 % yield) was isolated as a clear and colorless oil.

R_f = 0.39 (1:1, hexanes:DCM); ^{1}H NMR (500 MHz, $CDCl_3$) δ 7.48 – 7.22 (m, 10H), 5.45 (br s, 1H), 4.46 – 4.42 (m, 1H), 4.30 (br s, 1H), 4.07, 3.99 (ABq, J_{AB} = 14.0 Hz, 2H), 2.24 (dddd, J = 9.0, 5.0, 3.5, 2.5 Hz, 1H), 2.13 – 2.08 (m, 2H), 1.90 (app dp, J = 14.0, 3.5 Hz, 1H), 1.51 (dddd, J = 20.5, 14.0, 8.5, 2.5 Hz, 1H), 1.39 – 1.30 (m, 1H); ^{13}C NMR (100 MHz, $CDCl_3$) δ 145.8, 140.6, 137.7, 128.9, 128.4, 128.2, 127.8, 127.5, 127.1, 118.8, 72.8, 60.9, 27.4, 24.7, 19.4; IR (cast film, cm^{-1}) 3086, 3061, 3028, 3005, 2942, 2890, 2864, 2836, 1601; HRMS (ESI) calcd for $[M+H]^+$ $C_{20}H_{22}NO$: 292.1696, found: 292.1690.

Pertinent TROESY correlations for stereochemistry:

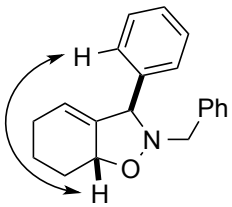

***Anti*-2-(2-Methylpropyl)-3-(propan-2-yl)-2,3,5,6,7,7a-hexahydro-1,2-benzoxazol-4-yl acetate (115a)**

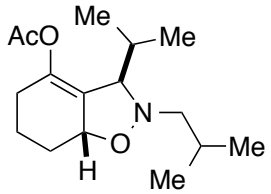

Using 80 mg of acetoxy silane **90a** and 140 mg of nitrone **113b** generated 21 mg of cycloadduct **115a** (40 % yield) was isolated as a clear and colorless oil.

R_f = 0.86 (9:1, hexanes:ethyl acetate); ^{1}H NMR (400 MHz, $CDCl_3$) δ 4.32 – 4.28 (m, 1H), 3.07 (dd, *J* = 7.6, 1.6 Hz, 1H), 2.67 (dd, *J* = 12.0, 5.6 Hz, 1H), 2.36 – 2.30 (m, 1H), 2.30 (dd, *J* = 12.0, 4.0 Hz, 1H), 2.31 – 2.16 (m, 2H), 2.13 (s, 3H), 1.97 – 1.92 (m, 1H), 1.85 – 1.55 (m, 3H), 1.30 – 1.20 (m, 1H), 1.01 (d, *J* = 6.8 Hz, 3H), 0.96 (d, *J* = 6.8 Hz, 3H), 0.92 (d, *J* = 6.4 Hz, 3H), 0.88 (d, *J* = 6.8 Hz, 3H); ^{13}C NMR (125 MHz, $CDCl_3$) δ 168.7, 142.2, 129.4, 75.9, 72.4, 68.6, 31.0, 29.4, 27.1, 26.0, 21.0, 21.0, 20.8, 19.8, 19.6, 19.3; IR (cast film, cm^{-1}) 2954, 2869, 1756; HRMS (ESI) calcd for $[M+H]^+$ $C_{16}H_{28}NO_3$: 282.2064, found: 282.2057.

Pertinent TROESY correlations for stereochemistry:

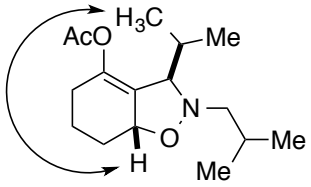

***Anti*-2-(2-Methylpropyl)-3-(propan-2-yl)-2,3,5,6,7,7a-hexahydro-1,2-benzoxazole (115b)**

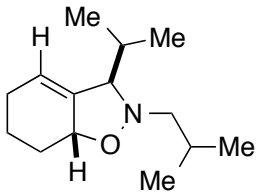

Using 63 mg of allylic silane **90b** and 125 mg of nitrone **113b** generated 21 mg of cycloadduct **115b** (54 % yield) was isolated as a clear and colorless oil.

R_f = 0.24 (1:1, hexanes:DCM); ^{1}H NMR (400 MHz, $CDCl_3$) δ 5.48 (s, 1H), 4.12 – 4.06 (m, 1H), 2.87 – 2.84 (m, 1H), 2.67 (dd, *J* = 12.4, 5.2 Hz, 1H), 2.31 (dd, *J* = 12.8, 8.8 Hz, 1H), 2.17 (dddd, *J* = 12.0, 5.6, 4.4, 3.2 Hz, 1H), 2.12 – 2.05 (m, 2H), 1.92 – 1.79 (m, 2H), 1.75 – 1.63 (m, 1H), 1.50 – 1.38 (m, 1H), 1.21 – 1.11 (m, 1H), 1.00 (d, *J* = 7.2 Hz, 3H), 0.97 (d, *J* = 6.4 Hz, 3H), 0.91 (d, *J* = 6.8 Hz, 3H), 0.90 (d, *J* = 6.8 Hz, 3H); ^{13}C NMR (125 MHz, $CDCl_3$) δ 142.6, 119.3, 75.5, 75.3, 68.0, 30.8, 28.5, 27.1, 24.8, 21.1, 20.9, 19.8, 19.4, 18.4; IR (cast film, cm^{-1}) 3055, 3007, 2953, 2868, 2838; HRMS (EI) calcd for $[M]^+$ $C_{14}H_{25}NO$: 223.1936, found: 223.1936.

Pertinent TROESY correlations for stereochemistry:

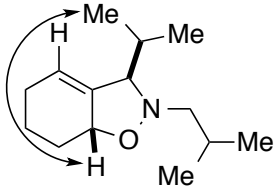

3,3-Dimethyl-2-(propan-2-yl)-2,3,5,6,7,7a-hexahydro-1,2-benzoxazol-4-yl acetate (116a)

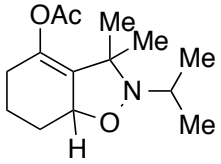

Using 55 mg of allylic silane **90a** and 76 mg of nitrone **113c** generated 9.2 mg of cycloadduct **116a** (20% yield) was isolated as a clear, colorless oil.

R_f = 0.23 (8:2, hexanes:ethyl acetate); ^{1}H NMR (400 MHz, $CDCl_3$) δ 4.32 – 4.27 (m, 1H), 3.12 – 3.01 (m, 1H), 2.22 – 2.09 (m, 2H), 2.17 (s, 3H), 1.99 – 1.91 (m, 2H), 1.70 – 1.58 (m, 2H) 1.41 (s, 3H), 1.30 (s, 3H), 1.23 (d, *J* = 6.4 Hz, 3H), 1.11 (d, *J* = 6.0 Hz, 3H); (Compound was not obtained in high enough purity to obtain ^{13}C NMR spectral data and experimental result could not be replicated); IR (cast film, cm^{-1}) 2974, 2942, 2869, 1759; HRMS (EI) calcd for $[M]^+$ $C_{14}H_{23}NO_3$: 253.1678, found: 253.1675.

3,3-Dimethyl-2-(propan-2-yl)-2,3,5,6,7,7a-hexahydro-1,2-benzoxazole (116b)

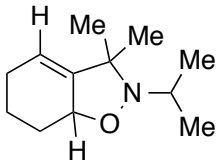

Using 30 mg of allylic silane **90b** and 50 mg of nitrone **113c** generated 9.2 mg of cycloadduct **116b** (58 % yield) was isolated as a clear and colorless oil.

R_f = 0.42 (9:1, hexanes:ethyl acetate); ^{1}H NMR (400 MHz, $CDCl_3$) δ 5.29 (ddd, *J* = 3.0, 3.0, 3.0 Hz, 1H), 4.20 (ddq, *J* = 10.4, 5.2, 2.8 Hz, 1H), 3.05 (app sept, *J* = 6.2 Hz, 1H), 2.15 – 2.06 (m, 2H), 2.05 – 1.95 (m, 1H), 1.88 – 1.81 (m, 1H), 1.46 (tddd, *J* = 13.8, 10.3, 7.0, 3.0 Hz, 1H), 1.32 (s, 3H), 1.29 – 1.15 (m, 1H), 1.21 (s, 3H), 1.21 (d, *J* = 6.0 Hz, 3H), 1.12 (d, *J* = 6.3 Hz, 3H); ^{13}C NMR (100 MHz, $CDCl_3$) δ 152.7, 114.1, 74.7, 64.0, 51.4, 27.5, 27.0, 24.4, 22.6, 22.4, 21.6, 19.4; IR (cast film, cm^{-1}) 2970, 2932, 2864, 1457; HRMS (EI) calcd for $[M]^+$ $C_{12}H_{21}NO$: 195.1623, found: 195.1619.

***Anti*-2-methyl-3-[(*E)*-2-phenylethenyl*]*-2,3,5,6,7,7a-hexahydro-1,2-benzoxazole (117b)**

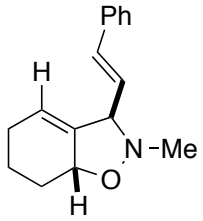

Using 25 mg of allylic silane **90b** and 57 mg of nitrone **113d** generated 4.8 mg of cycloadduct **117b** (29 % yield) was isolated as a clear, colorless oil.

R_f = 0.20 (9:1, hexane:ethyl acetate); ^{1}H NMR (400 MHz, $CDCl_3$) δ 7.42 – 7.39 (m, 2H), 7.34 – 7.29 (m, 2H), 7.26 – 7.22 (m, 1H), 6.56 (d, *J* = 16.0 Hz, 1H), 6.16 (dd, *J* = 15.6, 8.4 Hz, 1H), 5.48 (br s, 1H), 4.32 – 4.28 (m, 1H), 3.60 (br d, *J* = 7.6 Hz, 1H), 2.76 (s, 3H), 2.12 – 2.17 (m, 1H), 2.14 – 2.06 (m, 2H), 1.94 – 1.87 (m, 1H), 1.57 – 1.47 (m, 1H), 1.35 – 1.28 (m, 1H); ^{13}C NMR (125 MHz, $CDCl_3$) δ 144.8, 136.6, 132.8, 128.6, 127.8, 127.5, 126.5, 118.7, 76.5, 74.7, 43.6, 26.8, 24.7, 19.4; IR (cast film, cm^{-1}) 3026, 2930, 2864, 2844, 1678; HRMS (ESI) calcd for $[M+H]^+$ $C_{16}H_{20}NO$: 242.1539, found: 242.1535.

Pertinent TROESY correlations for stereochemistry:

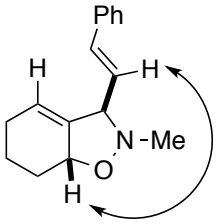

***Syn*-2-methyl-3-[(*E)*-2-phenylethenyl]-2,3,5,6,7,7a-hexahydro-1,2-benzoxazole (epi-117b)**

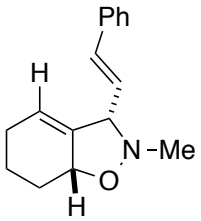

Using 25 mg of allylic silane **90b** and 57 mg of nitrone **113d** generated 2.2 mg of cycloadduct epi-**117b** (13 % yield) was isolated as a clear, colorless oil.

R_f = 0.39 (9:1, hexane:ethyl acetate); ^{1}H NMR (400 MHz, $CDCl_3$) δ 7.42 - 7.25 (m, 5H), 6.54 (d, *J* = 15.8 Hz, 1H), 6.08 (dd, *J* = 15.9, 8.5 Hz, 1H), 5.47 (br s, 1H), 4.53 (br s, 1H), 3.82 (br s, 1H), 2.80 (s, 3H), 2.19 – 2.01 (m, 3H), 1.93 – 1.86 (m, 1H), 1.58 – 1.46 (m, 1H), 1.39 – 1.27 (m, 1H); ^{13}C NMR (125 MHz, $CDCl_3$) δ 143.8, 136.6, 133.7, 128.6, 127.8, 126.8, 126.5, 119.8, 74.3, 72.6, 45.0, 27.8, 24.4, 19.3; IR (cast film, cm^{-1}) 3026, 2930, 2864, 2844, 1678; HRMS (ESI) calcd for $[M+H]^+$ $C_{16}H_{20}NO$: 242.1539, found: 242.1535.

Stereochemistry was tentatively assigned based on analogy from previous cycloadducts.

General Procedure for allene cycloaddition with azomethine imines.

The allylic silane **90a** or **90b**, and the appropriate azomethine imine **118a-d** (3 equiv) were added to a flask and an argon atmosphere was established via a purge needle. Acetonitrile (0.1 M) was added and cesium fluoride (5 equiv) was added to the reaction flask while maintaining the argon atmosphere via steady stream of argon from a purge needle. The reaction was monitored by TLC until completion, concentrated, and subjected to flash column chromatography on silica affording cycloadducts **119-122**.

***Anti*-3-Oxo-9-(propan-2-yl)-2,3,5,6,7,9-hexahydro-1*H*,4a*H*-pyrazolo[1,2-*a*]indazol-8-yl acetate (119a)**

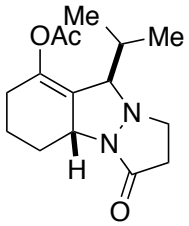

Using 35 mg of acetoxy silane **90a** and 36 mg of azomethine imine **118a** generated 10.1 mg of cycloadduct **119a** (44 % yield) was isolated as a clear, colorless oil.

R_f = 0.22 (ethyl acetate); ^{1}H NMR (400 MHz, $CDCl_3$) δ 3.87 (br s, 1H), 3.54 (td, *J* = 6.0, 2.0 Hz, 1H), 3.18 (dq, *J* = 3.8, 2.3 Hz, 1H), 2.87 – 2.76 (m, 3H), 2.59 – 2.50 (m, 1H), 2.34 – 2.27 (m, 1H), 2.17 – 2.10 (m, 1H), 2.13 (s, 3H), 2.04 – 1.99 (m, 1H), 1.81 (dqq, *J* = 7.0, 6.8, 4.0 Hz, 1H), 1.66 – 1.60 (m, 2H), 0.95 (d, *J* = 7.0 Hz, 3H), 0.93 (d, *J* = 6.8 Hz, 3H); ^{13}C NMR (125 MHz, $CDCl_3$) δ 168.4, 164.0, 142.8, 127.9, 72.1, 55.0, 54.5, 36.0, 31.7, 26.4, 25.1, 20.9, 20.4, 20.1, 17.2; IR (cast film, cm^{-1}) 2963, 2937, 2871, 2843, 1755, 1683; HRMS (EI) calcd for $[M]^+$ $C_{15}H_{22}N_2O_3$: 278.1630, found: 278.1628.

Pertinent TROESY correlations for stereochemistry:

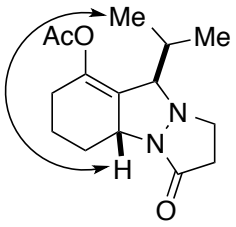

***Anti*-9-(Propan-2-yl)-1,2,5,6,7,9-hexahydro-3*H*,4a*H*-pyrazolo[1,2-*a*]indazol-3-one (119b)**

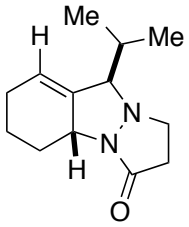

Using 25 mg of allylic silane **90b** and 29 mg of azomethine imine **118a** generated 9.4 mg of cycloadduct **119b** (63% yield) was isolated as a clear, colorless oil.

R_f = 0.17 (ethyl acetate); ^{1}H NMR (400 MHz, $CDCl_3$) δ 5.51 (br s, 1H), 3.71 (br s, *J* = 9.2 Hz, 1H), 3.61 – 3.53 (m, 1H), 2.98 – 2.95 (m, 1H), 2.87 – 2.75 (m, 3H), 2.64 – 2.52 (m, 1H), 2.19 – 2.02 (m, 2H), 1.94 – 1.87 (m, 1H), 1.78 (dsept, *J* = 6.9, 5.1 Hz, 1H), 1.59 – 1.37 (m, 2H), 0.96 (d, *J* = 6.8 Hz, 6H); ^{13}C NMR (125 MHz, $CDCl_3$) δ 163.9, 140.7, 120.8, 74.9, 54.3, 54.2, 36.0, 32.5, 25.2, 24.7, 19.7, 19.2, 18.1; IR (cast film, cm^{-1}) 2960, 2933, 2870, 2837, 1679; HRMS (EI) calcd for $[M]^+$ $C_{13}H_{20}N_2O$: 220.1575, found: 220.1580.

Pertinent TROESY correlations for stereochemistry:

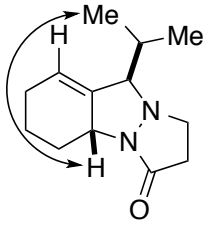

Anti-3-Oxo-9-phenyl-2,3,5,6,7,9-hexahydro-1*H*,4a*H*-pyrazolo[1,2-*a*]indazol-8-yl acetate (120a)

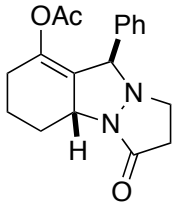

Using 50 mg of allylic silane **90a** and 63 mg of azomethine imine **118b** generated 12.5 mg of cycloadduct **120a** (51% yield) was isolated as a clear, colorless oil.

R_f = 0.25 (ethyl acetate); ^{1}H NMR (500 MHz, $CDCl_3$) δ 7.37 – 7.29 (m, 5H), 4.27 (br s, 1H), 4.20 (app q, *J* = 2.3 Hz, 1H), 3.45 (dt, *J* = 9.7, 6.2 Hz, 1H), 2.97 (app q, *J* = 9.8 Hz, 1H), 2.82 – 2.77 (m, 1H), 2.71 (dd, *J* = 9.8, 6.3 Hz, 2H), 2.37 – 2.30 (m, 1H), 2.17 – 2.04 (m, 2H), 1.81 – 1.67 (m, 2H), 1.74 (s, 3H); ^{13}C NMR (125 MHz, $CDCl_3$) δ 167.9, 166.9, 143.1, 137.9, 130.1, 128.7, 128.4, 128.4, 70.8, 55.3, 49.5, 35.4, 26.4, 25.2, 20.3, 20.1; IR (cast film, cm^{-1}) 3031, 2943, 2869, 2841, 1755, 1728, 1686; HRMS (EI) calcd for $[M]^+$ $C_{18}H_{20}N_2O_3$: 312.1474, found: 312.1468.

Pertinent ROESY correlations for stereochemistry:

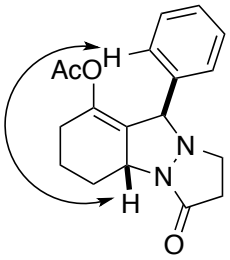

***Anti*-9-Phenyl-1,2,5,6,7,9-hexahydro-3*H*,4a*H*-pyrazolo[1,2-*a*]indazol-3-one (120b)**

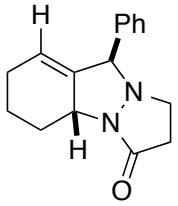

Using 32 mg of allylic silane **90b** and 44 mg of azomethine imine **118b** generated 10.3 mg of cycloadduct **120b** (46 % yield) was isolated as a clear, colorless oil that would crystalize upon prolonged evaporation to give long, clear, slightly yellow crystals.

R_f = 0.2 (ethyl acetate); mp = 100.4 – 104 °C; ^{1}H NMR (500 MHz, $CDCl_3$) δ 7.40 – 7.33 (m, 5H), 5.52 (app p, *J* = 3.4 Hz, 1H), 4.19 (br s, 1H), 4.10 (br s, *J* = 8.7 Hz, 1H), 3.43 (ddd, *J* = 9.7, 7.8, 5.1 Hz, 1H), 2.98 (app q, *J* = 9.7 Hz, 1H), 2.81 – 2.75 (m, 1H), 2.73 – 2.60 (m, 2H), 2.18 – 2.08 (m, 2H), 1.98 – 1.91 (m, 1H), 1.65 – 1.49 (m, 2H); ^{13}C NMR (125 MHz, $CDCl_3$) δ 167.8, 143.2, 139.3, 128.8, 128.1, 127.9, 121.6, 72.3, 54.7, 49.3, 35.4, 25.7, 24.4, 19.7; IR (cast film, cm^{-1}) 3058, 3029, 2939, 2865, 2836, 1696; HRMS (EI) calcd for $[M]^+$ $C_{16}H_{18}N_2O$: 254.1419, found: 254.1419.

X-ray quality crystals were grown via slow evaporation from a solution of ethyl acetate. Relative stereochemistry was determined by x-ray crystallography (Appendix IV).

***Anti*-3-oxo-9-(2-phenylethyl)-1H,2H,3H,4aH,5H,6H,7H,9H-pyrazolidino[1,2-a]indazol-8-yl acetate (121a)**

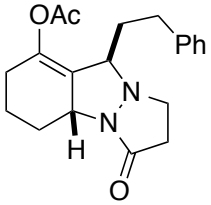

Using 38 mg of allylic silane **90a** and 56 mg of azomethine imine **118c** generated 16 mg of cycloadduct **121a** (46 % yield) was isolated as a slightly yellowish oil.

R_f = 0.20 (ethyl acetate); ^{1}H NMR (500 MHz, $CDCl_3$) δ 7.31 – 7.26 (m, 2H), 7.21 – 7.16 (m, 3H), 3.99 (br s, 1H), 3.64 (app. td, *J* = 8.5, 3.0 Hz, 1H), 3.39 (br s, 1H), 2.94 – 2.61 (m, 6H), 2.36 – 2.31 (m, 1H), 2.21 – 2.14 (m, 1H), 2.10 (s, 3H), 2.08 – 2.03 (m, 1H), 1.94 – 1.80 (m, 2H), 1.71 – 1.64 (m, 2H); ^{13}C NMR (125 MHz, $CDCl_3$) δ 168.4, 165.2, 142.6, 141.5, 128.5, 128.5, 128.4, 126.0, 65.5, 54.1, 52.4, 35.7, 34.4, 31.7, 26.3, 25.1, 20.8, 20.3; IR (cast film, cm^{-1}) 3085, 3060, 3026, 2936, 2864, 1753, 1678; HRMS (ESI) calcd for $[M]^+$ $C_{20}H_{24}N_2O_3$: 340.1786, found: 340.1787.

Stereochemistry was tentatively assigned based on analogy from previous cycloadducts.

Anti-9-(2-phenylethyl)-1H,2H,3H,4aH,5H,6H,7H,9H-pyrazolidino[1,2-a]indazol-3-one (121b)

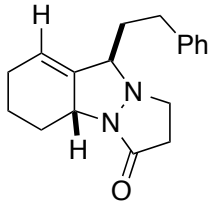

Using 30 mg of allylic silane **90b** and 47 mg of azomethine imine **118c** generated 21.9 mg of cycloadduct **121b** (76 % yield) was isolated as a clear, colorless oil, as a mixture of 2 isomers in an approximate 8:1 ratio.

Data is given for major isomer only. R_f = 0.20 (ethyl acetate); ^{1}H NMR (500 MHz, $CDCl_3$) δ 7.31 (m, 2H), 7.23 – 7.21 (m, 3H), 5.58 (br s, 1H), 3.87 (br s, 1H), 3.61 (app. td, *J* = 6.0, 2.0 Hz, 1H), 3.25 (br s, 1H), 2.94 – 2.63 (m, 5H), 2.20 – 2.06 (m, 2H), 1.98 – 1.82 (m, 3H), 1.62 – 1.49 (m, 3H); ^{13}C NMR (125 MHz, $CDCl_3$) δ 165.3, 141.9, 141.6, 128.5, 128.3, 126.0, 120.4, 68.1, 53.7, 51.7, 35.8, 35.3, 32.1, 25.4, 24.5, 19.7; IR (cast film, cm^{-1}) 3026, 2934, 2860, 1679; HRMS (ESI) calcd for $[M]^+$ $C_{18}H_{22}N_2O$: 282.1732, found: 282.1735.

Stereochemistry was tentatively assigned based on analogy from previous cycloadducts.

Mixture of *Syn*- and *Anti*-3-oxo-9-[(E)-2-phenylethenyl]-1H,2H,3H,4aH,5H,6H,7H,9H-pyrazolidino[1,2-a]indazol-8-yl acetate (122a)

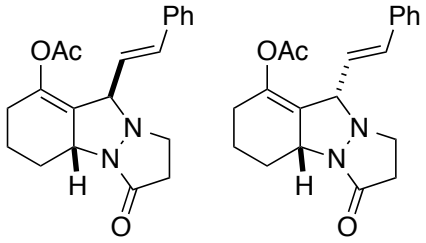

Using 30 mg of allylic silane **90a** and 45 mg of azomethine imine **118d** generated 15.6 mg of cycloadducts **122a** (65 % yield) was isolated as a 1:1 mixture of diastereomers as a yellowish oil.

Data is given for the two compounds, as the mixture was inseparable by flash column chromatography.

R_f = 0.10 (ethyl acetate); ^{1}H NMR (400 MHz, $CDCl_3$) δ 7.43 – 7.24 (m, 10H), 6.58 (d, *J* = 15.9 Hz, 1H), 6.57 (d, *J* = 15.7 Hz, 1H), 6.17 (dd, *J* = 15.9, 9.0 Hz, 1H), 6.04 (dd, *J* = 15.7, 8.7 Hz, 1H), 4.44 – 4.41 (m, 1H), 4.15 (app d, *J* = 9.6 Hz, 1H), 3.92 (d, *J* = 8.4 Hz, 1H), 3.61 (app dt, *J* = 9.1, 2.7 Hz, 1H), 3.57 – 3.51 (m, 2H), 3.06 – 2.95 (m, 2H), 2.87 – 2.78 (m, 1H), 2.74 – 2.62 (m, 4H), 2.40 – 2.30 (m, 2H), 2.29 – 1.98 (m, 5H), 1.96 (s, 3H), 1.81 – 1.59 (m, 3H), 1.71 (s, 3H), 1.50 – 1.40 (m, 1H); ^{13}C NMR (125 MHz, $CDCl_3$) δ 170.6, 169.0, 168.6, 168.0, 143.4, 142.2, 136.0, 134.1, 133.8, 128.8, 128.7, 128.3, 128.2, 128.1, 127.1, 126.5, 126.4, 125.0, 124.8, 70.7, 60.4, 54.5, 48.8, 35.1, 33.3, 27.1, 26.5, 26.3, 25.4, 21.1, 20.6, 20.5, 20.2, 19.6, 14.2 (One sp^2 hybridized carbon is missing, presumed to be coincidental with another signal); IR (cast film, cm^{-1}) 2925, 2855, 1757, 1644; HRMS (ESI) calcd for $[M+Na]^+$ $C_{20}H_{22}N_2NaO_3$: 361.1523, found: 361.1523.

Mixture of *Syn* and *Anti*-9-[(E)-2-phenylethenyl]-1H,2H,3H,4aH,5H,6H,7H,9H-pyrazolidino[1,2-a]indazol-3-one (122b)

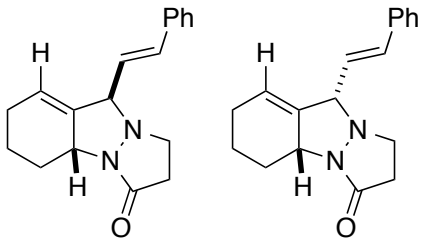

Using 32 mg of allylic silane **90b** and 55 mg of azomethine imine **118d** generated 10.3 mg of cycloadduct **122b** (99 % yield) was isolated as a slightly yellow oil in a 1:1 ratio of diastereomers.

Data is given for the two compounds, as the mixture was inseparable by flash column chromatography.

R_f = 0.15 (ethyl acetate); ^{1}H NMR (400 MHz, $CDCl_3$) δ 7.44 – 7.24 (m, 13H), 6.64 (d, *J* = 16.1 Hz, 1H), 6.59 (d, *J* = 15.9 Hz, 1H), 6.07 (dd, *J* = 15.7, 8.7 Hz, 1H), 6.04 (dd, *J* = 16.0, 8.1 Hz, 1H), 5.65 (br s, 1H), 5.57 (br s, 1H), 4.30 – 4.25 (m, 1H), 4.05 (br s, 1H), 3.88 (br d, *J* = 8.6 Hz, 1H), 3.65 – 3.57 (m, 1H), 3.52 – 3.46 (m, 1H), 3.11 (app q, *J* = 9.3 Hz, 1H), 3.01 (app q, *J* = 10.5 Hz, 1H), 2.93 – 2.84 (m, 1H), 2.78 – 2.62 (m, 4H, 2.43 – 2.37 (m, 1H), 2.21 – 2.05 (m, 4H), 1.96 – 1.88 (m, 2H), 1.67 – 1.46 (m, 4H), 1.40 – 1.24 (m, 2H); ^{13}C NMR (125 MHz, $CDCl_3$) δ 169.5, 168.5, 141.3, 141.1, 136.1, 135.8, 133.8, 128.7, 128.7, 128.3, 128.1, 126.6, 126.6, 125.2, 124.4, 121.8, 121.8, 71.8, 70.5, 53.8, 53.7, 50.0, 35.0, 33.8, 29.7, 27.5, 26.1, 24.4, 23.9, 19.9, 19.6 (One sp^2 hybridized carbon is missing, presumed to be coincidental with another signal); IR (cast film, cm^{-1}) 2925, 2855, 1745, 1662; HRMS (ESI) calcd for $[M+H]^+$ $C_{18}H_{21}N_2O$: 281.1648, found: 281.1644.

Cyclic allene/phenyl azide cycloaddition

Allylic silane **90b** and the appropriate azide **127a-g** (5 equiv) were added to a flask and an argon atmosphere was established via a purge needle. Dry acetonitrile (0.15 M) was added and cesium fluoride (5 equiv) was added to the reaction flask maintaining the argon atmosphere by a stream of argon from a purge needle. The reaction was left for 18 h, concentrated, and subjected to flash column chromatography on silica affording cycloadducts **128-134**.

1-(4-Nitrophenyl)-1,1a,2,3,4,4a,6,7,8,8a-decahydrobiphenyleno[1,8b-b]azirene (128)

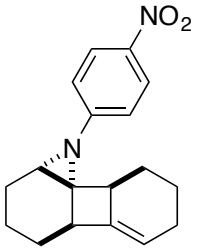

Using 50 mg of allylic silane **90b** and 115 mg of azide **127a** generated 10.6 mg of cycloadduct **128** was isolated as a slightly yellow oil, (52 % yield). Used (99:1, DCM:ethyl acetate) as the eluent for column chromatography.

R_f = 0.85 (8:2 hexanes:ethyl acetate); ^{1}H NMR (400 MHz, $CDCl_3$) δ 8.14 (m, 2H), 7.01 (m, 2H), 5.46 (app. p, *J* = 3.0 Hz, 1H), 3.46 (broad s, 1H), 3.21 (broad s, 1H), 2.57 (dd, *J* = 4.1, 1.5 Hz, 1H), 2.19 – 2.10 (m, 1H), 2.07 – 1.95 (m, 2H), 1.85 – 1.76 (m, 2H), 1.74 – 1.66 (m, 1H), 1.44 – 1.13 (m, 5H), 0.98 – 0.87 (m, 1H); ^{13}C NMR (125 MHz, $CDCl_3$) δ 157.8, 142.2, 139.7, 125.1, 120.2, 115.5, 51.3, 45.5, 43.4, 39.7, 25.5, 25.1, 25.0, 24.9, 21.1, 17.5; IR (cast film, cm^{-1}) 2932, 2858, 1630, 1597; HRMS (ESI) calcd for $[M+Na]^+$ $C_{18}H_{20}N_2NaO_2$: 319.1417, found: 319.1417.

Pertinent TROESY correlations for relative stereochemistry:

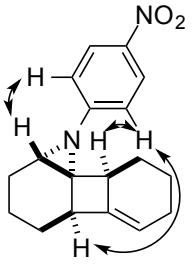

4-[(4-Nitrophenyl)amino]-dodecahydrobiphenylen-4a-ol (135)

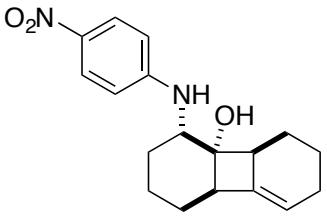

Allylic silane **90b** and azide **127a** (5 equiv) were added to a flask and an argon atmosphere was established via a purge needle. Dry acetonitrile (0.15 M) was added and cesium fluoride (5 equiv) was added to the reaction flask maintaining the argon atmosphere by a stream of argon from a purge needle. The reaction was left for 18 h, at

which point TLC analysis indicated the starting allylic silane had been consumed. 1M HCl (30 mL) was added to the reaction mixture in the fume hood and ether (30 mL) was added. The two layers were separated and the aqueous layer was further washed with ether (2 x 30 mL). The combined organic fractions were washed with distilled water (30 mL), brine (30 mL), dried with magnesium sulfate, filtered, concentrated, and subjected to flash column chromatography (99:1, DCM:ethyl acetate) on silica affording amino alcohol **135** (35 % yield) as a yellow oil.

Using 80 mg of allylic silane **90b** and 181 mg of azide **127a** generated 12 mg of amino alcohol **135** was obtained.

R_f = 0.30 (99:1, DCM:ethyl acetate); ^{1}H NMR (700 MHz, $CDCl_3$) δ 8.08 (d, *J* = 9.1 Hz, 2H), 6.47 (d, *J* = 9.1 Hz, 2H), 5.48 (br s, 1H), 5.45 (br d, *J* = 8.4 Hz, 1H), 3.53 (ddd, *J* = 11.9, 8.4, 2.8 Hz, 1H), 3.14 (br s, 1H), 2.70 – 2.68 (m, 1H), 2.10 (br s, 2H), 2.05 – 1.99 (m, 1H), ; ^{13}C NMR (175 MHz, $CDCl_3$) δ 152.3, 137.4, 133.5, 126.8, 115.3, 111.0, 74.3, 53.4, 53.3, 51.3, 25.5, 24.8, 22.2, 21.4, 21.3, 20.8, ; IR (cast film, cm^{-1}) 3471, 3405, 2929, 2857, 1604; HRMS (ESI) calcd for $[M+H]^+$ $C_{18}H_{23}N_2O_3$: 315.1703, found: 315.1702.

Ethyl 4-(2,3,4,4a,6,7,8,8a-octahydrobiphenyleno[1,8b-b]aziren-1(1aH)-yl)benzoate (129)

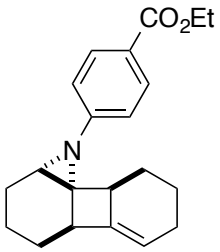

Using 65 mg of allylic silane **90b** and 172 mg of azide **127b** generated 14.8 mg of cycloadduct **129** (51 %) was isolated as a clear and slightly yellow oil. Used (99:1, DCM:ethyl acetate) as the eluent for column chromatography.

R_f = 0.38 (99:1, DCM/ethyl acetate); ^{1}H NMR (500 MHz, $CDCl_3$) δ 7.95 (m, 2H), 7.00 (m, 2H), 5.45 (app q, *J* = 2.9 Hz, 1H), 4.36 (q, *J* = 7.1 Hz, 2H), 3.46 (br s, 1H), 3.20 (br s, 1H), 2.54 (dd, *J* = 4.1, 1.5 Hz, 1H), 2.14 (app ddqd, *J* = 18.0, 6.4, 3.3, 1.4 Hz, 1H), 2.08 – 1.97 (m, 2H), 1.84 – 1.77 (m, 2H), 1.71 – 1.65 (m, 1H), 1.43 – 1.37 (m, 2H), 1.40 (t, *J* = 7.1 Hz, 3H), 1.34 – 1.19 (m, 2H), 1.12 (app. ddt, *J* = 12.3, 6.4, 3.5 Hz, 1H), 0.91 (dddd, *J*

= 13.4, 11.8, 10.3, 2.9 Hz, 1H); ^{13}C NMR (125 MHz, $CDCl_3$) δ 166.7, 155.8, 140.3, 130.7, 123.7, 120.1, 115.0, 60.6, 50.8, 45.7, 43.4, 39.1, 25.6, 25.2, 25.1, 25.0, 21.2, 17.6, 14.4; IR (cast film, cm^{-1}) 3041, 2980, 2932, 2857, 1712, 1603, 1507; HRMS (ESI) calcd for $[M+Na]^+$ $C_{21}H_{25}NNaO_2$: 346.1778, found: 346.1775.

Pertinent TROESY correlations for stereochemistry:

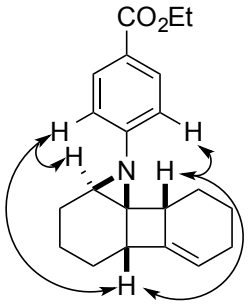

3-{13-Azatetracyclo[6.5.0.0^{1},^{12}.0^{2},^{7}]tridecan-13-yl}cyclohex-2-en-1-one (134)

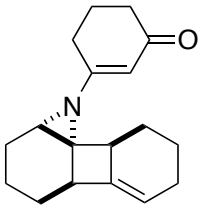

Using 50 mg of allylic silane **90b** and 92 mg of azide **127c** generated 3.4 mg of aziridine **134** (18 % yield) was obtained as a clear, colorless oil. Used (99:1, DCM:ethyl acetate) as the eluent for column chromatography.

R_f = 0.44 (1:1, diethyl ether:hexanes); ^{1}H NMR (500 MHz, $CDCl_3$) δ 5.56 (s, 1H), 5.45 (app p, *J* = 2.9, 1H), 3.40 (br s, 1H), 3.26 (m, 1H), 2.51 – 2.40 (m, 2H), 2.38 – 2.35 (m, 2H), 2.20 – 2.13 (m, 1H), 2.09 – 1.90 (m, 3H), 1.89 – 1.83 (m, 1H), 1.82 – 1.69 (m, 3H), 1.56 (dtd, *J* = 12.3, 6.4, 3.3, 1H), 1.50 – 1.35 (m, 2H), 1.30 – 1.15 (m, 3H), 1.08 – 1.00 (m, 1H); ^{13}C NMR (125 MHz, $CDCl_3$) δ 199.1, 139.6, 133.5, 115.3, 110.4, 50.6, 45.4, 44.3, 38.2, 37.0, 30.3, 29.1, 25.4, 25.1, 24.9, 22.4, 21.1, 17.2; IR (cast film, cm^{-1}) 3061, 3029, 2931, 2861, 1721; HRMS (ESI) calcd for $[M+H]^+$ $C_{18}H_{24}NO$: 270.1852, found: 270.1851.

Stereochemistry was tentatively assigned based on analogy from previous cycloadducts.

(E)-2-{13-Azatetracyclo[6.5.0.0^{1},^{12}.0^{2},^{7}]tridecan-13-yl}-1-phenylethenyl acetate (133)

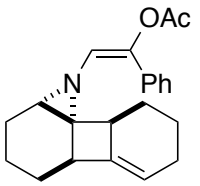

Using 50 mg of allylic silane **90b** and 135 mg of azide **127a** generated 4.8 mg of aziridine **133** (21 % yield) was obtained as a clear, yellow oil. Used (99:1, DCM:ethyl acetate) as the eluent for column chromatography.

R_f = 0.40 (9:1, DCM:ethyl acetate); ^{1}H NMR (500 MHz, $CDCl_3$) δ 7.32 – 7.29 (m, 4H), 7.24 – 7.21 (m, 1H), 6.27 (s, 1H), 5.44 (app p, *J* = 2.7 Hz, 1H), 3.27 (br s, 1H), 3.22 – 3.19 (m, 1H), 2.34 (s, 3H), 2.26 (br d, *J* = 4.1 Hz, 1H), 2.21 – 2.13 (m, 1H), 2.09 – 2.01 (m, 1H), 1.87 (br d, *J* = 14.5 Hz, 1H), 1.83 – 1.76 (m, 2H), 1.73 – 1.65 (m, 2H), 1.54 – 1.46 (m, 1H), 1.38 – 1.22 (m, 3H), 1.13 – 1.04 (m, 1H); ^{13}C NMR spectral data could not be obtained for the compound as it decomposed in chloroform to an intractable mixture; IR (cast film, cm^{-1}) 3062, 2925, 1699, 1653; HRMS (EI) calcd for $[M]^+$ $C_{22}H_{25}NO_2$: 335.1885, found: 335.1882.

Stereochemistry was tentatively assigned based on analogy from previous cycloadducts.

General Procedure for cyclic allene cycloaddition with α-azidostyrenes.

Allylic silane **90b**, and the appropriate α-azidostyrene **145a-d** (5 equiv) were added to a flask and an argon atmosphere was established via a purge needle. THF (0.6 M) was added and tetrabutylammonium fluoride (2 equiv of 1 M TBAF in THF was diluted to 0.2 M and added at a rate of 2 mL/h) was added via syringe pump. Once the addition was complete the reaction was stirred for an additional hour, concentrated, and subjected to flash column chromatography on silica affording cycloadducts **146-149**.

2-(4-MethoxyPhenyl)-4,5,6,7-tetrahydro-1*H*-indole (146)

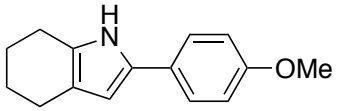

Using 21 mg of allylic silane **90b** and 52 mg of azide **145a** generated 8 mg of cycloadduct **146** (66 % yield) was isolated as a beige solid. The solid showed a melting point of 158 - 160 °C (uncorrected). Used (95:5:10, hexanes:ethyl acetate:DCM) as the eluent for column chromatography.

R_f = 0.26 (1:1 hexanes:DCM); ^{1}H NMR (500 MHz, $CDCl_3$) δ 7.85 (br s, 1H), 7.38 (m, 2H), 6.91 (m, 2H), 6.18 (d, *J* = 2.6 Hz, 1H), 3.84 (s, 3H), 2.65 (t, *J* = 6.2 Hz, 2H), 2.56 (t, *J* = 6.2 Hz, 2H), 1.89 – 1.77 (m, 4H); ^{13}C NMR (125 MHz, $CDCl_3$) δ 157.9, 130.3, 127.7, 126.4, 124.9, 118.7, 114.3, 104.1, 55.3, 23.8, 23.4, 22.9, 22.9; IR (cast film, cm^{-1}) 3436, 3389, 3062, 2922, 2850, 1739 1606; HRMS (EI) calcd for $[M]^+$ $C_{15}H_{17}NO$: 227.1310, found: 127.1309.

2-Phenyl-4,5,6,7-tetrahydro-1*H*-indole (147)

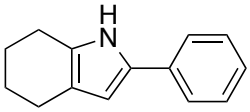

Using 20 mg of allylic silane **90b** and 41 mg of azide **145b** generated 6.0 mg of cycloadduct **147** (47 % yield) was isolated as an off-white solid. The solid showed a melting point of 107 - 108 °C (uncorrected). Used (95:5:10, hexanes:ethyl acetate:DCM) as the eluent for column chromatography.

R_f = 0.30 (9:1 hexanes:DCM); ^{1}H NMR (400 MHz, $CDCl_3$) δ 7.95 (br s, 1H), 7.46 – 7.43 (m, 2H), 7.37 – 7.32 (m, 2H), 7.19 – 7.15 (m, 1H), 6.30 (d, *J* = 2.7 Hz, 1H), 2.66 (broad t, *J* = 6.2 Hz, 2H), 2.57 (broad t, *J* = 6.1 Hz, 2H), 1.91 – 1.78 (m, 4H); ^{13}C NMR (100 MHz, $CDCl_3$) δ 133.2, 130.3, 128.8, 128.5, 125.5, 123.4, 119.0, 105.2, 23.8, 23.4, 22.9, 22.9; IR (cast film, cm^{-1}) 3287, 3062, 2930, 2852, 1670; HRMS (EI) calcd for $[M]^+$ $C_{14}H_{15}N$: 197.1204, found: 197.1204.

2-(Pyridin-2-yl)-4,5,6,7-tetrahydro-1*H*-indole (148)

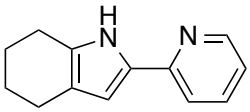

Using 20 mg of allylic silane **90b** and 38 mg of azide **145c** generated 1.7 mg of cycloadduct **148** (15 % yield) was isolated as a pinkish oil. Used (95:5:10, hexanes:ethyl acetate:DCM) as the eluent for column chromatography.

R_f = 0.25 (8:2, hexanes/ethyl acetate); ^{1}H NMR (400 MHz, $CDCl_3$) δ 9.17 (br s, 1H), 8.41 (ddd, *J* = 5.0, 1.8, 1.0 Hz, 1H), 7.57 (ddd, *J* = 9.2, 7.5, 1.9 Hz, 1H), 7.46 (ddd, *J* = 8.0, 1.0, 1.0 Hz, 1H), 6.96 (ddd, *J* = 7.3, 4.9, 1.1 Hz, 1H), 6.46 (d, *J* = 2.5 Hz, 1H), 2.63 (t, *J* = 6.0 Hz, 2H), 2.55 (t, *J* = 6.4 Hz, 2H), 1.87 – 1.74 (m, 4H); ^{13}C NMR (100 MHz, $CDCl_3$) δ 150.9, 148.7, 136.2, 129.9, 129.5, 119.7, 119.3, 117.5, 106.4, 23.8, 23.3, 22.9, 22.8; IR (cast film, cm^{-1}) 3208, 3164, 2925, 2851, 1598, 1509; HRMS (EI) calcd for $[M]^+$ $C_{13}H_{14}N_2$: 198.1156, found: 198.1156.

2-(3-Nitrophenyl)-4,5,6,7-tetrahydro-1*H*-indole (149)

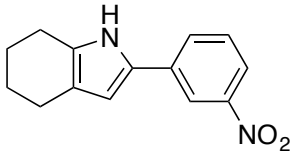

Using 30 mg of allylic silane **90b** and 80 mg of azide **145d** generated 9.4 mg of cycloadduct **149** (34 % yield) was isolated as a bright orange, powdery solid. The solid had a melting point of 163 – 165 °C (uncorrected). Used (95:5:10, hexanes:ethyl acetate:DCM) as the eluent for column chromatography.

R_f = 0.26 (1:1 hexanes:DCM); ^{1}H NMR (500 MHz, $CDCl_3$) δ 8.23 (dd, *J* = 2.0, 2.0 Hz, 1H), 8.12 (br s, 1H), 7.97 (ddd, *J* = 8.2, 2.3, 1.0 Hz, 1H), 7.72 (broad d, *J* = 8.1 Hz, 1H), 7.48 (dd, *J* = 8.0, 8.0 Hz, 1H), 6.43 (d, *J* = 2.7 Hz, 1H), 2.68 (broad t, *J* = 6.0 Hz, 2H), 2.57 (broad t, *J* = 6.1 Hz, 2H), 1.91 – 1.78 (m, 4H); ^{13}C NMR (125 MHz, $CDCl_3$) δ 134.7, 134.7, 130.4, 129.7, 128.7, 127.7, 119.7, 119.7 117.3, 107.3, 23.6, 23.2, 22.9, 22.8; IR (cast film, cm^{-1}) 3375, 3096, 2919, 2839, 1534; HRMS (EI) calcd for $[M]^+$ $C_{14}H_{14}N_2O_2$: 242.1055, found: 242.1054.

The alternate procedure employing cesium fluoride was also used:

Allylic silane **90b** and α-azido(3-nitro)styrene **136d** (5 equiv) were added to a flask and an argon atmosphere was established via a purge needle. Acetonitrile (0.2 M) and cesium fluoride (5 equiv) was added to the reaction flask maintaining the argon atmosphere. The

reaction was left for 18 h, concentrated, and subjected to flash column chromatography on silica affording cycloadduct **140** (43 %). Spectral data is the same as above.

2-Phenyl-3-methyl-4,5,6,7-tetrahydro-1*H*-indole (155)

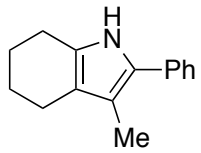

Using 32 mg of allylic silane **90b** and 70 mg of azide **154** generated 4.1 mg of cycloadduct **155** (22 % yield) was isolated as a clear and colorless oil. Used (95:5:10, hexanes:ethyl acetate:DCM) as the eluent for column chromatography.

R_f = 0.30 (9:1, hexanes/DCM); ^{1}H NMR (400 MHz, $CDCl_3$) δ 7.69 (br s, 1H), 7.43 – 7.37 (m, 4H), 7.23 – 7.19 (m, 1H), 2.64 (br t, *J* = 5.8 Hz, 2H), 2.51 – 2.48 (m, 2H), 2.18 (s, 3H), 1.89 – 1.80 (m, 4H). Other spectral data is unavailable due to the material decomposing and failure to reproduce the reaction.

2-Bromo-3-hydroxycyclohex-1-ene-1-carbonitrile (157)

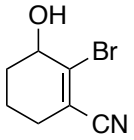

In a procedure modified from that of Agosta and Lowrance,[61] allylic alcohol **157** was prepared via the addition of diethylaluminum cyanide (5 equiv) to a toluene solution of 500 mg of ethoxy enone **156**. The reaction was monitored by TLC until the starting material had been consumed and the reaction was quenched with a 0.1 M sodium hydroxide solution. The aqueous layer was extracted with ethyl acetate (30 mL x 3), followed by washing the organic layers with 5% sodium carbonate solution, brine, and finally dried with sodium sulfate, and filtered.

Once concentrated the crude reaction mixture was dissolved in methanol (0.4 M), and cerium trichloride•heptahydrate (~1.1 equiv) was added to the solution. Once all the solids had dissolved, sodium borohydride (~1.1 equiv) was added to the solution carefully (caution: gas evolved). The reaction was stirred at room temperature for five minutes followed by quenching of the reaction with water and 1 M HCl (25 mL each).

The aqueous layer was extracted with diethyl ether (40 mL x 3). The organic layers were combined and washed successively with 1 M HCl, distilled water (40 mL x 3), and brine. The organic layer was dried with magnesium sulfate, filtered, and concentrated. The crude material was subjected to flash column chromatography (9:1, hexanes:ethyl acetate) on silica to yield 89.1 mg of a clear, colorless oil, allylic alcohol **157** (19 % yield over two steps).

R_f = 0.50 (7:3, hexanes/ethyl acetate); ^{1}H NMR (500 MHz, $CDCl_3$) δ 4.34 (br q, *J* = 5.0 Hz, 1H), 2.48 (d, *J* = 4.7 Hz, 1H), 2.41 (dtd, *J* = 17.7, 5.7, 1.7 Hz, 1H), 2.31 (dddd, *J* = 17.6, 7.5, 5.6, 1.5 Hz, 1H), 2.04 – 1.84 (m, 3H), 1.80 – 1.72 (m, 1H); ^{13}C NMR (125 MHz, $CDCl_3$) δ 140.4, 117.3, 117.0, 69.6, 30.8, 30.2, 17.5; IR (cast film, cm^{-1}) 3419, 2950, 2869, 2223, 1618; HRMS (EI) calcd for $[M]^+$ $C_7H_8NO^{79}Br$: 200.9789, found: 200.9786.

2-Bromo-3-cyanocyclohex-2-en-1-yl pyridine-2-carboxylate (158)

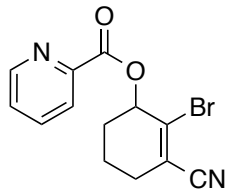

To a DCM (0.6 M) solution of dicyclohexylcarbodiimide (1.2 equiv) and picolinic acid (1.2 equiv) cooled to 0 °C was added solid DMAP (0.3 equiv). A DCM (0.6 M) solution of allylic alcohol **157** (89 mg) was then transferred via cannula to the cooled solution. The solution was warmed to room temperature, and stirred until the alcohol starting material had been consumed as determined by TLC. The reaction mixture was filtered through a pad of celite and concentrated. Subjecting the crude mixture to flash column chromatography (1:1, hexanes:ethyl acetate) on silica 68 mg of picolinic ester **158** (50 % yield) as a clear and colorless oil.

R_f = 0.31 (1:1, hexanes:ethyl acetate); ^{1}H NMR (500 MHz, $CDCl_3$) δ 8.58 (ddd, *J* = 4.8, 1.7, 0.9 Hz, 1H), 8.20 (app dt, *J* = 7.9, 1.01 Hz, 1H), 7.90 (app td, *J* = 7.7, 1.7, 1H), 7.55 (ddd, *J* = 7.7, 4.8, 1.3 Hz, 1H), 5.90 (app tt, *J* = 4.9, 1.6 Hz, 1H), 2.52 (app dtd, *J* = 17.9, 5.3, 1.6 Hz, 1H), 2.41 (dddd, *J* = 17.8, 8.2, 5.7, 1.6 Hz, 1H), 2.19 – 2.11 (m, 2H), 2.00 – 1.84 (m, 2H); ^{13}C NMR (125 MHz, $CDCl_3$) δ 163.9, 150.3, 147.4, 137.1, 134.7, 127.3,

125.6, 119.8, 117.2, 71.6, 30.1, 29.1, 17.6; IR (cast film, cm^{-1}) 3056, 2941, 2870, 2219, 1743, 1582; HRMS (ESI) calcd for $[M+H]^+$ $C_{13}H_{12}N_2O_2{}^{79}Br$: 307.0077, found: 307.0077.

2.8. References

(1) Schönbein, C. F. *Ber. Verh. Nat. Ges. Basel* **1847**, *7*, 4–7.

(2) Gothelf, K. V.; Jørgensen, K. A. *Chem. Rev.* **1998**, *98*, 863–910.

(3) Padwa, A.; Carter, S. P.; Chiacchio, U.; Kline, D. N. *Tetrahedron Lett.* **1986**, *27*, 2683–2686.

(4) Hayakawa, K.; Nishiyama, H.; Kanematsu, K. *J. Org. Chem.* **1985**, *50*, 512–517.

(5) Pinho e Melo, T. M. *Curr. Org. Chem.* **2009**, *13*, 1406–1431.

(6) Kolb, H. C.; Finn, M. G.; Sharpless, K. B. *Angew. Chem. Int. Ed. Engl.* **2001**, *40*, 2004–2021.

(7) Baskin, J. M.; Prescher, J. A.; Laughlin, S. T.; Agard, N. J.; Chang, P. V.; Miller, I. A.; Lo, A.; Codelli, J. A.; Bertozzi, C. R. *Proc. Natl. Acad. Sci. U S A* **2007**, *104*, 16793–16797.

(8) Ried, W.; Mengler, H. *Justus Liebigs Ann. Chem.* **1964**, *678*, 95–113.

(9) Bleiholder, R. F.; Schecter, H. *J. Am. Chem. Soc.* **1968**, *90*, 2131–2137.

(10) Wedegaertner, D. K.; Kattak, R. K.; Harrison, I.; Cristie, S. K. *J. Org. Chem.* **1991**, *56*, 4463–4467.

(11) Feldman, K. S.; Iyer, M. R. *J. Am. Chem. Soc.* **2005**, *127*, 4590–4591.

(12) López, C. S.; Faza, O. N.; Feldman, K. S.; Iyer, M. R.; Hester, D. K. *J. Am. Chem. Soc.* **2007**, *129*, 7638–7646.

(13) Padwa, A.; Craig, S. P.; Chiacchio, U.; Kline, D. N. *J. Org. Chem.* **1988**, *53*, 2232–2238.

(14) Beltrame, P.; Beltrame, P. L.; Cattania, M. G.; Zecchi, G. *J. Chem. Soc., Perkin Trans. 2* **1974**, 1301.

(15) Broggini, G.; Molteni, G. *J. Chem. Soc., Perkin Trans. 1* **2000**, 1685–1689.

(16) Braverman, S.; Mechoulam, H. *Isr. J. Chem.* **1967**, *5*, 71–74.

(17) Stirling, C. J. M. *Chem. Commun. (London)* **1967**, 131.

(18) Blackwell, G. B.; Haszeldine, R. N.; Taylor, D. R. *J. Chem. Soc., Perkin Trans. 1* **1983**, 1–5.

(19) Houk, K. N.; Sims, J.; Duke, R. E.; Strozier, R. W.; George, J. K. *J. Am. Chem.*

Soc. **1973**, *95*, 7287–7301.

(20) Houk, K. N.; Sims, J.; Watts, C. R.; Luskus, L. J. *J. Am. Chem. Soc.* **1973**, *95*, 7301–7315.

(21) Dolbier, W. R., Jr; Burkholder, C. R.; Winchester, W. R. *J. Org. Chem.* **1984**, *49*, 1518–1522.

(22) Dolbier, W. R.; Wicks, G. E.; Burkholder, C. R. *J. Org. Chem.* **1987**, *52*, 2196–2201.

(23) Dolbier, W. R., Jr; Purvis, G. D., III; Seabury, M. J.; Wicks, G. E.; Burkholder, C. R. *Tetrahedron* **1989**, *46*, 7991–8004.

(24) Padwa, A.; Bullock, W. H.; Kline, D. N.; Perumattam, J. *J. Org. Chem.* **1989**, *54*, 2862–2869.

(25) Dugovič, B.; Fišera, L.; Reißig, H.-U. *Eur. J. Org. Chem.* **2008**, 277–284.

(26) Balci, M.; Jones, W. M. *J. Am. Chem. Soc.* **1980**, *102*, 7607–7608.

(27) Johnson, R. P. *Chem. Rev.* **1989**, *89*, 1111–1124.

(28) Christl, M. in *Modern Allene Chemistry, Vol. 1* (Eds. N. Krause, A. S. K. Hashmi), Wiley–VCH Verlag: Weinheim, **2004**, pp. 243–357.

(29) Wittig, G.; Fritze, P. *Angew. Chem. Int. Ed.* **1966**, *5*, 846.

(30) Shakespeare, W. C.; Johnson, R. P. *J. Am. Chem. Soc.* **1990**, *112*, 8578–8579.

(31) Quintana, I.; Peña, D.; Pérez, D.; Guitián, E. *Eur. J. Org. Chem.* **2009**, 5519–5524.

(32) Wittig, G.; Fritze, P. *Liebigs Ann. Chem.* **1968**, *711*, 82–87.

(33) Hanessian, S.; Tyler, P. C.; Chapleur, Y. *Tetrahedron Lett.* **1981**, *22*, 4583–4586.

(34) Chorannat, J. A.; Mitchell, A. L.; Keogh, B. P. *Tetrahedron Lett.* **1990**, *31*, 315–318.

(35) Jastrzebski, J. T. B. H.; von Koten, G. Structures and Reactivities of Organocopper Compounds. In *Modern Organocopper Chemistry*; Krause, N., Ed.; Wiley-VCH Verlag GmbH: Weinheim, **2002**; Vol. 1; pp. 1-44.

(36) Piers, E.; de Waal, W.; Britton, R. W. *J. Am. Chem. Soc.* **1971**, *93*, 5113–5120.

(37) Marshall, J. A.; Hochstetler, A. R. *J. Am. Chem. Soc.* **1969**, *91*, 648–657.

(38) MacKenzie, D. A.; Sherratt, A. R.; Chigrinova, M.; Cheung, L. L.; Pezacki, J. P. *Curr. Op. Chem. Bio.* **2014**, *21*, 81–88.

(39) Dubrovskiy, A. V.; Larock, R. C. *Org. Lett.* **2010**, *12*, 1180–1183.

(40) Christl, M.; Fischer, H.; Arnone, M.; Engels, B. *Chem. Eur. J.* **2009**, *15*, 11266–11272.

(41) Christl, M.; Braun, M.; Fischer, H.; Groetsch, S.; Müller, G.; Leusser, D.; Deuerlein, S.; Stalke, D.; Arnone, M.; Engels, B. *Eur. J. Org. Chem.* **2006**, 5045–5058.

(42) Balci, M.; Jones, W. M. *J. Am. Chem. Soc.* **1981**, *103*, 2874–2876.

(43) Schmidt, M. W.; Angus, R. O.; Johnson, R. P. *J. Am. Chem. Soc.* **1982**, *104*, 6838–6839.

(44) Angus, R. O., Jr; Schmidt, M. W.; Johnson, R. P. *J. Am. Chem. Soc.* **1985**, *107*, 532–537.

(45) Engels, B.; Schöneboom, J. C.; Münster, A. F.; Groetsch, S.; Christl, M. *J. Am. Chem. Soc.* **2002**, *124*, 287–297.

(46) Daoust, K. J.; Hernandez, S. M.; Konrad, K. M.; Mackie, I. D.; Winstanley, J.; Johnson, R. P. *J. Org. Chem.* **2006**, *71*, 5708–5714.

(47) Werstiuk, N. H.; Roy, C. D.; Ma, J. *Can. J. Chem.* **1996**, *74*, 1903–1905.

(48) Nendel, M.; Tolbert, L. M.; Herring, L. E.; Islam, M. N.; Houk, K. N. *J. Org. Chem.* **1999**, *64*, 976–983.

(49) Dorn, H.; Otto, A. *Chem. Ber.* **1968**, *101*, 3287–3301.

(50) Dorn, H.; Otto, A. *Angew. Chem. Int. Ed. Engl.* **1968**, *7*, 214–215.

(51) Murahashi, S.-I.; Shiota, T. *Tetrahedron Lett.* **1987**, *28*, 2383–2386.

(52) Shintani, R.; Fu, G. C. *J. Am. Chem. Soc.* **2003**, *125*, 10778–10779.

(53) Moore, W. R.; Moser, W. R. *J. Org. Chem.* **1970**, *35*, 908–912.

(54) Huisgen, R.; Szeimies, G.; Möbius, L. *Chem. Ber.* **1967**, *100*, 2494–2507.

(55) Caubère, P. *Top. Curr. Chem.* **1978**, *73*, 49–103.

(56) Jimeno, C.; Renaud, P. In *Organic Azides: Syntheses and Applications*; Brase, S.; Banert, K., Eds.; John Wiley & Sons, Inc., Publication, 2010; pp. 239–267.

(57) Fleming, I. *Molecular Orbitals and Organic Chemical Reactions*; John Wiley & Sons, Inc., New York, 2011.

(58) Christl, M.; Schreck, M. *Chem. Ber.* **1987**, *120*, 915–920.

(59) Waali, E. E.; Jones, W. M. *J. Am. Chem. Soc.* **1973**, *95*, 8114–8118.

(60) Previous experience with synthesizing and isolating pyrrole products allowed the tentative assumption that the product was forming by TLC. [1] The R_f of the product, [2] the spot assumed to be the product turned bright red immediately upon exposure to anisaldehyde stain.

(61) Agosta, W. C.; Lowrance, J. W. W. *J. Org. Chem.* **1970**, *35*, 3851–3856.

(62) Neises, B.; Steglich, W. *Angew. Chem. Int. Ed. Engl.* **1978**, *17*, 522–524.

(63) Kobayashi, Y.; Feng, C.; Ikoma, A.; Ogawa, N.; Hirotsu, T. *Org. Lett.* **2014**, *16*, 760–763.

(64) Moore, H. W.; Decker, O. H. *Chem. Rev.* **1986**, *86*, 821–830.

(65) Saulnier, M. G.; Kadow, J. F.; Tun, M. M.; Langley, D. R.; Vyas, D. M. *J. Am. Chem. Soc.* **1989**, *111*, 8320–8321.

(66) Bode, J. W.; Hachisu, Y.; Matsuura, T.; Suzuki, K. *Tetrahedron Lett.* **2003**, *44*, 3555–3558.

(67) Moore, W. R.; Moser, W. R. *J. Am. Chem. Soc.* **1970**, *92*, 5469–5474.

(68) Tornøe, C. W.; Christensen, C.; Meldal, M. *J. Org. Chem.* **2002**, *67*, 3057–3064.

(69) Takeuchi, H.; Yanagida, S.; Ozaki, T.; Hagiwara, S.; Eguchi, S. *J. Org. Chem.* **1989**, *54*, 431–434.

(70) Tamura, Y.; Yoshimura, Y.; Kita, Y. *Chem. Pharm. Bull.* **1972**, *20*, 871–875.

(71) Hassner, A.; Fowler, F. W. *J. Org. Chem.* **1968**, *33*, 2686–2691.

(72) George, M. V.; Peterson, D. J.; Gilman, H. *J. Am. Chem. Soc.* **1960**, *82*, 403–406.

(73) Yoshida, Y.; Sakakura, Y.; Aso, N.; Okada, S.; Tanabe, Y. *Tetrahedron* **1999**, *55*, 2183–2192.

(74) Still, W. C.; Kahn, M.; Mitra, A. *J. Org. Chem.* **1978**, *43*, 2923–2925.

3. Enantiomeric Enrichment and Fidelity as a Mechanistic Probe for Cyclic Allene Cycloaddition Reactions

3.1. Structure of Cyclic Allenes

The structure of an allene is interesting insofar as it is a configurationally stable, chiral, tetrahedral functional groups; though spread over three carbon atoms rather than one. Following the Cahn-Ingold-Prelog priority rules as used with sp^3 hybridized chiral centers, due to spatial limitations even simple symmetrical, 1,3-disubstituted allenes are chiral due to the separation of the substituents on two different carbons. Figure 3.1 shows the priority and absolute configuration assignment to the two enantiomers of 2,3-pentadiene. Bent cyclic allenes are chiral as well as long as they are closed shell species and not planar conjugated radicals or zwitterionic compounds.

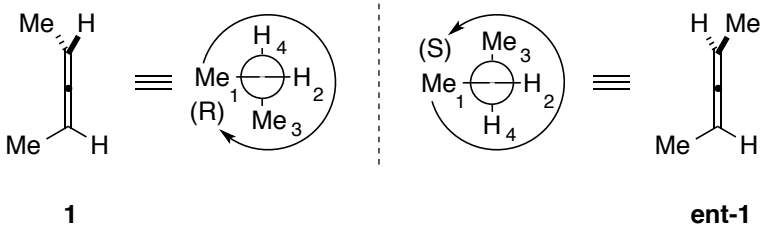

1 **ent-1**

Figure 3.1 - Absolute assignment of configuration to allenes using 2,3-pentadiene as example.

3.1.1. *In Situ* Observation of Cyclic Allenes

In order to analyze the structure of cyclic allenes, a number of techniques were used which gave conflicting results. Highly strained molecules are routinely observed using ultra-fast spectroscopy techniques.[1] These techniques are used to observe a fleeting reactive intermediate and are based upon the lifetime of the intermediate.

In 1981 Bock and coworkers reported on the generation of 1,2-propadiene from the thermolysis of cyclopropylacyl chloride **2**.[2] The group was attempting to optimize the formation of ketene intermediate **3** using photoelectron spectroscopy but only observed allene **5** (Scheme 3.1). Presumably the product arose from the extrusion of carbon monoxide to access the Doering-Moore-Skattebøl (DMS) reaction intermediate, **4,** leading to the formation of **5**.

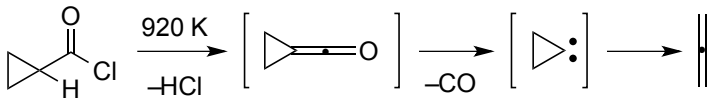

2 **3** **4** **5**

Scheme 3.1 - Mechanism for formation of propadiene from acyl chlorides under thermal conditions.

A similar method was then applied to the observation of 1,2-cyclohexadiene by Wentrup *et. al.*, whereby flash vacuum pyrolysis (FVP) of bicycloacyl chloride **6** was carried out at 800 °C (Scheme 3.2). The products were collected on a potassium bromide plate and characterized (11K in an argon matrix) by a sharp infrared absorption at 1886 cm^{-1} attributed to a weak allene stretch. If the reaction mixture was allowed to equilibrate to 170 K, only dimer **9** was produced which was verified by comparison with authentic samples prepared via the DMS reaction analogous to that reported by Moore and Moser.[3]

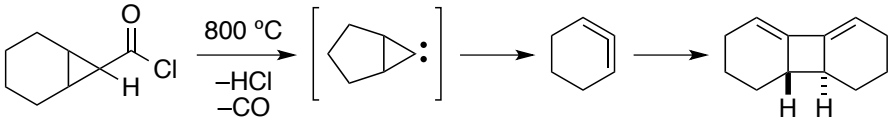

6 **7** **8** **9**

Scheme 3.2 - Attempted synthesis and observation of cyclic allenes by thermolysis of acyl chlorides.

Runge and Sander reported being unable to observe the same IR signal attributed to 1,2-cyclohexadiene (**8**) when analogous generation methods were employed. When trimethylstannylbromide **10** was subjected to flash vacuum pyrolysis (FVP) at 700 °C complete conversion of the starting material was achieved and the main products observed were trimethylstannyl bromide, 1-butene-3-yne, and ethylene. The latter two products most likely arose from the retro-dehydro-Diels-Alder reaction of 1,2-cyclohexadiene. Unable to detect the 1886 cm^{-1} IR frequency observed by Wentrup, the study did find a signal at 1829 cm^{-1} that the researchers attributed to cyclic allene **8**.

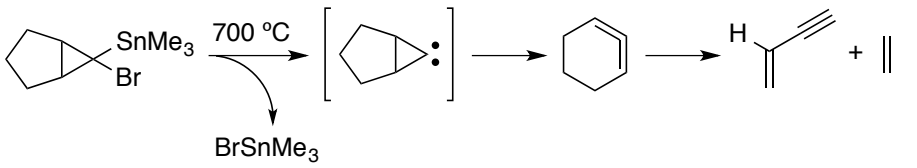

10 7 8 11 12

Scheme 3.3 - Thermolysis of tin-substituted cyclopropane.

Work done at the University of Gießen found the IR signal reported by Runge and Sander could be attributed to trimethylstannyl hydride during their attempted observation of 1,2-cyclohexadiene.[4] In the same studies using the DMS reaction of 6,6-dibromobicyclo[3.1.0]hexane (**16**) to prepare the cyclic allene *in situ*, an IR signal at 1976 cm^{-1} was tentatively assigned to cyclic allene **8**; however, the observation stands to be validated.

Werstiuk and coworkers reported the *in situ* generation of 1,2-cyclohexadiene by pyrolysis of the furan/cyclic allene Diels-Alder adduct (**13**).[5] Subtraction of the contributions of furan, and 1,3-cyclohexadiene from the photoelectron spectrum of the pyrolysis products showed signals in good correlation with the calculated four lowest ionization energies (8.60, 9.89, 11.40, 12.00 eV [HAM3]) as well as the negative of the energies of the four highest occupied molecular orbitals (8.64, 9.96, 12.61, 13.12 eV [HF/6-31G**]) of 1,2-cyclohexadiene (using Koopman's Theorem), providing support for a closed-shell, chiral, twisted cyclic allene. When the experiment was attempted using 6,6-dibromobicyclo[3.1.0]hexane (**16**), however, only decomposition was observed, with no evidence seen for the expected cycloallene **8** or its reaction products.[6]

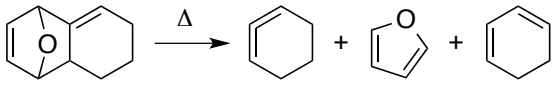

13 8 14 15

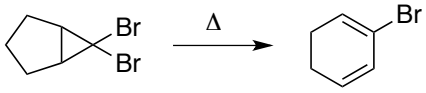

16 17

Scheme 3.4 - Laser-induced decomposition used to record the photoelectron spectrum of 1,2-cyclohexadiene.

3.2. Experimental Computational/Trapping Evidence for Cyclic Allene Ground State Electronic Configuration

A number of experimentalists have generated evidence for the ground state electronic configuration of 1,2-cyclohexadienes. The evidence compiled is in good agreement with the spectroscopic conclusions, that 1,2-cyclohexadiene is a closed-shell, twisted, potentially chiral cyclic allene intermediate.

3.2.1. Optically Active Cycloadducts of Cyclic Allenes from Base-Mediated Elimination

As seen in Figure 3.1 symmetrically substituted acyclic allenes are chiral, it should follow that 1,2-cyclohexadiene is also chiral. Though the activity of the intermediate depends on a number of factors including, but not limited to the method by which it is generated, and the substitution of the cyclic allene.

The first experiments to produce an optically active cycloadduct from an enantiomerically enriched cyclic allene were those of Balci and Jones via the use of enantiomerically enriched deuterated allene precursors, **18**.[7] Without the intermediacy of a closed-shell chiral intermediate, the enantiomeric enrichment of the starting materials could not be transferred to the cycloadducts (Table 3.1). The optical activity was found to drop, and eventually fell to zero upon raising the reaction temperature (entries 1, 3, and 5). The authors proposed this was consistent with the calculated barrier to racemization of 15 - 18 kcal/mol.[8,9] In all of these cases the absolute enantiomeric excess of the products or starting materials were not reported thus the degree to which the enantiomeric enrichment could be transferred/controlled was never evaluated. In a follow up publication the authors demonstrated the generation of the same proposed chiral cyclic allene intermediate using optically active potassium menthoxide as the base and vinylbromide **18-H** (entries 7 and 8).[10]

Table 3.1 - Trapping of optically active cyclic allenes with 1,3-diphenylisobenzofuran (DPIBF).

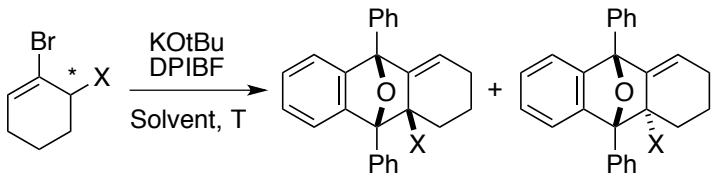

X = D, **18-D**
X = H, **18-H**

X = D, **19-D**
X = H, **19-H**

X = D, **19'-D**
X = H, **19'-H**

Entry	Vinyl Halide	Temperature (°C)	Solvent	Cycloadduct	Optical Activity $[\alpha]^{25}_{D}$ °
1	**18-D**	53	THF	**19-D**	-0.3 ± 0.09
2	**18-D**	53	THF	**19'-D**	+ 1.6 ± 0.11
3	**18-D**	80	diglyme	**19-D**	0.0 ± 0.11
4	**18-D**	80	diglyme	**19'-D**	+ 0.3 ± 0.2
5	**18-D**	100	diglyme	**19-D**	0.0 ± 0.06
6	**18-D**	100	diglyme	**19'-D**	0.0 ± 0.06
7	**18-H**	53	THF	**19-H**	-0.4 ± 0.11
8	**18-H**	100	THF	**19-H**	-0.0 ± 0.11

3.2.2. Enantiomerically Enriched Dihalocyclopropanes

The base-mediated elimination used by Balci and Jones demonstrated the potential chirality of cyclic allenes; however, the elimination does not take place to an appreciable extent at reaction temperature below 50 °C. In contrast the DMS reaction can be performed well below 0 °C which enabled greater control over the enantiomeric fidelity of the reaction.

Christl and coworkers proposed that a fused-phenyl ring would control the torquoselectivity of the cyclopropane ring opening.[11] Fluorobromocyclopropanes were used to ensure thermal stability of the requisite starting materials, and enantiomeric enrichment was established via preparative chiral HPLC. Though impractical, this gave access to both enantiomers of the starting material.

Upon subjecting indene-derived cyclopropane **20** to methyl lithium in the presence of 2,5-dimethylfuran, cycloadducts **22**/**22'** were isolated with an enantiomeric enrichment of ~70:30 (Scheme 3.5). This result was insensitive to temperature, dilution,

and steric crowding of the diene (use of 2-*t*-butyl-5-methylfuran, and 2,5-di*t*-butylfuran gave similar e.r.) leading the researchers to suggest that the fused-phenyl ring failed to absolutely control the torquoselectivity of the ring opening rather than suggesting the cyclic allene is undergoing inversion under the reaction conditions prior to the cycloaddition.

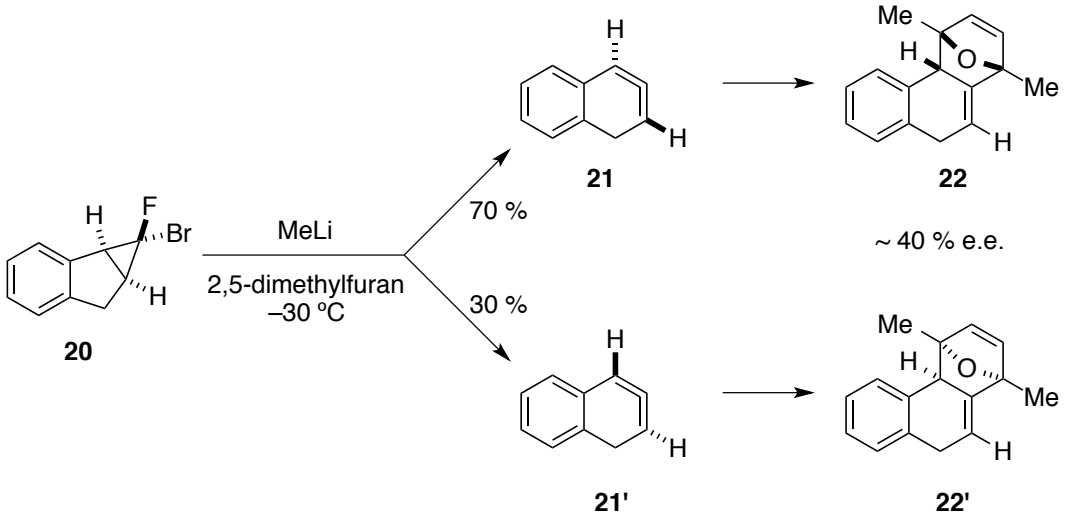

Scheme 3.5. - Furan trapping of chiral, enantiomerically enriched isonaphthalene cyclic allene

The use of 1-phenyl-6-bromo-6-fluorobicyclo[3.1.0]hexane **23** proved to better control the ring opening, giving consistently 100 % enantiomeric fidelity when the reaction was run in 2,5-dimethylfuran solvent.[12] The group proposed the absolute stereochemistry of both the starting materials and the cycloadducts using the predicted and experimentally determined electronic circular dichroism spectra. The enantiomeric transition states leading to the furan and styrene cycloadducts were discussed in light of the known absolute stereochemistry of the reactivity intermediate.

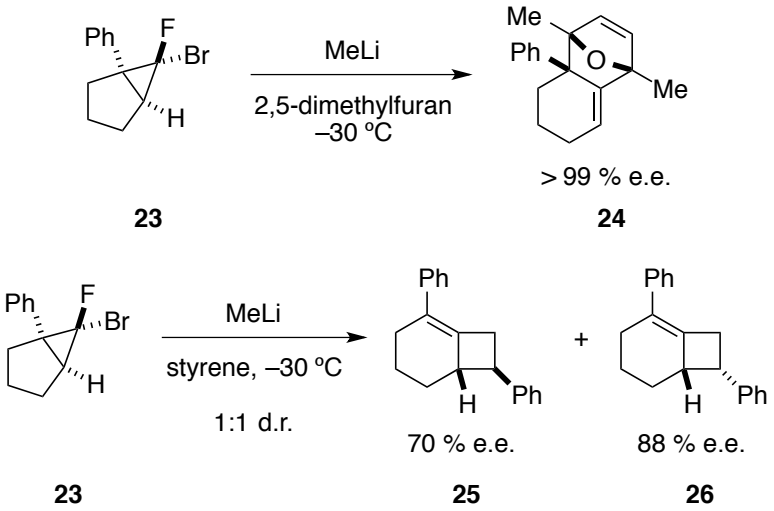

Scheme 3.6 – Highly enantiomerically fidelitous trapping of phenyl-substituted cyclic allene.

Christl and coworkers did find the enantiomeric excess of the products was dependent upon the trap employed. While the reaction with furans gave consistently high enantiomeric fidelity, the reaction with styrene saw a discernable erosion of enantiomeric enrichement. The reaction with styrene has been proposed to occur through diradical intermediates by Moore and Moser,[13] which could account for the erosion of the enantiomeric ratio of the chiral cyclic allene intermediate observed. The authors propose that the cycloaddition is fast enough to conserve the enantiomeric enrichment of the chiral intermediate and that the erosion of enantiomeric excess is better explained by a less sterically encumbered transition state for the initial bond forming step with styrene versus furan. In turn there is a decrease in the discrimination between the two enantiomeric faces of the allene in the reaction with styrene. Though there is a clear closed-shell allene intermediate, its interaction with the trapping molecule has strong influence on the course of the reaction and the subsequent enantiomeric ratio obtained.

The work described previously suggests that an accurate description of small carbocyclic allenes are closed shell, chiral intermediates. The conservation of enantiomeric enrichment or induction in these examples demonstrates the configurationally stability of the intermediate but also suggests that the mechanism of trapping is either fast enough to conserve the stereochemical information or occurs as a

concerted cycloaddition rather than a stepwise reaction with diradical or charged intermediates.

Chapter 2 dealt with an entirely new trapping modality of cyclic allenes, the [3+2] dipolar cycloaddition of cyclic allenes with a variety of 1,3-dipoles. In some cases high diastereoselectivity (for the *anti* isomer) was observed with no obvious reason for the high selectivity. We surmised this was partially due to a high degree of concertedness in the mechanism. In contrast *C*-styryl substituted 1,3-dipolar traps failed to show high diastereoselectivity. In consideration of the trapping studies already reported, the conservation of enantiomeric enrichment from an axially chiral cyclic allene to a [3+2] dipolar cycloadduct might shed light on the mechanism of the reactions. We propose that the conservation of enantiomeric enrichment would strongly imply a concerted cycloaddition. If a difference in the enantiomeric fidelity of the reaction with *C*-phenyl dipolar traps and *C*-styryl dipolar traps is observed, it could imply a difference in the mechanism of trapping.

With this in mind, we set out to adapt the fluoride-mediated silyl elimination strategy to the synthesis of axially enantiomerically enriched cyclic allenes. The production of the requisite allylic silanes would have application beyond our work thus warranting further exploration if successful. The previous work from Christl and coworkers on enantiomerically enriched dihalocyclopropane ring opening to chiral cyclic allene intermediates would be validated if new complementary methods for transferring central chirality to axially chiral cyclic allenes were achieved. Herein we describe our results toward these objectives.

3.3. Results and Discussion

3.3.1. Enantiomerically Enriched Allylic Silanes

Allylic silanes have been synthesized previously in an asymmetric fashion. The allylic silane most closely resembling the allylic silanes we employed previously for the racemic intermolecular trapping studies were used by Denmark *et. al.* when investigating the silyl-directed Nazarov reaction used enantiomerically enriched allylic silane **32**.[14] The enantiomerically enriched silanes were derived from racemic 1-bromo-6-trimethylsilylcyclohexene **27**, which was resolved via formation of diastereomeric amide

31 (Scheme 3.7), and thus not applicable to our needs. Interestingly, Professor Denmark mentions that the attempted preparation of non-racemic allylic silane **27** by silylcupration was unsuccessful though we hypothesized different methods could be employed to remedy the lack of enantiomeric enrichment.

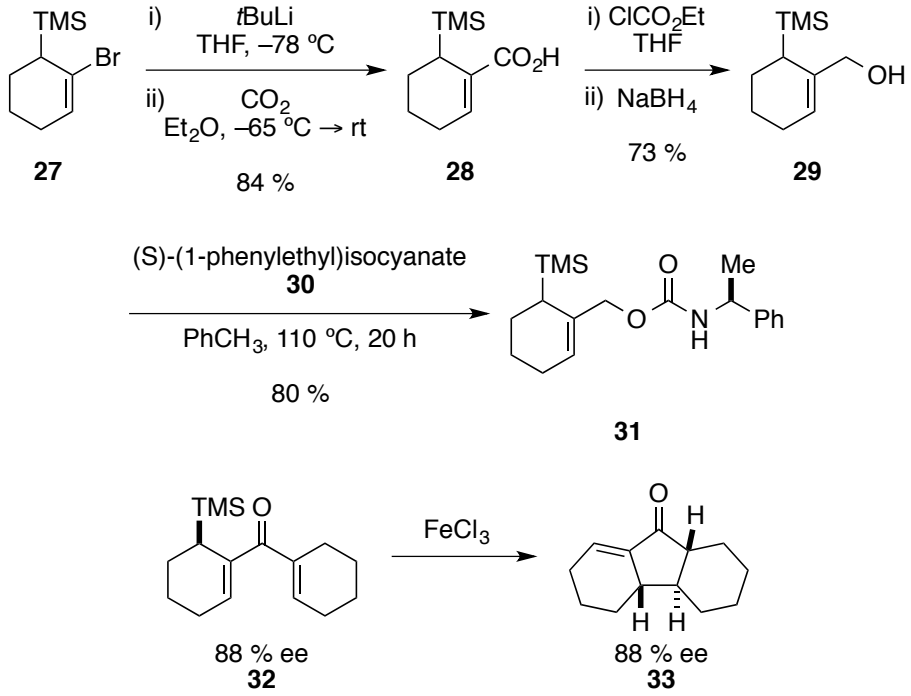

Scheme 3.7 - Denmark's synthesis of enantiomerically enriched allylic silanes.

Having previously developed the allylic silylation of 1-*O*-triflylcyclohexenes, it was assumed that using a enantiomerically enriched allylic leaving group would transfer the enantiomeric enrichmentity to the silane. From known 2-*O*-triflylcyclohex-2-enone (Scheme 3.8) Corey-Bakshi-Shibata[15] reduction with (R)-2-methyl-5,5-diphenyl-oxazaborolidine **35** furnished enantiomerically enriched allylic alcohol **36** in good yield but moderate enantioselectivity (as determined by chiral HPLC). Elaboration to the allylic tosylate and subsequent copper-mediated silylation generated 6-dimethylphenylsilyl-1-trifloylcyclohexene **37** with no optical activity. Starting from 2-bromocyclohex-2-enone, the analogous synthesis to give 6-dimethylphenylsilyl-1-bromocyclohexene **40** also provided optically inactive material. Formation of **37** and **40** as racemates was confirmed by determining the enantiomeric excess of their allene-derived cycloadducts with azomethine imines to be zero.

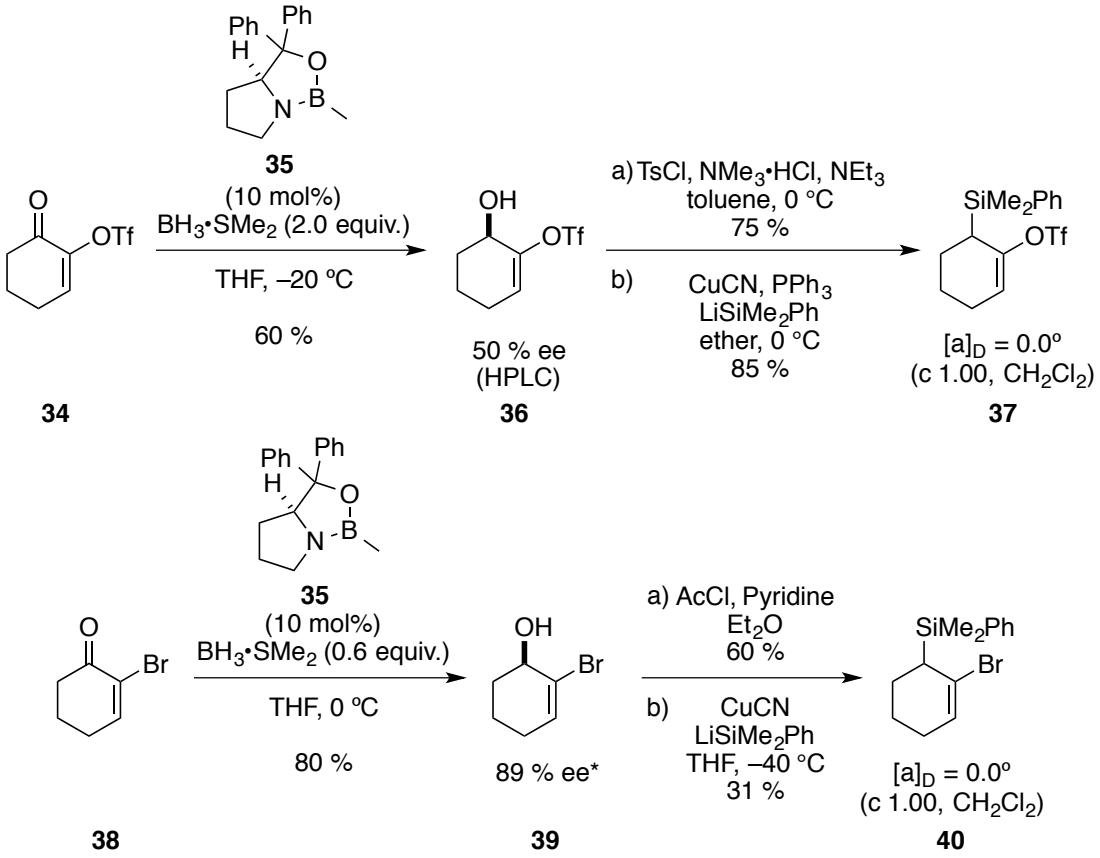

Scheme 3.8 - Attempted synthesis of enantiomerically enriched silanes on parent system.

Two mechanisms for the nucleophilic allylic displacement are possible (Scheme 3.9); a direct S_N2 nucleophilic displacement of the allylic leaving group can take place to give **43** or an S_N2' nucleophilic displacement can take place to give the regioisomer **41**. It was assumed one mechanism would prevail over the other allowing high stereochemical fidelity from the enantiomerically enriched starting materials. From the investigations of Fleming and others this assumption was not valid.[16-18] There are two ways to control the mechanism of the displacement; via unsymmetrically substituted olefins **44** or via a leaving group capable of directing the copper reagent **46** (Scheme 3.9).

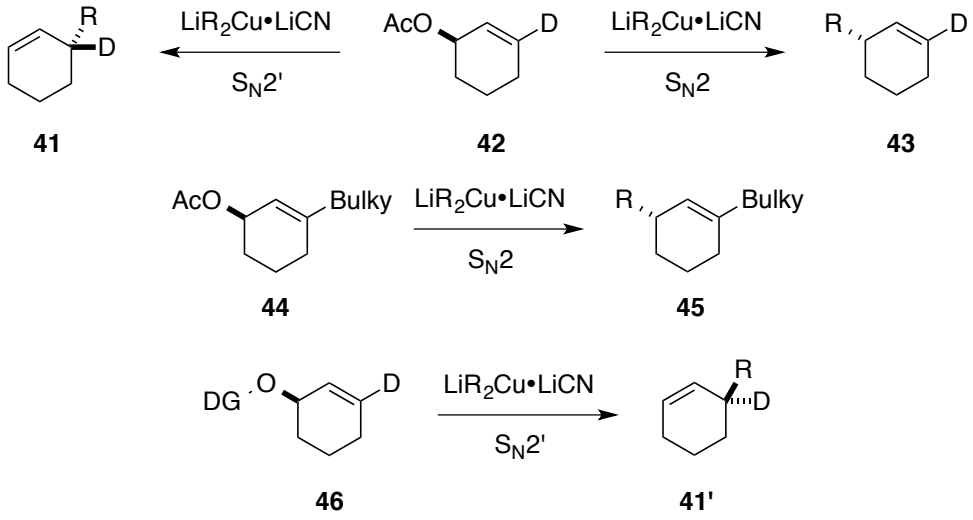

Scheme 3.9 - Two regiochemical outcomes of copper-mediated allylic displacement.

3.3.2. Controlling Cuprate-Addition with Substitution Pattern

In order to control the stereospecific addition of the silyl group to the cyclohexene scaffold, β-substituted cyclohexenes with allylic leaving groups were synthesized. The Stork-Danheiser alkylation enables the introduction of a number of different alkyl substituents via a nucleophilic addition/hydrolysis reaction as shown in Scheme 3.10.

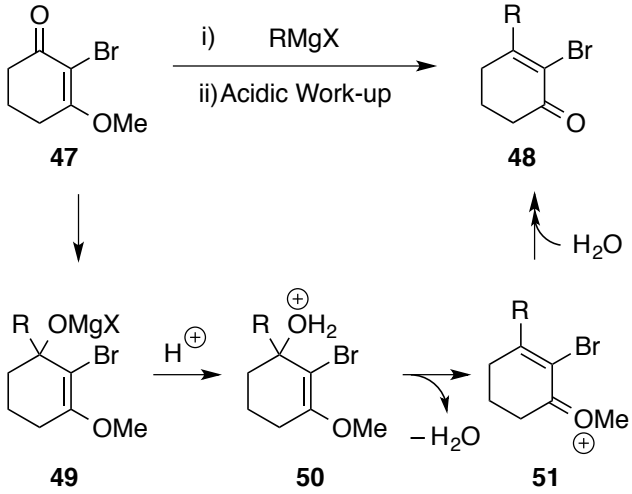

Scheme 3.10 - Mechanism of the Stork-Danheiser reaction.

2-Bromo-3-methylcyclohex-2-enone was synthesized by the addition of methylmagnesium bromide to bromo-enone **47** followed by a mildly acidic work-up. The allylic silane was obtained from the asymmetric Corey-Bakshi-Shibata reduction of

methylenone **52**, acetylation, and cuprate displacement under standard silylation conditions (Scheme 3.11). As expected, the regioisomer with the silyl group attached to the less substituted carbon of the allylic system was formed, albeit in low yield. The less substituted isomer forms due to the cuprate avoiding a steric clash with the alkyl substituent and consequently preserves the thermodynamically preferred tetrasubstituted olefin. The observed optical rotation of $[\alpha]_D$ – 3.30 verified that the material was enantiomerically enriched though we could not determine the absolute enantiomeric enrichment due to difficulties encountered trying to derivatize the material and separation of the two enantiomers was not successful using chiral high performance liquid chromatography.

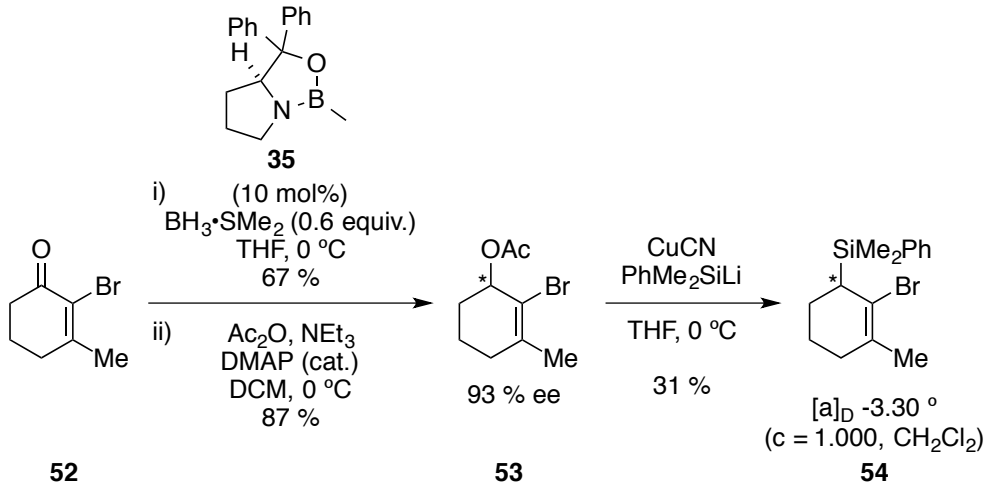

Scheme 3.11 - Synthesis of enantiomerically enriched, methyl-substituted allylic silane 54.

When enantiomerically enriched allylic silane **54** was subjected to the fluoride-mediated elimination/azomethine imine cycloaddition conditions used previously in Chapter 2 (Scheme 3.12) two cycloadducts, **56** and **57,** were formed as single diastereomers in a combined 16 % yield and 5.6:1 ratio of regioisomers. The major cycloadduct, **56**, resulted from cycloaddition across the lesser-substituted double bond of the allene. The regiochemistry was assigned based upon the presence or absence of vinylic sp^2 hybridized protons in the ^1H NMR spectral data; the presence of a proton bound to an sp^2 hybridized-carbon (signal at 5.53 ppm in the ^1H NMR spectrum) was

indicative of regioisomer **57** arising from cycloaddition across the more-substituted double bond of the cyclic allene.

HPLC analysis using a chiral stationary phase allowed the enantiomeric enrichment of the major regioisomer to be determined. The observed enantiomeric ratio of 64:36 indicated that the reaction took place with some degree of enantiomeric fidelity. Difficulties determining the enantiomeric excess of the resulting silane **54** warranted further investigation into the synthesis of different enantiomerically enriched allylic silanes.

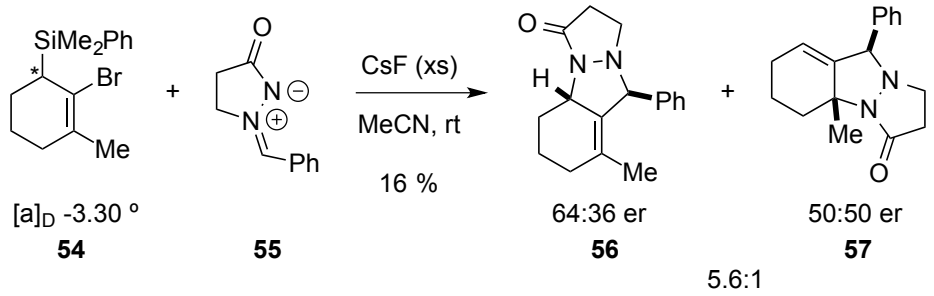

Scheme 3.12 - Trapping of enantiomerically enriched 1-methyl-1,2-cyclohexadiene with phenyl substituted azomethine imine 55.

3.3.3. Controlling Cuprate-Addition with Chelation

Gallina and Ciattini first demonstrated the ability of secondary lithium carbamates to control the copper-mediated allylic displacement of allylic leaving groups via an S_N2' type mechanism, with delivery of the cuprate from the same face as the leaving group (Scheme 3.13).[19] This precluded the presence of any other mildly acidic functional groups in the molecule that could possibly interfere with the deprotonation or the chelation of the carbamate to the copper species.

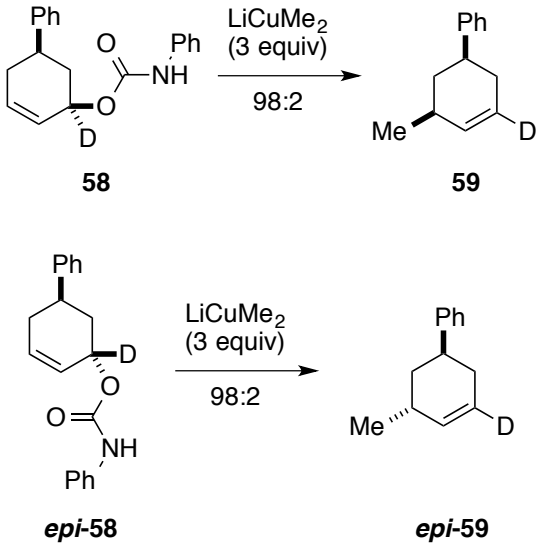

Scheme 3.13 - Gallina's carbamate directed allylic displacement with methyl-cuprate.

With the significant literature dedicated to the subject of controlling copper addition to allylic systems[20] we turned our attention toward a recent report from Kobayashi and coworkers whereby the stereochemistry of the allylic substituents is transferred to the products via the use of picolinic ester derivatives **60**/**62** as directing groups (Scheme 3.14).[21] Complementary to the observations of Gallina's group using carbamates, the picolinic ester gives products arising almost exclusively from *anti* delivery relative to the starting picolinate ester. Discouragingly, when Kobayashi and coworkers used lithium reagents to make the active cuprate, poor regioselectivity in the displacement was observed, though this was partially mitigated by the addition of a Lewis acid.

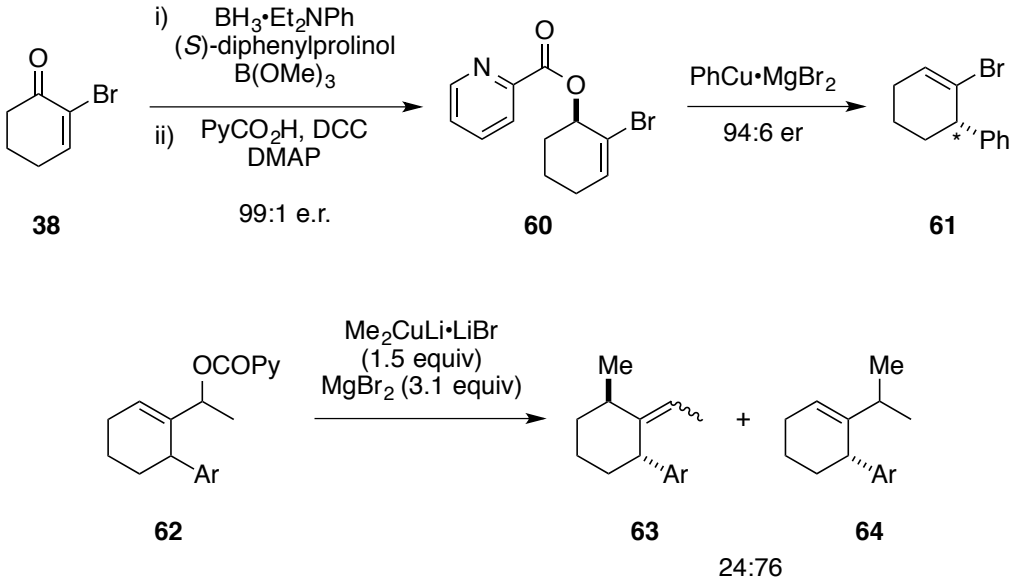

Scheme 3.14 - Picolinic ester as directing groups in cuprate displacement.

Previously, the silylation of allylic acetate **53** (Scheme 3.11) failed when using copper (I) bromide as the precursor, the reaction required the use of copper (I) cyanide to generate the higher order cuprate.[16] Starting with enantiomerically enriched picolinate ester (from the same allylic alcohol used in the synthesis of allylic acetate **53**), the optimization as shown in Table 3.2 shows that the regiochemistry of the addition was highly dependent upon the stoichiometry of both $MgBr_2•OEt_2$ and the number of equivalents of the silylating reagent (lower Lewis acid loading resulted in the formation of the less substituted isomer **54**). The use of freshly prepared Lewis acid improved the yield as well as the selectivity (entry 5).

Table 3.2 - Regioselectivity of silylation as mediated by $MgBr_2$•OEt_2.

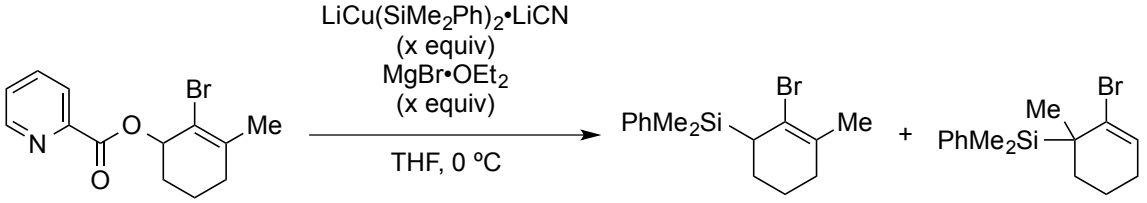

65 **54** **66**

Entry	Silylating Reagent (equiv)	Lewis Acid (equiv)	Yield (%)[c]	Ratio[d] (**54**:**66**)
1	1.1	4.0[a]	23	1:2
2	1.0	2.0[a]	43	1:1
3	1.0	3.0[a]	41	1:9
4	1.0	2.4[a]	18	1:9
5	0.99	3.0[b]	64	>5:95

[a] $MgBr_2$•OEt_2 (99 %) obtained from Sigma Aldrich was used for these reactions. [b] $MgBr_2$•OEt_2 was made by literature procedure (see experimental). [c] Yield is of purified mixture of **54** and **66**. [d] Ratio was determined by comparison of the integration of the silyl methyl groups in the ^{1}H NMR spectrum.

In order to understand the enantiomeric ratios obtained with the dipolar compounds, knowledge of the starting configuration is necessary. An understanding of the stereochemistry of the reduction and the regioselective silylation allows the educated assumption that the absolute stereochemistry of silane **66** was (*R*) as shown in Scheme 3.15.

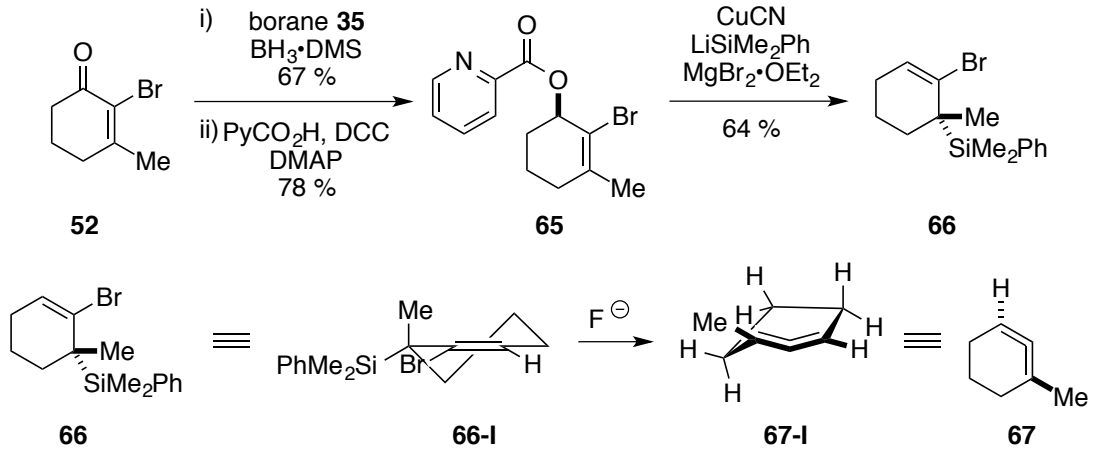

Scheme 3.15 - Proposed absolute configuration of the allylic silane and subsequent cyclic allene.

3.3.4. Determination of the Enantiomeric Excess of the Silane

With the stereochemistry of the silane addition controlled we turned our attention to the enantiomerically fidelitous nature of the reaction. Upon subjecting picolinic ester **65** to the silylation conditions, the enantiomerically enriched allylic silane (**66**) was generated in 64 % yield, with only minor impurities of the regioisomer **54**. Chiral HPLC was unsuccessful in separating the two enantiomers of the allylic silane **66**, therefore, derivatization via lithium/halogen exchange and quenching with benzoyl cyanide was employed to furnish benzoyl-substituted allylic silane **69** in 21 % yield. Chiral HPLC of benzoylated allylic silane **69** showed a high enantiomeric ratio of 97:3, a very satisfying result with which the enantiomeric fidelity of the dipolar cycloadditions could be tested.[22]

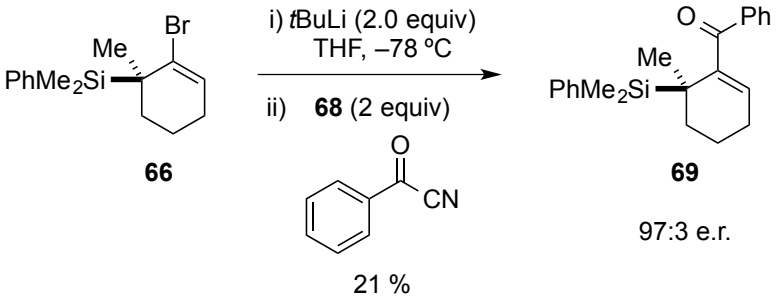

Scheme 3.16 - Derivatization of allylic silane 66 to facilitate HPLC analysis.

To test the ability of a fluoride-mediated elimination to transfer point chirality of the allylic silane to axial chirality of the allene, the reaction with furan was employed. From the work of Christl and coworkers, the cycloaddition of furan was found to show

high enantiomeric fidelity (Scheme 3.6).[12] Addition of TBAF to a furan solution of enantiomerically enriched allylic silane **66** at room temperature resulted in the formation of one major cycloadduct, **70** (Scheme 3.17). The site selectivity of the allene was assumed from a dearth of protons attached to sp^2-hybridized carbons, thus the cycloaddition occurred across the less-substituted double bond. Similar to the discussion in Chapter 2, the peaks at 0.54 ppm integrating to one (proton in red on structure **70-I**) indicate that the product had *anti* geometry resulting from an *endo* cycloaddition. Chiral HPLC analysis of purified **70** showed it to have an enantiomeric ratio of 87:13, indicating a small but significant erosion of enantiomeric enrichment from the starting allylic silane **66** (97:3 → 87:13). This is surprising considering the promising results Christl and coworkers reported with furan; however, the differences may be attributed to the substitution of the allenes formed. The phenyl-substituted cyclic allene studied by the Christl group may have a higher racemization barrier than the simple alkyl-substituted allene although this is addressed in Section 3.3.7. The result with furan provides a reference for the expected enantiomeric fidelity in the [3+2] dipolar cycloadditions studied. A difference in the enantiomeric ratio of the dipolar cycloadducts should be observed depending on the proficiency with which the dipolar compounds can trap the cyclic allene relative to furan.

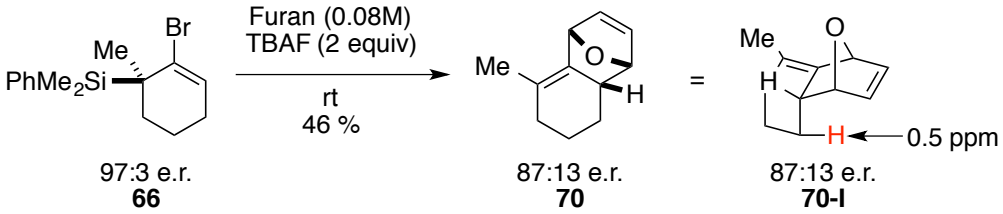

Scheme 3.17 - Diels-Alder reaction of an enantiomerically enriched, substituted allene with furan (the absolute stereochemistry is unknown).

3.3.5. The Reaction of Enantiomerically Enriched Allylic Silanes with Azomethine Imines

Initially the reaction of C-phenyl azomethine imine **72** with enantiomerically enriched allylic silane **66** proved extremely slow with cesium fluoride. Only partial consumption of the starting material took place in a 24 h period. The reaction was allowed to proceed for 5 days with regular monitoring, and when subjected to flash

column chromatography purification an 85 % yield of cycloadducts **74**/**75** could be obtained. TBAF proved to be a much more effective fluoride source: addition of a diluted solution of TBAF over the course of one hour allowed quantitative consumption of the starting material and excellent yield (98 %) of the cycloadducts in a 5:1 ratio (Scheme 3.18). The same regioisomers were obtained when azomethine imine **72** reacted with the regioisomeric allylic silane **54**, as shown in (Scheme 3.12).

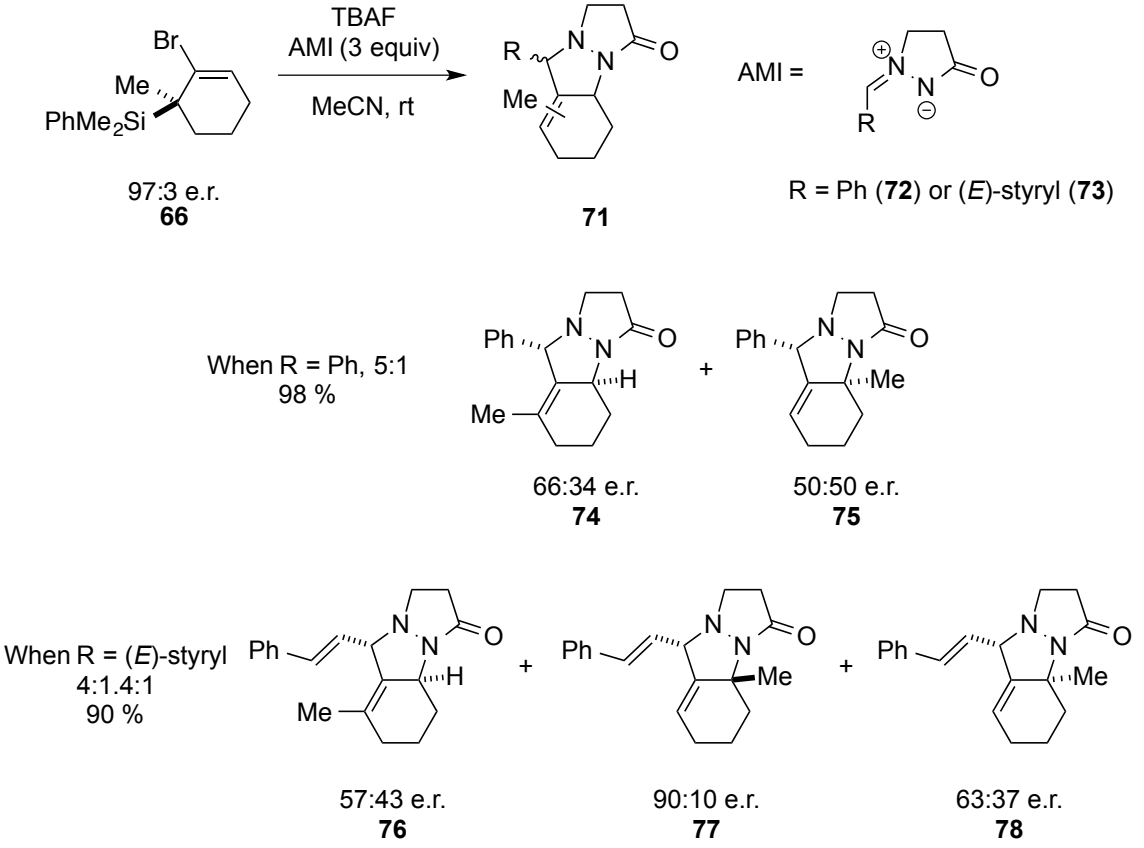

Scheme 3.18 - Trapping of enantiomerically enriched cyclic allenes with azomethine imines (absolute stereochemistry not known).

Contrary to the reactions encountered by Houk and Tolbert,[23] and Christl and Stalke,[24] the less-substituted double bond of the cyclic cumulene is more reactive. The reaction of 1-methyl cyclohexa-1,2-diene **67** at the less-substituted double bond most likely arises from avoidance of the bulky alkyl group by the 1,3-dipole, overriding the inductive activation of the double bond by the alkyl-substituent.

Considering the low diastereoselectivity observed with more conjugated azomethine imine traps in Chapter 2 (phenyl azomethine imine **72** gave >10:1, however

styryl azomethine imine **73** gave 1:1 diastereoselectivity), we assumed that the two different cycloaddition reactions would also give different degrees of enantiomeric fidelity from a common precursor. If the enantiomeric ratios obtained from the different cycloaddition reactions were different it may be possible to comment on the degree of concertedness of the reactions with differently substituted traps.

The regioisomers were formed as single diastereomers, however the enantiomeric ratio of the major regioisomer was a surprisingly low 66:34 as determined by chiral HPLC. This equates to a three-fold erosion of the enantiomeric ratio, a significant decrease relative to the reaction with furan. Even more troubling was the determination that the minor regioisomer **75** was obtained as a racemic mixture.

Bottini and coworkers reported competition experiments between a number of different traps with cyclic allenes under various generation conditions.[25] The relative rates of allene trapping show a correlation to the diastereoselectivity observed. The relatively faster trapping substrates (cyclopentadiene (1.5:1), styrene (2.2:1)) show little diastereoselectivity, whereas the slower traps showed much higher diastereoselectivity (furan (10:1), cyclohexadiene (3:1)). Given the high degree of diastereoselectivity observed in dipolar cycloadditions and assuming the correlation between the observed diastereoselectivity and the rate at which the traps react with the cyclic allene intermediates is true; the rate of capture of the cyclic allene by the 1,3-dipoles investigated must be slower than furan. The slow capture of the allene and premature inversion of the allene could account for the decrease in enantiomeric excess.

The reaction with the styryl substituted azomethine imine **73** gave mixed results. The major cycloadduct was obtained as a near racemic mixture, while the two regioisomeric diastereomers displayed higher enantiomeric ratios (the *syn* diastereomer being obtained in a 90:10 enantiomeric ratio, with relatively little stereochemical erosion from the original starting silane).

3.3.6. The Reaction of Enantiomerically Enriched Allylic Silanes with Nitrones

The [3+2] dipolar cycloaddition of nitrones and cyclic allenes shown in Chapter 2 displayed high diastereoselectivity with a number of differently substituted nitrones. (*E*)-Styryl substituted nitrone **82** however, showed a marked decrease in yield as well as diastereoselectivity. Similar to the investigation with differently substituted azomethine

imines a difference in enantiomeric fidelity was proposed to shed light on the mechanism of cycloaddition with differently substituted nitrones from a common enantiomerically enriched allylic silane (**66**). The selectivity and efficiency of two nitrones was scrutinized with allylic silane **66**, C-phenyl-N-benzylnitrone **79** and C-[(*E*)-styryl]-N-methylnitrone **82**.

The reaction of C-phenyl-N-benzylnitrone **79** with allylic silane **66** gave two regioisomers in an excellent 95 % yield in a 12:1 ratio of regioisomers (Scheme 3.19). Both regioisomers were isolated as single diastereomers. Surprisingly, the change from a vinyltriflate leaving group to a bromide leaving group resulted in two observations; first the reaction was significantly more efficient (95 % yield versus 62 %), and secondly TBAF was the preferred fluoride source considering the reaction with cesium fluoride took >3 days to consume the starting material. The products obtained were the regioisomers shown in Scheme 3.19, with the minor isomer resulting from a reaction at the more substituted alkene and the *anti* stereochemistry based upon TROESY correlations as shown in the experimental section.

Analogous to the previous reaction, exposure of allylic silane **66** to fluoride in the presence of excess C-(*E*)-styryl-N-methylnitrone **82** furnished two regioisomeric cycloadducts, **83** and **84** as single diastereomers. Similar to the unsubstituted cyclic allene used in Chapter 2, the reaction of 1-methyl-1,2-cyclohexadiene with the cinnamyl-derived nitrone showed a marked decrease in yield.

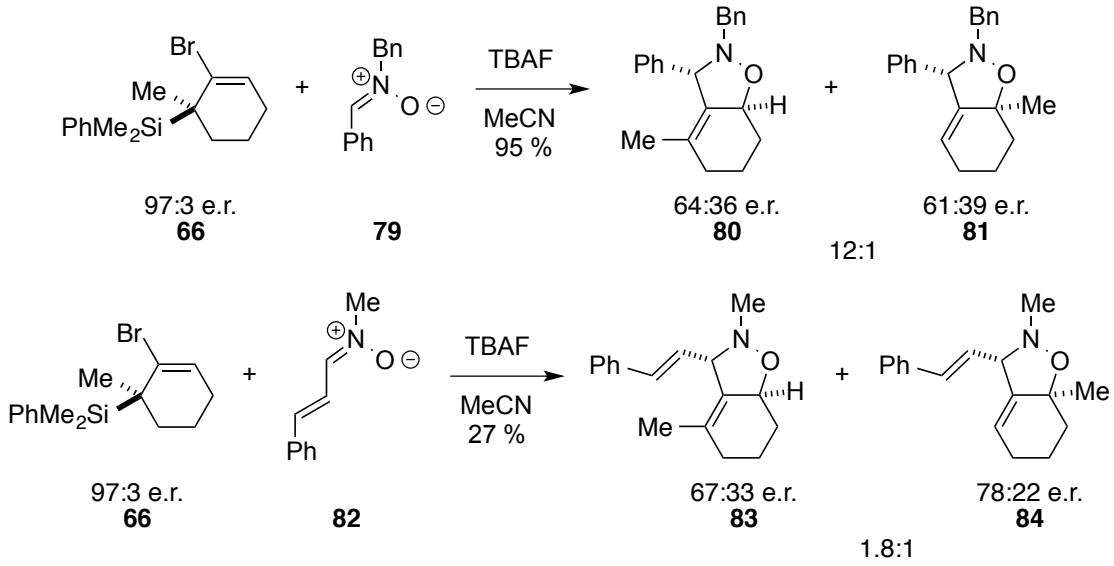

Scheme 3.19 - Intermolecular cycloaddition of nitrones and enantiomerically enriched cyclic allenes (absolute stereochemistry not known).

The cycloadditions showed exceptional control of diastereoselectivity, good regioselectivity; however, from the enantiomeric fidelity of the products mechanistic differences between the two differently substituted traps could not be drawn. Starting from the enantiomerically enriched allylic silane **66**, the two regioisomers show modest enantiomeric fidelity with enantiomeric ratios of 64:36 and 61:39. In comparison, the isomers of the cycloaddition with the cinnamaldehyde-derived nitrone **82** showed a similar enantiomeric ratio of 67:33 and 78:22. There appears to be no appreciable change in the enantiomeric fidelity of the reaction with respect to the substitution of the nitrone, regardless of the considerable change in reactivity/efficiency.

3.3.7. Addressing the Enantiomeric Fidelity of Dipolar Cycloadditions with Cyclic Allenes

Considering the significant loss in enantiomeric enrichment encountered, we envisioned two possible reasons for the loss in selectivity. One possible mechanism for stereochemical erosion is competition between the trapping of the enantiomerically enriched cyclic allene and the rate of racemization (**67**, **ent-67**). Alternatively the trap may fail to discriminate between the two faces of the chiral allene intermediate as it undergoes fast, reversible pseudo-chair flips (**67-I – 67-II**).

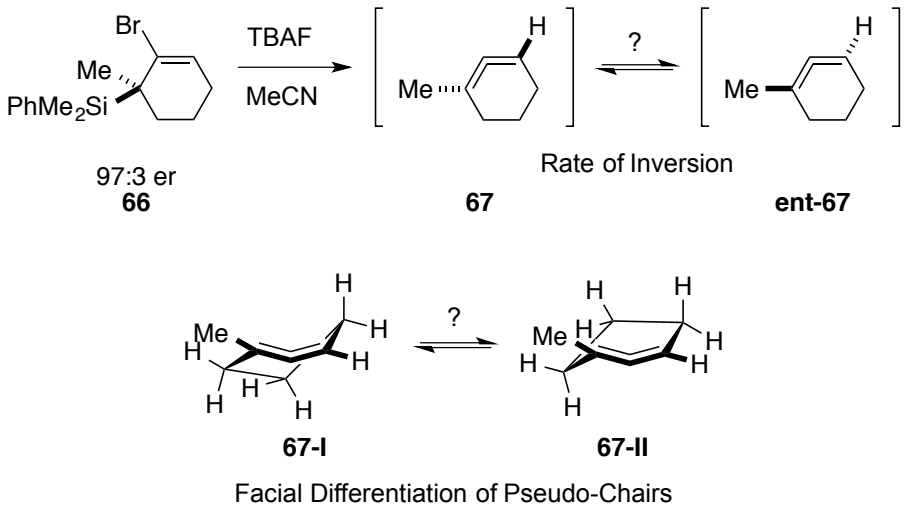

Scheme 3.20 – Two possible scenarios for loss of enantiomeric enrichment.

To discern if the allene is undergoing racemization during the reaction two control experiments were performed. The rate of inversion should vary with the reaction temperature such that lower e.e.'s will be obtained with higher reaction temperatures. (this is with the assumption the rate of trapping a cyclic allene intermediate with a 1,3-dipole is relatively unchanged). Conversely, at a lower temperature the racemization of the cyclic allene should slow relative to the trapping event leading to an increase in the enantiomeric excess observed. When the reaction was performed at –20 °C (entry 1), the enantiomeric ratio of the azomethine imine adducts **74** (64:36) was unaffected. Running the same trapping reaction at 60 °C, the yield decreased to 79 %, however the enantiomeric ratio of the regioisomers **74/75** was determined to be 62:38 and racemic, the same as running the reaction at room temperature. The lack of drift in the enantiomeric ratio across an 80 °C temperature regime suggests the cyclic allene is not undergoing inversion to an appreciable extent prior to trapping with the 1,3-dipole trap.

Table 3.3 - Enantiomeric excess as a function of temperature and number of equivalents of trap employed.

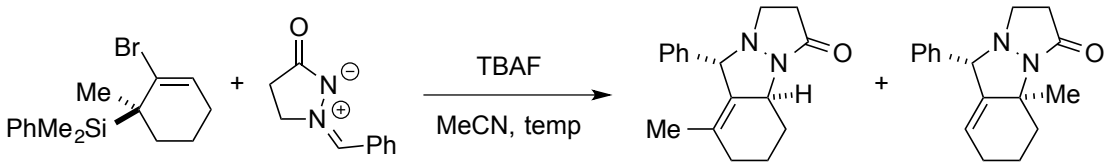

97:3 e.r.
66

equiv
72

74:ent-**74** e.r.
74

50:50 e.r.
75

Entry	Temperature (° C)	Equivalents of **72**	e.r. of **74**
1	rt	3	66:34
2	– 20 °C	3	64:36
3	+ 60 °C	3	62:38
4	rt	1	63:37

The seminal work of Christl, Stalke, and Engels using enantiopure Doering-Moore-Skattebøl starting materials **20** and trapping the resulting cyclic allene with 2,5-dimethylfuran showed the enantiomeric enrichment of the products was robust to changing the reaction temperature. Varying the temperature, substitution of the trap, as well as the dilution of the reaction mixture suggested that the stereochemical course of the reaction was more dependent upon the torquoselectivity of the cyclopropylcarbene ring opening than the rate of inversion (Scheme 3.21).

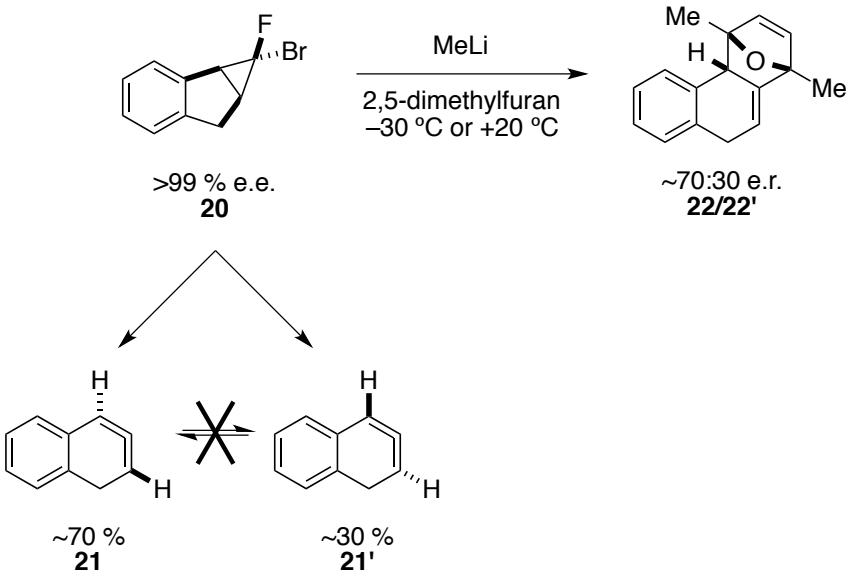

Scheme 3.21 – Investigation into the loss of enantiomeric enrichment in benzofused cyclic allenes.

In a separate experiment the stoichiometry (**68**:azomethine imine **72**) was reduced to 1:1 while keeping the concentration of the cyclic allene constant. Diluting the trapping molecule would allow more time for the allene to undergo inversion prior to trapping, allowing any racemization mechanism to erode the enantiomeric ratio further. The reaction remained remarkably efficient with a yield of 95 % of regioisomers **74** and **75**, in a 5.8:1 ratio respectively (by comparison of the benzylic protons in the ^{1}H NMR spectrum). The enantiomeric ratio of the regioisomers again remained unchanged with the major regioisomer **74** giving a 63:37 enantiomeric ratio. The stable enantiomeric ratios obtained disfavor the racemization of the cyclic allene (**Scheme 3.22**) prior to trapping similar to that observed by Christl.[11]

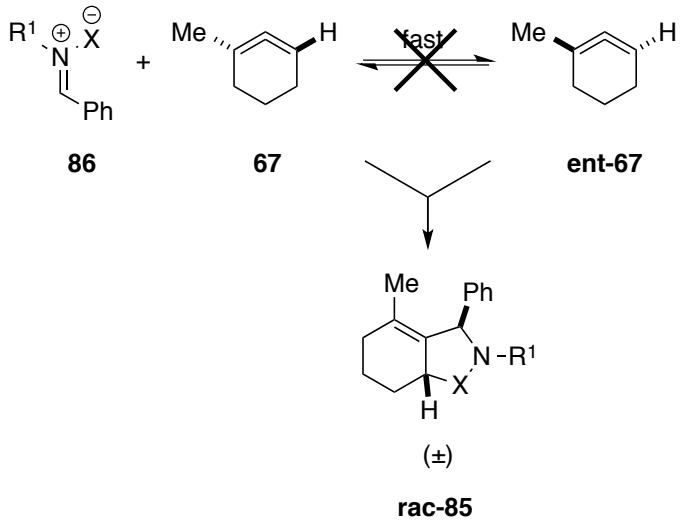

Scheme 3.22 – From control experiments inversion of allene is not likely occurring under the reaction conditions.

The poor enantiomeric ratios obtained across the substrates could also be accounted for by poor facial selectivity of the dipolar trap with respect to the cyclic allene, or poor energetic distinction between the enantiomeric transition states. As suggested in Figure 3.2 there is the possibility of two chair-like structures of the cyclic allene (**88-I** and **88-II**). For each pseudo-chair there are two possible enantiomeric reactive conformations (from diastereomer formation the cycloadducts **87** are assumed to come from an *endo*-like transition state **86**), leading to a total of four possible *endo*-like transition states.

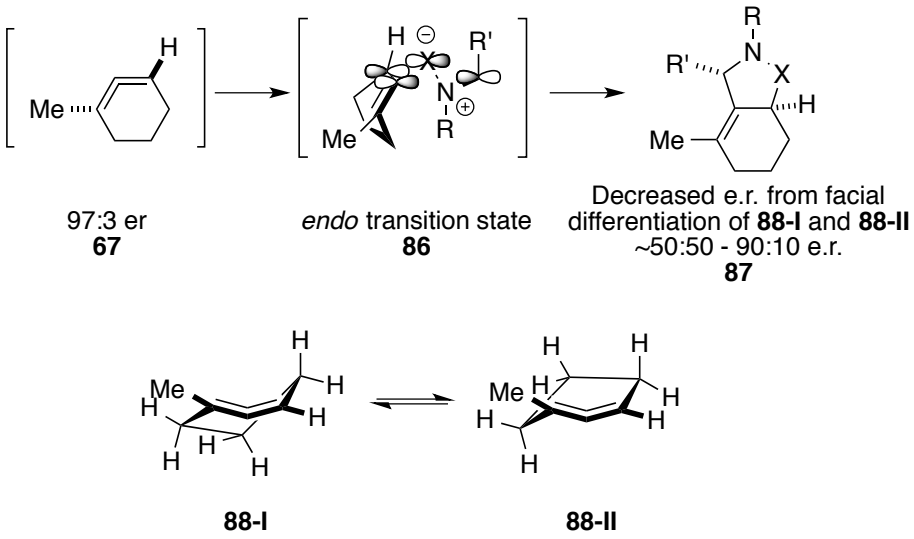

Figure 3.2 - The two possible chair conformations of the chiral cyclic allene intermediates (the absolute stereochemistry of the cycloadducts is unknown).

With regard to the observed enantiomeric ratios, the four postulated transition states (assuming a synchronous cycloaddition) give rise to the two possible enantiomers (Scheme 3.23). With a fast, reversible equilibrium between the two pseudo-chair conformations of the cyclic allene, the energy differences of the stereoisomeric transition states are influenced by two factors, the steric hindrance of the nitrogen and carbon substituents with the cyclic allene backbone (each gauche interaction contributing approximately 0.9 kcal/mol increase energy to the transition state),[26] and the conformation of the resulting cycloadducts (the unsubstituted half chair being favored over the boat by >5 kcal/mol)[27]. The reactions should be highly exergonic considering the strain energy of the cyclic allene intermediate and from the reactions with styrene the trapping events appear to be under kinetic rather than thermodynamic control.[28] Applying the Hammond postulate,[29] the predicted early transition states for the cycloadditions suggest the products have less impact on the regiochemical and stereochemical outcome of the reaction. When comparing the four predicted transition states for cycloaddition across the less-substituted olefin, obvious differences in the steric bias are not present (comparing **89-I**, **89-II**, **89-III**, and **89-IV**).

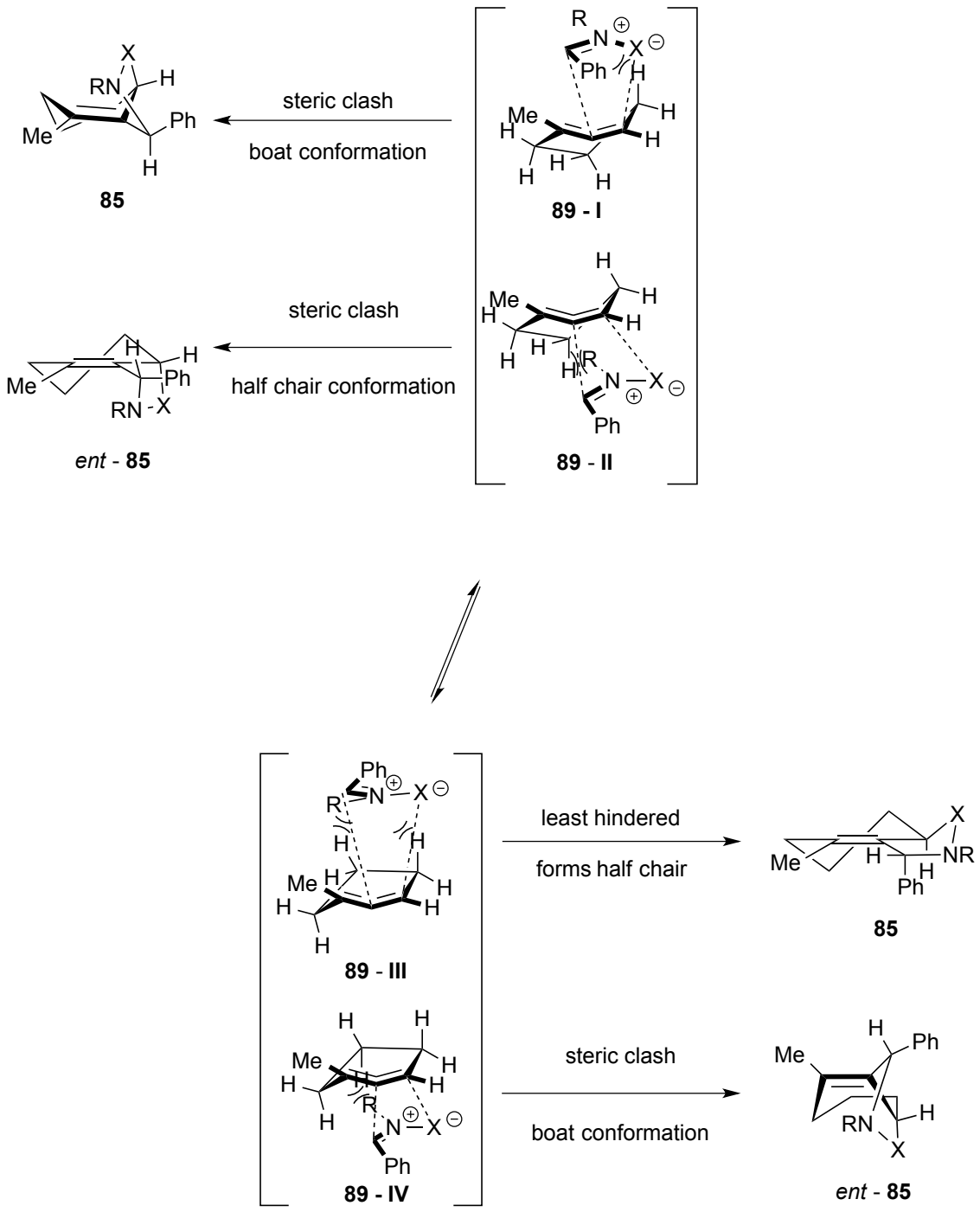

85 | 89 - I | 89 - II | ent - 85 | 89 - III | 85 | 89 - IV | ent - 85

Scheme 3.23 - Four different diastereo-/enantiomeric transition states.

If only a single gauche interaction separates the two transition states an approximate energy difference of 0.9 kcal/mol would be predicted. From the observed enantiomeric ratio of 63:37, an approximate 0.32 kcal/mol difference in transition state energies is predicted from the Gibbs-Helmholtz equation (Equation 3.1).[26] Assuming the

approximation is correct the cycloaddition transition states are very similar in energy. To account for the seemingly small difference in transition state energies more transition states need to be evaluated in addition to a more accurate computational model highlighting the steric interactions.

$$\frac{\mathbf{74}}{\mathbf{74'}} = e^{\frac{-\Delta\Delta G^{\ddagger}}{RT}}$$

Equation 3.1 - The Gibbs-Helmholtz equation (where 74' refers to the enantiomer of cycloadduct 74).

In collaboration with Joseph Cheramy and Yunjie Xu of the University of Alberta, the vibrational-circular dichroism spectrum of azomethine imine cycloadduct **74** was predicted using DFT calculations (B3LYP/6-31+G(d,p)) and compared with the experimentally determined spectrum (Figure 3.3).[22] The spectrum obtained of the enantiomerically enriched cycloadduct strongly suggests the stereochemistry of the major enantiomer is (*S,S*) as shown in Figure 3.3. If this model predicted the absolute stereochemistry of the major enantiomer accurately, the most favored transition state from chiral cyclic allene **67** would be **89-II** or **89-IV**. Further determination of the absolute stereochemistry of all the cycloadducts would allow a computational investigation of the pertinent transition states and evaluation of the facial selectivity that should be expected.

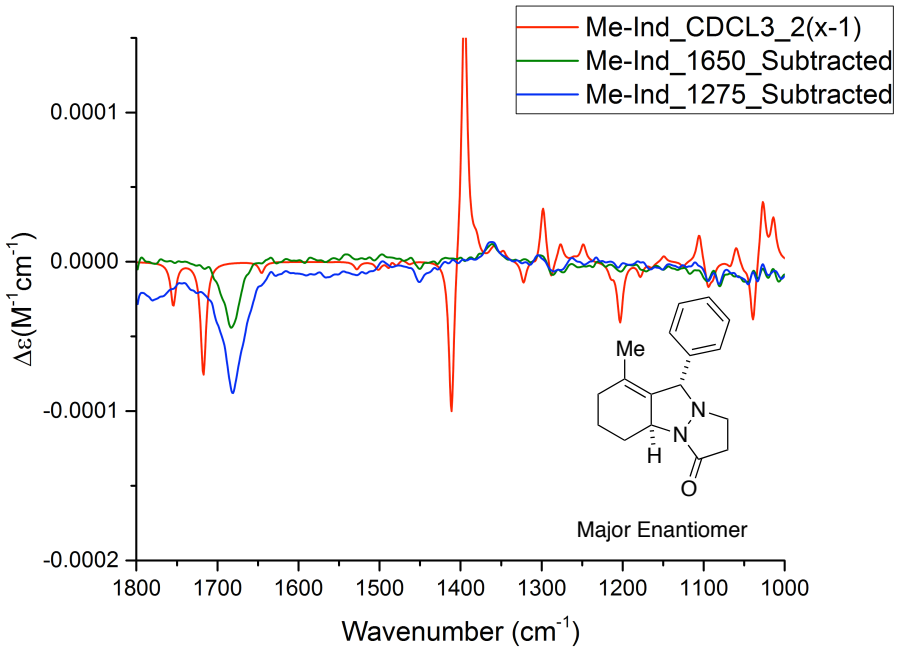

Figure 3.3 - Experimentally determined absolute stereochemistry of azomethine imine cycloadduct 74 by comparison of calculated and experimentally determined vCD spectra. (Calculations: DFT (B3LYP/6-31+G(d,p)) both gas phase and implicit solvation model in chloroform.)

Similar product distributions were observed for both *C*-phenyl azomethine imine **72** and *C*-phenyl nitrone **79**. This is presumably from the similar steric environments encountered in the cycloadditions. To explain the *anti* geometry of the cycloadducts the large phenyl-substituent is presumed to point away from the cyclic allene backbone, leaving the nitrogen substituent overlapping with the backbone. Both the nitrones and azomethine imines have significant aliphatic framework attached to the reactive nitrogen leading to congested transition states with little energy difference.

When dipolar traps bearing a *C*-[(*E*)-styryl]-substituent were used, significantly different cycloaddition results were encountered. The *C*-[(*E*)-styryl]-*N*-methyl nitrone reacted very similarly to the *C*-phenyl nitrone; however, the *C*-[(*E*)-styryl] azomethine imine gave now a mixture of regioisomers, as well as a mixture of diastereomers. The major isomer **76** (which has two tertiary stereocenters) was found to be almost racemic with an *anti* geometry. To account for the *anti* geometry, again the styryl-substituent is situated away from the cyclic allene ring. In the more congested regioisomers, the major

diastereomer has *syn* geometry, not seen previously in any of the cycloadditions with the methyl-substituted cyclic allene. To account for the geometry, the [(*E*)-styryl]-substituent must be situated over the cyclic allene ring (Figure 3.4), and the resulting enantiomeric ratio is much larger at 90:10 while the minor *anti* isomer gave a 63:37 enantiomeric ratio.

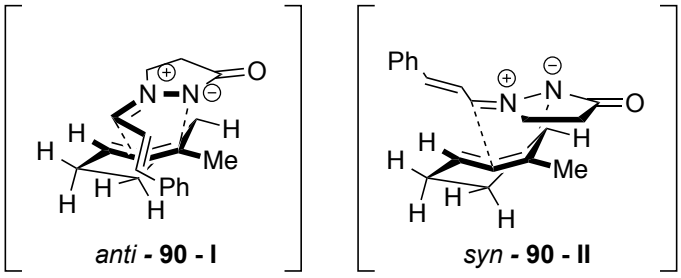

Figure 3.4 – Two possible transition states for *C*-styryl azomethine imine cycloaddition to give the minor regioisomers observed.

In order to have significant enantiomeric enrichment in the product, some energetic difference must exist between the transition states leading to the two different enantiomers. With the minimal knowledge of the absolute stereochemistry of the cycloadducts, a sophisticated discussion of the progression of the cycloadditions is not possible. However, at an elementary level, the proposed transition states in Scheme 3.23 show minimal steric preferences for any trajectory. Given the high diastereoselectivity over the generally large range of dipolar traps employed and the variable enantiomeric fidelity it is likely the cycloadditions are occurring in a similar fashion to that of furan, with some degree of concertedness. Significant interaction with the two reactive atoms of the dipolar trap in the transition state should lead to high diastereoselectivity; however, a very early transition state accounts for the low facial differentiation resulting in low enantiomeric fidelity.

3.4. Conclusion

Significant strides have been made in the study of cyclic allene cycloadditions including the synthesis of enantiomerically enriched allylic silanes by both substrate substitution control, and use of a new directing group. From these allylic silanes enantiomerically enriched cyclic allenes were presumably generated via the unprecedented fluoride-mediated silyl elimination, and trapped with a variety of allenophiles. Interestingly the efficient dipolar cycloadditions of azomethine imines and

nitrones displayed poor enantiomeric fidelity when compared to the cycloaddition with furan. Gratifyingly, the yields of the reactions were increased via the replacement of a triflate-leaving group with a bromide-leaving group. Extremely encouraging is the finding that by using a vinyl bromide-leaving group, changing the stoichiometry of the reaction to 1:1 in trap and allene precursor, high yields and selectivity was maintained.

To get a better understanding of the enantioselectivity a computational study looking in depth at the transition states should allow a quantification of the steric constraints of the different cycloadditions. This is complemented by the absolute stereochemistry of the cycloadducts being assigned using either X-ray crystallography or vibrational circular dichroism. The stereochemistry of the starting allylic silane **66** is hypothesized from the stereochemistry of the reduction/conjugate displacement.

3.5. Future Work

We were successful in the synthesis of enantiomerically enriched allylic silanes. The silanes were crucial to the investigation of axially chiral cyclic allene intermediates; nonetheless these substrates could be applied to the synthesis of other important chemicals. If the allylic silanes were applied to the synthesis of Denmark's dienones[14] (**32**, Scheme 3.24) it would decrease the number of steps required for the starting material synthesis considerably and avoid the use of chiral auxiliaries for the enantiomeric enrichment of the materials.

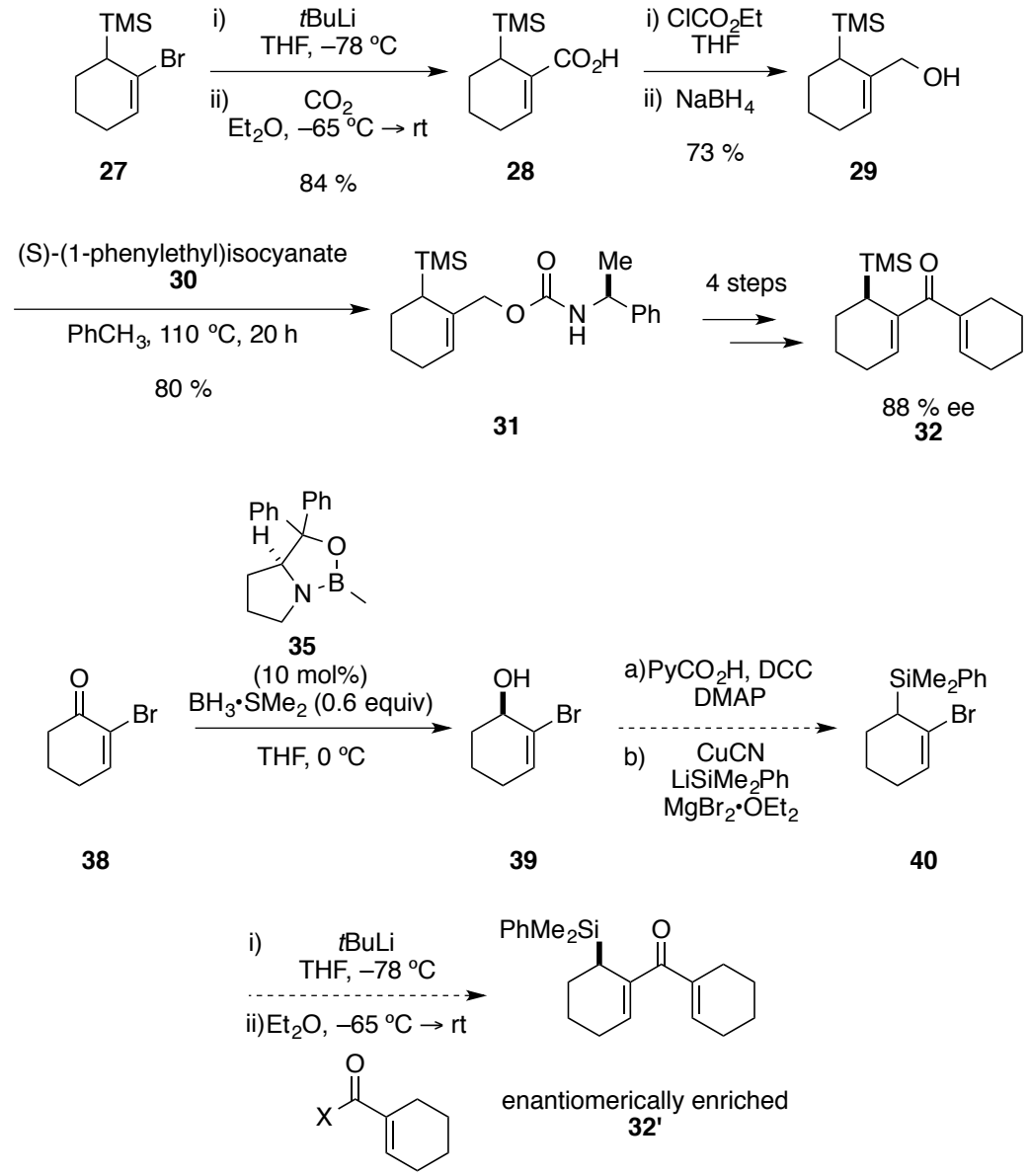

Scheme 3.24 - Use of enantiomerically enriched silanes to streamline synthesis of asymmetric Nazarov precursors.

Given the ability to make enantiomerically enriched allylic silanes, we were able to demonstrate the generation of enantiomerically enriched cyclic allenes and trap them in an enantiomerically fidelitous manner using furan, nitrones, and azomethine imines. Unfortunately, the observed enantiomeric ratio for the dipolar cycloadducts was low. To increase the enantiomeric ratio and regioselectivity, different substituents should be introduced (**91**). The effects of large substituents may allow greater enantiomeric fidelity in intermolecular trapping reactions (Scheme 3.25). Further substituting the backbone

should give interesting cycloadducts in terms of site selectivity on the cyclic allene as well as interesting diastereoselectivity (**95**).

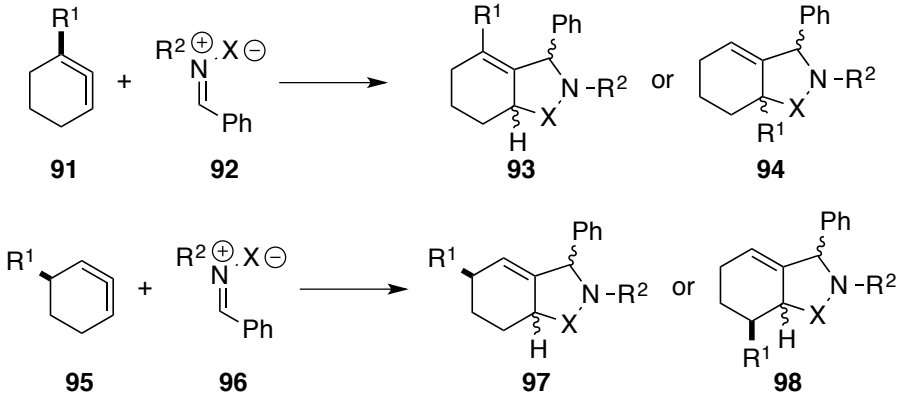

Scheme 3.25 - Effects of substituents on regio-, enantio-, and diastereoselectivity.

The promising enantiomeric fidelitous reactions may allow the application of a cyclic allene/1,3-dipole cycloaddition product to a natural product. This would showcase the techniques developed in the construction of the substrates in a straightforward manner, using catalytic enantiomeric induction (CBS reduction[15]), coupled with the efficient, enantiomerically faithful dipolar cycloadditions of cyclic allenes. One possible target is the natural product ibogamine **99** as shown in Scheme 3.26.[30-32] Starting from azomethine imine[33] **106** and a fluoride-mediated allylic silyl elimination dipolar cycloaddition incorporates all the carbon atoms of ibogamine. From **104** a number of steps are highlighted (**102** → **101**, **103** → **102**), which are unprecedented and leave areas for research and development.

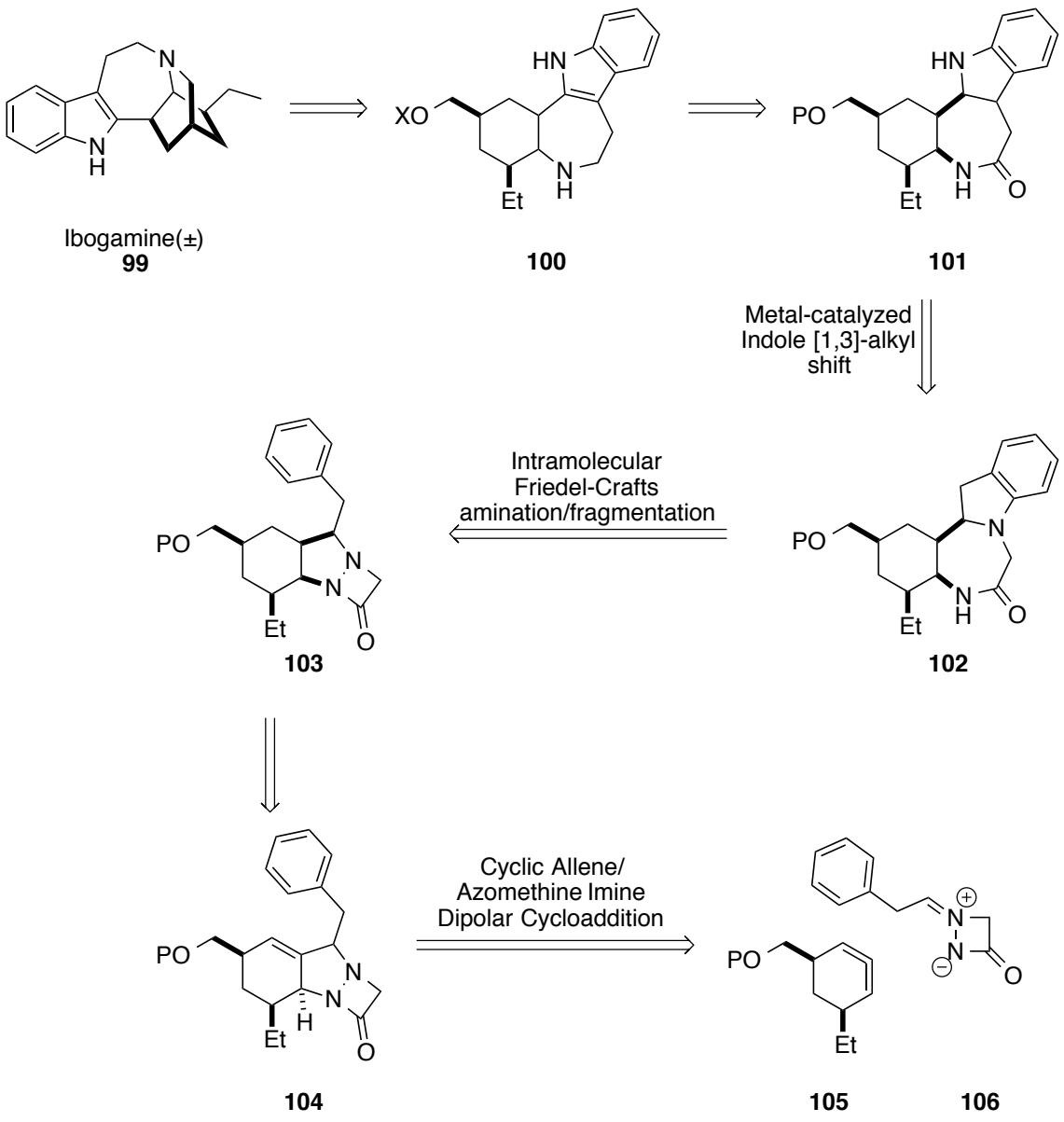

Scheme 3.26 - Proposed retrosynthesis of ibogamine (99).

3.6. Experimental

3.6.1. General Information

Reactions were carried out in oven (120 °C) or flame-dried glassware under a positive argon atmosphere unless otherwise stated. Transfer of anhydrous reagents was accomplished with oven-dried syringes or cannulae. Solvents were distilled before use: acetonitrile (CH_3CN), triethylamine (NEt_3), and dichloromethane (CH_2Cl_2) from calcium hydride, diethyl ether (Et_2O), and tetrahydrofuran (THF) from sodium/benzophenone,

toluene, and benzene (C_6H_6) from sodium metal. Thin layer chromatography was performed on glass plates pre-coated with 0.25 mm Kieselgel 60 F254 (Merck). Flash chromatography columns were packed with 230-400 mesh silica gel (Silicycle). Proton nuclear magnetic resonance spectra (^{1}H NMR) were recorded at 300 MHz, 400 MHz, or 500 MHz and coupling constants (*J*) are reported in Hertz (Hz). Carbon nuclear magnetic resonance spectra (^{13}C NMR) were recorded at 100 MHz or 125 MHz. The chemical shifts are reported on the δ scale (ppm) and referenced to the residual solvent peaks: $CDCl_3$ (7.26 ppm, ^{1}H; 77.06 ppm, ^{13}C) as internal standards. Standard notation is used to describe the multiplicity of the signals observed in ^{1}H NMR spectra: broad (br), apparent (app), multiplet (m), singlet (s), doublet (d), triplet (t), quartet (q), pentet (p), etc. Infrared (IR) spectra were measured with a Mattson Galaxy Series FT-IR 3000 spectrophotometer. High-resolution mass spectrometry (HRMS) data (APPI/APCI/ESI technique) were recorded using an Agilent Technologies 6220 oaTOF instrument. HRMS data (EI technique) were recorded using a Kratos MS50 instrument. (*S*)-(–)-2-Methyl-CBS-oxazaborolidine solution (1 M in toluene) from Sigma-Aldrich was used in these reactions. The enantiomeric excesses for chiral compounds were determined using an HPLC Agilent instrument with Chiralcel-IC column or reverse phase HPLC was run with an HPLC Agilent instrument with Chiralcel-IC or Chiralcel-AD-RH column.

Enone triflate **34**,[34] bromo enone **38**,[35] allylic alcohol **39**,[15] and methylenone **52**[36] are all known literature compounds, ^{1}H NMR and ^{13}C NMR spectral data matched those reported in the literature.

3.6.2. Physical Data

Phenyldimethylsilyl lithium

This reagent was prepared by a procedure similar to that employed by Gilman and coworkers: [37] See Chapter 2.

6-hydroxycyclohex-1-en-1-yl trifluoromethanesulfonate (36)

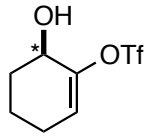

To a solution of (+)-CBS reagent[15,38] (0.1 equiv) in THF (0.09 M) was added a THF solution of enone **34** (0.6 M), and a THF solution of BH_3•SMe_2 (0.6 equiv, 0.38 M) simultaneously via a syringe pump over the course of 2 h at room temperature. Once the addition was completed the solution was stirred for a further 30 minutes after which careful addition of 10 mL of distilled water, an equal volume of ether and 10 mL of 1 M HCl quenched the reaction. The organic layers were separated and the aqueous layer was washed with ether (3 x 30 mL). The combined organic layers were combined, washed with water (30 mL), brine (30 mL), dried with magnesium sulfate, filtered, concentrated, and subjected to flash column chromatography (9:1, hexanes:ethyl acetate eluent) to furnish allylic alcohol **36** as a clear, and colorless oil.

Using 624 mg of enone **34**, 140 μL of BH_3•SMe_2, and 255 mL of 1 M solution of (+)-CBS reagent gave 379 mg of allylic alcohol **36** (60 % yield).

Spectral data matched that seen previously in Chapter 2.

R_f = 0.21 (9:1, hexanes:ethyl acetate); ^{1}H NMR (500 MHz, $CDCl_3$) δ 5.95 (dd, *J* = 7.0, 4.0 Hz, 1H), 4.35 (app dd, *J* = 4.5, 1.5 Hz, 1H), 2.31 (app dtd, *J* = 18.5, 5.0, 1.5 Hz, 1H), 2.19 (ddddd, *J* = 18.5, 9.0, 5.0, 3.5, 1.5 Hz, 1H), 2.06 (br d, *J* = 7.0 Hz, OH), 1.94-1.90 (m, 2H), 1.80-1.61 (m, 2H); ^{13}C NMR (100 MHz, $CDCl_3$) δ 149.4, 122.3, 118.5 (q, $^1J_{CF}$ = 318.1 Hz, 1C), 65.3, 31.9, 24.4, 17.1; IR (cast film, cm^{-1}) 3368, 2948, 2872, 1681; HRMS (ESI) calcd for $[M]^+$ $C_7H_9NaO_4S$: 269.0174, found: 269.0065.

2-{[(Trifluoromethyl)sulfonyl]oxy}cyclohex-2-en-1-yl 4-methylbenzenesulfonate (36')

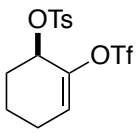

A dry, argon purged flask was charged with enantiomerically enriched allylic alcohol **36** and then dissolved in toluene (0.2 M). Solid trimethylamine hydrochloride was added (1

equiv) and the solution was cooled to 0 °C. To the cooled solution was added triethylamine (3 equiv) and the reaction was stirred for 20 min. Solid *p*-toluenesulfonyl chloride was added (0.75 equiv) and the solution was stirred for 2 hours. A second portion of *p*-toluenesulfonyl chloride (0.75 equiv) was added and the reaction was kept at 0 °C until TLC (9:1, hexanes:ethyl acetate) showed complete consumption of the starting alcohol. The reaction was quenched with 1 M HCl and extracted with diethyl ether (3 x 50 mL). The organic layers were washed with saturated sodium bicarbonate (30 mL), brine (30 mL), dried over magnesium sulfate, filtered, and concentrated. Careful gradient column chromatography (hexanes:ethyl acetate, 95:5 → 85:15 eluent) provided allylic tosylate **36'**, as a thermally unstable solid (the product was stored in the freezer if not used immediately).

Using 1.05 g of enone **89**, 408 mg of NMe_3•HCl, 1.29 g of NEt_3, and 1.22 g of tosyl chloride gave 1.29 g of allylic tosylate **36'** was isolated (75 % yield).

R_f = 0.23 (9:1, hexanes:ethyl acetate); ^{1}H NMR (500 MHz, $CDCl_3$) d 7.85 (d, *J* = 8.4 Hz, 2H), 7.38 (d, *J* = 8.4 Hz, 2H), 6.14 (dd, *J* = 5.4, 2.8 Hz, 1H), 5.08 (br s, 1H), 2.49 (s, 3H), 2.39-2.29 (m, 2H), 2.25-2.17 (m, 1H), 1.93-1.86 (m, 1H), 1.83-1.68 (m, 2H); ^{13}C NMR (125 MHz, $CDCl_3$) d 145.2, 143.9, 133.4, 129.9, 127.9, 126.5, 118.4 (q, $^1J_{CF}$ = 319.0 Hz, 1C) 74.4, 29.9, 24.1, 21.7, 15.6; IR (cast film, cm^{-1}) 3070, 2941, 2873, 1679, 1598; HRMS (ESI) calcd for $[M+Na]^+$ $C_{14}H_{15}F_3NaO_6S_2$: 423.0154, found: 423.0143.

6-(Phenyldimethylsilyl)cyclohex-1-en-1-yl trifluoromethanesulfonate (37)

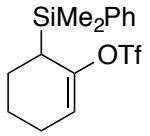

To a dry flask under argon atmosphere was added copper cyanide (0.1 equiv), triphenylphosphine (0.2 equiv), and allylic tosylate **36'**. The flask was charged with diethyl ether (0.15 M) and cooled to 0 °C using an ice/water bath. The previously prepared silyl anion solution (1.5 equiv) was added to the flask via a syringe pump at a rate that allowed the addition to be complete in 1 h.

Once the addition was complete, the reaction was kept at 0 °C for an additional 1 h. While cold the reaction was quenched with equal volumes (30 mL) of pH 7 - phosphate

buffer and hexanes. The layers were separated and the aqueous layer was further washed with hexanes (3 x 40 mL). The organic layer was washed with brine (30 mL), dried over magnesium sulfate, and filtered. Concentrating the organic layer, and careful flash column chromatography on silica (hex:DCM, 95:5 → 90:10) afforded allylic silane **37**.

Using 320 mg of allylic tosylate **36',** 7 mg of CuCN, 43 mg of PPh_3, and 2 mL of $PhMe_2SiCl$, 240 mg of allylic silane **37** (85 % yield) was isolated as a clear, and colorless oil.

R_f = 0.4 (9:1, hexanes:DCM); ^{1}H NMR (400 MHz, $CDCl_3$) δ 7.54 – 7.50 (m, 2H), 7.43 – 7.35 (m, 3H), 5.69 – 5.67 (m, 1H), 2.21 – 2.12 (m, 2H), 2.05 – 1.95 (m, 1H), 1.87 – 1.80 (m, 1H), 1.62 – 1.49 (m, 2H), 1.46 – 1.36 (m, 1H), 0.46 (s, 3H), 0.42 (s, 3H); ^{13}C NMR (125 MHz, $CDCl_3$) δ 152.2, 136.5, 133.9, 129.4, 127.9, 118.6 (q, $^1J_{CF}$ = 312.5 Hz, 1C), 115.9, 28.9, 25.7, 24.1, 20.8, -3.0, -3.9; IR (cast film, cm^{-1}) 3071, 3052, 2947, 2861, 1673; HRMS (EI) calcd for $[M]^+$ $C_{15}H_{19}F_3O_3SSi$: 364.0776, found: 364.0777.

(2-Bromocyclohex-2-en-1-yl)dimethylphenylsilane (40)

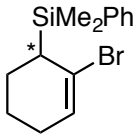

THF (0.37 M/CuCN) was added to a dry, argon purged flask and CuCN (1.1 equiv) was added. The THF was stirred vigorously during the addition to avoid clumps and unsuspended solids stuck to the flask. The resulting green solution was cooled to 0 °C for 10 minutes and the previously prepared solution of $LiSiMe_2Ph$ (2.15 equiv) was then added via cannula. This solution was orange to red in color and was stirred further at 0 °C for 15 minutes. Previously prepared known allylic acetate **39'**[21] (1 equiv) was dissolved with dry degassed THF (0.36 M) and this solution was then added via a syringe pump to the premixed solution of $LiCu(SiMe_2Ph)_2$•LiCN in THF maintained at 0 °C. The solution was added over the course of 1 h maintaining the temperature at 0 °C. Once addition was completed the reaction was stirred for a further 2 hours at 0 °C then quenched via the addition of pH 7-phosphate buffer (50 mL) and an equal volume of hexanes. The aqueous layer was extracted a further 3 times with hexanes (3 x 50 mL), dried over magnesium sulfate, filtered, concentrated, and subjected to column chromatography on silica (1 %

DCM:hexanes). Due to the number of spots by TLC and low polarity of the product an oversized column must be used with at least 4 times the recommended amount of silica.

Using 50 mg of allylic acetate **39'**, 22 mg of CuCN, and 875 μL of $PhMe_2SiCl$ gave 20 mg of allylic silane **40** (29 % yield) as a clear, and colorless oil.

The ^1H and ^{13}C NMR spectral data matched those of the reported compound.[39]

Compound was also synthesized in an enantiomerically enriched fashion via the known picolinic ester **60**[21] via the following procedure:

THF (0.37 M/CuCN) was added to a dry, argon purged flask and a mixture of solid $MgBr_2•OEt_2$ (3.0 equiv), and CuCN (0.9 equiv) was added. The THF was stirred vigorously during the addition to avoid clumps and unsuspended solids stuck to the flask. The resulting green solution was cooled to 0 °C for 10 minutes and the previously prepared solution of $LiSiMe_2Ph$ (1.75 equiv) was then added via cannula. This solution was orange to red in color and was stirred further at 0 °C for 15 minutes. Picolinic ester **60** was dissolved in dry degassed THF (0.36 M) and this solution was then added via a syringe pump to the premixed solution of $LiCu(SiMe_2Ph)_2•LiCN$ and $MgBr_2•OEt_2$ in THF maintained at 0 °C. The solution was added over the course of 1 h maintaining the temperature at 0 °C. Once addition was completed the reaction was stirred for a further 2 hours at 0 °C then quenched via the addition of pH 7-phosphate buffer (50 mL) and an equal volume of hexanes. The aqueous layer was extracted a further 3 times with hexanes (3 x 50 mL), dried over magnesium sulfate, filtered, concentrated, and subjected to column chromatography on silica (1 % DCM:hexanes). Due to the number of spots by TLC and low polarity of the product an oversized column must be used with at least 4 times the recommended amount of silica.

Using 585 mg of allylic picolinate **60**, 155 mg of CuCN, 564 mL of $PhMe_2SiCl$ and 1.30 g of $MgBr_2•OEt_2$ furnished 422 mg of allylic silane **40** (85 % yield) as a clear, and colorless oil.

The ^1H NMR and ^{13}C NMR spectral data matched the previously reported spectral data,[39] and in addition the material showed an $[\alpha]^{25}_D$ -9.1 c = 1.00 (DCM), though the ee was never determined.

2-Bromo-3-methylcyclohex-2-en-1-ol (52')

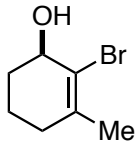

Known allylic alcohol **52'**[36] was synthesized via a known procedure:[15]

To a solution of (+)-CBS reagent[15,38] (0.1 equiv) in THF (0.09 M) was added a THF solution of enone **52** (0.6 M), and a THF solution of BH_3•SMe_2 (0.6 equiv, 0.38 M) simultaneously via a syringe pump over the course of 2 h at room temperature. Once the addition was completed the solution was stirred for a further 30 minutes after which careful addition of 10 mL of distilled water, an equal volume of ether and 10 mL of 1 M HCl quenched the reaction. The organic layers were separated and the aqueous layer was washed with ether (3 x 30 mL). The combined organic layers were combined, washed with water (30 mL), brine (30 mL), dried with magnesium sulfate, filtered, concentrated, and subjected to flash column chromatography (9:1, hexanes:ethyl acetate eluent).

Using 251 mg of enone **52**, 75 μL of BH_3•SMe_2, and 132 μL of 1 M solution of (+)-CBS reagent gave 168 mg of allylic alcohol **52'** (67 % yield) as a clear and colorless oil.

The ^{1}H NMR and ^{13}C NMR spectral data matched those reported for the compound.[36] $[\alpha]_D$ –64.2, c = 1.00 (DCM).

12-Bromo-3-methylcyclohex-2-en-1-yl acetate (53)

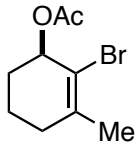

Allylic alcohol **52'** was added to a dry, argon purged flask. DCM (0.1 M) was added to dissolve the alcohol and the solution was cooled to 0 °C via an ice/water bath. To this solution was added acetic anhydride (1.5 equiv), triethylamine (2 equiv), and a catalytic amount of dimethylaminopyridine (1 crystal). The reaction was monitored by TLC analysis for consumption of the starting material and quenched by the addition of DCM (30 mL) and an equal volume of 1 M HCl. The organic layer was separated, the aqueous layer was washed with DCM (3 x 30mL), and the organic layers were combined. The organic layer was washed with distilled water (30 mL), brine (30 mL), dried over

magnesium sulfate, filtered, concentrated and subjected to column chromatography to furnish allylic acetate **53**.

Using 74 mg of allylic alcohol **52'**, 55 μL of acetic anhydride, 109 μL of NEt_3 and a crystal of DMAP furnished 84 mg of allylic acetate **53** (95 % yield) as a clear, and colorless oil.

R_f = 0.75 (9:1, hexanes:ethyl acetate); ^{1}H NMR (500 MHz, $CDCl_3$) δ 5.94 (br s, 1H), 2.25 – 2.11 (m, 2H), 2.13 (s, 3H), 1.96 – 1.90 (m, 1H), 1.90 (d, *J* = 1.0 Hz, 3H), 1.87 (ddd, *J* = 15.5, 4.5, 4.0 Hz, 1H), 1.80 – 1.67 (m, 2H); ^{13}C NMR (125 MHz, $CDCl_3$) δ 170.4, 140.2, 116.6, 72.9, 33.1, 30.2, 23.6, 21.2, 18.2; IR (cast film, cm^{-1}) 2939, 2869, 1738, 1657; HRMS (ESI) calcd for $[M+Na]^+$ $C_9H_{13}BrNaO_2$: 254.9991, found: 254.9991, $[\alpha]_D$ –94.8, c = 1.00 (DCM).

(2-bromo-3-methylcyclohex-2-en-1-yl)dimethylphenylsilane (54)

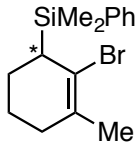

THF (0.37 M/CuCN) was added to a dry, argon purged flask and CuCN (0.95 equiv) was added. The THF was stirred vigorously during the addition to avoid clumps and unsuspended solids stuck to the flask. The resulting green solution was cooled to 0 °C for 10 minutes and the previously prepared solution of $LiSiMe_2Ph$ was then transferred via cannula. This solution was orange to red in color and was stirred further at 0 °C for 15 minutes. Allylic acetate **53** (1.05 equiv) was dissolved in dry degassed THF (0.36 M) and this solution was then added via a syringe pump to the premixed solution of $LiCu(SiMe_2Ph)_2$•LiCN in THF, maintained at 0 °C. The solution was added over the course of 1 h maintaining the temperature at 0 °C. Once addition was completed the reaction was stirred for a further 2 hours at 0 °C then quenched via the addition of pH 7-phosphate buffer (50 mL) and an equal volume of hexanes. The aqueous layer was extracted a further 3 times with hexanes (3 x 50 mL), dried over magnesium sulfate, filtered, concentrated, and subjected to column chromatography on silica (1 % DCM:hexanes). Due to the number of spots by TLC and low polarity of the product a

column four times the recommended size with 4 times the recommended amount of silica was used for the scale of the reaction was employed.[40]

Using 120 mg of allylic acetate **53**, 49 mg of CuCN, and 178 μL of $PhMe_2SiCl$, 23 mg of allylic silane **54** was obtained (31 %) as a clear and colorless oil.

R_f = 0.63 (hexanes); ^{1}H NMR (400 MHz, $CDCl_3$) δ 7.56 – 7.52 (m, 2H), 7.36 – 7.32 (m, 3H), 2.32 (app nonet, *J* = 1.9 Hz, 1H), 2.10 – 2.01 (m, 1H), 1.94 (dt, *J* = 17.5, 5.4 Hz, 1H), 1.78 (app t, *J* = 1.0 Hz, 3H), 1.73 (dd, *J* = 13.7, 5.7 Hz, 1H), 1.61 (app dq, *J* = 13.4, 4.6 Hz, 1H), 1.54 – 1.48 (m, 2H), 0.47 (s, 3H), 0.40 (s, 3H); ^{13}C NMR (125 MHz, $CDCl_3$) δ 138.9, 134.0, 129.6, 128.8, 127.6, 121.1, 36.3, 32.7, 27.9, 23.8, 21.9, –1.6, –2.5; IR (cast film, cm^{-1}) 3068, 3048, 2931, 2856, 1649; HRMS (ESI) calcd for $[M+Na]^+$ $C_{15}H_{21}BrNaSi$: 331.0488, found: 331.0491; $[\alpha]_D$ –3.3, c = 1.00 (DCM).

2-bromo-3-methylcyclohex-2-en-1-yl pyridine-2-carboxylate (65)

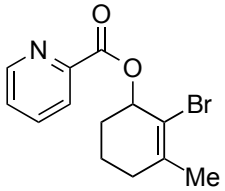

Allylic alcohol **52'** was dissolved in dry degassed DCM and transferred by cannula to a mixture of dicyclohexylcarbodiimide (1.1 equiv), dimethylaminopyridine (0.3 equiv), and picolinic acid (1.1 equiv) in DCM cooled to 0 °C. The mixture was stirred at 0 °C for 1 h and warmed to room temperature where it was stirred until the starting material had been consumed by TLC. The reaction was filtered through a pad of celite, washing the solid phase with DCM (3 x 30 mL), concentrated, subjected to flash column chromatography (8:2, hexanes:ethyl acetate) to afford picolinic ester **65** as a clear and colorless oil in 78 % yield.

R_f = 0.31 (7:3, hexanes:ethyl acetate); ^{1}H NMR (500 MHz, $CDCl_3$) δ 8.83 (dd, *J* = 4.8, 1.8, 0.9 Hz, 1H), 8.18 (dd, *J* = 7.9, 1.1 Hz, 1H), 7.87 (td, *J* = 7.8, 1.9 Hz, 1H), 7.49 (ddd, *J* = 7.7, 4.8, 1.3 Hz, 1H), 5.81 (br s, 1H), 2.29 – 2.09 (m, 3H), 2.03 (app tdd, *J* = 14.0, 4.5, 3.3 Hz, 1H), 1.92 (s, 3H), 1.90 (m, 1H), 1.77 – 1.71 (m, 1H); ^{13}C NMR (125 MHz, $CDCl_3$) δ 164.6, 150.1, 148.3, 140.7, 136.9, 126.8, 125.3, 116.2, 74.5, 33.2, 30.2, 23.7,

18.4; IR (cast film, cm^{-1}) 3055, 2944, 2867, 1717; HRMS (EI) calcd for $[M]^+$ $C_{13}H_{14}NO_2$: 216.10245, found: 216.10252; $[\alpha]_D$ -73.9, c = 1.00 (DCM).

{2-Bromo-1-[dimethyl(phenyl)silyl]cyclohex-2-en-1-e}methane (66)

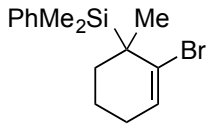

THF (0.37 M/CuCN) was added to a dry, argon purged flask and a mixture of solid $MgBr_2$•OEt_2 (3.0 equiv), and CuCN (0.95 equiv) was added. The THF was stirred vigorously during the addition to avoid clumps and unsuspended solids stuck to the flask. The resulting green solution was cooled to 0 °C for 10 minutes and the previously prepared solution of $LiSiMe_2Ph$ was then added via cannula. This solution was orange to red in color and was stirred further at 0 °C for 15 minutes. Picolinic ester **65** (1.05 equiv) was dissolved in dry degassed THF (0.36 M) and this solution was then added via a syringe pump to the premixed solution of $LiCu(SiMe_2Ph)_2$•LiCN and $MgBr_2$•OEt_2 in THF maintained at 0 °C. The solution was added over the course of 1 h maintaining the temperature at 0 °C. Once addition was completed the reaction was stirred for a further 2 hours at 0 °C then quenched via the addition of pH 7-phosphate buffer (50 mL) and an equal volume of hexanes. The aqueous layer was extracted a further 3 times with hexanes (3 x 50 mL), dried over magnesium sulfate, filtered, concentrated, and subjected to column chromatography on silica (1 % DCM:hexanes). Due to the number of spots by TLC and low polarity of the product a column four times the recommended size with 4 times the recommended amount of silica was used for the scale of the reaction was employed.[40]

[Note: The $MgBr_2$•OEt_2 was prepared by the addition of dibromoethane to an ethereal suspension of magnesium filings. The addition of dibromoethane caused the solution to boil. The reaction was heated to reflux until the filings had been consumed, then the suspension was transferred by cannula to a dry 1-neck round bottom flask. To the reaction flask was added another portion of ether and transferred by cannula to the 1-neck round bottom again. The suspension was concentrated and the solid was dried on a

Schlenk line overnight. The solid was then powdered in a mortar and pestle and stored in a dessicator until needed.]

Using 2.15 g of allylic picolinate **65**, 0.66 g of CuCN, 5.2 g of previously prepared $MgBr_2 \bullet OEt_2$, and 2.25 mL of $PhMe_2SiCl$ furnished 1.33 g of allylic silane **66** (64 % yield) was obtained as a clear and colorless oil (stable under argon for >3 months).

R_f = 0.57 (hexanes); ^{1}H NMR (500 MHz, $CDCl_3$) δ 7.61 – 7.59 (m, 2H), 7.39 – 7.36 (m, 3H), 6.01 (app t, *J* = 4.0 Hz, 1H), 2.01 (app dq, *J* = 17.8, 5.5 Hz, 1H), 1.94 – 1.86 (m, 1H), 1.80 – 1.75 (m, 1H), 1.54 – 1.49 (m, 2H), 1.40 – 1.35 (m, 1H), 1.29 (s, 3H), 0.49 (s, 3H), 0.46 (s, 3H); ^{13}C NMR (125 MHz, $CDCl_3$) δ 137.7, 134.6, 133.0, 128.9, 128.5, 127.5, 35.6, 33.0, 28.0, 23.3, 18.1, –3.1, –3.8; IR (cast film, cm^{-1}) 3069, 3048, 2938, 2863, 2836, 1624; HRMS (EI) calcd for $[M]^+$ $C_{15}H_{21}{}^{79}BrSi$: 308.05960, found: 308.05928; $[\alpha]_D$ +49.5, c = 1.73 (DCM).

(2-Benzoyl-1-methylcyclohex-2-en-1-yl)dimethylphenylsilane (69)

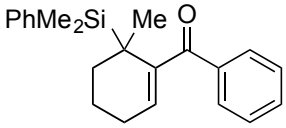

To a dry, argon purged flask was added allylic silane **66** and dry THF (0.2 M). The solution was cooled in a dry ice/acetone bath and *tert*-butyl lithium (1.7 M in pentane, 2.0 equiv) was added. The solution turned bright yellow. Maintaining the temperature at – 78 °C the reaction was monitored for 15 minutes or until the color dissipated at which point benzoyl cyanide (2.0 equiv) was added as a solid. The reaction was warmed to 0 °C using an ice bath and the reaction was stirred for 10 minutes at which point distilled water and ether were added to quench the reaction. The aqueous layer was extracted with ether (3 x 30 mL), and the combined organic layers were washed with distilled water (1 x 30 mL), brine (1 x 30 mL), dried over magnesium sulfate, filtered, concentrated, and subjected to column chromatography (1:3, DCM:hexanes eluent).

Using 107 mg of allylic silane **66**, 407 mL of 1.7 M *t*-BuLi (in pentanes), 91 mg of benzoyl cyanide furnished yielded 24 mg of benzoylated allylic silane **69** (21 %) as an oily white film.

R_f = 0.63 (1:1, DCM:hexanes); ^{1}H NMR (500 MHz, $CDCl_3$) δ 7.59 – 7.54 (m, 4H), 7.48 (app tt, *J* = 6.8, 1.2 Hz, 1H), 7.40 – 7.35 (m, 2H), 7.33 – 7.26 (m, 3H), 6.24 (app t, *J* = 4.0 Hz, 1H), 2.21 (app dtd, *J* = 19.6, 6.8, 4.4, 1H), 2.08 (app dtd, *J* = 19.6, 6.0, 4.0 Hz, 1H), 1.78 – 1.72 (m, 1H), 1.61 – 1.54 (m, 2H), 1.39 – 1.34 (m, 1H), 1.28 (s, 3H), 0.49 (s, 3H), 0.43 (s, 3H); ^{13}C NMR (125 MHz, $CDCl_3$) δ 199.2, 146.7, 140.8, 139.7, 139.4, 134.5, 131.5, 129.5, 128.5, 127.9, 127.4, 35.6, 26.7, 25.9, 23.4, 18.4, –2.3, –2.9; IR (cast film, cm^{-1}) 3067, 3024, 2938, 2861, 1650; HRMS (ESI) calcd for $[M+Na]^+$ $C_{22}H_{26}NaOSi$: 357.1645, found: 357.1642; $[\alpha]_D$ +95.5, c = 1.45; HPLC: IC column, 99.5:0.5, hexanes:IPA, 10 °C, ret. time = 7.15 min, 7.51 min (major), e.r. 97:3.

3-methyl-11-oxatricyclo[6.2.1.0^{2,7}]undeca-2,9-diene (70)

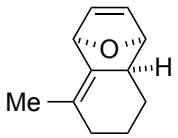

Allylic silane **66** was dissolved in furan (1M) and purged with argon. To the solution was added TBAF (1M, 3 equiv) and stirred for 1 hour. A small amount of silica was added to the solution, the stir bar was removed and the solution was concentrated. The residue was subjected to flash column chromatography (1:20, diethyl ether:hexanes eluent).

Using 90.1 mg of allylic silane **66** and 4 mL of furan yielded 21.6 mg (46 % yield) of Diels-Alder adduct **70** as a volatile colorless oil.

R_f = 0.33 (10:1, hexanes:diethyl ether); ^{1}H NMR (500 MHz, $CDCl_3$) δ 6.41 (dd, *J* = 5.5, 1.5 Hz, 1H), 6.03 (dd, *J* = 5.5, 1.5 Hz, 1H), 5.24 (s, 1H), 5.02 (ddd, *J* = 5.0, 1.0, 0.5 Hz, 1H), 2.36 – 2.32 (m, 1H), 2.06 (br dd, *J* = 15.5, 7.7 Hz, 1H), 1.94 (app dq, *J* = 11.6, 3.6 Hz, 1H), 1.85 – 1.80 (m, 2H), 1.68 (s, 3H), 1.59 – 1.52 (m, 1H), 0.33 (app qd, *J* = 11.8, 3.0 Hz, 1H); ^{13}C NMR (125 MHz, $CDCl_3$) δ 135.1, 132.7, 129.2, 125.0, 81.9, 78.9, 40.6, 30.5, 26.8, 23.2, 19.1; IR (cast film, cm^{-1}) 3071, 2999, 2928, 2856, 1560; HRMS (ESI) calcd for $[M+Na]^+$ $C_{11}H_{14}O$: 162.10446, found: 162.10431; HPLC: IC column, 95:5, hexanes:IPA, 20 °C, ret. time = 10.6 min (major), 12.6 min, e.r. 87:13.

Representative procedure for the reaction of allylic silanes with dipolar traps:

To a dry, argon purged flask was added allylic silane **54**. The flask was charged with dry acetonitrile (0.2 M), and the appropriate azomethine imine (**72** or **73**, 3 equiv) or nitrone (**79** or **82**, 5 equiv). The solution was stirred at room temperature as TBAF (3 equiv, diluted from 1 M to 0.17 M with acetonitrile) was added via a syringe pump over the course of one hour. Once the addition was completed the reaction was stirred until the starting material had been consumed as determined by TLC analysis. Upon consumption of the starting silane the stir bar was removed and the solution was concentrated. The residue was purified by flash column chromatography (see specific compound for eluent used).

Using 45 mg of allylic silane **66**, 76 mg of azomethine imine **72**, and 436 μL of TBAF furnished 38 mg of indazolones **74** and **75** as a partially separable mixture of regioisomers (5:1). Ethyl acetate (100 %) was used as the eluent to separate the two regioisomers.

***Anti*-8-methyl-9-phenyl-1H,2H,3H,4aH,5H,6H,7H,9H-pyrazolidino[1,2-a]indazol-3-one (56/74)**

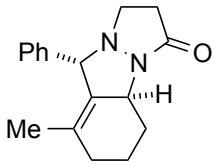

R_f = 0.2 (ethyl acetate); ^{1}H NMR (500 MHz, $CDCl_3$) δ 7.38 – 7.27 (m, 5H), 4.30 (br s, 1H), 4.14 (br s, 1H), 3.39 (td, *J* = 9.2, 4.1 Hz, 1H), 3.03 (app q, *J* = 9.9 Hz, 1H), 2.75 – 2.53 (m, 3H), 2.10 – 1.94 (m, 3H), 1.67 – 1.52 (m, 2H), 1.44 (s, 3H); ^{13}C NMR (125 MHz, $CDCl_3$) δ 166.6, 139.2, 135.2, 129.3, 128.8, 128.4, 128.0, 71.2, 55.4, 49.3, 35.3, 30.5, 26.0, 20.3, 19.0; IR (cast film, cm^{-1}) 3060, 2934, 2856, 1683; HRMS (EI) calcd for $[M]^+$ $C_{17}H_{20}N_2O$: 268.15756, found: 268.15756. HPLC: IC column, 75:25, hexanes:IPA, 22 °C, ret. time = 26.7 min (major), 37.6 min, e.r. 64:36.

TROESY correlations relevant to stereochemistry:

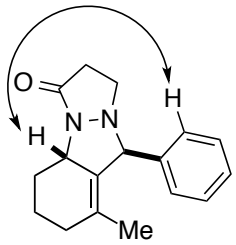

***Anti*-4a-methyl-9-phenyl-1H,2H,3H,4aH,5H,6H,7H,9H-pyrazolidino[1,2-a]indazol-3-one (57/75)**

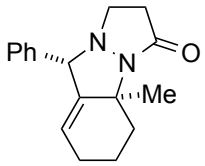

R_f = 0.36 (ethyl acetate); ^{1}H NMR (500 MHz, $CDCl_3$) δ 7.45 – 7.32 (m, 5H), 5.43 (app q, *J* = 3.8 Hz, 1H), 4.15 (app q, *J* = 2.7 Hz, 1H), 3.66 – 3.57 (m, 1H), 2.89 – 2.82 (m, 2H), 2.74 – 2.66 (m, 2H), 2.20 – 2.11 (m, 2H), 1.93 – 1.88 (m, 1H), 1.84 – 1.68 (m, 2H), 1.56 (s, 3H); ^{13}C NMR (125 MHz, $CDCl_3$) δ 163.8, 146.9, 39.7, 128.7, 127.9, 127.5, 120.6, 73.2, 58.3, 51.4, 36.4, 31.9, 23.6, 23.3, 17.4; IR (cast film, cm^{-1}) 3030, 2940, 2834, 1681; HRMS (EI) calcd for $[M]^+$ $C_{17}H_{20}N_2O$: 268.15756, found: 268.15689. HPLC: IC column, 75:25, hexanes:IPA, 22 °C, ret. time = 16.2 min, 30.6 min, e.r. 50:50.

TROESY correlations relevant to stereochemistry:

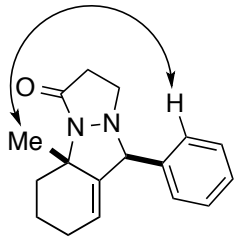

Using 50 mg of allylic silane **66**, 100 mg of azomethine imine **73**, and 480 μL of TBAF furnished 42.1 mg (95 % yield) of indazalones **76** and **77** and **78** as a clear and yellow oil, partially separable (4:1.4:1, **76**:**77**:**78** mixture of regioisomers). Ethyl acetate (100 %) was used as the eluent for chromatography.

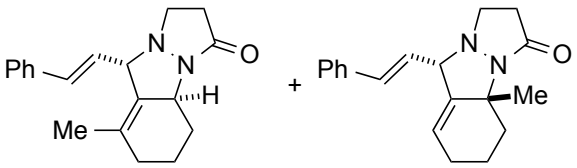

A mixture of **76** and **77** were partially separated by semi-preparative reverse phase HPLC, ACN C8 column 1:1:0.05%, H_2O:MeCN:TFA, 40 °C, ret. time = 10.2 min (**76**), 10.8 min (**77**), for the purpose of identification. Compound **76** partially decomposed upon subjecting it to semi-preparative HPLC and was further subjected to flash chromatography(ethyl acetate 100 % eluent).

***Anti*-4a-methyl-9-[(*E*)-2-phenylethenyl]-1H,2H,3H,4aH,5H,6H,7H,9H-pyrazolidino[1,2-a]indazol-3-one (76)**

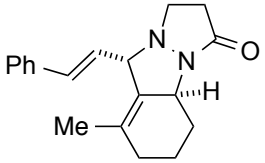

R_f = 0.19 (ethyl acetate); ^{1}H NMR (500 MHz, $CDCl_3$) δ 7.42 – 7.40 (m, 2H), 7.37 – 7.34 (m, 2H), 7.30 – 7.25 (m, 1H), 6.62 (d, *J* = 15.5 Hz, 1H), 6.07 (dd, *J* = 16.0, 9.5 Hz, 1H), 4.10 (br s, 2H), 3.53 – 3.47 (m, 1H), 3.19 (app q, *J* = Hz, 1H), 2.78 – 2.66 (m, 2H), 2.61 – 2.57 (m, 1H), 2.13 – 1.99 (m, 2H), 1.98 – 1.93 (m ,1H), 1.68 (s, 3H), 1.65 – 1.47 (m, 2H); ^{13}C NMR (125 MHz, $CDCl_3$) δ 168.7 (br), 136.9, 133.7, 133.5, 129.6, 128.7, 128.1, 126.5, 124.9 (br), 68.0 (br), 54.0, 47.6 (br), 35.0, 30.4, 26.4, 20.2, 19.0; IR (cast film, cm^{-1}) 3057, 3025, 2935, 2862, 1691; HRMS (ESI) calcd for $[M+H]^+$ $C_{19}H_{22}N_2O$: 295.1805, found: 295.1803; HPLC: IC column, 75:25, hexanes:IPA, 22 °C, ret. time = 24.9 min (major), 39.3 min, e.r. 57:43.

Pertinent TROESY correlations for relative stereochemistry:

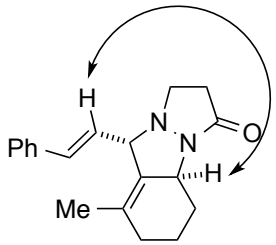

***Syn*-8-methyl-9-[(*E*)-2-phenylethenyl]-1H,2H,3H,4aH,5H,6H,7H,9H-pyrazolidino[1,2-a]indazol-3-one (77)**

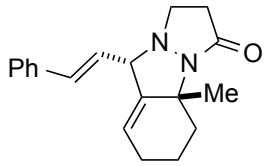

R_f = 0.15 (ethyl acetate); ^{1}H NMR (500 MHz, $CDCl_3$) δ 7.46 – 7.44 (m, 2H), 7.38 – 7.35 (m, 2H), 7.32 – 7.28 (m, 1H), 6.67 (d, *J* = 16.5 Hz, 1H), 6.06 (dd, *J* = 16.0, 8.0 Hz, 1H), 5.52 (app q, *J* = 3.5 Hz, 1H), 3.76 (m, 1H), 3.59 (t, *J* = 8.0 Hz, 1H), 3.00 – 2.84 (m, 2H), 2.61 (dd, *J* = 14.5, 7.0 Hz, 1H), 2.47 (dt, *J* = 12.0, 3.5 Hz, 1H), 2.18 – 2.12 (m, 2H), 1.89 – 1.85 (m, 1H), 1.76 – 1.58 (m, 2H), 1.66 (s, 3H); ^{13}C NMR (125 MHz, $CDCl_3$) δ 164.0, 144.7, 136.1, 135.7, 128.7, 128.2, 126.6, 124.2, 120.4, 69.7, 57.4, 53.2, 36.5, 32.4, 23.2, 23.1, 18.0; IR (cast film, cm^{-1}) 3026, 2974, 2941, 1676; HRMS (ESI) calcd for $[M+H]^+$ $C_{19}H_{23}N_2O$: 295.1805, found: 295.1801; HPLC: IC column, 75:25, hexanes:IPA, 22 °C, ret. time = 18.9 min, 22.0 min, e.r. 90:10.

Pertinent TROESY correlations for relative stereochemistry:

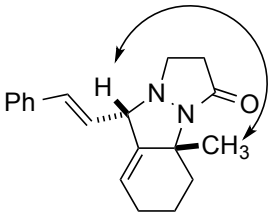

***Anti*-4a-methyl-9-[(*E*)-2-phenylethenyl]-1H,2H,3H,4aH,5H,6H,7H,9H-pyrazolidino[1,2-a]indazol-3-one (78)**

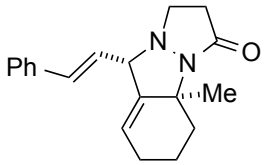

R_f = 0.20 (ethyl acetate); ^{1}H NMR (500 MHz, $CDCl_3$) δ 7.44 – 7.42 (m, 2H), 7.36 – 7.33 (m, 2H), 7.29 – 7.26 (m, 1H), 6.59 (d, *J* = 16.0 Hz, 1H), 6.18 (dd, *J* = 16.0, 8.5 Hz, 1H), 5.50 (app q, *J* = 4.0 Hz, 1H), 3.76 – 3.74 (m, 1H), 3.65 (td, *J* = 6.0, 2.5 Hz, 1H), 2.85 – 2.79 (m, 2H), 2.76 – 2.62 (m, 2H), 2.19 – 2.11 (m, 2H), 2.06 – 1.88 (m, 1H), 1.81 – 1.70 (m, 2H), 1.50 (s, 3H); ^{13}C NMR (125 MHz, $CDCl_3$) δ 163.6, 145.4, 136.4, 132.2, 128.6,

128.5, 127.9, 126.6, 120.8, 71.9, 58.1, 51.2, 36.3, 31.7, 23.7, 23.1, 17.5; IR (cast film, cm^{-1}) 3058, 3026, 2938, 2868, 1679; HRMS (ESI) calcd for $[M+H]^+$ $C_{19}H_{23}N_2O$: 295.1805, found: 295.18; HPLC: IC column, 75:25, hexanes:IPA, 20 °C, ret. time = 17.5 min, 30.0 min, e.r.: 34:66.

Pertinent TROESY correlations for relative stereochemistry:

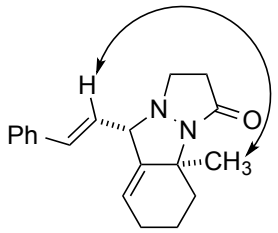

Using 45 mg of allylic silane **66**, 156 mg of nitrone **79**, and 440 mL of TBAF furnished 42 mg (95 % yield) of isoxazolines **80** and **81** as a clear and colorless oil, partially separable (12:1 mixture of regioisomers). 4:10:96, ethyl acetate:DCM:hexanes was used as the eluent for chromatography.

***Anti*-2-benzyl-3-phenyl-2,3,5,6,7,7a-hexahydro-1,2-benzoxazole (80)**

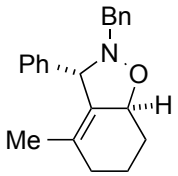

R_f = 0.19 (19:1, hexanes:ethyl acetate); ^{1}H NMR (500 MHz, $CDCl_3$) δ 7.42 – 7.21 (m, 10H), 4.47 – 4.43 (m, 1H), 4.38 (br s, 1H), 4.03, 4.01 (ABq, J_{AB} = 10.0 Hz, 2H), 2.23 (dddd, J = 11.5, 5.5, 4.0, 3.0 Hz, 1H), 2.04 – 2.02 (m, 2H), 1.94 – 1.88 (m, 1H), 1.61 – 1.51 (m, 1H), 1.52 (app q, J = 1.0 Hz, 3H), 1.30 (dddd, J = 14.0, 11.5, 10.5, 3.0 Hz, 1H); ^{13}C NMR (125 MHz, $CDCl_3$) δ 140.8, 138.2, 137.8, 128.9, 128.5, 128.3, 128.2, 127.3, 127.1, 126.7, 77.2, 71.5, 61.1, 30.7, 27.8, 19.8, 18.7; IR (cast film, cm^{-1}) 3061, 3028, 2940, 2864, 2830; HRMS (EI) calcd for $[M]^+$ $C_{21}H_{23}NO$: 305.17798, found: 305.17802, $[\alpha]_D$ +20.2, c = 1.28 (DCM); HPLC: Reverse Phase, OD-RH column, (0.05% acetic acid) H_2O/MeCN gradient: 1:9, H_2O:MeCN – 9:1, H_2O:MeCN, 30 °C, ret. time = 33.5 min, 34.6 min (major), 1 mL/min; e.r.: 37:63.

Pertinent TROESY correlations for stereochemistry:

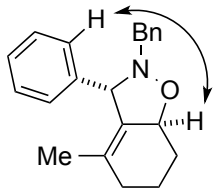

***Anti*-2-benzyl-7a-methyl-3-phenyl-2,3,5,6,7,7a-hexahydro-1,2-benzoxazole (81)**

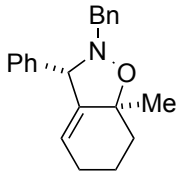

R_f = 0.29 (19:1, hexanes:ethyl acetate); ^{1}H NMR (500 MHz, $CDCl_3$) δ 7.51 – 7.49 (m, 2H), 7.44 – 7.42 (m, 2H), 7.36 – 7.21 (m, 6H), 5.42 – 5.40 (m, 1H), 4.31 (app q, *J* = 2.0 Hz, 1H), 4.10 (d, *J* = 15.0 Hz, 1H), 3.99 (d, *J* = 15.0 Hz, 1H), 2.16 – 2.11 (m, 2H), 1.95 (dt, *J* = 11.5, 3.5 Hz, 1H), 1.90 – 1.86 (m, 1H), 1.72 – 1.62 (m, 1H), 1.52 – 1.46 (m, 1H), 1.49 (s, 3H); ^{13}C NMR (125 MHz, $CDCl_3$) δ 148.1, 140.4, 138.1, 128.5, 128.4, 128.1, 127.8, 127.4, 126.9, 118.4, 79.3, 72.8, 60.3, 34.6, 24.5, 23.9, 18.8; IR (cast film, cm^{-1}) 3062, 3028, 2943, 2863, 1602; HRMS (ESI) calcd for $[M+H]^+$ $C_{21}H_{24}NO$: 306.1852, found: 306.1848; HPLC: Reverse Phase, AD-RH column, 0.1% AA/H_2O/MeCN gradient: 1:9, H_2O:MeCN – 9:1, H_2O:MeCN, (30 °C, 1 mL/min) 34.4 min (major) and 35.9 min, e.r.: 79:21.

Pertinent TROESY correlations for stereochemistry:

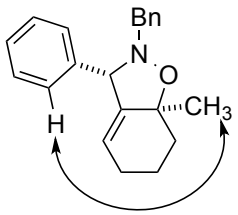

Using 54 mg of allylic silane **66**, 142 mg of nitrone **82**, and 430 μL of TBAF furnished a mixture of isoxazoles **83** (17 %) and **84** (10 %) as a partially separable mixture. 8:10:100, ethyl acetate:DCM:hexanes was used as the eluent for chromatography.

***Anti*-2,4-dimethyl-3-[(*E*)-2-phenylethenyl]-2,3,5,6,7,7a-hexahydro-1,2-benzoxazole (83)**

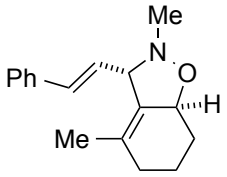

R_f = 0.16 (9:1, hexanes:ethyl acetate); ^{1}H NMR (500 MHz, $CDCl_3$) δ 7.44 – 7.42 (m, 2H), 7.35 – 7.32 (m, 2H), 7.28 – 7.24 (m, 1H), 6.59 (d, *J* = 16.0 Hz, 1H), 6.18 (dd, *J* = 16.0, 8.5 Hz, 1H), 4.31 (br s, 1H), 3.72 (br d, *J* = 7.5 Hz, 1H), 2.79 (s, 3H), 2.21 – 2.17 (m, 2H), 2.07 – 1.96 (m, 1H), 1.94 – 1.89 (m, 1H), 1.65 (s, 3H), 1.59 – 1.50 (m, 2H); ^{13}C NMR (125 MHz, $CDCl_3$) δ 136.8, 136.7, 132.8, 128.6, 127.9, 127.7, 127.2, 126.5, 73.5, 43.6, 31.0, 29.7, 26.9, 19.7, 18.1; IR (cast film, cm^{-1}) 3066, 3026, 2952, 2866, 2832, 1599; HRMS (ESI) calcd for $[M+H]^+$ $C_{17}H_{22}NO$: 256.1696, found: 256.1693; HPLC: Reverse Phase, IC column, 0.05% AA/H_2O/MeCN gradient: 1:9, H_2O:MeCN – 9:1, H_2O:MeCN, 30 °C, 1.0 mL/min, 37.0 min (major), 38.1 min, e.r.: 32:68.

Pertinent TROESY correlations for relative stereochemistry:

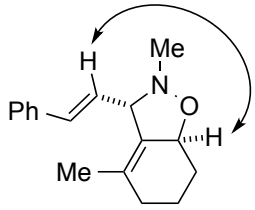

***Anti*-2,7a-dimethyl-3-[(*E*)-2-phenylethenyl]-2,3,5,6,7,7a-hexahydro-1,2-benzoxazole (84)**

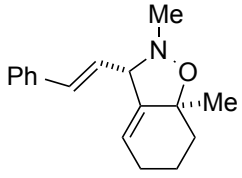

R_f = 0.25 (9:1, hexanes:ethyl acetate); ^{1}H NMR (400 MHz, $CDCl_3$) δ 7.42 – 7.38 (m, 2H), 7.34 – 7.30 (m, 2H), 7.25 – 7.22 (m, 1H), 6.54 (d, *J* = 15.6 Hz, 1H), 6.17 (dd, *J* = 15.6, 8.0 Hz, 1H), 5.39 (app q, *J* = 3.6 Hz, 1H), 3.60 – 3.58 (m, 1H), 2.75 (s, 3H), 2.15 – 2.04 (m, 2H), 1.98 – 1.86 (m, 2H), 1.69 – 1.62 (m, 1H), 1.47 – 1.35 (m, 1H), 1.45 (s, 3H);

^{13}C NMR (125 MHz, $CDCl_3$) δ 147.2, 136.7, 132.3, 128.6, 128.4, 127.7, 126.5, 118.0, 78.9, 74.7, 43.8, 33.6, 24.1, 23.8, 18.8; IR (cast film, cm^{-1}) 3059, 3026, 2929, 2862; HRMS (ESI) calcd for $[M+H]^+$ $C_{17}H_{21}NO$: 256.1696, found: 256.1694; HPLC: IC column, 95:5, hexanes:IPA, 5 °C, ret. time = 5.9 min, 6.9 min, e.r.: 25:75.

Pertinent TROESY correlations for relative stereochemistry:

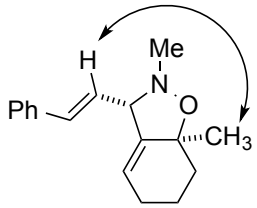

3.7. References

(1) American Institute of Physics. *Encyclopedia of Applied Physics*; Wiley-VCH, 1998.

(2) Bock, H.; Hirabayashi, T.; Mohmand, S. *Chem. Ber.* **1981**, *114*, 2595–2608.

(3) Moore, W. R.; Moser, W. R. *J. Am. Chem. Soc.* **1970**, *92*, 5469–5474.

(4) Christl, M. in *Modern Allene Chemistry, Vol. 1* (Eds. N. Krause, A. S. K. Hashmi), Wiley–VCH Verlag: Weinheim, **2004**, pp. 243–357.

(5) Werstiuk, N. H.; Roy, C. D.; Ma, J. *Can. J. Chem.* **1996**, *74*, 1903–1905.

(6) Werstiuk, N. H.; Roy, C. D.; Ma, J. *Can. J. Chem.* **1994**, *72*, 2537–2539.

(7) Balci, M.; Jones, W. M. *J. Am. Chem. Soc.* **1980**, *102*, 7607–7608.

(8) Engels, B.; Schöneboom, J. C.; Münster, A. F.; Groetsch, S.; Christl, M. *J. Am. Chem. Soc.* **2002**, *124*, 287–297.

(9) Schmidt, M. W.; Angus, R. O.; Johnson, R. P. *J. Am. Chem. Soc.* **1982**, *104*, 6838–6839.

(10) Balci, M.; Jones, W. M. *J. Am. Chem. Soc.* **1981**, *103*, 2874–2876.

(11) Christl, M.; Braun, M.; Fischer, H.; Groetsch, S.; Müller, G.; Leusser, D.; Deuerlein, S.; Stalke, D.; Arnone, M.; Engels, B. *Eur. J. Org. Chem.* **2006**, 5045–5058.

(12) Christl, M.; Fischer, H.; Arnone, M.; Engels, B. *Chem. Eur. J.* **2009**, *15*, 11266–11272.

(13) Moore, W. R.; Moser, W. R. *J. Org. Chem.* **1970**, *35*, 908–912.

(14) Denmark, S. E.; Wallace, M. A.; Walker, C. B., Jr. *J. Org. Chem.* **1990**, *55*, 5543–5545.

(15) Corey, E. J.; Bakshi, R. K.; Shibata, S.; Chen, C. P.; Singh, V. K. *J. Am. Chem. Soc.* **1987**, *109*, 7925–7926.

(16) Fleming, I. *e-EROS Encyclopedia Of Reagents for Organic Synthesis* **2009**, 1–3.

(17) Fleming, I.; Terrett, N. K. *J. Organomet. Chem.* **1984**, *264*, 99–118.

(18) Jastrzebski, J. T. B. H.; von Koten, G. Structures and Reactivities of Organocopper Compounds. In *Modern Organocopper Chemistry*; Krause, N., Ed.; Wiley-VCH Verlag GmbH: Weinheim, **2002**; Vol. 1; pp. 1-44.

(19) Gallina, C.; Ciattini, P. G. *J. Am. Chem. Soc.* **1979**, *101*, 1035–1036.

(20) Breit, B.; Demel, P. Copper-mediated Diastereoselective Conjugate Addition and Allylic Substitution Reactions. In *Modern Organocopper Chemistry*; Krause, N., Ed.; Wiley-VCH Verlag GmbH: Weinheim, **2002**; Vol. 1; pp. 188-223.

(21) Kobayashi, Y.; Feng, C.; Ikoma, A.; Ogawa, N.; Hirotsu, T. *Org. Lett.* **2014**, *16*, 760–763.

(22) Special Acknowledgement to Mr. Ed Fu and Professor Dennis Hall for the use of their Chiral HPLC machine, as well as for the training required to use the machine.

(23) Nendel, M.; Tolbert, L. M.; Herring, L. E.; Islam, M. N.; Houk, K. N. *J. Org. Chem.* **1999**, *64*, 976–983.

(24) Christl, M.; Schreck, M.; Fischer, T.; Rudolph, M.; Moigno, D.; Fischer, H.; Deuerlein, S.; Stalke, D. *Chem. Eur. J.* **2009**, *15*, 11256–11265.

(25) Bottini, A. T.; Hilton, L. L.; Plott, J. *Tetrahedron* **1975**, *31*, 1997–2001.

(26) Anslyn, E. V.; Dougherty, D. A. *Modern Physical Organic Chemistry.* University Science: Sausalito, CA, **2006**.

(27) Jensen, F. R.; Bushweller, C. H. *J. Am. Chem. Soc.* **1969**, *91*, 5774–5782.

(28) Christl, M.; Schreck, M. *Chem. Ber.* **1987**, *120*, 915–920.

(29) Hammond, G. S. *J. Am. Chem. Soc.* **1955**, *77*, 334–338.

(30) Hodgson, D. M.; Galano, J. M. *Org. Lett.* **2005**, *7*, 2221–2224.

(31) White, J. D.; Choi, Y. *Org. Lett.* **2000**, *2*, 2373–2376.

(32) Bartlett, M. F.; Dickel, D. F.; Taylor, W. I. *J. Am. Chem. Soc.* **1958**, *80*, 126–

136.

(33) Taylor, E. C.; Davies, H. M. L.; Clemens, R. J.; Yanagisawa, H.; Haley, N. F. *J. Am. Chem. Soc.* **1981**, *103*, 7660–7661.

(34) Saulnier, M. G.; Kadow, J. F.; Tun, M. M.; Langley, D. R.; Vyas, D. M. *J. Am. Chem. Soc.* **1989**, *111*, 8320–8321.

(35) Nicolaou, K. C.; Ding, H.; Richard, J.-A.; Chen, D. Y. K. *J. Am. Chem. Soc.* **2010**, *132*, 3815–3818.

(36) Hansson, M.; Arvidsson, P. I.; Lill, S. O. N.; Ahlberg, P. *J. Chem. Soc., Perkin Trans. 2 VL* - **2002**, 763–767.

(37) George, M. V.; Peterson, D. J.; Gilman, H. *J. Am. Chem. Soc.* **1960**, *82*, 403–406.

(38) Corey, E. J.; Bakshi, R. K.; Shibata, S. *J. Am. Chem. Soc.* **1987**, *109*, 5551–5553.

(39) Heerding, D. A.; Hong, C. Y.; Kado, N.; Look, G. C.; Overman, L. E. *J. Org. Chem.* **1993**, *58*, 6947–6948.

(40) Still, W. C.; Kahn, M.; Mitra, A. *J. Org. Chem.* **1978**, *43*, 2923–2925.

4. Intramolecular Capture of Cyclic Allene Intermediates

4.1. Intramolecularity Versus Intermolecularity

The formation of a product from the interaction of two reactants relies upon the favorable collision of the two molecules with a specific trajectory (i.e. *anti* attack of the nucleophile relative to the leaving group of the electrophile in an S_N2 reaction).[1] This event is dependent upon the charges of the molecules, the concentration, and the medium in which the reaction is performed, along with other factors. In order to create a more efficient reaction, concentration and temperature must be considered given that the likelihood of a favorable collision increases as the reaction mixture is concentrated or the temperature is raised. Increasing the concentration or temperature, however, can erode the stereoselectivity or chemoselectivity of the reaction.

In cases where the reactivity is more difficult to control, possibly due to the high reactivity of one reactant, or the transition state for a reaction is highly ordered, variations to the concentration and temperature of the reaction mixture can only partially mitigate low yield/selectivity. Intramolecular reactions usually show greater stereoselectivity by restricting the reactive conformations a substrate can assume. Intramolecularity can also generate higher yields, as the effective concentration of the substrates is high relative to intermolecular reactions. When one of the reactants is generated *in situ* due to its high energy, intramolecular reactions enable otherwise unobserved processes to take place. The two reactive portions of the molecule are forced into close proximity on a single molecule, increasing the probability of a favorable collision and decreasing the $\Delta S^{\ddagger}$ relative to an intermolecular reaction.

4.2. Intramolecular Reactions of Cyclic Allenes

The literature concerning the intramolecular reactivity of cyclic allenes is limited. Most of the examples use highly functionalized substrates, which contain groups stabilizing the cyclic allene intermediate and minimize dimerization due to steric encumbrance. As a strategy for increasing the complexity of the products, improving the

atom economy of the transformation, and enabling otherwise unrealized transformations, intramolecular capture is an attractive methodology.

4.2.1. Intramolecular Reactions in the Moore Cyclization

The first examples of trapping a cyclic allene intermediate in an intramolecular fashion are from the Moore group.[2] Recent calculations suggest the Moore cyclization occurs through a cyclic allene intermediate and not the previously assumed diradical or zwitterionic resonance structures.[3] With this in mind a number of interesting intramolecular trapping reactions have been reported of the Moore cyclization intermediates.

4.2.1.1 Olefin Capture of the Moore Intermediate

Several π-nucleophiles have shown to be proficient intramolecular traps for the Moore cyclization intermediate via a number of different mechanisms. *O*-Allyl cyclic allene intermediate **3** undergoes a Claisen [3,3]-sigmatropic rearrangement to give α-allyl quinone **4** (Scheme 4.1).[4] Similarly, *i*-propenyl-substituted cyclic allene **5** can undergo a 4π-electrocyclic-ring closure to give cyclobutene **6**.[5] The cyclobutene rearomatizes to furnish fused alkylidene cyclobutane **7**.

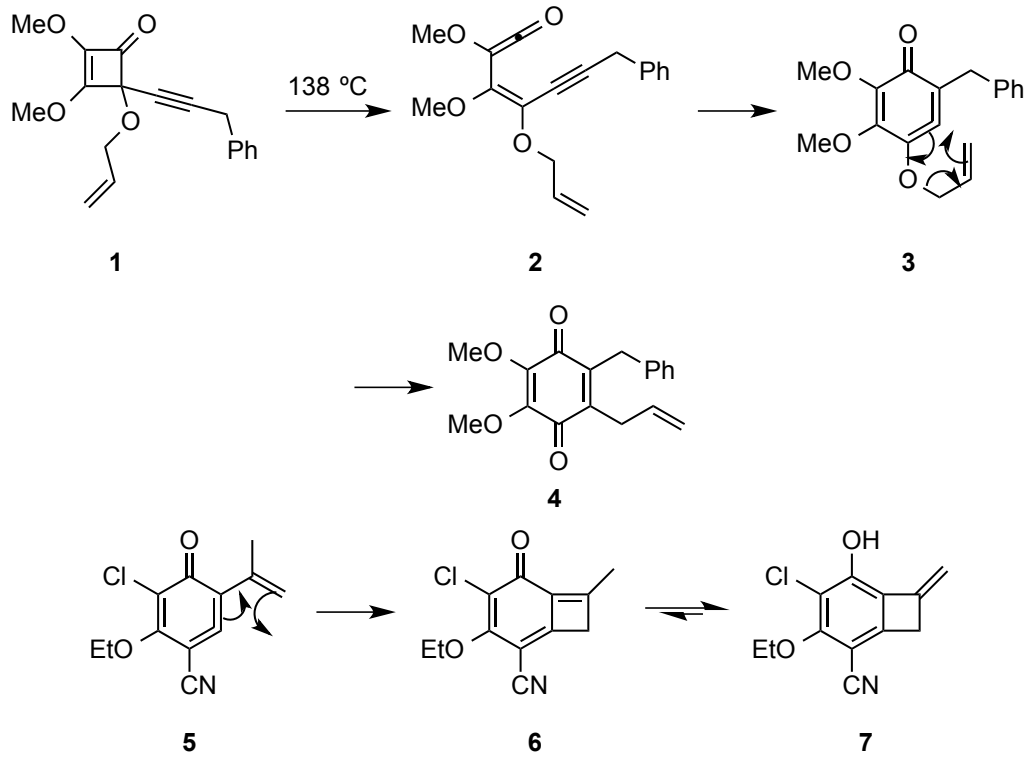

Scheme 4.1 – Pericyclic reactions of cyclic allene intermediates.

Moore and coworkers showed that when an alkyne is tethered to the cyclobutanone starting material (**7**) the addition of the cyclic allene onto the alkyne is observed (Scheme 4.2).[6] This differs from the intermolecular reaction with alkynes they reported earlier, which gave the [2+2] cycloadduct, cyclobutene **13** rather than the coniaene product (**11**).[2] Different reactivity was observed whether the reaction was intermolecular or intramolecular. This intramolecular strategy was amenable to the incorporation of heteroatoms in the linker such as nitrogen, and oxygen to make fused-aza/oxynaphthalene derivatives.[7]

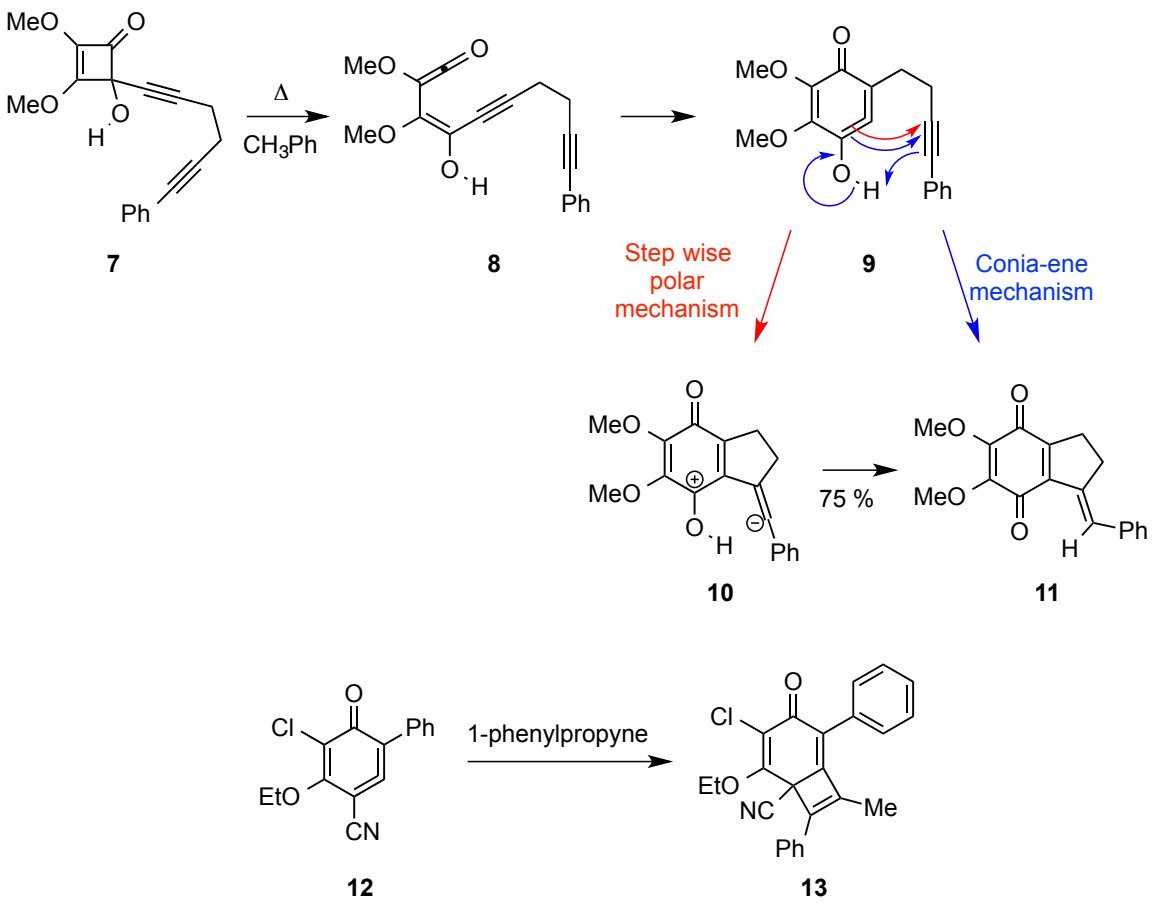

Scheme 4.2 – Intra/intermolecular reactions of cyclic allenes with alkynes.

The reactive π-system could also be part of an arene ring. There are a number of examples whereby a pendent aryl group traps a cyclic allene by a formal Friedel-Crafts reaction (Scheme 4.3).[2] Interestingly, only mild selectivity between arylation at C2 (**15**) versus C6 (**16**) on the indole ring was observed in the case of indole derivative **14**.[2,7] In the case of naphthyl substituted cyclic allene **19**, the arene is alkylated exclusively on C-8 of the naphthalene ring (**20**).

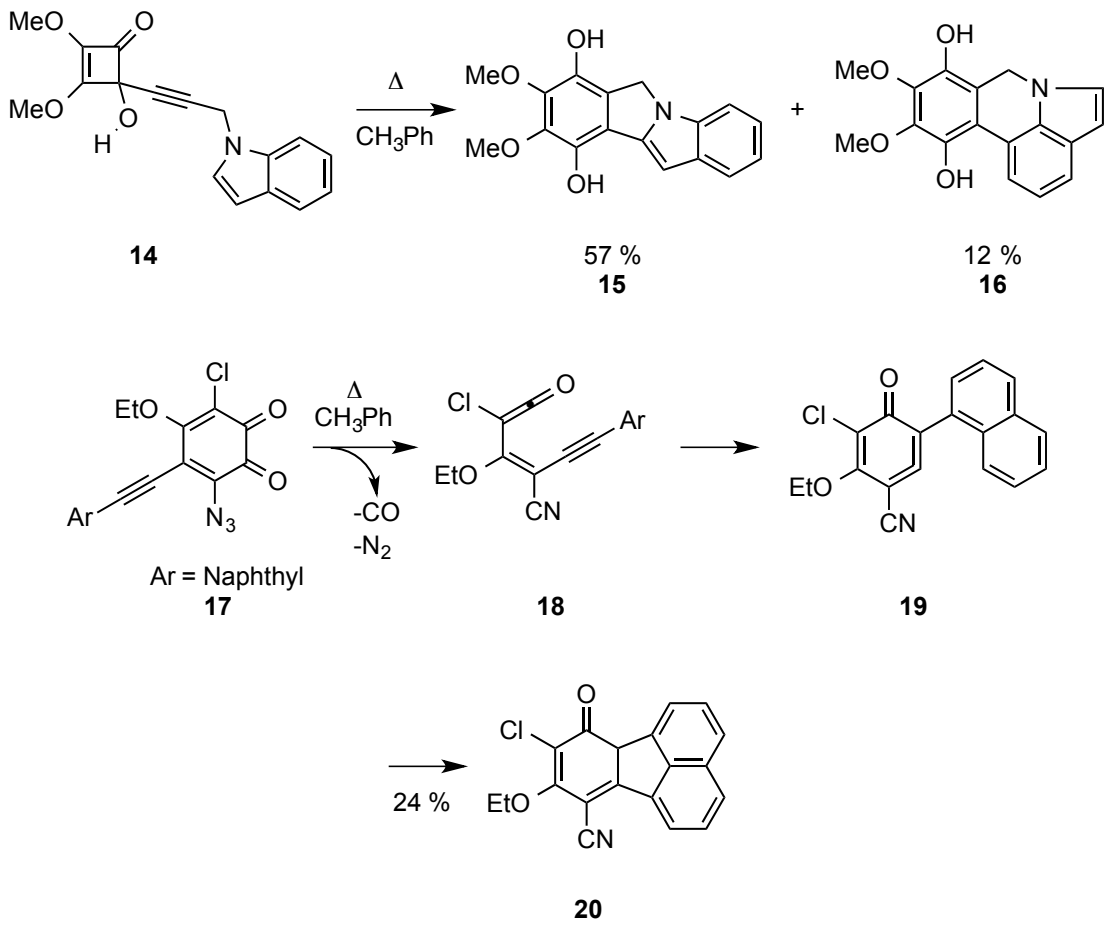

Scheme 4.3 - Intramolecular trapping of cyclic allenes by arene rings.

4.2.2. Intramolecular Capture of Hopf Cyclization Intermediates

Previously, Hopf showed that the theorized isobenzene cyclic allene intermediate of the Hopf cyclization could be trapped by styrene intermolecularly.[8] More recently, Fernandez and coworkers reported the intramolecular trapping of highly substituted isobenzene **24** (generated via a photolytic Hopf cyclization), by a retro-Brook-type[9] rearrangement to give silyl-cyclohexadienone **25**.[10] If the reaction was run in the presence of an amine, however, intermolecular sideproducts were observed.

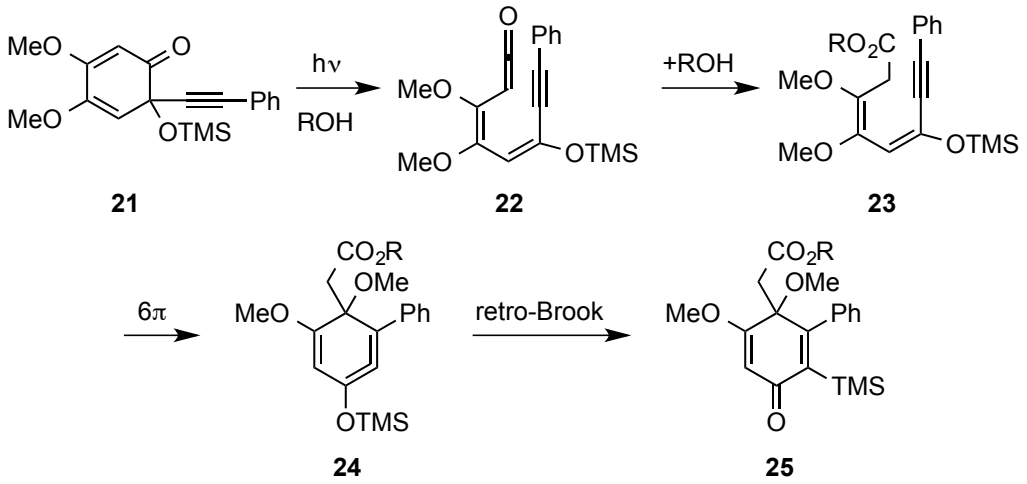

Scheme 4.4 - Retro-Brook migration of a silyl group to quench a cyclic allene.

4.2.3. Interrupted Dimerization of a Cyclic Allene

Although not a formal trapping of the cyclic allene intermediate, Christl reports the interrupted dimerization of phenyl-1,2-cyclohexadiene (**27**) (Scheme 4.5).[11] Upon addition of a strong base to a solution of 1-bromo-2-phenylcyclohexene (**26**) the cyclic allene formed and in the absence of a trap underwent dimerization to diradical **28** and intramolecular arylation to tricycle **29**. It may also be possible the reaction proceeds via a Diels-Alder-like transition state, given the precendent with furan and other dienes, it is likely the [4+2] cycloaddition is stepwise.

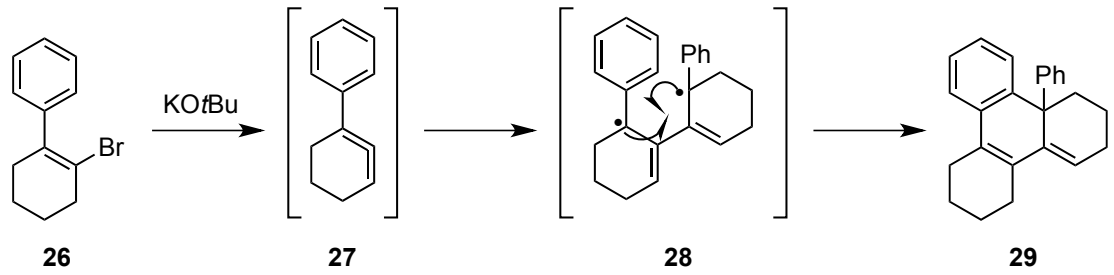

Scheme 4.5 - Dimerization of 1-phenyl-1,2-cyclohexadiene.

4.3. Intramolecular Capture of 1,2-Cyclohexadiene

The previously reported success with intramolecular cyclic allene capture has relied heavily upon sterically encumbered intermediates stabilized by heteroatoms. Considering the success of Moore and coworkers[2] it is a viable strategy for efficiently trapping cyclic allenes with relatively low trap concentrations (in an intramolecular reaction the stoichiometry is 1:1, trap:allene).

We became interested in intramolecular reactions of cyclic allenes to hopefully address the issue of using the trapping molecules in large excess, having highly efficient reactions, but using relatively minimally functionalized skeletons. When looking at the skeleton of the cyclic allenes synthesized via the copper-mediated silylation and subsequent fluoride-mediated elimination from Chapter 2, we proposed two possible strategies for trap incorporation. The first approach to intramolecular trapping reactions involves the replacement of the acetyl-protecting group on the enolate oxygen of **31** with acetyl equivalents that contain reactive moieties that are able to trap a cyclic allene intermediate (**30**, Figure 4.1). The second strategy, similar to the strategy employed in Chapter 3, relies upon the introduction of trapping moieties to the carbon skeleton at the β-position via a Stork-Danheiser alkylation (**32**).

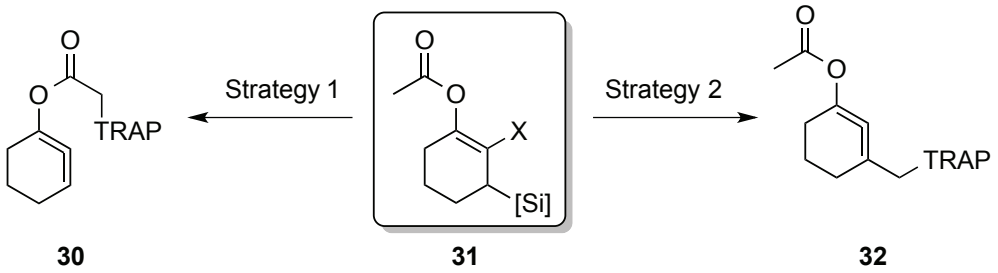

Figure 4.1 - Two strategies for trap incorporation using oxygen substituted cyclic allenes.

4.4. Results and Discussion

4.4.1. Functionalizing the Acyl-Enolate

Looking at the structure of the allene precursor **31**, the enol acetate seemed to be the easiest position to derivatize. Rather than functionalizing the carbon skeleton before or after the silylation reaction, we envisioned quenching the intermediate copper enolate with different acylium equivalents. This was demonstrated with a number of acyl chlorides as shown in Table 4.1 to generate cyclic allene precursors with different types of trapping functionalities within close proximity to the soon formed cyclic allene.

Table 4.1 - Quenching of the conjugate silyl cuprate addition with different acyl chlorides.

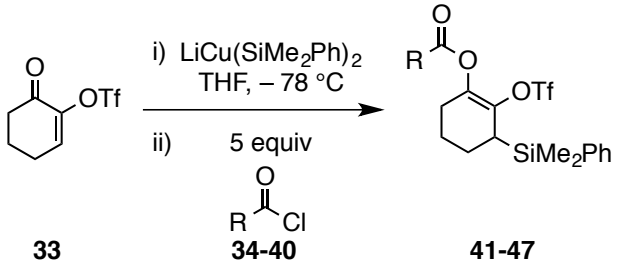

33 **34-40** **41-47**

Acyl Chloride	Acyl Chloride	Allene Precursor	Yield (%)[a]
Furoyl	**34**	**41**	89
Benzoyl	**35**	**42**	44
Cinnamoyl	**36**	**43**	61
4-MeOCinnamoyl	**37**	**44**	28
2-Chloroacetyl	**38**	**45**	quant.
2-Azidoacetyl	**39**	**46**	62
2-(2-Furyl)acetyl	**40**	**47**	58

[a] Yields are of isolated compounds.

Using α-chloroacetyl chloride to quench the reaction gave a quantitative yield of the α-chloroacetate derivative **45**, selective for *O*-acylation. Regrettably, under numerous nucleophilic substitution conditions (eg., sodium azide in DMSO, etc.) allylic silane **45** decomposed. For this reason, the alternative synthesis employing α-azidoacetyl chloride generated *in situ* was used to gain access to **46**. Cinnamoyl chloride and *p*-methoxycinnamoyl chloride both gave the *O*-protected enol derivatives **43** and **44**, respectively. Chemoselectivity between 1,4-addition and 1,2-addition to the acyl chloride of the α,β-unsaturated acyl chlorides cannot be ruled out given the low yield and the complicated crude ^{1}H NMR spectrum.

With the desired cyclic allene precursors in hand, all of the derivatives were then subjected to desilylative-elimination conditions. Regardless of the dilution, or fluoride source used (TBAF or CsF), none of the reactions yielded any signs of intramolecular

trapping products. The only products isolated were dimerized cyclic allenes (**48** and **49)** and in all of these cases the dimerization occurred across the less-substituted double bond to give the symmetrical products (Scheme 4.6). Azide-containing precursor **46** formed an intractable mixture of products, though infrared spectrophotometric analysis of several fractions indicated the presence of an azide functional group.

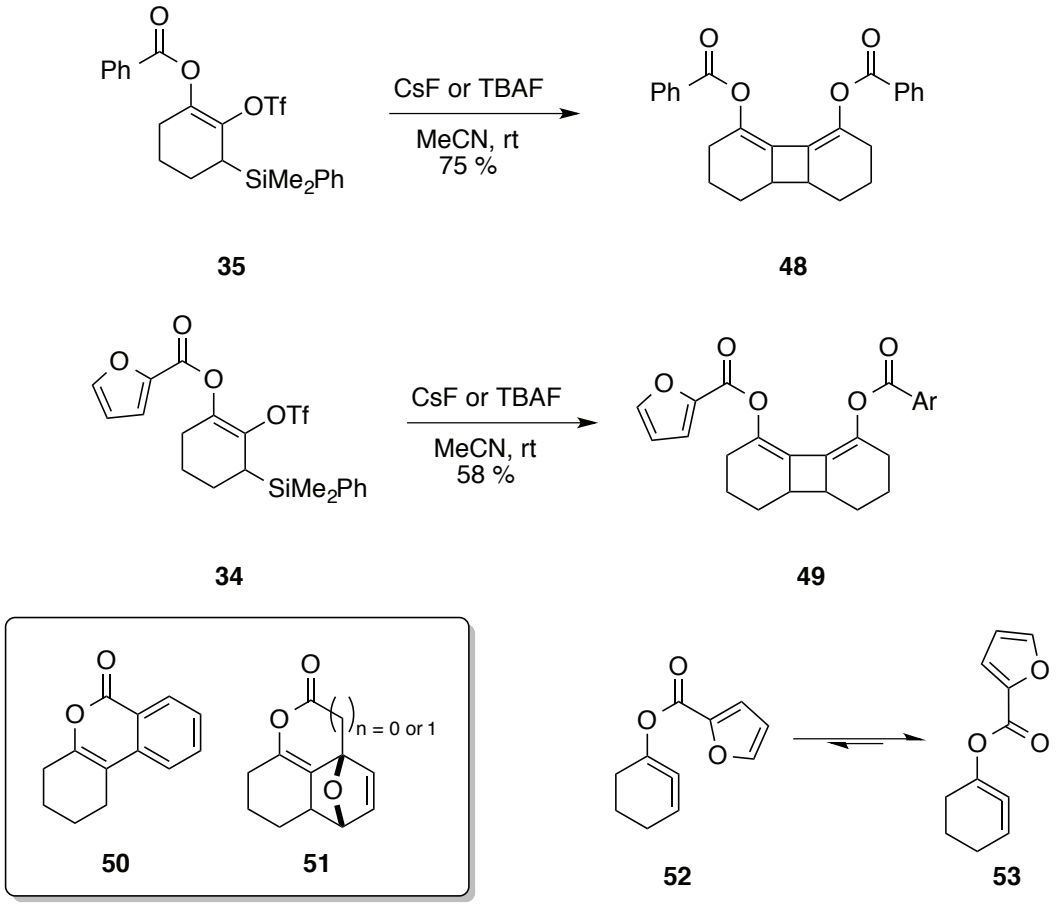

Scheme 4.6 - Attempted intramolecular trapping of cyclic allenes via acyl-linked traps.

From the structures of the predicted products (Scheme 4.6) it is not obvious whether they are more or less strained than the cyclic allene intermediate. We proposed that the strain of the allene being held within a six-membered ring (~ 32 kcal/mol)[12] should outweigh the strain of incorporation of even a fused alkylidene-cyclobutane ring (**52**). Assuming that the strain of the products minimally effects their formation, it is possible that the relative populations of *s-cis* and *s-trans* around the carbon-oxygen bond

of the ester prevents an intramolecular reaction between the acyl-substituent and the cyclic allene functional group (Scheme 4.6). In light of the failure of any acyl derivatives to trap the cyclic allene, work was focused on alternative strategies.

4.4.2. β-Substituted Cyclic Allenes

As an alternative to attaching the trapping moiety to the enolate oxygen, the next position derivatized with a tethered trapping molecule was the β-carbon on the enone sub-unit. Similar to the previous work with chiral cyclic allenes (Chapter 3), the Stork-Danheiser alkylation allowed ready incorporation of a new alkyl substituent on the β-carbon while conserving the brominated-enone moiety (Scheme 4.7). We envisioned a number of different nucleophiles could be added to generate a diverse series of substituted cyclic allene precursors.

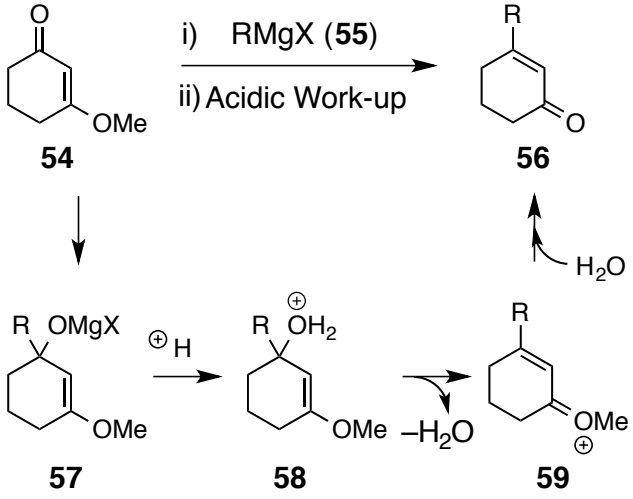

Scheme 4.7 - Mechanism of the Stork-Danheiser alkylation.

4.4.2.1 Common Synthetic Intermediate for a Cyclic Allene Precursor Library

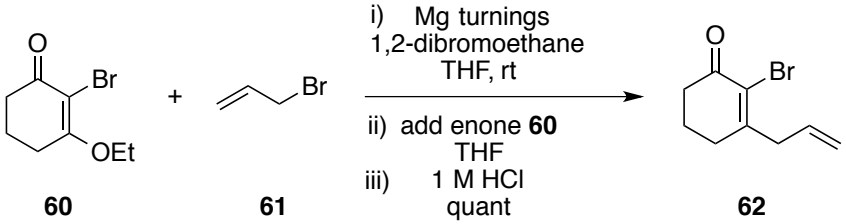

Scheme 4.8 - Allylation of enone 84 via the Stork-Danheiser alkylation.

In search of a common intermediate for the synthesis of a number of cyclic allene precursors, allylated enone **62** was chosen (Scheme 4.8). We envisioned a number of possible transformations whereby the pendent allyl group could be derivatized via different methods to incorporate different trapping moieties (Figure 4.2). The initial transformation explored was that of hydroboration/oxidation (**65**).[13]

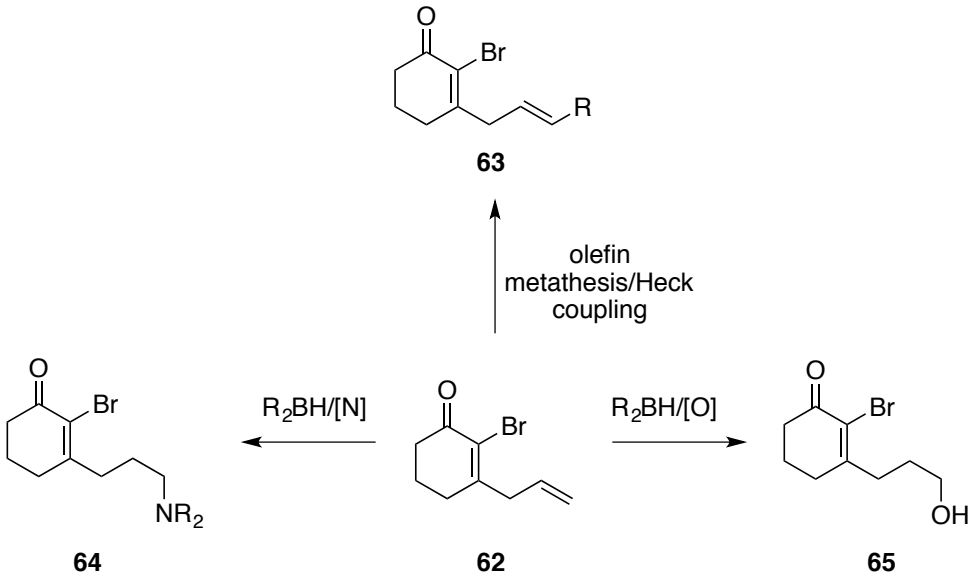

Figure 4.2 - Possible strategic compound for synthesis of cyclic allene precursors with intramolecular traps.

Following the initial allylation, hydroboration/oxidation was attempted with 9-BBN. The hindered borane-hydride was selected to control the regiochemistry of the hydroboration on the terminal olefin and discourage a reaction at the enone functionality. Unfortunately the only products observed were the known allylic alcohol **67** from 1,2-reduction of the enone, and an intractable mixture of other hydroboration/oxidation products (**66**). To circumvent over reduction of the starting material, silylation was carried out to give allylic silane **68** prior to hydroboration/oxidation to give tethered alcohol **69** (Scheme 4.9).

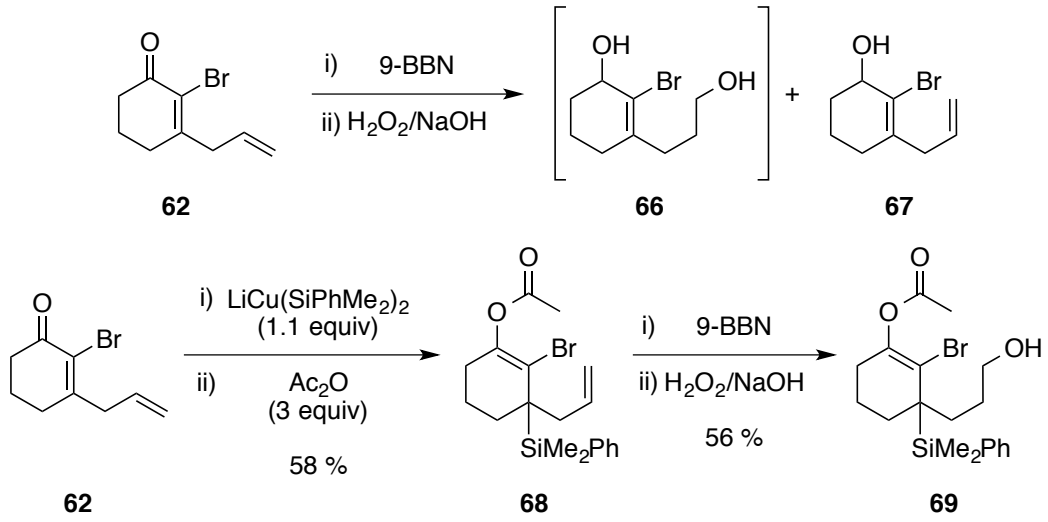

Scheme 4.9 - Hydroboration/oxidation of different allylated starting materials.

Alcohol **69** was then derivatized to the mesylate under standard conditions and immediately treated with sodium azide in DMSO to furnish tethered alkyl azide **70** (Scheme 4.10). If the substituted cyclic allene formed upon addition of fluoride, the azide-containing cyclic allene would be tetra-substituted (having both the alkyl group and the enol acetate group) shielding the terminal carbons of the cyclic allene. We hypothesized that the fully substituted allene would have a low probability of undergoing dimerization. Subjecting azide-tethered substrate **70** to fluoride-mediated elimination conditions gave intractable mixtures. Flash column chromatography of the crude material resulted in the isolation of multiple impure fractions, each of which contained signals at ~2200 cm^{-1} in the infrared spectrum attributed to an azide functional group. Considering the failure of the acetoxy-substituted cyclic allene to react with azides in an intermolecular fashion investigated in Chapter 2, it was not surprising though disappointing that the azide failed to trap the intermediate allene. In light of these results further characterization of the many products was abandoned.

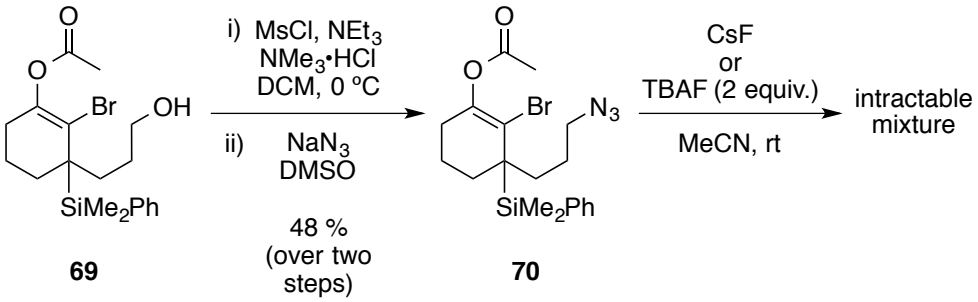

Scheme 4.10 - Nucleophilic exchange of a primary alcohol for an azide.

Primary alcohol **69** also allowed the *in situ* preparation of aliphatic aldehyde **71** via the oxidation with DMP. The instability of the aldehyde necessitated the immediate Wittig olefination with triphenylphosphoniumbenzyl bromide and potassium *t*-butoxide (Scheme 4.11). The reactions yielded an extremely complicated mixture of *cis* and *trans* olefins. Given these complications the substrates were further explored with undergraduate researcher Kyle McIntosh as part of a CHEM 401/403 project by an alternative strategy (Scheme 4.12).[14]

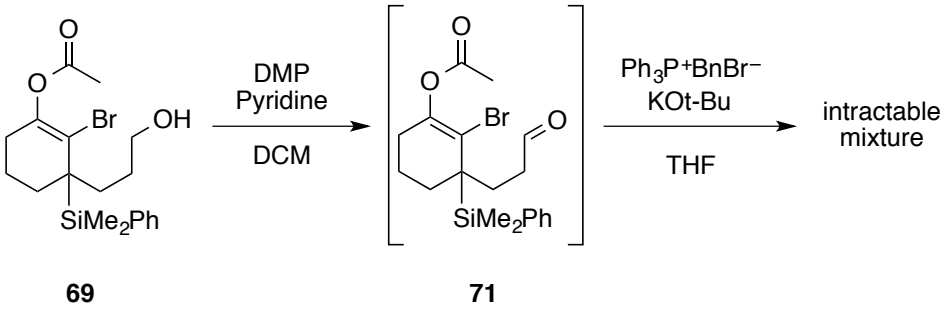

Scheme 4.11 - Attempted intramolecular capture of a cyclic allene with a tethered styrene.

Accessing tethered-styrene cyclic allene precursors **76/77** through a more straightforward approach Kyle was able to demonstrate the failure of substrates containing a tethered styrene moiety to cyclize under fluoride-mediated elimination conditions regardless of the length of the tethers (Scheme 4.12). Deacylated enones **78/79** were the only characterized products from the reaction mixtures. Typically low yields were reported when β-substituted styrenes were used to trap cyclic allenes.[15] To circumvent the poor reactivity of β-alkylstyrenes, α-linked substrate **80** was selected as a suitable candidate for further investigation.

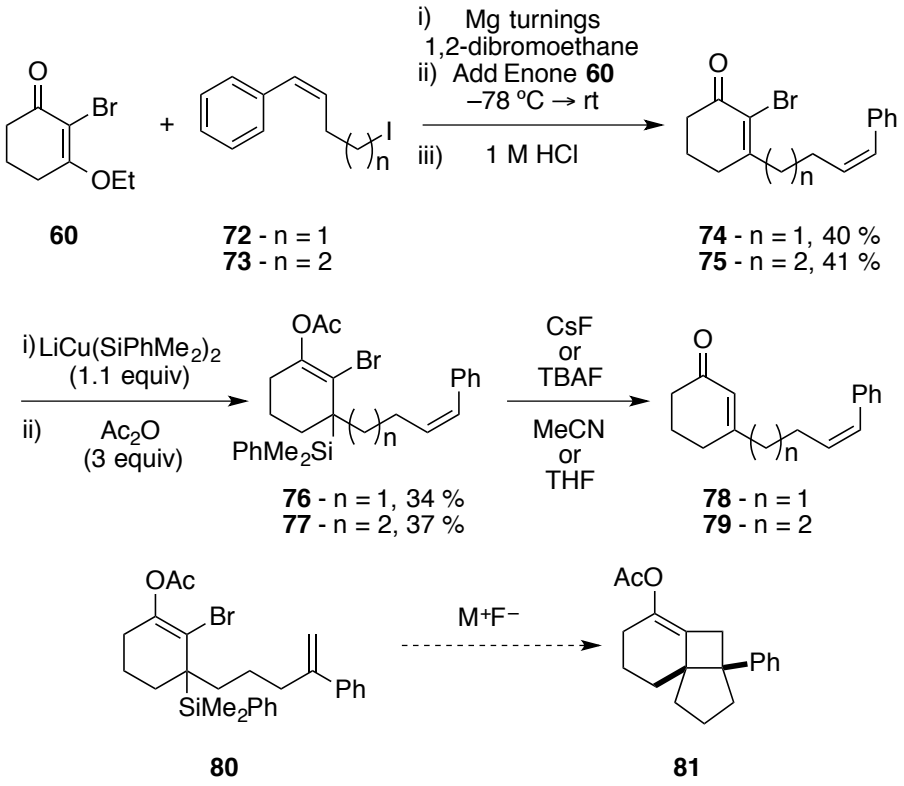

Scheme 4.12 - Synthesis of styrene-tethered intramolecular trapping substrates by Kyle McIntosh.[16]

4.4.2.2 Intramolecular Allene/Arene Reactions

The earliest work done by Wittig and Fritze showed cyclic allenes to be efficiently trapped by furans.[17,18] The formal Diels-Alder reaction was selective for the *endo* product and proceeded with a number of differently substituted furans.[19,20] While investigating the intramolecular cycloaddition reactions of arenes and acyclic allenes, Himbert and coworkers investigated the competitive Diels-Alder reaction between pendent anilines and pendent furans (Scheme 4.13).[21] The cycloaddition with furan was thermodynamically favored though it generated two isomers due to poor site selectivity with respect to the allene olefins and the reaction still required substantial heating. Given the previous success of intramolecular furan/allene cycloadditions[22-24] we surmised that the thermal activation barrier to the furan/allene intramolecular cycloaddition could be overcome with use of a strained cyclic allene.

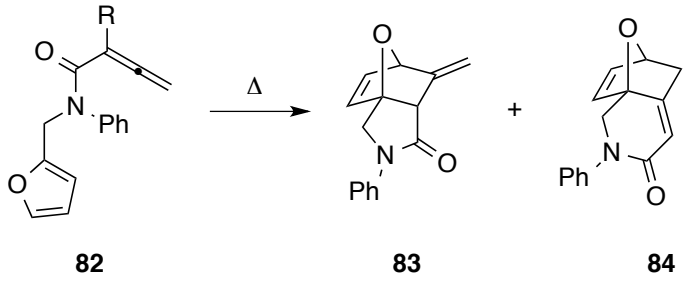

82 **83** **84**

Scheme 4.13 - Himbert [4+2] furan/allene cycloaddition.

4.4.2.3 The Intramolecular Cycloaddition of Furan with Cyclic Allenes

The initial focus was on the synthesis of lactam containing products similar to **85**. The retrosynthesis of tetracycle **85**, as shown in Figure 4.3, first relies upon an intramolecular Diels-Alder reaction initiated by formation of a cyclic allene by the fluoride-mediated desilylative elimination of **86**. Allylic silane **86** is synthesized from β-substituted enone **87**, which in turn is derived from the nucleophilic addition of amide **88** to bromo-enone **60**.[25,26]

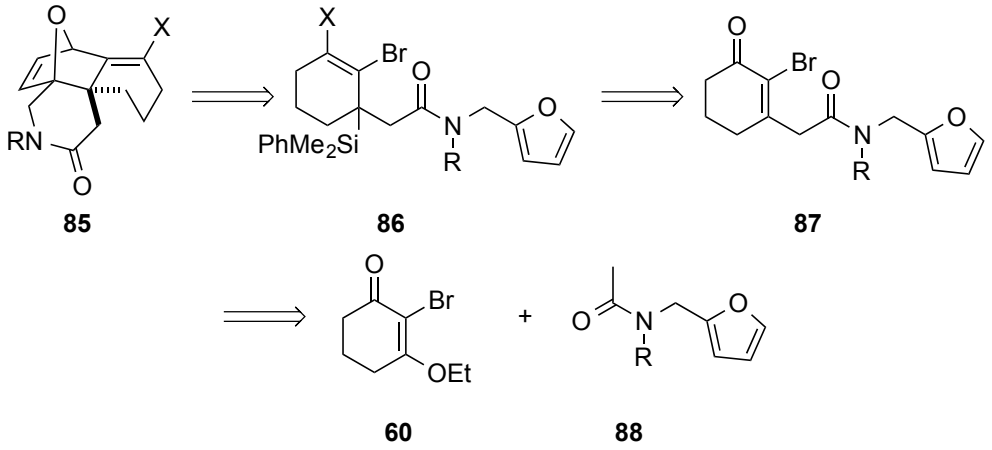

85 **86** **87**

60 **88**

Figure 4.3 - Retrosynthesis of proposed cyclic allene-derived Himbert cycloaddition.

The synthesis of the needed precursors began with a Stork-Danheiser alkylation to generate amides **90-92** (Table 4.2). This was demonstrated with a number of differently substituted amides: *N*-(furan-2-ylmethyl)-*N*-methyl, *N,N*-di(furan-2-ylmethyl), and *N*-methoxy-*N*-methyl acetamides. The ^{1}H NMR spectrum of (furan-2-ylmethyl)-substituted amides were significantly more complicated than expected due to the presence of rotamers. Weinreb amide derivative **90** was synthesized with the intent of performing a later stage derivatization, though due to the low yield it was not elaborated upon.

Table 4.2 - Synthesis of vinylogous amides via the Stork-Danheiser alkylation.

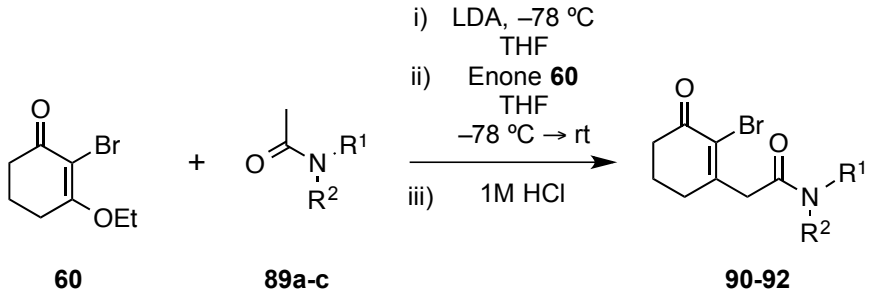

60 **89a-c** **90-92**

Amide	R^1	R^2	Product	Yield (%)[a]
89a	Me	OMe	**90**	15
89b	Me	furan-2-yl	**91**	90
89c	furan-2-yl	furan-2-yl	**92**	85

[a] Yields are of isolated products.

Subsequent silylation of the amides proved to be more difficult than previously experienced with the non-substituted enones (Chapter 2). Premature protonation of the cuprate enolate may occur, generating keto-amide **94** (Scheme 4.14); however, these compounds were not fully characterized. The source of the protons is unknown and in the case of bis(furan-2-ylmethyl)amide **92** no silylated acetates were isolated. Increasing the number of equivalents of the silyl cuprate reagent employed was detrimental to the yield of silyl amide **93**. No product formed if the acetic anhydride was added prior to the silyl cuprate reagent.

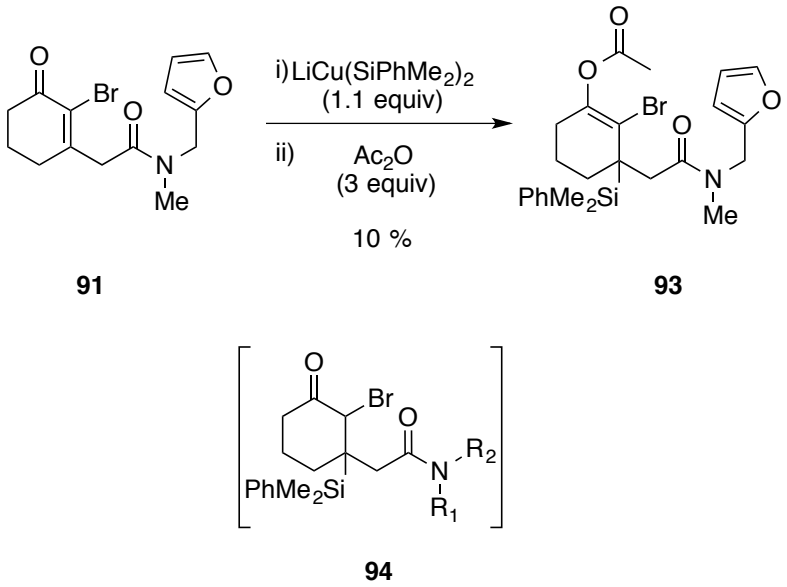

Scheme 4.14 - Silylation of amide 91.

Having synthesized the desired substituted cyclic allene precursors (albeit in poor yield), fluoride was added to an acetonitrile solution of silyl amide **93** (Scheme 4.15). Regrettably, none of the desired intramolecular trapping products were observed, although the starting materials were consumed. Enone **95** was the only isolated product from the reaction mixture, assumed to arise from a nucleophilic deacylation of cyclic allene **96** and subsequent protonation of vinyl anion **98** (Scheme 4.15).

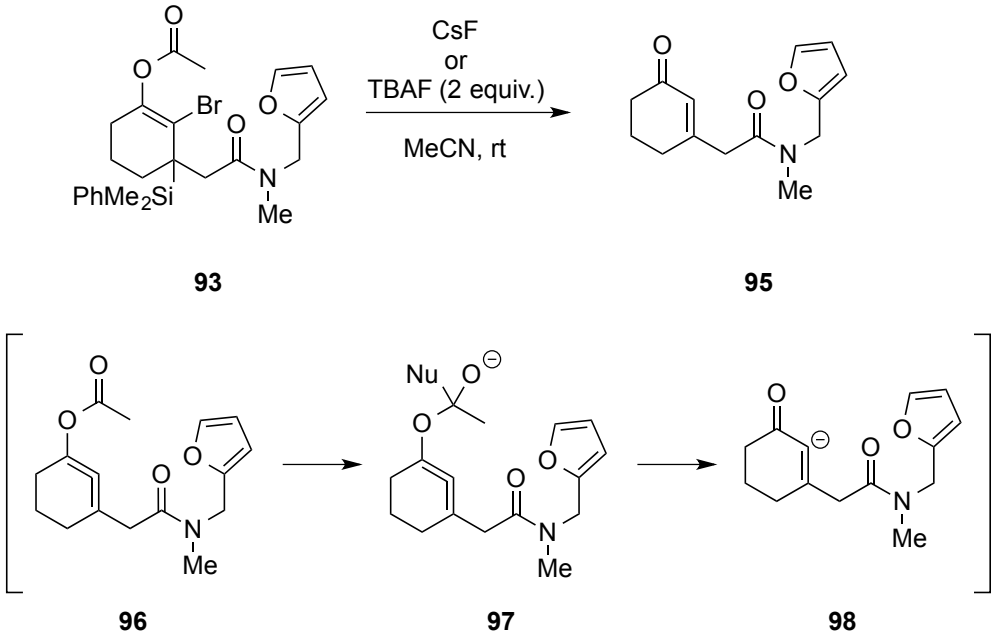

93 95

96 97 98

Scheme 4.15 - Attempted intramolecular trapping reaction with (furan-2-yl)-substituted amides.

The failure of cyclic allene **96** to undergo an intramolecular reaction was troubling considering the precedent for the trapping of cyclic allenes with furan in an intermolecular fashion.[17,19] More interesting than the failure to trap the allene is the lack of intermolecular reactivity of the cyclic allene. Whereas tri-substituted cyclic allene derivatives shown in Scheme 4.6 rapidly and preferentially undergo dimerization, these now tetra-substituted cyclic allenes show no tendency to dimerize or it occurred to such a small extent that it was undetected in the present experiments.

4.4.2.4 Aliphatic-Tethered Furan Intramolecular Trapping Substrates

We theorized the failure of *N*-(furan-2-ylmethyl)-*N*-methylacetamide derivative **93** to cyclize could be attributed to the conformational rigidity of the tether which prohibited the formation of a reactive conformation. Chapter 3 showed the methyl substituted cyclic allene could be trapped by 1,3-dipoles on either the unsubstituted olefin or the methyl-substituted olefin, therefore steric congestion of the reactive olefin was not considered to be problematic. To test whether the rigidity of the tether was hampering the reactivity, simple alkyl tethered substrate **100** was proposed (Figure 4.4). The furan ring would be tethered to the cyclic allene precursor by an unfunctionalized aliphatic chain.

The simple alkyl tether should have low barriers to sampling a high number of reactive conformations relative to the amide-linked substrate, and the allene could be trapped in an intramolecular fashion.

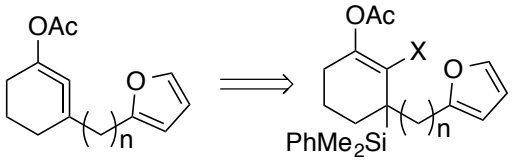

99 **100**

Figure 4.4 - Saturated aliphatic tether proposed for intramolecular allene capture.

Known alkyl halides **101/102** were converted to the required Grignard reagents under standard reduction conditions and were immediately added to a solution of enone **60** to yield furan-tethered enones **103/104** (Scheme 4.16). The substituted enones were silylated under the standard conditions developed in Chapter 2 to yield cyclic allene precursors **105/106**. Both the propylene and butylene tethered furans were synthesized to compare the effect of tether length on trapping efficiency.

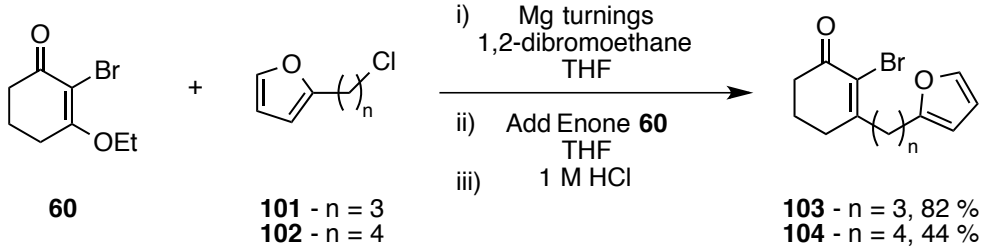

60

101 - n = 3
102 - n = 4

103 - n = 3, 82 %
104 - n = 4, 44 %

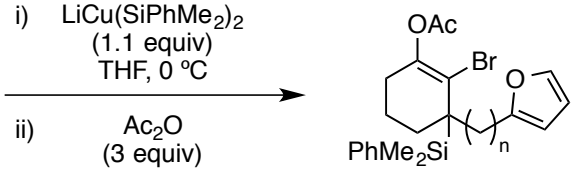

105 - n = 3, 80 %
106 - n = 4, 73 %

Scheme 4.16 - Synthesis of aliphatic-tethered furan cyclic allene precursor.

The addition of cesium fluoride to an acetonitrile solution of silane **105** gratifyingly yielded intramolecular cycloaddition product **107** (Scheme 4.17) as a single diastereomer (55 % yield). Using tetrabutylammonium fluoride as the fluoride source gave 67 % yield.

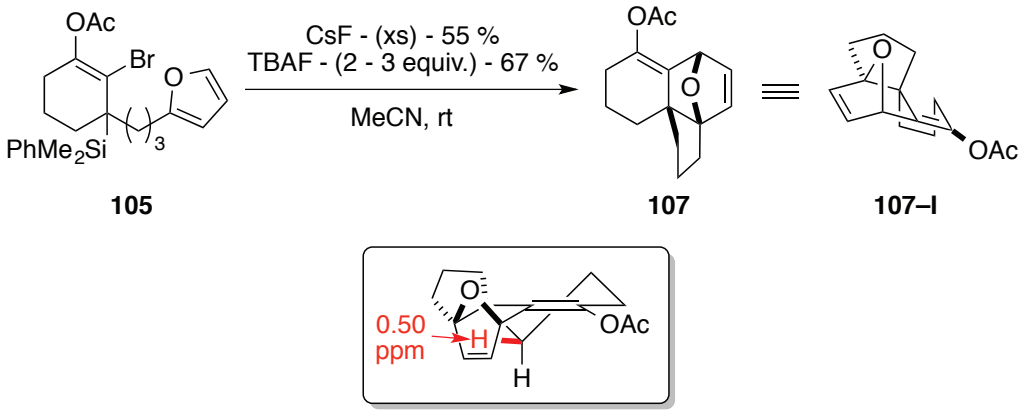

Scheme 4.17 - Intramolecular capture of 1-acetoxy-1,2-cyclohexadiene by a tethered furan.

The stereochemistry of the single diastereomer of **107** was more difficult to decipher than previous cycloadducts as the TROESY spectrum showed no meaningful correlations between any of the three rings. With this in mind there is a trend in furan cycloaddition chemistry associated with the *endo*-cycloadducts of furan. Bottini reports that only the *endo* intermolecular furan-cyclic allene cycloadducts show a peak at ~ 0.4 ppm, indicative of a proton shielded by the C9-C10 olefin of the *endo*-cycloadduct (**108**) (Figure 4.5).[19] For comparison *exo* isomer **109** has no proton signals upfield of 1.0 ppm.[19] From comparison of ^{1}H NMR spectral data, the stereochemistry of intramolecular cycloadduct **107** is assigned to be *endo* as shown in Scheme 4.17 based on the presence of an anomalously upfield proton resonance.

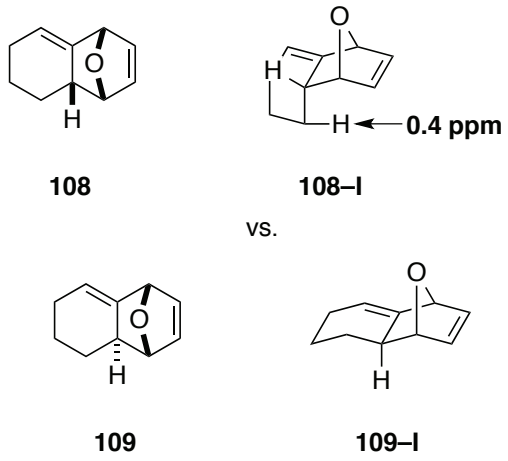

Figure 4.5 - 3D Representations of *endo* and *exo* furan adducts with 1,2-cyclohexadiene.

The butylene tethered homologous precursor **106** formed tetracyclic cycloadduct **110** in 21 % yield when a solution of TBAF was added (Scheme 4.18). The attenuated yield is most likely derived from the increased degrees of freedom in the longer tether, leading to slower formation of the six-membered ring. Similar to the propylene tethered substrate, a single diastereomer was observed and assigned an *endo* stereochemistry based upon the presence of a signal at 0.54 ppm in the ^{1}H NMR spectrum (**110–II**).

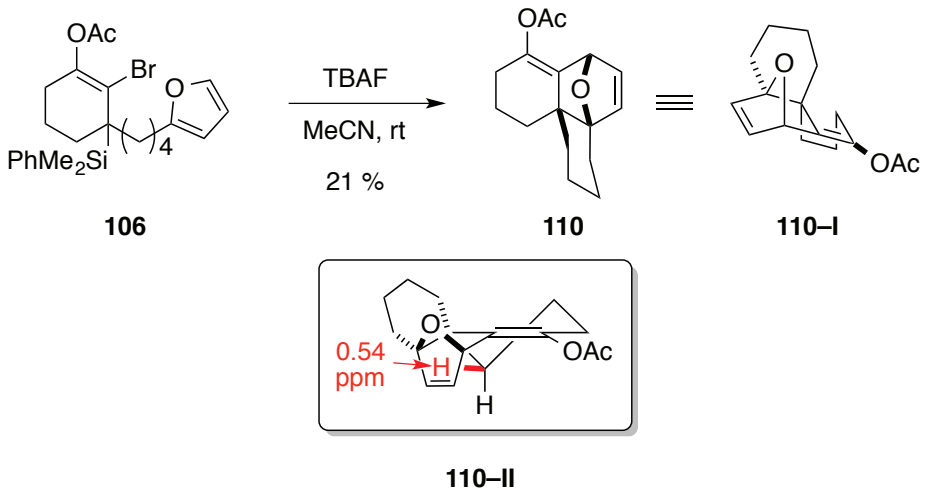

Scheme 4.18 - Intramolecular trapping with a four-carbon tether.

From the successful formation of intramolecular cycloadducts **107** and **110** it becomes apparent that the intramolecular trapping of a cyclic allene is not complicated though it is dependent on the lifetime of the intermediate. Simple alkyl tethers were

efficient considering the high substitution of the allene. The more substituted regioisomers were always formed in minor amounts in Chapter 3. In retrospect, it appears that thermodynamic conformational populations due to substituents on the tether greatly affected the efficiency of the intramolecular trapping of the cyclic allene due to the limited lifetime of the cyclic allene intermediate. The use of a *gem*-dimethyl group may facilitate greater efficiency in the butyl-tethered case, taking advantage of the Thorpe-Ingold effect,[27] though it has not been attempted as of yet.

4.5. Conclusions

The use of simple alkyl tethered furans enabled the demonstration of the intramolecular trapping of cyclic allenes not generated by an electrocyclization reaction. The intramolecular trapping products showcased the generation of molecular complexity quickly with excellent control of the stereochemistry and site selectivity on the cyclic allene. The Stork-Danheiser alkylation enabled quick construction of a number of substituted enones, which were transformed into a number of differently substituted cyclic allene precursors. The greatest success was achieved with a simple alkyl tether, though the synthesis of those substrates was longer and had no obvious branch point for diverse precursor synthesis other than enone **60**.

4.6. Future Directions

To increase the substrate scope and novelty of the transformations the reduction of the enone and silyl cuprate displacement of an allylic leaving group would be a simple way to generate less substituted derivatives **111–113** (Figure 4.6). It would be noteworthy to determine if removing the acetoxy group changes efficiency of the process or if dimerization of the less substituted cyclic allenes takes precedence.

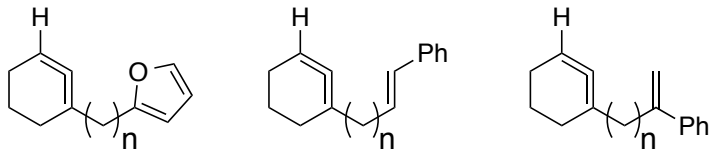

111 **112** **113**

Figure 4.6 - Cyclic allenes lacking a conjugated acetoxy group.

Part of the difficulty in silylating the precursors (especially prevalent in the amide-tethered cases) is assumed to arise from the steric crowding of the reactive enone functionality. To attenuate the low yields, the tethered trap could be moved one carbon away from the incipient allene (Scheme 4.19). This may complicate the process considering the possible stereoisomers formed in the silylation and alkylation; however, cuprate additions have been shown to be highly diastereoselective in conjugate additions.[28] The tethers could have heteroatoms and other substitution to increase complexity and facilitate the cyclization.

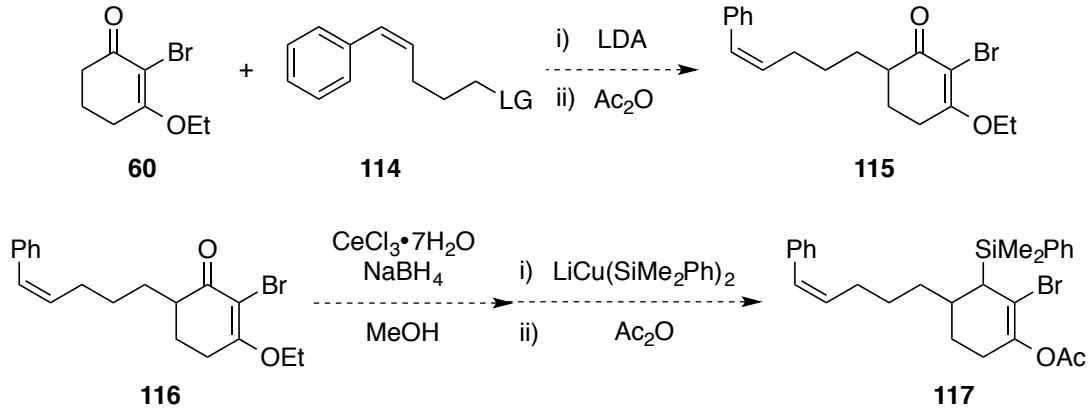

Scheme 4.19 - Possible incorporation of an allene trap at the γ-position.

The success of the furan cycloaddition was presumably due to the flexibility of the tether, therefore the rigidity of the amide linker hampers a successful reaction. To dodge these drawbacks the amide could be reduced to a simpler amine linker (**118**), increasing flexibility as well as the possibility for making piperidine spirocycles (**119**, Scheme 4.20).

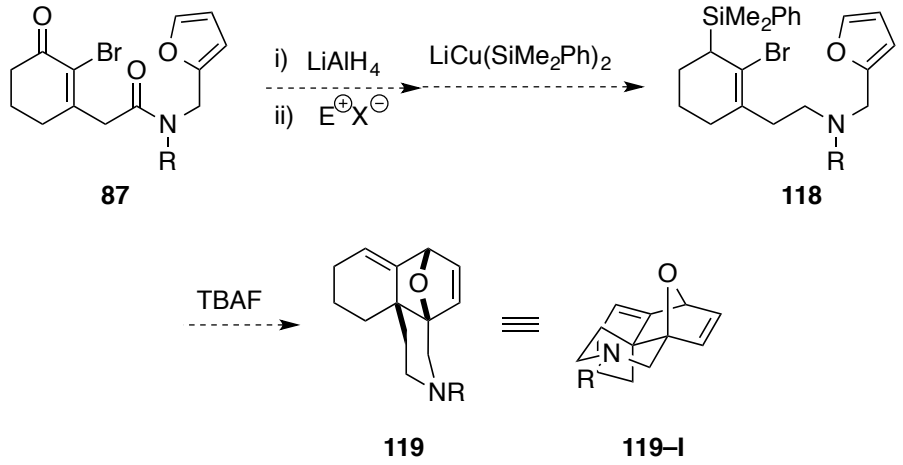

Scheme 4.20 - Reduction of amide-linker to facilitate an intramolecular reaction.

Finally, aldehyde **71** could be condensed with an *N*-alkyl-*N*-hydroxylamine **120** to generate a tethered nitrone (**121**). The previous success of intermolecular reactions with nitrones warrants the investigation into the intramolecular cycloadditions of nitrones with cyclic allenes (Scheme 4.21).

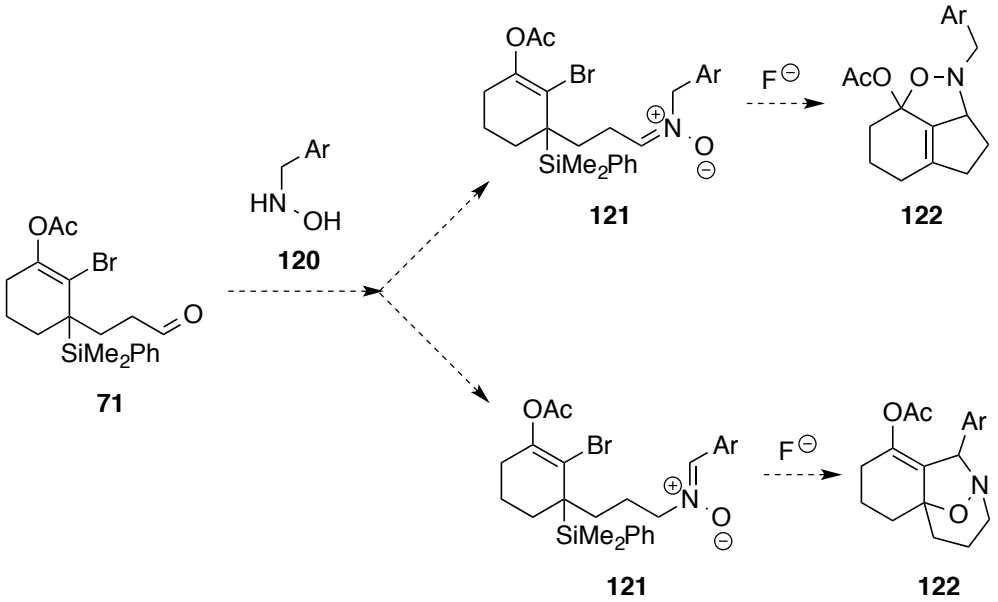

Scheme 4.21 - Possible intramolecular trapping of a cyclic allene with a nitrone.

4.7. Experimental

4.7.1. General Information

Reactions were carried out in oven (120 °C) or flame-dried glassware under a positive argon atmosphere unless otherwise stated. Transfer of anhydrous reagents was accomplished with oven-dried syringes or cannulae. Solvents were distilled before use: acetonitrile (CH_3CN), triethylamine (NEt_3), and dichloromethane (CH_2Cl_2) from calcium hydride, diethyl ether (Et_2O), and tetrahydrofuran (THF) from sodium/benzophenone, toluene, and benzene (C_6H_6) from sodium metal. Thin layer chromatography was performed on glass plates pre-coated with 0.25 mm Kieselgel 60 F254 (Merck). Flash chromatography columns were packed with 230-400 mesh silica gel (Silicycle). Proton nuclear magnetic resonance spectra (^{1}H NMR) were recorded at 300 MHz, 400 MHz, or 500 MHz and coupling constants (*J*) are reported in Hertz (Hz). Carbon nuclear magnetic resonance spectra (^{13}C NMR) were recorded at 100 MHz or 125 MHz. The chemical shifts are reported on the δ scale (ppm) and referenced to the residual solvent peaks: $CDCl_3$ (7.26 ppm, ^{1}H; 77.06 ppm, ^{13}C) as internal standards. Standard notation is used to describe the multiplicity of the signals observed in ^{1}H NMR spectra: broad (br), apparent (app), multiplet (m), singlet (s), doublet (d), triplet (t), quartet (q), pentet (p), etc. Infrared (IR) spectra were measured with a Mattson Galaxy Series FT-IR 3000 spectrophotometer. High-resolution mass spectrometry (HRMS) data (APPI/APCI/ESI technique) were recorded using an Agilent Technologies 6220 oaTOF instrument. HRMS data (EI technique) were recorded using a Kratos MS50 instrument.

Enone **33**,[29] 2-azido acetic acid **39**,[30] 2-(2-furyl)acetic acid **40**,[31] brominated enone **60,**[32] allylic alcohol **67**,[33] acetamides **89a-c**,[34] 2-(3-chloropropyl)furan **101**,[35] and 2-(4-chlorobutyl)furan **102**[36] are all known literature compounds, and their ^{1}H NMR and ^{13}C NMR spectral data matched those reported in the literature.

4.7.2. Physical Data

Phenyldimethylsilyl lithium

The reagent was prepared by a procedure similar to that employed by Gilman and coworkers:[37] See Chapter 2.

General procedure for the synthesis of acyl derivatives 41–47.

Two procedures were employed in the synthesis of the desired acyl derivatives dependent upon whether the acyl chloride was commercially available or not.

Using commercially available acyl chlorides:

To a dry flask under argon atmosphere was added copper bromide•dimethyl sulfide complex (1.25 equiv) which was suspended in THF, (0.15 M) and the flask was cooled to 0 °C using an ice-water bath. To this flask was added previously prepared lithium phenyldimethylsilyl anion (see previous entry, 2.5 equiv) via cannula transfer giving a deep red solution. The cuprate was stirred for 30 min maintaining the temperature at 0 °C. The cuprate solution was then cooled to -78 °C using a dry ice/acetone bath, and a cooled solution of enone **33** (1.0 equiv, 0.4 M in THF) was added via cannula. This solution was stirred at -78 °C for 5 hours. After 5 hours, the appropriate acyl chloride (5 equiv) was added via syringe (or in a solution of THF). The solution was maintained at -78 °C for a further 5 hours. To the solution was added a 30 mL portion of diethyl ether and a 25 mL portion of distilled water. The phases were separated and the aqueous layer was further extracted with diethyl ether (3 x 40 mL). The organic layer was washed with distilled water and brine, then dried over magnesium sulfate. The organic layer was filtered, concentrated and subjected to flash column chromatography to afford the appropriate compound.

From the carboxylic acids:

5 equivalents of the appropriate carboxylic acid was dissolved in dry DCM and cooled to 0 °C. To this solution was added 5.1 equivalents of oxalyl chloride and a single drop of dry dimethylformamide. The reaction was allowed to warm to room temperature and stir overnight. The solution was evaporated to dryness via the Schlenk line and dissolved in dry THF. This solution was added to the solution of enol cuprate as described in the previous section.

3-[Dimethyl(phenyl)silyl]-2-(trifluoromethanesulfonyloxy)cyclohex-1-en-1-yl furan-2-carboxylate (41)

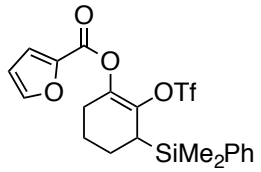

Using 70 mg of CuBr•SMe_2, 105 μL of $PhMe_2SiCl$, 100 μL of 2-furoyl chloride, and 50 mg of enone triflate **33**, furnished 86 mg of allylic silane **41** (89 % yield) as a clear, colorless oil. Eluent used for column chromatography was (1:1, hexanes:DCM)

R_f = 0.29 (1:1, hexanes:DCM); ^{1}H NMR (500 MHz, $CDCl_3$) δ 7.68 (dd, *J* = 1.7, 0.8 Hz, 1H), 7.58 – 7.55 (m, 2H), 7.44 – 7.39 (m, 3H), 7.34 (dd, *J* = 3.6, 0.7 Hz, 1H), 6.58 (dd, *J* 3.6, 1.7 = Hz, 1H), 2.41 – 2.36 (m, 2H), 2.29 – 2.25 (m, 1H), 1.89 – 1.83 (m, 1H), 1.70 – 1.56 (m, 3H), 0.48 (s, 6H); ^{13}C NMR (125 MHz, $CDCl_3$) δ 155.2, 147.4, 143.4, 140.4, 138.5, 136.4, 134.0, 129.5, 128.0, 119.9, 118.3 (q, $^1J_{C\text{-}F}$ = 320.5 Hz, 1C), 112.2, 27.9, 27.3, 25.4, 21.2, –2.8, –4.1; IR (cast film, cm^{-1}) 3056, 2954, 1750, 1577; HRMS (ESI) calcd for $[M+Na]^+$ $C_{20}H_{21}F_3NaO_6SSi$: 497.0672, found: 497.0665.

3-[Dimethyl(phenyl)silyl]-2-(trifluoromethanesulfonyloxy)cyclohex-1-en-1-yl benzoate (42)

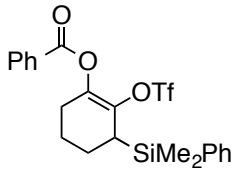

Using 70 mg of CuBr•SMe_2, 105 μL of $PhMe_2SiCl$, 140 μL of benzoyl chloride, and 50 mg of enone **33**, furnished 50 mg of allylic silane **42** (44 % yield) as a white waxy solid. mp = 93 – 95 °C. Eluent used for column chromatography was (1:1, hexanes:DCM)

R_f = 0.34 (1:1, hexanes:DCM); ^{1}H NMR (500 MHz, $CDCl_3$) δ 8.16 – 8.14 (m, 2H), 7.66 – 7.62 (m, 1H), 7.60 – 7.59 (m, 2H), 7.53 – 7.49 (m, 2H), 7.44 – 7.41 (m, 3H), 2.42 – 2.38 (m, 2H), 2.29 (app p, *J* = 2.5 Hz, 1H), 1.92 – 1.86 (m, 1H), 1.74 – 1.61 (m, 3H), 0.51 (s, 3H), 0.50 (s, 3H); ^{13}C NMR (125 MHz, $CDCl_3$) δ 163.6, 140.1, 139.1, 136.5, 134.0, 133.7, 130.3, 129.5, 128.7, 128.5, 128.0, 118.3 (q, $^1J_{C\text{-}F}$ = 318.2 Hz, 1C), 27.8,

27.3, 25.5, 21.2, –2.7, –4.1; IR (cast film, cm^{-1}) 3075, 2940, 2863, 1732, 1601; HRMS (ESI) calcd for $[M+Na]^+$ $C_{22}H_{23}F_3NaO_5SSi$: 507.088, found: 507.087.

3-[Dimethyl(phenyl)silyl]-2-(trifluoromethanesulfonyloxy)cyclohex-1-en-1-yl (2*E*)-3-phenylprop-2-enoate (43)

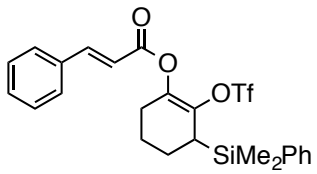

Using 63 mg of CuBr•SMe_2, 100 μL of $PhMe_2SiCl$, 160 mg of cinnamoyl chloride, and 50 mg of enone **33**, furnished 82.8 mg of allylic silane **43** (61 % yield) as a clear, colorless oil. Eluent used for column chromatography was (2:1, hexanes:DCM)

R_f = 0.49 (1:1, hexanes:DCM); ^{1}H NMR (500 MHz, $CDCl_3$) δ 7.84 (d, *J* = 16.0 Hz, 1H), 7.60 – 7.56 (m, 4H), 7.45 – 7.40 (m, 6H), 6.52 (d, *J* = 16.0 Hz, 1H), 2.42 – 2.31 (m, 2H), 2.26 (app p, *J* = 2.5 Hz, 1H), 1.89 – 1.83 (m, 1H), 1.70 – 1.57 (m, 3H), 0.50 (s, 6H); ^{13}C NMR (100 MHz, $CDCl_3$) δ 163.7, 147.2, 140.0, 139.0, 136.5, 134.1, 134.0, 130.8, 129.5, 129.0, 128.4, 128.0, 118.4 (q, $^1J_{C\text{-}F}$ = 318.5 Hz, 1C), 116.4, 27.8, 27.3, 25.4, 21.2, –2.8, –4.1; IR (cast film, cm^{-1}) 3070, 2953, 1737, 1635; HRMS (ESI) calcd for $[M+Na]^+$ $C_{24}H_{25}F_3NaO_5SSi$: 533.1036, found: 533.1025.

3-[Dimethyl(phenyl)silyl]-2-(trifluoromethanesulfonyloxy)cyclohex-1-en-1-yl (2*E*)-3-(4-methoxyphenyl)prop-2-enoate (44)

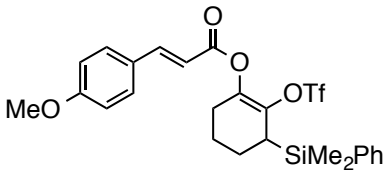

Using 126 mg of CuBr•SMe_2, 200 μL of $PhMe_2SiCl$, 402 mg of *p*-methoxycinnamoyl chloride and 100 mg of enone **33**, furnished 62.5 mg of allylic silane **44** (28 % yield) as a clear, colorless oil. Eluent used for column chromatography was (2:1, hexanes:DCM)

R_f = 0.54 (1:1, hexanes:DCM); ^{1}H NMR (500 MHz, $CDCl_3$) δ 7.76 (d, *J* = 16.0 Hz, 1H), 7.56 – 7.49 (m, 4H), 7.41 – 7.36 (m, 3H), 6.93 (app d, *J* = 6.8 Hz, 2H), 6.36 (d, *J* = 16.0 Hz, 1H), 3.87 (s, 3H), 2.37 – 2.32 (m, 2H), 2.27 – 2.22 (m, 1H), 1.88 – 1.80 (m, 1H), 1.70

– 1.54 (m, 3H), 0.48 (s, 6H); ^{13}C NMR (125 MHz, $CDCl_3$) δ 164.1, 161.8, 146.8, 139.9, 139.1, 136.5, 134.0, 130.1, 129.5, 128.0, 126.9, 118.4 (q, $^1J_{C\text{-}F}$ = 318.5 Hz, 1C), 114.4, 113.8, 55.4, 27.8, 27.3, 25.5, 21.2, –2.8, –4.1; IR (cast film, cm^{-1}) 3071, 3009, 2954, 1734, 1632; HRMS (ESI) calcd for $[M+Na]^+$ $C_{25}H_{27}F_3NaO_6SSi$: 563.114, found: 563.113.

3-[Dimethyl(phenyl)silyl]-2-(trifluoromethanesulfonyloxy)cyclohex-1-en-1-yl 2-chloroacetate (45)

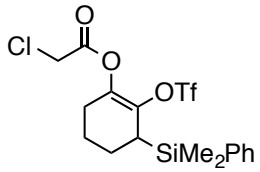

Using 70 mg of CuBr•SMe_2, 100 μL of $PhMe_2SiCl$, 163 μL of 2-chloroacetylchloride, and 50 mg of enone **33**, furnished 95 mg of allylic silane **45** (quantitative) as a clear, colorless oil. Eluent used for column chromatography was (2:1, hexanes:DCM)

R_f = 0.55 (1:1, hexanes:DCM); ^{1}H NMR (500 MHz, $CDCl_3$) δ 7.55 – 7.52 (m, 2H), 7.44 – 7.28 (m, 3H), 4.23, 4.22 (ABq, $^2J_{AB}$ = 15.5 Hz, 2H), 2.35 (app dtd, *J* = 17.1, 6.4, 2.6 Hz, 1H), 2.26 (app dtd, *J* = 16.8, 6.1, 2.9 Hz, 1H), 2.19 (app p, *J* = 2.5 Hz, 1H), 1.87 – 1.80 (m, 1H), 1.69 – 1.56 (m, 3H), 0.46 (s, 3H), 0.45 (s, 3H); ^{13}C NMR (125 MHz, $CDCl_3$) δ 164.4, 140.4, 138.7, 136.1, 133.9, 129.6, 128.0, 118.2 (q, $^1J_{C\text{-}F}$ = 320.4 Hz, 1C), 40.5, 27.7, 26.8, 25.3, 21.0, –2.9, –4.0; IR (cast film, cm^{-1}) 3072, 3051, 2956, 2865, 1785; HRMS (ESI) calcd for $[M+Na]^+$ $C_{17}H_{20}ClF_3NaO_5SSi$: 479.0334, found: 479.0322.

3-[Dimethyl(phenyl)silyl]-2-(trifluoromethanesulfonyloxy)cyclohex-1-en-1-yl 2-azidoacetate (46)

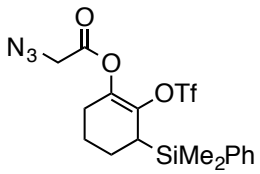

Using 270 mg of 2-azidoacetic acid, 126 mg of CuBr•SMe_2, 195 μL of $PhMe_2SiCl$, and 100mg of enone **33**, furnished 117 mg of allylic silane **46** (62 % yield) as a clear, colorless oil. Eluent used for column chromatography was (2:1, hexanes:DCM)

R_f = 0.55 (1:1, hexanes:DCM); ^{1}H NMR (500 MHz, $CDCl_3$) δ 7.74 – 7.52 (m, 2H), 7.43 – 7.39 (m, 3H), 4.05, 4.03 (ABq, $^2J_{AB}$ = 17.4 Hz, 2H), 2.37 (app dtd, J = 16.9, 6.3, 2.5 Hz, 1H), 2.29 – 2.23 (m, 1H), 2.19 (app p, J = 2.5 Hz, 1H), 1.89 – 1.81 (m, 1H), 1.70 – 1.56 (m, 3H), 0.47 (s, 3H), 0.46 (s, 3H); ^{13}C NMR (125 MHz, $CDCl_3$) δ 165.5, 140.3, 138.5, 136.1, 133.9, 129.6, 128.1, 118.2 (q, $^1J_{C\text{-}F}$ = 319.5 Hz, 1C), 50.1, 27.7, 27.0, 25.3, 21.0, –3.0, –4.0; IR (cast film, cm^{-1}) 3072, 3016, 2955, 2864, 2111, 1777; HRMS (ESI) calcd for $[M+Na]^+$ $C_{17}H_{20}F_3NaN_3O_5SSi$: 486.074, found: 486.073.

3-[Dimethyl(phenyl)silyl]-2-(trifluoromethanesulfonyloxy)cyclohex-1-en-1-yl 2-(furan-2-yl)acetate (47)

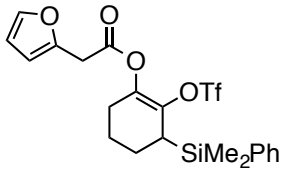

Using 100 mg of enone **33**, 130 mg of CuBr•SMe_2, 200 μL of $PhMe_2SiCl$, and 155 mg of homofuroic acid furnished 175 mg of allylic silane **47** (58 % yield) as a clear, colorless oil. Eluent used for column chromatography was (1:1, hexanes:DCM)

R_f = 0.29 (1:1, hexanes:DCM); ^{1}H NMR (500 MHz, $CDCl_3$) δ 7.63 – 7.51 (m, 2H), 7.42 – 7.36 (m, 4H), 6.38 (dd, J = 3.3, 1.9 Hz, 1H), 6.31 (dq, J = 3.2, 0.8 Hz, 1H), 3.86 (app s, 2H), 2.32 – 2.18 (m, 3H), 1.87 – 1.78 (m, 1H), 1.67 – 1.52 (m, 3H), 0.46 (s, 3H), 0.45 (s, 3H); ^{13}C NMR (125 MHz, $CDCl_3$) δ 166.4, 146.6, 140.1, 138.8, 136.4, 134.9, 133.9, 129.5, 128.0, 118.3 (q, $^1J_{C\text{-}F}$ = 320.6 Hz, 1C), 110.6, 108.6, 33.5, 27.7, 27.0, 25.4, 21.0, –2.8, –4.1; IR (cast film, cm^{-1}) 3071, 3050, 2954, 2864, 1772; HRMS (ESI) calcd for $[M+Na]^+$ $C_{21}H_{23}F_3NaO_6SSi$: 511.0829, found: 511.0824.

8-(Benzoyloxy)-2,3,4,4a,4b,5,6,7-octahydrobiphenylen-1-yl benzoate (48)

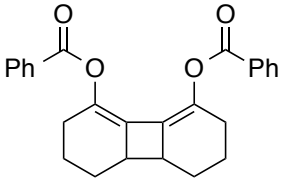

To an argon purged flask was added 38 mg of allylic silane **42** dissolved in 3 mL of acetonitrile. Tetrabutylammonium fluoride (2 equiv, 156 μL, 1 M in THF) was added to

the solution and once the addition was completed the reaction was concentrated and subjected to flash column chromatography (9:1:1 hexanes:ethyl acetate:DCM). Using 38 mg of allylic silane **42**, and 156 μL of TBAF (1 M) furnished 11.7 mg of dimer **48** (75 % yield) as a clear, colorless oil.

R_f = 0.27 (9:1, hexanes:ethyl acetate); ^{1}H NMR (300 MHz, $CDCl_3$) δ 7.70 – 7.66 (m, 4H), 7.38 – 7.35 (m, 2H), 7.18 – 7.12 (m, 4H), 2.75 – 2.70 (m, 2H), 2.45 (app dd, *J* = 18.3, 6.9, Hz, 2H), 2.27 – 2.14 (m, 2H), 2.03 – 1.92 (m, 4H), 1.75 – 1.59 (m, 2H), 1.37 – 1.23 (m, 2H); ^{13}C NMR (125 MHz, $CDCl_3$) δ 164.7, 139.8, 137.3, 132.7, 129.3, 127.7, 125.8, 47.0, 30.4, 27.1, 22.8; IR (cast film, cm^{-1}) 3063, 3033, 2930, 2861, 1730, 1601; HRMS (ESI) calcd for $[M+Na]^+$ $C_{26}H_{24}NaO_4$: 423.1567, found: 423.1557.

8-(Furan-2-carbonyloxy)-2,3,4,4a,4b,5,6,7-octahydrobiphenylen-1-yl furan-3-carboxylate (49)

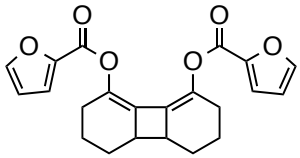

Allylic silane **65 (**62 mg) was dissolved in acetonitrile and a magnetic stirbar was added. Tetrabutylammonium fluoride (2 equiv, 286 μL, 1 M in THF) was added and once the addition was completed the reaction was pumped down and subjected to column chromatography (8:1:1, hexanes:DCM:ethyl acetate). Using 62 mg of allylic silane **65**, and 286 μL of TBAF (1 M) yielded 15 mg of dimer **41** (58 % yield) as a clear, colorless oil.

R_f = 0.25 (8:2, hexanes:ethyl acetate); ^{1}H NMR (500 MHz, $CDCl_3$) δ 7.41 (dd, *J* = 2.0, 1.0 Hz, 2H), 6.98 (dd, *J* = 3.5, 0.5 Hz, 2H), 6.36 (dd, *J* = 3.5, 2.0 Hz, 2H), 2.70 – 2.66 (m, 2H), 2.51 (dd, *J* = 17.5, 6.5 Hz, 2H), 2.22 – 2.15 (m, 2H), 2.0 – 1.93 (m, 4H), 1.71 – 1.59 (m, 2H), 1.31 – 1.22 (m, 2H); ^{13}C NMR (125 MHz, $CDCl_3$) δ 156.6, 146.4, 143.9, 137.0, 125.9, 118.4, 111.7, 46.9, 27.0, 26.7, 22.7; IR (cast film, cm^{-1}) 2939, 2852, 1732; HRMS (EI) calcd for $[M+Na]^+$ $C_{22}H_{20}NaO_6$: 403.1152, found: 403.1155.

2-Bromo-3-[dimethyl(phenyl)silyl]-3-(prop-2-en-1-yl)cyclohex-1-en-1-yl acetate (68)

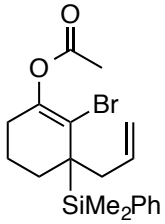

To a dry flask under argon atmosphere was added copper bromide•dimethyl sulfide complex (1.5 equiv) which was suspended in THF (0.15 M), and the flask was cooled to 0 °C using an ice-water bath. To this flask was added previously prepared lithium phenyldimethylsilyl anion (2.5 equiv) via cannula transfer giving a deep red solution. The cuprate was maintained at 0 °C for 20 min after which a cooled solution of 304 mg of enone **62** (1 equiv, 0.4 M in THF) was added via cannula. This solution was stirred at 0 °C for 5 hours. After 5 hours, acetic anhydride (5 equiv) was added via syringe. The solution was maintained at 0 °C for a further 5 hours. To the solution was added a 30 mL portion of diethyl ether and a 25 mL portion of distilled water. The phases were separated and the aqueous layer was further extracted with diethyl ether (3 x 40 mL). The organic layer was washed with distilled water and brine, then dried over magnesium sulfate, filtered, concentrated and subjected to flash column chromatography (3:1, hexanes:DCM). Using 265 mg of enone **62**, 358 mg of CuBr•SMe_2, and 575 μL of $PhMe_2SiCl$ furnished 264 mg of allylic silane **68** (58 % yield) as a yellow oil.

R_f = 0.55 (1:1, hexanes:DCM); ^{1}H NMR (500 MHz, $CDCl_3$) δ 7.61 – 7.59 (m, 2H), 7.43 – 7.37 (m, 3H), 5.81 (dtd, *J* = 18.2, 9.2, 5.3 Hz, 1H), 5.08 (m, 2H), 2.83 (dd, *J* = 14.2, 5.1 Hz, 1H), 2.24 – 2.08 (m, 3H), 2.21 (s, 3H), 1.71 – 1.63 (m, 4H), 0.54 (s, 3H), 0.49 (s, 3H); ^{13}C NMR (100 MHz, $CDCl_3$) δ 168.1, 145.0, 137.3, 135.4, 134.8, 129.1, 127.6, 120.1, 117.4, 40.6, 35.7, 31.8, 28.8, 20.8, 19.7, –2.7, –3.3; IR (cast film, cm^{-1}) 3070, 3012, 2940, 1762, 1654, 1636; HRMS (ESI) calcd for $[M+Na]^+$ $C_{19}H_{25}{}^{79}BrNaO_2Si$: 415.0699, found: 415.0699.

2-Bromo-3-[dimethyl(phenyl)silyl]-3-(3-hydroxypropyl)cyclohex-1-en-1-yl acetate (69)

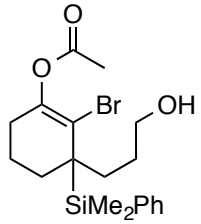

A 0.1 M THF solution of allylic silane **68** was cooled to 0 °C in a dry, argon purged flask. To this solution was added 9-BBN (2 equiv, 0.5 M in THF), and the solution was warmed to room temperature to stir for 2 h. The solution was cooled again to 0 °C and aqueous sodium hydroxide was added (2 M, 1.5 equiv), followed by aqueous hydrogen peroxide solution (30 % w/v, 10 equiv). The solution was allowed to warm to room temperature and stir overnight when the reaction was quenched via the addition of 1 M HCl and diethyl ether. The aqueous layer was extracted with ether (2 x 30 mL), the combined organic layers were washed with distilled water, brine, dried over magnesium sulfate, filtered, concentrated and subjected to flash column chromatography (4:1, hexanes:ethyl acetate) to give alcohol **69**. From 220 mg of allylic silane **68**, 1.46 mL of 9-BBN (0.5 M in THF), 702 μL of sodium hydroxide (2 M), and 560 μL of hydrogen peroxide (30 % w/w) furnished 130 mg of alcohol **69** (56 % yield) as a clear, colorless oil.

R_f = 0.64 (1:1, hexanes:ethyl acetate); ^{1}H NMR (500 MHz, $CDCl_3$) δ 7.61 – 7.58 (m, 2H), 7.42 – 7.36 (m, 3H), 3.71 – 3.63 (m, 2H), 2.26 – 2.20 (m, 1H), 2.21 (s, 3H), 2.13 – 1.99 (m, 2H), 1.75 – 1.51 (m, 7H), 1.47 (br s, 1H), 0.53 (s, 3H), 0.48 (s, 3H); ^{13}C NMR (125 MHz, $CDCl_3$) δ 168.1, 145.0, 137.4, 134.7, 129.1, 127.6, 120.4, 63.5, 35.5, 32.2, 31.5, 28.8, 27.9, 20.8, 20.2, –2.7, –3.1; IR (cast film, cm^{-1}) 3392, 3069, 2947, 2869, 1761; HRMS (ESI) calcd for $[M+Na]^+$ $C_{19}H_{27}{}^{79}BrNaO_3Si$: 433.0805, found: 433.0794.

3-(3-Azidopropyl)-2-bromo-3-[dimethyl(phenyl)silyl]cyclohex-1-en-1-yl acetate (70)

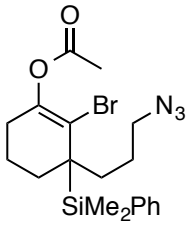

To a dry, argon purged flask 130 mg of alcohol **69** and 2.5 mL of DCM (0.15 M) were added. The flask was cooled to 0 °C for 10 minutes. Mesyl chloride (37 μL, 1.5 equiv) and triethylamine (110 μL, 2.5 equiv) were added in this order and the solution was stirred for 2 h until the starting material had been consumed as determined by TLC analysis. The reaction was quenched with 1 M HCl (30 mL) and extracted with DCM (6 x 30 mL). The combined organic fractions were combined, washed with distilled water, brine, dried with magnesium sulfate, filtered, concentrated, and a short silica plug was run (using 1:1 ethyl acetate:hexanes).

The solution was immediately pumped down and dissolved in a 0.5 M solution of sodium azide in DMSO (2 equiv of NaN_3, 1.5 mL). The reaction was stirred overnight. The solution was quenched with distilled water and extracted with diethyl ether (10 x 30 mL). The combined organic fractions were washed with distilled water (3 x 30 mL), brine (1 x 30 mL), dried over magnesium sulfate, filtered, concentrated, and subjected to flash column chromatography (10:1, hexanes:ethyl acetate) to give azide **70**. From 130 mg of alcohol **69**, 66 mg of azide **70** (48 % yield over two steps) was isolated as a clear, colorless oil.

R_f = 0.36 (9:1, hexanes:ethyl acetate); ^{1}H NMR (400 MHz, $CDCl_3$) δ 7.59 – 7.56 (m, 2H), .42 – 7.35 (m, 3H), 3.35 – 3.20 (m, 2H), 2.26 – 2.19 (m, 1H), 2.20 (s, 3H), 2.12 – 1.94 (m, 2H), 1.74 – 1.56 (m, 7H), 0.53 (s, 3H), 0.48 (s, 3H); ^{13}C NMR (100 MHz, $CDCl_3$) δ 168.0, 145.1, 137.1, 134.7, 129.2, 127.7, 120.0, 52.1, 35.5, 33.3, 31.5, 28.8, 24.2, 20.8, 20.2, –2.7, –3.2; IR (cast film, cm^{-1}) 3070, 2949, 2870, 2095, 1761, 1654; HRMS (ESI) calcd for $[M+Na]^+$ $C_{19}H_{26}{}^{79}BrNaN_3O_2Si$: 458.087, found: 458.086.

2-Bromo-3-[dimethyl(phenyl)silyl]-3-(3-oxopropyl)cyclohex-1-en-1-yl acetate (71)

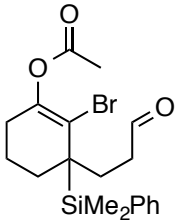

A dry, argon purged flask was charged with 282 mg of alcohol **69** and DCM (10 mL, 0.06 M), and cooled to 0 °C. Pyridine (94 μL, 1.7 equiv) and Dess-Martin periodinane (438mg, 1.4 equiv) were added successively and the reaction was stirred until the starting material was consumed as determined by TLC. The reaction was quenched via the addition of diethyl ether (30 mL) and 1 M HCl (30 mL). The aqueous layer was extracted with ether (2 x 30 mL), the combined organic fractions were washed with distilled water (30 mL), brine (30 mL), dried over magnesium sulfate, filtered, concentrated, and subjected to flash column chromatography (10:1, hexanes:ethyl acetate). Using 282 mg of alcohol **69**, 94 μL of pyridine, and 438 mg of DMP furnished 231 mg of aldehyde **71** (82 % yield) as a clear, colorless oil that decomposed rapidly, which prevented complete characterization.

R_f = 0.55 (8:2, hexanes:ethyl acetate); ^{1}H NMR (500 MHz, $CDCl_3$) δ 9.81 (t, *J* = 1.5 Hz, 1H), 7.59 – 7.56 (m, 2H), 7.42 – 7.36 (m, 3H), 2.51 – 2.46 (m, 2H), 2.37 – 2.31 (m, 1H), 2.26 – 2.19 (m, 1H), 2.20 (s, 3H), 2.09 – 2.04 (m, 1H), 1.83 – 1.77 (m, 1H), 1.72 – 1.59 (m, 3H), 1.53 – 1.47 (m, 1H), 0.54 (s, 3H), 0.49 (s, 3H); ^{13}C NMR (125 MHz, $CDCl_3$) δ 202.4, 168.1, 145.6, 136.9, 134.6, 129.3, 127.8, 119.4, 33.3, 35.0, 31.5, 28.8, 27.8, 20.8, 20.0, –2.7, –3.1.

General method to making enone amides 90–92:

A dry, argon purged flask was charged with THF and DIPA (1.7 equiv) then cooled to –78 °C in a dry ice/acetone bath. To this solution was added BuLi (2.4 M, 1.5 equiv.) via syringe and the solution was warmed to 0 °C for 5 minutes. The solution of LDA was cooled to –78 °C again and a 1M THF solution of the appropriate amide (**89a–c**) was added slowly via cannula. The solution initially took on a light pink color that intensified as the solution was warmed to 0 °C. The solution was stirred at 0 °C for 1 h (except in the

case of *N,O*-dimethylacetamide, which was stirred at –78 °C for 2 h due to low yields). The solution was recooled to –78 °C and a 1M THF solution of enone **60** (1 equiv) was added via cannula. The solution was allowed to warm to room temperature and stirred for 1 h, whereupon the majority of the color would dissipate over time. The reaction was then carefully quenched with 1M HCl and stirred for 5 minutes. DCM was added to the aqueous layer, the layers were separated, and the aqueous layer was washed with DCM (2 x 30 mL). The combined organic layers were washed with 1 M HCl (1 x 30 mL), saturated $NaHCO_3$ (2 x 30 mL), distilled water (1 x 30 mL), brine (1 x 30 mL), dried over magnesium sulfate, filtered, concentrated and finally subjected to flash column chromatography to give the desired enone amides (**90–92**).

2-(2-Bromo-3-oxocyclohex-1-en-1-yl)-N-methoxy-N-methylacetamide (90)

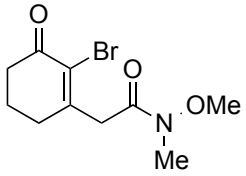

Using 500 mg of enone **60**, and 312 mg of amide **89a** furnished 96 mg of amide **90** (15 % yield) was isolated as an oil which solidified over time to a white solid. mp = 72 – 74 °C. R_f = 0.31 (9:1, DCM:ethyl acetate); ^{1}H NMR (500 MHz, $CDCl_3$) δ 3.78 (s, 3H), 3.74 (br s, 2H), 3.23 (s, 3H), 2.64 (dd, *J* = 7.6, 6.5 Hz, 2H), 2.60 (app t, *J* = 6.0 Hz, 2H), 2.09 – 2.04 (m, 2H); ^{13}C NMR (125 MHz, $CDCl_3$) δ 191.0, 169.0, 156.9, 125.1, 61.5, 42.8, 37.8, 33.0, 32.3, 21.8; IR (cast film, cm^{-1}) 2939, 1671, 1606; HRMS (ESI) calcd for $[M+H]^+$ $C_{10}H_{15}BrNO_3$: 276.023, found: 276.023.

2-(2-Bromo-3-oxocyclohex-1-en-1-yl)-*N*-(furan-2-ylmethyl)-*N*-methylacetamide (91)

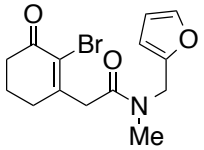

Using 205 mg of enone **60**, and 213 mg of amide **89b** furnished 273 mg of amide **91** (90 % yield) as a clear, colorless oil.

Note: NMR spectra at room temperature showed a mixture of amide rotamers. Complete coalescence could not be achieved at higher temperatures so the data are reported for the room temperature rotamer mixtures.

R_f = 0.32 (9:1, DCM:ethyl acetate); ^{1}H NMR (500 MHz, $CDCl_3$, rt) δ 7.42 (dd, *J* = 1.9, 0.8 Hz, 1H), 7.39 (dd, *J* = 1.8, 0.8 Hz, 1H), 6.39 (dd, *J* = 3.3, 1.9 Hz, 1H), 6.36 (dd, *J* = 3.3, 1.9 Hz, 1H), 6.30 – 6.29 (m, 2H), 4.61 (s, 2H), 4.50 (s, 2H), 3.82 (s, 2H), 3.66 (s, 2H), 3.08 (s, 3H), 3.01 (s, 3H), 2.67 – 2.63 (m, 8H), 2.11 – 2.05 (m, 4H); ^{13}C NMR (125 MHz, $CDCl_3$) δ 191.0, 191.0, 167.9, 167.8, 157.3, 157.3, 150.5, 149.5, 142.9, 142.4, 124.9, 124.9, 110.5, 110.4, 108.6, 108.3, 54.4, 47.0, 44.0, 43.9, 43.8, 37.9, 35.3, 33.8, 33.0, 32.9, 21.8, 21.8; IR (cast film, cm^{-1}) 3143, 3116, 2949, 1683, 1650, 1607; HRMS (EI) calcd for $[M]^+$ $C_{14}H_{16}{}^{79}BrNO_3$: 325.03134, found: 325.03223.

2-(2-Bromo-3-oxocyclohex-1-en-1-yl)-*N*,*N*-bis(furan-2-ylmethyl)acetamide (92)

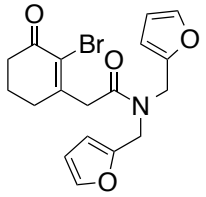

Using 400 mg of enone **60**, and 500 mg of amide **89c** furnished 606 mg of amide **92** (85 % yield) was isolated as a clear, colorless oil.

R_f = 0.25 (7:3, DCM:ethyl acetate); ^{1}H NMR (500 MHz, $CDCl_3$, rt) δ 7.41 (dd, *J* = 1.0, 0.5 Hz, 1H), 7.38 (dd, *J* = 1.0, 0.5 Hz, 1H), 6.37 (dd, *J* = 3.0, 2.0 Hz, 1H), 6.35 (dd, *J* = 3.0 2.0 Hz, 1H), 6.28 (d, *J* = 3.0 Hz, 1H), 6.26 (dd, *J* = 3.0, 0.5 Hz, 1H) 4.62 (s, 2H), 4.48 (s, 2H), 3.83 (s, 2H), 2.65 – 2.61 (m, 4H), 2.09 – 2.04 (m, 2H); ^{13}C NMR (125 MHz, $CDCl_3$) δ 191.0, 167.8, 157.2, 150.4, 149.4, 142.9, 142.4, 125.0, 110.5, 110.5, 109.0, 108.6, 44.1, 44.0, 41.3, 37.9, 32.9, 21.8; IR (cast film, cm^{-1}) 3117, 2949, 1683, 1652, 1607; HRMS (EI) calcd for $[M]^+$ $C_{18}H_{18}{}^{79}BrNO_4$: 391.04193, found: 391.04098.

2-Bromo-3-[dimethyl(phenyl)silyl]-3-{[(furan-2-ylmethyl)(methyl)carbamoyl]methyl}cyclohex-1-en-1-yl acetate (93)

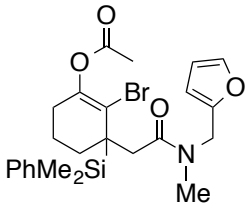

To a dry flask under argon atmosphere was added copper bromide•dimethyl sulfide complex (1.5 equiv) which was suspended in THF, (0.15 M) and the flask was cooled to 0 °C using an ice-water bath. To this flask was added previously prepared lithium phenyldimethylsilyl anion (2.9 equiv) via cannula transfer giving a deep red solution. The cuprate was maintained at 0 °C for 20 min and a cooled solution of 273 mg of amide **91** (1 equiv, 0.4 M in THF) was added via cannula. This solution was stirred at 0 °C for 5 hours. After 5 hours, acetic anhydride (5 equiv) was added via syringe. The solution was maintained at 0 °C for a further 5 hours after which a 30 mL portion of diethyl ether and a 25 mL portion of distilled water was added. The phases were separated and the aqueous layer was further extracted with diethyl ether (3 x 40 mL). The organic layer was washed with distilled water and brine, then dried over magnesium sulfate. The organic layer was filtered, concentrated and subjected to flash column chromatography (8:2:1, hexanes:ethyl acetate:DCM). Using 273 mg of amide **91**, 259 mg of CuBr•SMe_2, and 430 μL of $PhMe_2SiCl$ afforded 39 mg of allylic silane **93** (10 % yield) as a clear, colorless oil.

Note: NMR spectra at room temperature showed a mixture of amide rotamers. Complete coalescence could not be achieved at higher temperatures so the data are reported for the room temperature rotamer mixtures (i.e. in a 1:0.6 ratio, integrals are a reflection of ratio) R_f = 0.28 (8:2, hexanes:ethyl acetate); ^{1}H NMR (500 MHz, $CDCl_3$) δ 7.67 – 7.63 (m, 3.42H), 7.39 – 7.32 (m, 7.08H), 6.33 (dd, *J* = 3.1, 1.9 Hz, 1H), 6.31 (dd, *J* = 3.1, 1.9 Hz, 0.6H), 6.23 (d, *J* = 3.1 Hz, 1H), 6.04 (d, *J* = 3.1 Hz, 0.6H), 4.61 (d, *J* = 15.5 Hz, 1H), 4.46 (d, *J* = 15.2 Hz, 1H), 4.40 (d, *J* = 16.8 Hz, 0.7H), 4.27 (d, *J* = 16.8 Hz, 0.7H), 2.93 (s, 2.27H), 2.90 (s, 3H), 2.86, 2.83 (ABq, $^2J_{AB}$ = 16.0 Hz, 1.38H), 2.73, 2.70 (ABq, $^2J_{AB}$ = 16.0 Hz, 2H), 2.33 – 2.18 (m, 3.43H), 2.20 (s, 5.3H), 2.12 – 2.03 (m, 1.72H), 1.19 – 1.91 (m, 1.62H), 1.82 – 1.65 (m, 3.61H), 0.57 (s, 5H), 0.55 (s, 5H); ^{13}C NMR (125 MHz,

$CDCl_3$) δ 171.1, 170.9, 168.3, 168.2, 151.3, 150.4, 144.6, 144.4, 142.5, 142.0, 137.4, 137.4, 135.2, 135.2, 129.0, 127.4, 121.1, 121.1, 110.3, 110.3, 108.2, 107.6, 47.0, 43.6, 39.5, 39.4, 35.6, 35.5, 35.4, 33.9, 32.1, 32.0, 28.9, 28.9, 20.8, 19.6, 19.6, –1.7, –1.9, –2.8, –2.8 (Note: Three expected carbon resonances were not identified, presumably due to spectral overlap given the complex mixture of rotamers); IR (cast film, cm^{-1}) 3118, 3070, 2938, 1759, 1652; HRMS (EI) calcd for $[M]^+$ $C_{23}H_{27}{}^{79}BrNO_4Si$: 488.08926, found: 488.09014.

N-(Furan-2-ylmethyl)-N-methyl-2-(3-oxocyclohex-1-en-1-yl)acetamide (95)

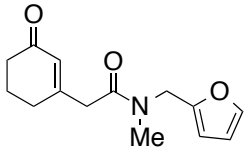

A dry, argon purged flask containing 39 mg of allylic silane **93** was charged with 1.5 mL of acetonitrile (0.01 M). To this solution was added 160 μL of TBAF (2 equiv, 1 M in THF diluted to 0.16 with MeCN) at a rate of 1 mL/h. The reaction was stirred a further 30 minutes following completion of the addition. The solution was concentrated and subjected to flash column chromatography (1:1, DCM:ethyl acetate). Using 39 mg of allylic silane **93**, and 160 μL of 1 M TBAF furnished 5.5 mg of enone **95** (28 % yield) as a clear, colorless oil.

Note: NMR spectra at room temperature showed a mixture of amide rotamers. Complete coalescence could not be achieved at higher temperatures so the data are reported for the room temperature rotamer mixtures (approximately 1:1 mixture).

R_f = 0.26 (1:1, DCM:ethyl acetate); ^{1}H NMR (400 MHz, $CDCl_3$) δ 7.39 (dd, *J* = 2.0, 0.8 Hz, 1H), 7.36 (dd, *J* = 1.6, 0.8 Hz, 1H), 6.35 (dd, *J* = 3.2, 2.0 Hz, 1H), 6.33 (dd, *J* = 3.2, 2.0 Hz, 1H), 6.26 (br d, 3.2 Hz, 1H), 6.23 (dd, *J* = 3.2, 0.4 Hz, 1H), 5.92 (br s, 1H), 5.90 (br s, 1H), 4.57 (s, 2H), 4.40 (s, 2H), 3.54 (s, 2H), 3.31 (s, 2H), 2.99 (s, 3H), 2.96 (s, 3H), 2.43 – 2.37 (m, 8H), 2.07 – 1.99 (m, 4H); ^{13}C NMR (100 MHz, $CDCl_3$) δ 199.4, 199.4, 168.5, 159.1, 158.7, 150.5, 142.9, 142.4, 131.2, 128.8, 121.1, 116.2, 110.4, 109.9, 108.6, 108.3, 47.1, 43.7, 43.2, 42.9, 37.2, 35.4, 33.6, 29.7, 29.6, 22.5 (Note: Two expected carbon resonances were not identified, presumably due to spectral overlap given the

complex mixture of rotamers); IR (cast film, cm^{-1}) 3116, 2936, 2864, 1650(br); HRMS (EI) calcd for $[M]^+$ $C_{14}H_{17}NO_3$: 247.12085, found: 247.12108.

2-Bromo-3-[3-(furan-2-yl)propyl]cyclohex-2-en-1-one (103)

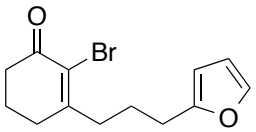

To a dry, argon purged flask was added magnesium filings (4.0 equiv). The flask was heated with a Bunsen burner under vacuum to activate the magnesium and cooled under a stream of argon. The flask was charged with THF and 0.1 equiv of dibromoethane was added to the solution. A prepared solution of 2-(3-chloropropyl)furan in THF (0.6 M) was added to the magnesium as the magnesium solution was heated to reflux over the course of an hour. The solution was further heated at reflux for 3 hours, then cooled to room temperature, at which point the solution was transferred by cannula to a previously prepared solution of enone **60** in THF (0.1 M) at –10 °C. The solution was warmed to room temperature, stirred for 1 hour, and quenched with 1M HCl. The reaction mixture was extracted with diethyl ether (4 x 30 mL) and the organic layers were combined. The organic layers were washed with 1 M HCl (1 x 30 mL), distilled water (1 x 30 mL), brine (1 x 30 mL), dried over magnesium sulfate, filtered, concentrated and subjected to flash column chromatography (9:1:1, hexanes:ethyl acetate:DCM). Using 107 mg of enone **60**, 106 mg of chloride **101**, and 60 mg of magnesium furnished 113 mg of enone **103** (82 % yield) as a clear, colorless oil.

R_f = 0.27 (8:2, hexanes:ethyl acetate); ^{1}H NMR (500 MHz, $CDCl_3$) δ 7.33, (dd, *J* = 2.0, 1.0 Hz, 1H), 6.31 (dd, *J* = 3.0, 1.5 Hz, 1H), 6.06 (dd, *J* = 3.0, 1.0 Hz, 1H), 2.74 (t, *J* = 7.5 Hz, 2H), 2.61 – 2.54 (m, 4H), 2.51 (t, *J* = 6.0 Hz, 2H), 2.00 (app p, *J* = 6.0 Hz, 2H), 1.92 (app p, *J* = 6.0 Hz, 2H); ^{13}C NMR (125 MHz, $CDCl_3$) δ 191.1, 163.2, 155.0, 141.1, 123.0, 110.2, 105.4, 38.7, 37.8, 32.4, 27.9, 25.2, 22.0; IR (cast film, cm^{-1}) 2938, 2867, 1683, 1596; HRMS (EI) calcd for $[M]^+$ $C_{13}H_{15}{}^{79}BrO_2$: 282.02554, found: 282.02484.

2-Bromo-3-[4-(furan-2-yl)butyl]cyclohex-2-en-1-one (104)

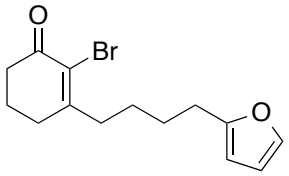

To a dry, argon purged flask was added magnesium filings (4.0 equiv). The flask was heated with a Bunsen burner under vacuum to activate the magnesium and cooled under a stream of argon. The flask was charged with THF and 0.1 equiv of dibromoethane was added to the solution. A prepared solution of 2-(4-chlorobutyl)furan in THF (0.6 M) was added to the magnesium as the magnesium solution was heated at reflux over the course of an hour. The solution was further heated to reflux for 3 hours, cooled to room temperature, at which point the solution was transferred by cannula to a previously prepared solution of 500 mg of enone **60** in THF (0.1 M) at –10 °C. The solution was warmed to room temperature, stirred for 1 hour, and quenched with 1 M HCl. The reaction mixture was extracted with diethyl ether (4 x 30 mL) and the organic layers were combined. The organic layers were washed with 1M HCl (1 x 30 mL), distilled water (1 x 30 mL), brine (1 x 30 mL), dried over magnesium sulfate, filtered, concentrated and subjected to flash column chromatography (9:1:1, hexanes:ethyl acetate:DCM). Using 500 mg of enone **60**, 500 mg of magnesium, 579 mg of chloride **102**, furnished 315 mg of enone **104** (44 % yield) as a clear, colorless oil.

R_f = 0.25 (8:2, hexanes:ethyl acetate); ^{1}H NMR (500 MHz, $CDCl_3$) δ 7.32 (dd, *J* = 1.9, 0.9 Hz, 1H), 6.30 (dd, *J* = 3.1, 1.9 Hz, 1H), 6.02 – 6.00 (m, 1H), 2.70 (t, *J* = 7.5 Hz, 2H), 2.60 (app t, *J* = 6.8 Hz, 2H), 2.56 (app t, *J* = 7.9 Hz, 2H), 2.50 (t, *J* = 6.1 Hz, 2H), 2.04 – 1.99 (m, 2H), 1.79 – 1.73 (m, 2H), 1.65 – 1.58 (m, 2H); ^{13}C NMR (125 MHz, $CDCl_3$) δ 191.2, 163.6, 155.6, 140.9, 122.8, 110.1, 105.0, 38.9, 37.9, 32.4, 27.9, 27.7, 26.2, 22.0; IR (cast film, cm^{-1}) 3115, 2935, 2863, 1683, 1595; HRMS (EI) calcd for $[M]^+$ $C_{14}H_{17}{}^{79}BrO_2$: 296.04120, found: 296.04059.

2-Bromo-3-[dimethyl(phenyl)silyl]-3-[3-(furan-2-yl)propyl]cyclohex-1-en-1-yl acetate (105)

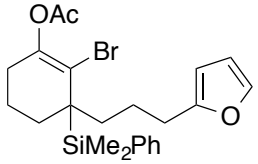

To a dry flask under argon atmosphere was added copper bromide•dimethyl sulfide complex (1.5 equiv) which was suspended in THF (0.15 M) and the flask was cooled to 0 °C using an ice-water bath. To this flask was added previously prepared lithium phenyldimethylsilyl anion (2.9 equiv) via cannula transfer giving a deep red solution. The cuprate was maintained at 0 °C for 20 min and a cooled solution of 130 mg of enone **103** (1 equiv, 0.4 M in THF) was added via cannula. This solution was stirred at 0 °C for 5 hours. After 5 hours, acetic anhydride (5 equiv) was added via syringe. The solution was maintained at 0 °C for a further 5 hours after which a 30 mL portion of diethyl ether and a 25 mL portion of distilled water was added. The phases were separated and the aqueous layer was further extracted with diethyl ether (3 x 40 mL). The organic layer was washed with distilled water and brine, then dried over magnesium sulfate. The organic layer was filtered, concentrated and subjected to flash column chromatography (3:1, hexanes:DCM). Using 200 mg of enone **103**, 187 mg of CuBr•SMe_2, 260 μL of $PhMe_2SiCl$, and 200 μL of acetic anhydride afforded 269 mg of allylic silane **105** (80 % yield) as a clear, colorless oil.

R_f = 0.66 (8:2, hexanes:ethyl acetate); ^{1}H NMR (400 MHz, $CDCl_3$) δ 7.57 – 7.55 (m, 2H), 7.38 – 7.31 (m, 3H), 7.30 (dd, *J* = 1.9, 0.8 Hz, 1H), 6.28 (dd, *J* = 3.2, 2.0 Hz, 1H), 5.98 (dd, *J* = 3.2, 0.9 Hz, 1H), 2.64 – 2.58 (m, 2H), 2.22 – 1.94 (m, 3H), 2.19 (s, 3H), 1.70 – 1.57 (m, 7H), 0.49 (s, 3H), 0.46 (s, 3H); ^{13}C NMR (125 MHz, $CDCl_3$) δ 168.1, 156.1, 144.8, 140.7, 137.5, 134.7, 129.1, 127.6, 120.5, 110.1, 104.8, 35.8, 35.8, 31.5, 28.8, 28.6, 23.2, 20.8, 20.2, –2.7, –3.2; IR (cast film, cm^{-1}) 3068, 3010, 2949, 2936, 2908, 1756; HRMS (EI) calcd for $[M]^+$ $C_{23}H_{29}{}^{79}BrO_3Si$: 460.10693, found: 460.10709.

2-Bromo-3-[dimethyl(phenyl)silyl]-3-[3-(furan-2-yl)butyl]cyclohex-1-en-1-yl acetate (106)

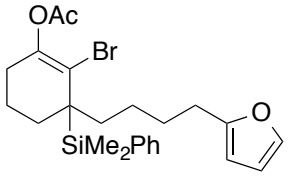

To a dry flask under argon atmosphere was added copper bromide•dimethyl sulfide complex (1.5 equiv) which was suspended in THF, (0.15 M) and the flask was cooled to 0 °C using an ice-water bath. To this flask was added previously prepared lithium phenyldimethylsilyl anion (2.9 equiv) via cannula transfer giving a deep red solution. The cuprate was maintained at 0 °C for 20 min and a cooled solution of 130 mg of enone **104** (1 equiv, 0.4 M in THF) was added via cannula. This solution was stirred at 0 °C for 5 hours. After 5 hours, acetic anhydride (5 equiv) was added via syringe. The solution was maintained at 0 °C for a further 5 hours after which a 30 mL portion of diethyl ether and a 25 mL portion of distilled water was added. The phases were separated and the aqueous layer was further extracted with diethyl ether (3 x 40 mL). The organic layer was washed with distilled water and brine, then dried over magnesium sulfate. The organic layer was filtered, concentrated and subjected to flash column chromatography (3:1, hexanes:DCM). Using 130 mg of enone **60**, 90 mg of CuBr•SMe_2, and 188 μL of $PhMe_2SiCl$ furnished 152 mg of allylic silane **106** (73 % yield) as a clear, colorless oil.

R_f = 0.63 (8:2, hexanes:ethyl acetate); ^{1}H NMR (500 MHz, $CDCl_3$) δ 7.58 – 7.55 (m, 2H), 7.38 – 7. 34 (m, 3H), 7.31 (dd, *J* = 1.5, 0.5 Hz, 1H), 6.29 (dd, *J* = 3.0, 2.0 Hz, 1H), 5.98 (dd, *J* = 3.0, 1.0 Hz, 1H), 2.70 – 2.58 (m, 2H), 2.24 – 2.18 (m, 1H), 2.20 (s, 3H), 2.13 – 2.07 (m, 1H), 1.94 (ddd, *J* = 13.7, 12.0, 4.1 Hz, 1H), 1.69 – 1.54 (m, 7H), 1.43 – 1.30 (m, 2H), 0.51 (s, 3H), 0.47 (s, 3H); ^{13}C NMR (125 MHz, $CDCl_3$) δ 168.1, 156.5, 144.7, 140.6, 137.6, 134.7, 129.0, 127.6, 120.7, 110.1, 104.5, 35.9, 35.9, 31.5, 28.8, 28.8, 28.0, 24.2, 20.8, 20.2, –2.6, –3.1; IR (cast film, cm^{-1}) 3069, 3048, 2942, 2860, 1761; HRMS (EI) calcd for $[M]^+$ $C_{24}H_{31}{}^{79}BrO_3Si$: 474.12259, found: 474.12284.

***Endo*-14-oxatetracyclo[9.2.1.0^{1},^{5}.0^{5},^{10}]tetradeca-9,12-dien-9-yl acetate (107)**

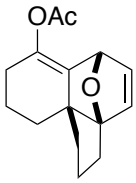

A dry, argon purged flask was charged with 80 mg of allylic silane **105** and 8 mL of acetonitrile (0.02M). To this solution was added TBAF (5 equiv, 1 M in THF) and the solution was stirred for 1 hour. The solution concentrated, and subjected to flash column chromatography (30:1, DCM: ethyl acetate). Using 80 mg of allylic silane **105**, and 870 μL of TBAF furnished 30 mg of cycloadduct **107** (67 % yield) as a clear, colorless oil.

R_f = 0.42 (19:1, DCM:ethyl acetate); ^{1}H NMR (500 MHz, $CDCl_3$) δ 6.45 (dd, *J* = 5.6, 1.8 Hz, 1H), 6.21 (d, *J* = 5.6 Hz, 1H), 5.22 (d, *J* = 1.5 Hz, 1H), 2.34 (ddd, *J* = 17.4, 5.2, 3.4 Hz, 1H), 2.17 (s, 3H), 2.16 – 1.83 (m, 8H), 1.73 (ddd, *J* = 12.5, 8.2, 3.1 Hz, 1H), 1.58 (app td, *J* = 11.7, 3.3 Hz, 1H), 0.51 (app dddd, *J* = 17.3, 11.6, 7.8, 1.6 Hz, 1H); ^{13}C NMR (125 MHz, $CDCl_3$) δ 169.2, 141.4, 136.7, 132.5, 131.5, 101.4, 77.9, 53.6, 33.4, 30.6, 26.5, 25.9, 23.5, 20.9, 20.8; IR (cast film, cm^{-1}) 2957, 2945, 2866, 1748; HRMS (EI) calcd for $[M]^+$ $C_{15}H_{18}O_3$: 246.12560, found: 246.12533.

***Endo*-15-oxatetracyclo[10.2.1.0^{1},^{6}.0^{6},^{11}]pentadeca-10,13-dien-10-yl acetate (110)**

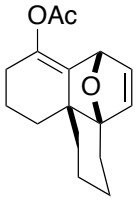

A dry, argon purged flask was charged with 177 mg of allylic silane **106** and 37 mL of acetonitrile (0.02 M). To this solution was added TBAF (5 equiv, 1 M in THF) and the solution was stirred for 1 hour. The solution was then concentrated, and subjected to flash column chromatography (column was run two times, 30:1, DCM:ethyl acetate). Using 177 mg of allylic silane **106**, and 1.49 mL of TBAF furnished 21 mg of cycloadduct **110** (21 % yield) as a clear, colorless oil.

R_f = 0.35 (19:1, DCM:ethyl acetate); ^{1}H NMR (500 MHz, $CDCl_3$) δ 6.40 (dd, *J* = 5.5, 2.0 Hz, 1H), 5.96 (d, *J* = 6.0 Hz, 1H), 5.23 (d, *J* = 1.5 Hz, 1H), 2.32 – 2.25 (m, 1H), 2.21 –

2.16 (m, 1H), 2.14 (s, 3H), 1.95 – 1.77 (m, 5 H), 1.73 (app dt, J = 13.6, 3.3 Hz, 1H), 1.68 – 1.59 (m, 4H), 1.46 – 1.37 (m, 1H), 0.57 – 0.51 (m, 1H); ^{13}C NMR (125 MHz, $CDCl_3$) δ 169.2, 139.5, 136.1, 135.4, 132.7, 90.8, 77.9, 43.0, 30.3, 27.9, 27.0, 25.1, 22.1, 22.1, 20.9, 19.8; IR (cast film, cm^{-1}) 3069, 3048, 2937, 2859, 1756, 1591; HRMS (ESI) calcd for $[M]^+$ $C_{16}H_{20}NaO_3$: 283.1305, found: 283.1300.

4.8. References

(1) Hughes, E. D.; Ingold, C. K. *J. Chem. Soc.* **1935**, 244.

(2) Moore, H. W.; Decker, O. H. *Chem. Rev.* **1986**, *86*, 821–830.

(3) Fernandez, M.; Hernandez, R.; Ramirez, A.; Ordonez, M. *Rev. Soc. Quim. Mex.* **2002,** *46*, 136–139.

(4) Perri, S. T.; Foland, L. D.; Decker, O. H.; Moore, H. W. *J. Org. Chem.* **1986**, *51*, 3067–3068.

(5) Moore, H. W.; Chow, K.; Nguyen, N. V. *J. Org. Chem.* **1987**, *52*, 2530–2537.

(6) Xiong, Y.; Xia, H.; Moore, H. W. *J. Org. Chem.* **1995**, *60*, 6460–6467.

(7) Xiong, Y.; Moore, H. W. *J. Org. Chem.* **1996**, *61*, 9168–9177.

(8) Hopf, H.; Berger, H.; Zimmermann, G.; Nüchter, U.; Jones, P. G.; Dix, I. *Angew. Chem. Int. Ed. Engl.* **1997**, *36*, 1187–1190.

(9) Brook, A. G. *Acc. Chem. Res.* **1974**, *7*, 77–84.

(10) Fernández-Zertuche, M.; Hernández-Lamoneda, R.; Ramírez-Solís, A. *J. Org. Chem.* **2000**, *65*, 5207–5211.

(11) Christl, M.; Schreck, M.; Fischer, T.; Rudolph, M.; Moigno, D.; Fischer, H.; Deuerlein, S.; Stalke, D. *Chem. Eur. J.* **2009**, *15*, 11256–11265.

(12) Daoust, K. J.; Hernandez, S. M.; Konrad, K. M.; Mackie, I. D.; Winstanley, J.; Johnson, R. P. *J. Org. Chem.* **2006**, *71*, 5708–5714.

(13) Brown, H. C.; Zweifel, G. *J. Am. Chem. Soc.* **1959**, *81*, 247–247.

(14) Compounds **72–79** were synthesized and characterized by Mr. Kyle McIntosh as part of a CHEM401/403 class.

(15) Christl, M.; Braun, M.; Müller, G. *Angew. Chem. Int. Ed. Engl.* **1992**, *31*,

473–476.

(16) Mr. Kyle McIntosh carried out this particular work as a CHEM401/403 project.

(17) Wittig, G.; Fritze, P. *Angew. Chem. Int. Ed.* **1966**, *5*, 846.

(18) Wittig, G.; Fritze, P. *Liebigs Ann. Chem.* **1968**, *711*, 82–87.

(19) Bottini, A. T.; Hilton, L. L.; Plott, J. *Tetrahedron* **1975**, *31*, 1997–2001.

(20) Christl, M.; Braun, M.; Fischer, H.; Groetsch, S.; Müller, G.; Leusser, D.; Deuerlein, S.; Stalke, D.; Arnone, M.; Engels, B. *Eur. J. Org. Chem.* **2006**, 5045–5058.

(21) Schlindwein, H.-J.; Himbert, G. *Chem. Ber.* **1989**, *122*, 2331–2339.

(22) Kurtz, P.; Gold, H.; Disselnkötter, H. *Justus Liebigs Ann. Chem.* **1959**, *624*, 1–25.

(23) Kozikowski, A. P.; Floyd, W. C.; Kuniak, M. P. *J. Chem. Soc., Chem. Commun.* **1977**, 582.

(24) Hayakawa, K.; Yamaguchi, Y.; Kanematsu, K. *Tetrahedron Lett.* **1985**, *26*, 2689–2692.

(25) Padwa, A.; Haffmanns, G.; Tomas, M. *Tetrahedron Lett.* **1983**, *24*, 4303–4306.

(26) Padwa, A.; Haffmanns, G.; Tomas, M. *J. Org. Chem.* **1984**, *49*, 3314–3322.

(27) Beesley, R. M.; Ingold, C. K.; Thorpe, J. F. *J. Chem. Soc., Trans.* **1915**, *107*, 1080–1106.

(28) **2002**, 1–36.

(29) Saulnier, M. G.; Kadow, J. F.; Tun, M. M.; Langley, D. R.; Vyas, D. M. *J. Am. Chem. Soc.* **1989**, *111*, 8320–8321.

(30) Choi, I.; Kim, Y.-K.; Min, D.-H.; Lee, S.; Yeo, W.-S. *J. Am. Chem. Soc.* **2011**, *133*, 16718–16721.

(31) Arena, G.; Cali, R.; Maccarone, E.; Passerini, A. *J. Chem. Soc., Perkin Trans. 2* **1993**, 1941–1945.

(32) Shepherd, R. G.; White, A. C. *J. Chem. Soc., Perkin Trans. 1* **1987**, 2153–2155.

(33) Beaulieu, P.; Ogilvie, W. W. *Tetrahedron Lett.* **2003**, *44*, 8883–8885.

(34) Kerr, W. J.; Morrison, A. J.; Pazicky, M.; Weber, T. *Org. Lett.* **2012**, *14*, 2250–2253.

(35) Naud, S.; Macnaughton, S. J.; Dyson, B. S.; Woollaston, D. J.; Dallimore, J. W. P.; Robertson, J. *Org. Biomol. Chem.* **2012**, *10*, 3506–3518.

(36) Föhlisch, B.; Herter, R. *Chem. Ber.* **1984**, *117*, 2580–2596.

(37) George, M. V.; Peterson, D. J.; Gilman, H. *J. Am. Chem. Soc.* **1960**, *82*, 403–406.

5. Efforts Toward the Synthesis of Asphaltene Model Compounds

5.1. Fossil Fuels and Asphaltenes

Oil sands and other more conventional fuel reserves are relied upon heavily to serve humankind's energy needs. On average, the international consumption of fossil fuels derived from these energy reserves reached 89.8 million barrels of oil every day in 2014 and is projected to continue rising.[1] Recovery and efficient utilization of the asphaltene component of bitumen has major implications for the world economy, as the more easily refined portions of bitumen reserves are pushed to the limit of current supply capabilities.

Refinement and consumption of the crude oil sands and bitumen requires the separation and upgrading of the hydrocarbons contained. The saturates, aromatics, resins, asphaltene (SARA) fractionation method (Figure 5.1), separates the heavy crude oil into saturated hydrocarbons (gasoline), smaller molecular weight aromatics (soluble aromatic compounds for upgrading and commercial retail), resins (soluble polar fractions), and asphaltenes.[2] The asphaltenes are removed from the easily refined fractions within the initial stages by the addition of aliphatic solvents to precipitate the most polar and largest molecular weight fractions. Differing compositions were obtained depending upon the solvent used and the volume of solvent used. Wang and coworkers found almost all asphaltene precipitated upon treating bitumen with a volume ratio of 30:1 or 40:1 of *n*-heptane to heavy oil.[3]

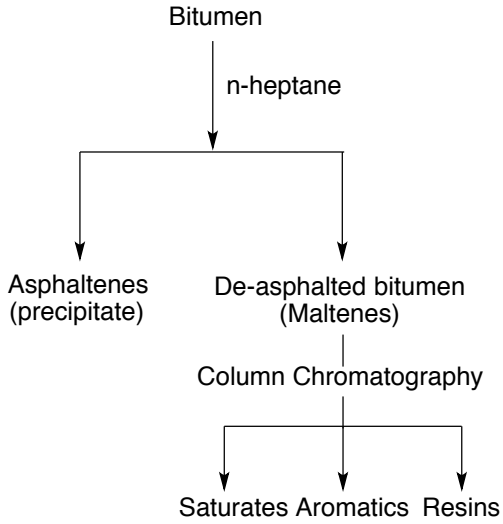

Figure 5.1 - SARA fractionation based upon solubility.

The precipitated asphaltenes have an extremely broad molecular diversity and no single compounds are in sufficient concentration to afford isolation and characterization. The molecular structure of a material determines the method by which the material can be upgraded (hydrogenated and cracked) and in turn determines the materials ultimate commercial value. Bulk asphaltene material has been characterized as having an average molecular weight of 750 – 1500 Da, and an atomic composition as shown in Table 5.1, with nickel, vanadium and other atoms making up smaller portions of the materials.[2,4]

Table 5.1 - Comparative atomic composition of Athabasca bitumen and asphaltene.[2]

	Carbon (%)	Hydrogen (%)	Nitrogen (%)	Oxygen (%)	Sulphur (%)
Bitumen	83.98	10.22	4.57	0.65	1.97
Asphaltene	81.31	7.88	7.53	1.06	2.79

The molecular architectures proposed for asphaltenes fitting the general physical characteristics described is a point of contention within the literature. Two factions disagree about the size and arrangement of the aromatic/aliphatic pieces of asphaltene structure, and it is not yet possible to characterize individual molecules of the asphaltene

mixture. Two models have been put forward, the continental model (**1**)[5] and the archipelago model (**2**)[6] (Figure 5.2).

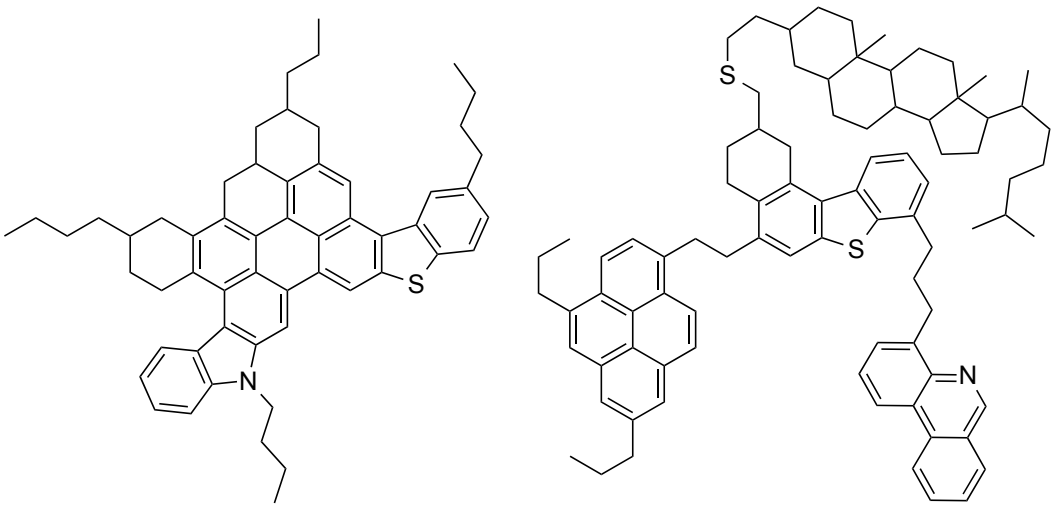

Figure 5.2 – Models of the continental (1) and archipelago (2) architectures.

The continental model (**1**) proposes that the structure of asphaltenes is comprised of large polycyclic aromatic molecules decorated on the periphery by aliphatic chains with heteroatoms dispersed throughout the structure. In contrast, the archipelago model (**2**) argues for the presence of small alkyl-decorated, aliphatic and aromatic polycyclic islands connected with saturated aliphatic linkers of varying length with heteroatoms dispersed throughout the molecules.

The limited solubility of asphaltenes is proposed to arise from intermolecular aggregation which in turn makes the refinement of the material difficult.[7] The different molecular structures present (polar functional groups, large polycyclic aromatics, and aliphatic chains) are suggested to form accumulative hydrophobic, hydrogen bonding interactions, π stacking, and polar intramolecular interactions creating supramolecular secondary, tertiary, and quaternary protein-like structures.[8] The stability of these aggregates is not attributed to any one of these interactions but more likely the sum of the intermolecular interactions.[2]

5.2. Asphaltene Model Compounds

Within the confines of such a complex mixture as bitumen and asphaltene, determining the individual molecular complexity and structure is a seemingly impossible feat. The nonrepeating structural diversity of asphaltenes has hampered efforts to understand the reasons behind their aggregation properties and in turn how to simplify the upgrading process.

Significant time and effort has been directed toward understanding the bulk asphaltene material.[2] Unfortunately, dependent upon the technique employed, and what physical feature of the material is being analyzed, different conclusions can be drawn.[9] The use of model compounds to calibrate specific techniques for bitumen/asphaltene samples has in part been impeded by the availability of appropriate calibration standards.

5.2.1. Previous Model Asphaltene Synthesis

Large polycyclic aromatic island synthesis has progressed significantly from the efforts of Müllen and coworkers applying Scholl aryl-aryl coupling conditions[10] (Scheme 5.1). Aryl-aryl bond formation under acidic oxidizing conditions as shown by Müllen's group demonstrates some of the upper boundaries of the synthetic technology, but also in the ability to make non-functionalized continental models.[11-15] However, the ability to obtain high quality spectral data for the largest continental compounds (**6**) was hampered due to the compound's limited solubility in organic solvents.

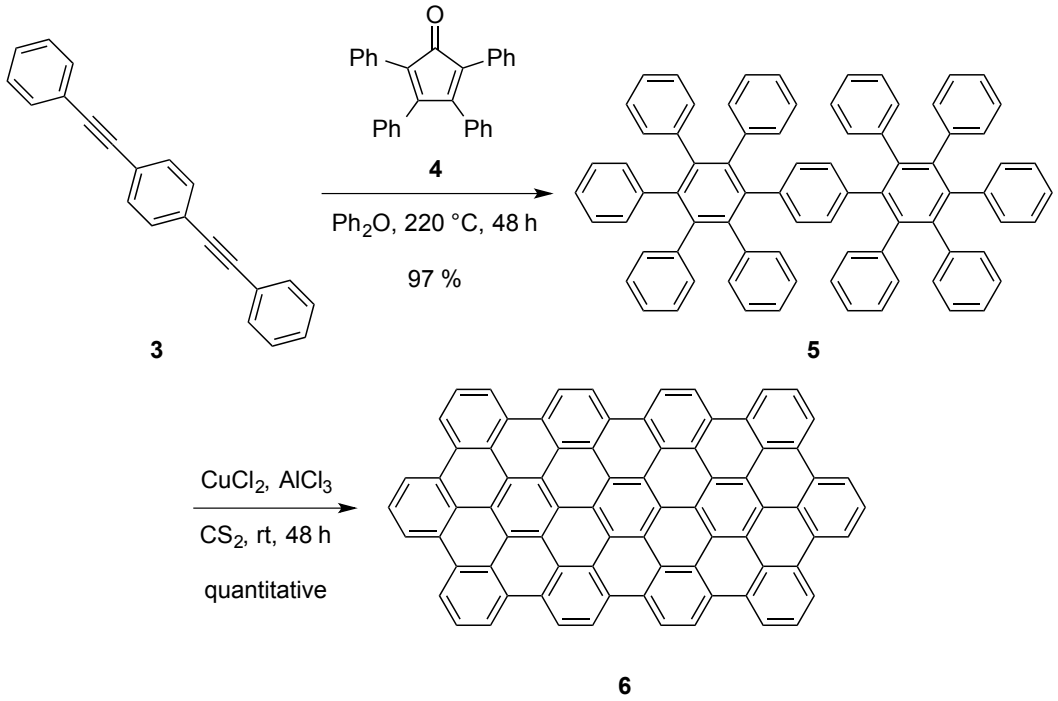

Scheme 5.1 - Synthesis of large polybenzenoid continental-like models.

Smaller, island-like, aliphatic-decorated, hexabenzocoronene structures were studied by Gray, Fenniri and coworkers to determine the propensity of the compounds to aggregate (Scheme 5.2).[16] Hexanesabenzocoronene derivatives decorated with long aliphatic chains were shown to form monomers, dimers and larger aggregates in toluene and *o*-dichlorobenzene using vapour-pressure osmometry. The dimers were shown to persist in *o*-dichlorobenzene even at 100 °C. In a similar manner to the strategy employed by Müllen, the coronenes were assembled by Lewis acid-mediated oxidative aryl-coupling.

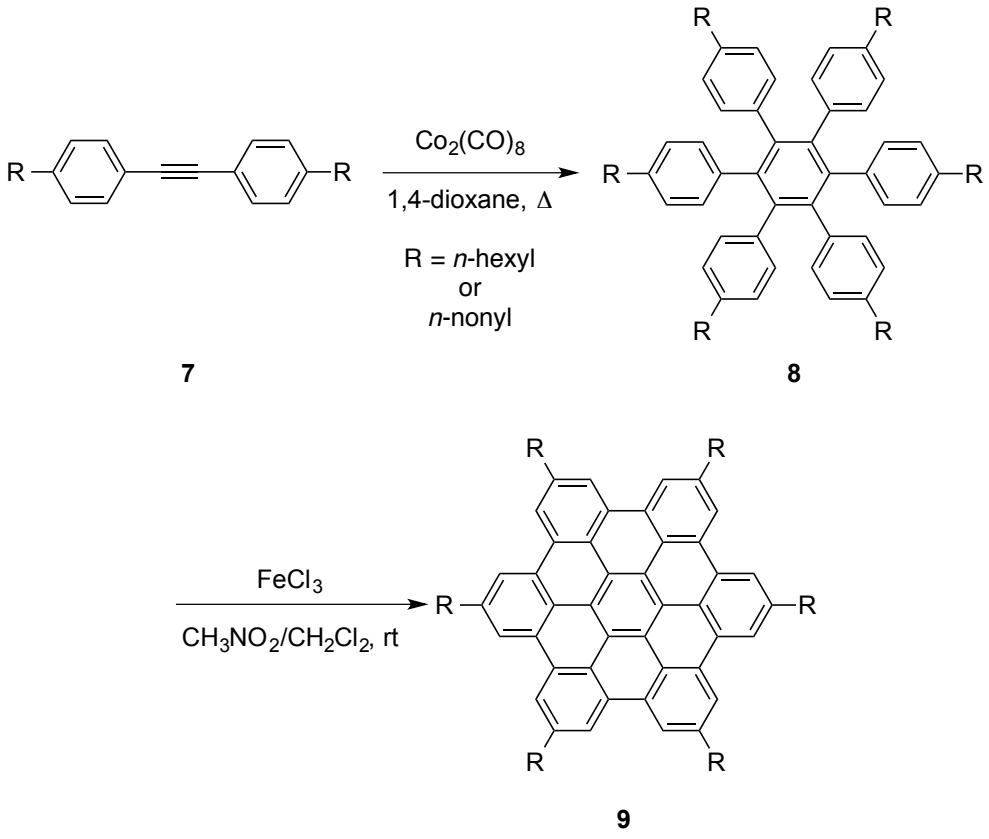

Scheme 5.2 - Synthesis of polyalkylated coronene continental models.

Mullins and coworkers have discussed the viability of the continental model in light of recent studies published on a comparison of the two models.[17] Mass spectrometry of the two types of model compounds showed significant fragmentation of the archipelago structures, not observed in natural asphaltene samples.[18] Using these unimolecular decomposition studies, NMR studies,[19,20] fluorescence measurements,[21,22] and the proficiency of the modified Yen model (single, aromatic island structures) to predict oil behavior,[23,24] Mullins and coworkers conclude that the major structural architecture of asphaltene is that of continental-like molecules rather than archipelago.

Archipelago model compounds have received significantly less attention in part due to the more complicated synthetic strategies required. Gray and coworkers have shown that simple two and three island structures can be synthesized in a linear strategy from halogenated aromatic compounds and Sonogashira coupling (Scheme 5.3).[25]

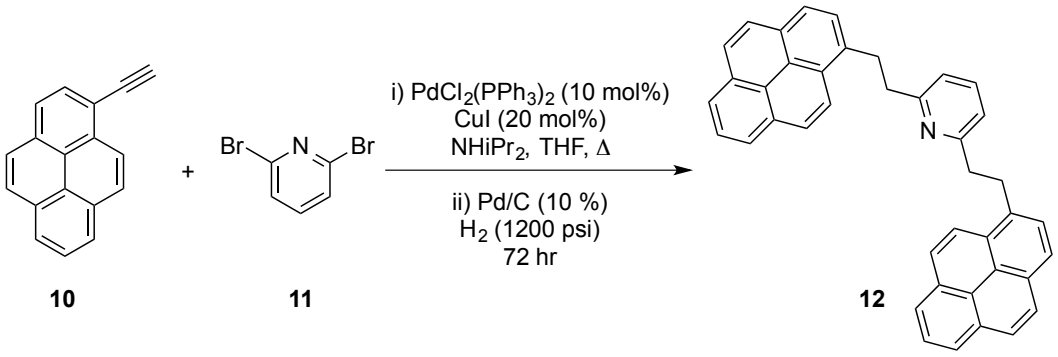

Scheme 5.3 - Synthesis of archipelago model compounds by Gray and coworkers.

Application of the linear Sonogashira strategy to a number of polycyclic aromatic hydrocarbon (PAH) terminal islands and heteroatom containing central islands has allowed the investigation of a number of archipelago architectures, by proton NMR,[26] thin film pyrolysis,[27] and mass spectrometry.[26] Gray found archipelago structures containing nitrogen have concentration dependent NMR spectra, attributed to persistent dimers, and oligomers.[28] These effects were not present in structures lacking a heteroatom substituent.

An important aspect of the study of asphaltenes that has not been addressed appropriately is the mass balance of the tests performed, tracking the material input and material output of the method employed. Gray and coworkers have recently disclosed the results of thermal cracking studies done with asphaltene model compounds **13 - 16** (Figure 5.3), finding during the process a number of addition products are formed from a proposed thermal radical processes.[29] This could be interpreted one of two ways: (1) the archipelago asphaltene structures are naturally occurring in crude asphaltenes or; (2) the \ archipelago structures proposed are produced during the industrial cracking process and not present in natural bitumen.

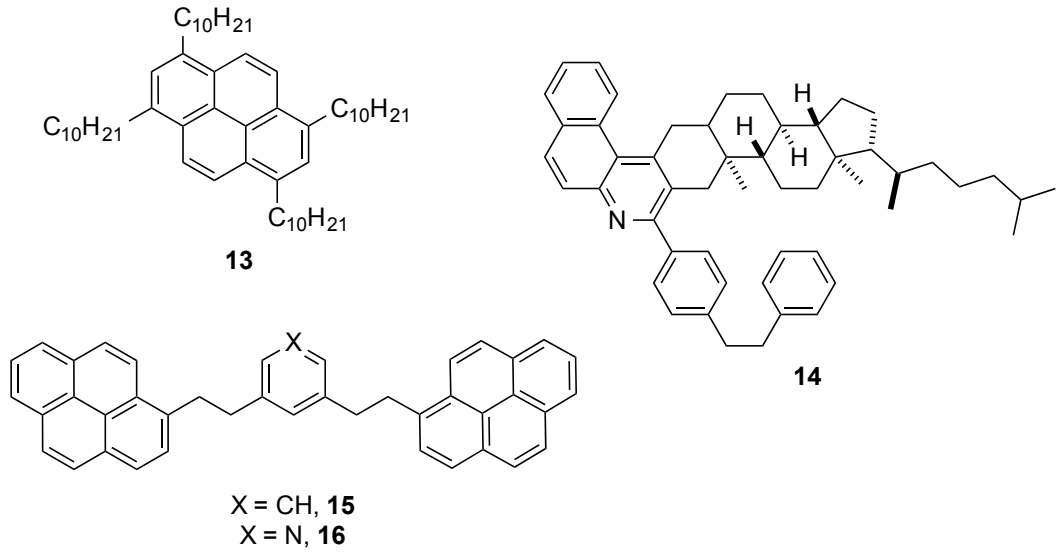

Figure 5.3 - Model asphaltene molecules subjected to thermal cracking.

Gray and coworkers reported access to a number of tetra-substituted pyrene-based archipelago structures relying upon the successive Kumada coupling of preformed Grignard reagents (Scheme 5.4).[30] Depending upon the order of bromination and subsequent Kumada coupling of the pyrene core, the strategy enabled access to a number of differently decorated pyrene derivatives.

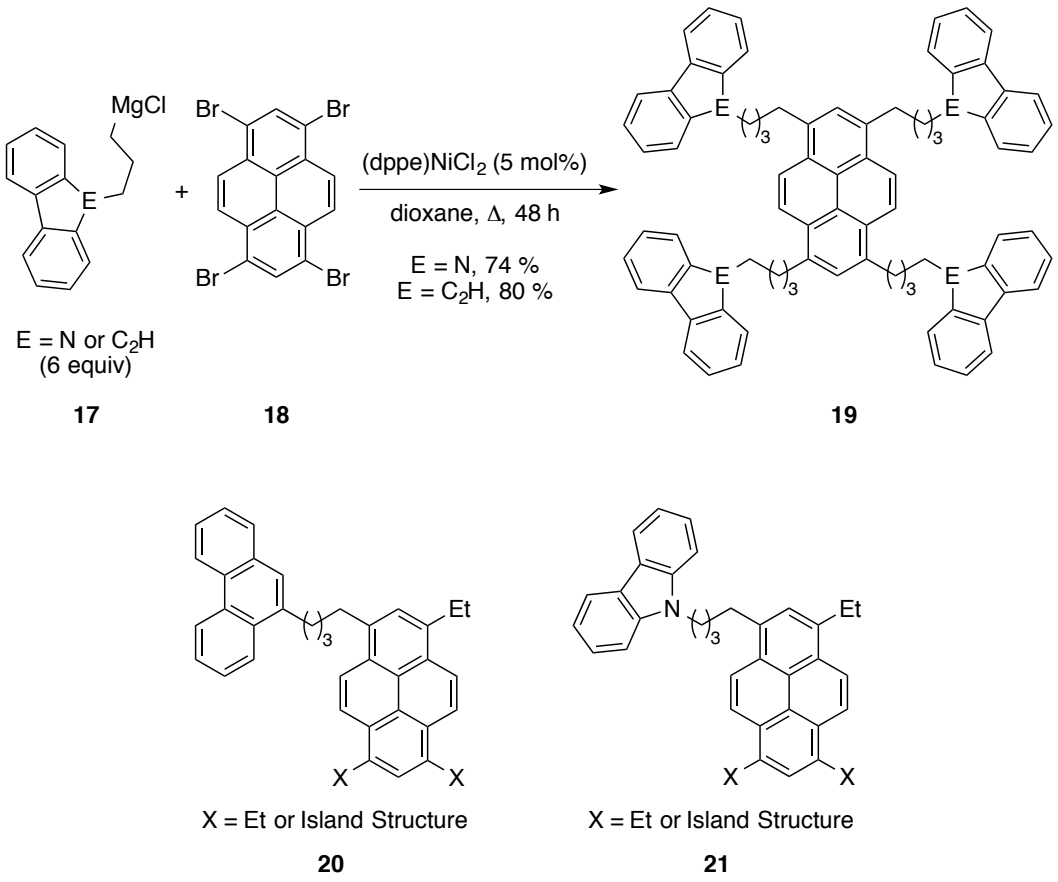

Scheme 5.4 - Archipelago model compounds with a pyrene core.

The availability of asphaltene model compounds with a variety of molecular architectures would enhance the understanding of asphaltene structure/aggregation dynamics. We focused on furthering the comprehension of intermolecular macromolecular association, insofar how the size of a molecule with few polar functionalities will aggregate strongly with other large non-polar molecules. The archipelago structures targeted (similar to those shown in Scheme 5.4) are poorly represented in the literature due to the difficulty in large molecules with few functionalized handles for retrosynthetic analysis. We hoped to develop a straightforward, scalable, short synthesis of a diverse number of three and four island structures with variable tether lengths to use as asphaltene model compounds. With the model compounds, a better understanding of the aggregative properties of large non-polar archipelago-like molecules would be possible by NMR spectral data analysis, mass spectrometry, and other techniques.

5.3. Results and Discussion

When constructing the archipelago model compounds it was important to plan for the inclusion of different central and terminals "islands", incorporation of different heteroatoms, and most importantly have the ability to have different tether lengths between islands. A family of compounds with different tether lengths will enable the study of solution phase dynamics as a function of the proximity of attached islands.

5.3.1. Strategy to Complex Archipelago Model Compounds

The synthetic route shown relies upon a transition metal-mediated [2+2+2] cycloaddition of alkynes and nitriles. Recent literature demonstrates that the construction of highly substituted heteroaromatics can be easily achieved via palladium, nickel, or cobalt catalysis.[31-35] Louie and coworkers have done exhaustive work developing the nickel catalyzed [2+2+2] reaction of tethered alkynes with activated and unactivated nitriles.[36] Using a cyclotrimerization to construct a nitrogen heterocycle would enable a convergent synthesis as shown in Figure 5.4.

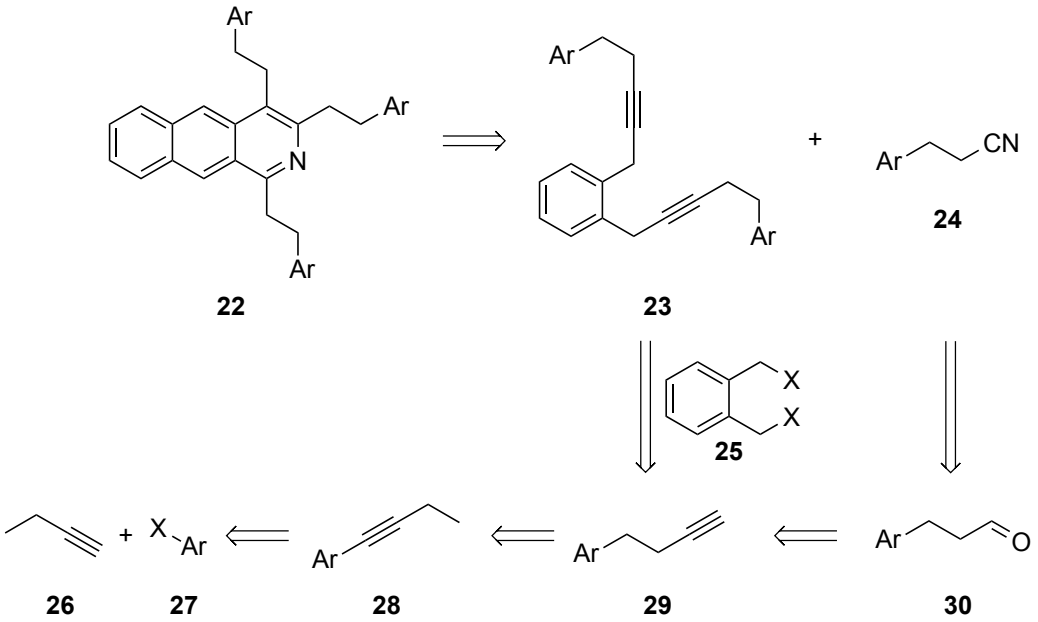

Figure 5.4 - Retrosynthesis of archipelago model compounds using a cyclotrimerization strategy (Ar here is different polycyclic aromatics; pyrene, phenanthrene, etc.).

To avoid mixtures of regiochemical cycloadducts in the cyclotrimerization step, the two alkynes would be tethered together as non-conjugated diyne (**23**) arising from the coupling of alkyne **29** with dihalogenated arene **25**. The alkynes were proposed to come from an alkyne-isomerization reaction (zipper reaction, **28** - **29**)[37] and could be derivatized to the desired nitriles as well.

5.3.2. Attempted Alkyne Zipper Reaction of Aryl Conjugated Alkynes

The anionic isomerization of an internal alkyne to a terminal alkyne has been applied in several scenarios,[37] but in particular the most interesting report is from the Hoye group.[38] Scheme 5.5 represents the only report of the zipper reaction being successfully applied to an internal alkyne conjugated with an aromatic ring.

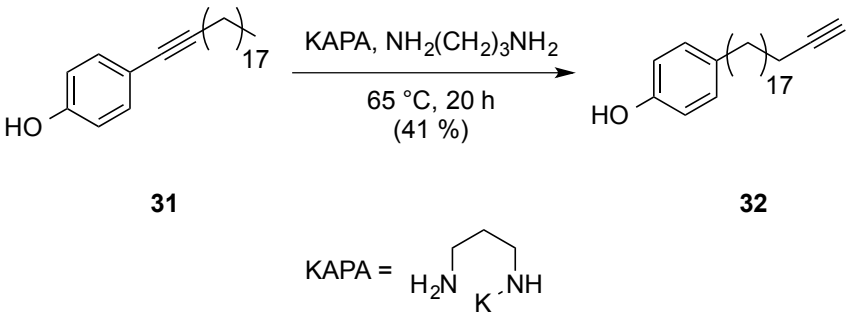

Scheme 5.5 - Application of the zipper reaction breaking conjugation from an aromatic ring.

When alkyne **33**[39] was subjected to various alkyne isomerization conditions no terminal alkynes were observed by analysis of the ^{1}H NMR spectra. The intractable mixtures were subjected to ^{1}H NMR spectroscopy in order to monitor the course of the reaction and numerous olefinic signals were observed. The predicted reaction mechanism as shown in Scheme 5.6 relies upon deprotonation of the allene **36** and subsequent protonation to form the one-carbon transposed alkyne **37**. Breaking the conjugation of the allene/alkyne with the aromatic system is a thermodynamically unfavourable process when considering the equilibrium between β-methylstyrene and allylbenzene favours the styrene by 5.6 kcal/mol,[40] which could prevent the chain walk of the alkyne.

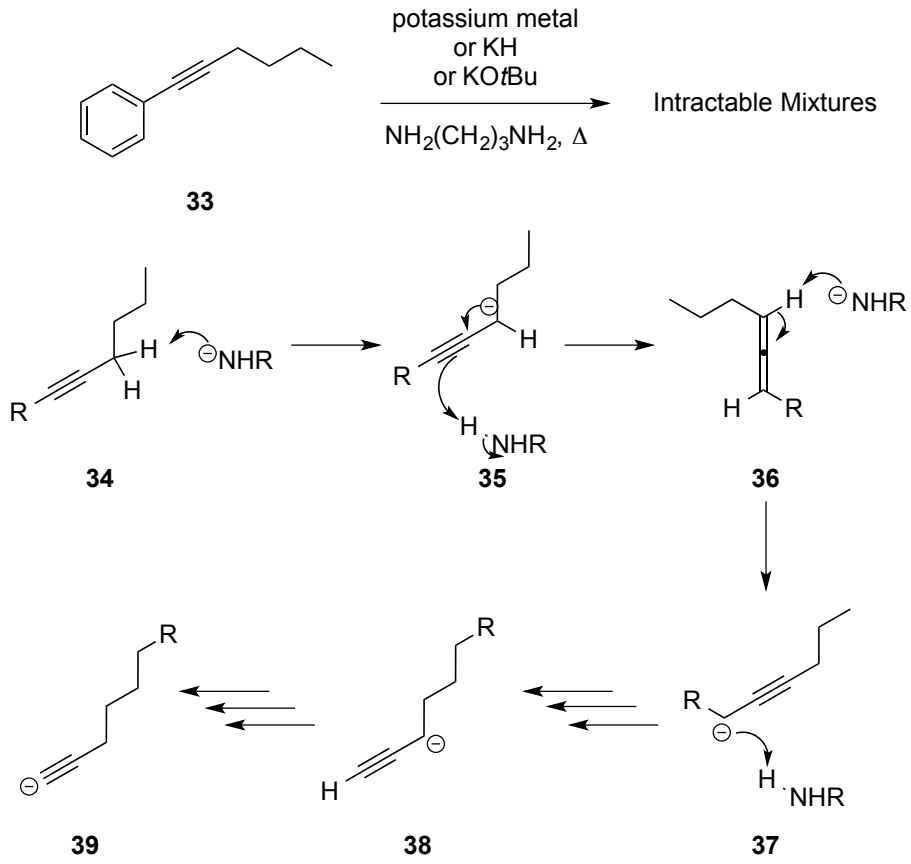

Scheme 5.6 - Proposed mechanism of the alkyne zipper reaction.

Failure to synthesize the desired terminal alkynes necessitated a revision of the synthetic strategy. At this time a communication from Colbon *et al.* reported the Heck-coupling/olefin isomerization of aryl bromides with non-conjugated enols to synthesize aryl-tethered aldehydes.[41] The Heck coupling/isomerization is a powerful strategy for incorporation of an aromatic group as well as an easily functionalized aldehyde.

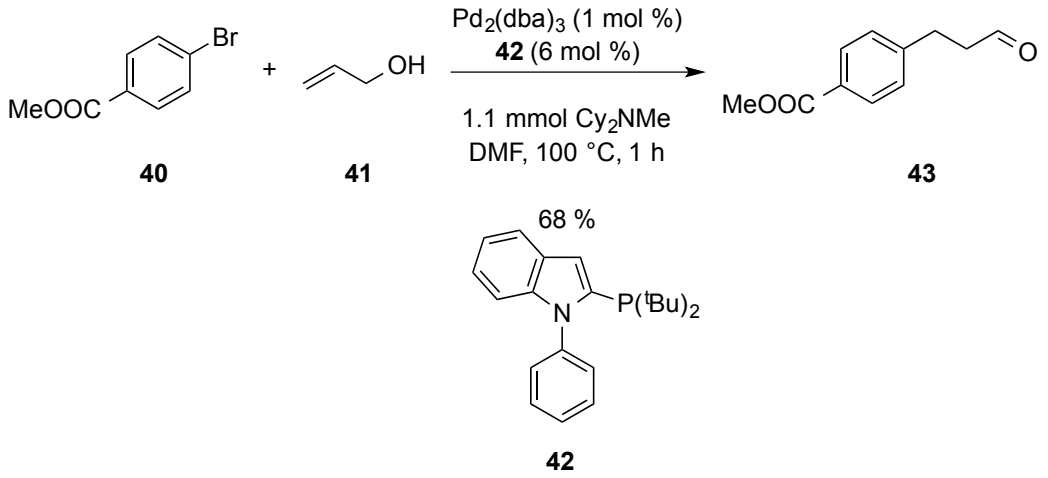

Scheme 5.7 - Heck coupling/olefin isomerization with aryl bromides.

Revision of the synthetic strategy incorporated the use of aryl-tethered aldehydes to act as the starting materials for both the tethered nitrile component (**24**) as well as the tethered alkyne (**29**) as shown in Scheme 5.8. The final model compounds would incorporate four island structures, three of which could be different. The ability to vary the tether length between islands would be easily achieved by varying the initial non-conjugated enol (**41**) used.

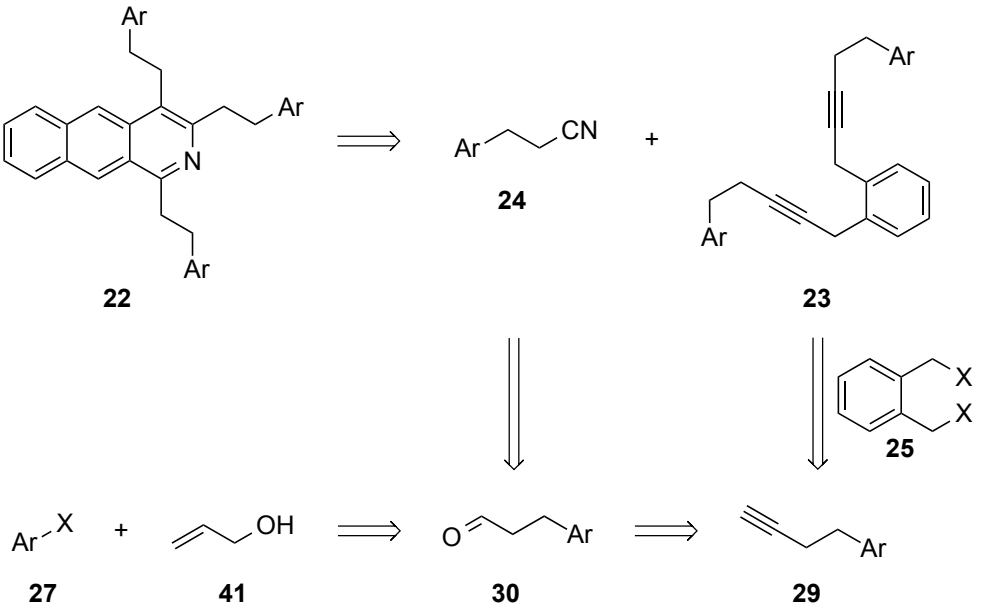

Scheme 5.8 - Revised retrosynthesis of archipelago model compounds.

5.3.3. Synthesis of Aryl-Tethered Aldehydes

Colbon's report relied upon expensive biaryl phosphine ligands to effect the Heck coupling/olefin isomerization under mild reaction conditions using aryl bromides. The prohibitive cost associated with the large-scale use of the ligands encouraged the search for more tenable reaction conditions. Historically, aryl iodides (while more difficult to synthesize) are more amenable to the Heck coupling/olefin isomerization reaction.[42] Specifically, a report from Jeffery shows an operationally simple and ligand-less palladium catalyzed reaction, providing excellent yields of tethered aldehydes even with electron poor aromatics.[43] Jeffery's reaction conditions were found to be the optimal reaction conditions (sodium bicarbonate as a base, palladium acetate, and tetrabutylammonium chloride as the phase transfer catalyst). Using these conditions a number of differently tethered phenanthrene and pyrene aldehydes were synthesized (Table 5.2).

Table 5.2 - Synthesis of family of tethered aryl aldehydes.

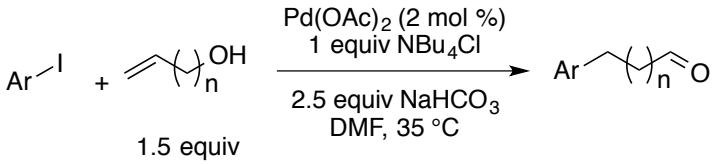

44 **45-47** **48-53**

Aryl – Iodide	n =	Alcohol	Aldehyde	Yield (%)[a]
Phenanthrene	1	**45**	**48**	84
Phenanthrene	2	**46**	**49**	74
Phenanthrene	3	**47**	**50**	37
Pyrene	1	**45**	**51**	85
Pyrene	2	**46**	**52**	77
Pyrene	3	**47**	**53**	73

[a] Yields are of purified compounds.

Consistent with the results of Larock,[44] Heck,[45] and Jeffery[43] the choice of phase transfer catalyst, and base is very important for the reaction. Amatore found that in the presence of chloride anions, the oxidative addition of iodobenzene to palladium occurs faster through a proposed anionic, chloride-ligated palladium species.[46] Hartwig found

similar effects studying the oxidative addition of aryl sulfonates in the presence of anionic additives.[47]

In addition to the longer reaction time required in the in the case of 4-penten-1-ol (**47**), another aldehyde product was observed. This is consistent with the observations of Larock and coworkers.[44] Depending upon the regiochemistry of the initial migratory insertion event into the olefin (either formation of **III** or **V**), there are theoretically two regioisomeric aldehydes that can result (Figure 5.5), easily distinguishable by the number of methylene groups present. The isomeric aldehyde was not isolated but comparing the integration of formyl group protons in the crude NMR spectrum the aldehydes were isolated in a 10:1 mixture of isomers.

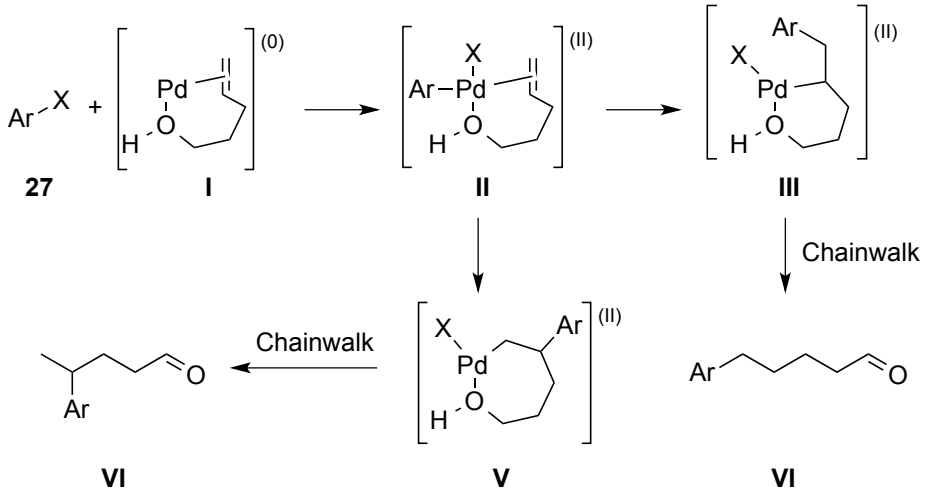

Figure 5.5 - Formation of isomeric aldehydes when pentenol 47 is used in aldehyde synthesis.

5.3.4. Synthesis of the Tethered Alkynes

With the tethered aldehydes in hand the homologation of the aldehydes to the terminal alkynes was investigated. There were two different methods considered for the homologation reaction, the Corey-Fuchs reaction[48] or the Gilbert-Seyferth/Bestmann-Ohira homologation.[49,50] Whilst the Corey-Fuchs reaction can be performed using reagents that are commonly available in a synthetic chemistry laboratory, it is a two-step process complicated by the removal of triphenyl phosphine oxide during synthesis of the 1,1-dibromoolefin, and the use of excess *n*-butyl lithium for the Fritsch-Buttenberg-Wiechell rearrangement.[51-53]

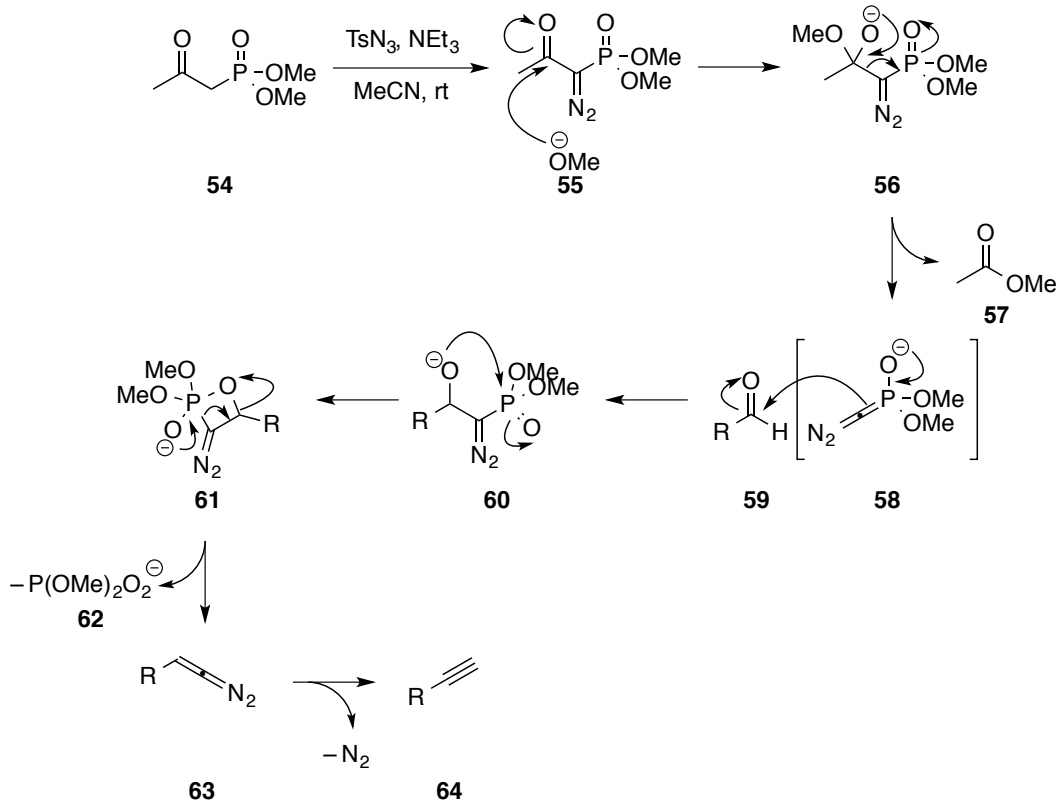

Figure 5.6 – Aldehyde-alkyne homologation using the Bestmann-Ohira reagent (55).

Using the Bestmann-Ohira reagent for alkyne synthesis is a single step transformation under mild reaction conditions (Figure 5.6). Unfortunately the synthesis of (1-diazo-2-oxo-propyl)-phosphonic acid dimethyl ester (55) is not trivial and the reagent is prohibitively expensive. More recently, the one-pot diazo transfer/homologation was reported, in which diazo **55** is generated *in situ*.[54] Initially, subjecting the aldehydes to diazo **55** generated *in situ* failed to provide satisfactory yields; this is assumed to be a direct result of the *p*-toluenesulfonylamine present in the reaction mixture. Subjecting the aldehydes **48**, **50**, and **51** to basic methanol in the presence of 1.5 equivalents of previously isolated diazo **55** furnished terminal alkynes **65** – **67** in good to excellent yields (Table 5.3).

Table 5.3 - Synthesis of tethered alkynes via the Bestmann-Ohira reaction.

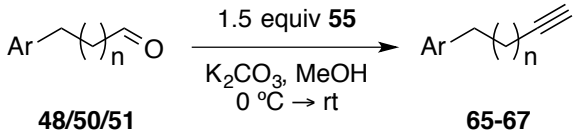

48/50/51 65-67

Aryl Aldehyde	n =	Alkyne	Yield (%)[a]
Phenanthrene (**48**)	1	**65**	75
Phenanthrene (**50**)	3	**66**	80
Pyrene (**51**)	1	**67**	93

[a] Yields are of purified compounds.

Interestingly, the aldehyde failed to dissolve in methanol at the outset of the reaction; only over several hours did the suspension become homogeneous. Hoping to mitigate the solubility problem and facilitate shorter reaction times the reaction was performed in anhydrous ethanol. Initial inspection of the crude reaction mixture showed a significantly more complicated mixture of products when compared to running the reaction in methanol. Given the difficulties using ethanol as a solvent the previous reaction conditions were employed further.

5.3.5. Synthesis of Tethered Nitriles

Tethered aldehydes **48** – **53** also act as the starting material for the tethered nitriles. Traditionally, attempted condensation of aldoximes results in the formation of amides via a Beckmann rearrangement.[55] Several methods have been developed to aid in the second condensation step, avoiding the formation of the amide side product (Scheme 5.9). The simplicity of the microwave protocol encouraged the application of Chakraborti's method to the synthesis of the desired nitriles.[56]

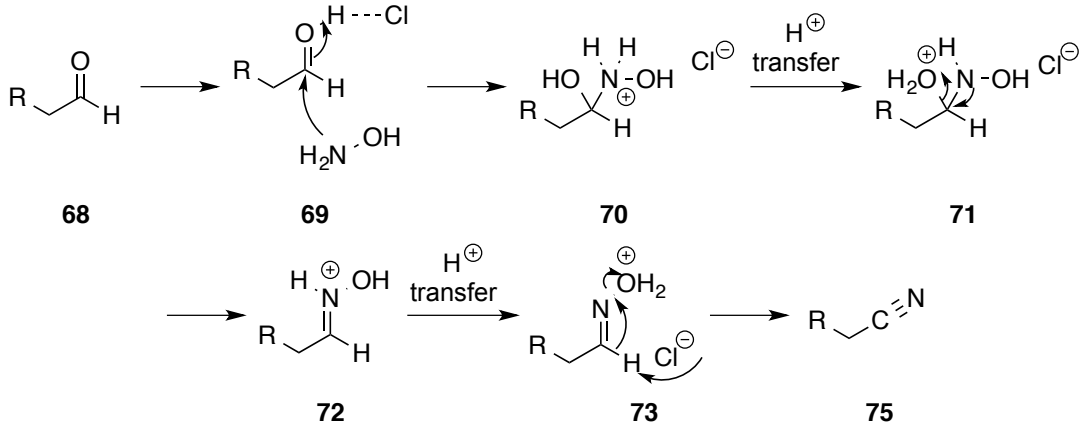

Scheme 5.9 - Beckmann fragmentation to furnish nitriles from aldehydes.

Subjecting the tethered aldehydes to N-hydroxylamine hydrochloride in N-methylpyrrolidinone (NMP) under microwave irradiation provided the desired nitriles in moderate yields (Table 5.4). The reaction with pyrene-tethered aldehydes gave lower yields that were attributed to the difference in solubility of the different aromatic islands in NMP. Increasing the amount of solvent used did not adversely affect the reaction, although a homogeneous solution was not attained until after the reaction mixture had been heated in the microwave reactor.

Table 5.4 - Synthesis of tethered nitriles.

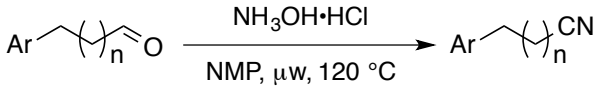

48-53 **76-81**

Aryl Aldehyde	n =	Nitrile	Yield (%)[a]
Phenanthrene (**48**)	1	**76**	79
Phenanthrene (**49**)	2	**77**	90
Phenanthrene (**50**)	3	**78**	80
Pyrene (**51**)	1	**79**	85
Pyrene (**52**)	2	**80**	58
Pyrene (**53**)	3	**81**	39

[a] Yields are based on purified products.

As the length of the tether increased the yield dropped off dramatically. Inspection of the crude reaction mixture by TLC analysis and ^{1}H NMR spectral data showed incomplete consumption of the starting material in the case of the pyrene-tethered aldehydes. Resealing the microwave tube and subjecting it to further irradiation did not result in further conversion. Due to the time constraints on this project the procedure was never optimized for the latter substrates, although the starting aldehydes could be recovered from the reaction mixture.

5.3.6. Synthesis of 1,2-Dipropargylic Arenes

Benzylic alkynes are not trivial substrates to synthesize. Given the stability gained from conjugating with an aromatic ring[40] and the increased acidity of the benzylic protons with the electron withdrawing alkyne attached the products have been observed to readily decompose.[57] If the benzylic proton is deprotonated the alkyne can isomerize to the aryl conjugated allene. For the synthesis of the model asphaltene compounds proposed previously (Scheme 5.8), two benzylic alkynes would have to be installed on the same aromatic ring adjacent to one another.

5.3.6.1. 1,2-Dipropargylic Arenes by Nucleophilic Substitution

Takahashi and coworkers have reported that simple lithium acetylides can be added to a low temperature THF/DMPU solution of 1,2-bis(bromomethyl)benzene, furnishing the benzylic acetylene compounds in good yields (Scheme 5.10).[58] This is contrary to the findings of Brandsma, who reported that 4-substituted-butyne derivatives were poor nucleophiles for benzylic substitution reactions because the products could decompose under strongly basic conditions.[59] With more demanding substrates the addition of catalytic copper chloride to a solution of the metallated acetylides was found to facilitate formation of the 1,2-dipropargylic arenes (**89**) in good yields (Scheme 5.10).

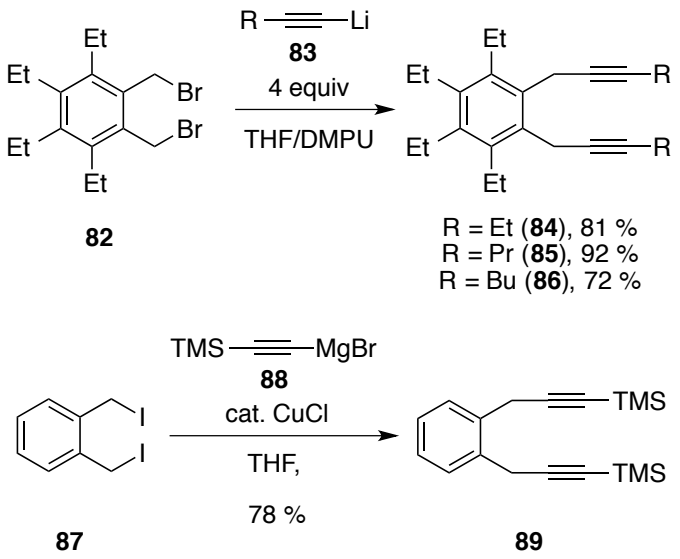

Scheme 5.10 - 1,2-Dipropargylic arenes by nucleophilic substitution.

The conditions of Takahashi and coworkers were applied to the synthesis of 1,2-dipropargylic arenes using 1,2-(bisbromomethyl)benzene (**91**) and metallated 4-phenyl-1-butyne (**90**). This gave an inseparable mixture of the starting alkyne and the wanted arene (**92**). Decreasing the number of equivalents of acetylide to sub-stoichiometric quantities increased the yield of dialkyne **92** though the material was still contaminated with 4-phenyl-1-butyne (Scheme 5.11). In addition to the problems with purifying the product, the transformation proved difficult to reproduce, with poor, and variable yields (ranging from 0 – 30 %).

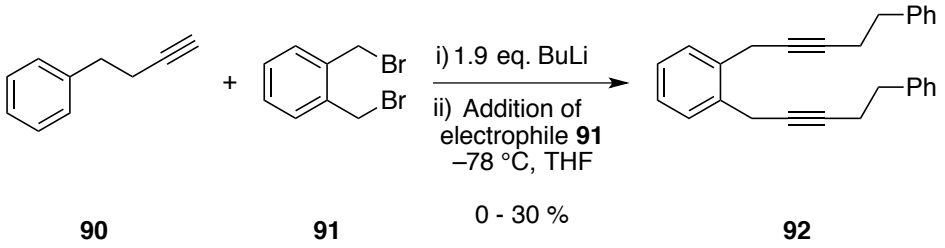

Scheme 5.11 - Synthesis of starting 1,2-dipropargylic arenes by nucleophlic substitution.

This impure material that was obtained was carried through to attempt the cyclotrimerization with tethered nitriles. In 2008 Alexander Deiter's group reported the synthesis of substituted benzoisoquinolines using microwave irradiation and a cobalt

catalyst.[60] As the benzyl alkynes synthesized most closely resemble Deiter's substrates, these reaction conditions were applied. Impure 1,2-dipropargylic arene **92** was mixed with ten equivalents of adiponitrile (**93**), and one equivalent of cyclopentadienylcobalt (I) biscarbonyl (**94**) in toluene and subjected to microwave irradiation. From the complex mixture, benzo[g]isoquinoline **95** was tentatively isolated (Scheme 5.12). Isoquinoline **95** contains a nitrile group not usually associated with asphaltene structures; however, this was included with the hopes of hydrolyzing the nitrile to a carboxylic acid. Further efforts toward replicating the experiment and making derivatives led only to intractable mixtures.

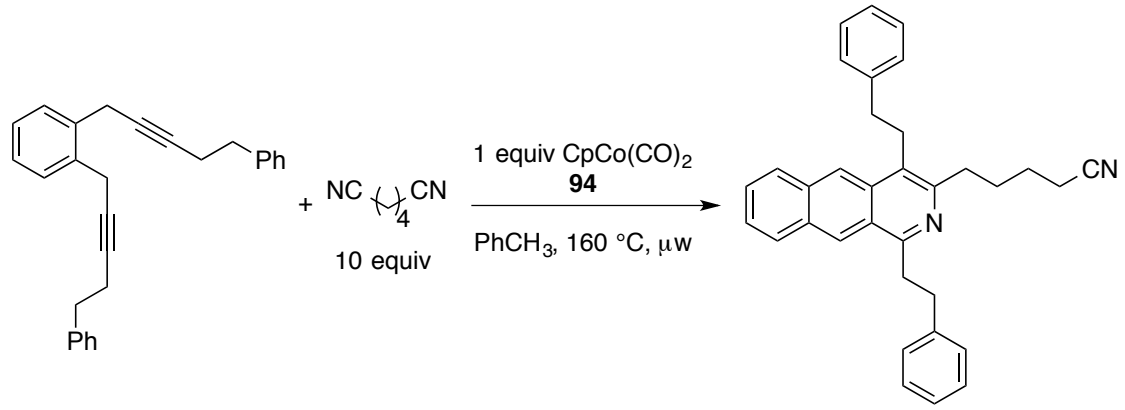

92 **93** **95**

Scheme 5.12 - Cyclotrimerization of the 1,2-dipropargylic arene with adiponitrile.

When this protocol was applied to the pyrene-linked alkyne **96**, the addition of *n*-butyllithium to a solution of the alkyne furnished a deep blue solution (Scheme 5.13). The blue color is consistent with the observations of Müllen and coworkers when characterizing the alkali metal reduction of pyrene and derivatives.[61] Quenching the reaction and workup resulted in recovery of the starting alkyne **96**. The lithiation and derivatization of the more complex polycyclic aromatic alkynes was not possible by this method.

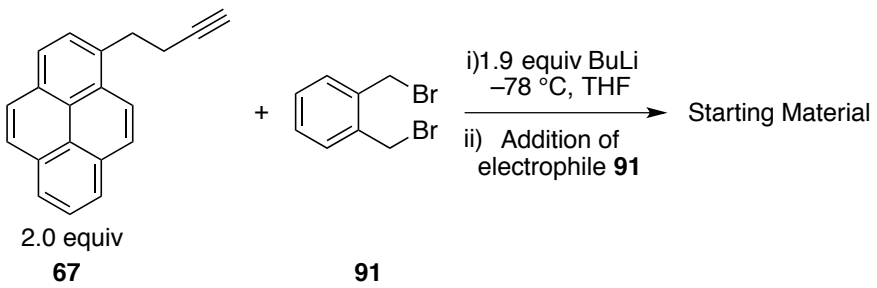

Scheme 5.13 - Attempted alkynylation using pyrene-linked acetylene.

Copper-catalyzed benzylic coupling of the alkyne is also reported on these substrates as in the coupling of trimethylsilylacetylene magnesium bromide with *o*-bis(bromomethyl)benzene to furnish the 1,2-dipropargylic derivative **89** (Scheme 5.10).[62] Initial application of the benzylic Castro-Stevens-like coupling to 4-(9-phenanthryl)-1-butyne coupling with *o*-bis(bromomethyl)benzene generated a yellow precipitate, completely insoluble in all solvents. Washing the solid with a saturated aqueous solution of ammonium chloride, the solid changed from a bright yellow solid, to a chalky, white solid. Similarly, 4-(1-pyrenyl)-1-butyne under the analogous reaction conditions furnished a similar yellow precipitate displaying no solubility in organic solvents (Scheme 5.14).

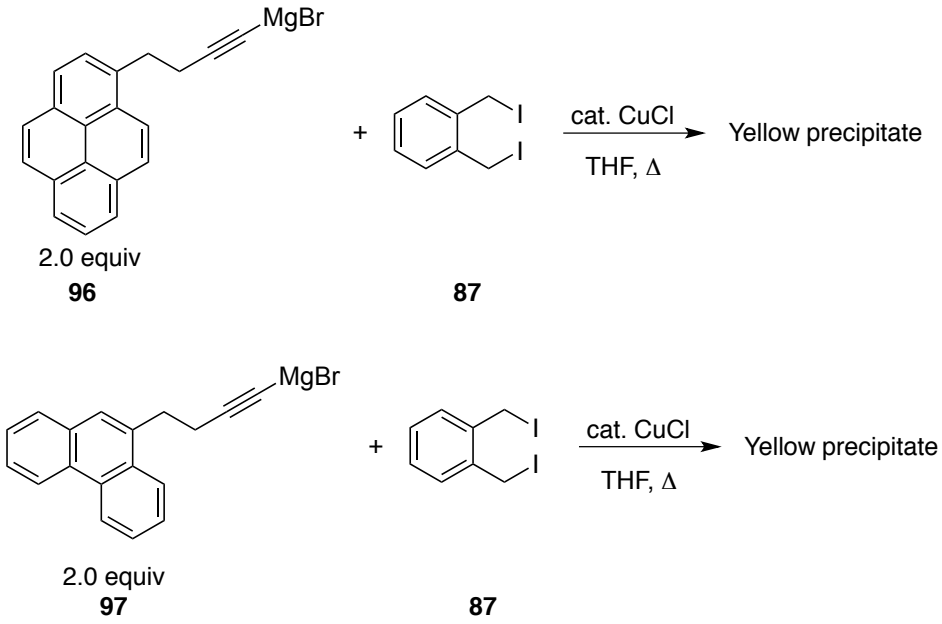

Scheme 5.14 – Use of catalytic copper in synthesis of 1,2-dipropargylic arenes.

In the absence of further characterization, the solid obtained from the reaction with phenanthrene was subjected to [2+2+2] cyclotrimerization with different nitriles under the cyclotrimerization conditions reported by Deiters. Microwave irradiation of the yellow precipitate in the presence of ten eqivalents of 5-(9-phenanthryl)-1-pentanenitrile gave a complex mixture of products. Both ^{1}H NMR spectral data and mass spectrometry of partially purified fractions suggested the product was present; however, the sample contained severe contamination by diethyl phthalates that could not be removed by further chromatography. Due to the scale (less than 1 mg recovered) and contamination, further purification and characterization was abandoned.

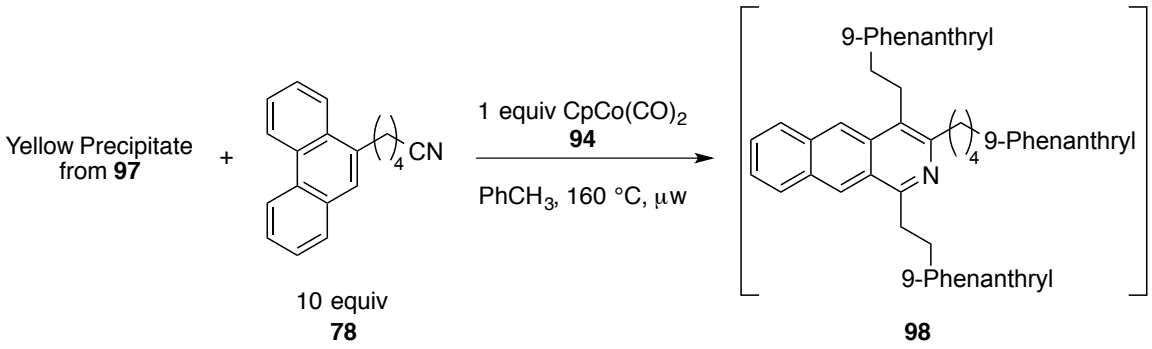

Scheme 5.15 - Use of non-characterized yellow precipitate in cyclotrimerization chemistry.

5.3.6.2. Palladium-Catalyzed Benzyl-Alkynylation

Upon further consideration of a compatible method of generating the 1,2-dipropargylic arenes, we noted that Buchwald *et al.* described a palladium-catalyzed method whereby careful choice of ligand (XPhos) and base (Cs_2CO_3, 1.1 equiv.) furnished the sought benzylic alkynes in good to excellent yields from the benzylic chlorides and terminal alkynes (Scheme 5.16).[63] If the conditions were changed slightly by using acetonitrile as the solvent and increasing the number of equivalents of base the researchers reported the efficient coupling to give the allene in good to excellent yields. Though there are many reports of palladium being used to generate a benzyl-alkyne bond, Buchwald's procedure did not require the synthesis or preformation of an organometallic reagent,[64,65] an alkynoic ester,[66] or a carboxylic acid[67] prior to the reaction.

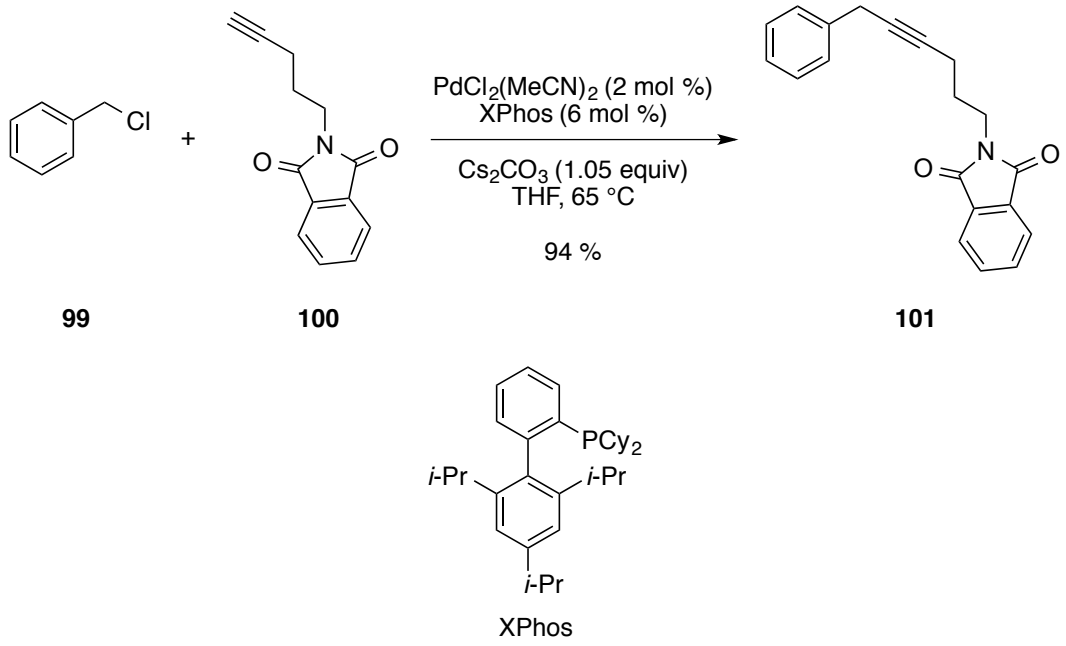

99 **100** **101** **102**

Scheme 5.16 - Buchwald coupling to synthesize propargylic arenes.

In the event, of Buchwald's palladium-catalyzed benzylic Heck alkynylation proved to be unsuitable for generating the desired product. Inspection of the crude reaction mixture showed no consumption of either starting material (Scheme 5.17). Most likely the presence of two benzyl chloride functionalities adjacent on the benzene ring caused decomposition of the palladium catalyst.

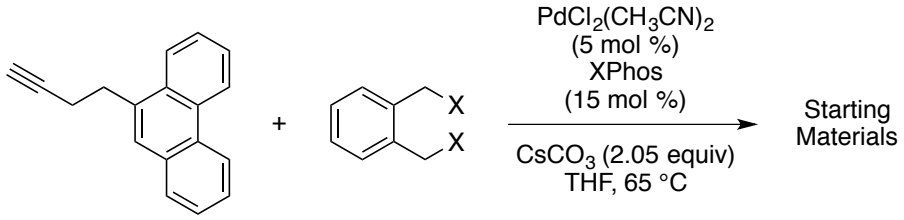

65 X = Cl **103**
X = Br, **91**

Scheme 5.17 - Attempted Heck alkynylation using Buchwald's optimized conditions.

5.3.6.3. Cobalt-Catalyzed Benzyl-Alkynylation

Following the attempts to use palladium and copper we turned to a report from Tunge and coworkers who reported the benzylic coupling of magnesium acetylides with

simple cobalt salts.[68] Trimethylsilyl acetylide as well as hexynal acetylide were shown to couple efficiently with a number of different electronically demanding benzylic chlorides and benzyl bromide. The alkyl acetylides failed to give satisfactory yields with any of the benzylic chlorides but a modest 70 % yield was obtained with benzyl bromide. Most notable about Tunge's report is the formation of the 1,2-dipropargylic arenes **89** (Scheme 5.18), very similar to the substrates targeted by our group.

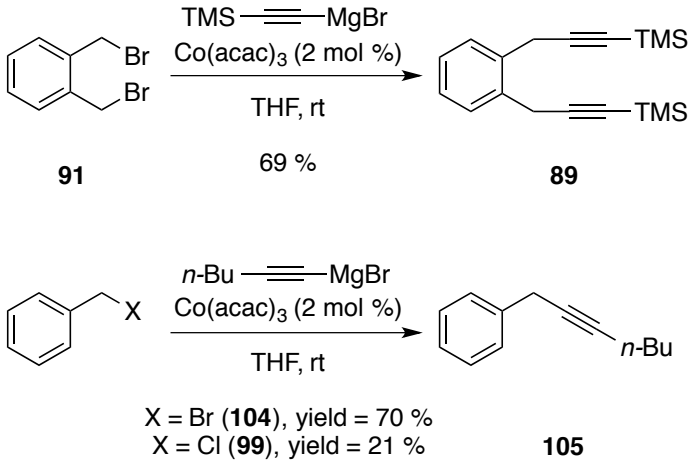

Scheme 5.18 - Cobalt-catalyzed nucleophilic benzylic alkynylation.

Application of cobalt-catalyzed nucleophilic benzylic substitution with metallated alkynes was attempted using 4-phenyl-1-butyne (Scheme 5.19). Following column chromatography, inspection of the ^{1}H NMR spectral analysis showed a complicated mixture of nonpolar compounds with multiple olefin signals. Portion-wise addition of the Grignard reagent did not change the complex mixture obtained, therefore the reaction was abandoned.

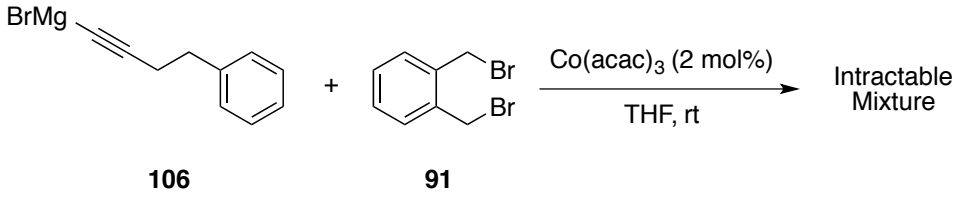

Scheme 5.19 - Attempt at using Co(acac)$_3$ as a nucleophilic catalyst.

Other methods that relied upon Brønsted acids[69] and DDQ oxidation[70] exist, however were not explored due to the limited substrate scopes reported. This is the

extent of the study that could be completed as a change of focus took place within my research, which was discussed within the previous chapters.

5.4. Conclusions

Given the difficulties encountered synthesizing the 1,2-dipropargylic arenes the synthesis of a library of archipelago model compounds could not be completed. The use of transition metal-catalyzed Heck olefination/Larock isomerization did allow the facile synthesis of a number of aryl-tethered aldehydes with variable tether lengths, which could subsequently be transformed into the desired nitriles and alkynes in a single step.

5.5. Alternative Strategies

In retrospect, the highly functionalized scaffolds that were the basis of the strategy were fragile and incompatible with the scale or efficiency demanded in further reactions. One final strategy is then offered, this time relying upon more robust intermediates. Selenium esters **100** are accessible from the previously synthesized tethered aldehydes. These esters would be used in the radical acylation of pyridazine to give diketone **102** (or aldol product **103**). The key to the success of this strategy is the retro-aldol/condensation reaction with terminal amine **104**. If this were to work, the synthesis could then be completed with a Diels-Alder/retro-Diels-Alder reaction with benzopyridazine **105** to give the highly substituted, unsymmetrical, four-island model compound **107**.[71] Further development of the radical acylation of the pyridazine scaffold would be required; however, it would enable a significant library of model compounds to be synthesized.

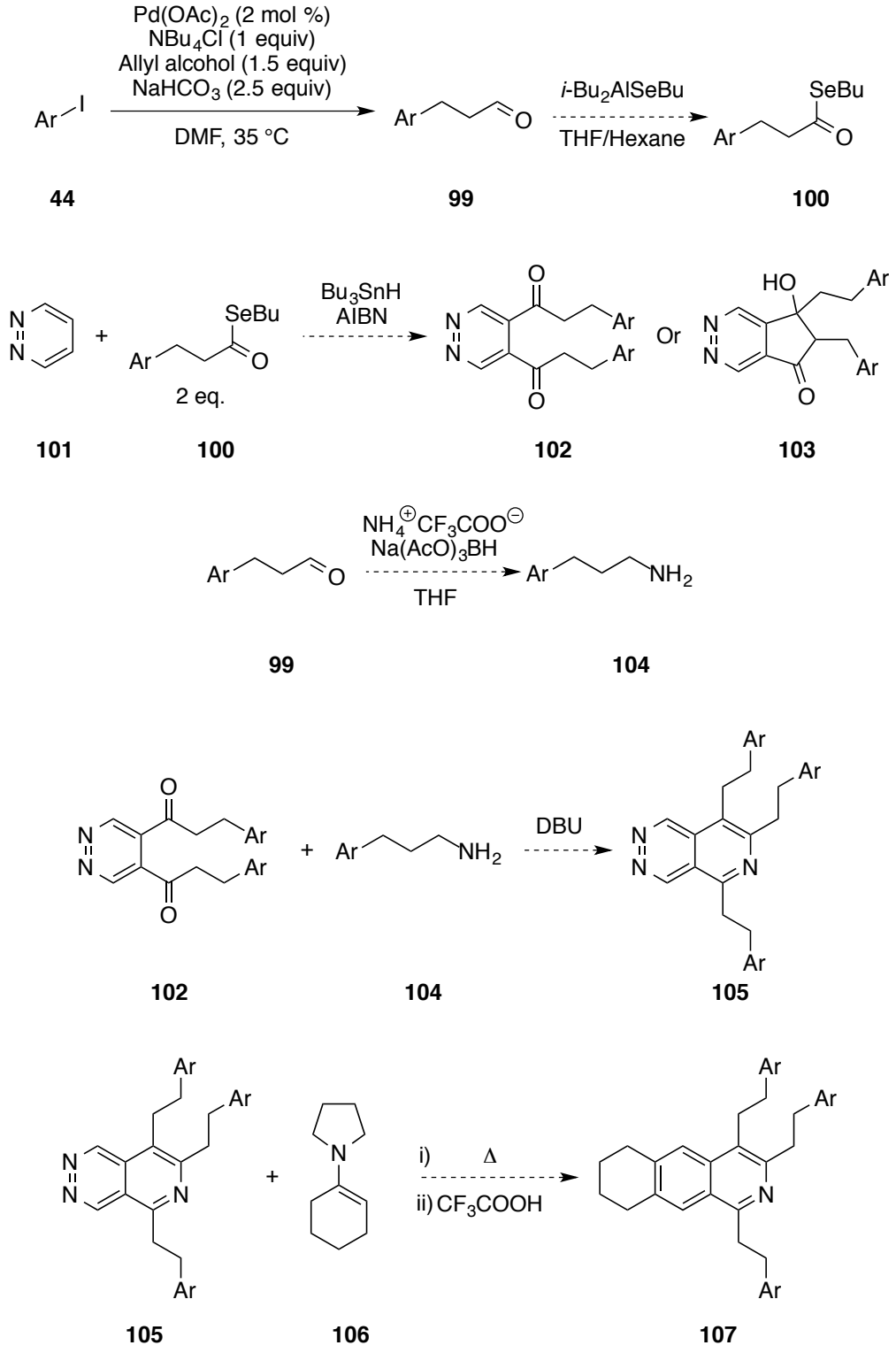

Scheme 5.20 - Revised synthetic strategy to four island archipelagos.[72-75]

5.6. Experimental

5.6.1. General Information

Reactions were carried out in oven (120 °C) or flame-dried glassware under a positive argon atmosphere unless otherwise stated. Transfer of anhydrous reagents was accomplished with oven-dried syringes or cannulae. Solvents were distilled before use: acetonitrile (CH_3CN), triethylamine (NEt_3), and dichloromethane (CH_2Cl_2) from calcium hydride, diethyl ether (Et_2O), and tetrahydrofuran (THF) from sodium/benzophenone, toluene, and benzene (C_6H_6) from sodium metal. Thin layer chromatography was performed on glass plates pre-coated with 0.25 mm Kieselgel 60 F254 (Merck). Flash chromatography columns were packed with 230-400 mesh silica gel (Silicycle). Proton nuclear magnetic resonance spectra (^{1}H NMR) were recorded at 300 MHz, 400 MHz, or 500 MHz and coupling constants (*J*) are reported in Hertz (Hz). Carbon nuclear magnetic resonance spectra (^{13}C NMR) were recorded at 100 MHz or 125 MHz. The chemical shifts are reported on the δ scale (ppm) and referenced to the residual solvent peaks: $CDCl_3$ (7.26 ppm, ^{1}H; 77.06 ppm, ^{13}C) as internal standards. Standard notation is used to describe the multiplicity of the signals observed in ^{1}H NMR spectra: broad (br), apparent (app), multiplet (m), singlet (s), doublet (d), triplet (t), quartet (q), pentet (p), etc. Infrared (IR) spectra were measured with a Mattson Galaxy Series FT-IR 3000 spectrophotometer. High-resolution mass spectrometry (HRMS) data (APPI/APCI/ESI technique) were recorded using an Agilent Technologies 6220 oaTOF instrument. HRMS data (EI technique) were recorded using a Kratos MS50 instrument.

Alkyne **33**[39] is a known literature compound and the ^{1}H NMR and ^{13}C NMR spectral data matched those reported in the literature.

5.6.2. Physical data

Synthesis of tethered aldehydes by Heck coupling/isomerization (General Procedure I): To a flame-dried Schlenk flask under an argon atmosphere was added aryl iodide (1 equiv.), tetrabutylammonium chloride (1 equiv.), palladium acetate (0.025 equiv.), and sodium bicarbonate (2.5 equiv.). To the mixture of solids was added simultaneously, DMF (0.5 M in iodide), and the appropriate aliphatic ene-ol (1.5 equiv.).

The solution was heated to 30 °C for 24 – 48 hours, until completion of the reaction by TLC. The solution was quenched with distilled water and extracted with ethyl acetate (3 x 75 mL). The combined extracts were washed with water (2 x 25 mL), and brine (25 mL). The organic layer was dried over magnesium sulfate, filtered, and concentrated under vacuum. The oily product is initially by purified by recrystallization minimal benzene (cooled in the fridge); the remaining mother liquor is purified by flash column chromatography.

3-(9-Phenanthryl)propanal (48)

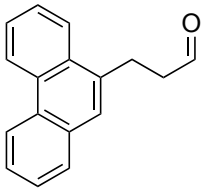

According to General Procedure (I), 9-iodophenanthrene was coupled with 2-propen-1-ol yielding **48** (84 %). R_f (4:1 hexanes:ethyl acetate) 0.35; ^{1}H NMR (300 MHz, $CDCl_3$) δ 9.94 (t, *J* = 1.5 Hz, 1H), 8.75 (m, 1H), 8.66 (app. d, *J* = 7.2 Hz, 1H), 8.06 (m, 1H), 7.83 (m, 1H), 7.68-7.56 (m, 5H), 3.48 (t, *J* = 7.8 Hz, 2H), 2.99 (dt, *J* = 7.2, 1.5 Hz, 2H); ^{13}C NMR (125 MHz, $CDCl_3$) δ 201.5, 134.4, 131.7, 130.9, 130.8, 129.8, 128.2, 126.8, 126.8, 126.4, 126.4, 126.4, 123.9, 123.5, 122.5, 44.1, 25.5; IR (cast film, cm^{-1}) 3065, 2939, 2895, 2824, 2723, 1722; HRMS calcd for $[M]^+$ $C_{17}H_{14}O$: 234.1044, found: 234.1046.

4-(9-Phenanthryl)butanal (49)

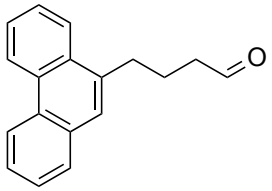

According to General Procedure (I), 9-iodophenanthrene was coupled with 3-buten-1-ol yielding **49** (74 %). R_f (4:1 hexanes:ethyl acetate) 0.49; ^{1}H NMR (500 MHz, $CDCl_3$) δ 9.85 (t, *J* = 1.5 Hz, 1H), 8.77 (m, 1H), 8.69 (dd, *J* = 8.0, 0.5 Hz, 1H), 8.15 (m, 1H), 7.86 (dd, *J* = 7.5, 1.5 Hz, 1H), 7.72-7.60 (m, 5H), 3.21 (t, *J* = 7.0 Hz, 2H), 2.63 (dt, *J* = 7.0,

1.5 Hz, 2H), 2.21 (tt, J = 7.0, 7.0 Hz, 2H); ^{13}C NMR (125 MHz, $CDCl_3$) δ 202.2, 135.4, 131.7, 131.0, 130.8, 129.8, 128.1, 126.7, 126.7, 126.5, 126.3, 126.2, 124.4, 123.3, 122.5, 43.6, 32.6, 22.5; IR (cast film, cm^{-1}) 3062, 2934, 2895, 2816, 2727, 1720; HRMS calcd for $[M]^+$ $C_{18}H_{16}O$: 248.1201, found: 248.1202.

5-(9-Phenanthryl)pentanal (50)

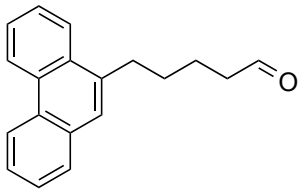

According to General Procedure (I), 9-iodophenanthrene was coupled with 4-penten-1-ol yielding **50** (37 %). R_f (4:1 hexanes:ethyl acetate) 0.40; ^{1}H NMR (500 MHz, $CDCl_3$) δ 9.82 (t, J = 2.0 Hz, 1H), 8.77 (m, 1H), 8.69 (app. d, J = 8.0 Hz, 1H), 8.11 (m, 1H), 7.86 (m, 1H), 7.72-7.60 (m, 5H), 3.19 (t, J = 6.5 Hz, 2H), 2.54 (dt, J = 7.5, 2.0 Hz, 2H), 1.94-1.81 (m, 4H) ^{13}C NMR (125 MHz, $CDCl_3$) δ 202.5, 159.6, 136.0, 131.9, 131.2,130.8, 129.7, 128.1, 126.7, 126.6, 126.2, 126.2, 126.0, 124.3, 123.3, 122.5, 43.8, 33.2, 29.7, 22.2; IR (cast film, cm^{-1}) 3076, 2928, 2884, 2862, 2823, 2723, 1720; HRMS calcd for $[M]^+$ $C_{19}H_{18}O$: 262.1357, found: 262.1352.

3-(1-Pyrenyl)propanal (51)

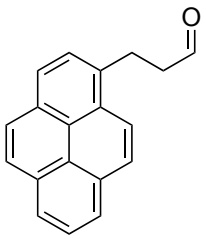

According to General Procedure (I), 1-iodopyrene was coupled with 2-propen-1-ol yielding **51** (84 %). R_f (4:1 hexanes:ethyl acetate) 0.34; ^{1}H NMR (500 MHz, $CDCl_3$) δ 9.97 (t, J = 1.0 Hz, 1H), 8.25 (d, J = 9.5 Hz, 1H), 8.23-8.20 (m, 2H), 8.17 (d, J = 9.0 Hz, 1H), 8.16 (d, J = 7.5 Hz, 1H), 8.07 (s, 2H), 8.04 (t, J = 7.5 Hz, 1H), 7.92 (d, J = 8.0 Hz, 1H), 3.73 (t, J = 7.5 Hz, 2H), 3.06 (dt, J = 7.5, 1.0 Hz, 2H) ^{13}C NMR (125 MHz, $CDCl_3$) δ 201.4, 134.4, 131.4, 130.8, 130.2, 128.6, 127.8, 127.5, 127.0, 126.9, 126.0, 125.2,

125.1, 125.0, 125.0, 125.0, 122.8, 45.5, 25.7; IR (cast film, cm^{-1}) 3038, 2944, 2896, 2853, 2750, 1712; HRMS calcd for $[M]^+$ $C_{19}H_{14}O$: 258.1044, found: 258.1044.

4-(1-Pyrenyl)butanal (52)

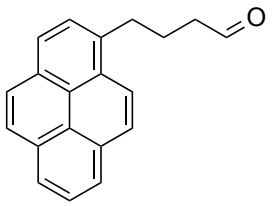

According to General Procedure (I), 1-iodopyrene was coupled with 3-buten-1-ol yielding **52** (77 %). R_f (4:1 hexanes:ethyl acetate) 0.45; ^1H NMR (500 MHz, $CDCl_3$) δ 9.81 (t, *J* = 1.5 Hz, 1H), 8.29 (d, *J* = 9.0 Hz, 1H), 8.18-8.16 (m, 2H), 8.12 (d, *J* = 9.5 Hz, 1H), 8.11 (d, *J* = 7.5 Hz, 1H), 8.03 (s, 2H), 8.00 (t, *J* = 7.5 Hz, 1H), 7.85 (d, *J* = 8.0 Hz, 1H), 3.40 (app. t, *J* = 7.5 Hz, 2H), 2.58 (dt, *J* = 7.0, 1.5 Hz, 2H), 2.21 (tt, *J* = 8.0, 8.0 Hz, 2H). ^{13}C NMR (125 MHz, $CDCl_3$) δ 202.2, 135.5, 131.5, 130.9, 130.1, 128.8, 127.5, 127.5, 127.3, 126.8, 125.9, 125.2, 125.0, 124.9, 124.8, 123.2, 43.5, 32.6, 24.0; IR (cast film, cm^{-1}) 3040, 2939, 2877, 2819, 2719, 1721; HRMS calcd for $[M]^+$ $C_{20}H_{16}O$: 272.1201, found: 272.1209.

5-(1-Pyrenyl)pentanal (53)

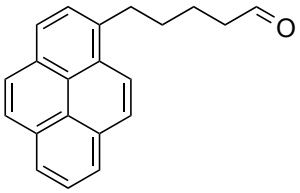

According to General Procedure (I), 1-iodopyrene was coupled with 4-penten-1-ol yielding **53** (73 %). R_f (4:1 hexanes:ethyl acetate) 0.50; ^1H NMR (500 MHz, $CDCl_3$) δ 9.81 (t, *J* = 2.0 Hz, 1H), 8.28 (d, *J* = 9.0 Hz, 1H), 8.20 (d, *J* = 8.0 Hz, 1H), 8.19 (d, *J* = 7.5 Hz, 1H), 8.14 (d, *J* = 8.0 Hz, 2H), 8.06 (s, 1H), 8.06 (s, 1H), 8.03 (t, *J* = 8.0 Hz, 1H), 7.90 (d, *J* = 7.5 Hz, 1H), 3.42 (t, *J* = 7.0 Hz, 2H), 2.54 (dt, *J* = 7.5, 2.0 Hz, 2H), 1.98-1.91 (m, 2H), 1.89-1.82 (m, 2H); ^{13}C NMR (125 MHz, $CDCl_3$) δ 202.4, 136.2, 131.5, 130.9, 129.9, 128.6, 127.5, 127.3, 127.2, 126.7, 125.9, 125.1, 125.1, 124.9, 124.8, 124.8,

123.3, 43.8, 33.3, 31.3, 22.2; IR (cast film, cm^{-1}) 3043, 2940, 2880, 2871, 2813, 2712, 1720; HRMS calcd for $[M]^+$ $C_{21}H_{18}O$: 286.1358, found: 286.1361.

General Procedure for the synthesis of the tethered alkynes using the Bestmann-Ohira reaction: Tethered aldehyde (1 equiv.) and dimethyl (1-diazo-2-oxopropyl)phosphonate (1.5 equiv.) were suspended in dry, degassed methanol in a flame dried Schlenk flask under argon. The solution was cooled to 0 °C by ice bath and solid potassium carbonate (2.5 equiv.) was added. The mixture was stirred at room temperature for 18 h. After completion of the reaction the mixture was quenched with distilled water and extracted with diethyl ether (3 x 50 mL). The combined organic extracts were washed with water (50 mL) and brine (50 mL) then dried with magnesium sulfate, and filtered.. The organic solution was concentrated then purified by silica plug eluting with 1:1 DCM:hexanes.

4-(9-Phenanthryl)-1-butyne (65)

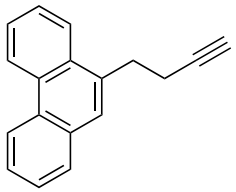

According to General Procedure (II), 3-(9-phenanthryl)propanal yields **65** (75 %). R_f (4:1 hexanes:ethyl acetate) 0.66; ^1H NMR (500 MHz, $CDCl_3$) δ 8.78 (m, 1H), 8.69 (app. d, *J* = 8.5 Hz, 1H), 8.12 (m, 1H), 7.88 (dd, *J* = 7.5, 2.0 Hz, 1H), 7.72-7.60 (m, 5H), 3.42 (t, *J* = 7.5 Hz, 2H), 2.74 (td, *J* = 7.5, 3.0 Hz, 2H), 2.08 (t, *J* = 3.0, 1H); ^{13}C NMR (125 MHz, $CDCl_3$) δ 134.4, 131.7, 130.8, 130.7, 129.9, 128.3, 126.7, 126.7, 126.6, 126.3, 126.3, 124.0, 123.4, 122.5, 83.9, 69.3, 32.5, 19.4; IR (cast film, cm^{-1}) 3272, 3062, 2932, 2915, 2846, 2111; HRMS calcd for $[M]^+$ $C_{18}H_{14}$: 230.1096, found: 230.1096.

6-(9-Phenanthryl)-1-hexyne (66)

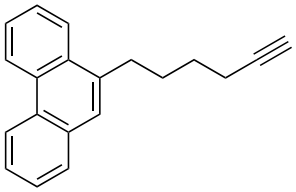

According to General Procedure (II), 5-(9-phenanthryl)pentanal yields **66** (80 %); ^{1}H NMR (500 MHz, $CDCl_3$) δ 8.78 (m, 1H), 8.70 (d, *J* = 8.0 Hz, 1H), 8.15 (m, 1H), 7.87 (m, 1H), 7.72-7.60 (m, 5H), 3.19 (app. t, *J* = 8.0 Hz, 2H), 2.33 (td, *J* = 7.0, 2.5 Hz, 2H), 2.03-1.97 (m, 3H), 1.77 (tt, *J* = 7.0, 7.0 Hz, 2H); ^{13}C NMR (125 MHz, $CDCl_3$) δ 136.3, 131.9, 131.3, 130.8, 129.7, 128.1, 126.6, 126.5, 126.2, 126.1, 126.0, 124.4, 123.3, 122.5, 84.4, 68.5, 32.9, 29.2, 28.5, 18.4; IR (cast film, cm^{-1}) 3275, 3062, 2945, 2910, 2852, 2113; HRMS calcd for $[M]^+$ $C_{20}H_{18}$: 258.1408, found: 258.1408.

4-(1-Pyrenyl)-1-butyne (67)

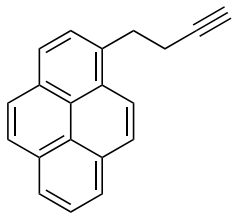

According to General Procedure (II), 3-(1-pyrenyl)propanal yields **67** (93 %); ^{1}H NMR (500 MHz, $CDCl_3$) δ 8.30 (d, *J* = 9.0 Hz, 1H), 8.22 (d, *J* = 7.5 Hz, 1H), 8.21 (d, *J* = 7.5 Hz, 1H), 8.16 (d, *J* = 8.0 Hz, 1H), 8.15 (d, *J* = 9.0 Hz, 1H), 8.08 (s, 2H), 8.04, (app. t, *J* = 7.5, 7.5 Hz, 1H), 7.96 (d, *J* = 7.5 Hz, 1H), 3.64 (t, *J* = 8.0 Hz, 2H), 2.79 (td, *J* = 8.0, 2.5 Hz, 2H), 2.11 (t, *J* = 2.5 Hz, 1H); ^{13}C NMR (125 MHz, $CDCl_3$) δ 134.4, 131.4, 130.9, 130.3, 128.7, 127.6, 127.5, 127.3, 126.9, 125.9, 125.1, 125.0, 124.9, 124.8, 123.0, 83.9, 69.4, 32.6, 20.8; IR (cast film, cm^{-1}); HRMS calcd for $[M]^+$ $C_{20}H_{14}$: 254.1096, found: 254.1094.

General Procedure for the synthesis of tethered nitriles via a copper catalyzed Beckman condensation: Tethered aldehyde (1 equiv.), hydroxyamine hydrochloride (1.5 equiv.) and N-methylpyrrolidinone were combined in an appropriately sized microwave vial with a stir bar, flushed with argon and sealed. The mixture was irradiated in a Biotage microwave reactor for 15 minutes at 160 °C. Upon completion of the reaction, distilled water (50 mL) was added. The aqueous layer was washed with diethyl ether (4 x 25 mL) and the combined organic extracts were washed with distilled water (3 x 25 mL) and brine (50 mL). The organic layer was dried over magnesium sulfate, filtered, and

concentrated. Further purification was not necessary in most cases but could be achieved via silica plug.

3-(9-Phenanthryl)propanenitrile (76)

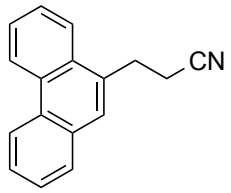

According to General Procedure (III), 3-(9-phenanthryl)propanal yields **76** (79 %); ^{1}H NMR (500 MHz, $CDCl_3$) δ 8.81 (d, *J* = 7.5 Hz, 1H), 8.71 (d, *J* = 8.5 Hz, 1H), 8.01 (d, *J* = 8 Hz, 1H), 7.91 (d, *J* = 8.0 Hz, 1H), 7.76-7.63 (m, 5H), 3.54 (t, *J* = 7.5 Hz, 2H), 2.88 (t, *J* = 8.0 Hz, 2H); ^{13}C NMR (125 MHz, $CDCl_3$) δ 132.1, 131.4, 131.0, 130.1, 130.1, 128.5, 127.2, 127.1, 127.0, 126.9, 126.7, 123.7, 123.3, 122.5, 119.2, 29.3, 18.1; IR (cast film, cm^{-1}) 3105, 3066, 3050, 3033, 2954, 2917, 2854, 2250; HRMS calcd for $[M]^+$ $C_{17}H_{13}N$: 231.1048, found: 231.1049.

4-(9-Phenanthryl)butanenitrile (77)

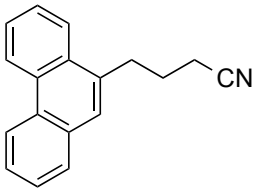

According to General Procedure (III), 4-(9-phenanthryl)butanal yields **77** (90 %); ^{1}H NMR (500 MHz, $CDCl_3$) δ 8.75 (m, 1H), 8.66 (d, *J* = 7.5 Hz, 1H), 8.04 (m, 1H), 7.85 (m, 1H), 7.70-7.59 (m, 5H), 3.28 (t, *J* = 7.5 Hz, 2H), 2.39 (t, *J* = 7.0 Hz, 2H), 2.16 (tt, *J* = 7.0, 7.0 Hz, 2H); ^{13}C NMR (125 MHz, $CDCl_3$) δ 133.8, 131.6, 130.9, 130.7, 129.9, 128.2, 127.0, 126.9, 126.8, 126.5, 126.4, 124.0, 123.5,122.5, 119.6, 32.0, 25.7, 16.9; IR (cast film, cm^{-1}) 3064, 2958, 2940, 2875, 2243; HRMS calcd for $[M]^+$ $C_{18}H_{15}N$: 245.1204, found: 245.1206.

5-(9-Phenanthryl)pentanenitrile (78)

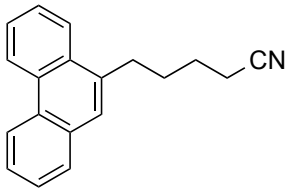

According to General Procedure (III), 4-(9-phenanthryl)pentanal yields **78** (80 %); ^{1}H NMR (500 MHz, $CDCl_3$) δ 8.78 (m, 1H), 8.69 (d, *J* = 7.0 Hz, 1H), 8.09 (m, 1H), 7.86 (m, 1H), 7.72-7.59 (m, 5H), 3.20 (t, *J* = 7.5 Hz, 2H), 2.43 (t, *J* = 7.0 Hz, 2H), 2.03 (tt, *J* = 8.0, 7.5 Hz, 2H), 1.86 (tt, *J* = 8.0, 7.0 Hz, 2H); ^{13}C NMR (125 MHz, $CDCl_3$) δ 135.3, 131.7, 131.0, 130.8, 129.8, 128.1, 126.8, 126.7, 126.4, 126.3, 126.2, 124.2, 123.4, 122.5, 119.6, 32.6, 29.1, 25.4, 17.2; IR (cast film, cm^{-1}) 3076, 2937, 2919, 2248; HRMS calcd for $[M]^+$ $C_{19}H_{17}N$: 259.1361, found: 259.1357.

3-(1-Pyrenyl)propanenitrile (79)

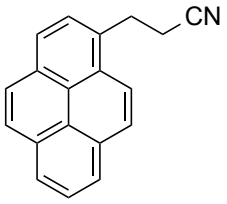

According to General Procedure (III), 3-(1-Pyrenyl)propanal yields **79** (85 %); ^{1}H NMR (400 MHz, $CDCl_3$) δ 8.22-8.15 (m, 5H), 8.07-8.01 (m, 3H), 7.92 (d, *J* = 8.0 Hz, 1H), 3.73 (t, *J* = 7.6 Hz, 2H), 2.87 (t, *J* = 7.6 Hz, 2H); ^{13}C NMR (125MHz, $CDCl_3$) δ 131.7, 131.4, 130.9, 130.7, 128.5, 128.3, 127.4, 127.4, 127.1, 126.2, 125.5, 125. 3, 125.2, 125.1, 124.9, 122.0, 119.1, 29.3, 19.3; IR (cast film, cm^{-1}) 3041, 2952, 2245; HRMS calcd for $[M]^+$ $C_{19}H_{13}N$: 255.1048, found: 255.1053.

4-(1-Pyrenyl)butanenitrile (80)

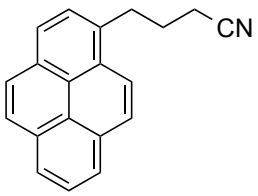

According to General Procedure (III), 4-(1-Pyrenyl)butanal yields **80** (58 %); ^{1}H NMR (500 MHz, $CDCl_3$) δ 8.25-7.99 (m, 8H), 7.84 (d, *J* = 8.0 Hz, 1H), 3.47 (t, *J* = 7.5 Hz, 2H), 2.36 (t, *J* = 7.0 Hz, 2H), 2.18 (tt, *J* = 7.5, 7.5 Hz, 2H) ^{13}C NMR (125 MHz, $CDCl_3$) δ 133.7, 131.4, 130.8, 130.4, 128.7, 127.8, 127.5, 127.3, 127.1, 126.1, 125.2, 125.2, 125.0, 124.9, 124.9, 122.8, 119.6, 32.0, 27.2, 16.8; IR (cast film, cm^{-1}) 3041, 2939, 2876, 2245; HRMS calcd for $[M]^+$ $C_{20}H_{15}N$: 269.1204, found: 269.1201.

5-(1-Pyrenyl)pentanenitrile (81)

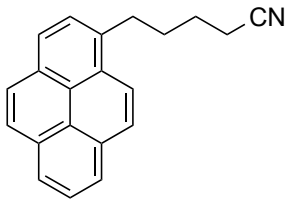

According to General Procedure (III), 5-(1-Pyrenyl)pentanal yields **81** (39 %); ^{1}H NMR (500 MHz, $CDCl_3$) δ 8.24 (d, *J* = 9.0 Hz, 1H), 8.18 (d, *J* = 2.5 Hz, 1H), 8.17 (d, *J* = 2.5 Hz, 1H), 8.13 (d, *J* = 2.0 Hz, 1H), 8.11 (s, 1H), 8.03 (s, 2H), 8.00 (dd, *J* = 8.0, 8.0 Hz, 1H), 7.85 (d, *J* = 8.0 Hz, 1H), 3.40 (t, *J* = 7.5 Hz, 2H), 2.36 (t, *J* = 7.0 Hz, 2H), 2.03 (m, 2H), 1.82 (tt, *J* = 7.5, 8.0 Hz, 2H); ^{13}C NMR (125 MHz, $CDCl_3$) δ 135.4, 131.5, 130.9, 130.1, 128.6, 127.5, 127.5, 127.2, 126.8, 125.9, 125.2, 125.1, 125.0, 124.9, 124.9, 123.1, 119.6, 32.6, 30.6, 25.3, 17.2; IR (cast film, cm^{-1}) 3040, 3012, 2934, 2865, 2246; HRMS calcd for $[M]^+$ $C_{21}H_{17}N$: 283.1361, found: 283.1361.

1,4-(2-Phenylethyl)-3-(4-cyanobutyl)benzo[g]isoquinoline (95)

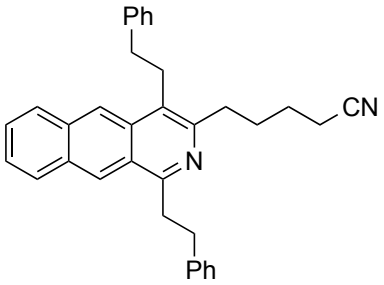

A flame dried Schlenk flask under argon was charged with 0.352 g (2.7 mmol, 2.2 equiv.) of 4-phenyl-1-butyne and 6.5 mL of dry degassed THF. The solution was cooled to -78 °C in a dry ice/acetone bath and 1.5 mL of 1.7 M n-BuLi (2.6 mmol, 2.1 equiv.) was

added. The solution was left to warm to room temperature over the course of 1 hour. After warming to room temperature the solution was cooled to -78 °C and 0.325 g (1.2 mmol, 1 equiv.) of *o*-bis(bromomethyl)benzene was added as a solid. The solution was allowed to warm to room temperature over the course of 1 h and warmed to 40 °C for 3h. The solution was cooled to room temperature, quenched with the addition of NH_4Cl (50 mL), and washed with diethyl ether (3 x 50 mL). The combined organic extracts were washed with water (50 mL) and brine (50 mL). The organic phase was dried with magnesium sulfate, filtered, and concentrated to a clear, colorless oil. The oil was subjected to flash column chromatography (hexanes:ethyl acetate, 1:0 → 19:1). Inconsistent yields were obtained between 0 % and 35 %, obtained as a mixture of compound and starting alkyne.

In order to obtain a usable product a number of precautions were necessary:

(1) The *n*-BuLi used must be freshly titrated to avoid having excess base in the reaction mixture.

(2) Note that there is a small excess of the terminal alkyne used relative to the stoichiometry to avoid the presence of excess *n*-BuLi

(3) The dibromomethylbenzene electrophile used was recrystallized from benzene and kept in a desiccator wrapped in aluminum foil.

1,2-bis(5-phenyl-2-pentynyl)benzene, **92**; ^{1}H NMR (500 MHz, $CDCl_3$) δ 7.36-7.19 (m, 14H), 3.51 (t, J = 2.5 Hz, 4H), 2.83 (t, J = 7.5 Hz, 4H), 2.50 (tt, J = 7.5, 2.5 Hz, 4H).

100 mg of the previous material was added to a flame dried 2-5 mL microwave vial within a drybox. To this was added 300 mg (2.75 mmol, 10 equiv.) of degassed adiponitrile, and 4 mL of toluene. Before capping the vial 50 mg (0.275 mmol, 1 equiv.) of $CpCo(CO)_2$ was added by microliter syringe. The vial was quickly capped and sealed and subjected to microwave irradiation, 160 ^{o}C for 3 hrs. Once the reaction is completed the mixture is poured into a round bottom flask and the solid extracted with DCM 4 x 10 mL. This mixture is concentrated on a rotary evaporator and the extract is subjected to column chromatography 3 times (gradient 1:4/ethyl acetate:hexanes with 1% triethylamine to 3:7/ ethyl acetate:hexanes with 1% triethylamine) to give 7.9 mg (6.1 %)

of a clear, yellow oil **95**. This material is very sensitive to decomposition in air as well as in chloroform.

1,4-(2-Phenylethyl)-3-(4-cyanobutyl)benzo[g]isoquinoline: ^{1}H NMR (500 MHz, $CDCl_3$) δ 8.77 (s, 1H), 8.57 (s, 1H), 8.07 (d, *J* = 8.0 Hz, 1H), 8.06 (d, *J* = 8.5 Hz, 1H), 7.60 (td, *J* = 7.0, 1.5 Hz, 1H), 7.54 (td, *J* = 6.5, 1.0 Hz, 1H), 7.39 – 7.23 (m, 10H), 3.77 (app. t, *J* = 8.0 Hz, 2H), 3.48 (app. t, *J* = 8.5 Hz, 2H), 3.33 (app. t, *J* = 8.0 Hz, 2H), 3.07 (app. t, *J* = 8.0 Hz, 2H), 2.93 (t, *J* = 7.5 Hz, 2H), 2.40 (t, *J* = 7.0 Hz, 2H), 1.91 (app p, *J* = 6.0 Hz, 2H), 1.78 (app p, *J* = 7.5 Hz, 2H); ^{13}C NMR (125 MHz, $CDCl_3$) δ 159.8, 148.1, 142.2, 141.7, 133.8, 132.3, 131.1, 128.9, 128.6, 128.6, 128.4, 128.4, 128.2, 127.3, 126.3, 126.0, 125.8, 125.5, 124.3, 124.1, 122.0, 119.9, 37.1, 36.7, 34.8, 33.8, 30.0, 28.7, 25.4, 17.1; IR (cast film, cm^{-1}) 3059, 3025, 2927, 2861, 2245; HRMS (ESI) calcd for $[M]^+$ $C_{34}H_{32}N_2$: 468.2566, found: 468.2575.

5.7. References

(1) International Energy Agency. *Oil Medium-term Market Report 2012*; 2012.

(2) *Strausz, O. P.;* Lown, E. M., *The Chemistry of Alberta Oil Sands Bitumens and Heavy Oils*; Alberta Energy: Calgary; 2003, 1-695.

(3) Wang, J.; Buckley, J. *J. Disper. Sci. Technol.* **2007**, *28*, 425–430.

(4) Qian, K.; Edwards, K. E.; Siskin, M.; Olmstead, W. N.; Mennito, A. S.; Dechert, G. J.; Hoosain, N. E. *Energ. Fuel.* **2007**, *21*, 1042–1047.

(5) Groenzin, H.; Mullins, O. C. *Energ. Fuel.* **2000**, *14*, 677–684.

(6) Jaffe, S. B.; Freund, H.; Olmstead, W. N. *Ind. Eng. Chem. Res.* **2005**, *44*, 9840–9852.

(7) Kuznicki, T.; Masliyah, J. H.; Bhattacharjee, S. *Energ. Fuel.* **2008**, *22*, 2379–2389.

(8) Andersen, S. I.; Birdi, K. S. *J. Colloid Interf. Sci.* **1991**, *142*, 497–502.

(9) Strausz, O. P.; Safarik, I.; Lown, E. M.; Morales-Izquierdo, A. *Energ. Fuel.* **2008**, *22*, 1156–1166.

(10) Scholl, R.; Seer, C.; Weitzenböck, R. *Chem. Ber.* **1910**, *43*, 2202–2209.

(11) Müller, M.; Mauermann-Düll, H.; Wagner, M.; Enkelmann, V.; Müllen, K. *Angew. Chem. Int. Ed. Engl.* **1995**, *34*, 1583–1586.

(12) Müller, M.; Petersen, J.; Strohmaier, R.; Günther, C.; Karl, N.; Müllen, K.

Angew. Chem. Int. Ed. Engl. **1996**, *35*, 886–888.

(13) Müller, M.; Iyer, V. S.; Kübel, C.; Enkelmann, V.; Müllen, K. *Angew. Chem. Int. Ed. Engl.* **1997**, *36*, 1607–1610.

(14) Iyer, V. S.; Wehmeier, M.; Brand, J. D.; Keegstra, M. A.; Müllen, K. *Angew. Chem. Int. Ed. Engl.* **1997**, *36*, 1604–1607.

(15) Müller, M.; Kübel, C.; Müllen, K. *Chem. Eur. J.* **1998**, *4*, 2099–2109.

(16) Rakotondradany, F.; Fenniri, H.; Rahimi, P.; Gawrys, K. L.; Kilpatrick, P. K.; Gray, M. R. *Energ. Fuel.* **2006**, *20*, 2439–2447.

(17) Mullins, O. C.; Sabbah, H.; Eyssautier, J.; Pomerantz, A. E.; Barré, L.; Andrews, A. B.; Ruiz-Morales, Y.; Mostowfi, F.; McFarlane, R.; Goual, L.; Lepkowicz, R.; Cooper, T.; Orbulescu, J.; Leblanc, R. M.; Edwards, J.; Zare, R. N. *Energ. Fuel.* **2012**, *26*, 3986–4003.

(18) Sabbah, H.; Morrow, A. L.; Pomerantz, A. E.; Zare, R. N. *Energ. Fuel.* **2011**, *25*, 1597–1604.

(19) Sharma, A.; Groenzin, H.; Tomita, A.; Mullins, O. C. *Energ. Fuel.* **2002**, *16*, 490–496.

(20) Scotti, R.; Montanari, L. Molecular Structure and Intermolecular Interaction of Asphaltenes by NMR, IR, and ESR. In *Structures and Dynamics of Asphaltenes*; Mullins, O. C.; Sheu, E. Y., Eds.; Springer-Verlag GmbH, Heidelberg, **1998**; 79–114.

(21) Ruiz-Morales, Y.; Mullins, O. C. *Energ. Fuel.* **2009**, *23*, 1169–1177.

(22) Klee, T.; Masterson, T.; Miller, B.; Barrasso, E.; Bell, J.; Lepkowicz, R.; West, J.; Haley, J. E.; Schmitt, D. L.; Flikkema, J. L.; Cooper, T. M.; Ruiz-Morales, Y.; Mullins, O. C. *Energ. Fuel.* **2011**, *25*, 2065–2075.

(23) Buckley, J.; Wang, J.; Creek, J., Solubility of the Least-Soluble Asphaltenes. In *Asphaltenes, Heavy Oils, And Petroleomics*; Mullins, O.; Sheu, E.; Hammami, A.; Marshall, A., Eds.; Springer New York, **2007**; pp. 401–437.

(24) Buckley, J. S.; Hirasaki, G. J.; Liu, Y.; Drasek, Von, S.; Wang, J.-X.; Gill, B. S. *Pet. Sci. Technol.* **1998**, *16*, 251–285.

(25) Sabbah, H.; Morrow, A. L.; Pomerantz, A. E.; Mullins, O. C.; Tan, X.; Gray, M. R.; Azyat, K.; Tykwinski, R. R.; Zare, R. N. *Energ. Fuel.* **2010**, *24*, 3589–3594.

(26) Tan, X.; Fenniri, H.; Gray, M. R. *Energ. Fuel.* **2008**, *22*, 715–720.

(27) Karimi, A.; Qian, K.; Olmstead, W. N.; Freund, H.; Yung, C.; Gray, M. R. *Energ. Fuel.* **2011**, *25*, 3581–3589.

(28) Personal correspondance with Professor Murray R. Gray, Department of Chemical and Materials Engineering, University of Alberta.

(29) Alshareef, A. H.; Scherer, A.; Tan, X.; Azyat, K.; Stryker, J. M.; Tykwinski, R. R.; Gray, M. R. *Energ. Fuel.* **2011**, *25*, 2130–2136.

(30) Diner, C.; Scott, D. E.; Tykwinski, R. R.; Gray, M. R.; Stryker, J. M. *J. Org. Chem.* **2015**, *80*, 1719–1726.

(31) LeBoeuf, D.; Gandon, V.; Malacria, M. In *Handbook of cyclization reactions*; Wiley-VCH: Weinheim, 2010; pp. 367–406.

(32) Lautens, M.; Klute, W.; Tam, W. *Chem. Rev.* **1996**, *96*, 49–92.

(33) Chopade, P. R.; Louie, J. *Adv. Synth. Catal.* **2006**, *348*, 2307–2327.

(34) Nakamura, I.; Yamamoto, Y. *Chem. Rev.* **2004**, *104*, 2127–2198.

(35) Domínguez, G.; Pérez-Castells, J. *Chem. Soc. Rev.* **2011**, *40*, 3430–3444.

(36) Kumar, P.; Prescher, S.; Louie, J. *Angew. Chem. Int. Ed.* **2011**, *50*, 10694–10698.

(37) Brown, C. A.; Yamashita, A. *J. Am. Chem. Soc.* **1975**, *97*, 891–892.

(38) Hoye, R. C.; Baigorria, A. S.; Danielson, M. E.; Pragman, A. A.; Rajapakse, H. A. *J. Org. Chem.* **1999**, *64*, 2450–2453.

(39) Cheng, J.; Sun, Y.; Wang, F.; Guo, M.; Xu, J.-H.; Pan, Y.; Zhang, Z. *J. Org. Chem.* **2004**, *69*, 5428–5432.

(40) Taskinen, E.; Lindholm, N. *J. Phys. Org. Chem.* **1994**, *7*, 256–258.

(41) Colbon, P.; Ruan, J.; Purdie, M.; Mulholland, K.; Xiao, J. *Org. Lett.* **2011**, *13*, 5456–5459.

(42) Muzart, J. *Tetrahedron* **2005**, *61*, 4179–4212.

(43) Jeffery, T. *J. Chem. Soc., Chem. Commun.* **1984**, 1287–1289.

(44) Larock, R. C.; Leung, W.-Y.; Stolz-Dunn, S. *Tetrahedron Lett.* **1989**, *30*, 6629–6632.

(45) Heck, R. F. *J. Am. Chem. Soc.* **1968**, *90*, 5526–5531.

(46) Amatore, C.; Jutand, A.; Suarez, A. *J. Am. Chem. Soc.* **1993**, *115*, 9531–9541.

(47) Roy, A. H.; Hartwig, J. F. *Organometallics* **2004**, *23*, 194–202.

(48) Corey, E. J.; Fuchs, P. L. *Tetrahedron Lett.* **1972**, *13*, 3769–3772.

(49) Seyferth, D.; Marmor, R. S.; Hilbert, P. *J. Org. Chem.* **1971**, *36*, 1379–1386.

(50) Müller, S.; Liepold, B.; Roth, G. J.; Bestmann, H. J. *Synlett* **1996**, 521–522.

(51) Fritsch, P. *Justus Liebigs Ann. Chem.* **1894**, *279*, 319–323.

(52) Buttenberg, W. P. *Justus Liebigs Ann. Chem.* **1894**, *279*, 324–337.

(53) Wiechell, H. *Justus Liebigs Ann. Chem.* **1894**, *279*, 337–344.

(54) Roth, G.; Liepold, B.; Müller, S.; Bestmann, H. *Synthesis* **2004**, 59–62.

(55) Gawley, R. E. The Beckmann Reactions: Rearrangements, Eliminations-Additions, Fragmentations, and Rearrangement-Cyclizations. In *Organic Reactions*; John Wiley & Sons, Inc.: New York; **2004,** 1-406.

(56) Chakraborti, A. K.; Kaur, G. *Tetrahedron* **1999**, *55*, 13265–13268.

(57) Bowden, K.; Cook, R. S. *J. Chem. Soc., Perkin Trans. 2* **1972**, 1407–1411.

(58) Takahashi, T.; Li, S.; Huang, W.; Kong, F.; Nakajima, K.; Shen, B.; Ohe, T.; Kanno, K.-I. *J. Org. Chem.* **2006**, *71*, 7967–7977.

(59) Brandsma, L. *Preparative Acetylenic Chemistry*. 1st ed.; Elsevier: Amsterdam, **1988,** 1-321.

(60) Zou, Y.; Young, D. D.; Cruz-Montanez, A.; Deiters, A. *Org. Lett.* **2008**, *10*, 4661–4664.

(61) Schnieders, C.; Müllen, K.; Huber, W. *Tetrahedron* **1984**, *40*, 1701–1711.

(62) Rossi, R.; Carpita, A.; Lippolis, V.; Benetti, M. *Gazz. Chim. Ital.* **1990**, *120*, 783.

(63) Larsen, C.; Anderson, K.; Tundel, R.; Buchwald, S. *Synlett* **2006**, *2006*, 2941–2946.

(64) Pérez, I.; Sestelo, J. P.; Sarandeses, L. A. *J. Am. Chem. Soc.* **2001**, *123*, 4155–4160.

(65) Qian, M.; Negishi, E.-I. *Tetrahedron Lett.* **2005**, *46*, 2927–2930.

(66) Torregrosa, R. R. P.; Ariyarathna, Y.; Chattopadhyay, K.; Tunge, J. A. *J. Am. Chem. Soc.* **2010**, *132*, 9280–9282.

(67) Zhang, W.-W.; Zhang, X.-G.; Li, J.-H. *J. Org. Chem.* **2010**, *75*, 5259–5264.

(68) Kuno, A.; Saino, N.; Kamachi, T.; Okamoto, S. *Tetrahedron Lett.* **2006**, *47*, 2591–2594.

(69) Xiang, S.-K.; Zhang, L.-H.; Jiao, N. *Chem. Commun.* **2009**, 6487–6489.

(70) Correia, C. A.; Li, C.-J. *Adv. Synth. Catal.* **2010**, *352*, 1446–1450.

(71) Haider, N. *Tetrahedron* **1992**, *48*, 7173–7184.

(72) Inoue, T.; Takeda, T.; Kambe, N.; Ogawa, A.; Ryu, I.; Sonoda, N. *J. Org. Chem.* **1994**, *59*, 5824–5827.

(73) Boger, D. L.; Mathvink, R. J. *J. Org. Chem.* **1992**, *57*, 1429–1443.

(74) Heinisch, G.; Jentzsch, A.; Pailer, M. *Monatsh. Chem.* **1974**, *105*, 648–652.

(75) Abdel-Magid, A. F.; Mehrman, S. J. *Org. Process Res. Dev.* **2006**, *10*, 971–1031.

Compiled References

Chapter 1

(1) Allen, A. E.; MacMillan, D. W. C. *Chem. Sci.* **2012**, *3*, 633.

(2) Gillespie, R. J.; Nyholm, R. S. *Q. Rev., Chem. Soc.* **1957**, *11*, 339.

(3) Anslyn, E. V.; Dougherty, D. A. *Modern Physical Organic Chemistry*. University Science: Sausalito, CA, **2006**.

(4) Walsh, A. D. *Nature* **1947**, *159*, 712.

(5) Shea, K. J. *Tetrahedron* **1980**, *36*, 1683–1715.

(6) House, H. O.; Kleschick, W. A.; Zaiko, E. J. *J. Org. Chem.* **1978**, *43*, 3653–3661.

(7) Gampe, C. M.; Carreira, E. M. *Angew. Chemie. Int. Ed.* **2012**, *51*, 3766–3778.

(8) Gampe, C. M.; Boulos, S.; Carreira, E. M. *Angew. Chemie. Int. Ed.* **2010**, *49*, 4092–4095.

(9) Gampe, C. M.; Carreira, E. M. *Angew. Chemie. Int. Ed.* **2011**, *50*, 2962–2965.

(10) Kolb, H. C.; Finn, M. G.; Sharpless, K. B. *Angew. Chem. Int. Ed. Engl.* **2001**, *40*, 2004–2021.

(11) Huisgen, R. *Proc Chem. Soc.***1961**, 357–396.

(12) Huisgen, R. *Angew. Chem. Int. Ed. Engl.* **1963**, *2*, 565–598.

(13) Wittig, G.; Krebs, A. *Chem. Ber.* **1961**, *94*, 3260–3275.

(14) Baskin, J. M.; Prescher, J. A.; Laughlin, S. T.; Agard, N. J.; Chang, P. V.; Miller, I. A.; Lo, A.; Codelli, J. A.; Bertozzi, C. R. *Proc. Natl. Acad. Sci. U S A* **2007**, *104*, 16793–16797.

(15) Agard, N. J.; Prescher, J. A.; Bertozzi, C. R. *J. Am. Chem. Soc.* **2004**, *126*, 15046–15047.

(16) Hoffmann, R. W. *Dehydrobenzene and Cycloalkynes*; 1st ed.; Elsevier, 2012.

(17) Moss, R. A.; Platz, M. S.; Maitland Jones, J. *Reactive Intermediate Chemistry*; John Wiley & Sons, 2004.

(18) Wittig, G.; Fritze, P. *Angew. Chemie. Int. Ed.* **1966**, *5*, 846.

(19) Wittig, G.; Mayer, U. *Chem. Ber.* **1963**, *96*, 342–348.

(20) Christl, M. Cyclic Allenes up to Seven-Membered Rings. In *Modern Allene Chemistry*, Vol. 1; Krause, N., Hashmi A. K. S., Ed.; Wiley-VCH: Weinheim,

Germany, 2005; 243–357.

(21) Johnson, R. P. *Chem. Rev.* **1989**, *89*, 1111–1124.

(22) Balci, M.; Taskesenligil, Y. In *Advances in Strained and Interesting Organic Molecules*; Halton, B., Ed.; JAI Press: Stamford, Connecticut, 1999; Vol. 8, pp. 43–82.

(23) Angus, R. O., Jr; Schmidt, M. W.; Johnson, R. P. *J. Am. Chem. Soc.* **1985**, *107*, 532–537.

(24) Skraba, S. L.; Johnson, R. P. *J. Org. Chem.* **2012**, *77*, 11096–11100.

(25) Levek, T. J.; Kiefer, E. F. *J. Am. Chem. Soc.* **1976**, *98*, 1875–1879.

(26) Dowd, P. *J. Am. Chem. Soc.* **1966**, *88*, 2587–2589.

(27) Dowd, P.; Chang, W.; Paik, Y. H. *J. Am. Chem. Soc.* **1986**, *108*, 7416–7417.

(28) Bottini, A. T.; Cabral, L. J.; Dev, V. *Tetrahedron Lett.* **1977**, 615–618.

(29) Moore, W. R.; Moser, W. R. *J. Am. Chem. Soc.* **1970**, *92*, 5469–5474.

(30) Christl, M.; Schreck, M. *Chem. Ber.* **1987**, *120*, 915–920.

(31) Ceylan, M.; Budak, Y. *J. Chem. Res.* **2002**, *2002*, 416–419.

(32) Tolbert, L. M.; Islam, M. N.; Johnson, R. P.; Loiselle, P. M.; Shakespeare, W. C. *J. Am. Chem. Soc.* **1990**, *112*, 6416–6417.

(33) Christl, M.; Schreck, M.; Fischer, T.; Rudolph, M.; Moigno, D.; Fischer, H.; Deuerlein, S.; Stalke, D. *Chem. Eur. J.* **2009**, *15*, 11256–11265.

(34) Hoffmann, H. *Angew. Chem. Int. Ed. Engl.* **1969**, *8*, 556–577.

(35) Wittig, G.; Fritze, P. *Liebigs Ann. Chem.* **1968**, *711*, 82–87.

(36) Martin, J. G.; Hill, R. K. *Chem. Rev.* **1961**, *61*, 537–562.

(37) Williamson, K. L.; Hsu, Y.-F. L. *J. Am. Chem. Soc.* **1970**, *92*, 7385–7389.

(38) Kobuke, Y.; Sugimoto, T.; Furukawa, J.; Fueno, T. *J. Am. Chem. Soc.* **1972**, *94*, 3633–3635.

(39) Bottini, A. T.; Hilton, L. L.; Plott, J. *Tetrahedron* **1975**, *31*, 1997–2001.

(40) Balci, M.; Jones, W. M. *J. Am. Chem. Soc.* **1980**, *102*, 7607–7608.

(41) Schöneboom, J. C.; Groetsch, S.; Christl, M.; Engels, B. *Chem. Eur. J.* **2003**, *9*, 4641–4649.

(42) Engels, B.; Schöneboom, J. C.; Münster, A. F.; Groetsch, S.; Christl, M. *J. Am. Chem. Soc.* **2002**, *124*, 287–297.

(43) Nendel, M.; Tolbert, L. M.; Herring, L. E.; Islam, M. N.; Houk, K. N. *J. Org. Chem.* **1999**, *64*, 976–983.

(44) Schmidt, M. W.; Angus, R. O.; Johnson, R. P. *J. Am. Chem. Soc.* **1982**, *104*, 6838–6839.

(45) Daoust, K. J.; Hernandez, S. M.; Konrad, K. M.; Mackie, I. D.; Winstanley, J.; Johnson, R. P. *J. Org. Chem.* **2006**, *71*, 5708–5714.

(46) Burrell, R. C.; Daoust, K. J.; Bradley, A. Z.; DiRico, K. J.; Johnson, R. P. *J. Am. Chem. Soc.* **1996**, *118*, 4218–4219.

(47) Christl, M.; Fischer, H.; Arnone, M.; Engels, B. *Chem. Eur. J.* **2009**, *15*, 11266–11272.

(48) Balci, M.; Jones, W. M. *J. Am. Chem. Soc.* **1981**, *103*, 2874–2876.

(49) Bergman, R. G.; Rajadhyaksha, V. J. *J. Am. Chem. Soc.* **1970**, *92*, 2163–2164.

(50) Groetsch, S.; Spuziak, J.; Christl, M. *Tetrahedron* **2000**, *56*, 4163–4171.

(51) Miller, B.; Shi, X. *J. Am. Chem. Soc.* **2001**, *109*, 578–579.

(52) Christl, M.; Groetsch, S. *Eur. J. Org. Chem.* **2000**, 1871–1874.

(53) Wittig, G.; Harborth, G. *Chem. Ber.* **1944**, *77*, 306–314.

(54) Scardiglia, F.; Roberts, J. D. *Tetrahedron* **1957**, *1*, 343–344.

(55) Roberts, J. D. *J. Am. Chem. Soc.* **1960**, *82*, 4750–4751.

(56) Montgomery, L. K.; Scardiglia, F.; Roberts, J. D. *J. Am. Chem. Soc.* **1965**, *87*, 1917–1925.

(57) Montgomery, L. K.; Applegate, L. E. *J. Am. Chem. Soc.* **1967**, *89*, 2952–2960.

(58) Montgomery, L. K.; Clouse, A. O.; Crelier, A. M.; Applegate, L. E. *J. Am. Chem. Soc.* **1967**, *89*, 3453–3457.

(59) Bottini, A. T.; Corson, F. P.; Fitzgerald, R.; Frost, I. K. A. *Tetrahedron* **1972**, *28*, 4883–4904.

(60) Wittig, G. *Naturwissenschaften* **1942**, *30*, 696–703.

(61) Roberts, J. D.; Simmons, H. E., Jr.; Carlsmith, L. A.; Vaughan, C. W. *J. Am. Chem. Soc.* **1953**, *75*, 3290–3291.

(62) Caubère, P.; Brunet, J. J. *Tetrahedron Lett.* **1969**, *14,* 3323–3326.

(63) Caubère, P.; Brunet, J. J. *Tetrahedron* **1972**, *28*, 4835–4845.

(64) Caubère, P.; Brunet, J. J. *Tetrahedron* **1972**, *28*, 4847–4857.

(65) Brunet, J. J.; Fixari, B.; Caubère, P. *Tetrahedron* **1974**, *30*, 1237–1243.

(66) Fixari, B.; Brunet, J. J.; Caubère, P. *Tetrahedron* **1976**, *32*, 927–934.

(67) Doering, W. V. E.; Hoffman, A. K. *J. Am. Chem. Soc.* **1954**, *76*, 6162–6165.

(68) Skell, P. S.; Garner, A. Y. *J. Am. Chem. Soc.* **1956**, *78*, 5430–5433.

(69) Doering, W. V. E.; LaFlamme, P. M. *Tetrahedron* **1958**, *2*, 75–79.

(70) Moore, W. R.; Ward, H. R. *J. Org. Chem.* **1960**, *25*, 2073.

(71) Skattebol, L. *Tetrahedron Lett.* **1961**, *5*, 167–172.

(72) Skattebol, L.; Solomon, S. *Org. Synth.* **1969**, *49*, 35–38.

(73) Voukides, A. C.; Cahill, K. J.; Johnson, R. P. *J. Org. Chem.* **2013**, *78*, 11815–11823.

(74) Moore, W. R.; Moser, W. R. *J. Org. Chem.* **1970**, *35*, 908–912.

(75) Harnos, S.; Tivakornpannarai, S.; Waali, E. E. *Tetrahedron Lett.* **1986**, *27*, 3701–3704.

(76) Christl, M.; Braun, M.; Müller, G. *Angew. Chem. Int. Ed. Engl.* **1992**, *31*, 473–476.

(77) Squillacote, M. E.; Sheridan, R. S.; Chapman, O. L.; Anet, F. *J. Am. Chem. Soc.* **1979**, *101*, 3657–3659.

(78) Viehe, H. G.; Janousek, Z.; Merényi, R. *Substituent Effects in Radical Chemistry*; D. Reidel Publishing Company: Dordrecht, Holland, 1986.

(79) Christl, M.; Schreck, M. *Angew. Chem. Int. Ed. Engl.* **1987**, *26*, 449–451.

(80) Bottini, A. T.; Hilton, L. L. *Tetrahedron* **1975**, *31*, 2003–2004.

(81) Kostikov, R.; Molchanov, A.; Hopf, H. *Top. Curr. Chem.* **1990**, *155*, 41–73.

(82) Untch, K. G.; Martin, D. J.; Castellucci, N. T. *J. Org. Chem.* **1965**, *30*, 3572–3573.

(83) Fedoryński, M. *Chem. Rev.* **2003**, *103*, 1099–1132.

(84) Christl, M.; Braun, M.; Fischer, H.; Groetsch, S.; Müller, G.; Leusser, D.; Deuerlein, S.; Stalke, D.; Arnone, M.; Engels, B. *Eur. J. Org. Chem.* **2006**, 5045–5058.

(85) Algi, F.; Ozen, R.; Balci, M. *Tetrahedron Lett.* **2002**, *43*, 3129–3131.

(86) Boyden, F. M. Ph.D. Dissertation, University of the Pacific: Stockton, California, 1969.

(87) Shakespeare, W. C.; Johnson, R. P. *J. Am. Chem. Soc.* **1990**, *112*, 8578–8579.

(88) Quintana, I.; Peña, D.; Pérez, D.; Guitián, E. *Eur. J. Org. Chem.* **2009**, *2009*, 5519–5524.

(89) Dykstra, H. B. *J. Am. Chem. Soc.* **1934**, *56*, 1625–1628.

(90) Blomquist, A. T.; Marvel, C. S. *J. Am. Chem. Soc.* **1933**, *55*, 1655–1662.

(91) Butz, L. W.; Gaddis, A. M.; Butz, E. W.; Davis, R. E. *J. Org. Chem.* **1940**, *5*, 379–388.

(92) Butz, L. W.; Joshel, L. M. *J. Am. Chem. Soc.* **1941**, *63*, 3344–3347.

(93) Butz, L. W.; Joshel, L. M. *J. Am. Chem. Soc.* **1942**, *64*, 1311–1313.

(94) Nudenberg, W.; Butz, L. W. *J. Am. Chem. Soc.* **1943**, *65*, 2059–2060.

(95) Butz, L. W.; Gaddis, A. M.; Butz, E. W. *J. Am. Chem. Soc.* **1947**, *69*, 924–925.

(96) Joshel, L. M.; Butz, L. W.; Feldman, J. *J. Am. Chem. Soc.* **1941**, *63*, 3348–3349.

(97) Danheiser, R. L.; Gould, A. E.; Fernandez de la Pradilla, R.; Helgason, A. L. *J. Org. Chem.* **1994**, *59*, 5514–5515.

(98) Robinson, J. M.; Tlais, S. F.; Fong, J.; Danheiser, R. L. *Tetrahedron* **2011**, *67*, 9890–9898.

(99) Hayes, M. E.; Shinokubo, H.; Danheiser, R. L. *Org. Lett.* **2005**, *7*, 3917–3920.

(100) Werstiuk, N. H.; Roy, C. D.; Ma, J. *Can. J. Chem.* **1996**, *74*, 1903–1905.

(101) Hopf, H.; Musso, H. *Angew. Chem. Int. Ed. Engl.* **1969**, *8*, 680–680.

(102) Scott, L. T.; Hashemi, M. M.; Meyer, D. T.; Warren, H. B. *J. Am. Chem. Soc.* **1991**, *113*, 7082–7084.

(103) Rabideau, P. W.; Abdourazak, A. H.; Folsom, H. E.; Marcinow, Z.; Sygula, A.; Sygula, R. *J. Am. Chem. Soc.* **1994**, *116*, 7891–7892.

(104) Brown, R. F. C.; Harrington, K. J.; McMullen, G. L. *J. Chem. Soc., Chem. Commun.* **1974**, 123.

(105) Hopf, H.; Berger, H.; Zimmermann, G.; Nüchter, U.; Jones, P. G.; Dix, I. *Angew. Chem. Int. Ed. Engl.* **1997**, *36*, 1187–1190.

(106) Kitaguchi, H.; Ohkubo, K.; Ogo, S.; Fukuzumi, S. *J. Am. Chem. Soc.* **2005**, *127*, 6605–6609.

(107) Fernández-Zertuche, M.; Hernández-Lamoneda, R.; Ramírez-Solís, A. *J. Org.*

Chem. **2000**, *65*, 5207–5211.

(108) Moore, H. W.; Decker, O. H. *Chem. Rev.* **1986**, *86*, 821–830.

(109) Chow, K.; Van, N. N.; Moore, H. W. *J. Org. Chem.* **1990**, *55*, 3876–3880.

(110) Perri, S. T.; Foland, L. D.; Decker, O. H.; Moore, H. W. *J. Org. Chem.* **1986**, *51*, 3067–3068.

(111) Karlsson, J. O.; Nguyen, N. V.; Foland, L. D.; Moore, H. W. *J. Am. Chem. Soc.* **1985**, *107*, 3392–3393.

(112) Fernandez, M.; Hernandez, R.; Ramirez, A.; Ordonez, M. *J. Mex. Chem. Soc.* **2002,** *46,* 136-139.

(113) Angus, R. O. J.; Johnson, R. P. *J. Org. Chem.* **1984**, *49*, 2880–2883.

(114) Moore, H. W.; Chow, K.; Nguyen, N. V. *J. Org. Chem.* **1987**, *52*, 2530–2537.

(115) Xiong, Y.; Xia, H.; Moore, H. W. *J. Org. Chem.* **1995**, *60*, 6460–6467.

(116) Xiong, Y.; Moore, H. W. *J. Org. Chem.* **1996**, *61*, 9168–9177.

(117) Freeman, P. K.; Swenson, K. E. *J. Org. Chem.* **1982**, *47*, 2033–2039.

(118) Klumpp, G. W.; van Dijk, P. M. *Recl. Trav. Chim. Pays B.* **1971**, *90*, 381–384.

(119) Wehage, H.; Heesing, A. *Chem. Ber.* **1992**, *125*, 209–215.

(120) Hartwig, J. F., Ed. *Organotransition Metal Chemistry*; Univ Science Books: Sausalito, CA., 2010.

(121) Masai, H.; Sonogashira, K.; Hagihara, N. *Bull. Chem. Soc. Jpn.* **1968**, *41*, 750–751.

(122) Kolomnikov, I. S.; Loveeva, T. S.; Gorbachevskaya, V. V.; Aleksandrov, G. G.; Struckhov, Y. T.; Vol'pin, M. E. *J. Chem. Soc. D* **1971**, 972.

(123) Boekel, C. P.; Teuben, J. H.; de Liefde Meijer, H. J. *J. Organomet. Chem.* **1975**, *102*, 161–165.

(124) Boekel, C. P.; Teuben, J. H.; de Liefde Meijer, H. J. *J. Organomet. Chem.* **1974**, *81*, 371–377.

(125) Buchwald, S. L.; Lum, R. T.; Dewan, J. C. *J. Am. Chem. Soc.* **1986**, *108*, 7441–7442.

(126) Buchwald, S. L.; Nielsen, R. B. *Chem. Rev.* **1988**, *88*, 1047–1058.

(127) Yin, J.; Abboud, K. A.; Jones, W. M. *J. Am. Chem. Soc.* **1993**, *115*, 3810–3811.

(128) Yin, J.; Jones, W. M. *Tetrahedron* **1995**, *51*, 4395–4406.

Chapter 2

(1) Schönbein, C. F. *Ber. Verh. Nat. Ges. Basel* **1847**, *7*, 4–7.

(2) Gothelf, K. V.; Jørgensen, K. A. *Chem. Rev.* **1998**, *98*, 863–910.

(3) Padwa, A.; Carter, S. P.; Chiacchio, U.; Kline, D. N. *Tetrahedron Lett.* **1986**, *27*, 2683–2686.

(4) Hayakawa, K.; Nishiyama, H.; Kanematsu, K. *J. Org. Chem.* **1985**, *50*, 512–517.

(5) Pinho e Melo, T. M. *Curr. Org. Chem.* **2009**, *13*, 1406–1431.

(6) Kolb, H. C.; Finn, M. G.; Sharpless, K. B. *Angew. Chem. Int. Ed. Engl.* **2001**, *40*, 2004–2021.

(7) Baskin, J. M.; Prescher, J. A.; Laughlin, S. T.; Agard, N. J.; Chang, P. V.; Miller, I. A.; Lo, A.; Codelli, J. A.; Bertozzi, C. R. *Proc. Natl. Acad. Sci. U S A* **2007**, *104*, 16793–16797.

(8) Ried, W.; Mengler, H. *Justus Liebigs Ann. Chem.* **1964**, *678*, 95–113.

(9) Bleiholder, R. F.; Schecter, H. *J. Am. Chem. Soc.* **1968**, *90*, 2131–2137.

(10) Wedegaertner, D. K.; Kattak, R. K.; Harrison, I.; Cristie, S. K. *J. Org. Chem.* **1991**, *56*, 4463–4467.

(11) Feldman, K. S.; Iyer, M. R. *J. Am. Chem. Soc.* **2005**, *127*, 4590–4591.

(12) López, C. S.; Faza, O. N.; Feldman, K. S.; Iyer, M. R.; Hester, D. K. *J. Am. Chem. Soc.* **2007**, *129*, 7638–7646.

(13) Padwa, A.; Craig, S. P.; Chiacchio, U.; Kline, D. N. *J. Org. Chem.* **1988**, *53*, 2232–2238.

(14) Beltrame, P.; Beltrame, P. L.; Cattania, M. G.; Zecchi, G. *J. Chem. Soc., Perkin Trans. 2* **1974**, 1301.

(15) Broggini, G.; Molteni, G. *J. Chem. Soc., Perkin Trans. 1* **2000**, 1685–1689.

(16) Braverman, S.; Mechoulam, H. *Isr. J. Chem.* **1967**, *5*, 71–74.

(17) Stirling, C. J. M. *Chem. Commun. (London)* **1967**, 131.

(18) Blackwell, G. B.; Haszeldine, R. N.; Taylor, D. R. *J. Chem. Soc., Perkin Trans. 1* **1983**, 1–5.

(19) Houk, K. N.; Sims, J.; Duke, R. E.; Strozier, R. W.; George, J. K. *J. Am. Chem. Soc.* **1973**, *95*, 7287–7301.

(20) Houk, K. N.; Sims, J.; Watts, C. R.; Luskus, L. J. *J. Am. Chem. Soc.* **1973**, *95*,

7301–7315.

(21) Dolbier, W. R., Jr; Burkholder, C. R.; Winchester, W. R. *J. Org. Chem.* **1984**, *49*, 1518–1522.

(22) Dolbier, W. R.; Wicks, G. E.; Burkholder, C. R. *J. Org. Chem.* **1987**, *52*, 2196–2201.

(23) Dolbier, W. R., Jr; Purvis, G. D., III; Seabury, M. J.; Wicks, G. E.; Burkholder, C. R. *Tetrahedron* **1989**, *46*, 7991–8004.

(24) Padwa, A.; Bullock, W. H.; Kline, D. N.; Perumattam, J. *J. Org. Chem.* **1989**, *54*, 2862–2869.

(25) Dugovič, B.; Fišera, L.; Reißig, H.-U. *Eur. J. Org. Chem.* **2008**, 277–284.

(26) Balci, M.; Jones, W. M. *J. Am. Chem. Soc.* **1980**, *102*, 7607–7608.

(27) Johnson, R. P. *Chem. Rev.* **1989**, *89*, 1111–1124.

(28) Christl, M. in *Modern Allene Chemistry, Vol. 1* (Eds. N. Krause, A. S. K. Hashmi), Wiley–VCH Verlag: Weinheim, **2004**, pp. 243–357.

(29) Wittig, G.; Fritze, P. *Angew. Chem. Int. Ed.* **1966**, *5*, 846.

(30) Shakespeare, W. C.; Johnson, R. P. *J. Am. Chem. Soc.* **1990**, *112*, 8578–8579.

(31) Quintana, I.; Peña, D.; Pérez, D.; Guitián, E. *Eur. J. Org. Chem.* **2009**, 5519–5524.

(32) Wittig, G.; Fritze, P. *Liebigs Ann. Chem.* **1968**, *711*, 82–87.

(33) Hanessian, S.; Tyler, P. C.; Chapleur, Y. *Tetrahedron Lett.* **1981**, *22*, 4583–4586.

(34) Chorannat, J. A.; Mitchell, A. L.; Keogh, B. P. *Tetrahedron Lett.* **1990**, *31*, 315–318.

(35) Jastrzebski, J. T. B. H.; von Koten, G. Structures and Reactivities of Organocopper Compounds. In *Modern Organocopper Chemistry*; Krause, N., Ed.; Wiley-VCH Verlag GmbH: Weinheim, **2002**; Vol. 1; pp. 1-44.

(36) Piers, E.; de Waal, W.; Britton, R. W. *J. Am. Chem. Soc.* **1971**, *93*, 5113–5120.

(37) Marshall, J. A.; Hochstetler, A. R. *J. Am. Chem. Soc.* **1969**, *91*, 648–657.

(38) MacKenzie, D. A.; Sherratt, A. R.; Chigrinova, M.; Cheung, L. L.; Pezacki, J. P. *Curr. Op. Chem. Bio.* **2014**, *21*, 81–88.

(39) Dubrovskiy, A. V.; Larock, R. C. *Org. Lett.* **2010**, *12*, 1180–1183.

(40) Christl, M.; Fischer, H.; Arnone, M.; Engels, B. *Chem. Eur. J.* **2009**, *15*, 11266–

11272.

(41) Christl, M.; Braun, M.; Fischer, H.; Groetsch, S.; Müller, G.; Leusser, D.; Deuerlein, S.; Stalke, D.; Arnone, M.; Engels, B. *Eur. J. Org. Chem.* **2006**, 5045–5058.

(42) Balci, M.; Jones, W. M. *J. Am. Chem. Soc.* **1981**, *103*, 2874–2876.

(43) Schmidt, M. W.; Angus, R. O.; Johnson, R. P. *J. Am. Chem. Soc.* **1982**, *104*, 6838–6839.

(44) Angus, R. O., Jr; Schmidt, M. W.; Johnson, R. P. *J. Am. Chem. Soc.* **1985**, *107*, 532–537.

(45) Engels, B.; Schöneboom, J. C.; Münster, A. F.; Groetsch, S.; Christl, M. *J. Am. Chem. Soc.* **2002**, *124*, 287–297.

(46) Daoust, K. J.; Hernandez, S. M.; Konrad, K. M.; Mackie, I. D.; Winstanley, J.; Johnson, R. P. *J. Org. Chem.* **2006**, *71*, 5708–5714.

(47) Werstiuk, N. H.; Roy, C. D.; Ma, J. *Can. J. Chem.* **1996**, *74*, 1903–1905.

(48) Nendel, M.; Tolbert, L. M.; Herring, L. E.; Islam, M. N.; Houk, K. N. *J. Org. Chem.* **1999**, *64*, 976–983.

(49) Dorn, H.; Otto, A. *Chem. Ber.* **1968**, *101*, 3287–3301.

(50) Dorn, H.; Otto, A. *Angew. Chem. Int. Ed. Engl.* **1968**, *7*, 214–215.

(51) Murahashi, S.-I.; Shiota, T. *Tetrahedron Lett.* **1987**, *28*, 2383–2386.

(52) Shintani, R.; Fu, G. C. *J. Am. Chem. Soc.* **2003**, *125*, 10778–10779.

(53) Moore, W. R.; Moser, W. R. *J. Org. Chem.* **1970**, *35*, 908–912.

(54) Huisgen, R.; Szeimies, G.; Möbius, L. *Chem. Ber.* **1967**, *100*, 2494–2507.

(55) Caubère, P. *Top. Curr. Chem.* **1978**, *73*, 49–103.

(56) Jimeno, C.; Renaud, P. In *Organic Azides: Syntheses and Applications*; Brase, S.; Banert, K., Eds.; John Wiley & Sons, Inc., Publication, 2010; pp. 239–267.

(57) Fleming, I. *Molecular Orbitals and Organic Chemical Reactions*; John Wiley & Sons, Inc., New York, 2011.

(58) Christl, M.; Schreck, M. *Chem. Ber.* **1987**, *120*, 915–920.

(59) Waali, E. E.; Jones, W. M. *J. Am. Chem. Soc.* **1973**, *95*, 8114–8118.

(60) Previous experience with synthesizing and isolating pyrrole products allowed the tentative assumption that the product was forming by TLC. [1] The R_f of the

product, [2] the spot assumed to be the product turned bright red immediately upon exposure to anisaldehyde stain.

(61) Agosta, W. C.; Lowrance, J. W. W. *J. Org. Chem.* **1970**, *35*, 3851–3856.

(62) Neises, B.; Steglich, W. *Angew. Chem. Int. Ed. Engl.* **1978**, *17*, 522–524.

(63) Kobayashi, Y.; Feng, C.; Ikoma, A.; Ogawa, N.; Hirotsu, T. *Org. Lett.* **2014**, *16*, 760–763.

(64) Moore, H. W.; Decker, O. H. *Chem. Rev.* **1986**, *86*, 821–830.

(65) Saulnier, M. G.; Kadow, J. F.; Tun, M. M.; Langley, D. R.; Vyas, D. M. *J. Am. Chem. Soc.* **1989**, *111*, 8320–8321.

(66) Bode, J. W.; Hachisu, Y.; Matsuura, T.; Suzuki, K. *Tetrahedron Lett.* **2003**, *44*, 3555–3558.

(67) Moore, W. R.; Moser, W. R. *J. Am. Chem. Soc.* **1970**, *92*, 5469–5474.

(68) Tornøe, C. W.; Christensen, C.; Meldal, M. *J. Org. Chem.* **2002**, *67*, 3057–3064.

(69) Takeuchi, H.; Yanagida, S.; Ozaki, T.; Hagiwara, S.; Eguchi, S. *J. Org. Chem.* **1989**, *54*, 431–434.

(70) Tamura, Y.; Yoshimura, Y.; Kita, Y. *Chem. Pharm. Bull.* **1972**, *20*, 871–875.

(71) Hassner, A.; Fowler, F. W. *J. Org. Chem.* **1968**, *33*, 2686–2691.

(72) George, M. V.; Peterson, D. J.; Gilman, H. *J. Am. Chem. Soc.* **1960**, *82*, 403–406.

(73) Yoshida, Y.; Sakakura, Y.; Aso, N.; Okada, S.; Tanabe, Y. *Tetrahedron* **1999**, *55*, 2183–2192.

(74) Still, W. C.; Kahn, M.; Mitra, A. *J. Org. Chem.* **1978**, *43*, 2923–2925.

Chapter 3

(1) American Institute of Physics. *Encyclopedia of Applied Physics*; Wiley-VCH, 1998.

(2) Bock, H.; Hirabayashi, T.; Mohmand, S. *Chem. Ber.* **1981**, *114*, 2595–2608.

(3) Moore, W. R.; Moser, W. R. *J. Am. Chem. Soc.* **1970**, *92*, 5469–5474.

(4) Christl, M. in *Modern Allene Chemistry, Vol. 1* (Eds. N. Krause, A. S. K. Hashmi), Wiley–VCH Verlag: Weinheim, **2004**, pp. 243–357.

(5) Werstiuk, N. H.; Roy, C. D.; Ma, J. *Can. J. Chem.* **1996**, *74*, 1903–1905.

(6) Werstiuk, N. H.; Roy, C. D.; Ma, J. *Can. J. Chem.* **1994**, *72*, 2537–2539.

(7) Balci, M.; Jones, W. M. *J. Am. Chem. Soc.* **1980**, *102*, 7607–7608.

(8) Engels, B.; Schöneboom, J. C.; Münster, A. F.; Groetsch, S.; Christl, M. *J. Am. Chem. Soc.* **2002**, *124*, 287–297.

(9) Schmidt, M. W.; Angus, R. O.; Johnson, R. P. *J. Am. Chem. Soc.* **1982**, *104*, 6838–6839.

(10) Balci, M.; Jones, W. M. *J. Am. Chem. Soc.* **1981**, *103*, 2874–2876.

(11) Christl, M.; Braun, M.; Fischer, H.; Groetsch, S.; Müller, G.; Leusser, D.; Deuerlein, S.; Stalke, D.; Arnone, M.; Engels, B. *Eur. J. Org. Chem.* **2006**, 5045–5058.

(12) Christl, M.; Fischer, H.; Arnone, M.; Engels, B. *Chem. Eur. J.* **2009**, *15*, 11266–11272.

(13) Moore, W. R.; Moser, W. R. *J. Org. Chem.* **1970**, *35*, 908–912.

(14) Denmark, S. E.; Wallace, M. A.; Walker, C. B., Jr. *J. Org. Chem.* **1990**, *55*, 5543–5545.

(15) Corey, E. J.; Bakshi, R. K.; Shibata, S.; Chen, C. P.; Singh, V. K. *J. Am. Chem. Soc.* **1987**, *109*, 7925–7926.

(16) Fleming, I. *e-EROS Encyclopedia Of Reagents for Organic Synthesis* **2009**, 1–3.

(17) Fleming, I.; Terrett, N. K. *J. Organomet. Chem.* **1984**, *264*, 99–118.

(18) Jastrzebski, J. T. B. H.; von Koten, G. Structures and Reactivities of Organocopper Compounds. In *Modern Organocopper Chemistry*; Krause, N., Ed.; Wiley-VCH Verlag GmbH: Weinheim, **2002**; Vol. 1; pp. 1-44.

(19) Gallina, C.; Ciattini, P. G. *J. Am. Chem. Soc.* **1979**, *101*, 1035–1036.

(20) Breit, B.; Demel, P. Copper-mediated Diastereoselective Conjugate Addition and Allylic Substitution Reactions. In *Modern Organocopper Chemistry*; Krause, N., Ed.; Wiley-VCH Verlag GmbH: Weinheim, **2002**; Vol. 1; pp. 188-223.

(21) Kobayashi, Y.; Feng, C.; Ikoma, A.; Ogawa, N.; Hirotsu, T. *Org. Lett.* **2014**, *16*, 760–763.

(22) Special Acknowledgement to Mr. Ed Fu and Professor Dennis Hall for the use of their Chiral HPLC machine, as well as for the training required to use the machine.

(23) Nendel, M.; Tolbert, L. M.; Herring, L. E.; Islam, M. N.; Houk, K. N. *J. Org. Chem.* **1999**, *64*, 976–983.

(24) Christl, M.; Schreck, M.; Fischer, T.; Rudolph, M.; Moigno, D.; Fischer, H.; Deuerlein, S.; Stalke, D. *Chem. Eur. J.* **2009**, *15*, 11256–11265.

(25) Bottini, A. T.; Hilton, L. L.; Plott, J. *Tetrahedron* **1975**, *31*, 1997–2001.

(26) Anslyn, E. V.; Dougherty, D. A. *Modern Physical Organic Chemistry.* University Science: Sausalito, CA, **2006**.

(27) Jensen, F. R.; Bushweller, C. H. *J. Am. Chem. Soc.* **1969**, *91*, 5774–5782.

(28) Christl, M.; Schreck, M. *Chem. Ber.* **1987**, *120*, 915–920.

(29) Hammond, G. S. *J. Am. Chem. Soc.* **1955**, *77*, 334–338.

(30) Hodgson, D. M.; Galano, J. M. *Org. Lett.* **2005**, *7*, 2221–2224.

(31) White, J. D.; Choi, Y. *Org. Lett.* **2000**, *2*, 2373–2376.

(32) Bartlett, M. F.; Dickel, D. F.; Taylor, W. I. *J. Am. Chem. Soc.* **1958**, *80*, 126–136.

(33) Taylor, E. C.; Davies, H. M. L.; Clemens, R. J.; Yanagisawa, H.; Haley, N. F. *J. Am. Chem. Soc.* **1981**, *103*, 7660–7661.

(34) Saulnier, M. G.; Kadow, J. F.; Tun, M. M.; Langley, D. R.; Vyas, D. M. *J. Am. Chem. Soc.* **1989**, *111*, 8320–8321.

(35) Nicolaou, K. C.; Ding, H.; Richard, J.-A.; Chen, D. Y. K. *J. Am. Chem. Soc.* **2010**, *132*, 3815–3818.

(36) Hansson, M.; Arvidsson, P. I.; Lill, S. O. N.; Ahlberg, P. *J. Chem. Soc., Perkin Trans. 2 VL* - **2002**, 763–767.

(37) George, M. V.; Peterson, D. J.; Gilman, H. *J. Am. Chem. Soc.* **1960**, *82*, 403–406.

(38) Corey, E. J.; Bakshi, R. K.; Shibata, S. *J. Am. Chem. Soc.* **1987**, *109*, 5551–5553.

(39) Heerding, D. A.; Hong, C. Y.; Kado, N.; Look, G. C.; Overman, L. E. *J. Org. Chem.* **1993**, *58*, 6947–6948.

(40) Still, W. C.; Kahn, M.; Mitra, A. *J. Org. Chem.* **1978**, *43*, 2923–2925.

Chapter 4

(1) Hughes, E. D.; Ingold, C. K. *J. Chem. Soc.* **1935**, 244.

(2) Moore, H. W.; Decker, O. H. *Chem. Rev.* **1986**, *86*, 821–830.

(3) Fernandez, M.; Hernandez, R.; Ramirez, A.; Ordonez, M. *Rev. Soc. Quim. Mex.* **2002,** *46*, 136–139.

(4) Perri, S. T.; Foland, L. D.; Decker, O. H.; Moore, H. W. *J. Org. Chem.* **1986**, *51*, 3067–3068.

(5) Moore, H. W.; Chow, K.; Nguyen, N. V. *J. Org. Chem.* **1987**, *52*, 2530–2537.

(6) Xiong, Y.; Xia, H.; Moore, H. W. *J. Org. Chem.* **1995**, *60*, 6460–6467.

(7) Xiong, Y.; Moore, H. W. *J. Org. Chem.* **1996**, *61*, 9168–9177.

(8) Hopf, H.; Berger, H.; Zimmermann, G.; Nüchter, U.; Jones, P. G.; Dix, I. *Angew. Chem. Int. Ed. Engl.* **1997**, *36*, 1187–1190.

(9) Brook, A. G. *Acc. Chem. Res.* **1974**, *7*, 77–84.

(10) Fernández-Zertuche, M.; Hernández-Lamoneda, R.; Ramírez-Solís, A. *J. Org. Chem.* **2000**, *65*, 5207–5211.

(11) Christl, M.; Schreck, M.; Fischer, T.; Rudolph, M.; Moigno, D.; Fischer, H.; Deuerlein, S.; Stalke, D. *Chem. Eur. J.* **2009**, *15*, 11256–11265.

(12) Daoust, K. J.; Hernandez, S. M.; Konrad, K. M.; Mackie, I. D.; Winstanley, J.; Johnson, R. P. *J. Org. Chem.* **2006**, *71*, 5708–5714.

(13) Brown, H. C.; Zweifel, G. *J. Am. Chem. Soc.* **1959**, *81*, 247–247.

(14) Compounds **72–79** were synthesized and characterized by Mr. Kyle McIntosh as part of a CHEM401/403 class.

(15) Christl, M.; Braun, M.; Müller, G. *Angew. Chem. Int. Ed. Engl.* **1992**, *31*, 473–476.

(16) Mr. Kyle McIntosh carried out this particular work as a CHEM401/403 project.

(17) Wittig, G.; Fritze, P. *Angew. Chem. Int. Ed.* **1966**, *5*, 846.

(18) Wittig, G.; Fritze, P. *Liebigs Ann. Chem.* **1968**, *711*, 82–87.

(19) Bottini, A. T.; Hilton, L. L.; Plott, J. *Tetrahedron* **1975**, *31*, 1997–2001.

(20) Christl, M.; Braun, M.; Fischer, H.; Groetsch, S.; Müller, G.; Leusser, D.; Deuerlein, S.; Stalke, D.; Arnone, M.; Engels, B. *Eur. J. Org. Chem.* **2006**, 5045–5058.

(21) Schlindwein, H.-J.; Himbert, G. *Chem. Ber.* **1989**, *122*, 2331–2339.

(22) Kurtz, P.; Gold, H.; Disselnkötter, H. *Justus Liebigs Ann. Chem.* **1959**, *624*, 1–25.

(23) Kozikowski, A. P.; Floyd, W. C.; Kuniak, M. P. *J. Chem. Soc., Chem. Commun.* **1977**, 582.

(24) Hayakawa, K.; Yamaguchi, Y.; Kanematsu, K. *Tetrahedron Lett.* **1985**, *26*, 2689–2692.

(25) Padwa, A.; Haffmanns, G.; Tomas, M. *Tetrahedron Lett.* **1983**, *24*, 4303–4306.

(26) Padwa, A.; Haffmanns, G.; Tomas, M. *J. Org. Chem.* **1984**, *49*, 3314–3322.

(27) Beesley, R. M.; Ingold, C. K.; Thorpe, J. F. *J. Chem. Soc., Trans.* **1915**, *107*, 1080–1106.

(28) **2002**, 1–36.

(29) Saulnier, M. G.; Kadow, J. F.; Tun, M. M.; Langley, D. R.; Vyas, D. M. *J. Am. Chem. Soc.* **1989**, *111*, 8320–8321.

(30) Choi, I.; Kim, Y.-K.; Min, D.-H.; Lee, S.; Yeo, W.-S. *J. Am. Chem. Soc.* **2011**, *133*, 16718–16721.

(31) Arena, G.; Cali, R.; Maccarone, E.; Passerini, A. *J. Chem. Soc., Perkin Trans. 2* **1993**, 1941–1945.

(32) Shepherd, R. G.; White, A. C. *J. Chem. Soc., Perkin Trans. 1* **1987**, 2153–2155.

(33) Beaulieu, P.; Ogilvie, W. W. *Tetrahedron Lett.* **2003**, *44*, 8883–8885.

(34) Kerr, W. J.; Morrison, A. J.; Pazicky, M.; Weber, T. *Org. Lett.* **2012**, *14*, 2250–2253.

(35) Naud, S.; Macnaughton, S. J.; Dyson, B. S.; Woollaston, D. J.; Dallimore, J. W. P.; Robertson, J. *Org. Biomol. Chem.* **2012**, *10*, 3506–3518.

(36) Föhlisch, B.; Herter, R. *Chem. Ber.* **1984**, *117*, 2580–2596.

(37) George, M. V.; Peterson, D. J.; Gilman, H. *J. Am. Chem. Soc.* **1960**, *82*, 403–406.

Chapter 5

(1) International Energy Agency. *Oil Medium-term Market Report 2012*; 2012.

(2) *Strausz, O. P.;* Lown, E. M., *The Chemistry of Alberta Oil Sands Bitumens and Heavy Oils*; Alberta Energy: Calgary; 2003, 1-695.

(3) Wang, J.; Buckley, J. *J. Disper. Sci. Technol.* **2007**, *28*, 425–430.

(4) Qian, K.; Edwards, K. E.; Siskin, M.; Olmstead, W. N.; Mennito, A. S.; Dechert, G. J.; Hoosain, N. E. *Energ. Fuel.* **2007**, *21*, 1042–1047.

(5) Groenzin, H.; Mullins, O. C. *Energ. Fuel.* **2000**, *14*, 677–684.

(6) Jaffe, S. B.; Freund, H.; Olmstead, W. N. *Ind. Eng. Chem. Res.* **2005**, *44*, 9840–9852.

(7) Kuznicki, T.; Masliyah, J. H.; Bhattacharjee, S. *Energ. Fuel.* **2008**, *22*, 2379–2389.

(8) Andersen, S. I.; Birdi, K. S. *J. Colloid Interf. Sci.* **1991**, *142*, 497–502.

(9) Strausz, O. P.; Safarik, I.; Lown, E. M.; Morales-Izquierdo, A. *Energ. Fuel.* **2008**, *22*, 1156–1166.

(10) Scholl, R.; Seer, C.; Weitzenböck, R. *Chem. Ber.* **1910**, *43*, 2202–2209.

(11) Müller, M.; Mauermann-Düll, H.; Wagner, M.; Enkelmann, V.; Müllen, K. *Angew. Chem. Int. Ed. Engl.* **1995**, *34*, 1583–1586.

(12) Müller, M.; Petersen, J.; Strohmaier, R.; Günther, C.; Karl, N.; Müllen, K. *Angew. Chem. Int. Ed. Engl.* **1996**, *35*, 886–888.

(13) Müller, M.; Iyer, V. S.; Kübel, C.; Enkelmann, V.; Müllen, K. *Angew. Chem. Int. Ed. Engl.* **1997**, *36*, 1607–1610.

(14) Iyer, V. S.; Wehmeier, M.; Brand, J. D.; Keegstra, M. A.; Müllen, K. *Angew. Chem. Int. Ed. Engl.* **1997**, *36*, 1604–1607.

(15) Müller, M.; Kübel, C.; Müllen, K. *Chem. Eur. J.* **1998**, *4*, 2099–2109.

(16) Rakotondradany, F.; Fenniri, H.; Rahimi, P.; Gawrys, K. L.; Kilpatrick, P. K.; Gray, M. R. *Energ. Fuel.* **2006**, *20*, 2439–2447.

(17) Mullins, O. C.; Sabbah, H.; Eyssautier, J.; Pomerantz, A. E.; Barré, L.; Andrews, A. B.; Ruiz-Morales, Y.; Mostowfi, F.; McFarlane, R.; Goual, L.; Lepkowicz, R.; Cooper, T.; Orbulescu, J.; Leblanc, R. M.; Edwards, J.; Zare, R. N. *Energ. Fuel.* **2012**, *26*, 3986–4003.

(18) Sabbah, H.; Morrow, A. L.; Pomerantz, A. E.; Zare, R. N. *Energ. Fuel.* **2011**, *25*,

1597–1604.

(19) Sharma, A.; Groenzin, H.; Tomita, A.; Mullins, O. C. *Energ. Fuel.* **2002**, *16*, 490–496.

(20) Scotti, R.; Montanari, L. Molecular Structure and Intermolecular Interaction of Asphaltenes by NMR, IR, and ESR. In *Structures and Dynamics of Asphaltenes*; Mullins, O. C.; Sheu, E. Y., Eds.; Springer-Verlag GmbH, Heidelberg, **1998**; 79–114.

(21) Ruiz-Morales, Y.; Mullins, O. C. *Energ. Fuel.* **2009**, *23*, 1169–1177.

(22) Klee, T.; Masterson, T.; Miller, B.; Barrasso, E.; Bell, J.; Lepkowicz, R.; West, J.; Haley, J. E.; Schmitt, D. L.; Flikkema, J. L.; Cooper, T. M.; Ruiz-Morales, Y.; Mullins, O. C. *Energ. Fuel.* **2011**, *25*, 2065–2075.

(23) Buckley, J.; Wang, J.; Creek, J., Solubility of the Least-Soluble Asphaltenes. In *Asphaltenes, Heavy Oils, And Petroleomics*; Mullins, O.; Sheu, E.; Hammami, A.; Marshall, A., Eds.; Springer New York, **2007**; pp. 401–437.

(24) Buckley, J. S.; Hirasaki, G. J.; Liu, Y.; Drasek, Von, S.; Wang, J.-X.; Gill, B. S. *Pet. Sci. Technol.* **1998**, *16*, 251–285.

(25) Sabbah, H.; Morrow, A. L.; Pomerantz, A. E.; Mullins, O. C.; Tan, X.; Gray, M. R.; Azyat, K.; Tykwinski, R. R.; Zare, R. N. *Energ. Fuel.* **2010**, *24*, 3589–3594.

(26) Tan, X.; Fenniri, H.; Gray, M. R. *Energ. Fuel.* **2008**, *22*, 715–720.

(27) Karimi, A.; Qian, K.; Olmstead, W. N.; Freund, H.; Yung, C.; Gray, M. R. *Energ. Fuel.* **2011**, *25*, 3581–3589.

(28) Personal correspondance with Professor Murray R. Gray, Department of Chemical and Materials Engineering, University of Alberta.

(29) Alshareef, A. H.; Scherer, A.; Tan, X.; Azyat, K.; Stryker, J. M.; Tykwinski, R. R.; Gray, M. R. *Energ. Fuel.* **2011**, *25*, 2130–2136.

(30) Diner, C.; Scott, D. E.; Tykwinski, R. R.; Gray, M. R.; Stryker, J. M. *J. Org. Chem.* **2015**, *80*, 1719–1726.

(31) LeBoeuf, D.; Gandon, V.; Malacria, M. In *Handbook of cyclization reactions*; Wiley-VCH: Weinheim, 2010; pp. 367–406.

(32) Lautens, M.; Klute, W.; Tam, W. *Chem. Rev.* **1996**, *96*, 49–92.

(33) Chopade, P. R.; Louie, J. *Adv. Synth. Catal.* **2006**, *348*, 2307–2327.

(34) Nakamura, I.; Yamamoto, Y. *Chem. Rev.* **2004**, *104*, 2127–2198.

(35) Domínguez, G.; Pérez-Castells, J. *Chem. Soc. Rev.* **2011**, *40*, 3430–3444.

(36) Kumar, P.; Prescher, S.; Louie, J. *Angew. Chem. Int. Ed.* **2011**, *50*, 10694–10698.

(37) Brown, C. A.; Yamashita, A. *J. Am. Chem. Soc.* **1975**, *97*, 891–892.

(38) Hoye, R. C.; Baigorria, A. S.; Danielson, M. E.; Pragman, A. A.; Rajapakse, H. A. *J. Org. Chem.* **1999**, *64*, 2450–2453.

(39) Cheng, J.; Sun, Y.; Wang, F.; Guo, M.; Xu, J.-H.; Pan, Y.; Zhang, Z. *J. Org. Chem.* **2004**, *69*, 5428–5432.

(40) Taskinen, E.; Lindholm, N. *J. Phys. Org. Chem.* **1994**, *7*, 256–258.

(41) Colbon, P.; Ruan, J.; Purdie, M.; Mulholland, K.; Xiao, J. *Org. Lett.* **2011**, *13*, 5456–5459.

(42) Muzart, J. *Tetrahedron* **2005**, *61*, 4179–4212.

(43) Jeffery, T. *J. Chem. Soc., Chem. Commun.* **1984**, 1287–1289.

(44) Larock, R. C.; Leung, W.-Y.; Stolz-Dunn, S. *Tetrahedron Lett.* **1989**, *30*, 6629–6632.

(45) Heck, R. F. *J. Am. Chem. Soc.* **1968**, *90*, 5526–5531.

(46) Amatore, C.; Jutand, A.; Suarez, A. *J. Am. Chem. Soc.* **1993**, *115*, 9531–9541.

(47) Roy, A. H.; Hartwig, J. F. *Organometallics* **2004**, *23*, 194–202.

(48) Corey, E. J.; Fuchs, P. L. *Tetrahedron Lett.* **1972**, *13*, 3769–3772.

(49) Seyferth, D.; Marmor, R. S.; Hilbert, P. *J. Org. Chem.* **1971**, *36*, 1379–1386.

(50) Müller, S.; Liepold, B.; Roth, G. J.; Bestmann, H. J. *Synlett* **1996**, 521–522.

(51) Fritsch, P. *Justus Liebigs Ann. Chem.* **1894**, *279*, 319–323.

(52) Buttenberg, W. P. *Justus Liebigs Ann. Chem.* **1894**, *279*, 324–337.

(53) Wiechell, H. *Justus Liebigs Ann. Chem.* **1894**, *279*, 337–344.

(54) Roth, G.; Liepold, B.; Müller, S.; Bestmann, H. *Synthesis* **2004**, 59–62.

(55) Gawley, R. E. The Beckmann Reactions: Rearrangements, Eliminations-Additions, Fragmentations, and Rearrangement-Cyclizations. In *Organic Reactions*; John Wiley & Sons, Inc.: New York; **2004,** 1-406.

(56) Chakraborti, A. K.; Kaur, G. *Tetrahedron* **1999**, *55*, 13265–13268.

(57) Bowden, K.; Cook, R. S. *J. Chem. Soc., Perkin Trans. 2* **1972**, 1407–1411.

(58) Takahashi, T.; Li, S.; Huang, W.; Kong, F.; Nakajima, K.; Shen, B.; Ohe, T.;

Kanno, K.-I. *J. Org. Chem.* **2006**, *71*, 7967–7977.

(59) Brandsma, L. *Preparative Acetylenic Chemistry*. 1st ed.; Elsevier: Amsterdam, **1988,** 1-321.

(60) Zou, Y.; Young, D. D.; Cruz-Montanez, A.; Deiters, A. *Org. Lett.* **2008**, *10*, 4661–4664.

(61) Schnieders, C.; Müllen, K.; Huber, W. *Tetrahedron* **1984**, *40*, 1701–1711.

(62) Rossi, R.; Carpita, A.; Lippolis, V.; Benetti, M. *Gazz. Chim. Ital.* **1990**, *120*, 783.

(63) Larsen, C.; Anderson, K.; Tundel, R.; Buchwald, S. *Synlett* **2006**, *2006*, 2941–2946.

(64) Pérez, I.; Sestelo, J. P.; Sarandeses, L. A. *J. Am. Chem. Soc.* **2001**, *123*, 4155–4160.

(65) Qian, M.; Negishi, E.-I. *Tetrahedron Lett.* **2005**, *46*, 2927–2930.

(66) Torregrosa, R. R. P.; Ariyarathna, Y.; Chattopadhyay, K.; Tunge, J. A. *J. Am. Chem. Soc.* **2010**, *132*, 9280–9282.

(67) Zhang, W.-W.; Zhang, X.-G.; Li, J.-H. *J. Org. Chem.* **2010**, *75*, 5259–5264.

(68) Kuno, A.; Saino, N.; Kamachi, T.; Okamoto, S. *Tetrahedron Lett.* **2006**, *47*, 2591–2594.

(69) Xiang, S.-K.; Zhang, L.-H.; Jiao, N. *Chem. Commun.* **2009**, 6487–6489.

(70) Correia, C. A.; Li, C.-J. *Adv. Synth. Catal.* **2010**, *352*, 1446–1450.

(71) Haider, N. *Tetrahedron* **1992**, *48*, 7173–7184.

(72) Inoue, T.; Takeda, T.; Kambe, N.; Ogawa, A.; Ryu, I.; Sonoda, N. *J. Org. Chem.* **1994**, *59*, 5824–5827.

(73) Boger, D. L.; Mathvink, R. J. *J. Org. Chem.* **1992**, *57*, 1429–1443.

(74) Heinisch, G.; Jentzsch, A.; Pailer, M. *Monatsh. Chem.* **1974**, *105*, 648–652.

(75) Abdel-Magid, A. F.; Mehrman, S. J. *Org. Process Res. Dev.* **2006**, *10*, 971–1031.

Appendix I: Selected NMR Spectra

(Chapter 2)

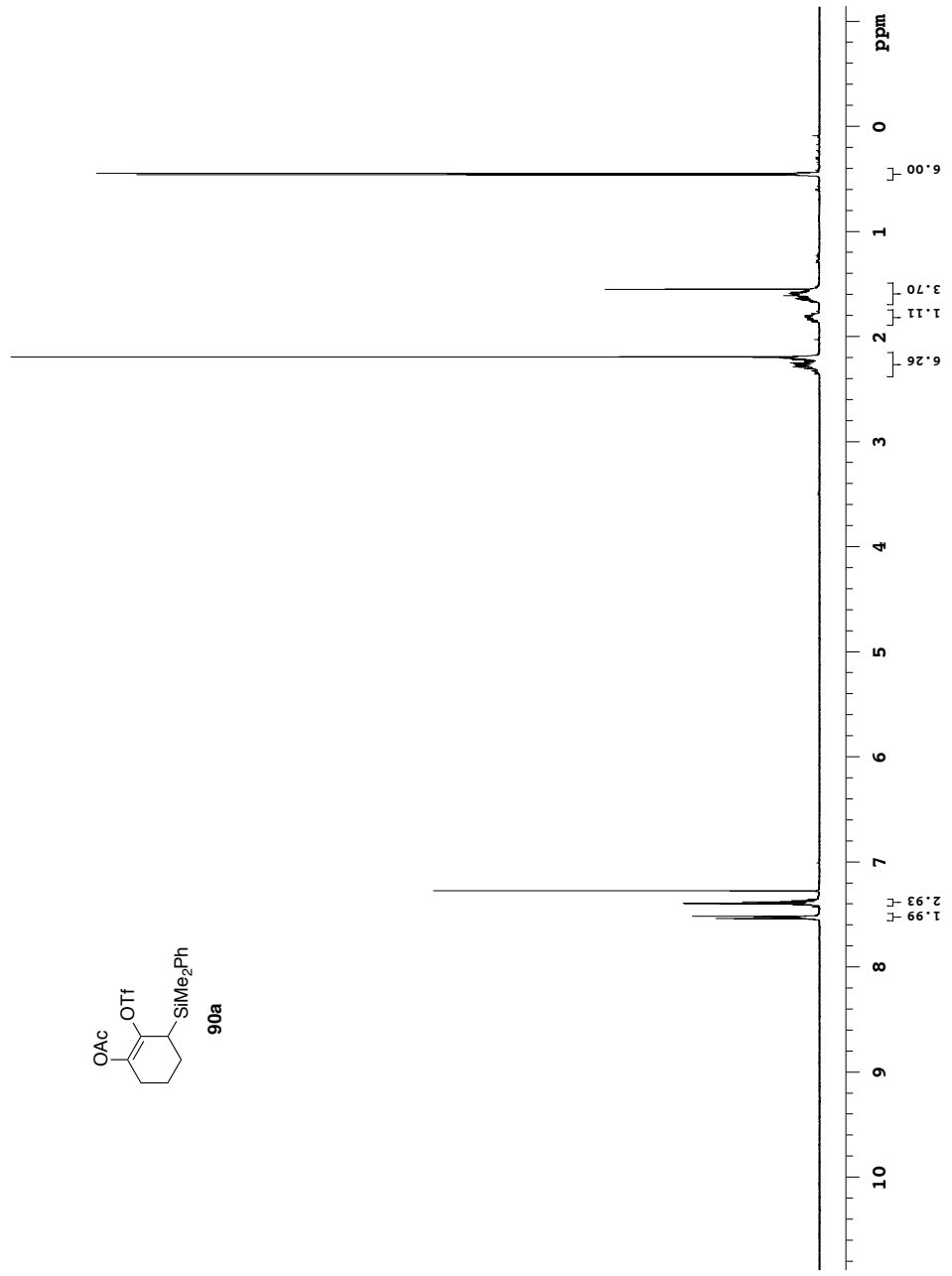
OAc
OTf
SiMe2Ph
90a
ppm
0
1
2
3
4
5
6
7
8
9
10
6.00
3.70
1.11
6.26
1.99
2.93

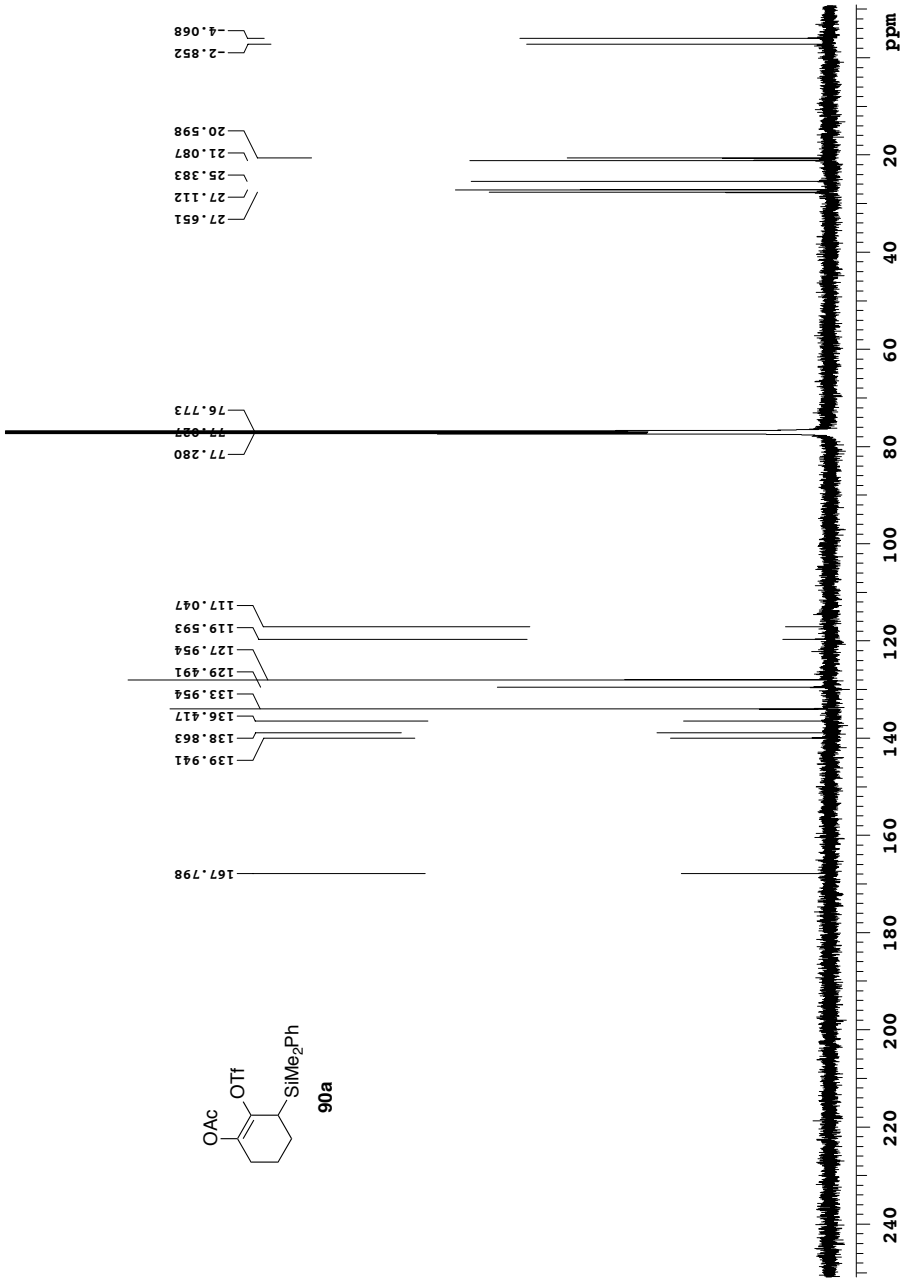
-4.068
-2.852
20.598
21.087
25.383
27.112
27.651
76.773
77.037
77.280
117.047
119.593
127.954
129.491
133.954
136.417
138.863
139.941
167.798
ppm
20
40
60
80
100
120
140
160
180
200
220
240
OAc
OTf
SiMe2Ph
90a

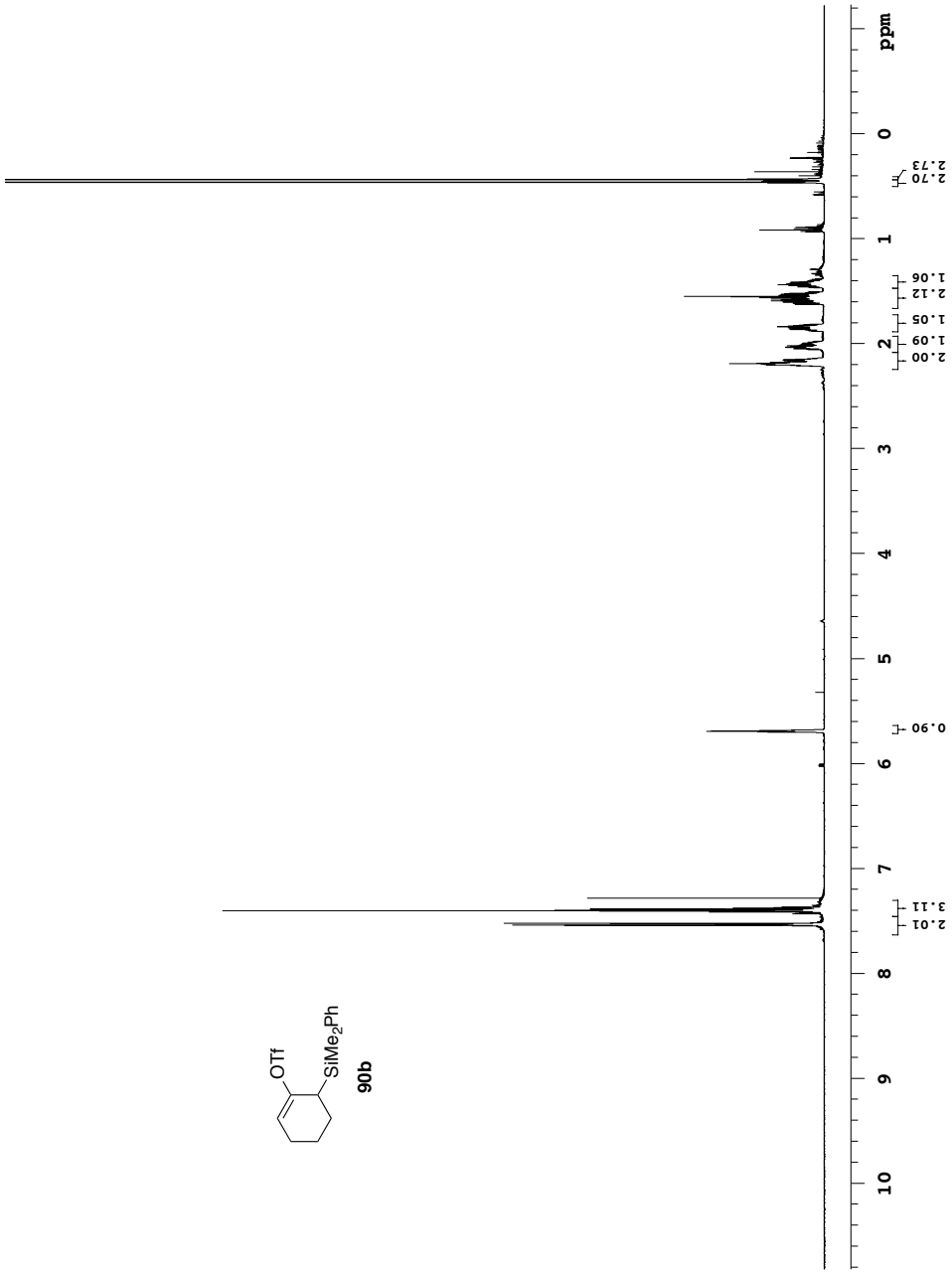
OTf
SiMe2Ph
90b
ppm
0
1
2
3
4
5
6
7
8
9
10
2.73
2.70
1.06
2.12
1.05
1.09
2.00
0.90
3.11
2.01

Verner, VL-10_allylic_silyl_vinyltriflate
125.691 MHz C13[H1] 1D in cdcl3 (ref. to CDCl3 @ 77.06 ppm), temp 27.7 C -> actual temp = 27.0 C, colddual probe

date: Feb 5 2015 sweep width: 32895Hz acq.time: 2.5s relax.time: 0.2s # scans: 296 dig.res.: 0.3 Hz/pt hz/mm:137.1
spectrometer:ibdw file:/mnt/d600/home13/westnmr/nmrdata/Verner/Book10/2015.02.5.u5_VL-10_allylic_silyl_vinyltriflate_loc7_10.55_C13_1D

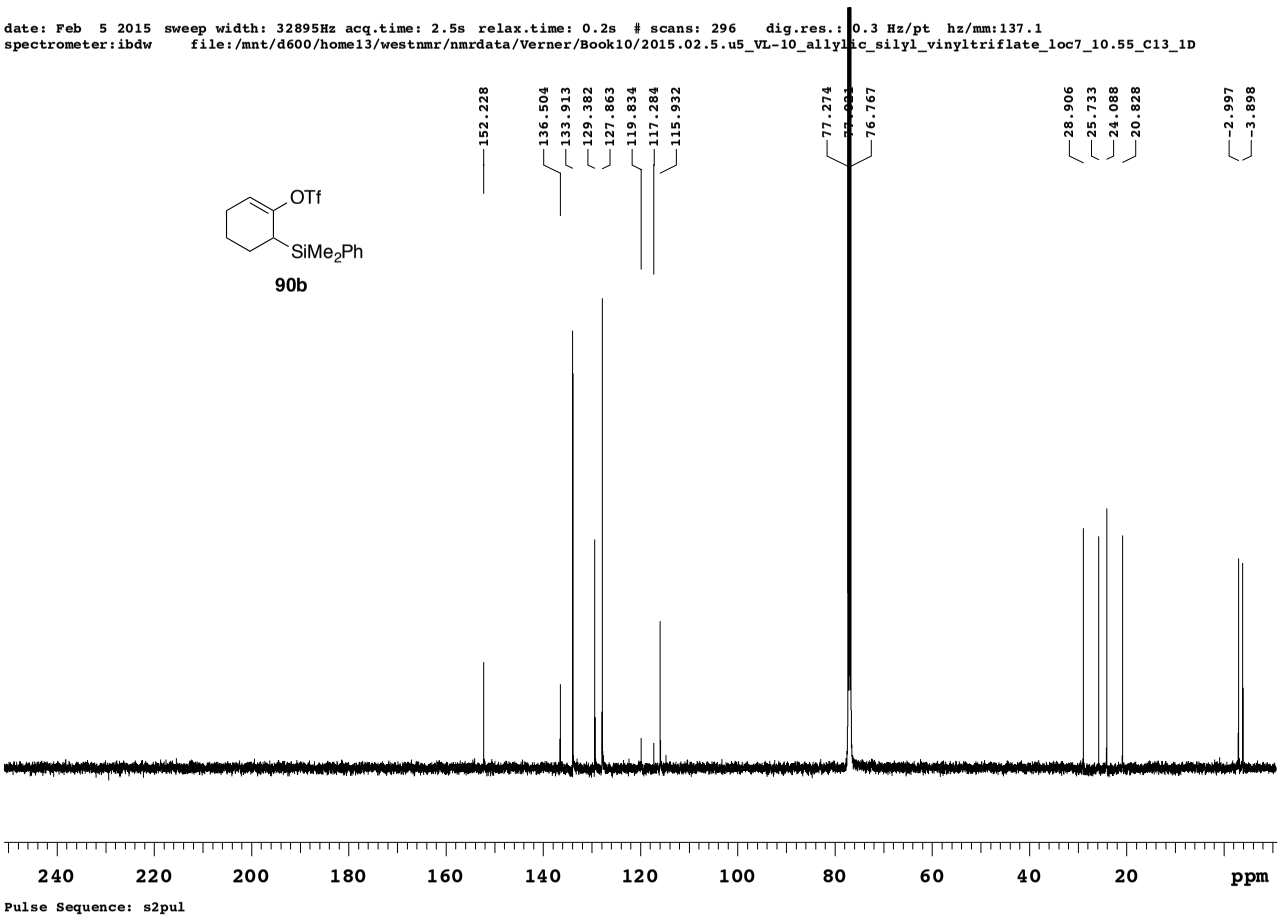

Pulse Sequence: s2pul

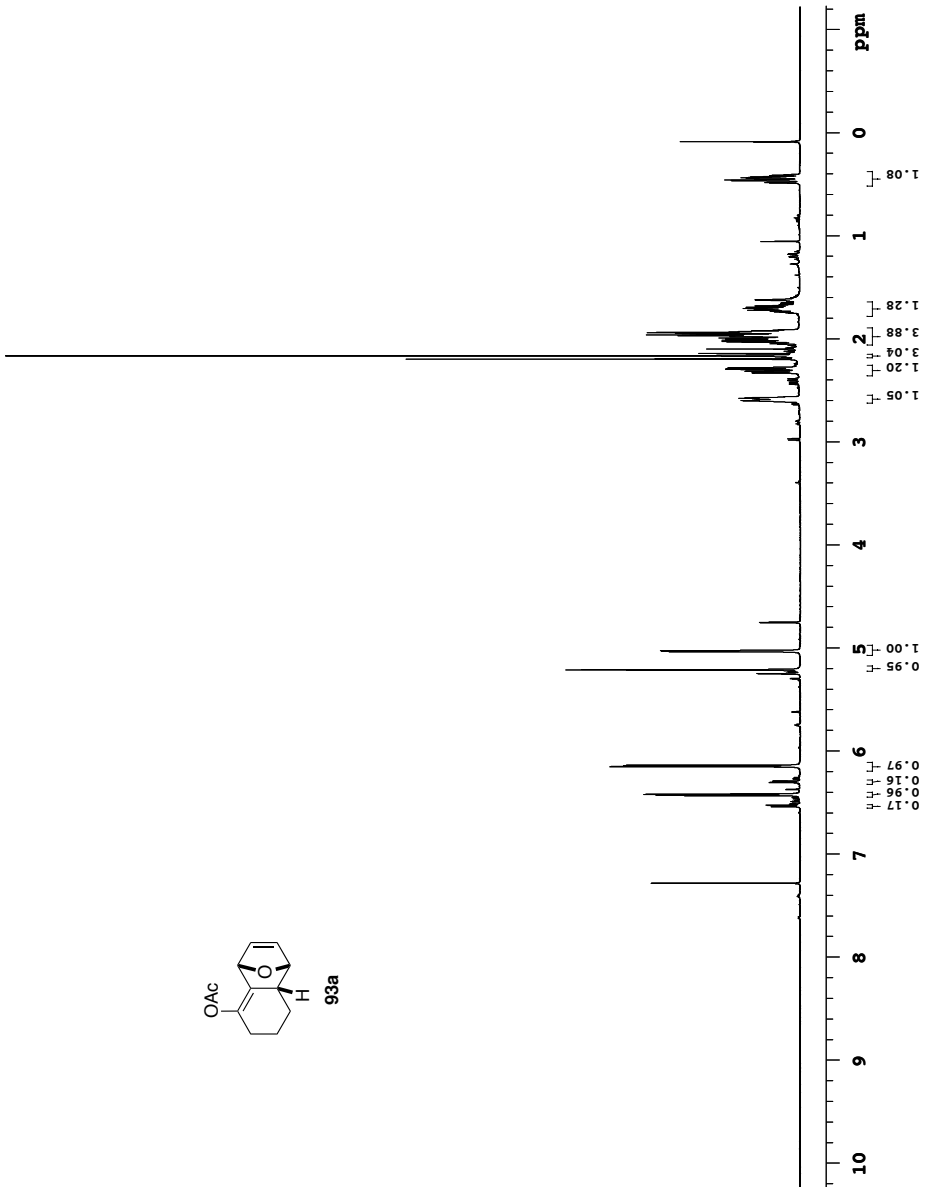
OAc
O
H
93a
ppm
0 1 2 3 4 5 6 7 8 9 10
1.08
1.28
3.88
3.04
1.20
1.05
1.00
0.95
0.97
0.16
0.96
0.17

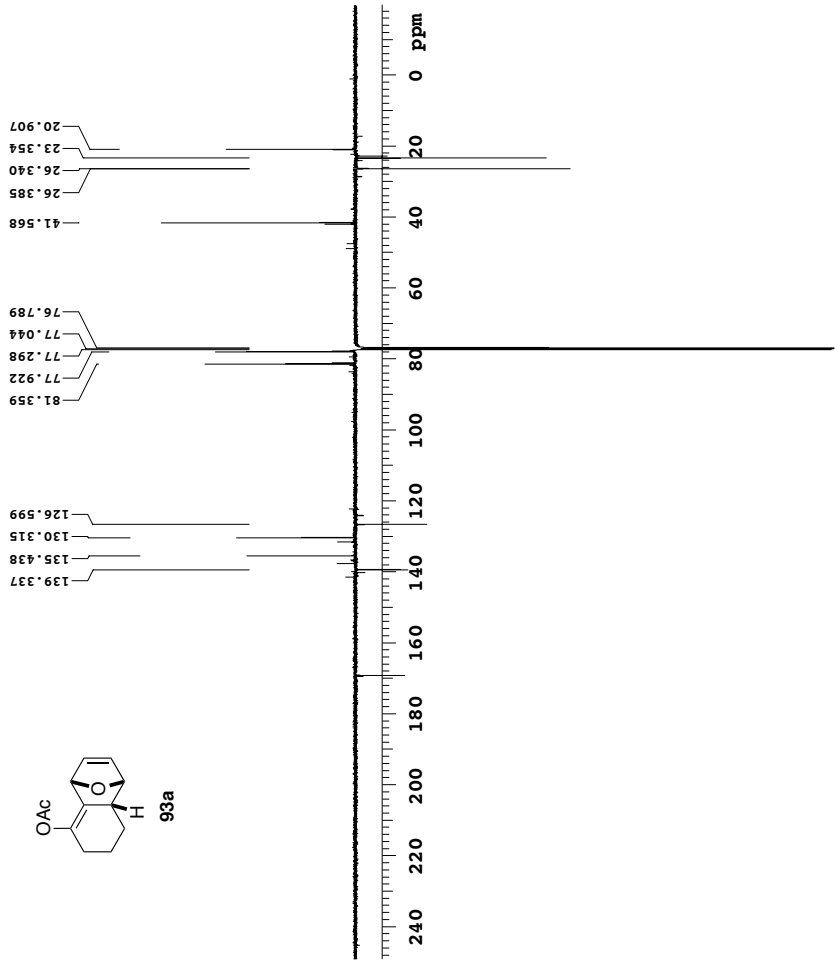
20.907
23.354
26.340
26.385
41.568
76.789
77.044
77.298
77.922
81.359
126.599
130.315
135.438
139.337
0 ppm
20
40
60
80
100
120
140
160
180
200
220
240
OAc
O
H
93a

Me
Me
Me
OAc
N
O
95a
ppm
0
1
2
3
4
5
6
7
8
9
10
3.13
1.18
1.21
2.20
6.15
5.74
1.04
1.00
2.30

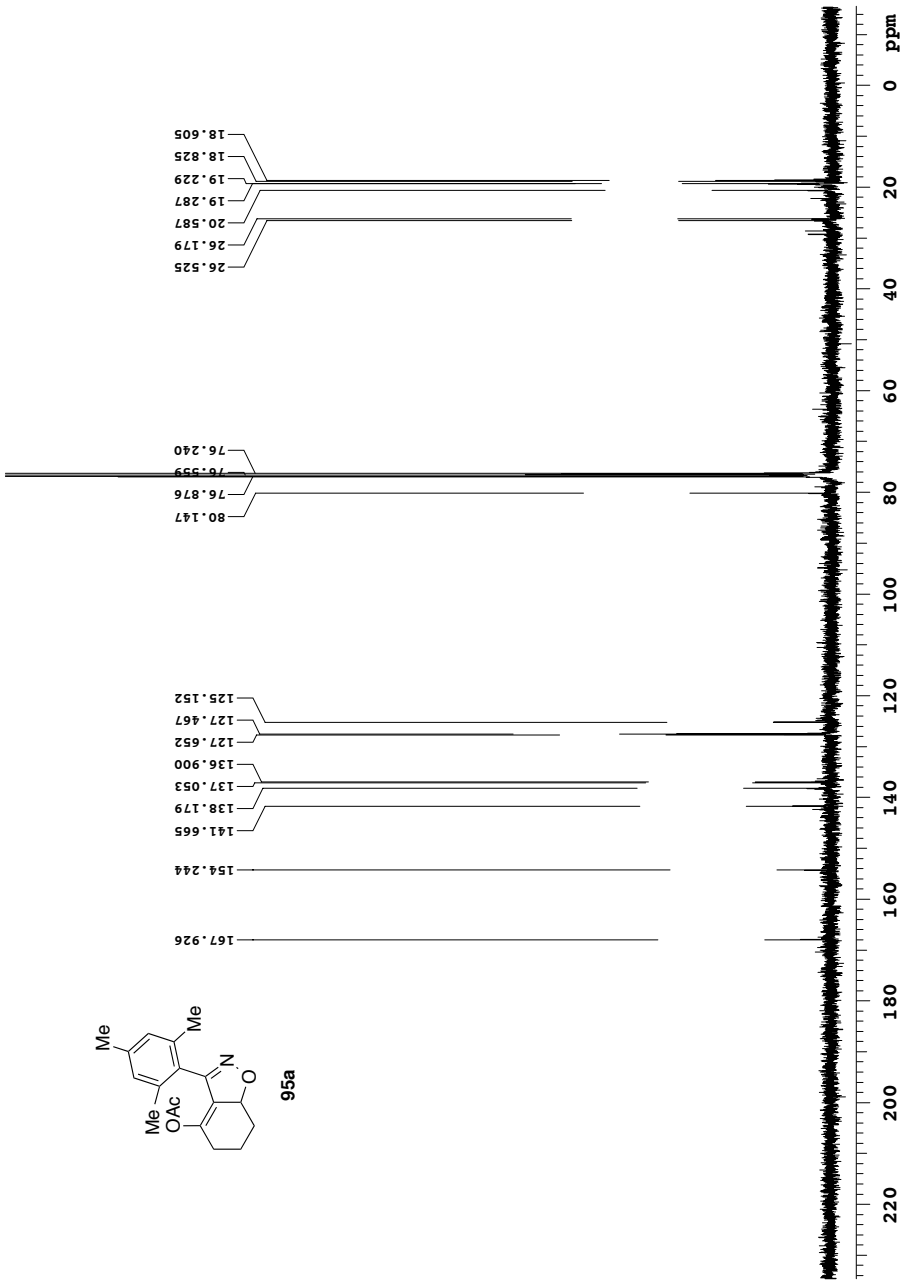
18.605
18.825
19.229
19.287
20.587
26.179
26.525
76.240
76.559
76.876
80.147
125.152
127.467
127.652
136.900
137.053
138.179
141.665
154.244
167.926
Me
Me
Me
OAc
N
O
95a
ppm
0
20
40
60
80
100
120
140
160
180
200
220

VL-5-64 trap with nitrone
399.794 MHz H1 1D in cdcl3 (ref. to CDCl3 @ 7.26 ppm), temp 27.0 C -> actual temp = 27.0 C, autoxdb probe

date: Mar 5 2013 sweep width: 4802Hz acq.time: 5.0s relax.time: 0.1s # scans: 16 dig.res.: 0.1 Hz/pt hz/mm:20.0
spectrometer:d300 file:/mnt/d600/home13/westnmr/nmrdata/Verner/Book5/2013.03.05.i4_VL-5-64_allene_and_nitrone_dibenzyl__H1_1D

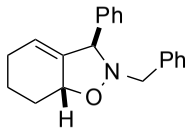

114b

Pulse Sequence: s2pul

Verner,
100.690 MHz C13[H1] 1D in cdcl3 (ref. to CDCl3 @ 77.06 ppm), temp 27.0 C -> actual temp = 27.0 C, m400gz probe

date: Jun 5 2013 sweep width: 27174Hz acq.time: 2.0s relax.time: 0.1s # scans: 512 dig.res.: 0.2 Hz/pt hz/mm:113.2
spectrometer:d300 file:/mnt/d600/home13/westnmr/nmrdata/Verner/Book5/2013.06.5.m4_VL-5-179_11.29_C13_1D

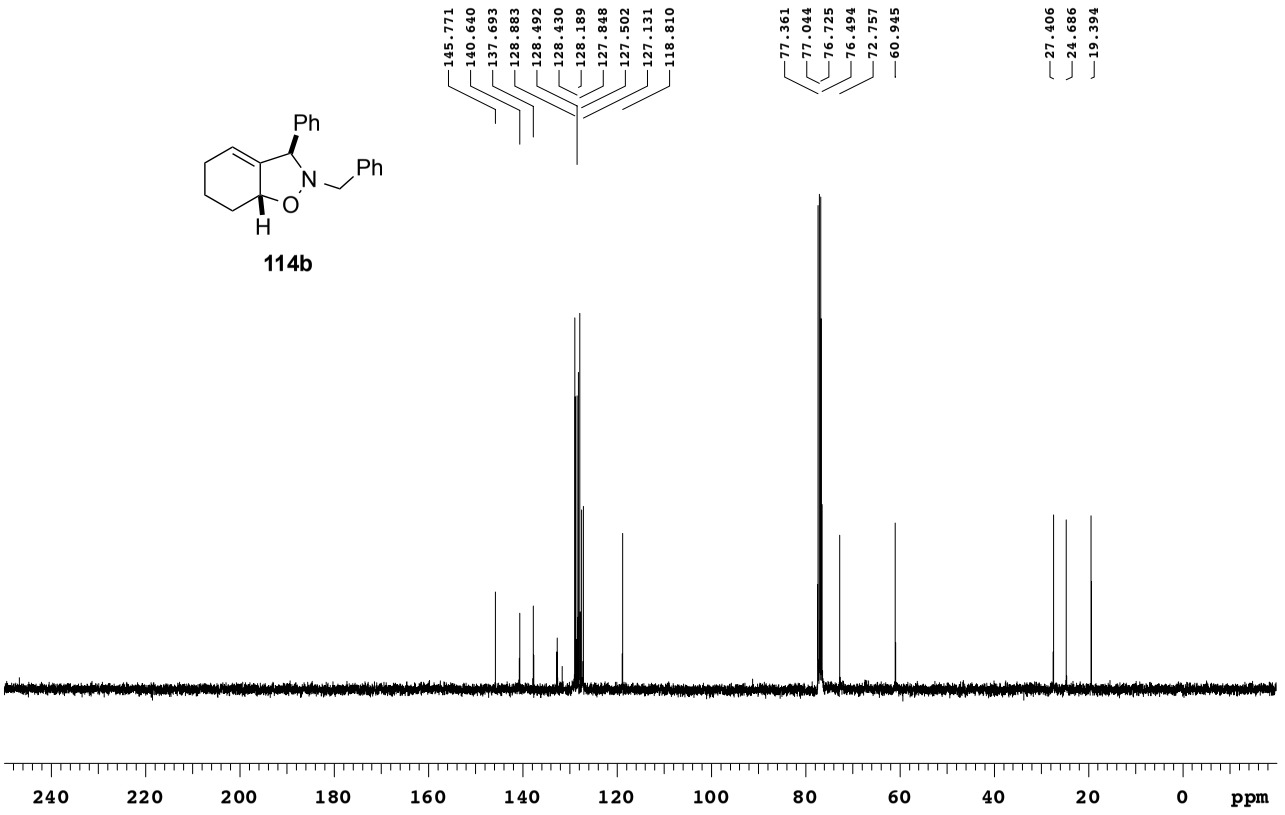

114b

Pulse Sequence: s2pul

Verner, VL-DBN
399.947 MHz H1 ROESY in cdcl3
temp 25.5C --> actual temp = 26.9, sw400 probe

Temp. 25.5 C / 298.6 K
Operator: nmrlab

Relax. delay 1.000 sec
Acq. time 1.000 sec
Width 4801.9 Hz
2D Width 4801.9 Hz
32 repetitions
2 x 256 increments
OBSERVE H1, 399.9447601 MHz
DATA PROCESSING
Sq. sine bell 0.250 sec
Shifted by -0.250 sec
F1 DATA PROCESSING
Sq. sine bell 0.053 sec
Shifted by -0.053 sec
FT size 8192 x 1024
Total time 11 hr, 2 min

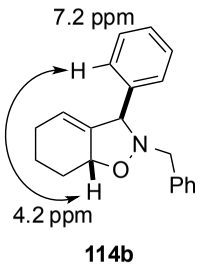

114b

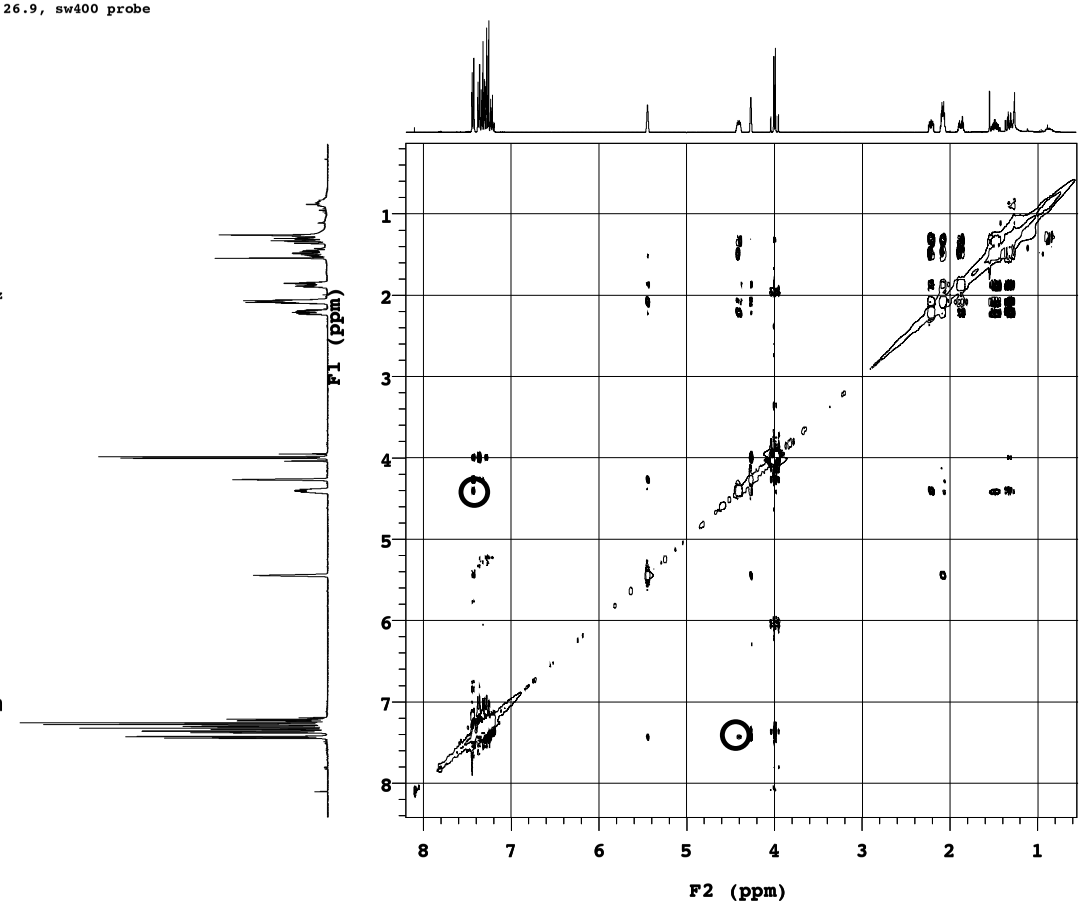

Pulse Sequence: ROESY

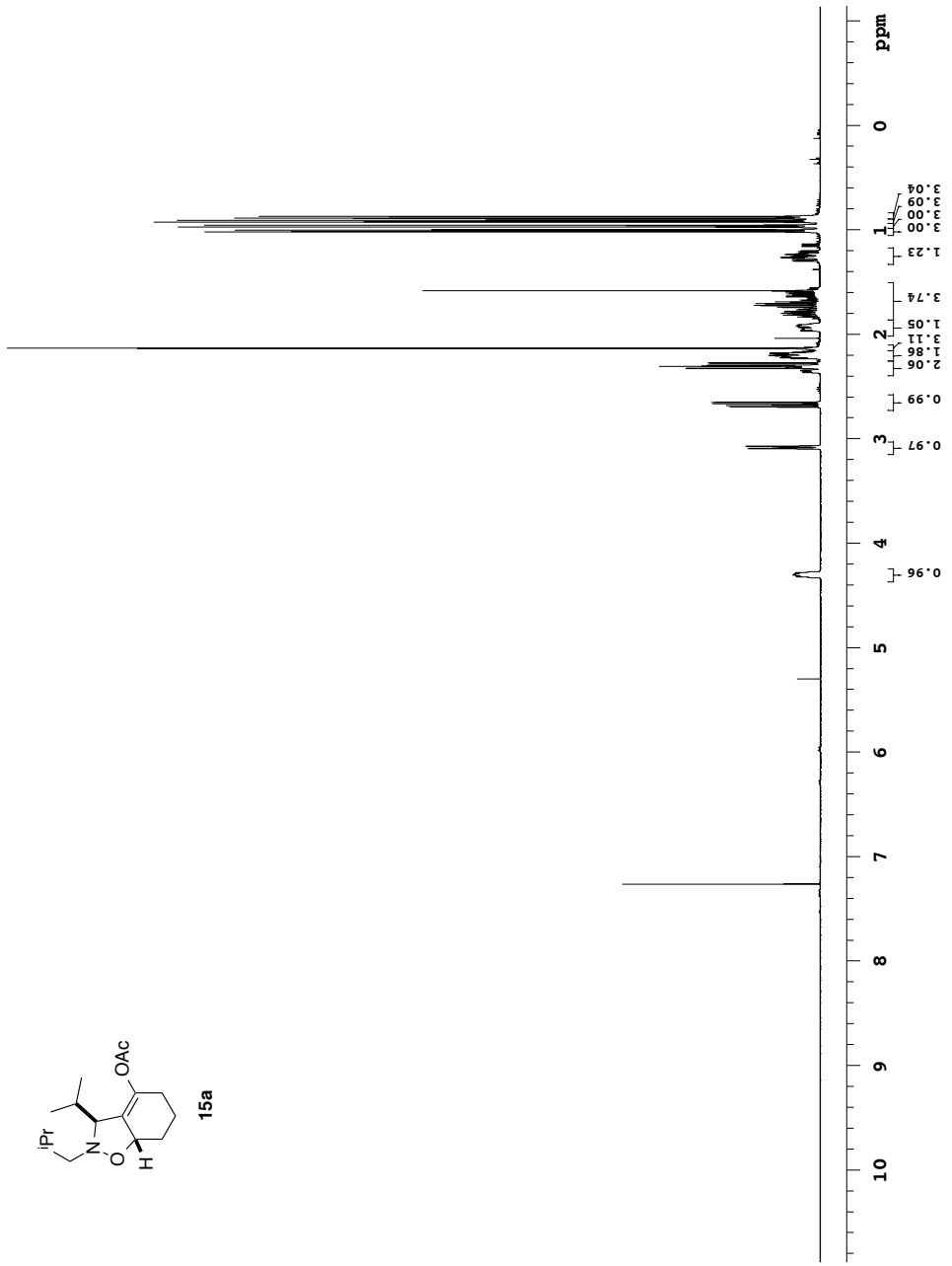
OAc
iPr
N
O
H
15a
ppm
0
1
2
3
4
5
6
7
8
9
10
3.04
3.09
3.00
3.00
1.23
3.74
1.05
3.11
1.86
2.06
0.99
0.97
0.96

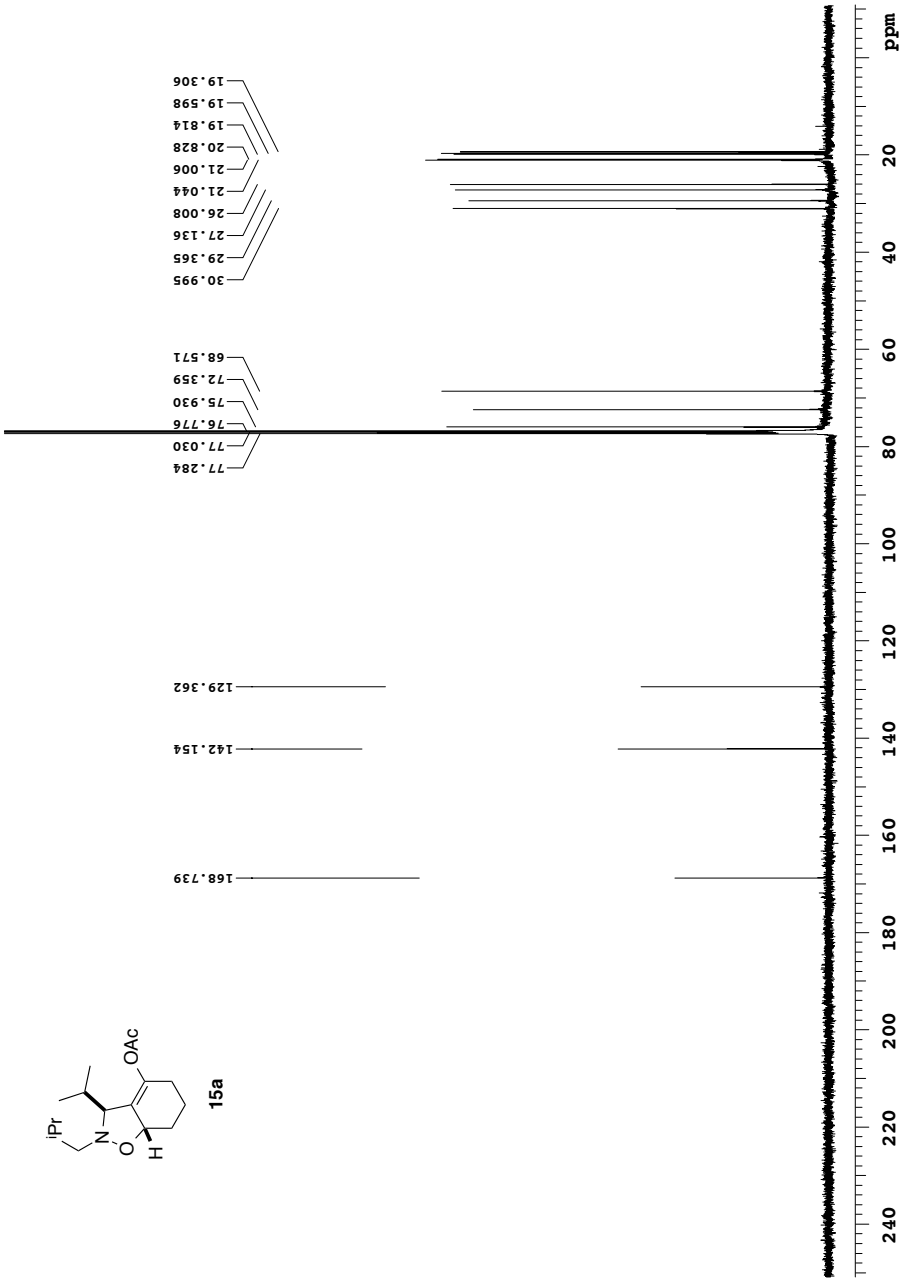
ppm
20
40
60
80
100
120
140
160
180
200
220
240
19.306
19.598
19.814
20.828
21.006
21.044
26.008
27.136
29.365
30.995
68.571
72.359
75.930
76.776
77.030
77.284
129.362
142.154
168.739
OAc
iPr
N
O
H
15a

499.806 MHz H1 ROESY in cdcl3 (ref. to CDCl3 @ 7.26 ppm), temp 27.7 C -> actual temp = 27.0 C, colddual probe

Temp. 27.7 C / 300.9 K
Operator: nmrlab

Relax. delay 1.000 sec
Acq. time 1.000 sec
Width 2500.0 Hz
2D Width 2500.0 Hz
64 repetitions
2 x 178 increments
OBSERVE H1, 499.8039202 MHz
DATA PROCESSING
Sq. sine bell 0.250 sec
Shifted by -0.250 sec
F1 DATA PROCESSING
Sq. sine bell 0.007 sec
Shifted by -0.007 sec
FT size 8192 x 1024
Total time 15 hr, 25 min

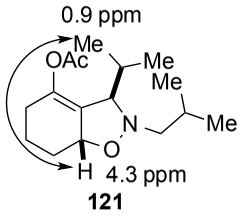

121

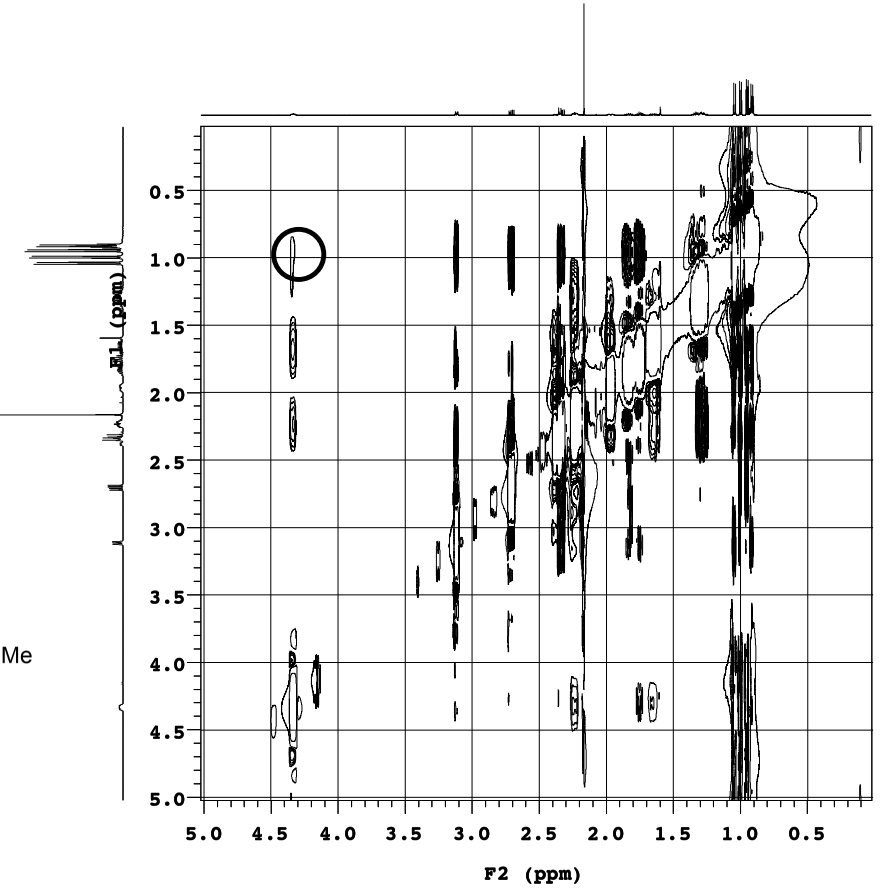

Pulse Sequence: ROESY

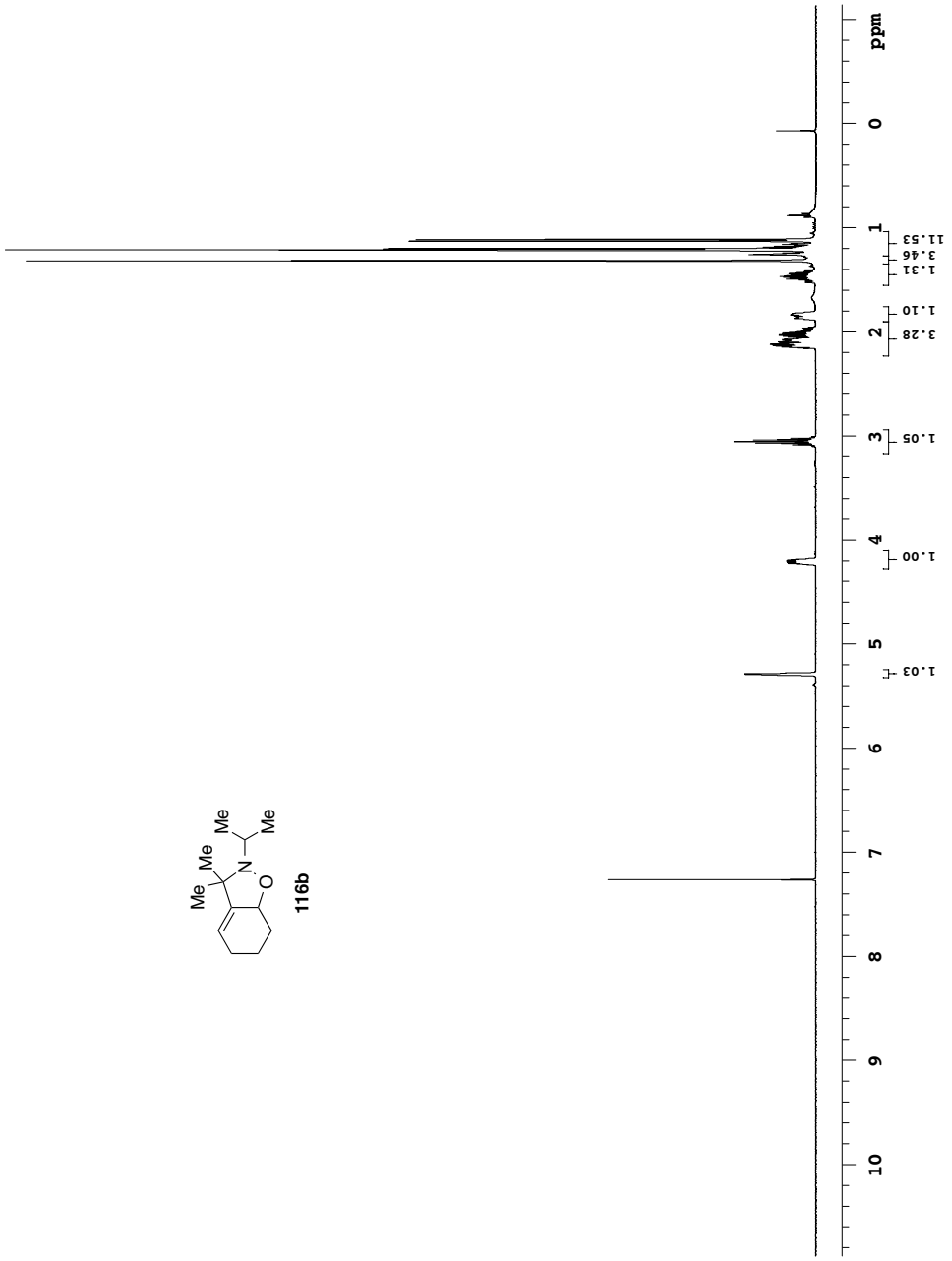
Me
Me
Me
Me
N
O
116b
ppm
0
1
2
3
4
5
6
7
8
9
10
11.53
3.46
1.31
1.10
3.28
1.05
1.00
1.03

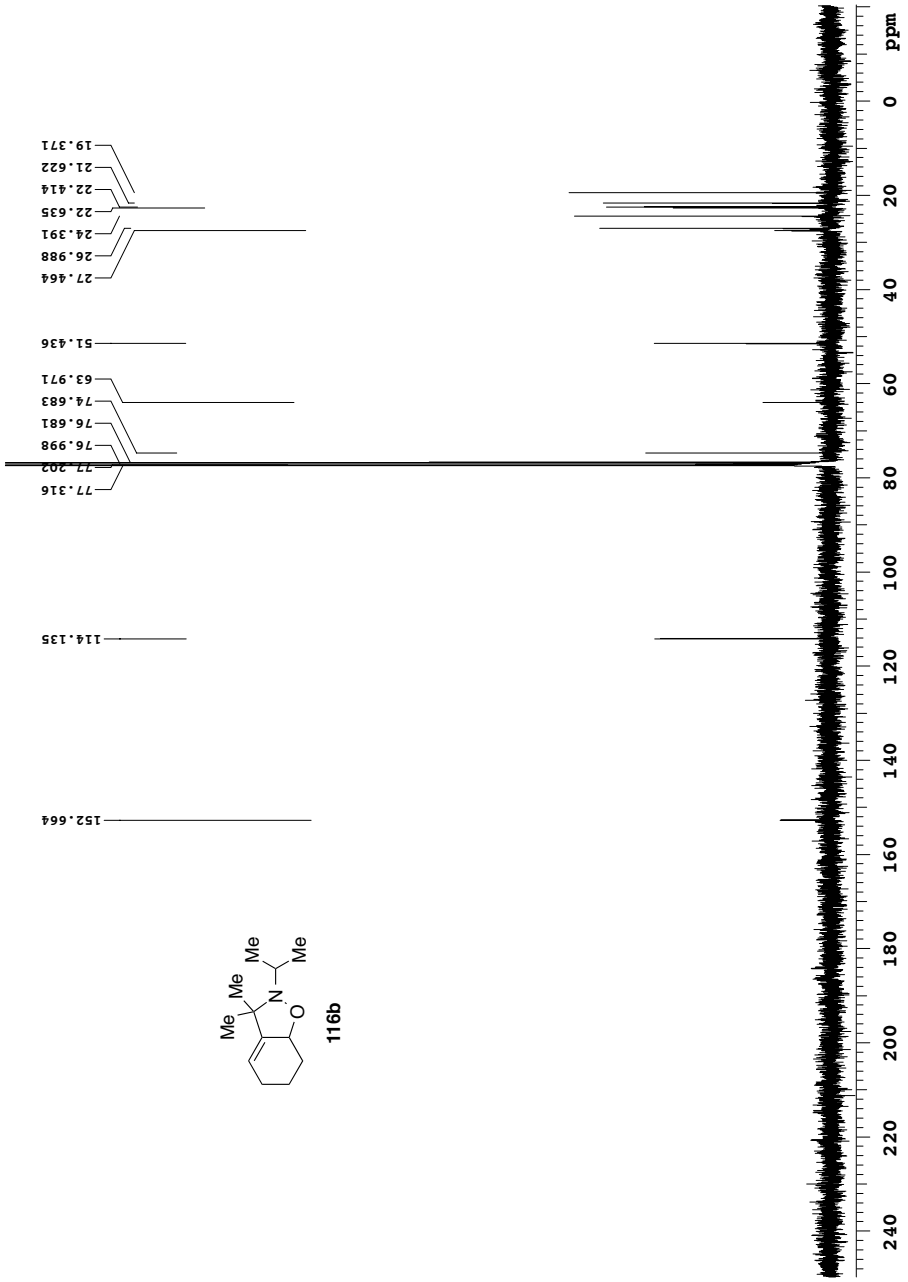
19.371
21.622
22.414
22.635
24.391
26.988
27.464
51.436
63.971
74.683
76.681
76.998
77.202
77.316
114.135
152.664
Me
Me
Me
Me
N
O
116b
ppm
0
20
40
60
80
100
120
140
160
180
200
220
240

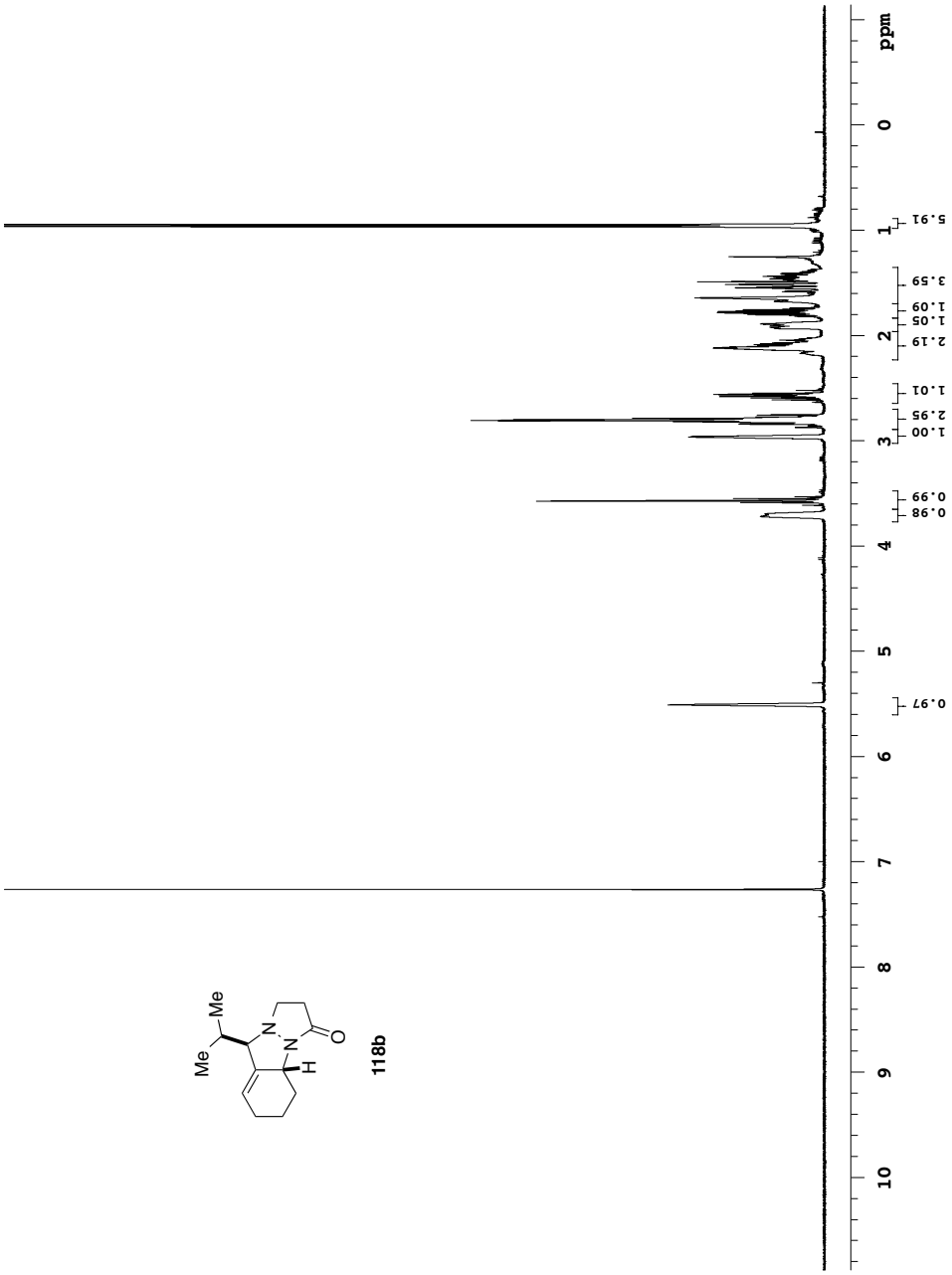
ppm
0
1
2
3
4
5
6
7
8
9
10
5.91
3.59
1.09
1.05
2.19
1.01
2.95
1.00
0.99
0.98
0.97
Me
Me
N
N
O
H
118b

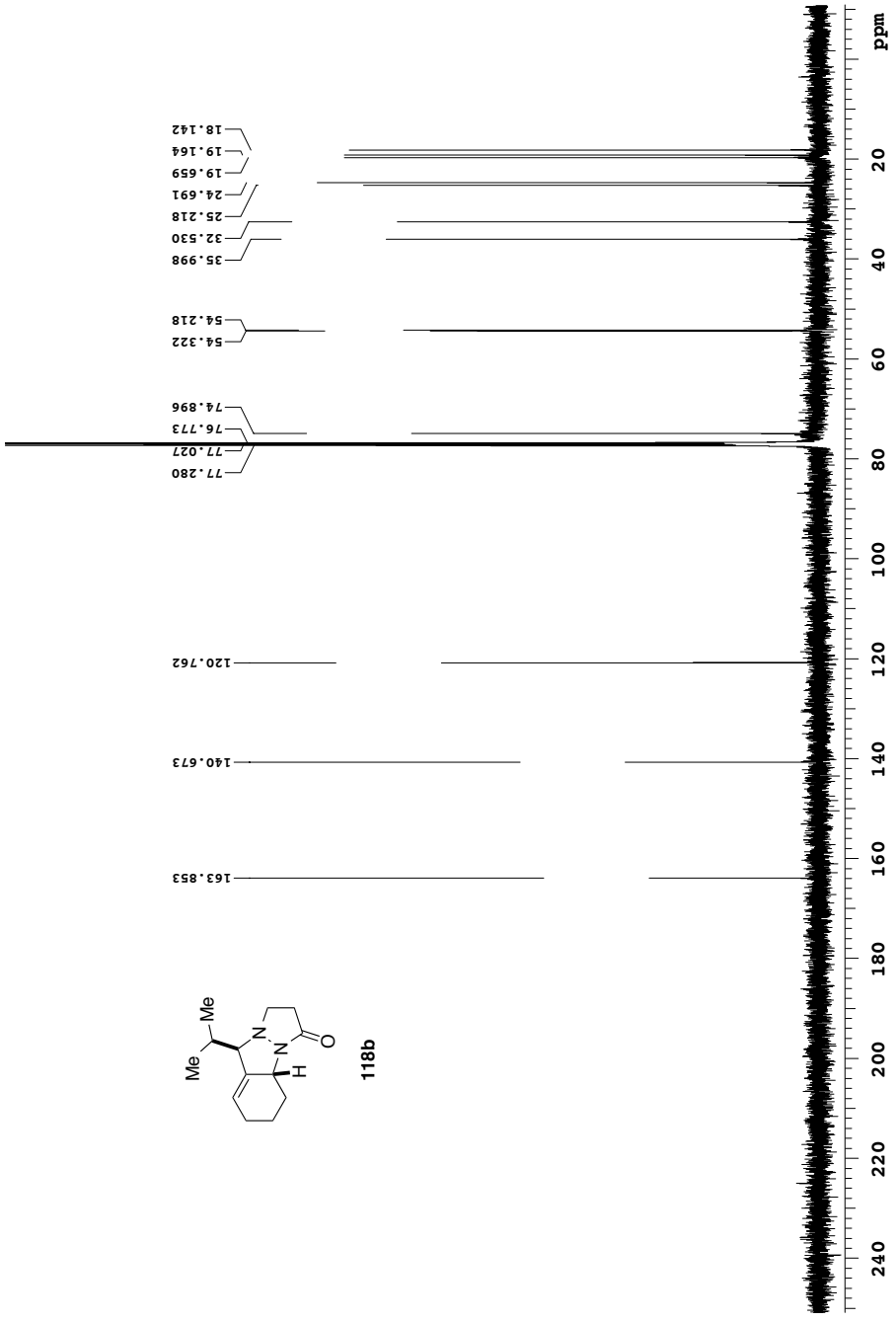
163.853
140.673
120.762
77.280
77.027
76.773
74.896
54.322
54.218
35.998
32.530
25.218
24.691
19.659
19.164
18.142
ppm
20
40
60
80
100
120
140
160
180
200
220
240
Me
Me
N
N
O
H
118b

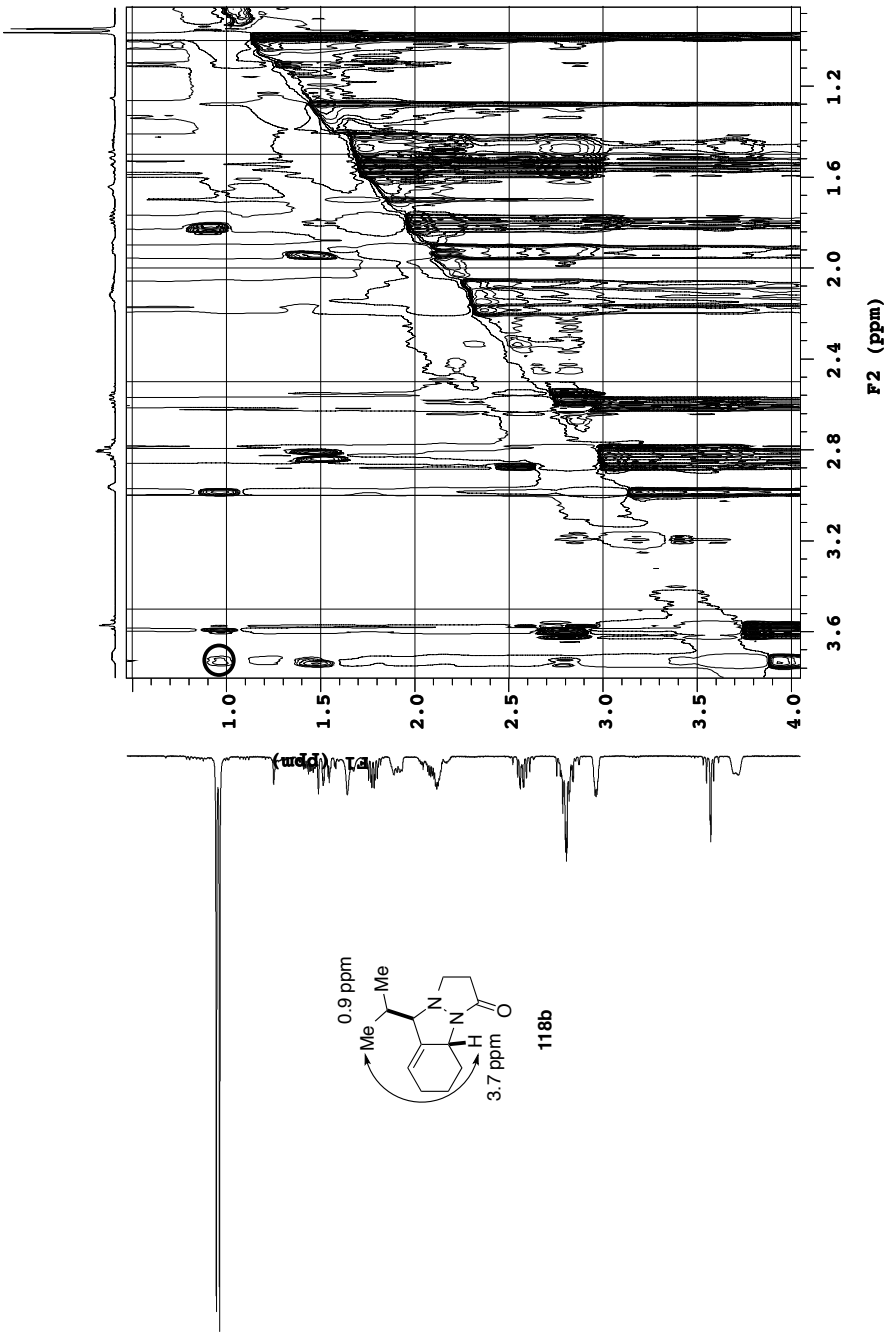
F2 (ppm)
1.0
1.5
2.0
2.5
3.0
3.5
4.0
1.2
1.6
2.0
2.4
2.8
3.2
3.6
0.9 ppm
Me
Me
N
N
H
O
3.7 ppm
118b

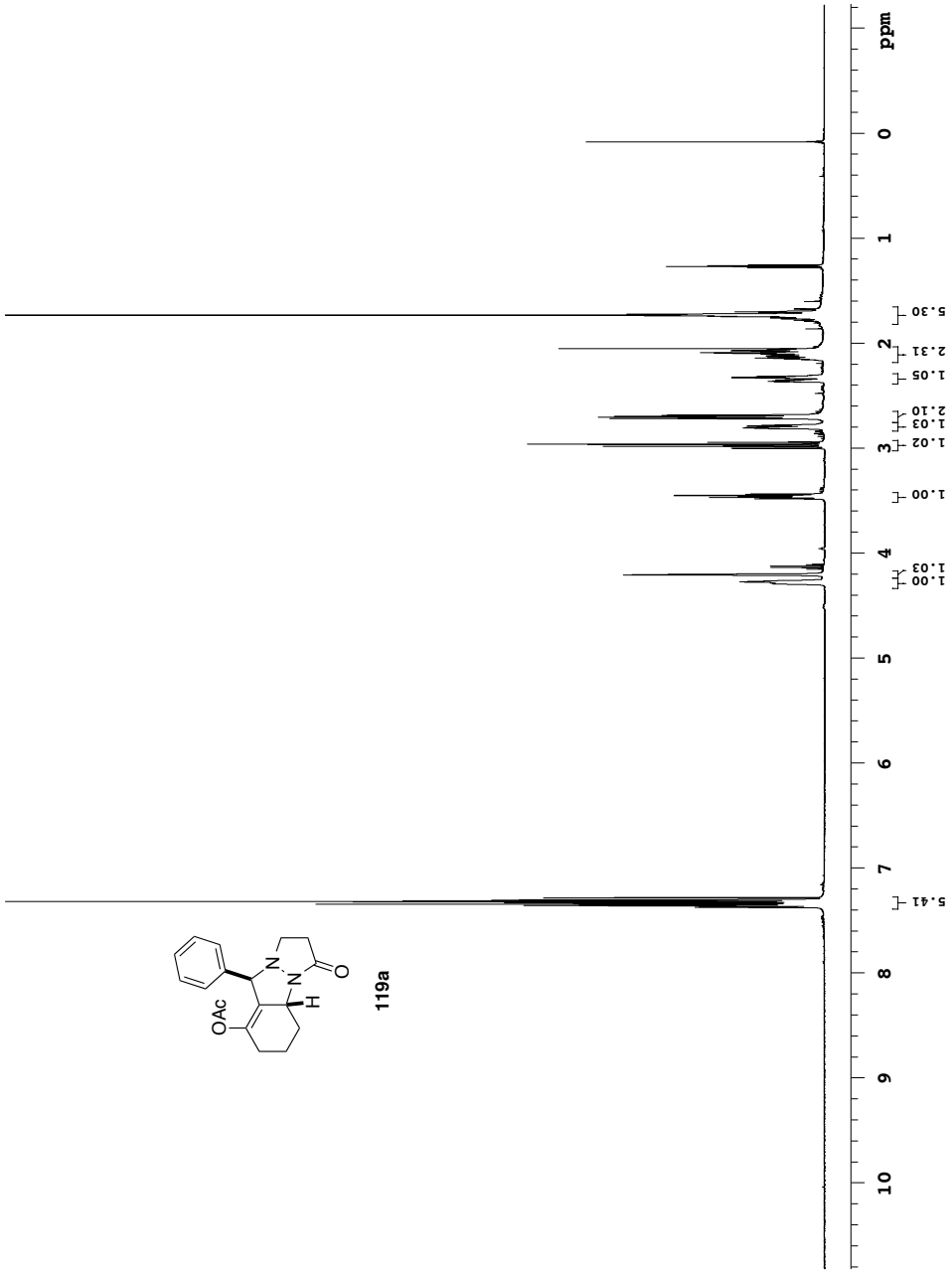
ppm
0
1
2
3
4
5
6
7
8
9
10
5.30
2.31
1.05
2.10
1.03
1.02
1.00
1.00
1.03
5.41
OAc
N
N
H
O
119a

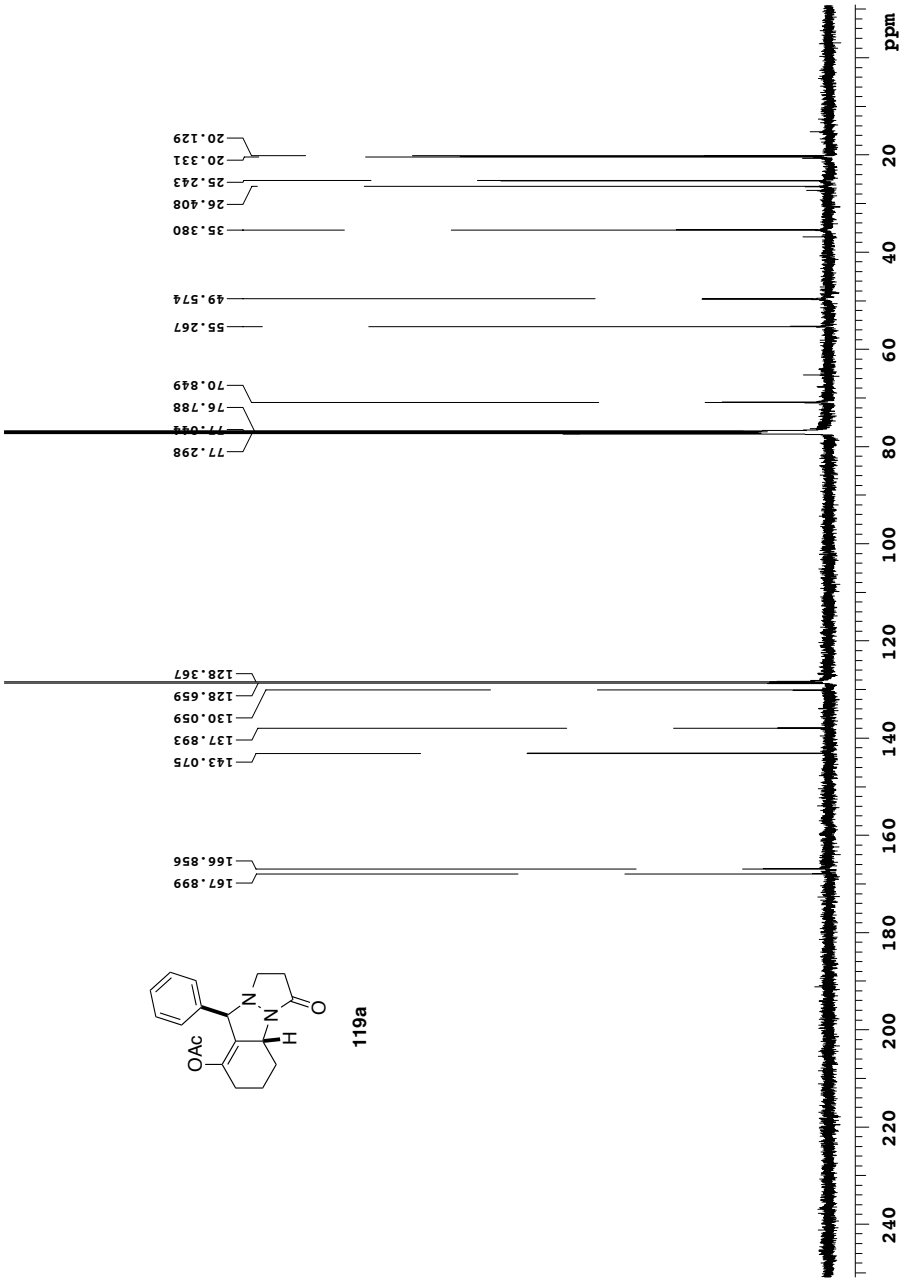
20.129
20.331
25.243
26.408
35.380
49.574
55.267
70.849
76.788
77.044
77.298
128.367
128.659
130.059
137.893
143.075
166.856
167.899
ppm
20
40
60
80
100
120
140
160
180
200
220
240
N
N
O
H
OAc

119a

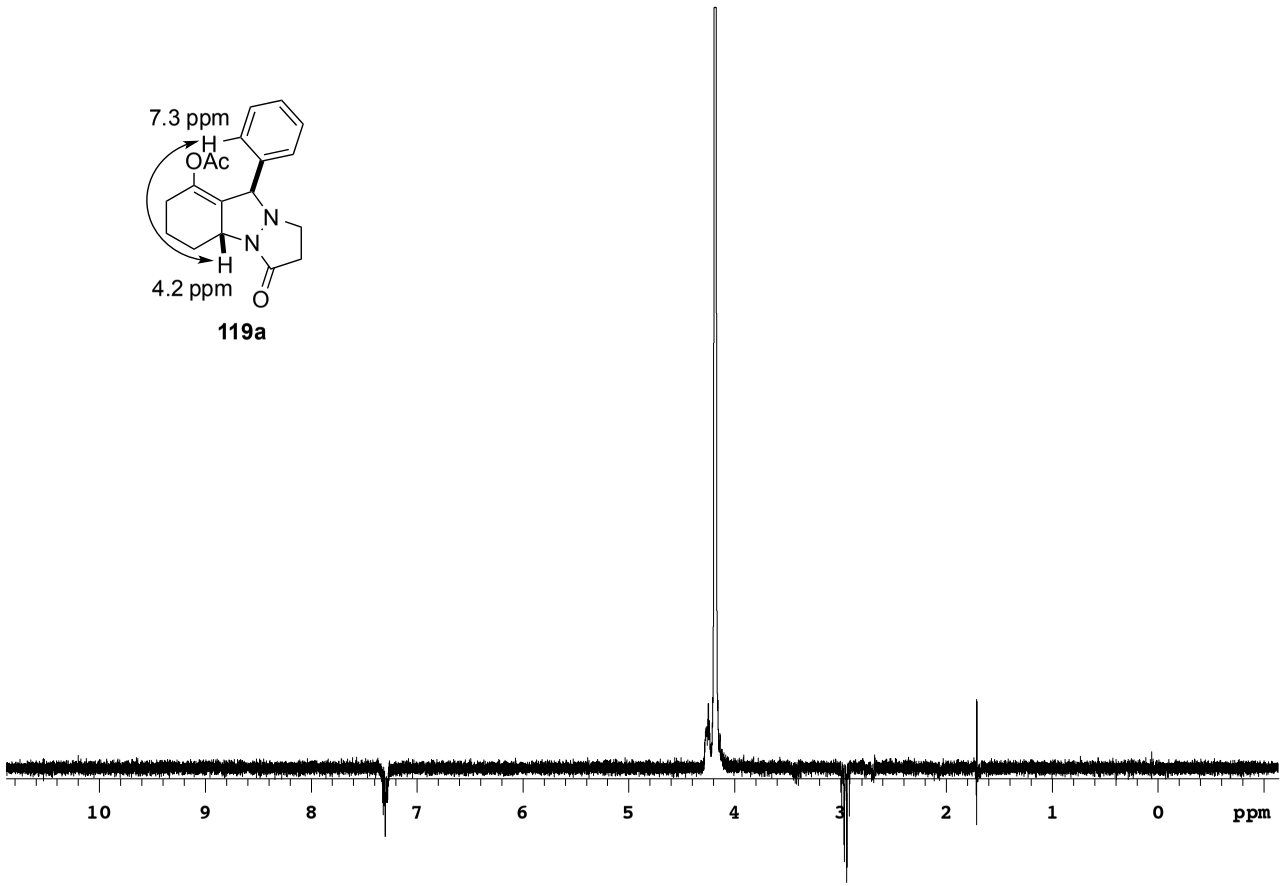

119a

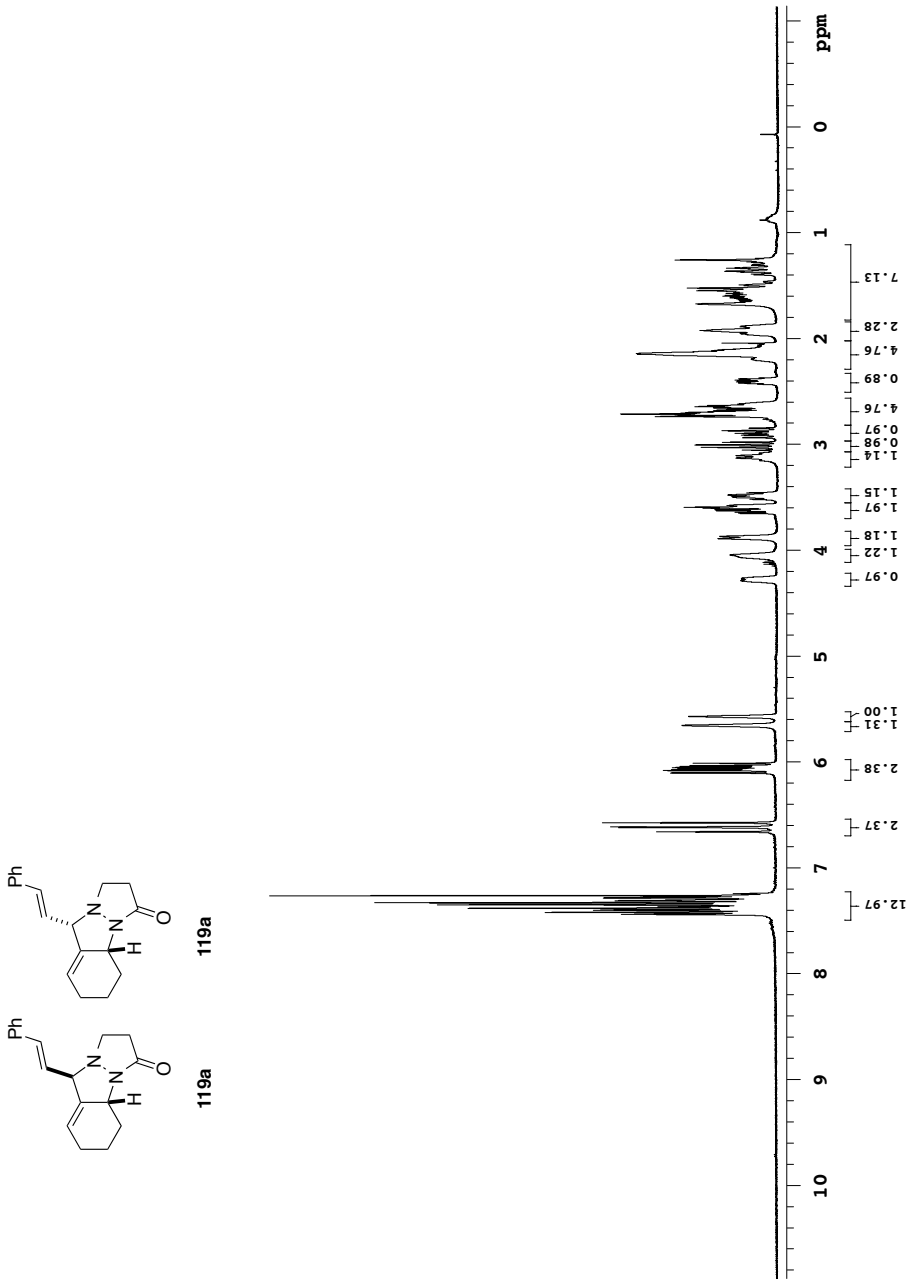
Ph
N
N
H
O
119a
Ph
N
N
H
O
119a
ppm
0
1
2
3
4
5
6
7
8
9
10
12.97
2.37
2.38
1.31
1.00
0.97
1.22
1.18
1.97
1.15
1.14
0.98
0.97
4.76
0.89
4.76
2.28
7.13

Verner, VL-8-117_allene_w_cinnamaldehyde_AMI
125.691 MHz C13[H1] 1D in cdcl3 (ref. to CDCl3 @ 77.06 ppm), temp 27.7 C -> actual temp = 27.0 C, colddual probe

date: May 16 2014 sweep width: 32895Hz acq.time: 2.5s relax.time: 0.2s # scans: 128 dig.res.: 0.3 Hz/pt hz/mm:137.1
spectrometer:d300 file:/mnt/d600/home13/westnmr/nmrdata/Verner/Book8/2014.05.16.u5_VL-8-117_allene_w_cinnamaldehyde_AMI_15.11_C13_1D

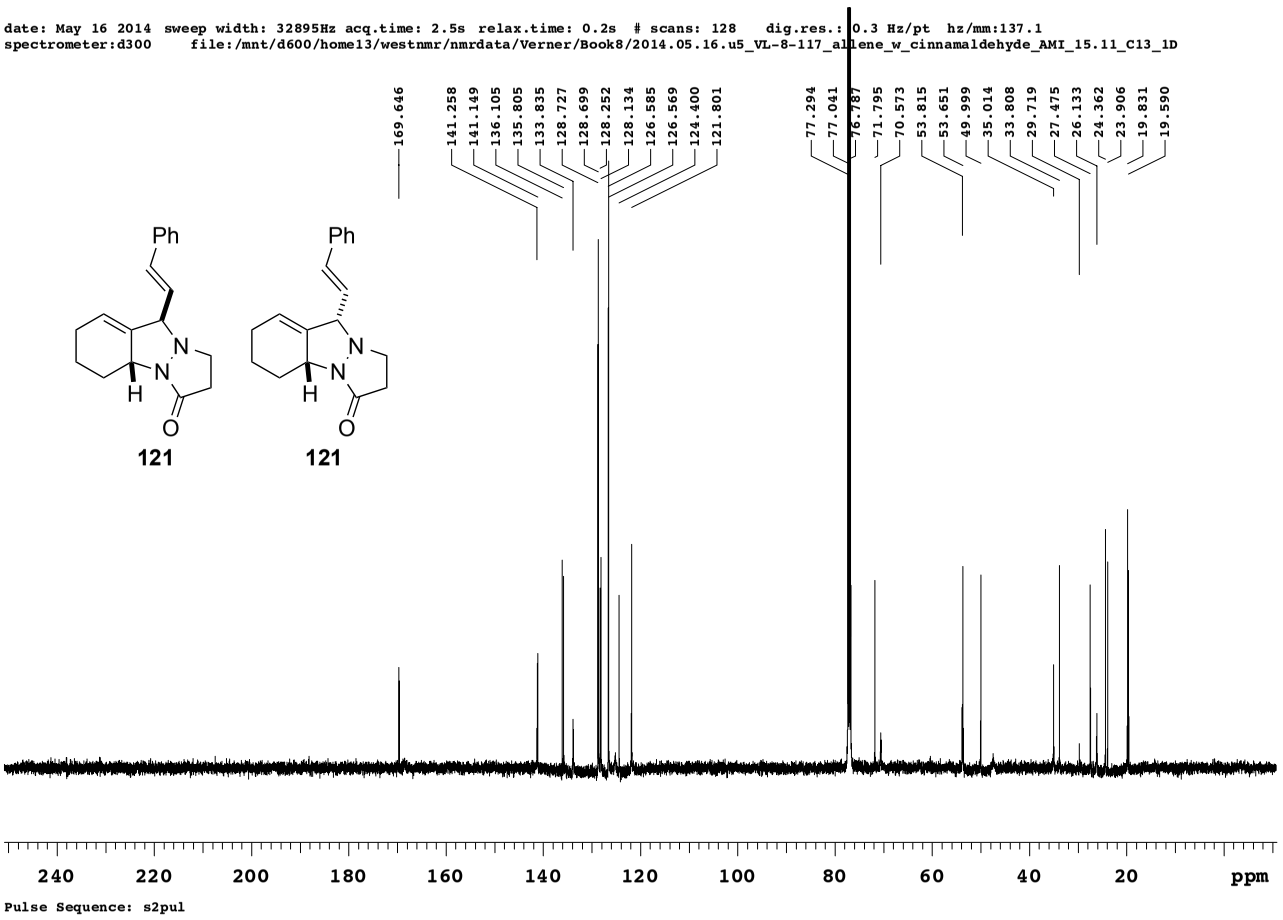

121

121

Pulse Sequence: s2pul

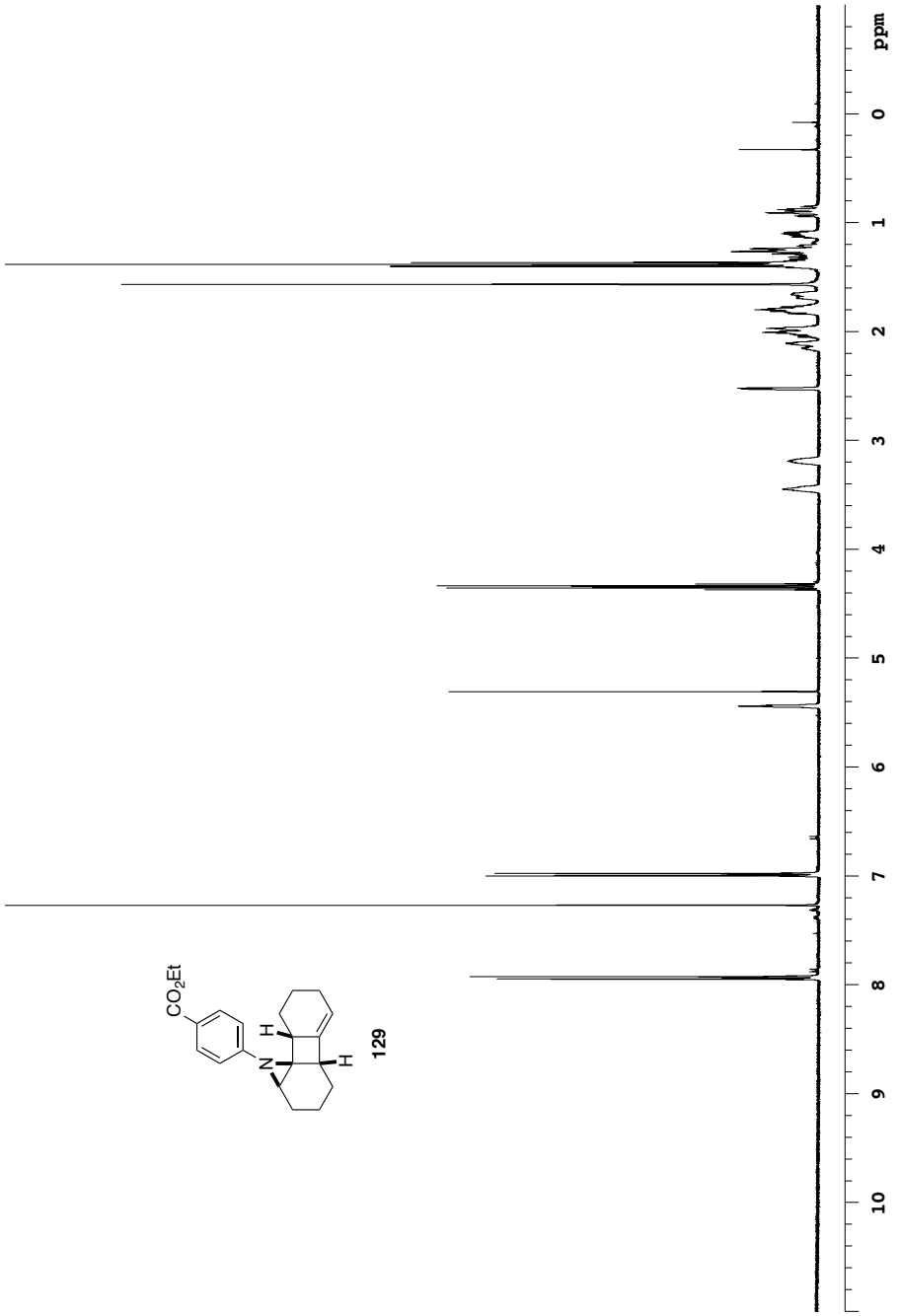
CO2Et
H
N
H
129
ppm
0
1
2
3
4
5
6
7
8
9
10

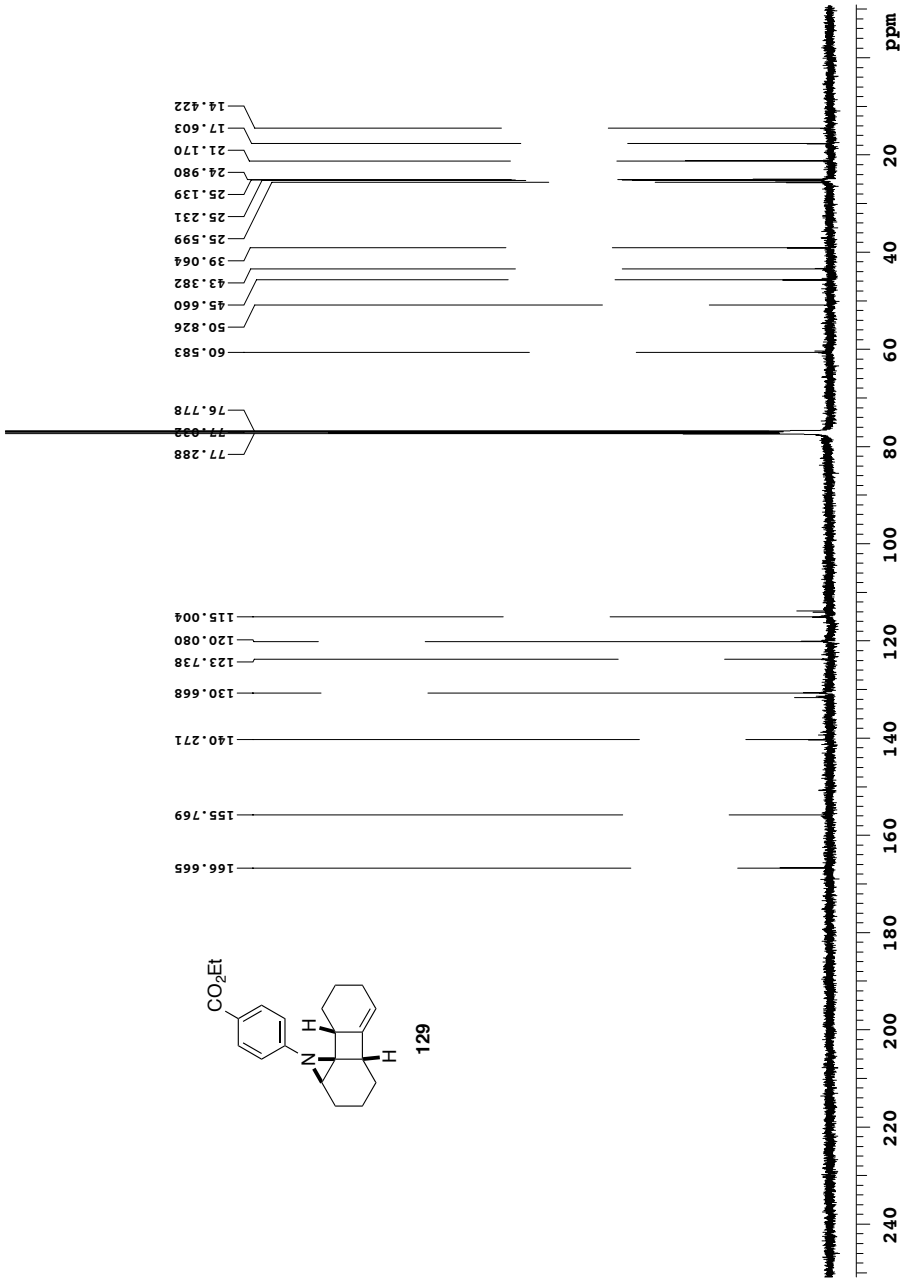
14.422
17.603
21.170
24.980
25.139
25.231
25.599
39.064
43.382
45.660
50.826
60.583
76.778
77.032
77.288
115.004
120.080
123.738
130.668
140.271
155.769
166.665
ppm
20
40
60
80
100
120
140
160
180
200
220
240
CO2Et
H
N
H
129

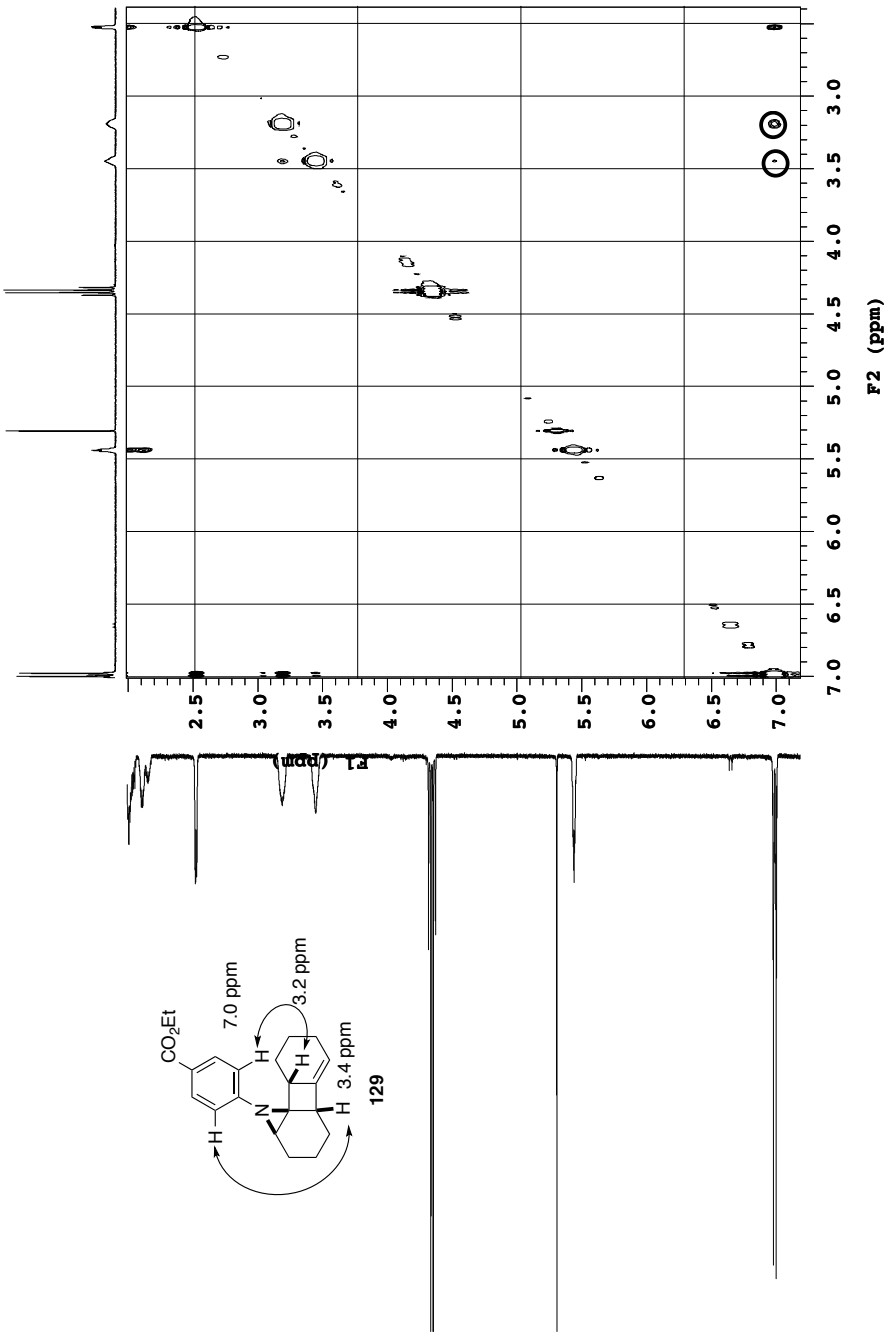
F2 (ppm)
F1 (ppm)
CO2Et
7.0 ppm
3.2 ppm
3.4 ppm
H
H
H
N
H
129

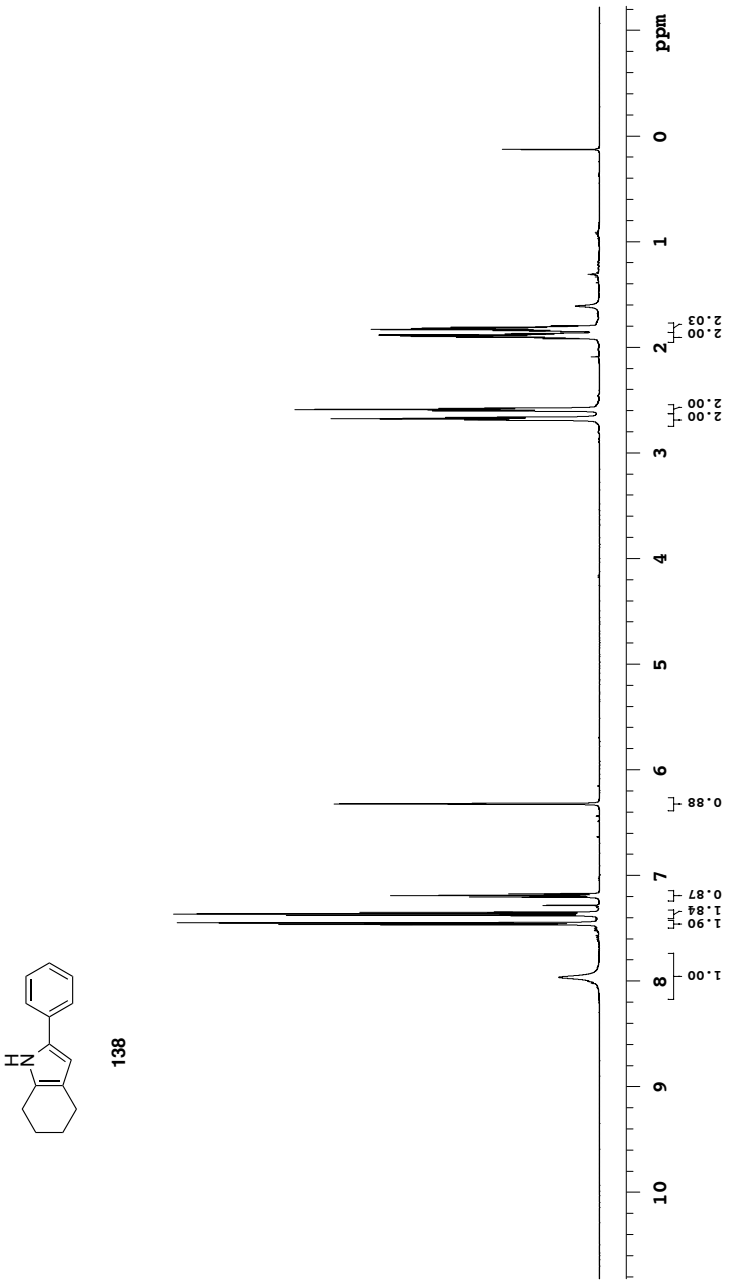
138
ppm
0
1
2
3
4
5
6
7
8
9
10
2.03
2.00
2.00
2.00
0.88
0.87
1.84
1.90
1.00

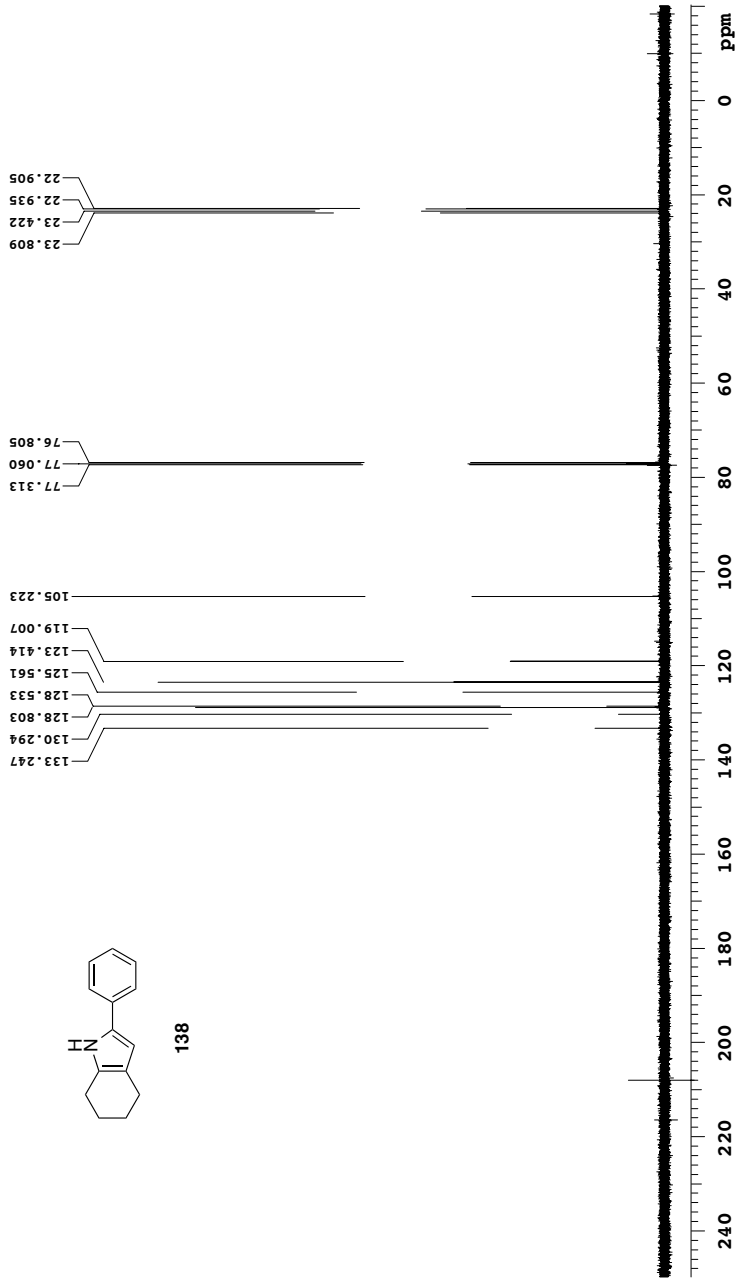
22.905
22.935
23.422
23.809
76.805
77.060
77.313
105.223
119.007
123.414
125.561
128.533
128.803
130.294
133.247
ppm
0
20
40
60
80
100
120
140
160
180
200
220
240
NH
138

Appendix II: Selected NMR Spectra

(Chapter 3)

499.806 MHz H1 PRESAT in cdcl3 (ref. to CDCl3 @ 7.26 ppm), temp 27.7 C -> actual temp = 27.0 C, colddual probe

date: Aug 15 2014 sweep width: 6010Hz acq.time: 5.0s relax.time: 2.1s # scans: 16 dig.res.: 0.2 Hz/pt hz/mm:25.0
spectrometer:ibdw file:/mnt/d600/home13/westnmr/nmrdata/Verner/Book9/2014.08.15.u5_VL-9-57_bromomethylcyclohexene_acetoxy_loc2_13.25_H1_1D

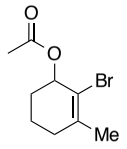

53

Pulse Sequence: PRESAT

125.691 MHz C13[H1] 1D in cdcl3 (ref. to CDCl3 @ 77.06 ppm), temp 27.7 C -> actual temp = 27.0 C, colddual probe

date: Aug 15 2014 sweep width: 32895Hz acq.time: 2.5s relax.time: 0.2s # scans: 128 dig.res.: 0.3 Hz/pt hz/mm:137.1
spectrometer:ibdw file:/mnt/d600/home13/westnmr/nmrdata/Verner/Book9/2014.08.15.u5_VL-9-57_bromomethylcyclohexene_acetoxy_loc2_13.27_C13_1D

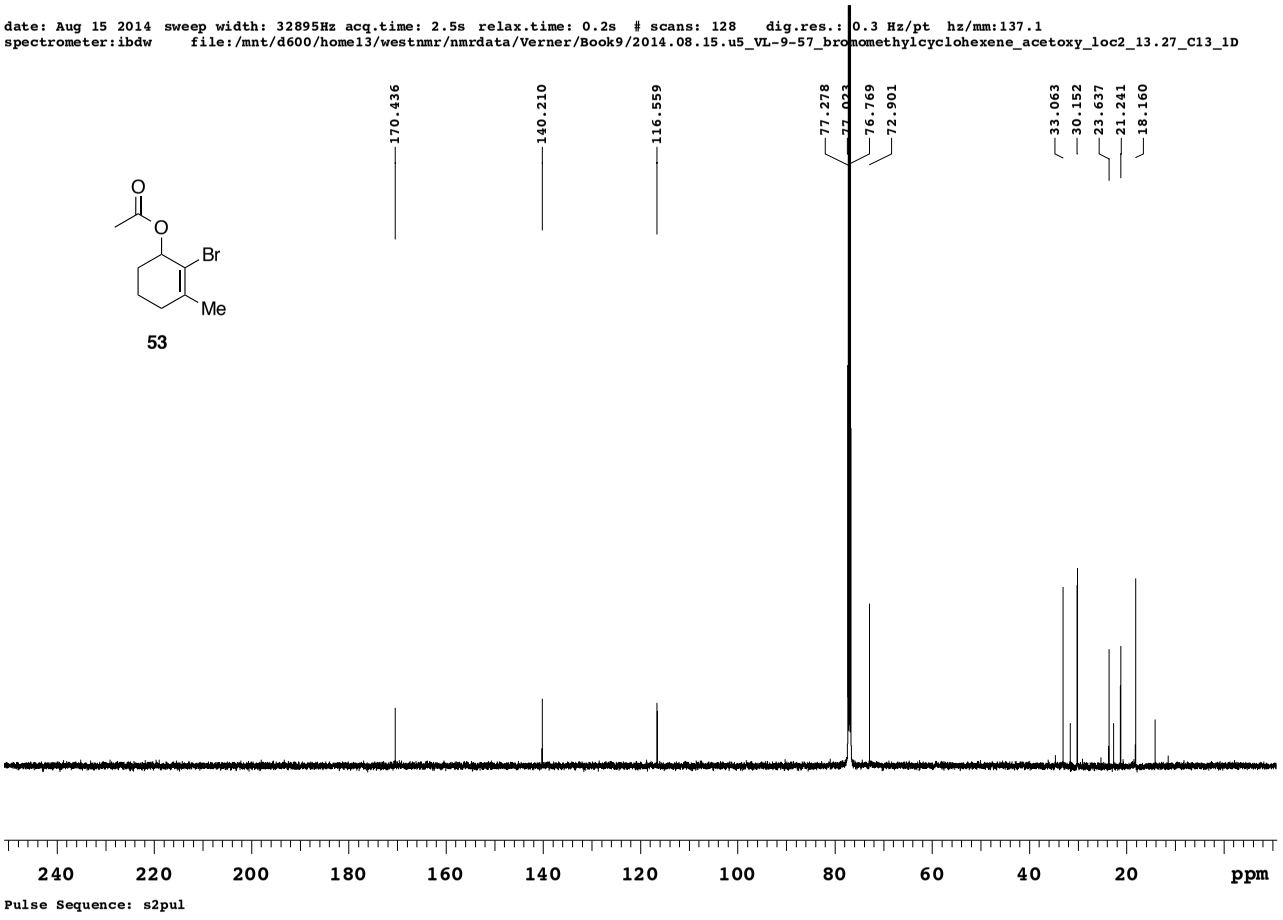

Pulse Sequence: s2pul

399.984 MHz H1 1D in cdcl3 (ref. to CDCl3 @ 7.26 ppm), temp 25.9 C -> actual temp = 27.0 C, onenmr probe

date: Aug 11 2014 sweep width: 4808Hz acq.time: 5.0s relax.time: 0.1s # scans: 16 dig.res.: 0.1 Hz/pt hz/mm:20.0
spectrometer:ibdw file:/mnt/d600/home13/westnmr/nmrdata/Verner/Book9/2014.08.11.mr4_VL-9-45_silylation_of_acetoxy_methylbromocyclohexene_H1_1D

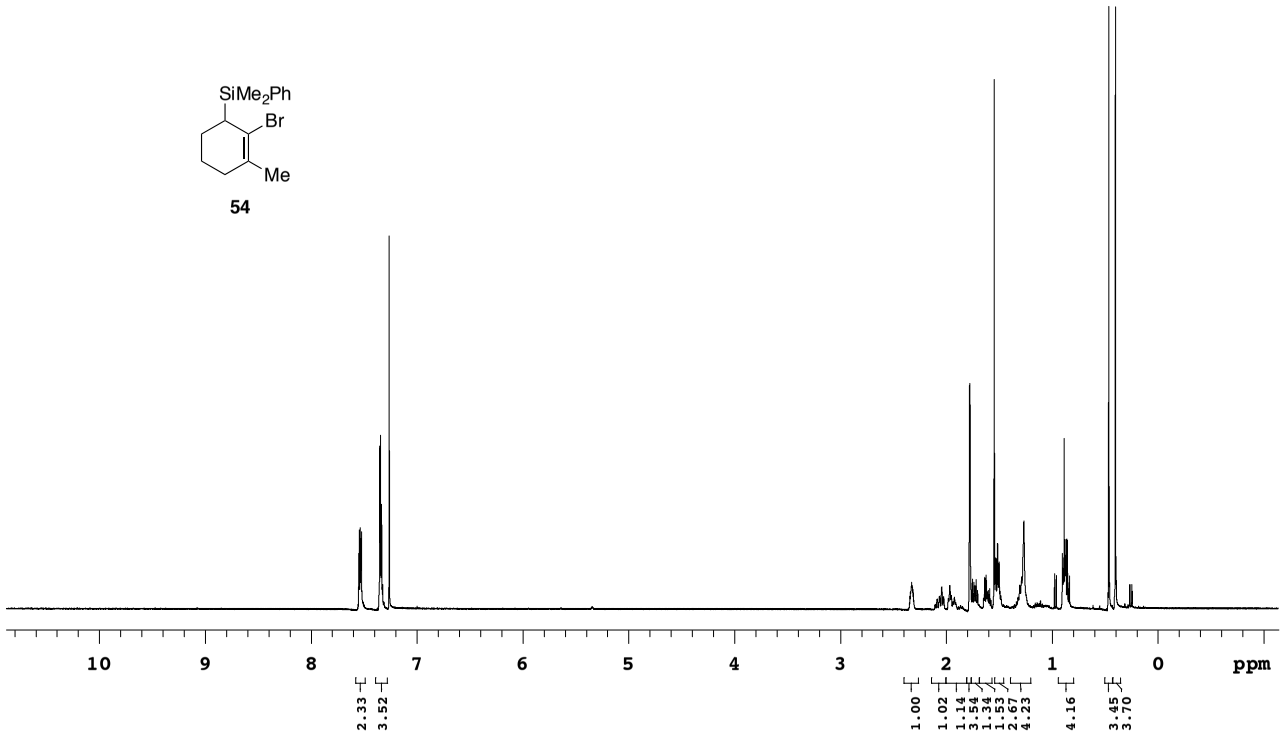

Pulse Sequence: s2pul

Verner, VL-9-45_silylation_acetoxy_bromomethylcyclohexene
125.691 MHz C13[H1] 1D in cdcl3 (ref. to CDCl3 @ 77.06 ppm), temp 27.7 C -> actual temp = 27.0 C, colddual probe

date: Aug 11 2014 sweep width: 32895Hz acq.time: 2.5s relax.time: 0.2s # scans: 128 dig.res.: 0.3 Hz/pt hz/mm:137.1
spectrometer:ibdw file:/mnt/d600/home13/westnmr/nmrdata/Verner/Book9/2014.08.11.u5_VL-9-45_silylation_acetoxy_bromomethylcyclohexene_loc2_12.54_C13_1D

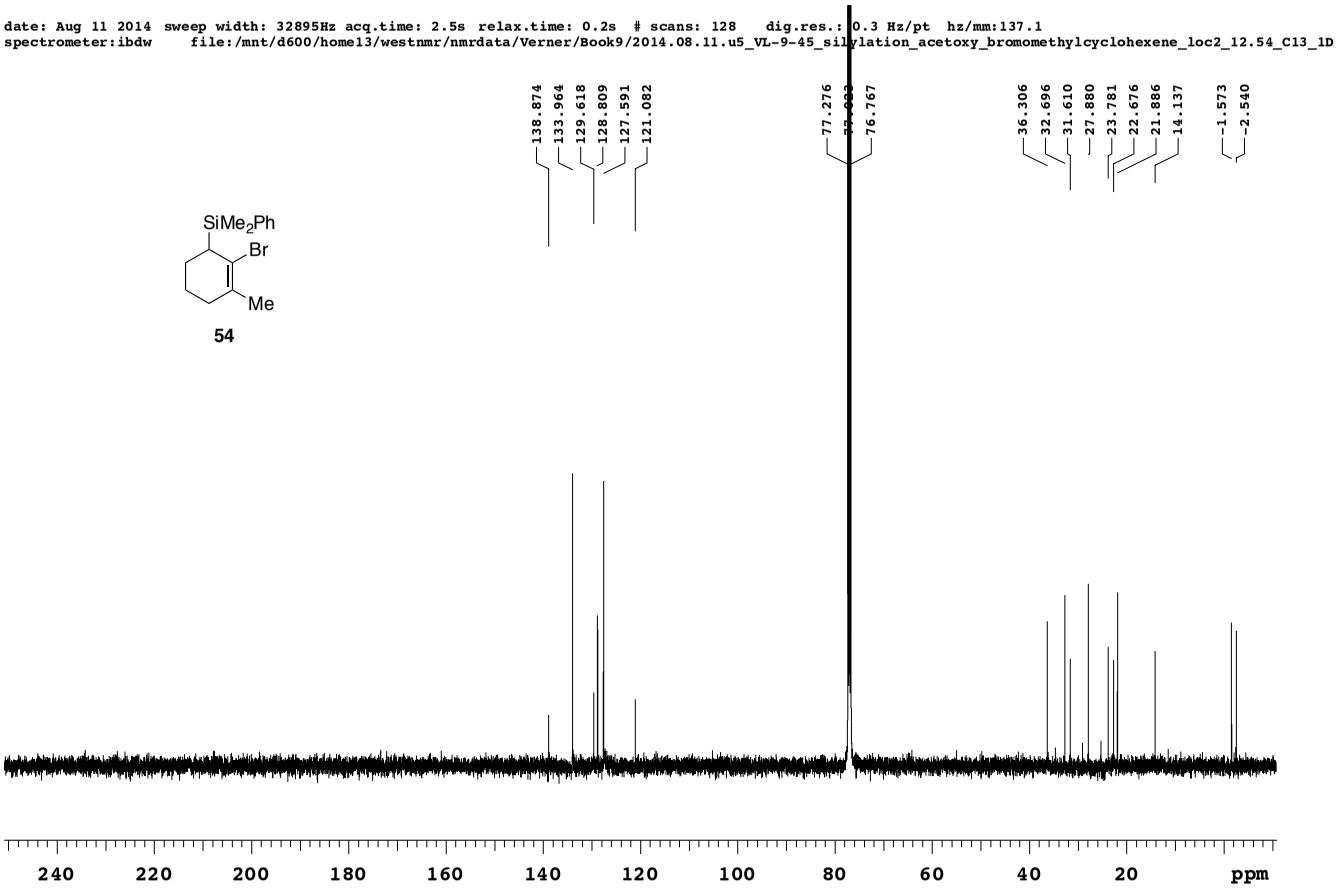

Pulse Sequence: s2pul

VL-9-187 methylbromocyclohexene picolinic ester
399.984 MHz H1 1D in cdcl3 (ref. to CDCl3 @ 7.26 ppm), temp 25.9 C -> actual temp = 27.0 C, onenmr probe

date: Oct 30 2014 sweep width: 4808Hz acq.time: 5.0s relax.time: 0.1s # scans: 16 dig.res.: 0.1 Hz/pt hz/mm:20.0
spectrometer:ibdw file:/mnt/d600/home13/westnmr/nmrdata/Verner/Book9/2014.10.30.mr4_VL-9-187_methylbromocyclohexene_picolinic_ester_H1_1D

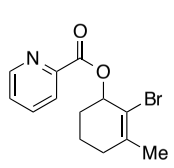

65

Pulse Sequence: s2pul

Verner, VL-9-93_picolinic_ester_methylbromocyclohexene
125.691 MHz C13[H1] 1D in cdcl3 (ref. to CDCl3 @ 77.06 ppm), temp 27.7 C -> actual temp = 27.0 C, colddual probe

date: Aug 29 2014 sweep width: 32895Hz acq.time: 2.5s relax.time: 0.2s # scans: 128 dig.res.: 0.3 Hz/pt hz/mm:137.1
spectrometer:ibdw file:/mnt/d600/home13/westnmr/nmrdata/Verner/Book9/2014.08.29.u5_VL-9-93_picolinic_ester_methylbromocyclohexene_loc3_10.52_C13_1D

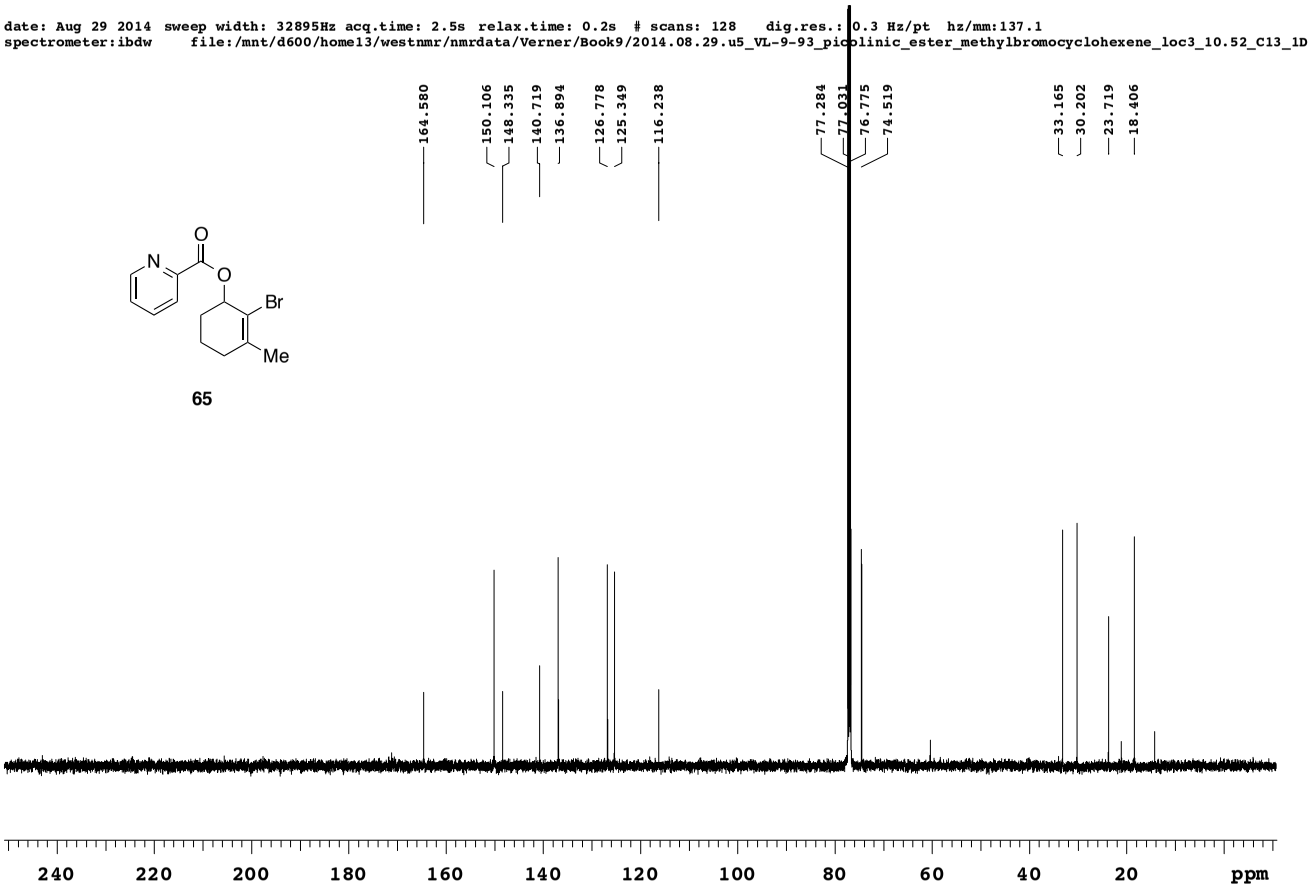

65

Pulse Sequence: s2pul

399.984 MHz H1 1D in cdcl3 (ref. to CDCl3 @ 7.26 ppm), temp 25.9 C -> actual temp = 27.0 C, onenmr probe

date: Oct 30 2014 sweep width: 4808Hz acq.time: 5.0s relax.time: 0.1s # scans: 16 dig.res.: 0.1 Hz/pt hz/mm:20.0
spectrometer:ibdw file:/mnt/d600/home13/westnmr/nmrdata/Verner/Book9/2014.10.30.mr4_VL-9-181_bromomethylcyclohexene_silyl_H1_1D

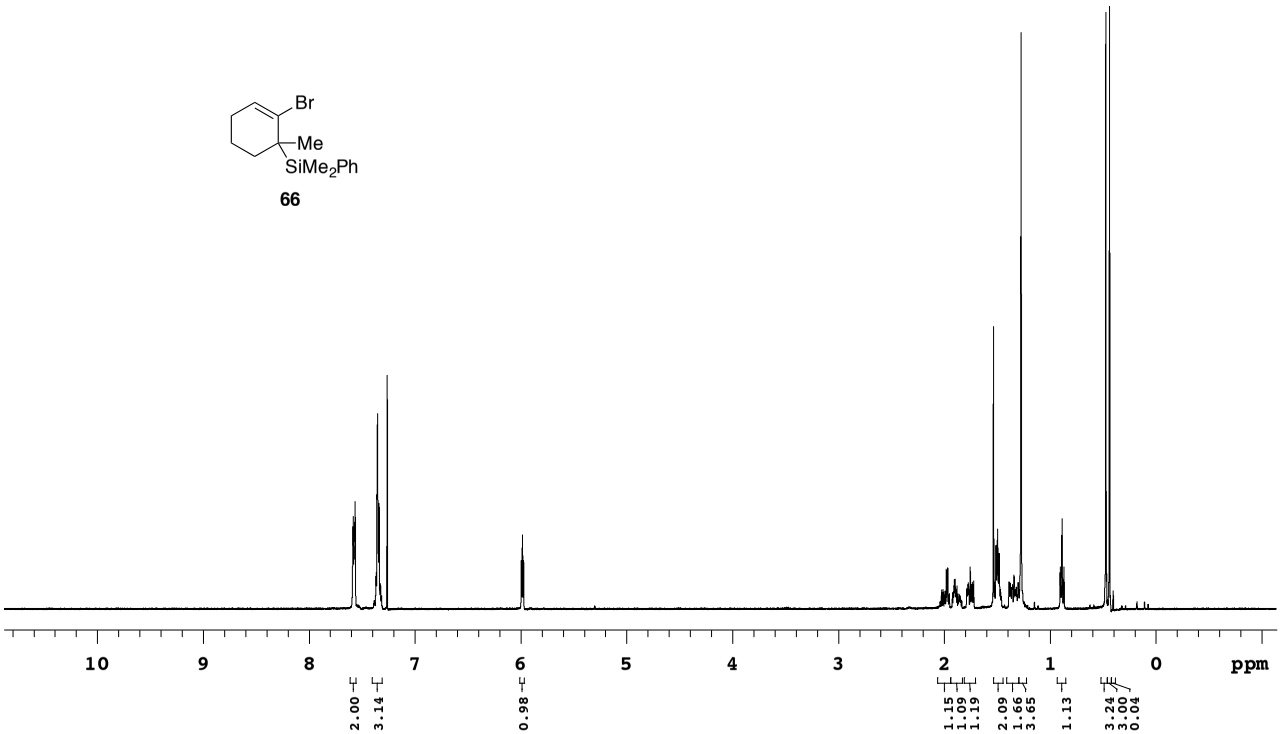

Pulse Sequence: s2pul

125.266 MHz C13[H1] 1D in cdcl3 (ref. to CDCl3 @ 77.06 ppm), temp 26.4 C -> actual temp = 27.0 C, autoxdb probe

date: Feb 17 2015 sweep width: 33827Hz acq.time: 2.5s relax.time: 0.1s # scans: 480 dig.res.: 0.3 Hz/pt hz/mm:140.9
spectrometer:d300 file:/mnt/d600/home13/westnmr/nmrdata/Verner/Book9/2015.02.17.i5_VL-9-18_mallene_precursor__tertiary_silane__C13_1D

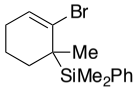

66

Pulse Sequence: s2pul

399.984 MHz H1 1D in cdcl3 (ref. to CDCl3 @ 7.26 ppm), temp 25.9 C -> actual temp = 27.0 C, onenmr probe

date: Dec 19 2014 sweep width: 4808Hz acq.time: 5.0s relax.time: 0.1s # scans: 16 dig.res.: 0.1 Hz/pt hz/mm:20.0
spectrometer:ibdw file:/mnt/d600/home13/westnmr/nmrdata/Verner/Book9/2014.12.19.mr4_VL-9-201_mallene_precursor_benzoylated_H1_1D

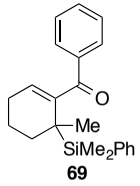

69

Pulse Sequence: s2pul

125.691 MHz C13[H1] 1D in cdcl3 (ref. to CDCl3 @ 77.06 ppm), temp 27.7 C -> actual temp = 27.0 C, colddual probe

date: Oct 16 2014 sweep width: 32895Hz acq.time: 2.5s relax.time: 0.2s # scans: 128 dig.res.: 0.3 Hz/pt hz/mm:137.1
spectrometer:ibdw file:/mnt/d600/home13/westnmr/nmrdata/Verner/Book9/2014.10.16.u5_VL-9-173_silylmethylcyclohexene_benzoyl_loc6_09.25_C13_1D

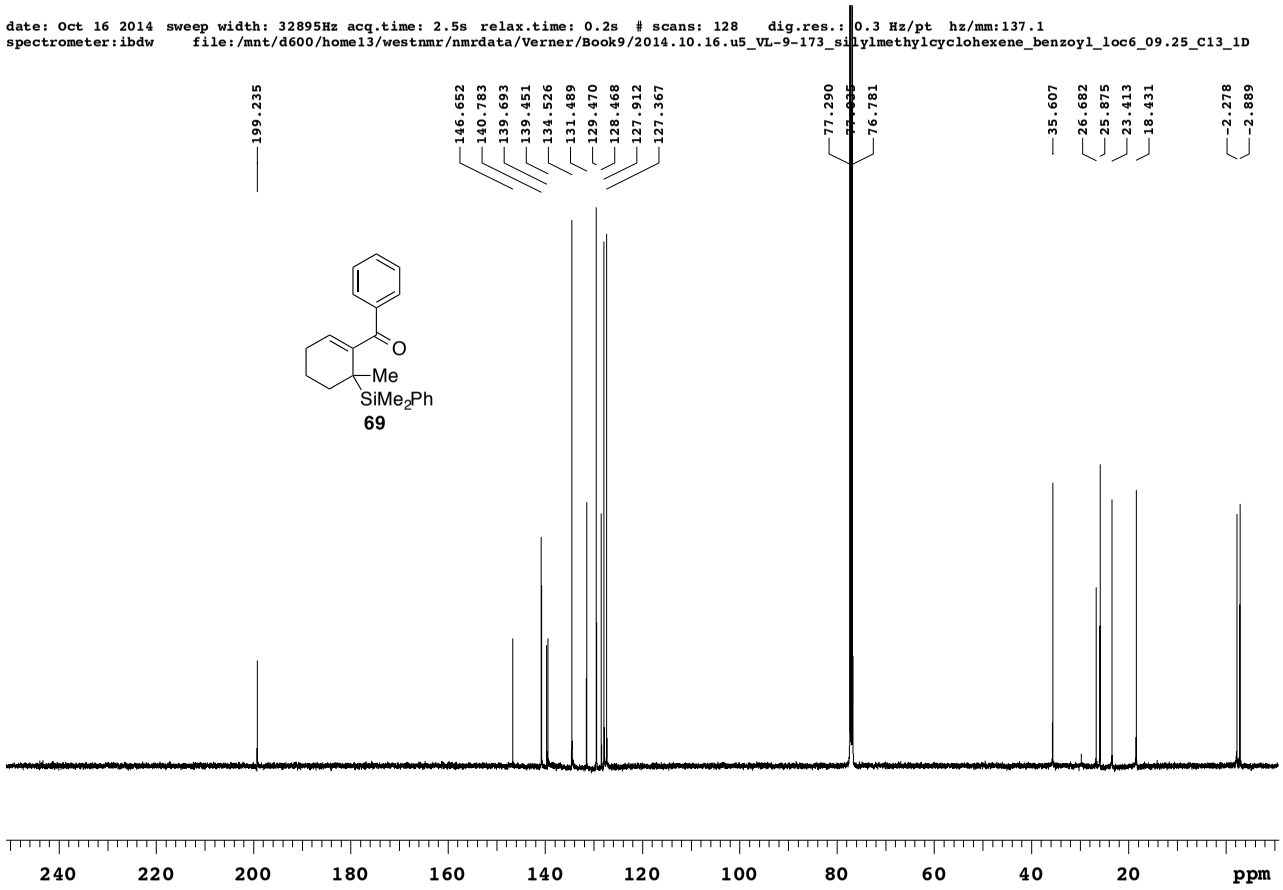

Pulse Sequence: s2pul

498.118 MHz H1 1D in cdcl3 (ref. to CDCl3 @ 7.26 ppm), temp 26.4 C -> actual temp = 27.0 C, autoxdb probe

date: Sep 11 2014 sweep width: 6001Hz acq.time: 5.0s relax.time: 0.1s # scans: 16 dig.res.: 0.1 Hz/pt hz/mm:25.0
spectrometer:ibdw file:/mnt/d600/home13/westnmr/nmrdata/Verner/Book9/2014.09.11.i5_VL-9-107_chiral_mallene_benzaldehyde_AMI_major_isomer_H1_1D

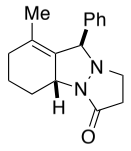

74

Pulse Sequence: s2pul

125.691 MHz C13[H1] 1D in cdcl3 (ref. to CDCl3 @ 77.06 ppm), temp 27.7 C -> actual temp = 27.0 C, colddual probe

date: Sep 11 2014 sweep width: 32895Hz acq.time: 2.5s relax.time: 0.2s # scans: 128 dig.res.: 0.3 Hz/pt hz/mm:137.1
spectrometer:ibdw file:/mnt/d600/home13/westnmr/nmrdata/Verner/Book9/2014.09.11.u5_VL-9-107_chiral_mallene_benzaldehyde_AMI_major_isomer_loc4_13.48_C13_1D

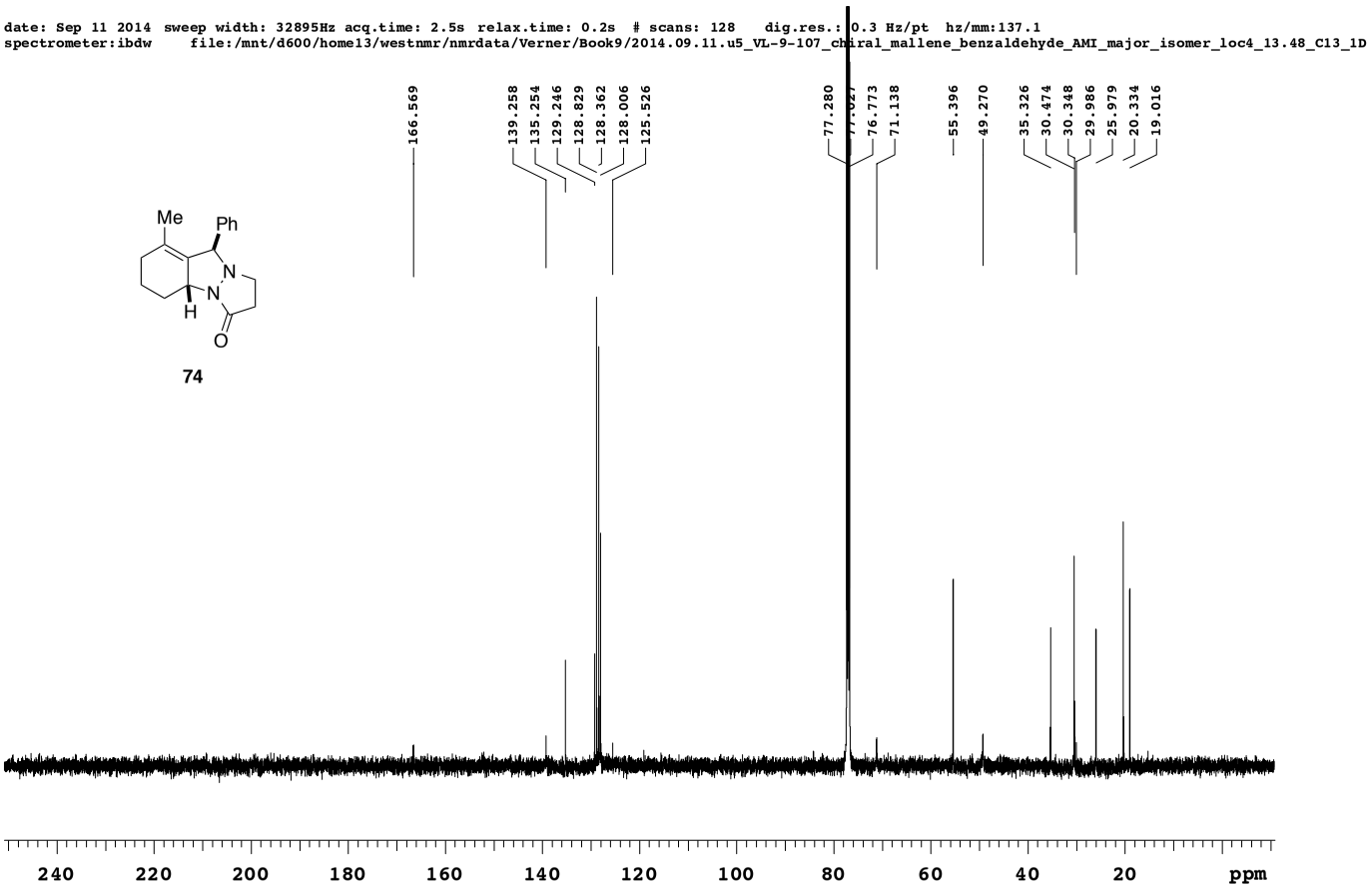

74

Pulse Sequence: s2pul

Verner, VL-9-107_C-mallene_Benzaldehyde_AMI_major
499.806 MHz H1 ROESY in cdcl3 (ref. to CDCl3 @ 7.26 ppm), temp 27.7 C -> actual temp = 27.0 C, colddual probe

Temp. 27.7 C / 300.9 K
Sample #6, Operator: WEST

Relax. delay 1.000 sec
Acq. time 1.000 sec
Width 6009.6 Hz
2D Width 8012.8 Hz
16 repetitions
2 x 170 increments
OBSERVE H1, 499.8039263 MHz
DATA PROCESSING
Sq. sine bell 0.250 sec
Shifted by -0.250 sec
F1 DATA PROCESSING
Sq. sine bell 0.021 sec
Shifted by -0.021 sec
FT size 8192 x 1024
Total time 3 hr, 38 min

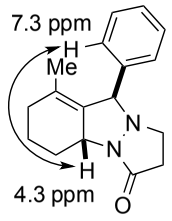

74

Pulse Sequence: ROESY

499.806 MHz H1 PRESAT in cdcl3 (ref. to CDCl3 @ 7.26 ppm), temp 27.7 C -> actual temp = 27.0 C, colddual probe

date: Dec 23 2014 sweep width: 6010Hz acq.time: 5.0s relax.time: 2.1s # scans: 16 dig.res.: 0.2 Hz/pt hz/mm:25.0
spectrometer:ibdw file:/mnt/d600/home13/westnmr/nmrdata/Verner/Book9/2014.12.23.u5_VL-9-203_m-allene_benzAMI_minor_loc6_15.04_H1_1D

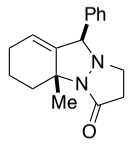

75

Pulse Sequence: PRESAT

125.691 MHz C13[H1] 1D in cdcl3 (ref. to CDCl3 @ 77.06 ppm), temp 27.7 C -> actual temp = 27.0 C, colddual probe

date: Dec 23 2014 sweep width: 32895Hz acq.time: 2.5s relax.time: 0.2s # scans: 128 dig.res.: 0.3 Hz/pt hz/mm:137.1
spectrometer:ibdw file:/mnt/d600/home13/westnmr/nmrdata/Verner/Book9/2014.12.23.u5_VL-9-203_m-allene_benzAMI_minor_loc6_15.05_C13_1D

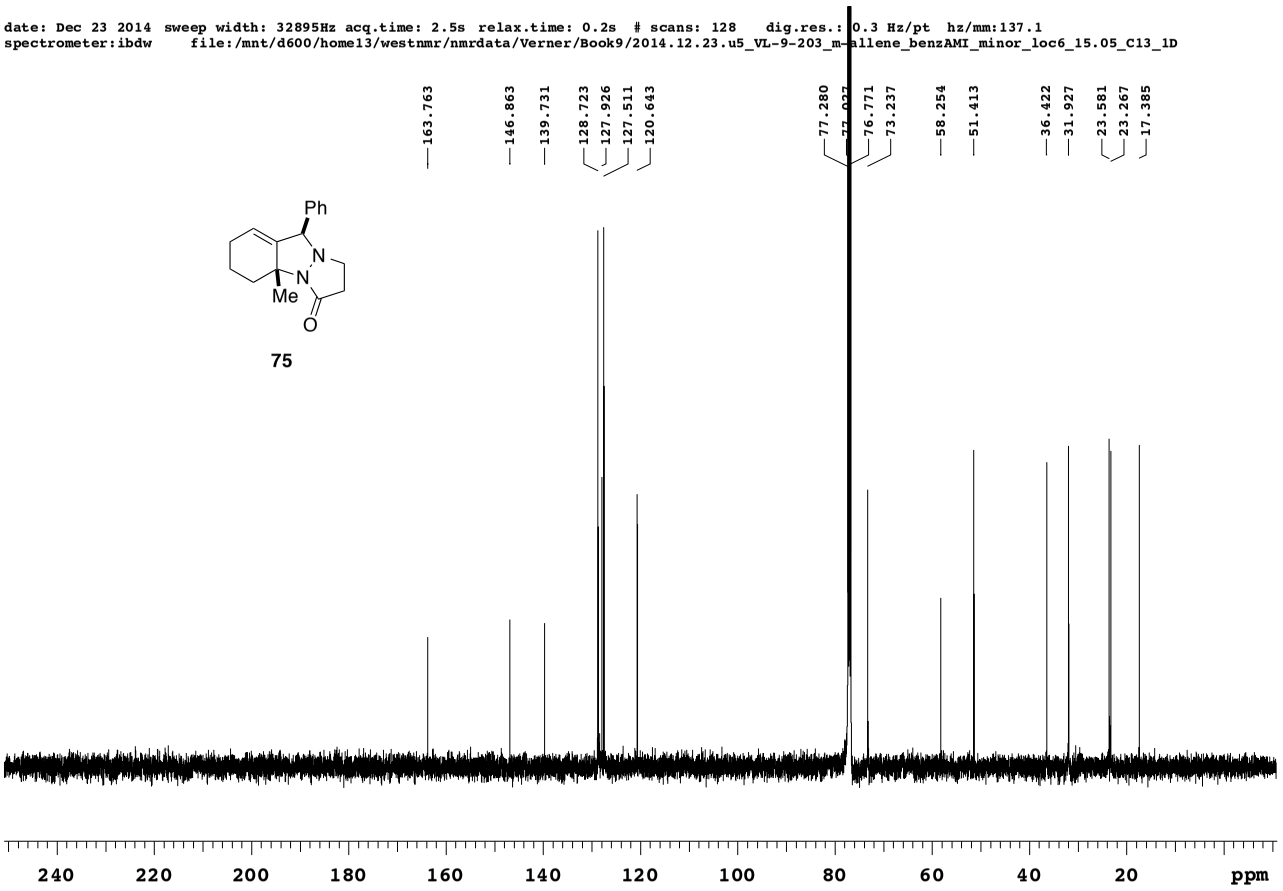

75

Pulse Sequence: s2pul

Verner, VL-9-107_C_mallene_benzaldehyde_AMI_minor
499.806 MHz H1 ROESY in cdcl3 (ref. to CDCl3 @ 7.26 ppm), temp 27.7 C -> actual temp = 27.0 C, colddual probe

Temp. 27.7 C / 300.9 K
Sample #7, Operator: WEST

Relax. delay 1.000 sec
Acq. time 1.000 sec
Width 6009.6 Hz
2D Width 8012.8 Hz
16 repetitions
2 x 170 increments
OBSERVE H1, 499.8039392 MHz
DATA PROCESSING
Sq. sine bell 0.250 sec
Shifted by -0.250 sec
F1 DATA PROCESSING
Sq. sine bell 0.021 sec
Shifted by -0.021 sec
FT size 8192 x 1024
Total time 3 hr, 38 min

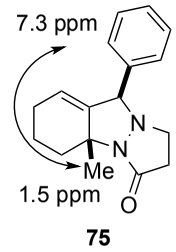

75

Pulse Sequence: ROESY

498.118 MHz H1 1D in cdcl3 (ref. to CDCl3 @ 7.26 ppm), temp 26.4 C -> actual temp = 27.0 C, autoxdb probe

date: Nov 4 2014 sweep width: 6001Hz acq.time: 5.0s relax.time: 0.1s # scans: 16 dig.res.: 0.1 Hz/pt hz/mm:25.0
spectrometer:ibdw file:/mnt/d600/home13/westnmr/nmrdata/Verner/Book9/2014.11.04.i5_VL-9-194_cm-allene_cinnamaldehyde_AMI_regioisomer_2_H1_1D

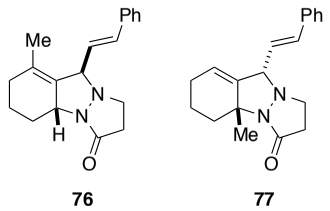

76

77

Pulse Sequence: s2pul

498.118 MHz H1 1D in cdcl3 (ref. to CDCl3 @ 7.26 ppm), temp 26.4 C -> actual temp = 27.0 C, autoxdb probe

date: Jan 26 2015 sweep width: 6001Hz acq.time: 5.0s relax.time: 0.1s # scans: 16 dig.res.: 0.1 Hz/pt hz/mm:25.0
spectrometer:ibdw file:/mnt/d600/home13/westnmr/nmrdata/Verner/Book9/2015.01.26.i5_VL-9-207_mallene_cinAMI_major__F2__H1_1D

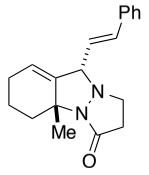

77

Pulse Sequence: s2pul

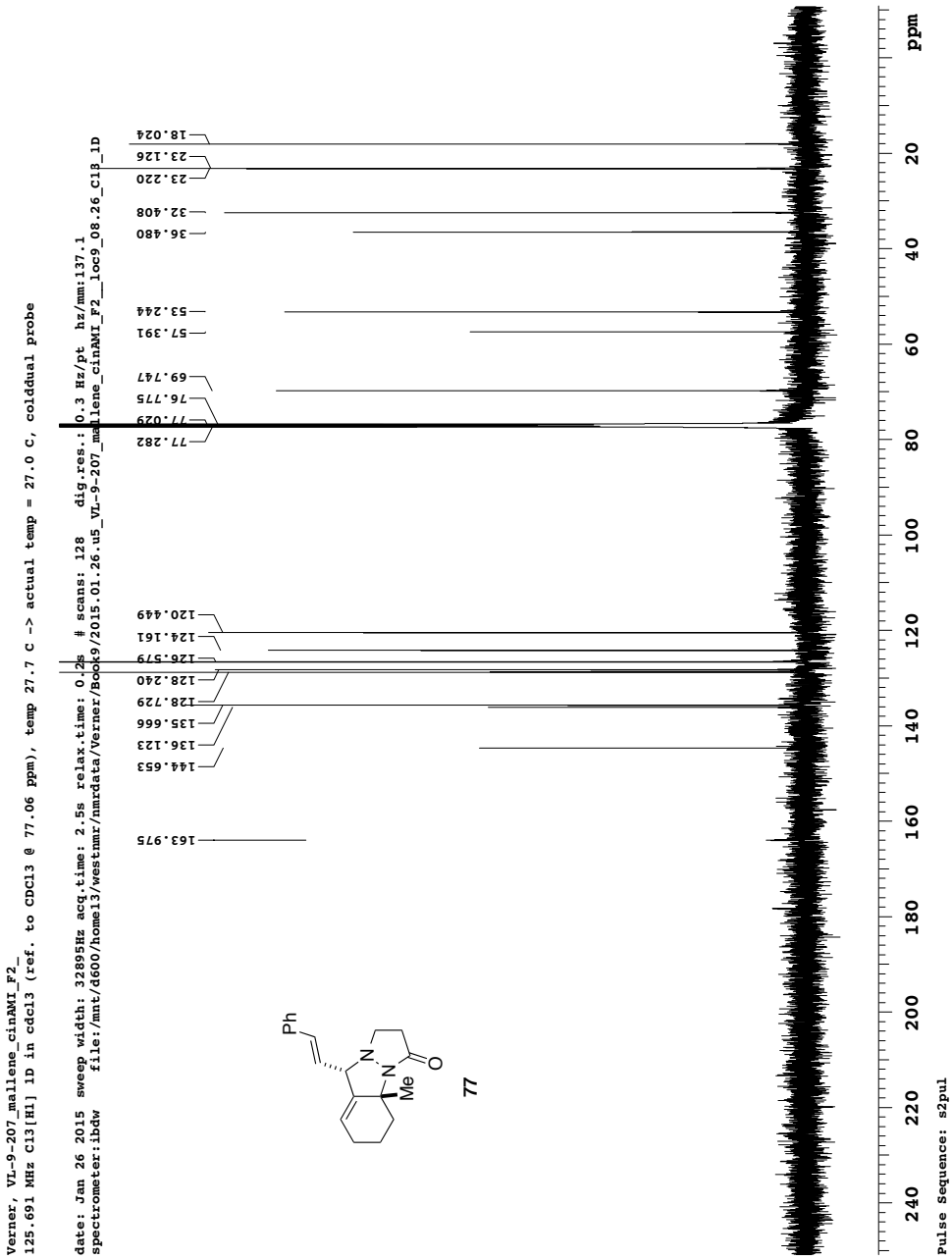
Verner, VL-9-207_mallene_cinAMI_F2_
125.691 MHz C13[H1] 1D in cdcl3 (ref. to CDCl3 @ 77.06 ppm), temp 27.7 C -> actual temp = 27.0 C, colddual probe
date: Jan 26 2015 sweep width: 32895Hz acq.time: 2.5s relax.time: 0.2s # scans: 128 dig.res.: 0.3 Hz/pt hz/mm:137.1
spectrometer:ibdw file:/mnt/d600/home13/westmnr/nmrdata/Verner/Book9/2015.01.26.u5_VL-9-207_mallene_cinAMI_F2__loc9_08.26_C13_1D
18.024
23.126
23.220
32.408
36.480
53.244
57.391
69.747
76.775
77.029
77.282
120.449
124.161
126.579
128.240
128.729
135.666
136.123
144.653
163.975
Ph
N
N
Me
O
77
240
220
200
180
160
140
120
100
80
60
40
20
ppm
Pulse Sequence: s2pul

VL-9-207 mallene cinAMI major (F2)
498.118 MHz H1 ROESY in cdcl3 (ref. to CDCl3 @ 7.26 ppm), temp 26.4 C -> actual temp = 27.0 C, autoxdb probe

Temp. 26.4 C / 299.6 K
Operator: nmrlab

Relax. delay 1.000 sec
Acq. time 1.000 sec
Width 6000.6 Hz
2D Width 6000.6 Hz
16 repetitions
2 x 365 increments
OBSERVE H1, 498.1154023 MHz
DATA PROCESSING
Sq. sine bell 0.250 sec
Shifted by -0.250 sec
F1 DATA PROCESSING
Sq. sine bell 0.009 sec
Shifted by -0.009 sec
FT size 8192 x 1024
Total time 7 hr, 53 min

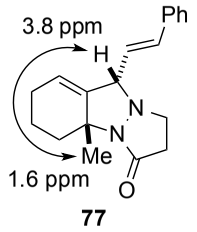

77

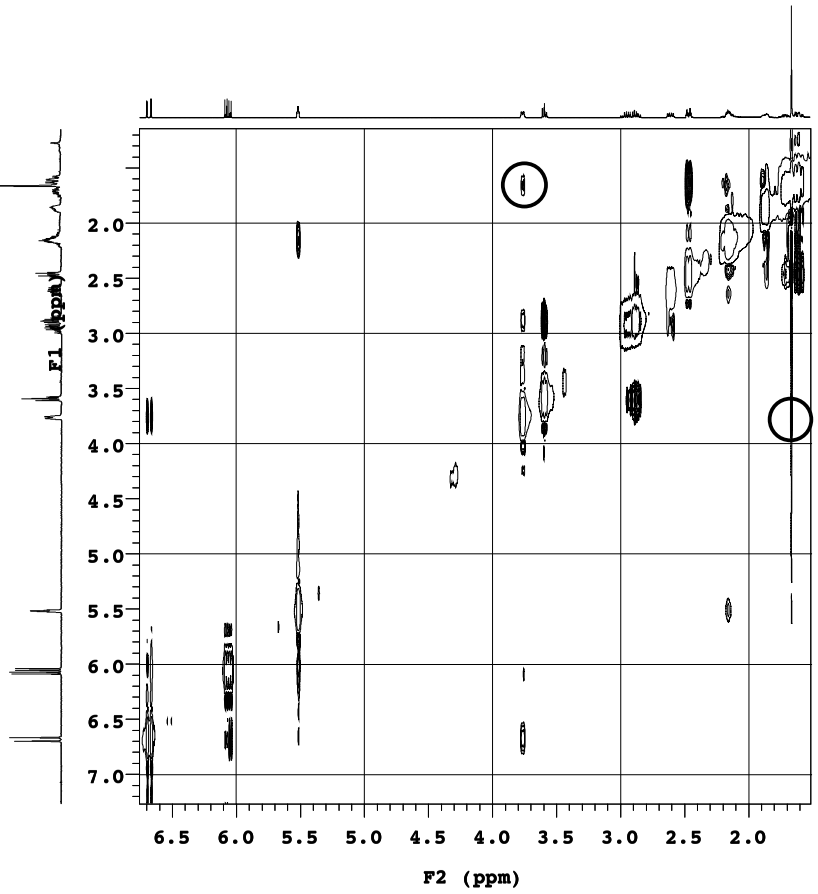

Pulse Sequence: ROESY

125.691 MHz C13[H1] 1D in cdcl3 (ref. to CDCl3 @ 77.06 ppm), temp 27.7 C -> actual temp = 27.0 C, colddual probe

date: Jan 22 2015 sweep width: 32895Hz acq.time: 2.5s relax.time: 0.2s # scans: 628 dig.res.: 0.3 Hz/pt hz/mm:137.1
spectrometer:ibdw file:/mnt/d600/home13/westnmr/nmrdata/Verner/Book9/2015.01.22.u5_VL-9-207_mallene_cinAMI_minor_R1__loc12_07.37_C13_1D

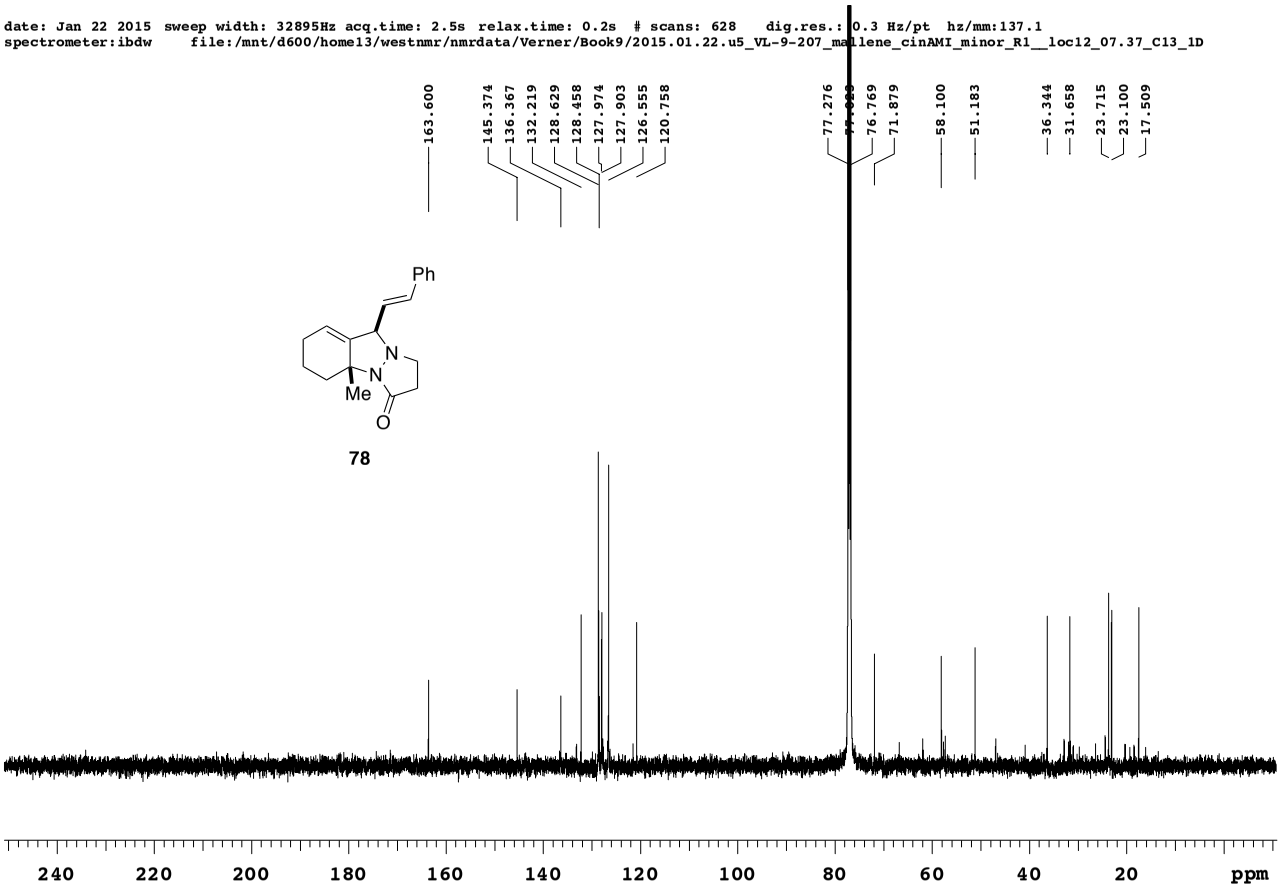

78

Pulse Sequence: s2pul

Verner, VL-9-207_mallene_cinAMI_minor_R1_
499.806 MHz H1 ROESY in cdcl3 (ref. to CDCl3 @ 7.26 ppm), temp 27.7 C -> actual temp = 27.0 C, colddual probe

Temp. 27.7 C / 300.9 K
Sample #2, Operator: WEST

Relax. delay 1.000 sec
Acq. time 1.000 sec
Width 6009.6 Hz
2D Width 8012.8 Hz
16 repetitions
2 x 170 increments
OBSERVE H1, 499.8039258 MHz
DATA PROCESSING
Sq. sine bell 0.250 sec
Shifted by -0.250 sec
F1 DATA PROCESSING
Sq. sine bell 0.021 sec
Shifted by -0.021 sec
FT size 8192 x 1024
Total time 3 hr, 38 min

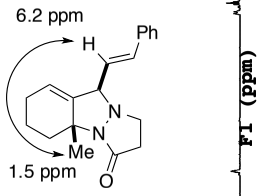

78

Pulse Sequence: ROESY

VL-9-93 m-allene dibenzyl nitrone
498.118 MHz H1 1D in cdcl3 (ref. to CDCl3 @ 7.26 ppm), temp 26.4 C -> actual temp = 27.0 C, autoxdb probe

date: Sep 2 2014 sweep width: 6001Hz acq.time: 5.0s relax.time: 0.1s # scans: 16 dig.res.: 0.1 Hz/pt hz/mm:25.0
spectrometer:ibdw file:/mnt/d600/home13/westnmr/nmrdata/Verner/Book9/2014.09.02.i5_VL-9-93_m-allene_dibenzyl_nitrone_H1_1D

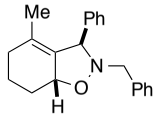

80

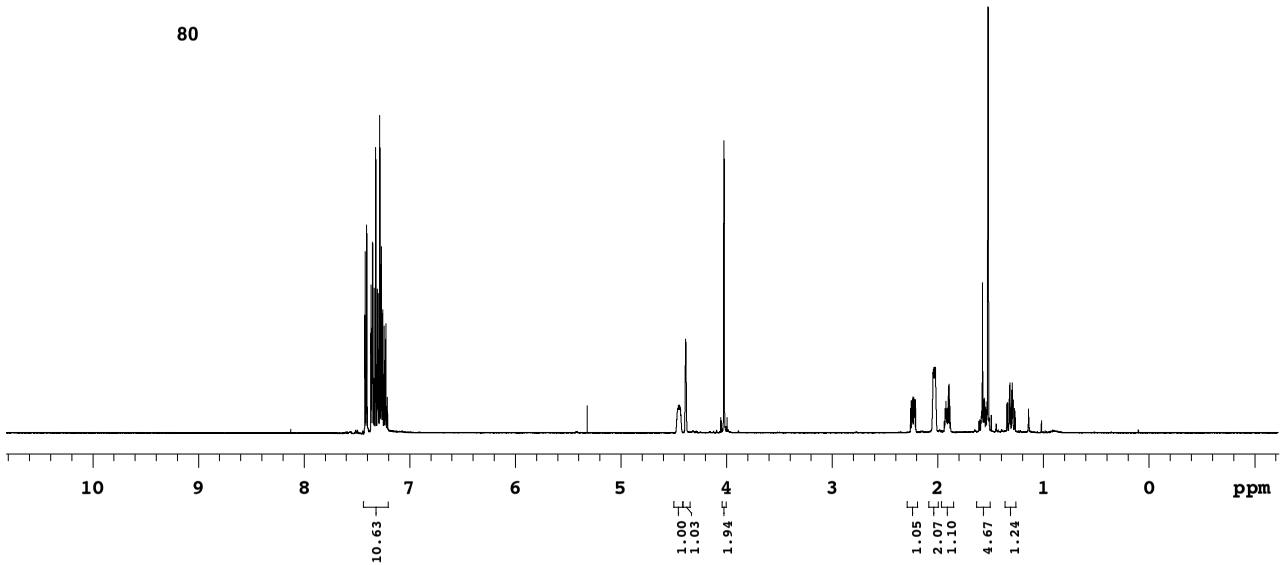

Pulse Sequence: s2pul

125.691 MHz C13[H1] 1D in cdcl3 (ref. to CDCl3 @ 77.06 ppm), temp 27.7 C -> actual temp = 27.0 C, colddual probe

date: Sep 2 2014 sweep width: 32895Hz acq.time: 2.5s relax.time: 0.2s # scans: 128 dig.res.: 0.3 Hz/pt hz/mm:137.1
spectrometer:ibdw file:/mnt/d600/home13/westnmr/nmrdata/Verner/Book9/2014.09.2.u5_VL-9-93_m-allene_dibenzylnitrone_loc3_12.55_C13_1D

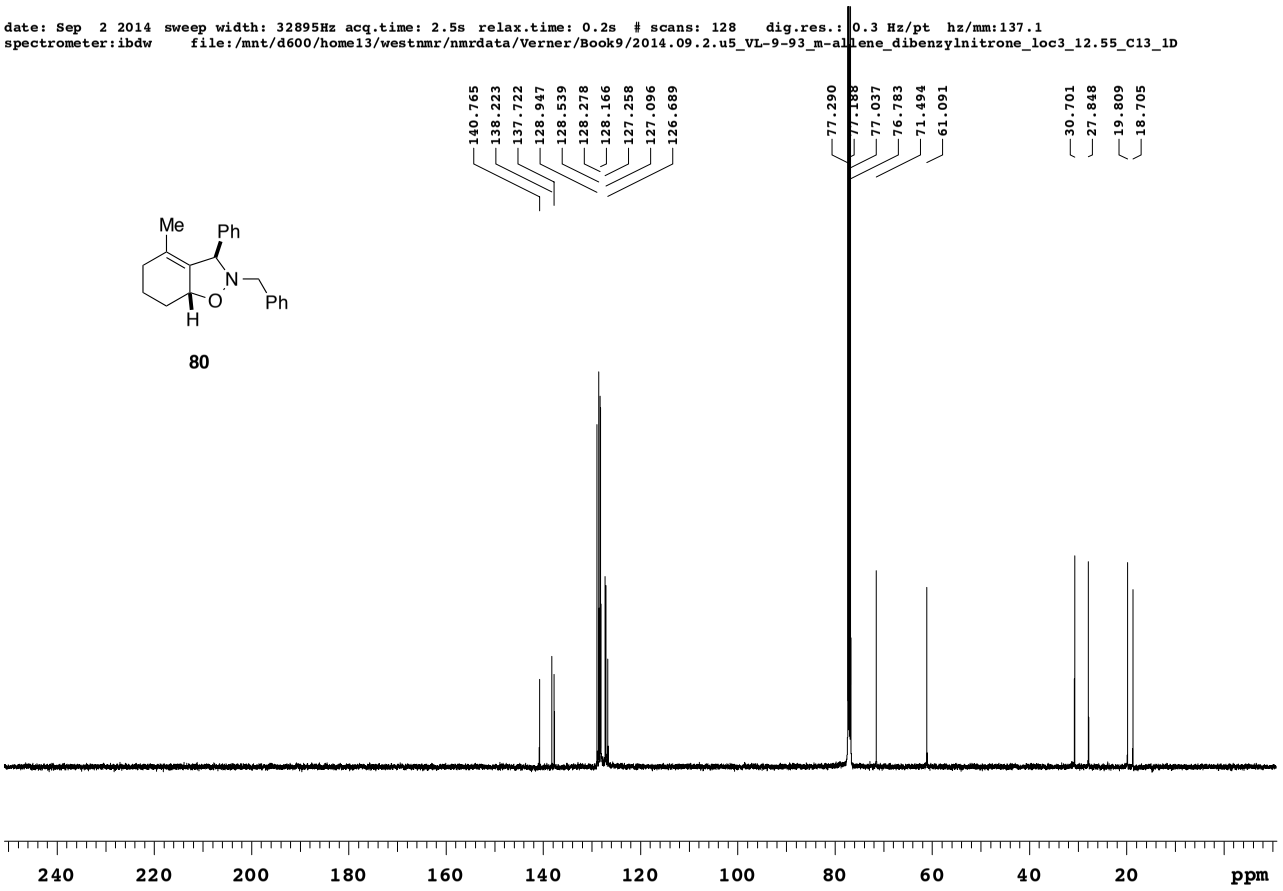

80

Pulse Sequence: s2pul

498.118 MHz H1 1D in cdcl3 (ref. to CDCl3 @ 7.26 ppm), temp 26.4 C -> actual temp = 27.0 C, autoxdb probe

date: Sep 4 2014 sweep width: 6001Hz acq.time: 5.0s relax.time: 0.1s # scans: 16 dig.res.: 0.1 Hz/pt hz/mm:25.0
spectrometer:ibdw file:/mnt/d600/home13/westnmr/nmrdata/Verner/Book9/2014.09.04.i5_VL-9-95_m-allene_dibenzylnitrone_regioisomer_H1_1D

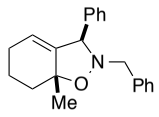

81

Pulse Sequence: s2pul

125.691 MHz C13[H1] 1D in cdcl3 (ref. to CDCl3 @ 77.06 ppm), temp 27.7 C -> actual temp = 27.0 C, colddual probe

date: Sep 4 2014 sweep width: 32895Hz acq.time: 2.5s relax.time: 0.2s # scans: 128 dig.res.: 0.3 Hz/pt hz/mm:137.1
spectrometer:ibdw file:/mnt/d600/home13/westnmr/nmrdata/Verner/Book9/2014.09.4.u5_VL-9-95_m-allene_dibenzylnitrone_regioisomer_loc4_08.03_C13_1D

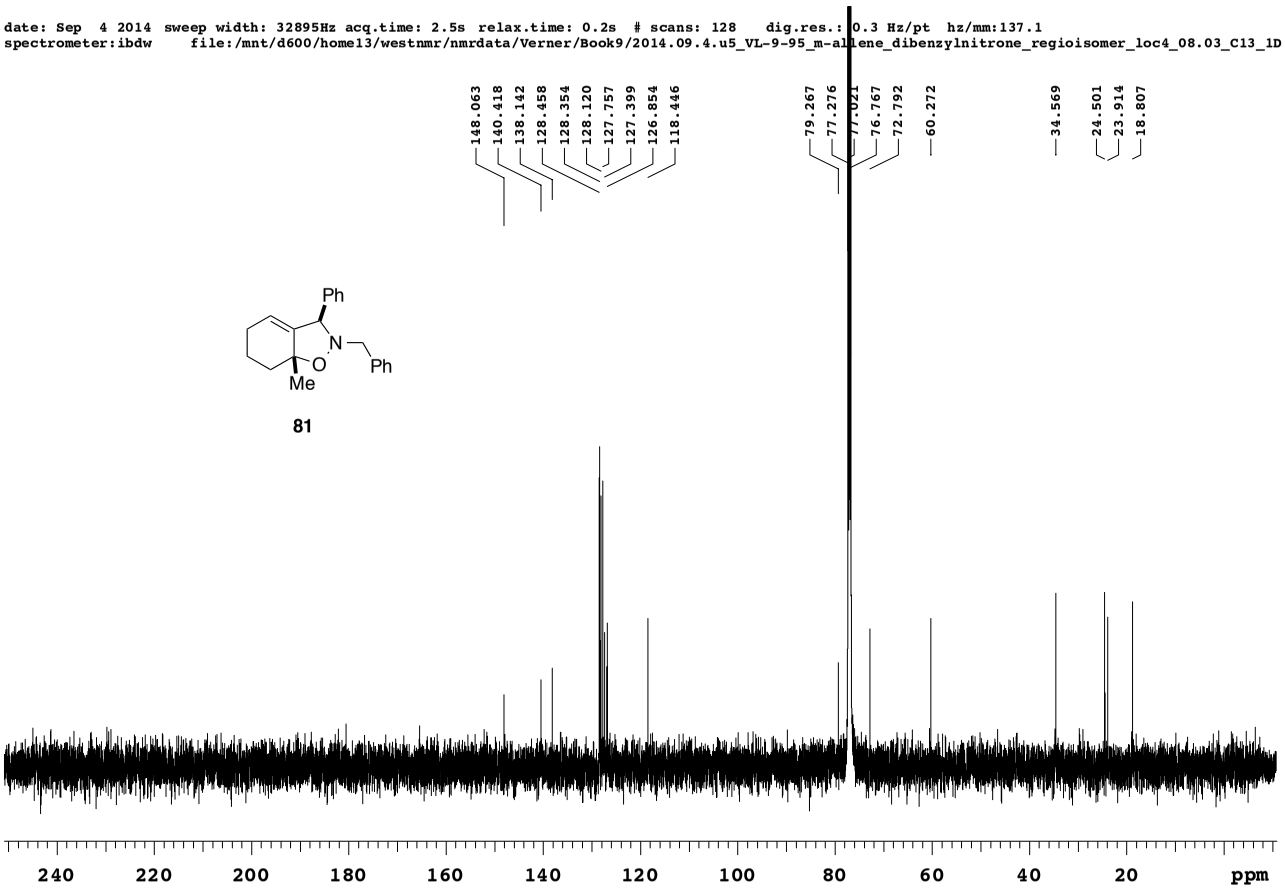

81

Pulse Sequence: s2pul

498.118 MHz H1 1D in cdcl3 (ref. to CDCl3 @ 7.26 ppm), temp 26.4 C -> actual temp = 27.0 C, autoxdb probe

date: Oct 1 2014 sweep width: 6001Hz acq.time: 5.0s relax.time: 0.1s # scans: 16 dig.res.: 0.1 Hz/pt hz/mm:25.0
spectrometer:ibdw file:/mnt/d600/home13/westnmr/nmrdata/Verner/Book9/2014.10.01.i5_VL-9-131_c-mallene_cinnamaldehyde_nitrone__major__with_EU_1_H1_1D

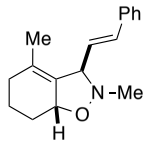

83

Pulse Sequence: s2pul

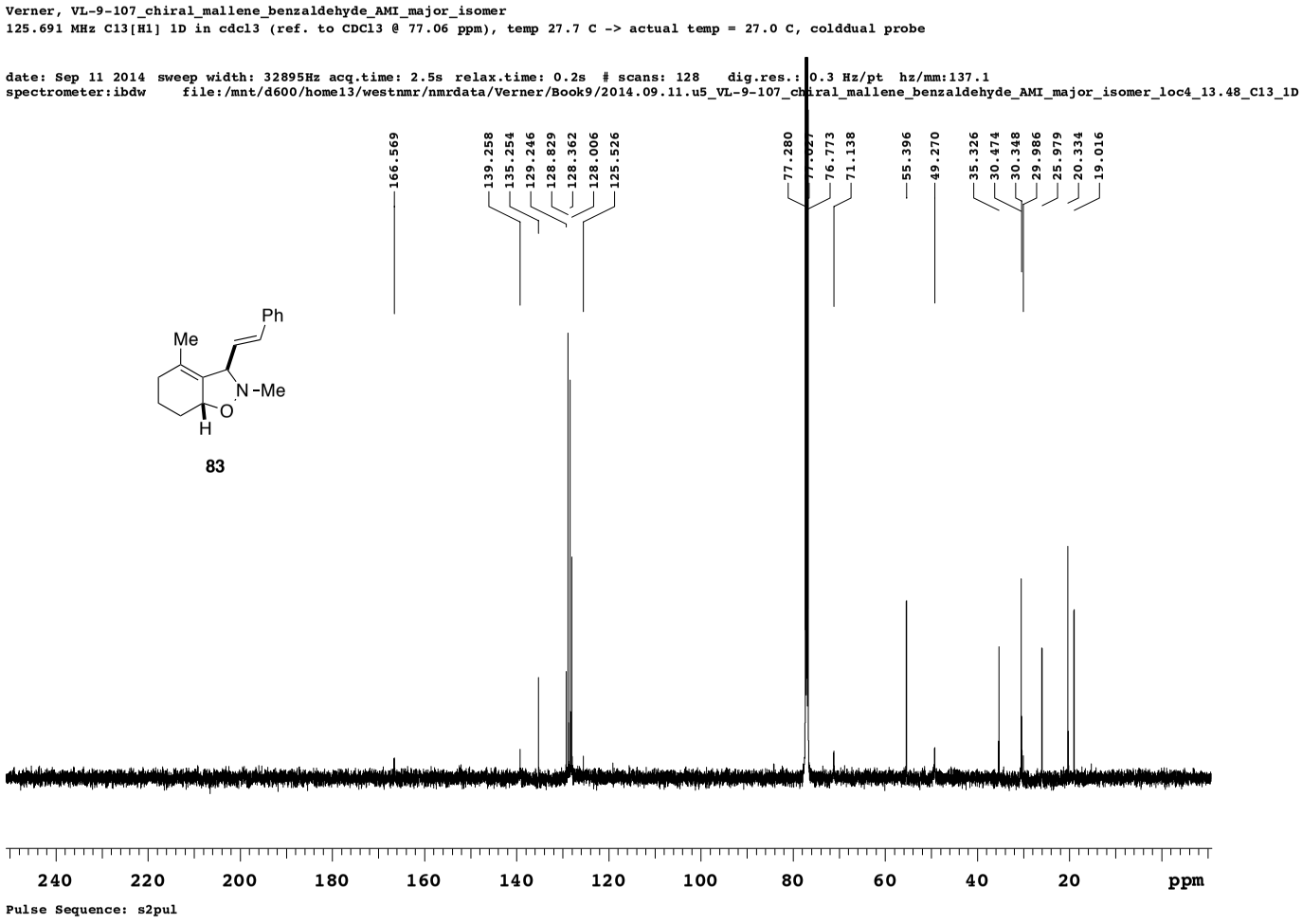
Verner, VL-9-107_chiral_mallene_benzaldehyde_AMI_major_isomer
125.691 MHz C13[H1] 1D in cdcl3 (ref. to CDCl3 @ 77.06 ppm), temp 27.7 C -> actual temp = 27.0 C, colddual probe
date: Sep 11 2014 sweep width: 32895Hz acq.time: 2.5s relax.time: 0.2s # scans: 128 dig.res.: 0.3 Hz/pt hz/mm:137.1
spectrometer:ibdw file:/mnt/d600/home13/westnmr/nmrdata/Verner/Book9/2014.09.11.u5_VL-9-107_chiral_mallene_benzaldehyde_AMI_major_isomer_loc4_13.48_C13_1D
166.569
139.258
135.254
129.246
128.829
128.362
128.006
125.526
77.280
77.067
76.773
71.138
55.396
49.270
35.326
30.474
30.348
29.986
25.979
20.334
19.016
Ph
Me
N-Me
O
H
83
240
220
200
180
160
140
120
100
80
60
40
20
ppm
Pulse Sequence: s2pul

Verner, VL-9-131_c-mallene_cinnamaldehyde_nitrone_fraction_2
499.806 MHz H1 ROESY in cdcl3 (ref. to CDCl3 @ 7.26 ppm), temp 27.7 C -> actual temp = 27.0 C, colddual probe

Temp. 27.7 C / 300.9 K
Sample #9, Operator: WEST

Relax. delay 1.000 sec
Acq. time 1.000 sec
Width 6009.6 Hz
2D Width 8012.8 Hz
16 repetitions
2 x 170 increments
OBSERVE H1, 499.8039257 MHz
DATA PROCESSING
Sq. sine bell 0.250 sec
Shifted by -0.250 sec
F1 DATA PROCESSING
Sq. sine bell 0.021 sec
Shifted by -0.021 sec
FT size 8192 x 1024
Total time 3 hr, 38 min

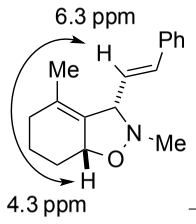

83

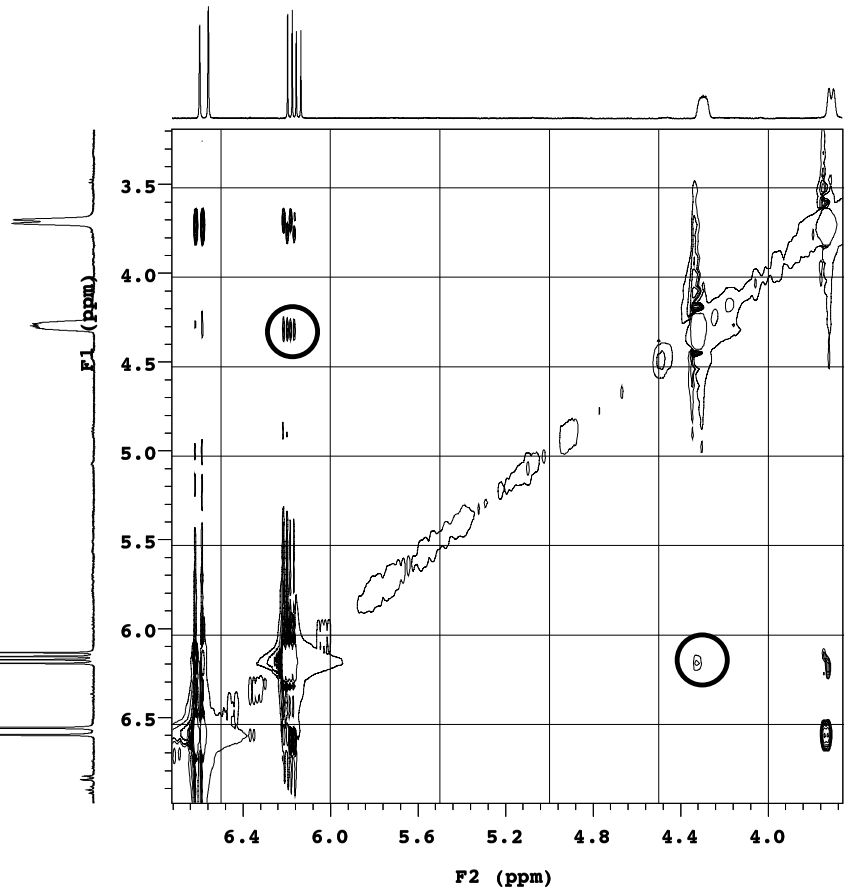

Pulse Sequence: ROESY

498.118 MHz H1 1D in cdcl3 (ref. to CDCl3 @ 7.26 ppm), temp 26.4 C -> actual temp = 27.0 C, autoxdb probe

date: Nov 4 2014 sweep width: 6001Hz acq.time: 5.0s relax.time: 0.1s # scans: 16 dig.res.: 0.1 Hz/pt hz/mm:25.0
spectrometer:ibdw file:/mnt/d600/home13/westnmr/nmrdata/Verner/Book9/2014.11.04.i5_VL-9-195_cm-allene_cinnamaldehyde_nitrone_regioisomer_1_H1_1D

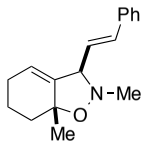

84

Pulse Sequence: s2pul

125.691 MHz C13[H1] 1D in cdcl3 (ref. to CDCl3 @ 77.06 ppm), temp 27.7 C -> actual temp = 27.0 C, colddual probe

date: Jan 23 2015 sweep width: 32895Hz acq.time: 2.5s relax.time: 0.2s # scans: 1288 dig.res.: 0.3 Hz/pt hz/mm:137.1
spectrometer:ibdw file:/mnt/d600/home13/westnmr/nmrdata/Verner/Book9/2015.01.23.u5_VL-9-208_mallene_cinN_minor_F2__loc1_07.41_C13_1D

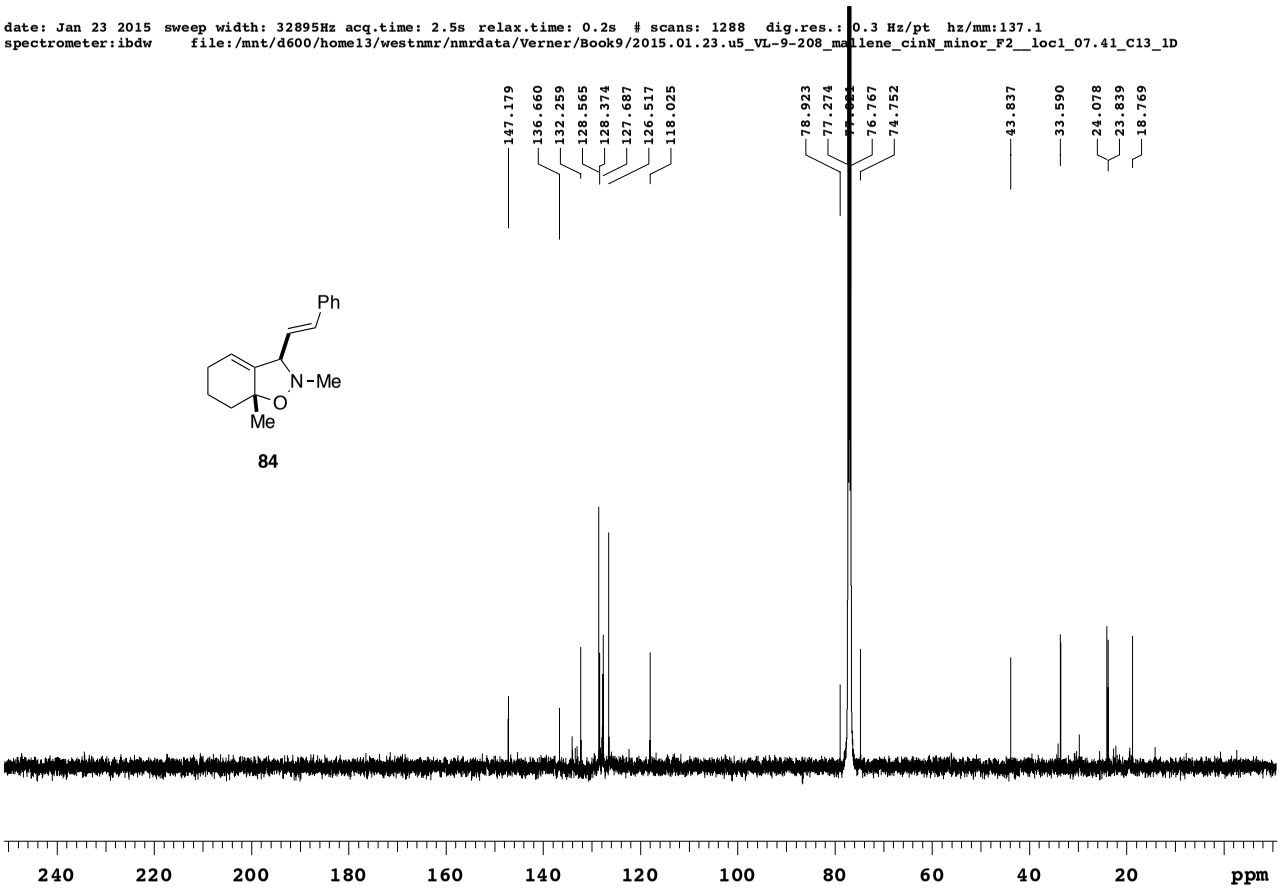

84

Pulse Sequence: s2pul

Verner, VL-9-208_mallene_cinN_minor
499.806 MHz H1 ROESY in cdcl3 (ref. to CDCl3 @ 7.26 ppm), temp 27.7 C -> actual temp = 27.0 C, colddual probe

Temp. 27.7 C / 300.9 K
Sample #12, Operator: WEST

Relax. delay 1.000 sec
Acq. time 1.000 sec
Width 6009.6 Hz
2D Width 8012.8 Hz
16 repetitions
2 x 170 increments
OBSERVE H1, 499.8039268 MHz
DATA PROCESSING
Sq. sine bell 0.250 sec
Shifted by -0.250 sec
F1 DATA PROCESSING
Sq. sine bell 0.021 sec
Shifted by -0.021 sec
FT size 8192 x 1024
Total time 3 hr, 38 min

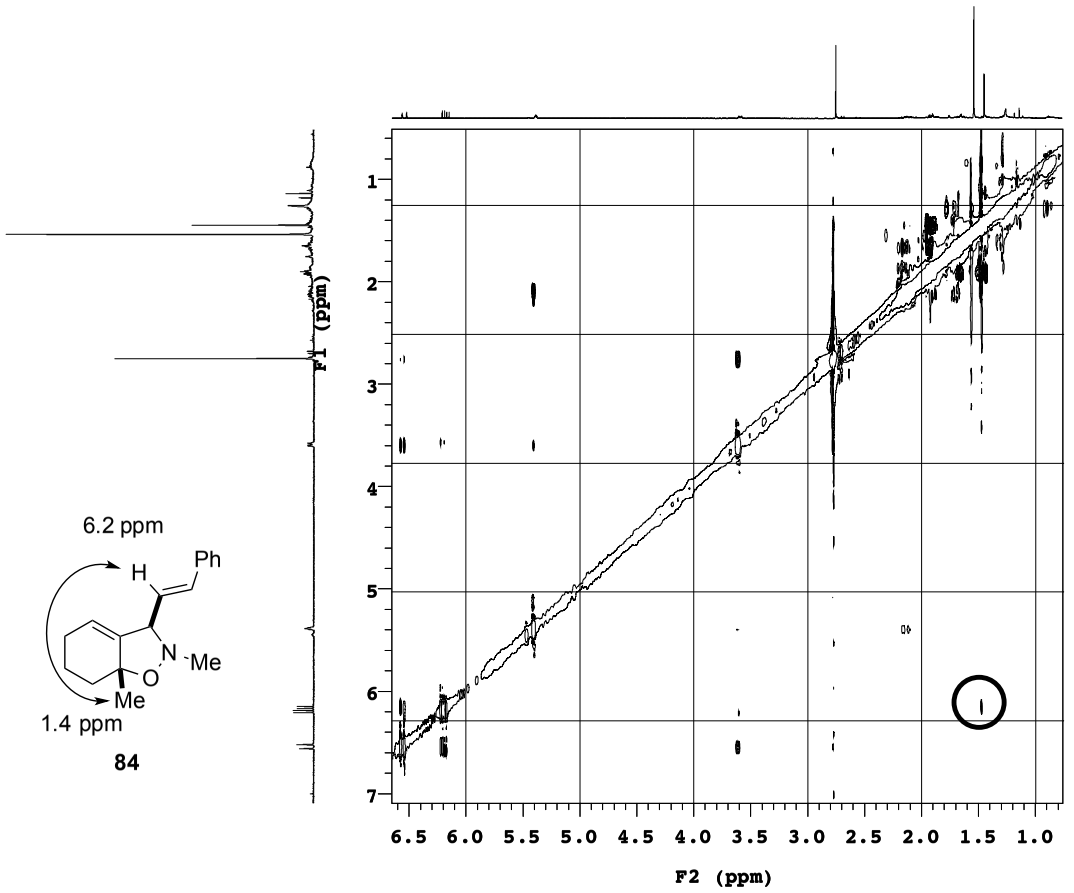

84

Pulse Sequence: ROESY

Appendix III: Selected NMR Spectra

(Chapter 4)

VL-4-182 Furoyl chloride quench of conjugate addition
498.118 MHz H1 1D in cdcl3 (ref. to CDCl3 @ 7.26 ppm), temp 27.2 C -> actual temp = 27.0 C, autoxdb probe

date: Nov 21 2012 sweep width: 6010Hz acq.time: 5.0s relax.time: 0.1s # scans: 16 dig.res.: 0.1 Hz/pt hz/mm:17.0
spectrometer:ibdw file:/mnt/d600/home13/westnmr/nmrdata/Verner/Book4/2012.11.21.i5_VL-4-182_Furoylchloride_w_enonetriflate_conjugate_add_H1_1D

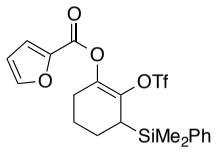

41

Pulse Sequence: s2pul

Verner, VL-4-182_furoyl_chloride_w_conjugate_enone_add
125.693 MHz C13[H1] 1D in cdcl3 (ref. to CDCl3 @ 77.06 ppm), temp 27.7 C -> actual temp = 27.0 C, colddual probe

date: Nov 21 2012 sweep width: 32895Hz acq.time: 2.5s relax.time: 0.2s # scans: 628 dig.res.: 0.3 Hz/pt hz/mm:137.1
spectrometer:ibdw file:/mnt/d600/home13/westnmr/nmrdata/Verner/Book4/2012.11.21.u5_VL-4-182_furoyl_chloride_w_conjugate_enone_add_14.30_C13_1D

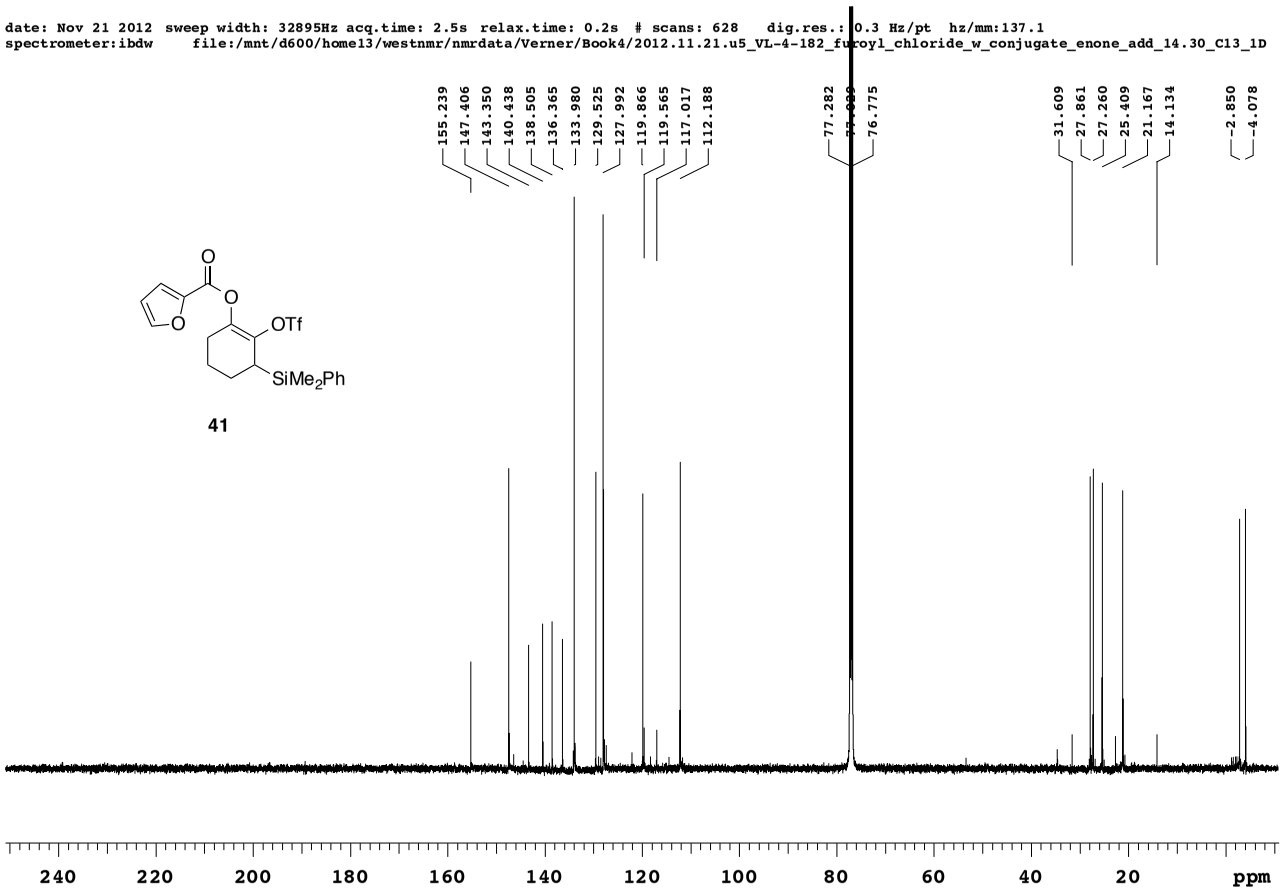

41

Pulse Sequence: s2pul

VL-4-207 methoxycinnamyl ester
299.971 MHz H1 1D in cdcl3 (ref. to CDCl3 @ 7.26 ppm), temp 27.0 C -> actual temp = 27.0 C, id300 probe

date: Jan 4 2013 sweep width: 3598Hz acq.time: 5.0s relax.time: 0.1s # scans: 16 dig.res.: 0.1 Hz/pt hz/mm:15.0
spectrometer:ibdw file:/mnt/d600/home13/westnmr/nmrdata/Verner/Book4/2013.01.04.i3_VL-4-207_methoxy_cinammyl_ester_H1_1D

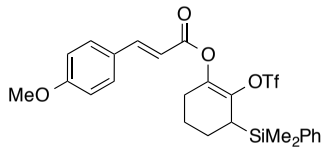

44

Pulse Sequence: s2pul

VL-4-207 methoxy cinnamic ester
125.266 MHz C13[H1] 1D in cdcl3 (ref. to CDCl3 @ 77.06 ppm), temp 27.2 C -> actual temp = 27.0 C, autoxdb probe

date: Dec 13 2012 sweep width: 33827Hz acq.time: 2.5s relax.time: 0.1s # scans: 1444 dig.res.: 0.3 Hz/pt hz/mm:140.9
spectrometer:ibdw file:/mnt/d600/home13/westnmr/nmrdata/Verner/Book4/2012.12.13.i5_VL-4-207_methoxy_cinnamic_ester_C13_1D

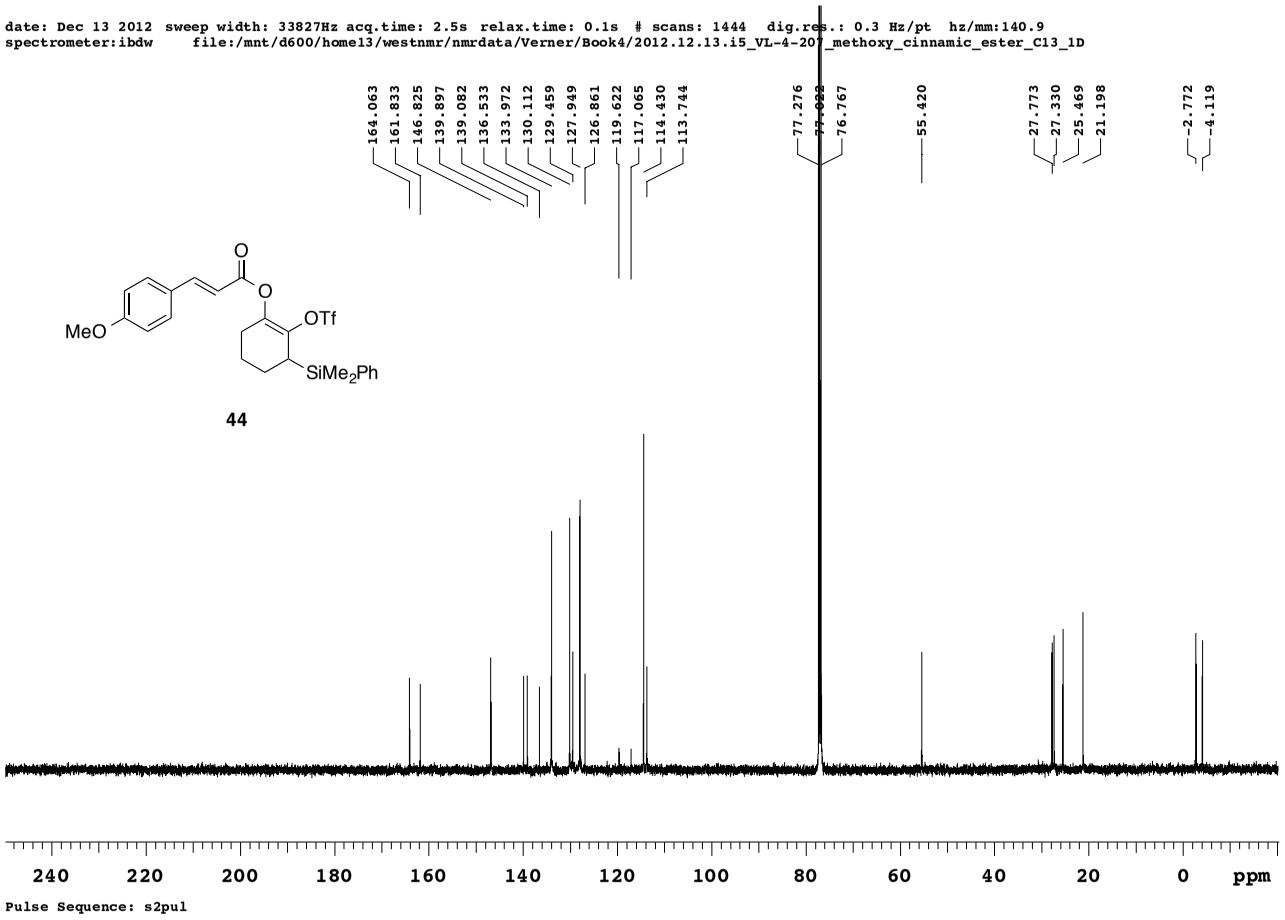

44

Pulse Sequence: s2pul

498.118 MHz H1 1D in cdcl3 (ref. to CDCl3 @ 7.26 ppm), temp 27.2 C -> actual temp = 27.0 C, autoxdb probe

date: Nov 23 2012 sweep width: 6010Hz acq.time: 5.0s relax.time: 0.1s # scans: 16 dig.res.: 0.1 Hz/pt hz/mm:25.0
spectrometer:ibd5 file:/mnt/d600/home13/westnmr/nmrdata/Verner/Book4/2012.11.23.i5_VL-4-185_furyl_dimer_H1_1D

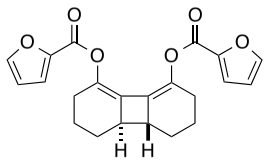

49

Pulse Sequence: s2pul

125.693 MHz C13[H1] 1D in cdcl3 (ref. to CDCl3 @ 77.06 ppm), temp 27.7 C -> actual temp = 27.0 C, colddual probe

date: Nov 23 2012 sweep width: 32895Hz acq.time: 2.5s relax.time: 0.2s # scans: 628 dig.res.: 0.3 Hz/pt hz/mm:137.1
spectrometer:ibd5 file:/mnt/d600/home13/westnmr/nmrdata/Verner/Book4/2012.11.23.u5_VL-4-185_fraction_2_furyl_allene_08.35_C13_1D

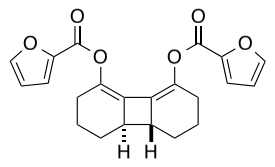

49

Pulse Sequence: s2pul

VL-6-76 silyl allyl conjugate
498.118 MHz H1 1D in cdcl3 (ref. to CDCl3 @ 7.26 ppm), temp 26.4 C -> actual temp = 27.0 C, autoxdb probe

date: Aug 20 2013 sweep width: 6001Hz acq.time: 5.0s relax.time: 0.1s # scans: 16 dig.res.: 0.1 Hz/pt hz/mm:25.0
spectrometer:ibdw file:/mnt/d600/home13/westnmr/nmrdata/Verner/Book6/2013.08.20.i5_VL-6-76_allyl_silyl_conjugate_H1_1D

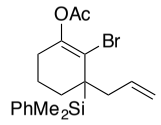

68

Pulse Sequence: s2pul

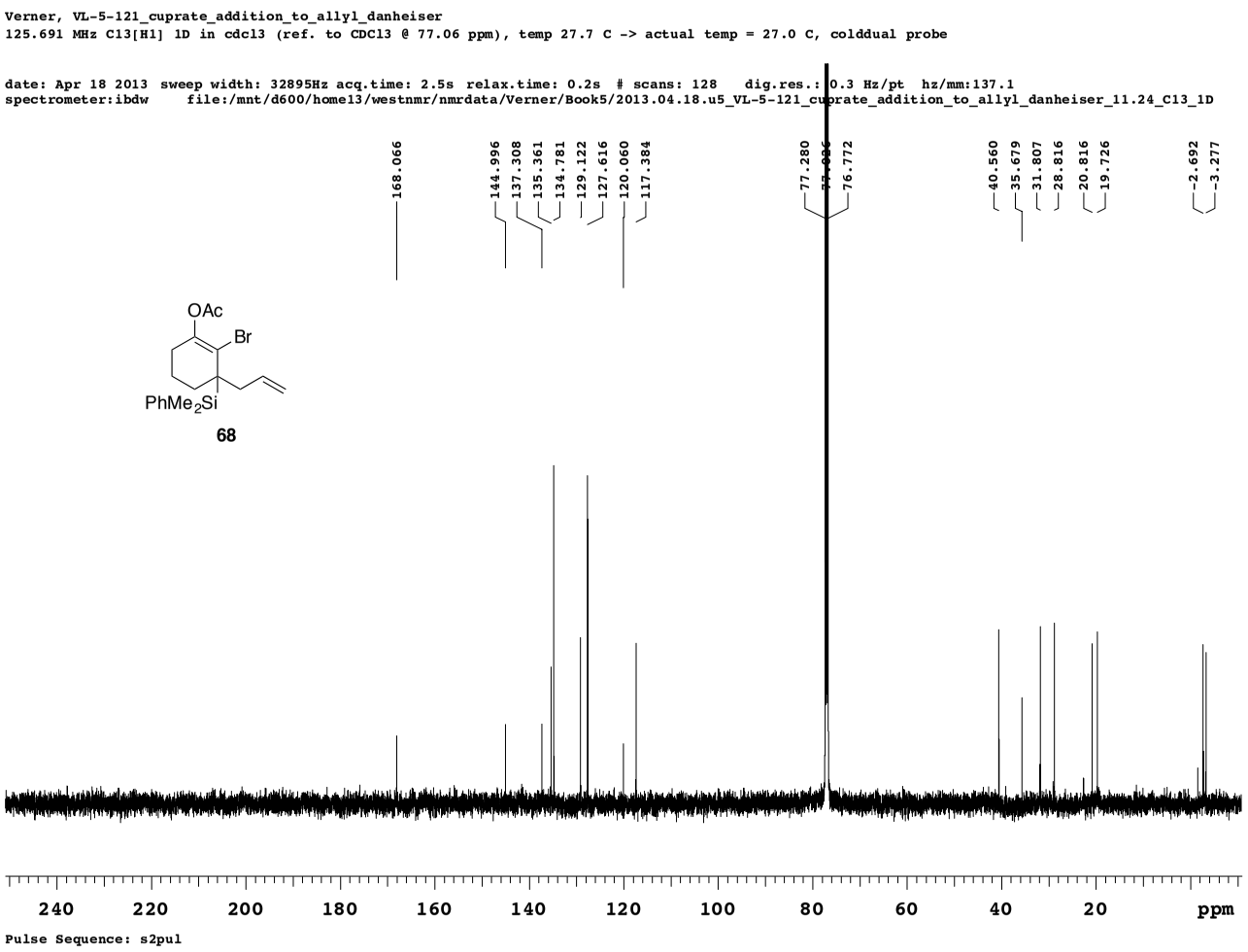
Verner, VL-5-121_cuprate_addition_to_allyl_danheiser
125.691 MHz C13[H1] 1D in cdcl3 (ref. to CDCl3 @ 77.06 ppm), temp 27.7 C -> actual temp = 27.0 C, colddual probe
date: Apr 18 2013 sweep width: 32895Hz acq.time: 2.5s relax.time: 0.2s # scans: 128 dig.res.: 0.3 Hz/pt hz/mm:137.1
spectrometer:ibdw file:/mnt/d600/home13/westnmr/nmrdata/Verner/Book5/2013.04.18.u5_VL-5-121_cuprate_addition_to_allyl_danheiser_11.24_C13_1D
168.066
144.996
137.308
135.361
134.781
129.122
127.616
120.060
117.384
77.280
77.086
76.772
40.560
35.679
31.807
28.816
20.816
19.726
-2.692
-3.277
OAc
Br
PhMe2Si
68
240
220
200
180
160
140
120
100
80
60
40
20
ppm
Pulse Sequence: s2pul

Verner, VL-5-126_hydroboration_oxidation_of_conjugate_allyl_danheiser
499.806 MHz H1 PRESAT in cdcl3 (ref. to CDCl3 @ 7.26 ppm), temp 27.7 C -> actual temp = 27.0 C, colddual probe

date: Apr 19 2013 sweep width: 6010Hz acq.time: 5.0s relax.time: 2.1s # scans: 16 dig.res.: 0.2 Hz/pt hz/mm: 20.8
spectrometer:ibdw file:/mnt/d600/home13/westnmr/nmrdata/Verner/Book5/2013.04.19.u5_VL-5-126_hydroboration_oxidation_of_conjugate_allyl_danheiser_16.43_H1_1D

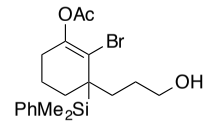

69

Pulse Sequence: PRESAT

Verner, VL-5-126_hydroboration_oxidation_of_conjugate_allyl_danheiser
125.691 MHz C13[H1] 1D in cdcl3 (ref. to CDCl3 @ 77.06 ppm), temp 27.7 C -> actual temp = 27.0 C, colddual probe

date: Apr 19 2013 sweep width: 32895Hz acq.time: 2.5s relax.time: 0.2s # scans: 128 dig.res.: 0.3 Hz/pt hz/mm:137.1
spectrometer:ibdw file:/mnt/d600/home13/westnmr/nmrdata/Verner/Book5/2013.04.19.u5_VL-5-126_hydroboration_oxidation_of_conjugate_allyl_danheiser_16.45_C13_1D

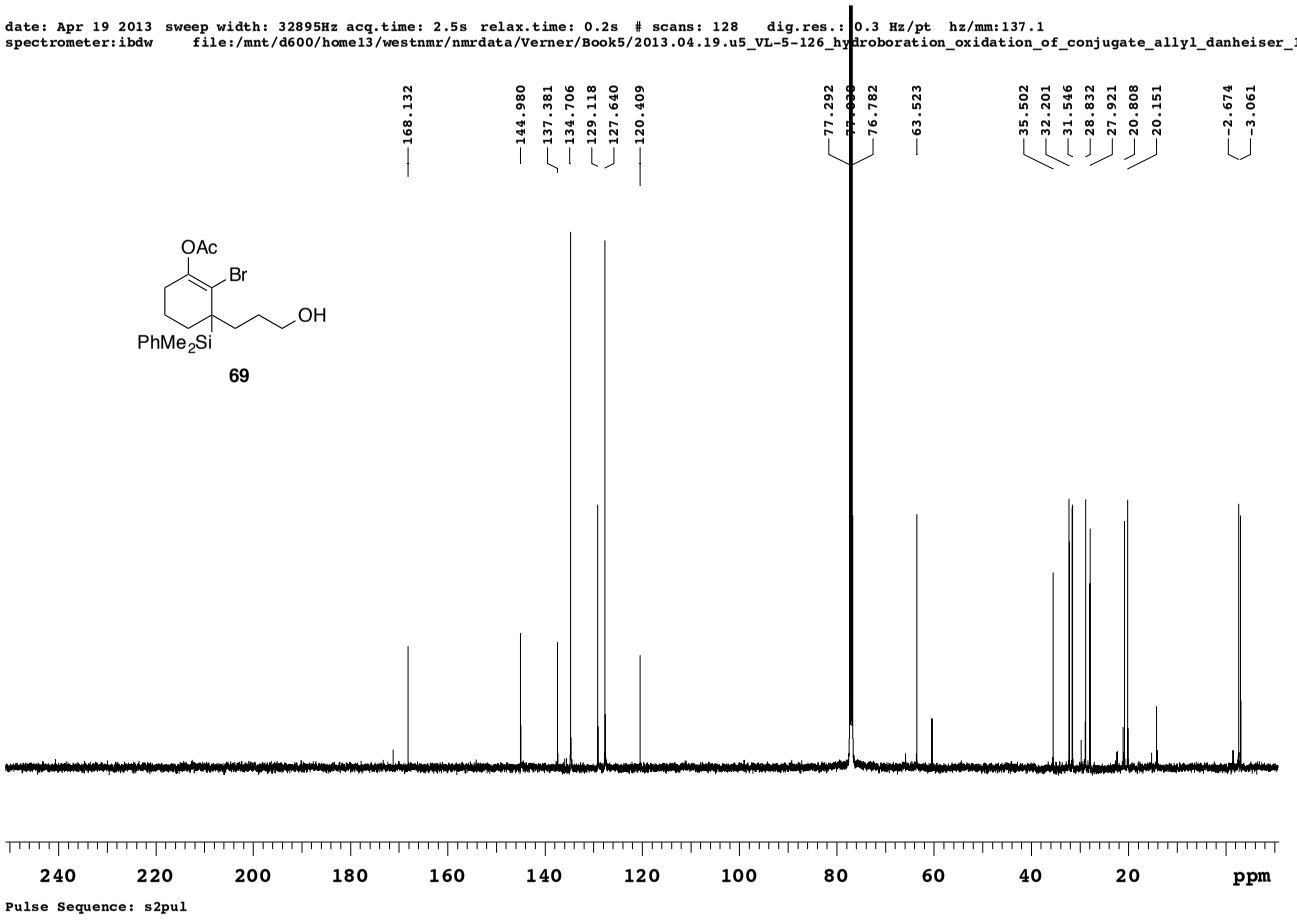

69

Pulse Sequence: s2pul

VL-5-131 tethered azide
399.794 MHz H1 1D in cdcl3 (ref. to CDCl3 @ 7.26 ppm), temp 26.5 C -> actual temp = 27.0 C, autoxdb probe

date: Apr 24 2013 sweep width: 4802Hz acq.time: 5.0s relax.time: 0.1s # scans: 16 dig.res.: 0.1 Hz/pt hz/mm:20.0
spectrometer:ibdw file:/mnt/d600/home13/westnmr/nmrdata/Verner/Book5/2013.04.24.i4_VL-5-131_tethered_azide_H1_1D

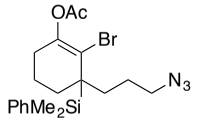

70

Pulse Sequence: s2pul

Verner, VL-5-131_tethered_azide
100.690 MHz C13[H1] 1D in cdcl3 (ref. to CDCl3 @ 77.06 ppm), temp 27.0 C -> actual temp = 27.0 C, m400gz probe

date: Apr 24 2013 sweep width: 27174Hz acq.time: 2.0s relax.time: 0.1s # scans: 704 dig.res.: 0.2 Hz/pt hz/mm:113.2
spectrometer:ibdw file:/mnt/d600/home13/westnmr/nmrdata/Verner/Book5/2013.04.24.m4_VL-5-131_tethered_azide_11.03_C13_1D

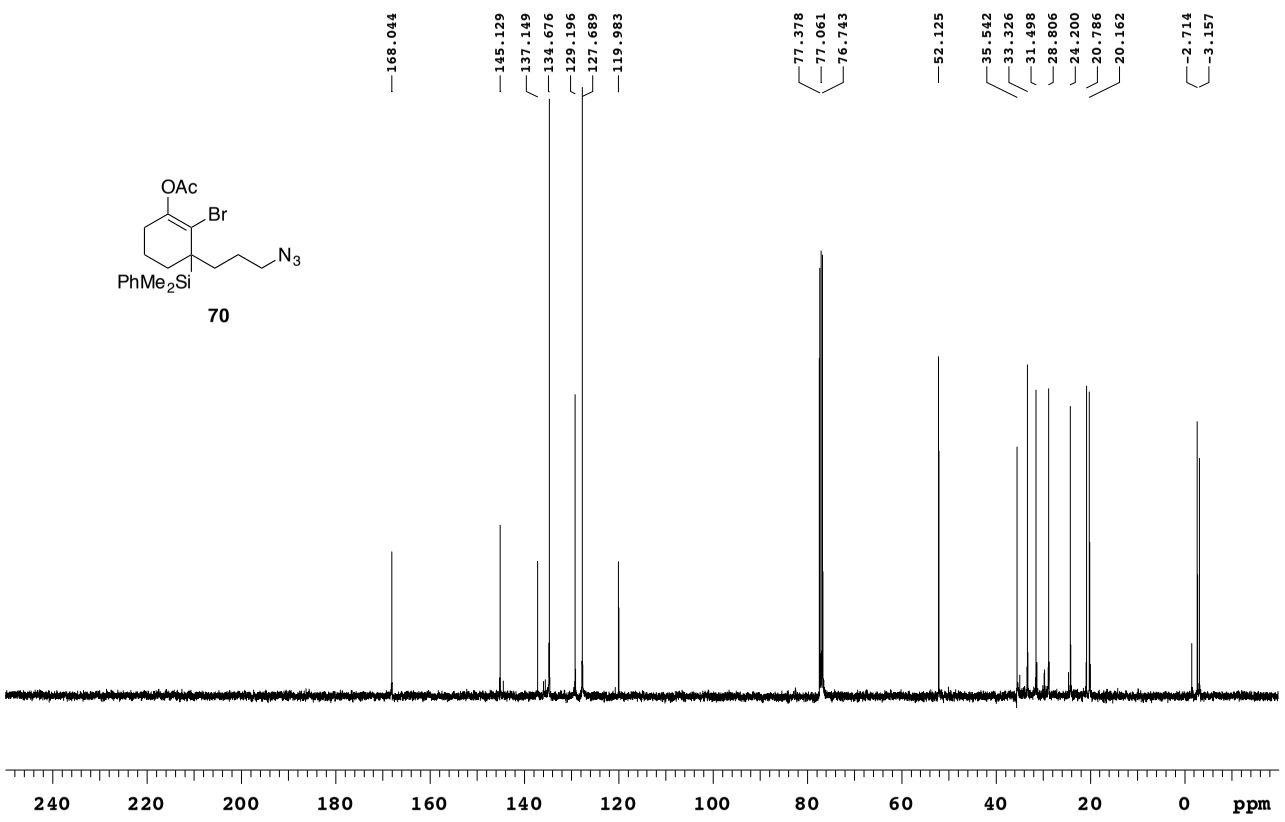

70

Pulse Sequence: s2pul

VL-8-45 SD methylfurfurylacetamide
499.806 MHz H1 1D in cdcl3 (ref. to CDCl3 @ 7.26 ppm), temp 27.7 C -> actual temp = 27.0 C, colddual probe

date: Apr 3 2014 sweep width: 6010Hz acq.time: 5.0s relax.time: 0.1s # scans: 16 dig.res.: 0.1 Hz/pt hz/mm:25.0
spectrometer:ibdw file:/mnt/d600/home13/westnmr/nmrdata/Verner/Book8/2014.04.03.u5_VL-8-45_SD_methylfurfurylacetamide_H1_1D

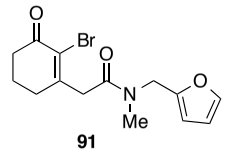

91

Pulse Sequence: s2pul

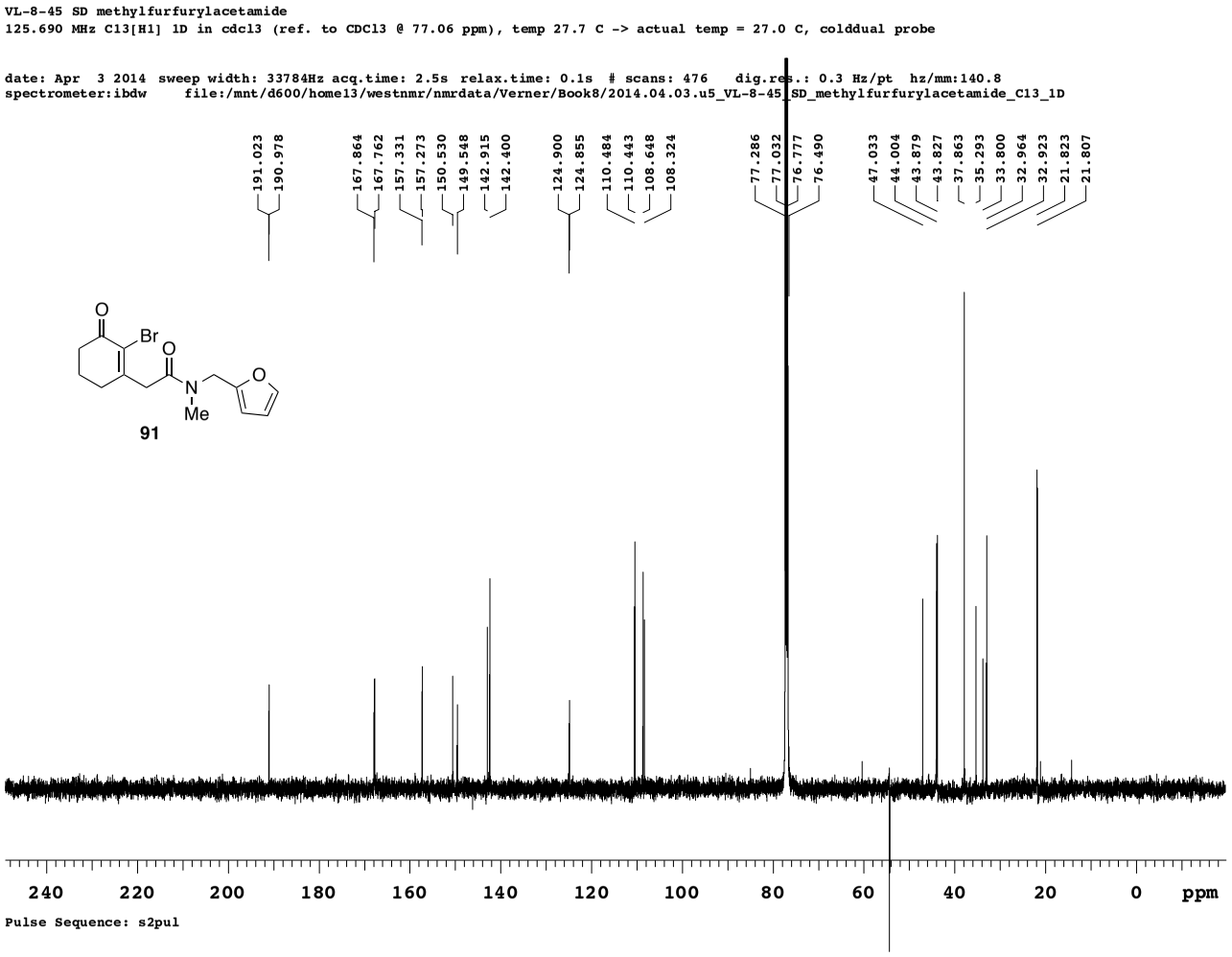
VL-8-45 SD methylfurfurylacetamide
125.690 MHz C13[H1] 1D in cdcl3 (ref. to CDCl3 @ 77.06 ppm), temp 27.7 C -> actual temp = 27.0 C, colddual probe
date: Apr 3 2014 sweep width: 33784Hz acq.time: 2.5s relax.time: 0.1s # scans: 476 dig.res.: 0.3 Hz/pt hz/mm:140.8
spectrometer:ibdw file:/mnt/d600/home13/westnmr/nmrdata/Verner/Book8/2014.04.03.u5_VL-8-45_SD_methylfurfurylacetamide_C13_1D
191.023
190.978
167.864
167.762
157.331
157.273
150.530
149.548
142.915
142.400
124.900
124.855
110.484
110.443
108.648
108.324
77.286
77.032
76.777
76.490
47.033
44.004
43.879
43.827
37.863
35.293
33.800
32.964
32.923
21.823
21.807
O
Br
O
N
Me
O
91
240
220
200
180
160
140
120
100
80
60
40
20
0
ppm
Pulse Sequence: s2pul

VL-8-47 silylation SD methylfufurylacetamide
499.806 MHz H1 1D in cdcl3 (ref. to CDCl3 @ 7.26 ppm), temp 27.7 C -> actual temp = 27.0 C, colddual probe

date: Apr 4 2014 sweep width: 6010Hz acq.time: 5.0s relax.time: 0.1s # scans: 16 dig.res.: 0.1 Hz/pt hz/mm:25.0
spectrometer:ibdw file:/mnt/d600/home13/westnmr/nmrdata/Verner/Book8/2014.04.04.u5_VL-8-47_silylation_SD_methylfufurylacetamide_H1_1D

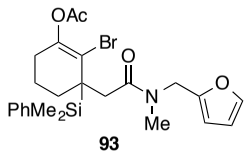

93

Pulse Sequence: s2pul

VL-8-47 silylation SD methylfufurylacetamide
125.690 MHz C13[H1] 1D in cdcl3 (ref. to CDCl3 @ 77.06 ppm), temp 27.7 C -> actual temp = 27.0 C, colddual probe

date: Apr 4 2014 sweep width: 33784Hz acq.time: 2.5s relax.time: 0.1s # scans: 128 dig.res.: 0.3 Hz/pt hz/mm:140.8
spectrometer:ibdw file:/mnt/d600/home13/westnmr/nmrdata/Verner/Book8/2014.04.04.u5_VL-8-47_silylation_SD_methylfufurylacetamide_C13_1D

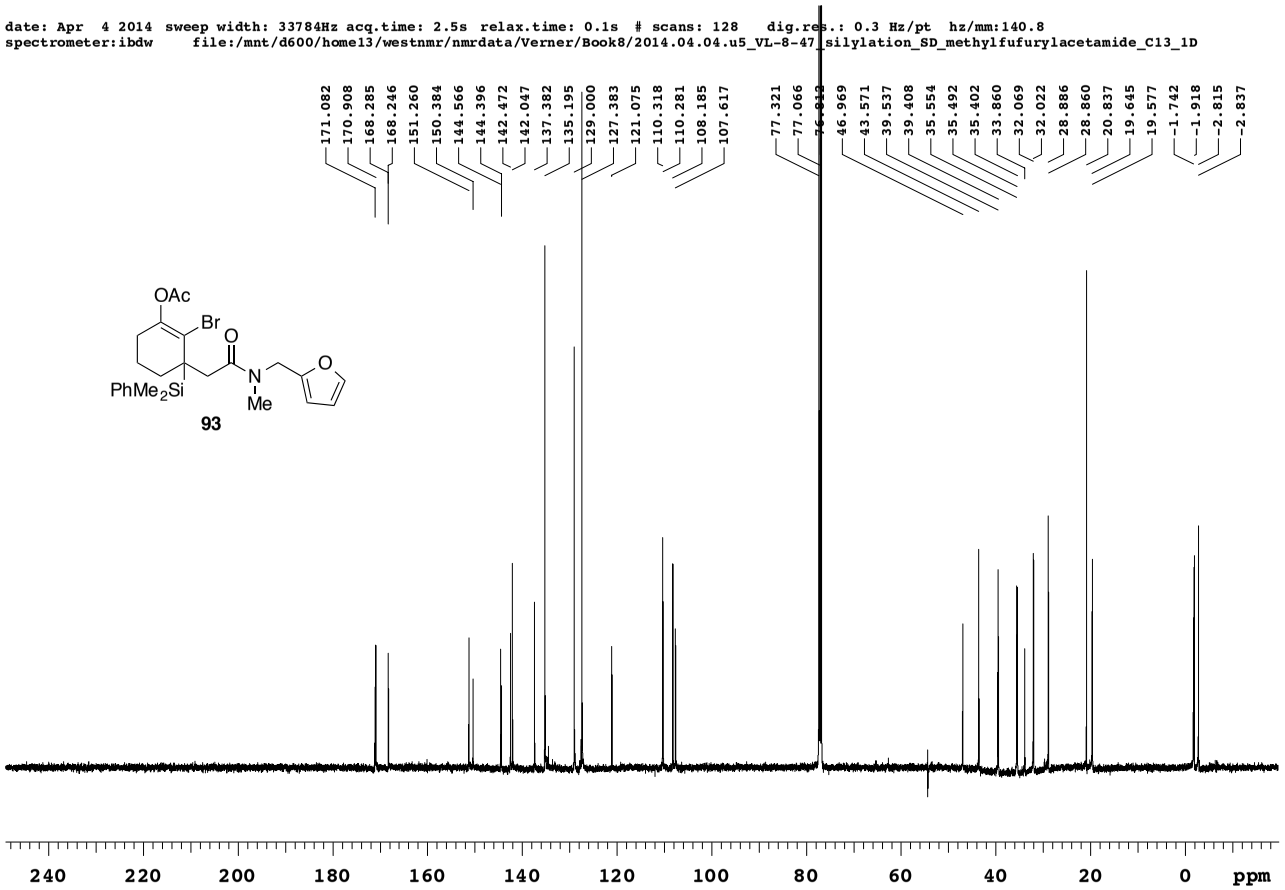

93

Pulse Sequence: s2pul

VL-8-59 Intra furan acetamide Aallene
399.984 MHz H1 1D in cdcl3 (ref. to CDCl3 @ 7.26 ppm), temp 25.9 C -> actual temp = 27.0 C, onenmr probe

date: Apr 8 2014 sweep width: 4808Hz acq.time: 5.0s relax.time: 0.1s # scans: 16 dig.res.: 0.1 Hz/pt hz/mm:20.0
spectrometer:ibdw file:/mnt/d600/home13/westnmr/nmrdata/Verner/Book8/2014.04.08.mr4_VL-8-59_Intra_furan_acetamide_Aallene_H1_1D

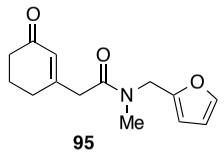

95

Pulse Sequence: s2pul

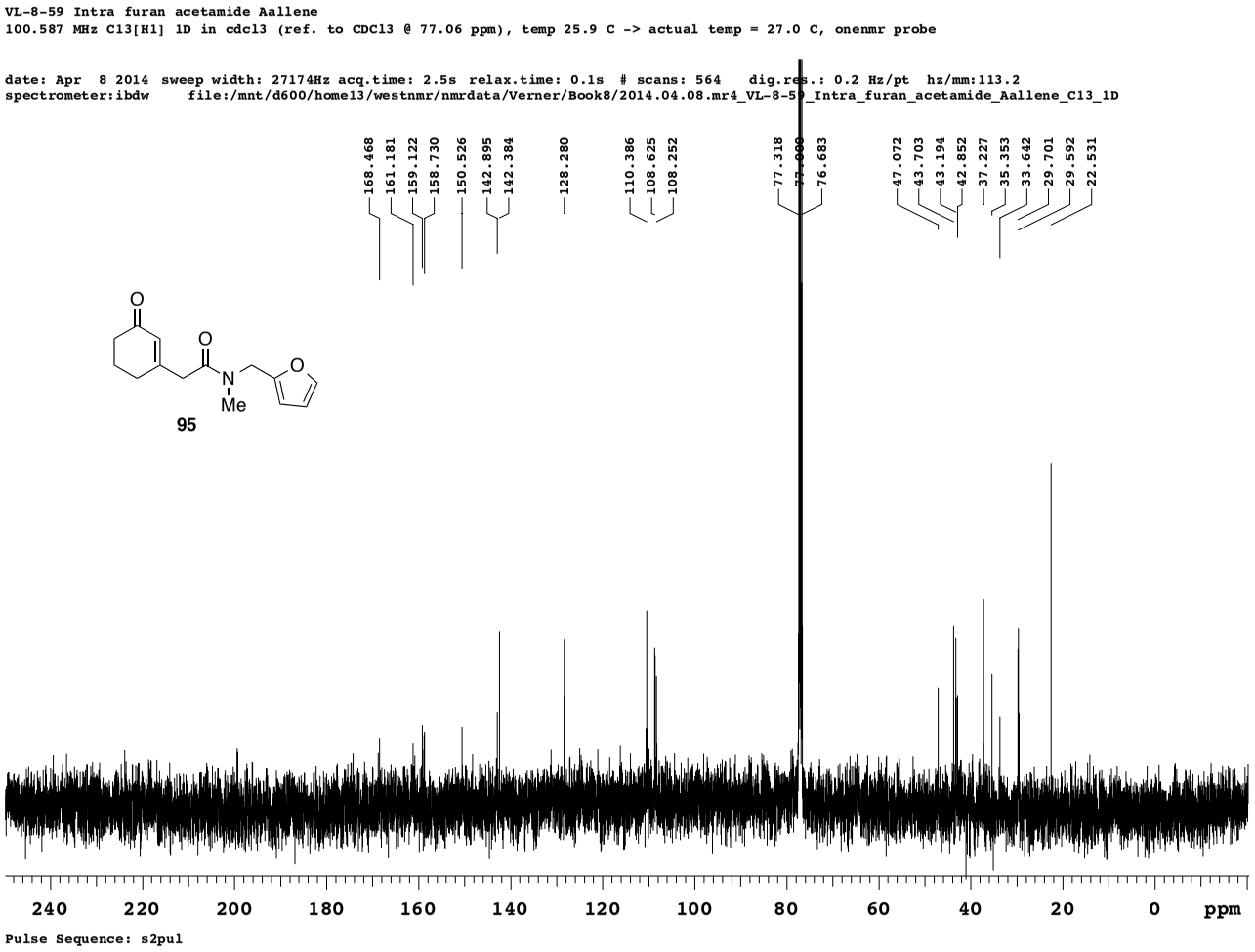
VL-8-59 Intra furan acetamide Aallene
100.587 MHz C13[H1] 1D in cdcl3 (ref. to CDCl3 @ 77.06 ppm), temp 25.9 C -> actual temp = 27.0 C, onenmr probe
date: Apr 8 2014 sweep width: 27174Hz acq.time: 2.5s relax.time: 0.1s # scans: 564 dig.res.: 0.2 Hz/pt hz/mm:113.2
spectrometer:ibdw file:/mnt/d600/home13/westnmr/nmrdata/Verner/Book8/2014.04.08.mr4_VL-8-59_Intra_furan_acetamide_Aallene_C13_1D
168.468
161.181
159.122
158.730
150.526
142.895
142.384
128.280
110.386
108.625
108.252
77.318
77.060
76.683
47.072
43.703
43.194
42.852
37.227
35.353
33.642
29.701
29.592
22.531
O
O
N
Me
O
95
240
220
200
180
160
140
120
100
80
60
40
20
0
ppm
Pulse Sequence: s2pul

VL-5-52 major spot of danheiser reaction with propyl furan
498.118 MHz H1 1D in cdcl3 (ref. to CDCl3 @ 7.26 ppm), temp 27.2 C -> actual temp = 27.0 C, autoxdb probe

date: Feb 15 2013 sweep width: 6001Hz acq.time: 5.0s relax.time: 0.1s # scans: 16 dig.res.: 0.1 Hz/pt hz/mm:25.0
spectrometer:ibdw file:/mnt/d600/home13/westnmr/nmrdata/Verner/Book5/2013.02.15.i5_VL-5-52_major_spot_H1_1D

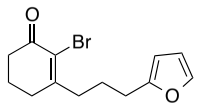

103

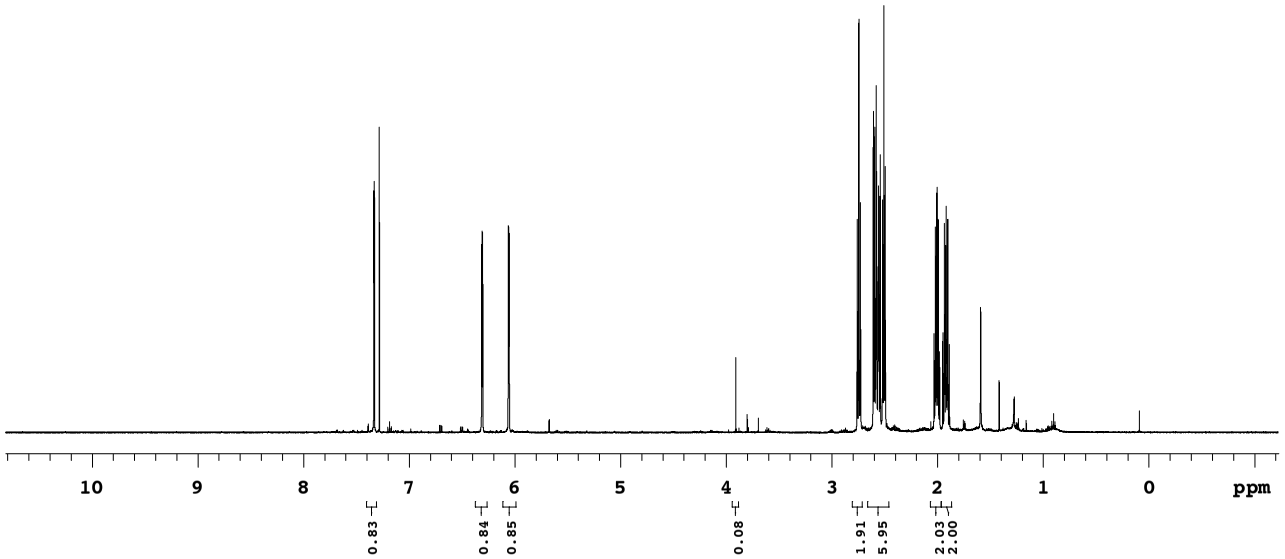

Pulse Sequence: s2pul

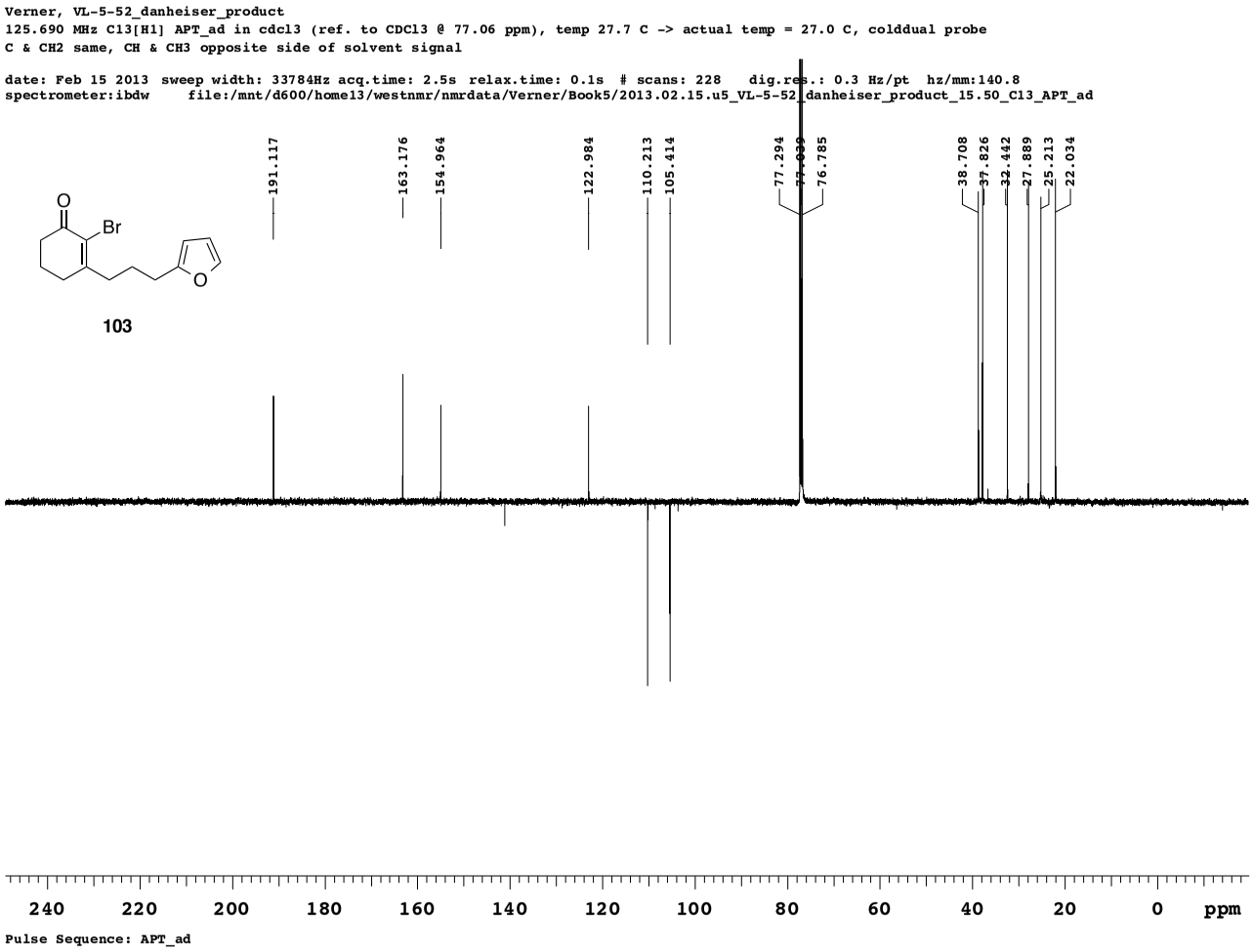
Verner, VL-5-52_danheiser_product
125.690 MHz C13[H1] APT_ad in cdcl3 (ref. to CDCl3 @ 77.06 ppm), temp 27.7 C -> actual temp = 27.0 C, colddual probe
C & CH2 same, CH & CH3 opposite side of solvent signal
date: Feb 15 2013 sweep width: 33784Hz acq.time: 2.5s relax.time: 0.1s # scans: 228 dig.res.: 0.3 Hz/pt hz/mm:140.8
spectrometer:ibdw file:/mnt/d600/home13/westnmr/nmrdata/Verner/Book5/2013.02.15.u5_VL-5-52_danheiser_product_15.50_C13_APT_ad
191.117
163.176
154.964
122.984
110.213
105.414
77.294
77.039
76.785
38.708
37.826
32.442
27.889
25.213
22.034
O
Br
O
103
240
220
200
180
160
140
120
100
80
60
40
20
0
ppm
Pulse Sequence: APT_ad

VL-5-80 conjugate to butyl danheiser product
498.118 MHz H1 1D in cdcl3 (ref. to CDCl3 @ 7.26 ppm), temp 26.4 C -> actual temp = 27.0 C, autoxdb probe

date: Mar 21 2013 sweep width: 6001Hz acq.time: 5.0s relax.time: 0.1s # scans: 16 dig.res.: 0.1 Hz/pt hz/mm:25.0
spectrometer:ibdw file:/mnt/d600/home13/westnmr/nmrdata/Verner/Book5/2013.03.21.i5_VL-5-80_conjugate_to_butylfuryl_danheiser_H1_1D

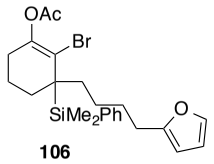

106

Pulse Sequence: s2pul

Verner, VL-5-80_conjugate_to_butylfuryl_danheiser
125.691 MHz C13[H1] 1D in cdcl3 (ref. to CDCl3 @ 77.06 ppm), temp 27.7 C -> actual temp = 27.0 C, colddual probe

date: Mar 21 2013 sweep width: 32895Hz acq.time: 2.5s relax.time: 0.2s # scans: 128 dig.res.: 0.3 Hz/pt hz/mm:137.1
spectrometer:ibdw file:/mnt/d600/home13/westnmr/nmrdata/Verner/Book5/2013.03.21.u5_VL-5-80_conjugate_to_butylfuryl_danheiser_20.03_C13_1D

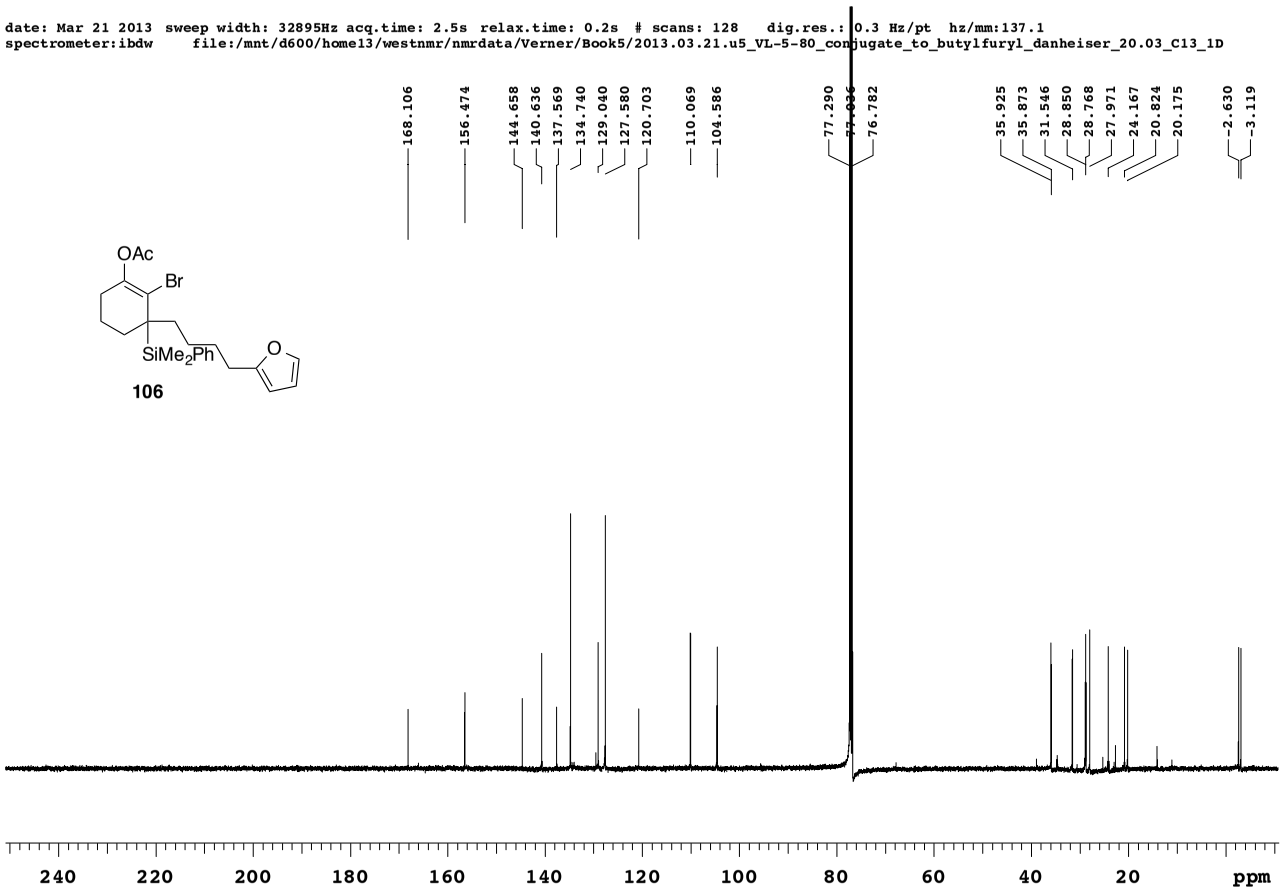

Pulse Sequence: s2pul

Verner, VL-5-72b_danheiser_intra
499.806 MHz H1 PRESAT in cdcl3 (ref. to CDCl3 @ 7.26 ppm), temp 27.7 C -> actual temp = 27.0 C, colddual probe

date: Mar 14 2013 sweep width: 6010Hz acq.time: 5.0s relax.time: 2.1s # scans: 16 dig.res.: 0.2 Hz/pt hz/mm:25.0
spectrometer:ibdw file:/mnt/d600/home13/westnmr/nmrdata/Verner/Book5/2013.03.14.u5_VL-5-72b_danheiser_intra_11.30_H1_1D

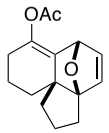

107

Pulse Sequence: PRESAT

Verner, VL-5-72b_danheiser_intra
125.691 MHz C13[H1] 1D in cdcl3 (ref. to CDCl3 @ 77.06 ppm), temp 27.7 C -> actual temp = 27.0 C, colddual probe

date: Mar 14 2013 sweep width: 32895Hz acq.time: 2.5s relax.time: 0.2s # scans: 128 dig.res.: 0.3 Hz/pt hz/mm:137.1
spectrometer:ibdw file:/mnt/d600/home13/westnmr/nmrdata/Verner/Book5/2013.03.14.u5_VL-5-72b_danheiser_intra_11.32_C13_1D

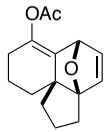

107

Pulse Sequence: s2pul

Appendix IV: Selected NMR Spectra

(Chapter 5)

VL-3-Unknown crystals in fridge
299.971 MHz H1 1D in cdcl3 (ref. to CDCl3 @ 7.26 ppm), temp 27.0 C -> actual temp = 27.0 C, id300 probe

date: Apr 19 2012 sweep width: 3601Hz acq.time: 5.0s relax.time: 0.1s # scans: 16 dig.res.: 0.1 Hz/pt hz/mm:15.0
spectrometer:ibdw file:/mnt/d600/home13/westnmr/nmrdata/Verner/Book3/2012.04.19.i3_VL-3-phenanthrylpropanal_H1_1D

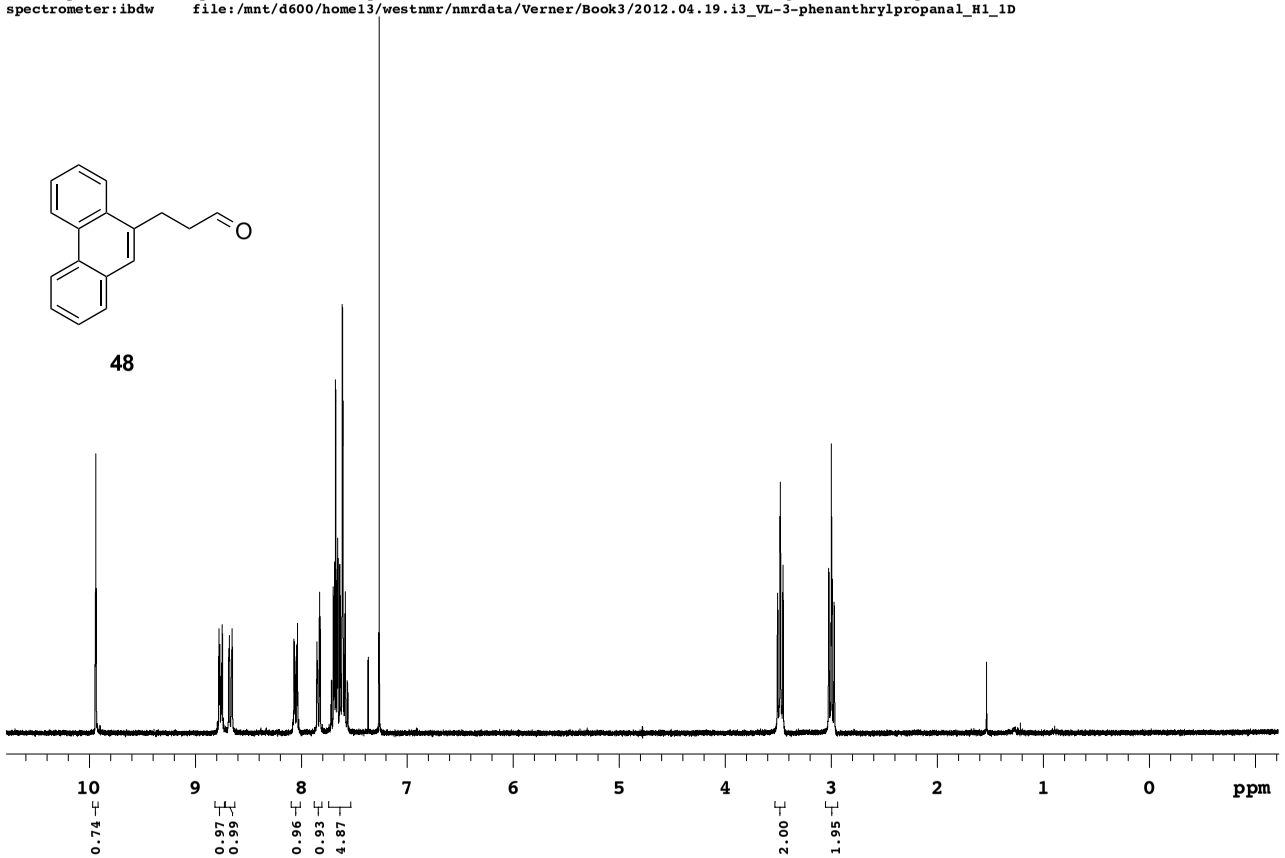

Pulse Sequence: s2pul

VL-3-Phenanthrylpropanal
125.690 MHz C13[H1] 1D in cdcl3 (ref. to CDCl3 @ 77.06 ppm), temp 27.7 C -> actual temp = 27.0 C, colddual probe

date: Apr 19 2012 sweep width: 33784Hz acq.time: 2.5s relax.time: 0.1s # scans: 244 dig.res.: 0.3 Hz/pt hz/mm:140.8
spectrometer:ibdw file:/mnt/d600/home13/westnmr/nmrdata/Verner/Book3/2012.04.19.u5_VL-3-Phenanthrylpropanal_C13_1D

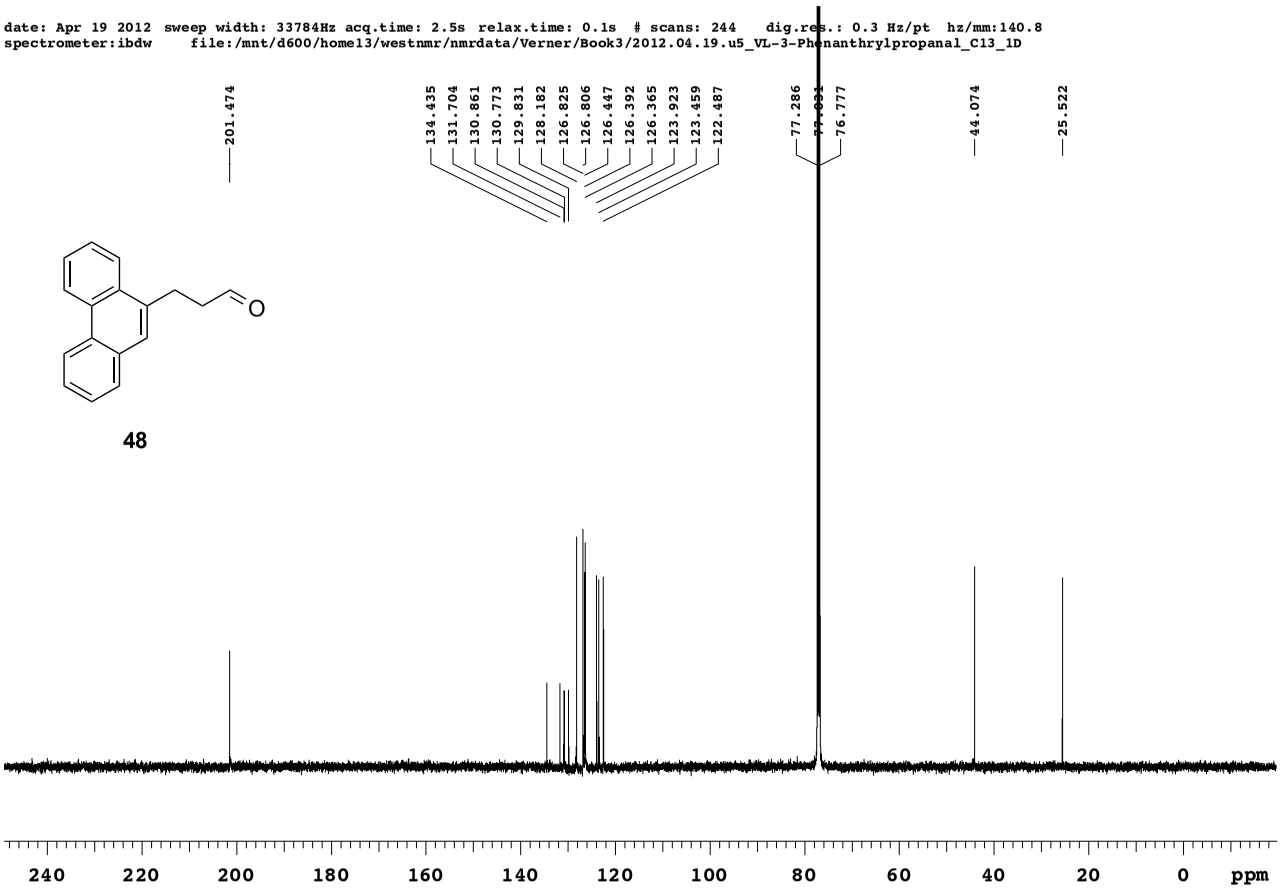

48

Pulse Sequence: s2pul

VL-3-pyrene butanal
498.122 MHz H1 1D in cdcl3 (ref. to CDCl3 @ 7.26 ppm), temp 27.2 C -> actual temp = 27.0 C, autoxdb probe

date: Jan 18 2012 sweep width: 6001Hz acq.time: 5.0s relax.time: 0.1s # scans: 16 dig.res.: 0.1 Hz/pt hz/mm:25.0
spectrometer:ibdw file:/mnt/d600/home13/westnmr/nmrdata/Verner/Book3/2012.01.18.i5_VL-3-Pyrenebutanal_H1_1D

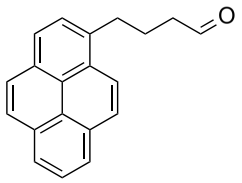

52

Pulse Sequence: s2pul

Verner, VL-3-Pyrenylbutanal
125.693 MHz C13[H1] 1D in cdcl3 (ref. to CDCl3 @ 77.06 ppm), temp 27.7 C -> actual temp = 27.0 C, colddual probe

date: Jun 25 2012 sweep width: 32895Hz acq.time: 2.5s relax.time: 0.2s # scans: 628 dig.res.: 0.3 Hz/pt hz/mm:137.1
spectrometer:ibdw file:/mnt/d600/home13/westnmr/nmrdata/Verner/Book3/2012.06.25.u5_VL-3-Pyrenylbutanal_14.29_C13_1D

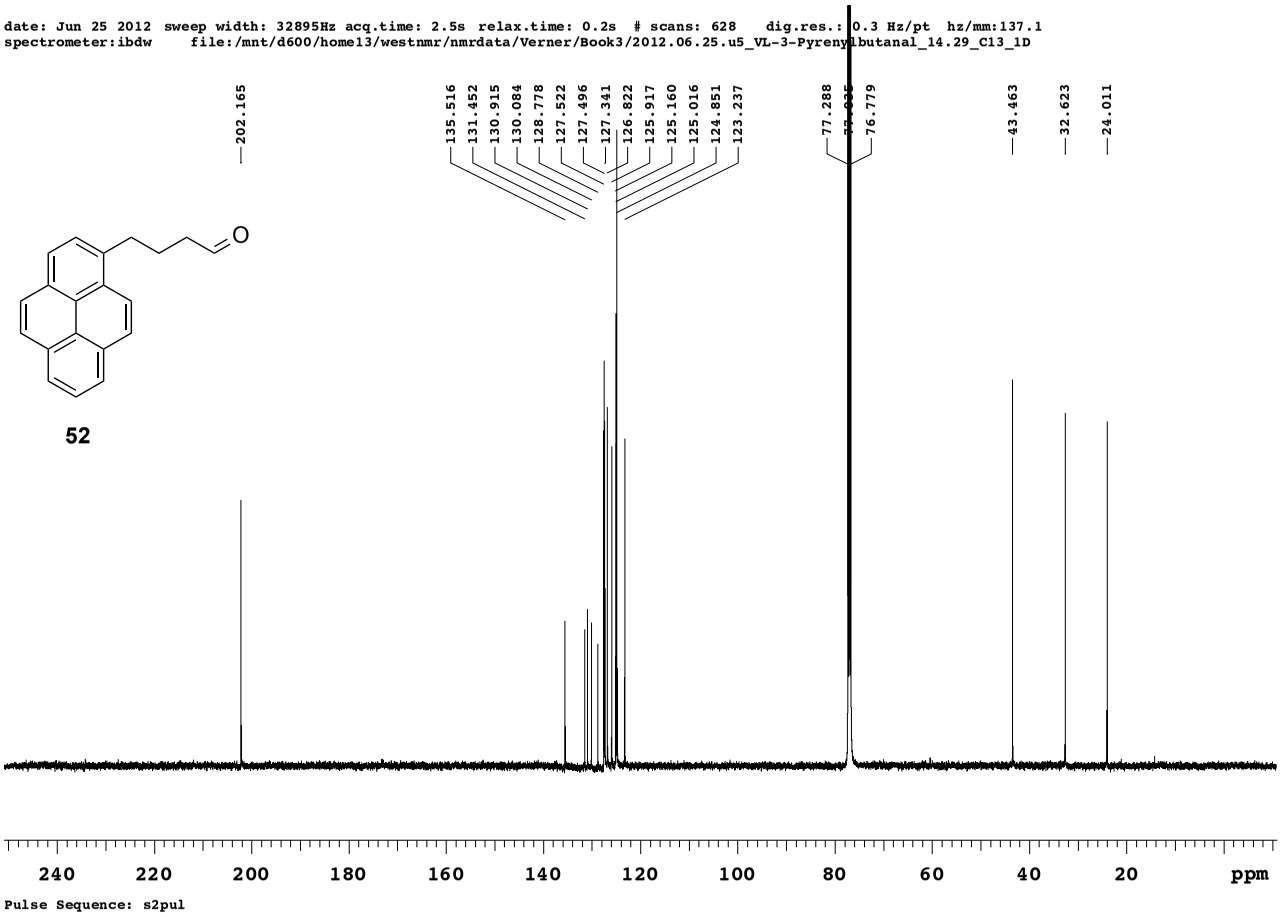

52

Pulse Sequence: s2pul

Verner, VL-3-PhenPenAlk
499.815 MHz H1 PRESAT in cdcl3 (ref. to CDCl3 @ 7.26 ppm), temp 27.7 C -> actual temp = 27.0 C, colddual probe

date: May 22 2012 sweep width: 6010Hz acq.time: 5.5s relax.time: 2.1s # scans: 16 dig.res.: 0.2 Hz/pt hz/mm:20.8
spectrometer:ibdw file:/mnt/d600/home13/westnmr/nmrdata/Verner/Book3/2012.05.22.u5_VL-3-PhenPenAlk_13.44_H1_1D

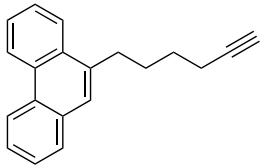

66

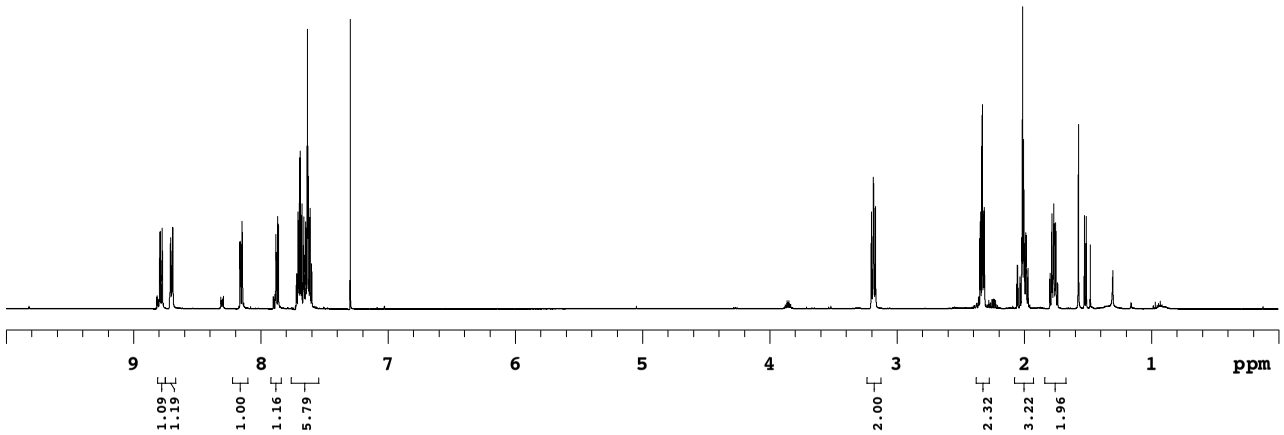

Pulse Sequence: PRESAT

Verner, VL-3-PhenPenAlk
125.693 MHz C13[H1] 1D in cdcl3 (ref. to CDCl3 @ 77.06 ppm), temp 27.7 C -> actual temp = 27.0 C, colddual probe

date: May 22 2012 sweep width: 32895Hz acq.time: 2.5s relax.time: 0.2s # scans: 128 dig.res.: 0.3 Hz/pt hz/mm:137.1
spectrometer:ibdw file:/mnt/d600/home13/westnmr/nmrdata/Verner/Book3/2012.05.22.u5_VL-3-PhenPenAlk_13.46_C13_1D

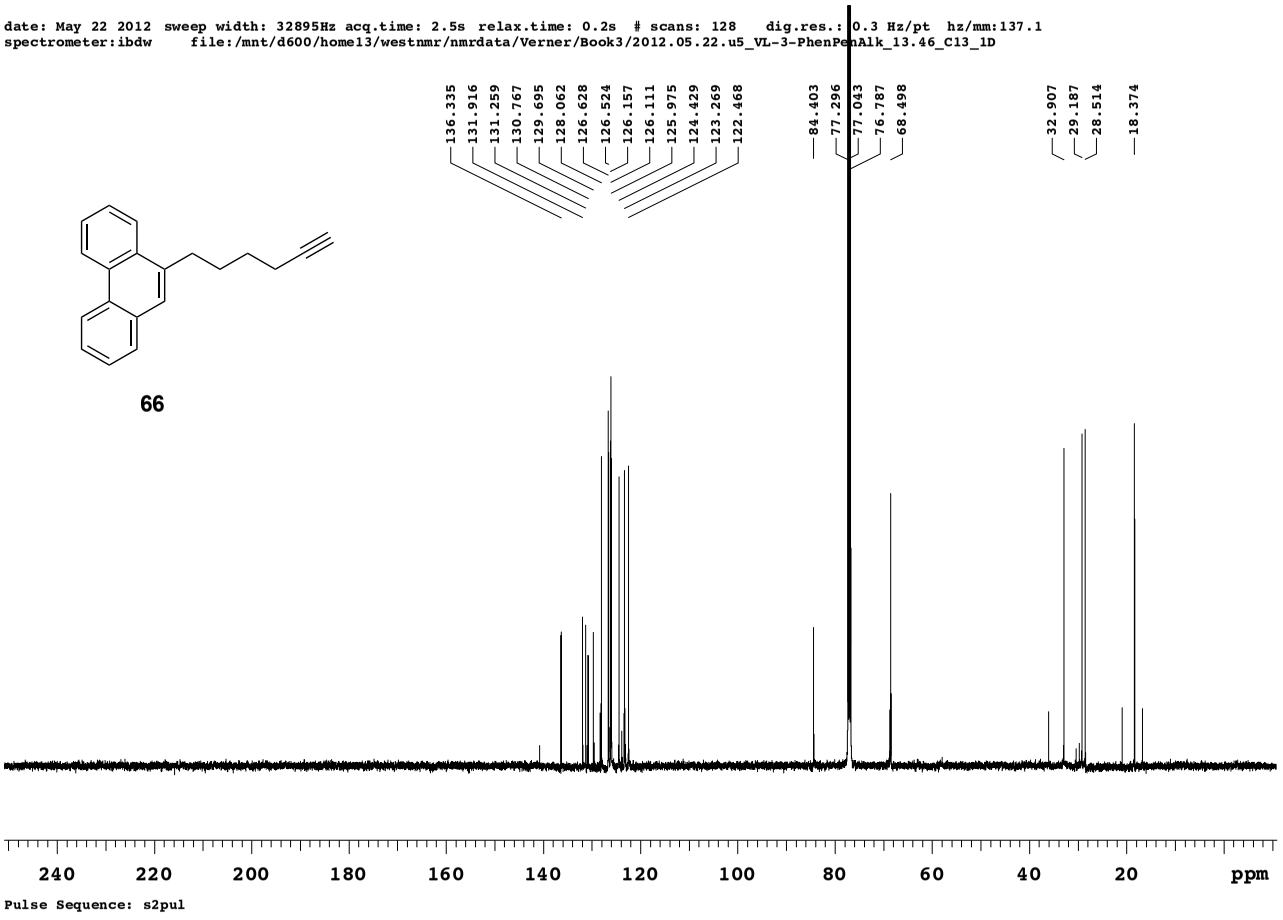

66

Pulse Sequence: s2pul

Verner, VL-3-PyPrAlk
499.815 MHz H1 PRESAT in cdcl3 (ref. to CDCl3 @ 7.26 ppm), temp 27.7 C -> actual temp = 27.0 C, colddual probe

date: May 22 2012 sweep width: 6010Hz acq.time: 5.5s relax.time: 2.1s # scans: 16 dig.res.: 0.2 Hz/pt hz/mm:20.8
spectrometer:ibdw file:/mnt/d600/home13/westnmr/nmrdata/Verner/Book3/2012.05.22.u5_VL-3-PyPrAlk_13.26_H1_1D

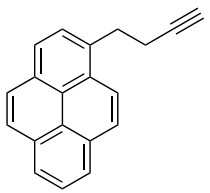

67

Pulse Sequence: PRESAT

Verner, VL-3-PyPrAlk
125.693 MHz C13[H1] 1D in cdcl3 (ref. to CDCl3 @ 77.06 ppm), temp 27.7 C -> actual temp = 27.0 C, colddual probe

date: May 22 2012 sweep width: 32895Hz acq.time: 2.5s relax.time: 0.2s # scans: 128 dig.res.: 0.3 Hz/pt hz/mm:137.1
spectrometer:ibdw file:/mnt/d600/home13/westnmr/nmrdata/Verner/Book3/2012.05.22.u5_VL-3-PyPrAlk_13.28_C13_1D

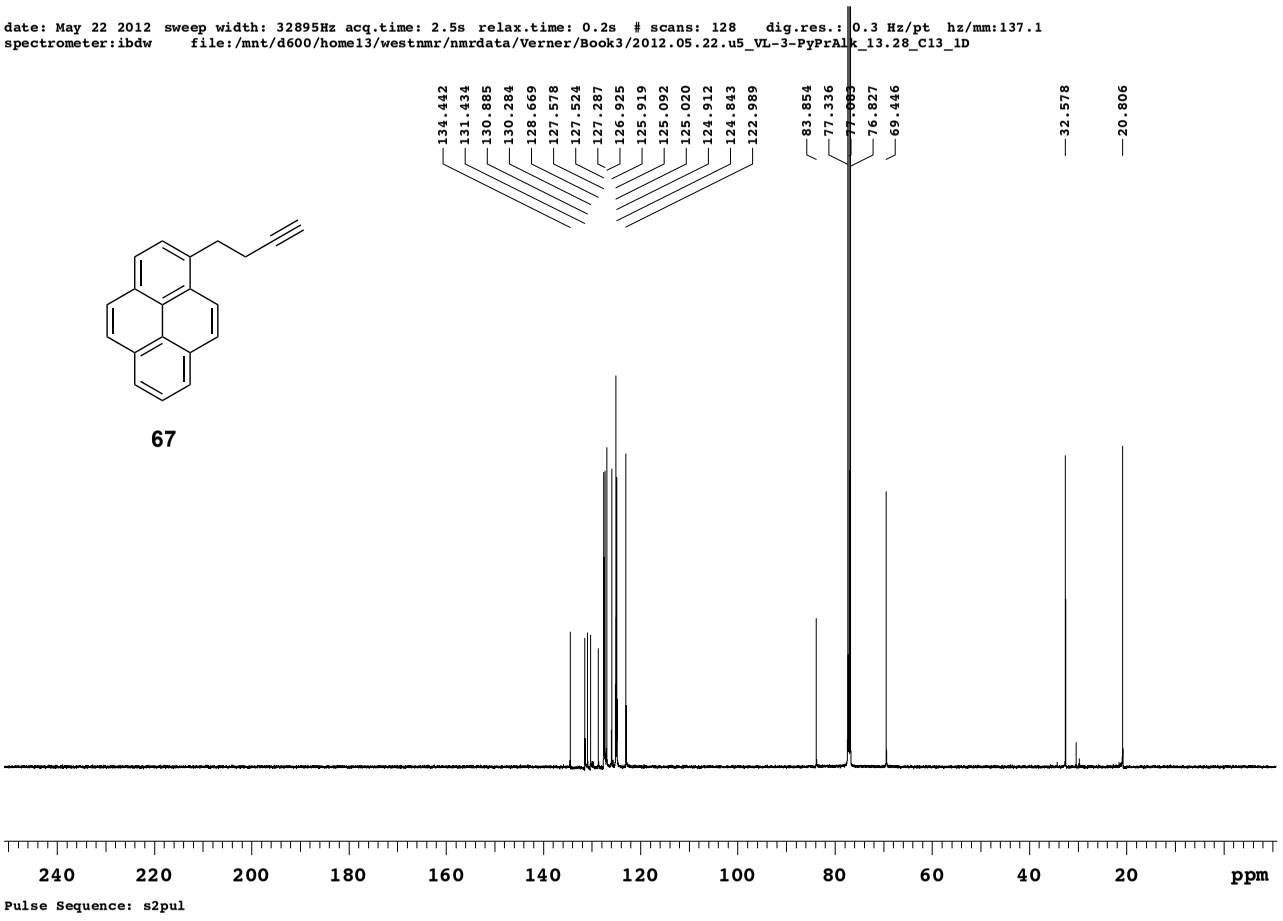

67

Pulse Sequence: s2pul

VL-3-phenanthrene propyl nitrile
498.122 MHz H1 1D in cdcl3 (ref. to CDCl3 @ 7.26 ppm), temp 27.2 C -> actual temp = 27.0 C, autoxdb probe

date: Jan 18 2012 sweep width: 6001Hz acq.time: 5.0s relax.time: 0.1s # scans: 16 dig.res.: 0.1 Hz/pt hz/mm:25.0
spectrometer:ibdw file:/mnt/d600/home13/westnmr/nmrdata/Verner/Book3/2012.01.18.i5_VL-3-phenanthrene_propyl_nitrile_H1_1D

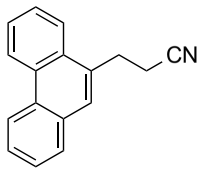

76

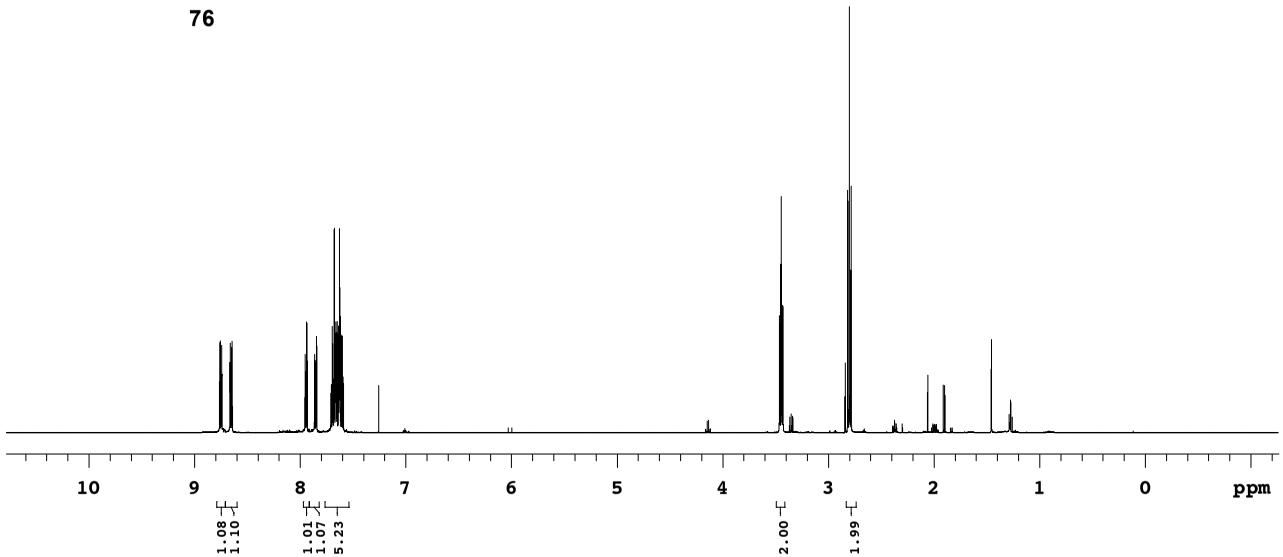

Pulse Sequence: s2pul

Verner, VL-phenprnit
125.693 MHz C13[H1] 1D in cdcl3 (ref. to CDCl3 @ 77.06 ppm), temp 27.7 C -> actual temp = 27.0 C, colddual probe

date: May 23 2012 sweep width: 32895Hz acq.time: 2.5s relax.time: 0.2s # scans: 512 dig.res.: 0.3 Hz/pt hz/mm:137.1
spectrometer:ibdw file:/mnt/d600/home13/westnmr/nmrdata/Verner/Book3/2012.05.23.u5_VL-phenprnit_15.40_C13_1D

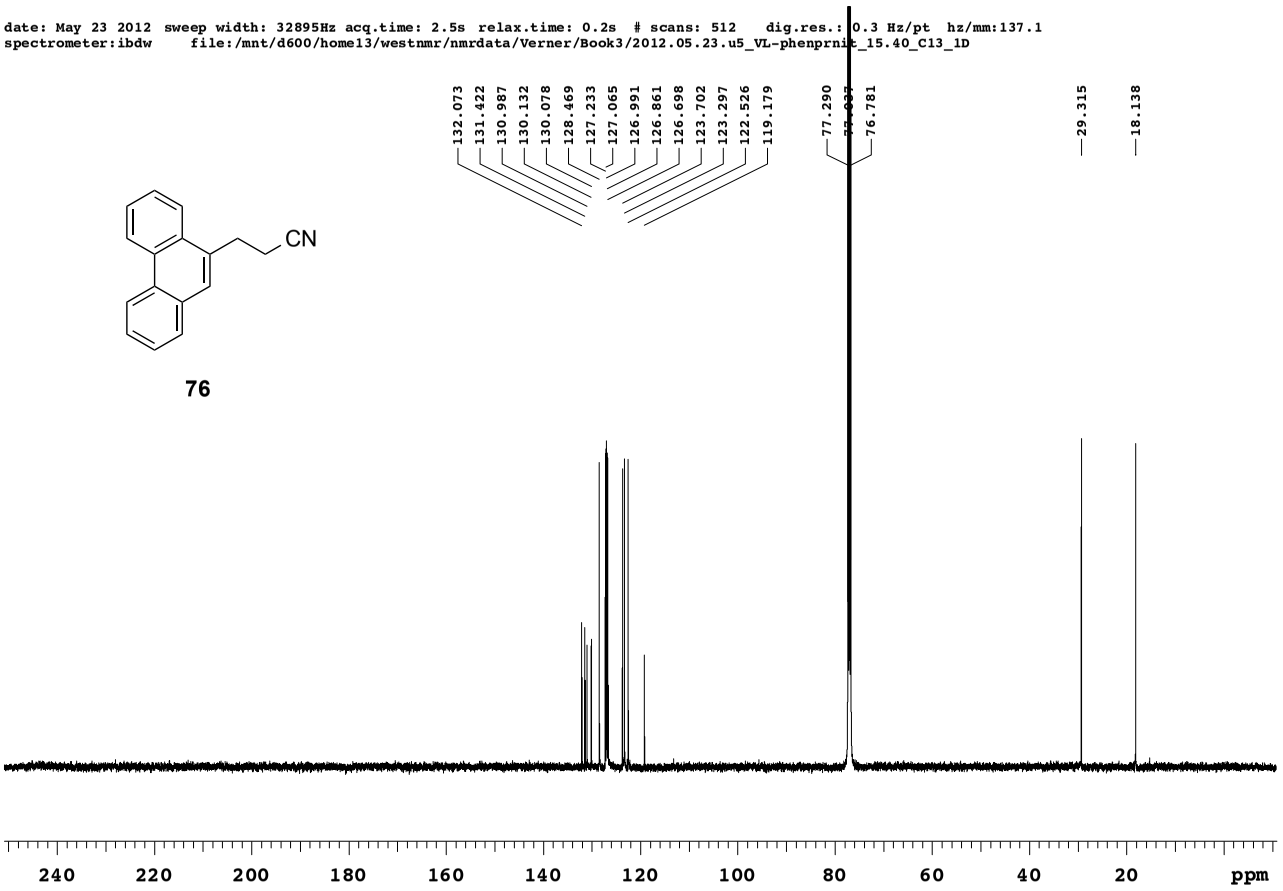

76

Pulse Sequence: s2pul

Verner, VL-PyBuN
499.815 MHz H1 PRESAT in cdcl3 (ref. to CDCl3 @ 7.26 ppm), temp 27.7 C -> actual temp = 27.0 C, colddual probe

date: Dec 18 2012 sweep width: 6010Hz acq.time: 5.0s relax.time: 2.1s # scans: 16 dig.res.: 0.2 Hz/pt hz/mm:25.0
spectrometer:ibdw file:/mnt/d600/home13/westnmr/nmrdata/Verner/Book3/2012.12.18.u5_VL-PyBuN_12.20_H1_1D

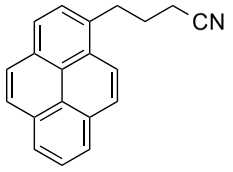

80

Pulse Sequence: PRESAT

Verner, VL-PyBuN
125.693 MHz C13[H1] 1D in cdcl3 (ref. to CDCl3 @ 77.06 ppm), temp 27.7 C -> actual temp = 27.0 C, colddual probe

date: Dec 18 2012 sweep width: 32895Hz acq.time: 2.5s relax.time: 0.2s # scans: 188 dig.res.: 0.3 Hz/pt hz/mm:137.1
spectrometer:ibdw file:/mnt/d600/home13/westnmr/nmrdata/Verner/Book3/2012.12.18.u5_VL-PyBuN_12.22_C13_1D

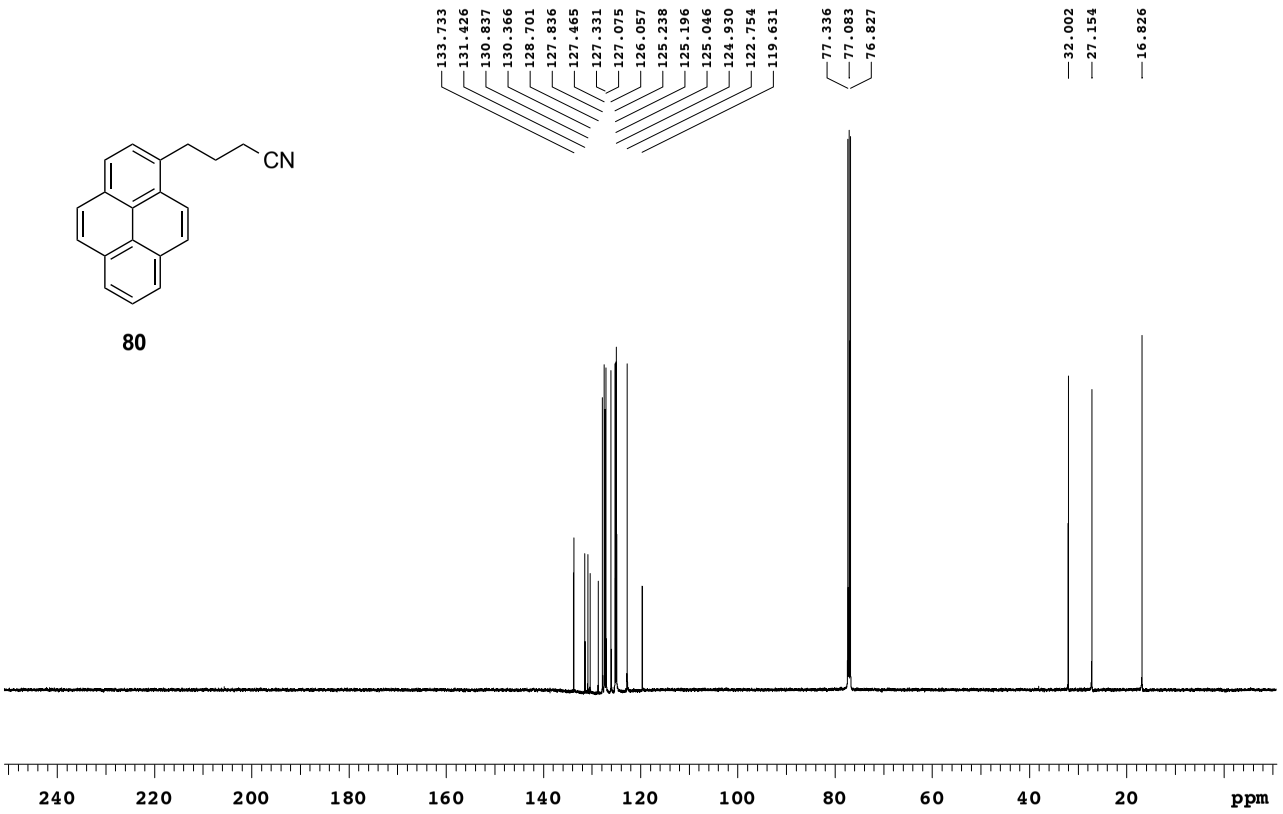

80

Pulse Sequence: s2pul

499.815 MHz H1 1D in cdcl3 (ref. to CDCl3 @ 7.26 ppm), temp 27.7 C -> actual temp = 27.0 C, colddual probe

date: Sep 23 2011 sweep width: 6010Hz acq.time: 5.0s relax.time: 0.1s # scans: 16 dig.res.: 0.1 Hz/pt hz/mm:25.0
spectrometer:ibdw file:/mnt/d600/home13/westnmr/nmrdata/Verner/Book2/2011.09.23.u5_cyclizationwithdinitrile_H1_1D

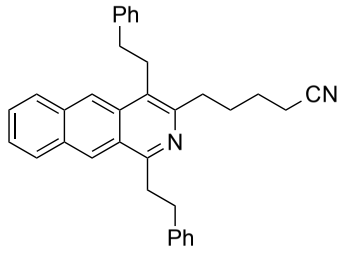

95

Pulse Sequence: s2pul

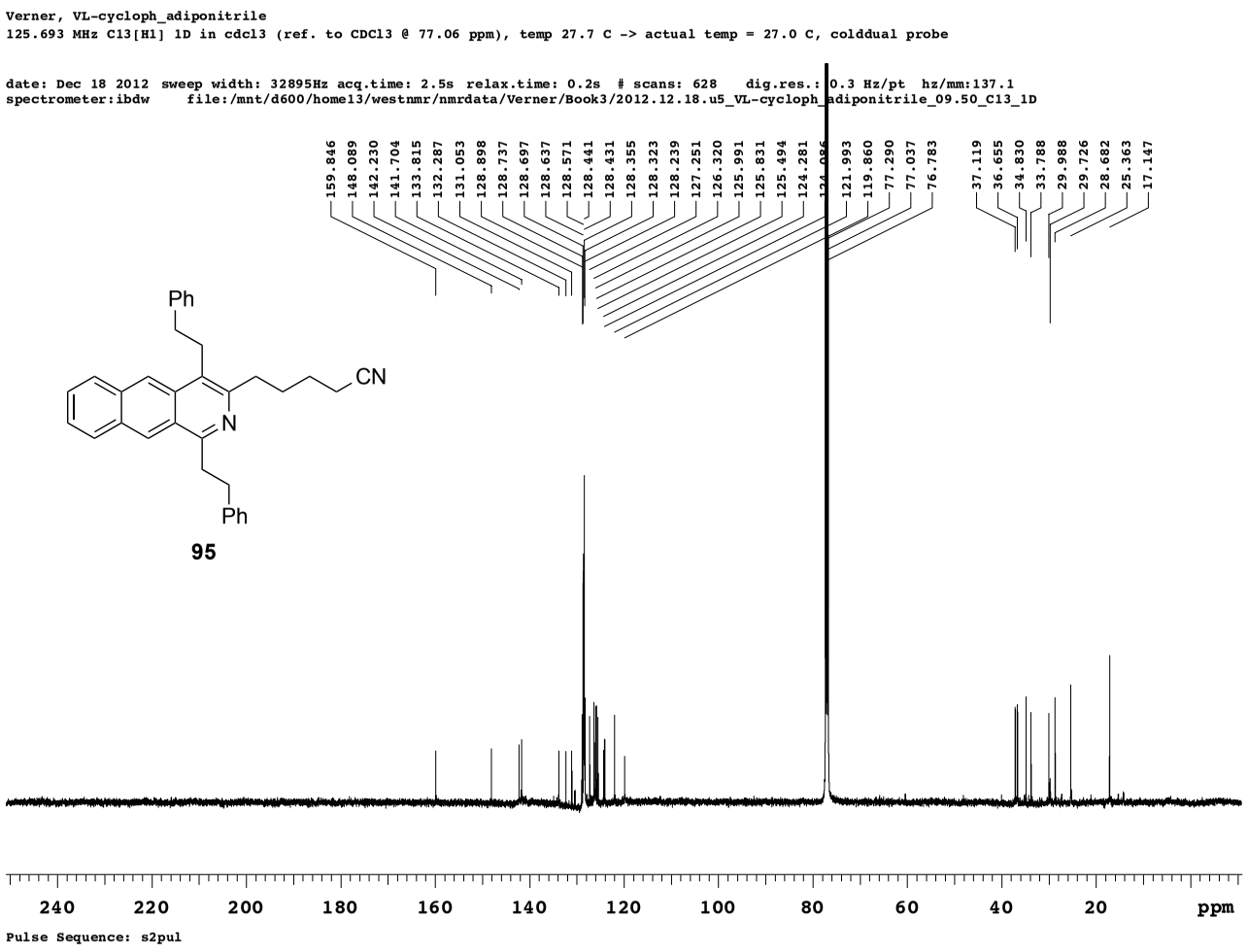
Verner, VL-cycloph_adiponitrile
125.693 MHz C13[H1] 1D in cdcl3 (ref. to CDCl3 @ 77.06 ppm), temp 27.7 C -> actual temp = 27.0 C, colddual probe
date: Dec 18 2012 sweep width: 32895Hz acq.time: 2.5s relax.time: 0.2s # scans: 628 dig.res.: 0.3 Hz/pt hz/mm:137.1
spectrometer:ibdw file:/mnt/d600/home13/westnmr/nmrdata/Verner/Book3/2012.12.18.u5_VL-cycloph_adiponitrile_09.50_C13_1D
159.846
148.089
142.230
141.704
133.815
132.287
131.053
128.898
128.737
128.697
128.637
128.571
128.441
128.431
128.355
128.323
128.239
127.251
126.320
125.991
125.831
125.494
124.281
121.993
119.860
77.290
77.037
76.783
37.119
36.655
34.830
33.788
29.988
29.726
28.682
25.363
17.147
Ph
CN
N
Ph
95
240
220
200
180
160
140
120
100
80
60
40
20
ppm
Pulse Sequence: s2pul

Appendix V: Sample HPLC Data for Chiral Cycloadducts

(Chapter 3)

VL-9-silylketoneR OD Hex/IPA 99.5/0.5 VL99_10.m 141104

```
==========================================================================
Injection Date  : 11/4/2014 3:03:47 PM          Seq. Line :   3
Sample Name     : VL-9-silylketonR               Location : Vial 21
Acq. Operator   : Verner                            Inj :   1
Acq. Instrument : Instrument 1                 Inj Volume : 5 µl
Different Inj Volume from Sequence !     Actual Inj Volume : 0.5 µl
Acq. Method     : C:\HPCHEM\1\METHODS\VL995_10.M
Last changed    : 11/4/2014 3:01:23 PM by Verner
Analysis Method : C:\HPCHEM\1\METHODS\EDH90.M
Last changed    : 4/1/2015 10:10:55 AM by Taras
                  (modified after loading)
```

DAD1 A, Sig=210,8 Ref=360,100 (VERNER\14110403.D)

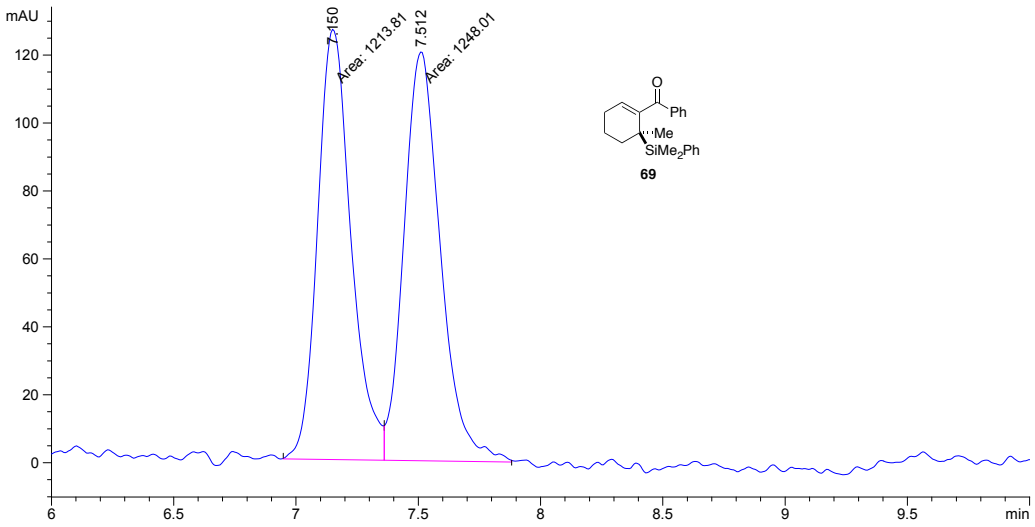


```
==========================================================================
                        Area Percent Report
==========================================================================

Sorted By             :      Signal
Multiplier            :      1.0000
Dilution              :      1.0000
Use Multiplier & Dilution Factor with ISTDs


Signal 1: DAD1 A, Sig=210,8 Ref=360,100

Peak RetTime Type  Width     Area      Height     Area
  #   [min]        [min]   [mAU*s]     [mAU]       %
----|-------|----|-------|----------|----------|--------|
   1   7.150 MF    0.1596 1213.81079  126.77758  49.3054
   2   7.512 FM    0.1726 1248.01062  120.49529  50.6946

Totals :                  2461.82141  247.27287


==========================================================================
                        *** End of Report ***
```

VL-9-193 chiral silylbenzoyl derivative
IC column 99.5:0.5 Hex:IPA 10 celcius

```
==================================================================
Injection Date  : 11/13/2014 2:29:47 PM          Seq. Line :   1
Sample Name     : 9-193                           Location : Vial 21
Acq. Operator   : Verner                             Inj :   1
Acq. Instrument : Instrument 1                  Inj Volume : 5 µl
Different Inj Volume from Sequence !     Actual Inj Volume : 0.5 µl
Acq. Method     : C:\HPCHEM\1\METHODS\VL995_10.M
Last changed    : 11/13/2014 2:28:36 PM by Verner
Analysis Method : C:\HPCHEM\1\METHODS\EDH90.M
Last changed    : 4/1/2015 10:10:55 AM by Taras
                  (modified after loading)
```

DAD1 B, Sig=254,8 Ref=360,100 (VERNER\VL141131.D)

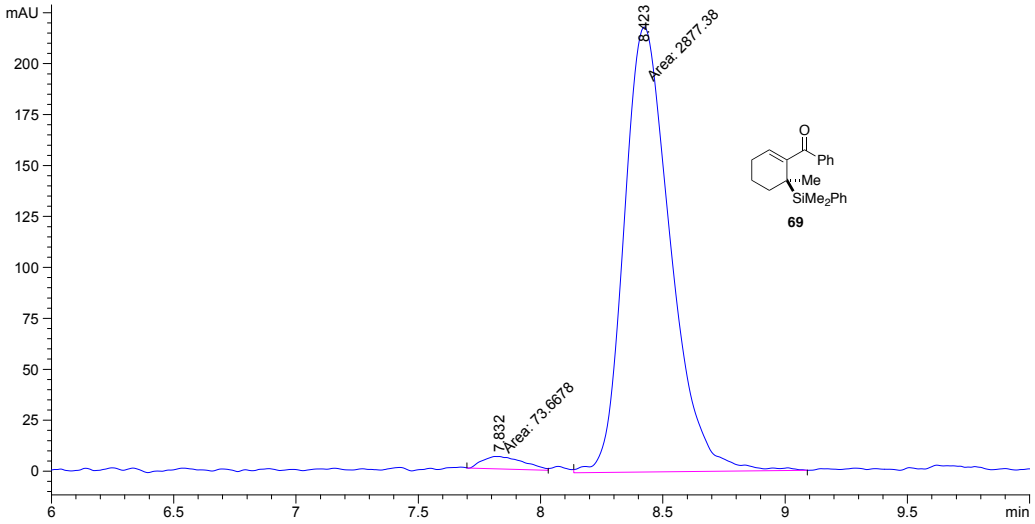


```
==================================================================
                        Area Percent Report
==================================================================

Sorted By             :      Signal
Multiplier            :      1.0000
Dilution              :      1.0000
Use Multiplier & Dilution Factor with ISTDs


Signal 1: DAD1 B, Sig=254,8 Ref=360,100

Peak RetTime Type  Width     Area      Height     Area
  #   [min]        [min]   [mAU*s]     [mAU]       %
----|-------|----|-------|----------|----------|--------|
   1   7.832 MM    0.1986   73.66780    6.18154   2.4963
   2   8.423 MM    0.2194 2877.38354  218.57042  97.5037

Totals :                  2951.05135  224.75196

==================================================================
                        *** End of Report ***
```

VL-9-199 racemic furan adduct
IC column 95:5 hex ipa
20 celcius
0.5mL/min
feb 26 2015

```
======================================================================
Injection Date  : 2/26/2015 11:01:19 AM          Seq. Line :   1
Sample Name     : VL-9-199 R                      Location : Vial 31
Acq. Operator   : Verner                             Inj :   1
Acq. Instrument : Instrument 1                  Inj Volume : 5 µl
Different Inj Volume from Sequence !     Actual Inj Volume : 1 µl
Acq. Method     : C:\HPCHEM\1\METHODS\VL95.M
Last changed    : 2/26/2015 11:36:40 AM by Verner
                  (modified after loading)
Analysis Method : C:\HPCHEM\1\METHODS\EDH90.M
Last changed    : 4/1/2015 10:13:43 AM by Taras
                  (modified after loading)
```

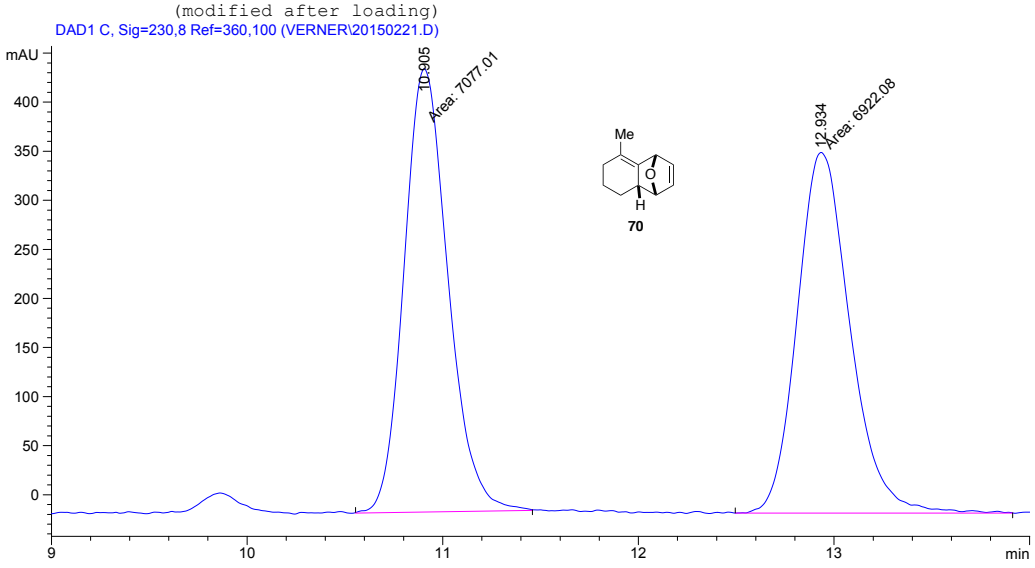


```
======================================================================
                        Area Percent Report
======================================================================

Sorted By             :      Signal
Multiplier            :      1.0000
Dilution              :      1.0000
Use Multiplier & Dilution Factor with ISTDs


Signal 1: DAD1 C, Sig=230,8 Ref=360,100

Peak RetTime Type  Width     Area      Height     Area
  #   [min]        [min]   [mAU*s]     [mAU]       %
----|-------|----|-------|----------|----------|--------|
   1  10.905 MM    0.2609 7077.00928  452.14902  50.5533
   2  12.934 MM    0.3137 6922.08301  367.78052  49.4467

Totals :                  1.39991e4   819.92953
```

VL-9-198 chiral furan adduct
IC column 95:5 hex ipa
20 celcius
0.5 mL/min
feb 26 2015

```
==================================================================
Injection Date  : 2/26/2015 11:43:29 AM          Seq. Line :   2
Sample Name     : VL-9-198 C                      Location : Vial 32
Acq. Operator   : Verner                             Inj :   1
Acq. Instrument : Instrument 1                  Inj Volume : 5 µl
Different Inj Volume from Sequence !     Actual Inj Volume : 1 µl
Acq. Method     : C:\HPCHEM\1\METHODS\VL95.M
Last changed    : 2/26/2015 12:03:25 PM by Verner
                  (modified after loading)
Analysis Method : C:\HPCHEM\1\METHODS\EDH90.M
Last changed    : 4/1/2015 10:13:43 AM by Taras
                  (modified after loading)
```

DAD1 C, Sig=230,8 Ref=360,100 (VERNER\20150222.D)

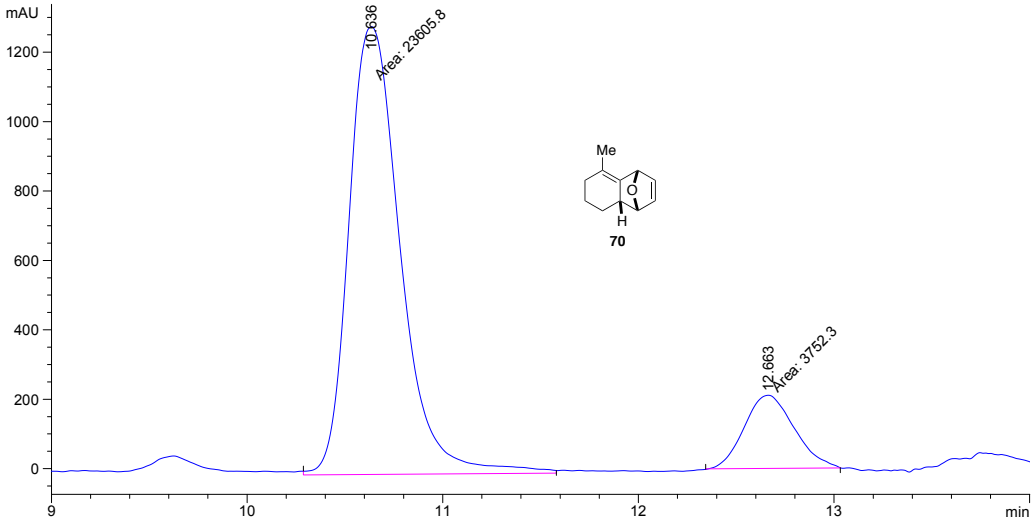


```
==================================================================
                        Area Percent Report
==================================================================

Sorted By             :      Signal
Multiplier            :      1.0000
Dilution              :      1.0000
Use Multiplier & Dilution Factor with ISTDs


Signal 1: DAD1 C, Sig=230,8 Ref=360,100

Peak RetTime Type  Width     Area      Height     Area
  #   [min]        [min]   [mAU*s]     [mAU]       %
----|-------|----|-------|----------|----------|--------|
   1  10.636 MM    0.3048 2.36058e4  1290.88745  86.2845
   2  12.663 MM    0.2961 3752.30420  211.18797  13.7155

Totals :                  2.73581e4  1502.07542
```

Data File C:\HPCHEM\1\DATA\VERNER\15032000.D Sample Name: VL-malBAMImaj

IC IPR:HEX 25:75 20C 0.7 mL/min

```
==========================================================================
Injection Date  : 3/19/2015 5:59:21 PM          Seq. Line :   1
Sample Name     : VL-malBAMImaj                  Location : Vial 21
Acq. Operator   : Verner                            Inj :   1
Acq. Instrument : Instrument 1                  Inj Volume : 1 µl
Acq. Method     : C:\HPCHEM\1\METHODS\VL75.M
Last changed    : 11/13/2014 2:10:34 PM by Verner
Analysis Method : C:\HPCHEM\1\METHODS\EDH90.M
Last changed    : 4/1/2015 10:17:49 AM by Taras
                  (modified after loading)
```

DAD1 A, Sig=210,8 Ref=360,100 (VERNER\15032000.D)

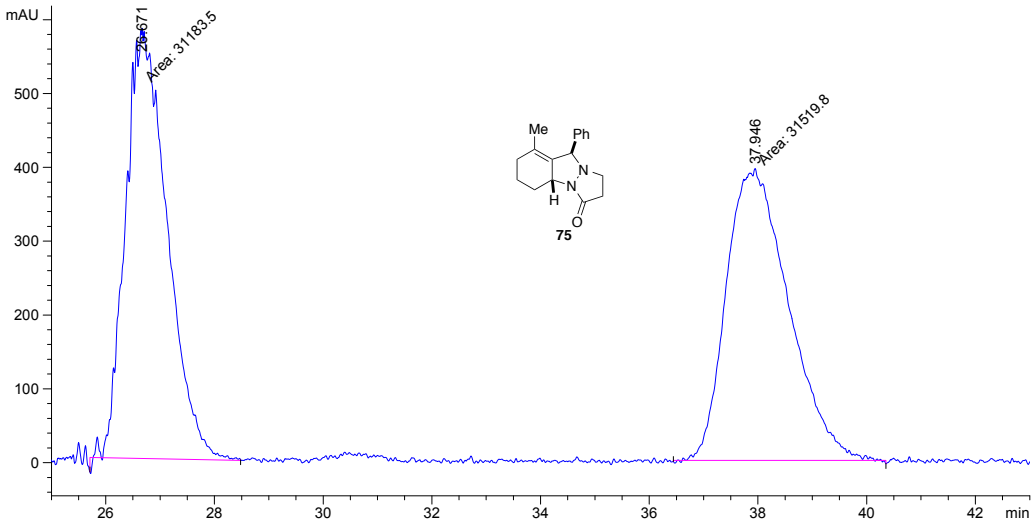


```
==========================================================================
                          Area Percent Report
==========================================================================

Sorted By             :      Signal
Multiplier            :      1.0000
Dilution              :      1.0000
Use Multiplier & Dilution Factor with ISTDs


Signal 1: DAD1 A, Sig=210,8 Ref=360,100

Peak RetTime Type  Width     Area      Height     Area
  #   [min]        [min]   [mAU*s]     [mAU]       %
----|-------|----|-------|----------|----------|--------|
   1  26.671 MM    0.8917 3.11835e4   582.86346  49.7318
   2  37.946 MM    1.3277 3.15198e4   395.65768  50.2682

Totals :                  6.27033e4   978.52115

==========================================================================
                          *** End of Report ***
```

VL-9-190 R2 chiral m-allene benzyl AMI
IC column 75:25 Hex:IPA 22

```
==========================================================================
Injection Date  : 11/13/2014 5:29:15 PM          Seq. Line :   5
Sample Name     : 9-190 R2                        Location : Vial 23
Acq. Operator   : Verner                             Inj :   1
Acq. Instrument : Instrument 1                  Inj Volume : 1 µl
Acq. Method     : C:\HPCHEM\1\METHODS\VL75.M
Last changed    : 11/13/2014 2:10:34 PM by Verner
Analysis Method : C:\HPCHEM\1\METHODS\EDH90.M
Last changed    : 4/1/2015 10:17:49 AM by Taras
                  (modified after loading)
```

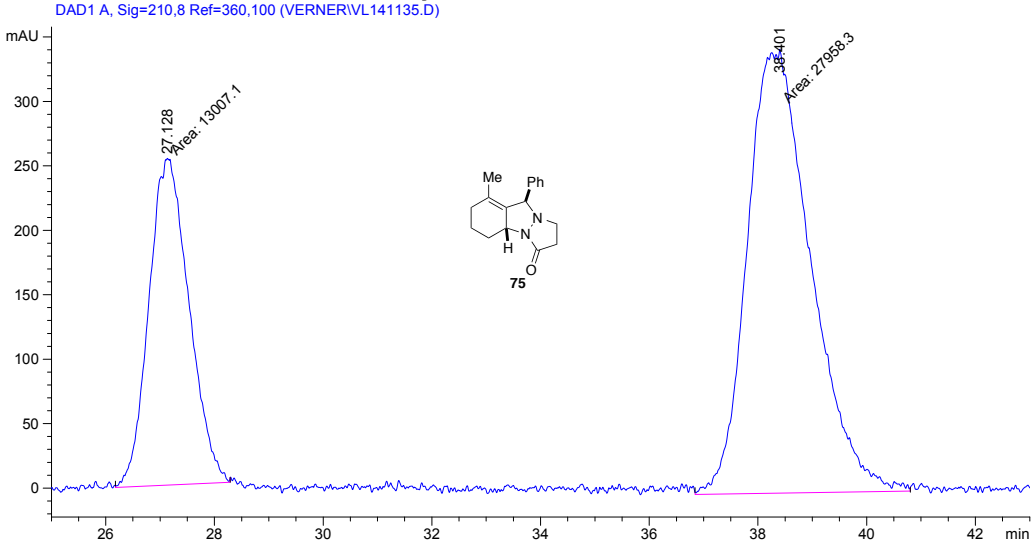


```
==========================================================================
                          Area Percent Report
==========================================================================

Sorted By             :      Signal
Multiplier            :      1.0000
Dilution              :      1.0000
Use Multiplier & Dilution Factor with ISTDs


Signal 1: DAD1 A, Sig=210,8 Ref=360,100

Peak RetTime Type  Width     Area      Height     Area
  #   [min]        [min]   [mAU*s]     [mAU]       %
----|-------|----|-------|----------|----------|--------|
   1  27.128 MM    0.8548 1.30071e4   253.59607  31.7513
   2  38.401 MM    1.3522 2.79583e4   344.60544  68.2487

Totals :                  4.09654e4   598.20151


==========================================================================
                          *** End of Report ***
```

IC IPR:HEX 25:75 20C 0.7 mL/min

```
==========================================================================
Injection Date  : 3/19/2015 7:00:30 PM          Seq. Line :   2
Sample Name     : VL-malBAMImin                  Location : Vial 22
Acq. Operator   : Verner                            Inj :   1
Acq. Instrument : Instrument 1                 Inj Volume : 1 µl
Acq. Method     : C:\HPCHEM\1\METHODS\VL75.M
Last changed    : 11/13/2014 2:10:34 PM by Verner
Analysis Method : C:\HPCHEM\1\METHODS\EDH90.M
Last changed    : 4/1/2015 10:21:58 AM by Taras
                  (modified after loading)
```

DAD1 C, Sig=230,8 Ref=360,100 (VERNER\15032001.D)

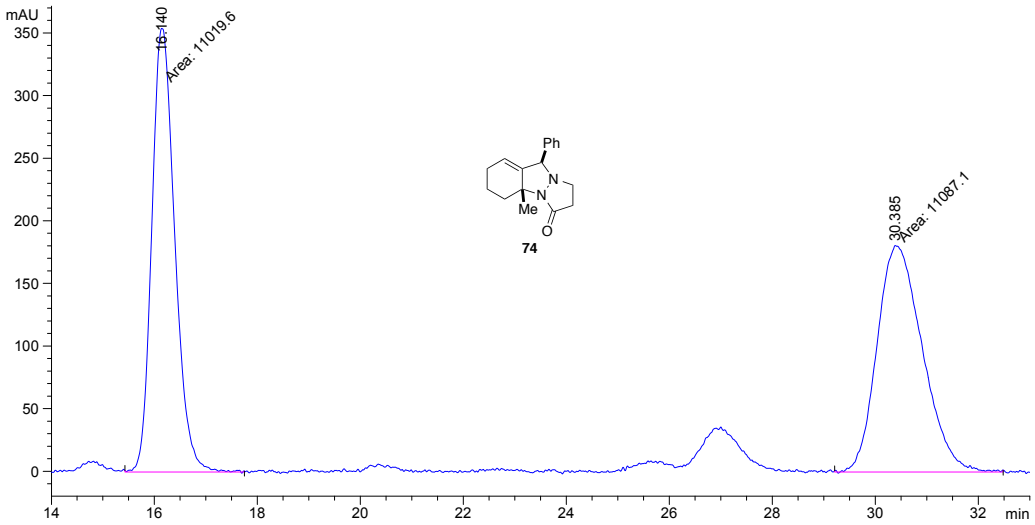


```
==========================================================================
                          Area Percent Report
==========================================================================

Sorted By             :      Signal
Multiplier            :      1.0000
Dilution              :      1.0000
Use Multiplier & Dilution Factor with ISTDs


Signal 1: DAD1 C, Sig=230,8 Ref=360,100

Peak RetTime Type  Width     Area      Height     Area
  #   [min]        [min]   [mAU*s]     [mAU]       %
----|-------|----|-------|----------|----------|--------|
   1  16.140 MM    0.5183 1.10196e4   354.36923  49.8473
   2  30.385 MM    1.0212 1.10871e4   180.95213  50.1527

Totals :                  2.21067e4   535.32137

==========================================================================
                          *** End of Report ***
```

VL-9-190 mallene BAMI minor
IC column 75:25 hex:ipr
20 c

```
======================================================================
Injection Date  : 1/29/2015 1:47:27 PM          Seq. Line :   1
Sample Name     : VL9-190                        Location : Vial 11
Acq. Operator   : Verner                             Inj :   1
Acq. Instrument : Instrument 1                 Inj Volume : 1 µl
Acq. Method     : C:\HPCHEM\1\METHODS\VL75.M
Last changed    : 11/13/2014 2:10:34 PM by Verner
Analysis Method : C:\HPCHEM\1\METHODS\EDH90.M
Last changed    : 4/1/2015 10:21:58 AM by Taras
                  (modified after loading)
```

DAD1 C, Sig=230,8 Ref=360,100 (VERNER\01291501.D)

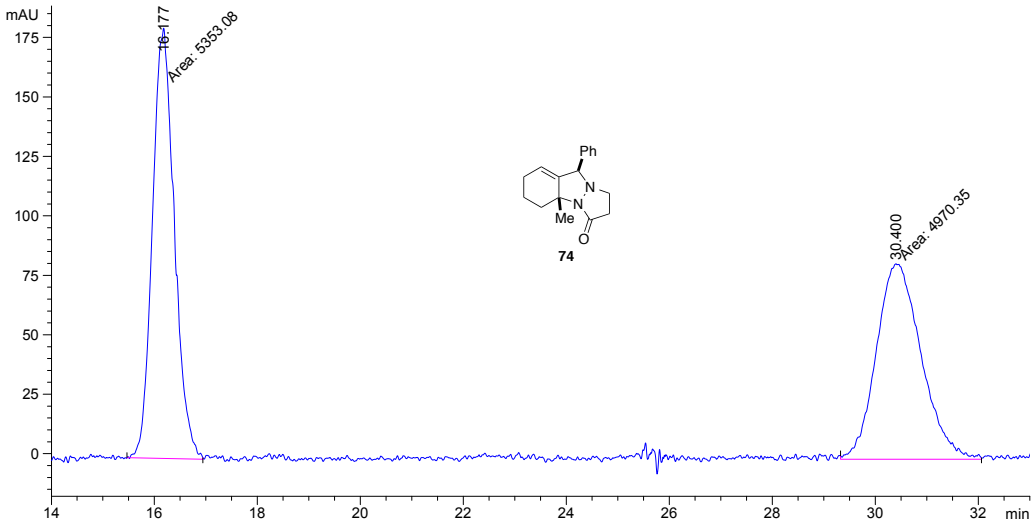


```
======================================================================
                        Area Percent Report
======================================================================

Sorted By             :      Signal
Multiplier            :      1.0000
Dilution              :      1.0000
Use Multiplier & Dilution Factor with ISTDs


Signal 1: DAD1 C, Sig=230,8 Ref=360,100

Peak RetTime Type  Width     Area      Height     Area
  #   [min]        [min]   [mAU*s]     [mAU]       %
----|-------|----|-------|----------|----------|--------|
   1  16.177 MM    0.4931 5353.07910  180.93117  51.8537
   2  30.400 MM    1.0077 4970.35449   82.20432  48.1463

Totals :                  1.03234e4   263.13549

======================================================================
                        *** End of Report ***
```

VL-9-207 F3 mallene cinAMI
IC column 75:25 hex:ipr
20 c

```
==========================================================================
Injection Date  : 1/29/2015 3:49:45 PM          Seq. Line :   3
Sample Name     : VL9-207F3                      Location : Vial 13
Acq. Operator   : Verner                            Inj :   1
Acq. Instrument : Instrument 1                  Inj Volume : 1 µl
Acq. Method     : C:\HPCHEM\1\METHODS\VL75.M
Last changed    : 11/13/2014 2:10:34 PM by Verner
Analysis Method : C:\HPCHEM\1\METHODS\EDH90.M
Last changed    : 4/1/2015 10:24:12 AM by Taras
                  (modified after loading)
```

DAD1 A, Sig=210,8 Ref=360,100 (VERNER\01291503.D)

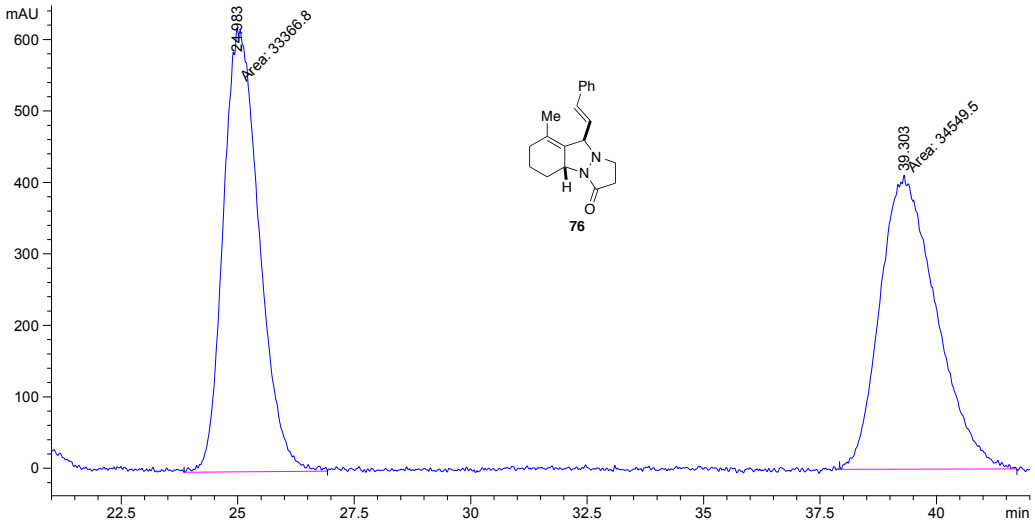


```
==========================================================================
                          Area Percent Report
==========================================================================

Sorted By             :      Signal
Multiplier            :      1.0000
Dilution              :      1.0000
Use Multiplier & Dilution Factor with ISTDs


Signal 1: DAD1 A, Sig=210,8 Ref=360,100

Peak RetTime Type  Width     Area      Height     Area
  #   [min]        [min]   [mAU*s]     [mAU]       %
----|-------|----|-------|----------|----------|--------|
   1  24.983 MM    0.8950 3.33668e4   621.37579  49.1293
   2  39.303 MM    1.3983 3.45495e4   411.80890  50.8707

Totals :                  6.79163e4  1033.18469

==========================================================================
                          *** End of Report ***
```

VL-9-194 R2 chiral m-allene cinammyl AMI
IC column 75:25 Hex:IPA 22

```
==========================================================================
Injection Date  : 11/13/2014 7:31:34 PM          Seq. Line :   7
Sample Name     : 9-194 R2                        Location : Vial 25
Acq. Operator   : Verner                             Inj :   1
Acq. Instrument : Instrument 1                  Inj Volume : 1 µl
Acq. Method     : C:\HPCHEM\1\METHODS\VL75.M
Last changed    : 11/13/2014 2:10:34 PM by Verner
Analysis Method : C:\HPCHEM\1\METHODS\EDH90.M
Last changed    : 4/1/2015 10:24:12 AM by Taras
                  (modified after loading)
```

DAD1 B, Sig=254,8 Ref=360,100 (VERNER\VL141137.D)

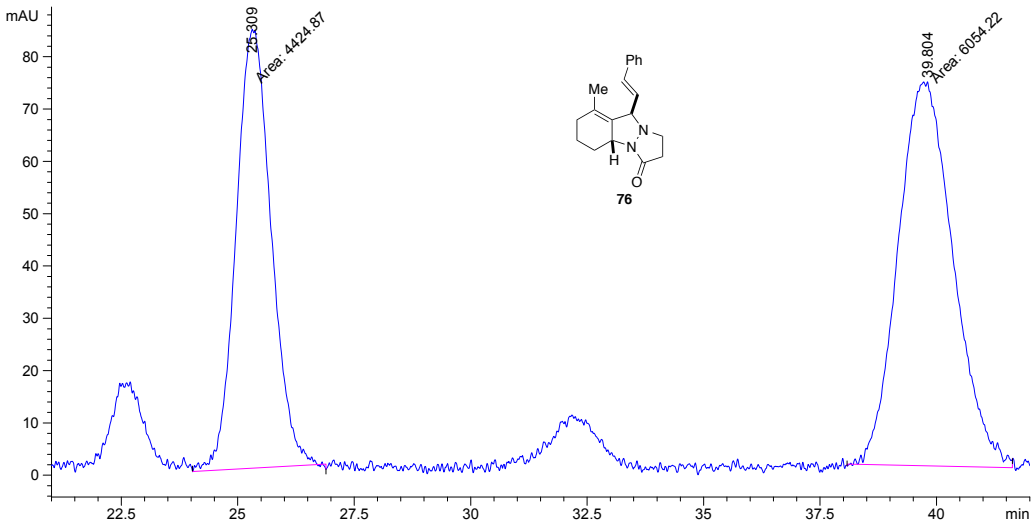


```
==========================================================================
                        Area Percent Report
==========================================================================

Sorted By             :      Signal
Multiplier            :      1.0000
Dilution              :      1.0000
Use Multiplier & Dilution Factor with ISTDs


Signal 1: DAD1 B, Sig=254,8 Ref=360,100

Peak RetTime Type  Width     Area      Height     Area
  #   [min]        [min]   [mAU*s]     [mAU]       %
----|-------|----|-------|----------|----------|--------|
   1  25.309 MM    0.8786 4424.87305   83.93762  42.2257
   2  39.804 MM    1.3736 6054.22217   73.46134  57.7743

Totals :                  1.04791e4   157.39896


==========================================================================
                        *** End of Report ***
```

VL-9-207 mallene cinAMI F2
IC column 75 25 hex IPA 22 C

```
==========================================================================
Injection Date  : 1/26/2015 4:34:24 PM          Seq. Line :   3
Sample Name     : VL-9-207F2                     Location : Vial 13
Acq. Operator   : Verner                            Inj :   1
Acq. Instrument : Instrument 1                 Inj Volume : 1 µl
Acq. Method     : C:\HPCHEM\1\METHODS\VL75.M
Last changed    : 11/13/2014 2:10:34 PM by Verner
Analysis Method : C:\HPCHEM\1\METHODS\EDH90.M
Last changed    : 4/1/2015 10:28:24 AM by Taras
                  (modified after loading)
```

DAD1 B, Sig=254,8 Ref=360,100 (VERNER\15012603.D)

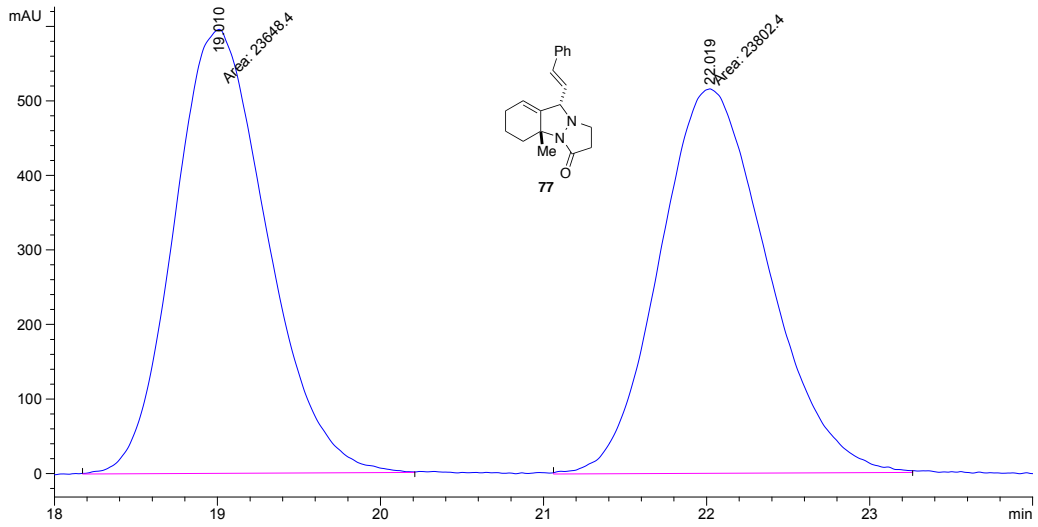


```
==========================================================================
                          Area Percent Report
==========================================================================

Sorted By             :      Signal
Multiplier            :      1.0000
Dilution              :      1.0000
Use Multiplier & Dilution Factor with ISTDs


Signal 1: DAD1 B, Sig=254,8 Ref=360,100

Peak RetTime Type  Width     Area      Height     Area
  #   [min]        [min]   [mAU*s]     [mAU]       %
----|-------|----|-------|----------|----------|--------|
   1  19.010 MM    0.6612 2.36484e4   596.08929  49.8377
   2  22.019 MM    0.7687 2.38024e4   516.04401  50.1623

Totals :                  4.74508e4  1112.13330


==========================================================================
                          *** End of Report ***
```

VL-9-194 R2 chiral m-allene cinammyl AMI
IC column 75:25 Hex:IPA 22

```
==========================================================================
Injection Date  : 11/13/2014 7:31:34 PM          Seq. Line :   7
Sample Name     : 9-194 R2                        Location : Vial 25
Acq. Operator   : Verner                             Inj :   1
Acq. Instrument : Instrument 1                  Inj Volume : 1 µl
Acq. Method     : C:\HPCHEM\1\METHODS\VL75.M
Last changed    : 11/13/2014 2:10:34 PM by Verner
Analysis Method : C:\HPCHEM\1\METHODS\EDH90.M
Last changed    : 4/1/2015 10:28:24 AM by Taras
                  (modified after loading)
```

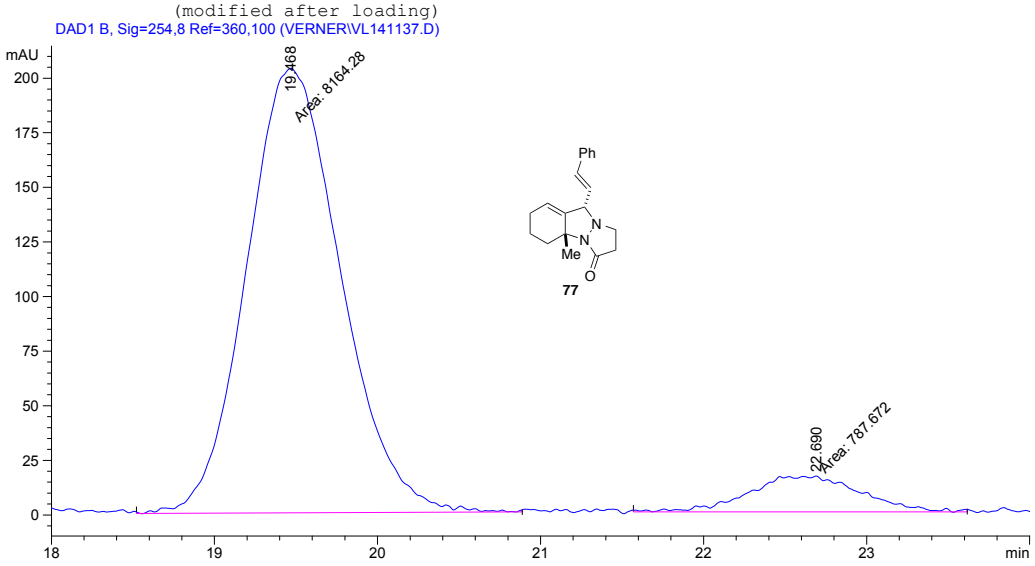


```
==========================================================================
                        Area Percent Report
==========================================================================

Sorted By             :      Signal
Multiplier            :      1.0000
Dilution              :      1.0000
Use Multiplier & Dilution Factor with ISTDs


Signal 1: DAD1 B, Sig=254,8 Ref=360,100

Peak RetTime Type  Width     Area      Height     Area
  #   [min]        [min]   [mAU*s]     [mAU]       %
----|-------|----|-------|----------|----------|--------|
   1  19.468 MM    0.6683 8164.28271  203.60756  91.2011
   2  22.690 MM    0.7976  787.67151   16.45898   8.7989

Totals :                  8951.95422  220.06654


==========================================================================
                        *** End of Report ***
```

VL-9-207 R1 racemic mallene cinAMI
IC column 75:25 hex:ipr
20 c

```
==========================================================================
Injection Date  : 1/29/2015 2:48:36 PM          Seq. Line :   2
Sample Name     : VL9-207R1                      Location : Vial 12
Acq. Operator   : Verner                             Inj :   1
Acq. Instrument : Instrument 1                 Inj Volume : 1 µl
Acq. Method     : C:\HPCHEM\1\METHODS\VL75.M
Last changed    : 11/13/2014 2:10:34 PM by Verner
Analysis Method : C:\HPCHEM\1\METHODS\EDH90.M
Last changed    : 4/1/2015 10:31:21 AM by Taras
                  (modified after loading)
```

DAD1 D, Sig=230,16 Ref=360,100 (VERNER\01291502.D)

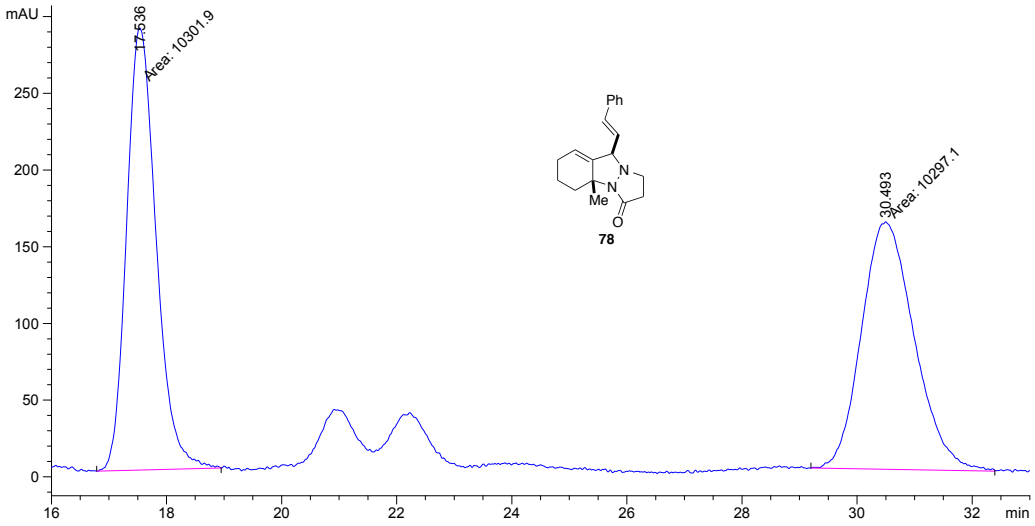


```
==========================================================================
                          Area Percent Report
==========================================================================

Sorted By             :      Signal
Multiplier            :      1.0000
Dilution              :      1.0000
Use Multiplier & Dilution Factor with ISTDs


Signal 1: DAD1 D, Sig=230,16 Ref=360,100

Peak RetTime Type  Width     Area      Height     Area
  #   [min]        [min]   [mAU*s]     [mAU]       %
----|-------|----|-------|----------|----------|--------|
   1  17.536 MM    0.5957 1.03019e4   288.23123  50.0117
   2  30.493 MM    1.0635 1.02971e4   161.37090  49.9883

Totals :                  2.05990e4   449.60213

==========================================================================
                          *** End of Report ***
```

VL-9-194 R1 chiral m-allene cinammyl AMI
IC column 75:25 Hex:IPA 22

```
==========================================================================
Injection Date  : 11/13/2014 6:30:25 PM          Seq. Line :   6
Sample Name     : 9-194 R1                        Location : Vial 24
Acq. Operator   : Verner                             Inj :   1
Acq. Instrument : Instrument 1                  Inj Volume : 1 µl
Acq. Method     : C:\HPCHEM\1\METHODS\VL75.M
Last changed    : 11/13/2014 2:10:34 PM by Verner
Analysis Method : C:\HPCHEM\1\METHODS\EDH90.M
Last changed    : 4/1/2015 10:31:21 AM by Taras
                  (modified after loading)
```

DAD1 D, Sig=230,16 Ref=360,100 (VERNER\VL141136.D)

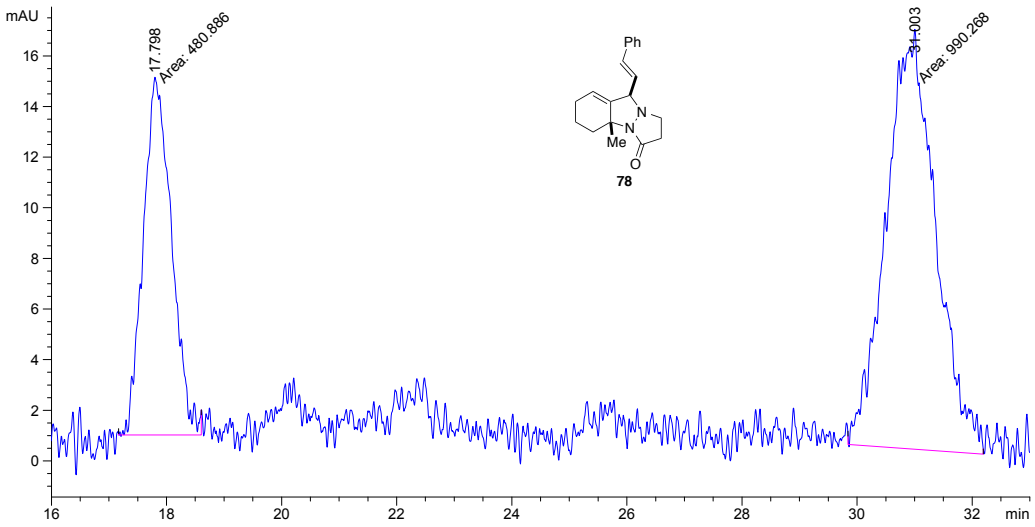


```
==========================================================================
                          Area Percent Report
==========================================================================

Sorted By             :      Signal
Multiplier            :      1.0000
Dilution              :      1.0000
Use Multiplier & Dilution Factor with ISTDs


Signal 1: DAD1 D, Sig=230,16 Ref=360,100

Peak RetTime Type  Width     Area      Height     Area
  #   [min]        [min]   [mAU*s]     [mAU]       %
----|-------|----|-------|----------|----------|--------|
   1  17.798 MM    0.5666  480.88571   14.14417  32.6877
   2  31.003 MM    0.9943  990.26788   16.59977  67.3123

Totals :                  1471.15359   30.74394


==========================================================================
                          *** End of Report ***
```

0.1% AA in aq and ACN GEN_OD1.m AD-RH column NOV 13, 2014

```
==========================================================================
Injection Date  : 11/13/2014 4:50:21 PM          Seq. Line :   3
Sample Name     : 9-191 R2                        Location : P1-C-02
Acq. Operator   : Ed                                  Inj :   1
Acq. Instrument : 1100LC                        Inj Volume : 1 µl
Different Inj Volume from Sequence !     Actual Inj Volume : 5 µl
Acq. Method     : C:\HPCHEM\1\METHODS\GEN_OD1.M
Last changed    : 11/13/2014 3:37:01 PM by Ed
                  (modified after loading)
Analysis Method : C:\HPCHEM\1\METHODS\EDH90.M
Last changed    : 4/2/2015 10:26:43 AM by Taras
                  (modified after loading)
```

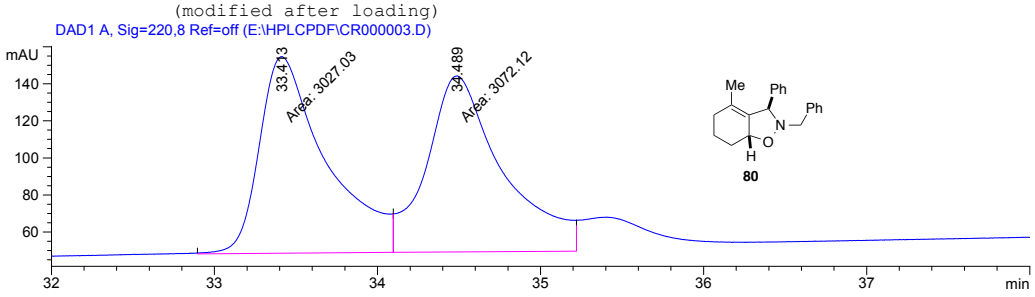


```
==========================================================================================
                              Fraction Information
==========================================================================================
Fraction collection off
==========================================================================================
No Fractions found.
==========================================================================================
==========================================================================
                           Area Percent Report
==========================================================================

Sorted By             :      Signal
Multiplier            :      1.0000
Dilution              :      1.0000
Use Multiplier & Dilution Factor with ISTDs


Signal 1: DAD1 A, Sig=220,8 Ref=off

Peak RetTime Type  Width     Area      Height     Area
  #   [min]        [min]   [mAU*s]     [mAU]       %
----|-------|----|-------|----------|----------|--------|
   1  33.413 MF    0.4744 3027.03076  106.34895  49.6304
   2  34.489 FM    0.5380 3072.11572   95.17728  50.3696

Totals :                  6099.14648  201.52623

==========================================================================
                           *** End of Report ***
```

0.1% AA aq and ACN GEN_OD1.m Oct 15, 2014 AD-RH colimn

```
==================================================================
Injection Date  : 10/15/2014 5:42:29 PM          Seq. Line :   3
Sample Name     : 9-99-R1                         Location : P1-C-03
Acq. Operator   : Ed                                  Inj :   1
Acq. Instrument : 1100LC                        Inj Volume : 1 µl
Acq. Method     : C:\HPCHEM\1\METHODS\GEN_OD1.M
Last changed    : 10/15/2014 3:03:44 PM by Ed
Analysis Method : C:\HPCHEM\1\METHODS\EDH90.M
Last changed    : 4/2/2015 10:26:43 AM by Taras
                  (modified after loading)
```

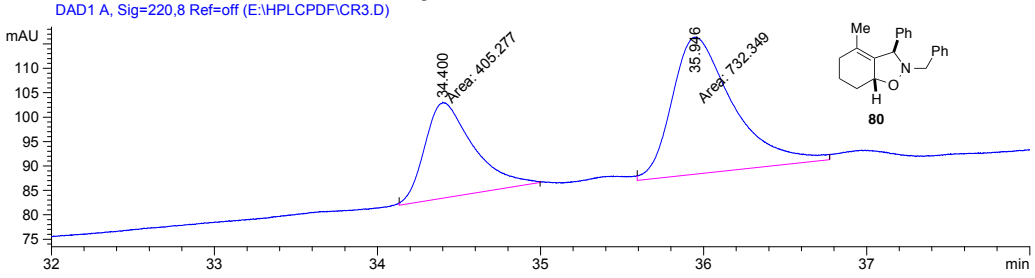


```
==========================================================================
                          Fraction Information
==========================================================================
Fraction collection off
==========================================================================
No Fractions found.
==========================================================================
==================================================================
                        Area Percent Report
==================================================================

Sorted By             :      Signal
Multiplier            :      1.0000
Dilution              :      1.0000
Use Multiplier & Dilution Factor with ISTDs


Signal 1: DAD1 A, Sig=220,8 Ref=off

Peak RetTime Type  Width     Area      Height     Area
  #   [min]        [min]   [mAU*s]     [mAU]       %
----|-------|----|-------|----------|----------|--------|
   1  34.400 MM    0.3441  405.27698   19.63156  35.6248
   2  35.946 MM    0.4346  732.34869   28.08663  64.3752

Totals :                  1137.62567   47.71819


==================================================================
                        *** End of Report ***
```

0.1% AA aq and ACN GEN_OD1.m Feb 17, 2015

```
==========================================================================
Injection Date  : 2/18/2015 10:06:56 AM          Seq. Line :   1
Sample Name     : 10-3 minor                      Location : P1-E-01
Acq. Operator   : Ed                                  Inj :   1
Acq. Instrument : 1100LC                        Inj Volume : 1 µl
Different Inj Volume from Sequence !     Actual Inj Volume : 10 µl
Acq. Method     : C:\HPCHEM\1\METHODS\GEN_OD1.M
Last changed    : 2/18/2015 10:09:45 AM by Ed
                  (modified after loading)
Analysis Method : C:\HPCHEM\1\METHODS\EDH90.M
Last changed    : 4/2/2015 10:37:10 AM by Taras
                  (modified after loading)
```

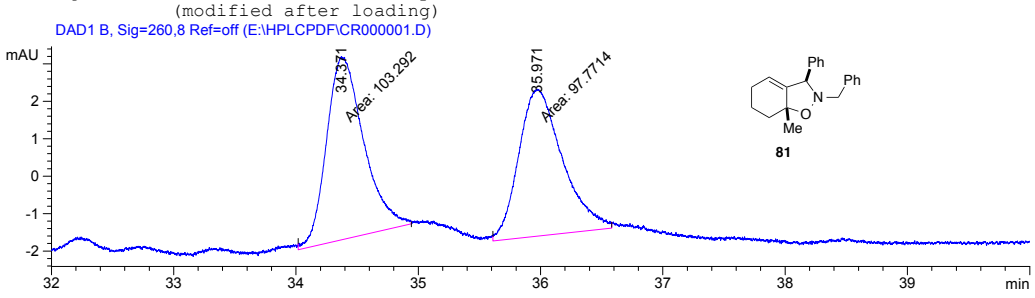


```
==========================================================================================
                              Fraction Information
==========================================================================================
Fraction collection off
==========================================================================================
No Fractions found.
==========================================================================================
==========================================================================
                           Area Percent Report
==========================================================================

Sorted By             :      Signal
Multiplier            :      1.0000
Dilution              :      1.0000
Use Multiplier & Dilution Factor with ISTDs


Signal 1: DAD1 B, Sig=260,8 Ref=off

Peak RetTime Type  Width     Area      Height     Area
  #   [min]        [min]   [mAU*s]     [mAU]       %
----|-------|----|-------|----------|----------|--------|
   1  34.371 MM    0.3515  103.29161    4.89748  51.3728
   2  35.971 MM    0.4149   97.77140    3.92727  48.6272

Totals :                   201.06301    8.82475

==========================================================================
                           *** End of Report ***
```

H2O and IPA AD-RH GEN_OD1.m JAN 28, 2015

```
==========================================================================
Injection Date  : 1/28/2015 3:52:15 PM          Seq. Line :  12
Sample Name     : MAll-DBN                       Location : P1-D-03
Acq. Operator   : Ed                                Inj :   1
Acq. Instrument : 1100LC                       Inj Volume : 1 µl
Different Inj Volume from Sequence !     Actual Inj Volume : 5 µl
Acq. Method     : C:\HPCHEM\1\METHODS\GEN_OD1.M
Last changed    : 10/16/2014 8:58:00 AM by Ed
Analysis Method : C:\HPCHEM\1\METHODS\EDH90.M
Last changed    : 4/2/2015 10:34:33 AM by Taras
                  (modified after loading)
```

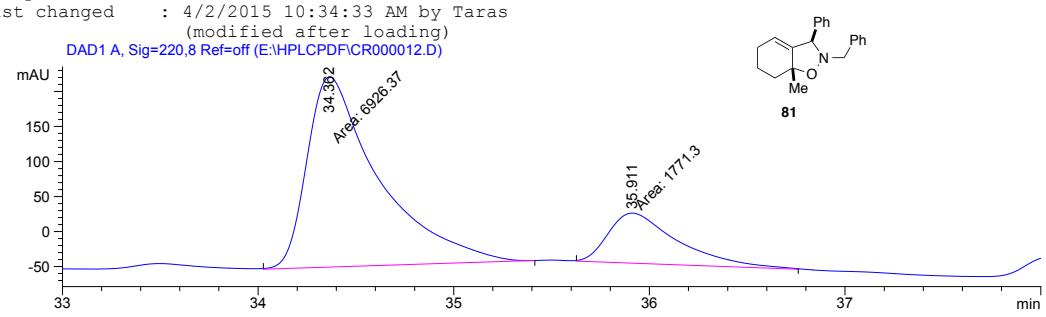


```
==========================================================================================
                              Fraction Information
==========================================================================================
Fraction collection off
==========================================================================================
No Fractions found.
==========================================================================================
==========================================================================
                            Area Percent Report
==========================================================================

Sorted By             :      Signal
Multiplier            :      1.0000
Dilution              :      1.0000
Use Multiplier & Dilution Factor with ISTDs


Signal 1: DAD1 A, Sig=220,8 Ref=off

Peak RetTime Type  Width     Area      Height     Area
  #   [min]        [min]   [mAU*s]     [mAU]       %
----|-------|----|-------|----------|----------|--------|
   1  34.362 MM    0.4246 6926.36572  271.88876  79.6347
   2  35.911 MM    0.4121 1771.30371   71.64355  20.3653

Totals :                  8697.66943  343.53232


==========================================================================
                           *** End of Report ***
```

0.1% AA aq and ACN GEN_OD1.m Mar 31, 2015

```
======================================================================
Injection Date  : 4/2/2015 12:35:29 PM          Seq. Line :   1
Sample Name     : Mall_UN_Major                  Location : P1-F-09
Acq. Operator   : Ed                                Inj :   1
Acq. Instrument : 1100LC                       Inj Volume : 1 µl
Different Inj Volume from Sequence !     Actual Inj Volume : 5 µl
Acq. Method     : C:\HPCHEM\1\METHODS\GEN_OD1.M
Last changed    : 3/23/2015 4:21:39 PM by Ed
Analysis Method : C:\HPCHEM\1\METHODS\EDH90.M
Last changed    : 4/9/2015 3:17:35 PM by Taras
                  (modified after loading)
```

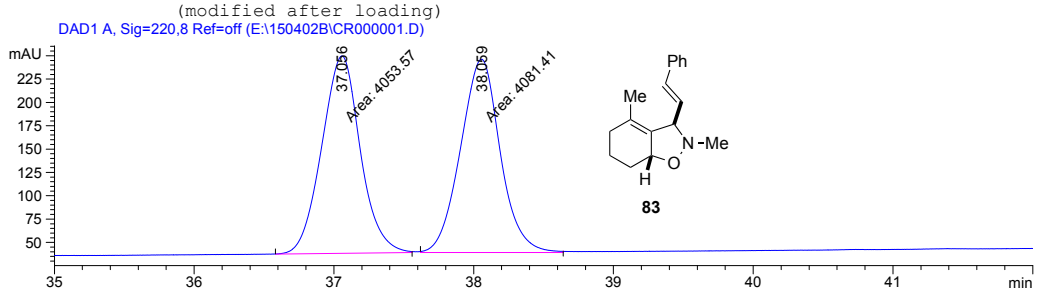


```
================================================================================
                          Fraction Information
================================================================================
Fraction collection off
================================================================================
No Fractions found.
================================================================================
======================================================================
                        Area Percent Report
======================================================================

Sorted By             :      Signal
Multiplier            :      1.0000
Dilution              :      1.0000
Use Multiplier & Dilution Factor with ISTDs


Signal 1: DAD1 A, Sig=220,8 Ref=off

Peak RetTime Type  Width     Area      Height     Area
  #   [min]        [min]   [mAU*s]     [mAU]       %
----|-------|----|-------|----------|----------|--------|
   1  37.056 MM    0.3191 4053.56738  211.69261  49.8289
   2  38.059 MM    0.3284 4081.40527  207.13354  50.1711

Totals :                  8134.97266  418.82616


======================================================================
                          *** End of Report ***
```

0.1% AA aq and ACN GEN_OD1.m Mar 31, 2015

```
==========================================================================
Injection Date  : 4/2/2015 1:33:58 PM            Seq. Line :   2
Sample Name     : VL-10-29-Major                  Location : P1-F-08
Acq. Operator   : Ed                                 Inj :   1
Acq. Instrument : 1100LC                        Inj Volume : 1 µl
Different Inj Volume from Sequence !     Actual Inj Volume : 3 µl
Acq. Method     : C:\HPCHEM\1\METHODS\GEN_OD1.M
Last changed    : 3/23/2015 4:21:39 PM by Ed
Analysis Method : C:\HPCHEM\1\METHODS\EDH90.M
Last changed    : 4/9/2015 3:17:35 PM by Taras
                  (modified after loading)
```

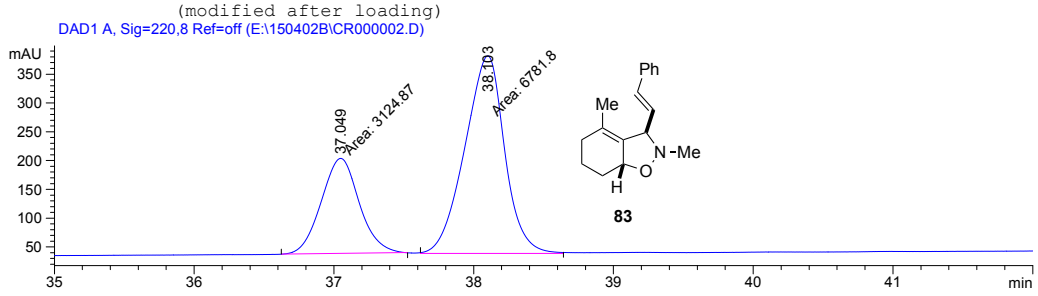


```
==========================================================================================
                              Fraction Information
==========================================================================================
Fraction collection off
==========================================================================================
No Fractions found.
==========================================================================================
==========================================================================
                            Area Percent Report
==========================================================================

Sorted By             :      Signal
Multiplier            :      1.0000
Dilution              :      1.0000
Use Multiplier & Dilution Factor with ISTDs


Signal 1: DAD1 A, Sig=220,8 Ref=off

Peak RetTime Type  Width     Area      Height     Area
  #   [min]        [min]   [mAU*s]     [mAU]       %
----|-------|----|-------|----------|----------|--------|
   1  37.049 MM    0.3152 3124.87256  165.25400  31.5431
   2  38.103 MM    0.3294 6781.79688  343.18680  68.4569

Totals :                  9906.66943  508.44080


==========================================================================
                           *** End of Report ***
```

```
======================================================================
Injection Date  : 01-Apr-15, 09:57:20          Seq. Line :   1
Sample Name     : VLmallciNminor                Location : Vial 21
Acq. Operator   : Verner                            Inj :   1
Acq. Method     : EDH95-5.M
Analysis Method : C:\HPCHEM\1\METHODS\EDH90.M
Last changed    : 4/1/2015 10:07:22 AM by Taras
                  (modified after loading)
```

DAD1 B, Sig=254,8 Ref=360,100 (SNAPSHOT.D)

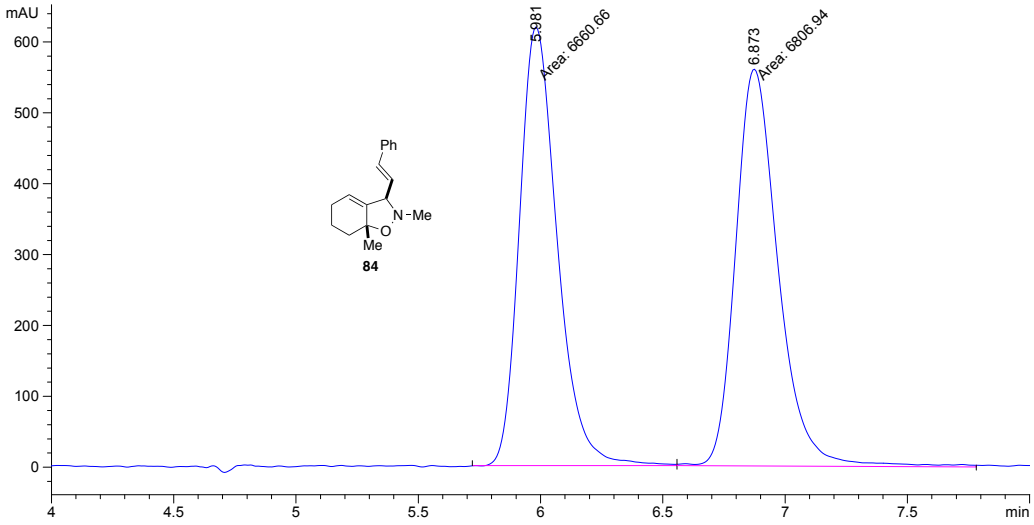


```
======================================================================
                        Area Percent Report
======================================================================

Sorted By             :      Signal
Multiplier            :      1.0000
Dilution              :      1.0000
Use Multiplier & Dilution Factor with ISTDs


Signal 1: DAD1 B, Sig=254,8 Ref=360,100

Peak RetTime Type  Width     Area      Height     Area
  #   [min]        [min]   [mAU*s]     [mAU]       %
----|-------|----|-------|----------|----------|--------|
   1   5.981 MM    0.1793 6660.66455  619.22931  49.4569
   2   6.873 MM    0.2025 6806.93994  560.19275  50.5431

Totals :                  1.34676e4  1179.42206

======================================================================
                        *** End of Report ***
```

Hex:IPA = 95:5 5C IC column Feb 04, 2015

```
======================================================================
Injection Date  : 2/4/2015 2:55:53 PM          Seq. Line :   3
Sample Name     : 208                           Location : Vial 12
Acq. Operator   : ED                                Inj :   1
Acq. Instrument : Instrument 1                Inj Volume : 5 µl
Different Inj Volume from Sequence !     Actual Inj Volume : 2 µl
Acq. Method     : C:\HPCHEM\1\METHODS\EDH95-5.M
Last changed    : 2/4/2015 3:19:17 PM by ED
                  (modified after loading)
Analysis Method : C:\HPCHEM\1\METHODS\EDH90.M
Last changed    : 4/1/2015 10:35:52 AM by Taras
                  (modified after loading)
```

DAD1 B, Sig=254,8 Ref=360,100 (VERNER\15020303.D)

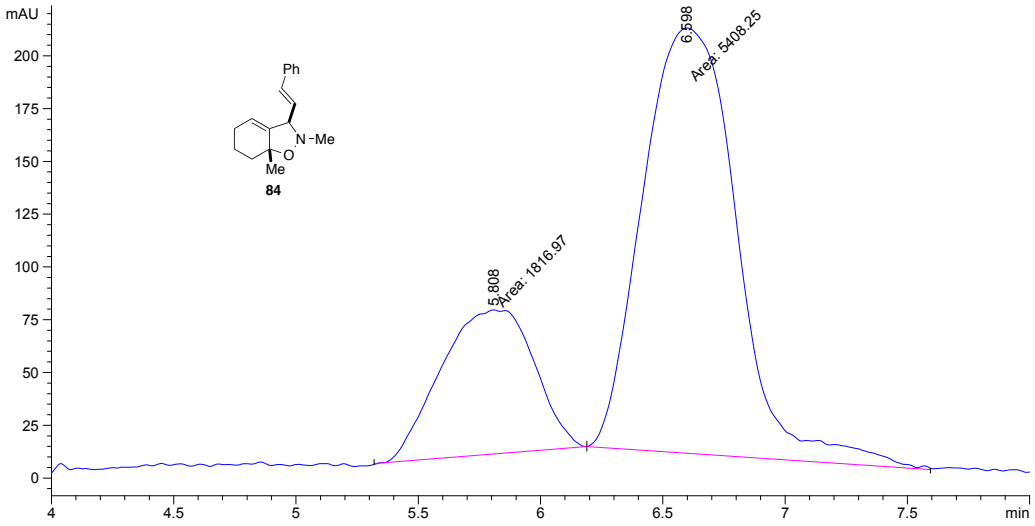


```
======================================================================
                        Area Percent Report
======================================================================

Sorted By             :      Signal
Multiplier            :      1.0000
Dilution              :      1.0000
Use Multiplier & Dilution Factor with ISTDs


Signal 1: DAD1 B, Sig=254,8 Ref=360,100

Peak RetTime Type  Width     Area      Height     Area
  #   [min]        [min]   [mAU*s]     [mAU]       %
----|-------|----|-------|----------|----------|--------|
   1   5.808 MM    0.4429 1816.97266   68.38134  25.1476
   2   6.598 MM    0.4473 5408.25146  201.51224  74.8524

Totals :                  7225.22412  269.89358

======================================================================
                        *** End of Report ***
```

Appendix VI: X-ray Crystallographic Data for Compound 119b

(Chapter 2)

STRUCTURE REPORT

XCL Code: FGW1404 **Date:** 24 April 2014

Compound: 9-Phenyl-1,2,5,6,7,9-hexahydro-3*H*,4a*H*-pyrazolo[1,2-*a*]indazol-3-one
Formula: $C_{16}H_{18}N_2O$

Supervisor: F. G. West **Crystallographer:** R. McDonald

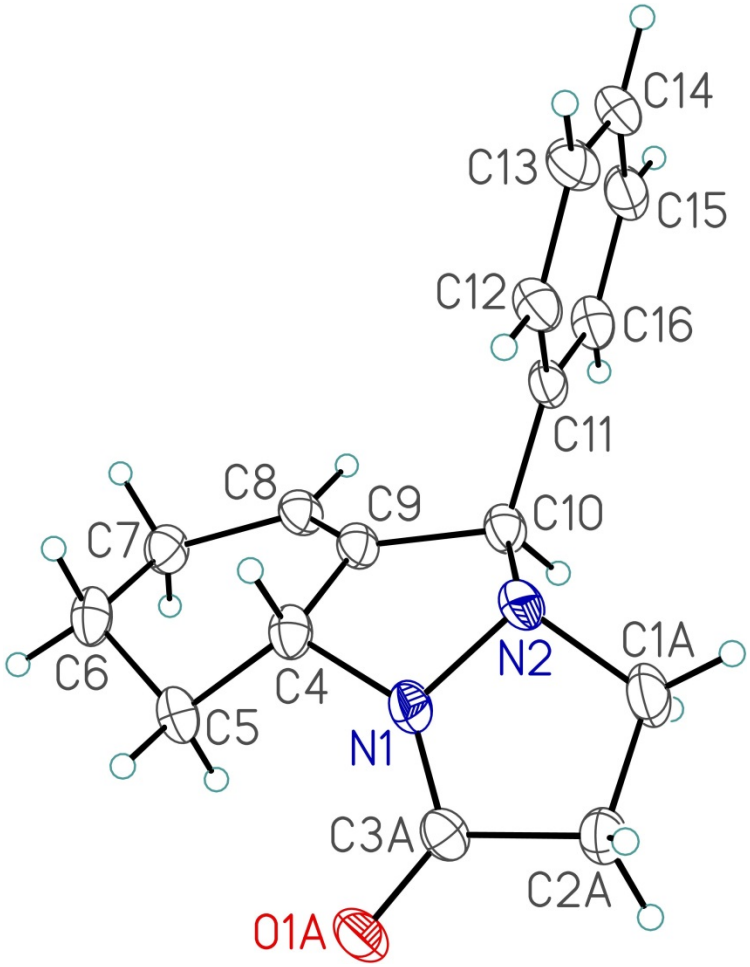

9-Phenyl-1,2,5,6,7,9-hexahydro-3*H*,4a*H*-pyrazolo[1,2-*a*]indazol-3-one (119b)

Figure Legends

Figure 1. Perspective view of the 9-phenyl-1,2,5,6,7,9-hexahydro-3*H*,4a*H*-pyrazolo[1,2-*a*]indazol-3-one molecule showing the atom labelling scheme. Non-hydrogen atoms are represented by Gaussian ellipsoids at the 30% probability level. Hydrogen atoms are shown with arbitrarily small thermal parameters.

Figure 2. Alternate view of the molecule.

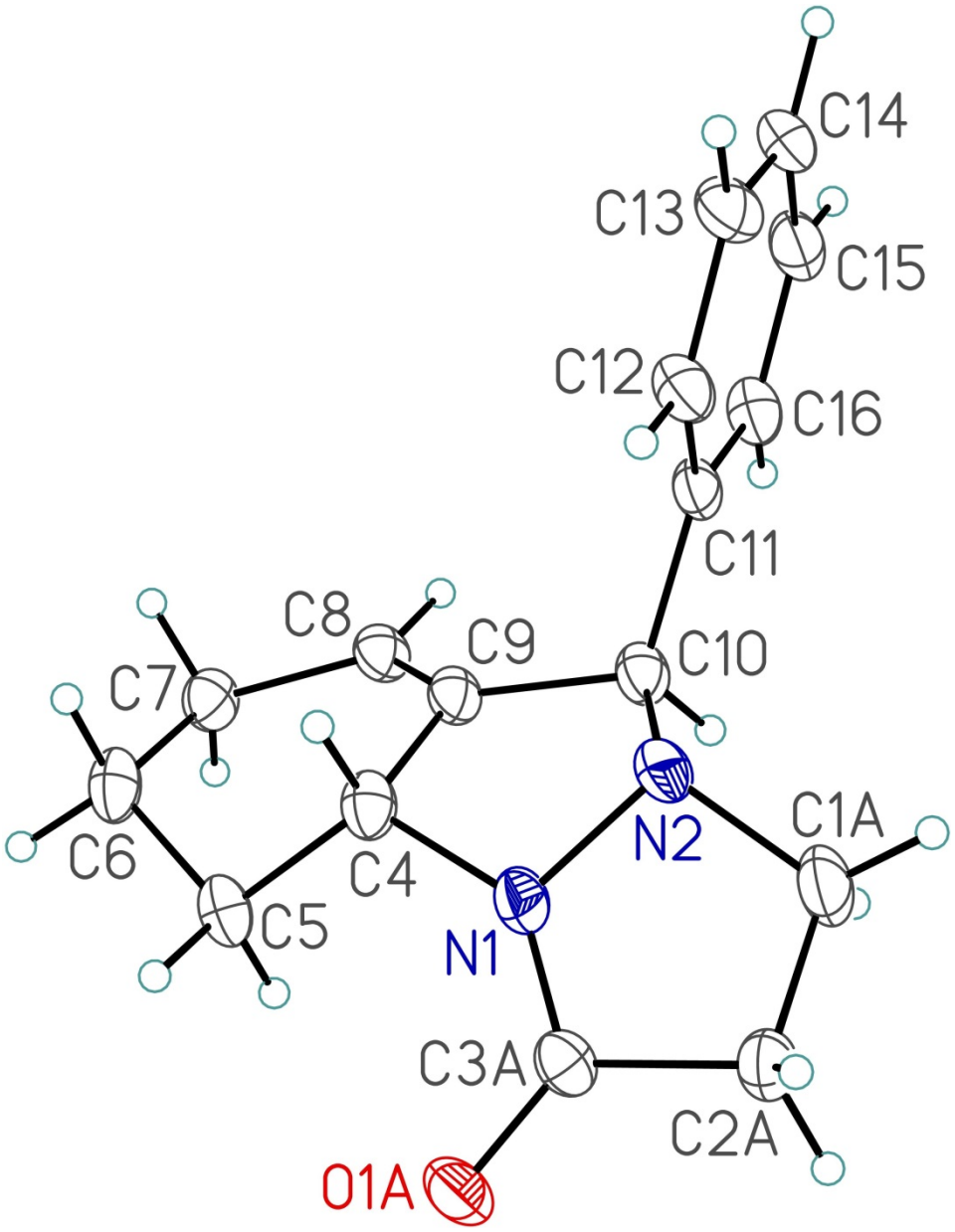
C14
C13
C15
C12
C16
C11
C8
C9
C10
C7
N2
C1A
C6
C4
C5
N1
C3A
C2A
O1A

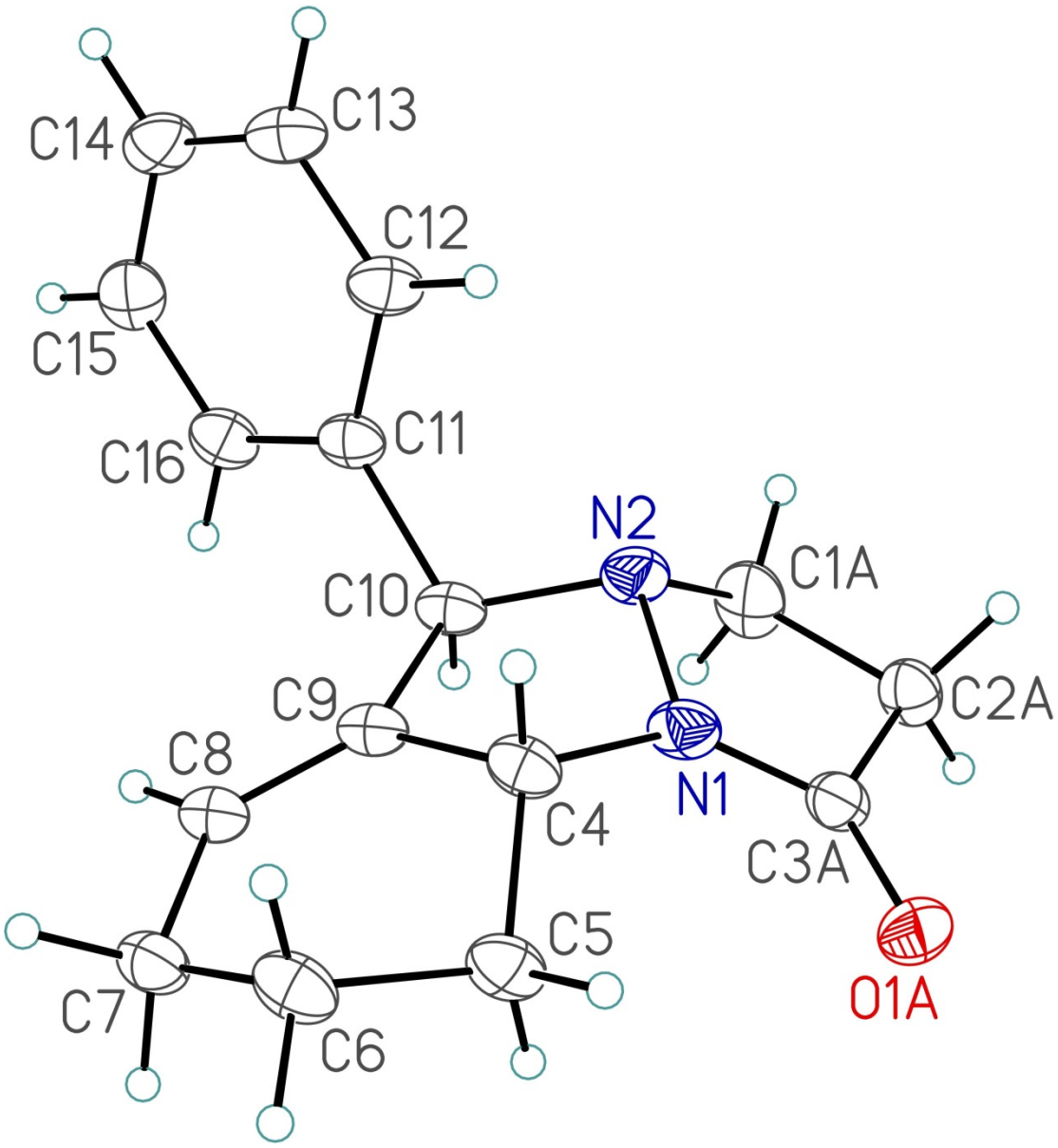
C14
C13
C12
C15
C11
C16
N2
C10
C1A
C9
C2A
C8
N1
C4
C3A
C5
O1A
C7
C6

List of Tables

Table 1. Crystallographic Experimental Details

A. Crystal Data	
formula	$C_{16}H_{18}N_2O$
formula weight	254.32
crystal dimensions (mm)	0.20 × 0.11 × 0.05
crystal system	triclinic
space group	$P\bar{1}$ (No. 2)
unit cell parameters[a]	
a (Å)	6.1406 (2)
b (Å)	10.4845 (4)
c (Å)	11.5339 (4)
α (deg)	65.566 (3)
β (deg)	89.799 (3)
γ (deg)	79.090 (3)
V (Å^3)	661.51 (4)
Z	2
ρ_{calcd} (g cm^{-3})	1.277
μ (mm^{-1})	0.635
B. Data Collection and Refinement Conditions	
diffractometer	Bruker D8/APEX II CCD[b]
radiation (λ [Å])	Cu Kα (1.54178) (microfocus source)
temperature (°C)	–100
scan type	ω and ϕ scans (1.0°) (5 s exposures)
data collection 2θ limit (deg)	146.65
total data collected	4524 (-7 ≤ h ≤ 7, -12 ≤ k ≤ 12, -14 ≤ l ≤ 14)
independent reflections	2535 (R_{int} = 0.0250)
number of observed reflections (*NO*)	2033 [$F_o^2 \geq 2\sigma(F_o^2)$]
structure solution method	direct methods/dual space (*SHELXD*[c])
refinement method	full-matrix least-squares on F^2 (*SHELXL–2013*[d])
absorption correction method	Gaussian integration (face-indexed)
range of transmission factors	1.0000–0.8630
data/restraints/parameters	2535 / 0 / 208
goodness-of-fit (*S*)[e] [all data]	1.026
final R indices[f]	
R_1 [$F_o^2 \geq 2\sigma(F_o^2)$]	0.0416
wR_2 [all data]	0.1149
largest difference peak and hole	0.167 and –0.146 e Å^{-3}

[a]Obtained from least-squares refinement of 4212 reflections with 8.44° < 2θ < 144.50°.

[b]Programs for diffractometer operation, data collection, data reduction and absorption correction were those supplied by Bruker.

[c]Schneider, T. R.; Sheldrick, G. M. *Acta Crystallogr.* **2002**, *D58*, 1772-1779.

[d]Sheldrick, G. M. *Acta Crystallogr.* **2008**, *A64*, 112–122.

[e]$S = [\Sigma w(F_o^2 - F_c^2)^2/(n - p)]^{1/2}$ (n = number of data; p = number of parameters varied; $w = [\sigma^2(F_o^2) + (0.0507P)^2 + 0.1250P]^{-1}$ where $P = [\text{Max}(F_o^2, 0) + 2F_c^2]/3$).

[f]$R_1 = \Sigma||F_o| - |F_c||/\Sigma|F_o|$; $wR_2 = [\Sigma w(F_o^2 - F_c^2)^2/\Sigma w(F_o^4)]^{1/2}$.